ASPECTS OF THE THERMAL HISTORY OF THE EASTERN MARGIN OF CANADA BASED ON APATITE FISSION TRACK AND (U-TH)/HE THERMOCHRONOLOGY

by

Alexander Michael Grist

Submitted in partial fulfillment of the requirements for the degree of
Doctor of Philosophy

at

Dalhousie University
Halifax, Nova Scotia
August, 2004

© Copyright by Alexander M. Grist, 2004

National Library
of Canada

Acquisitions and
Bibliographic Services

395 Wellington Street
Ottawa ON K1A 0N4
Canada

Bibliothèque nationale
du Canada

Acquisisitons et
services bibliographiques

395, rue Wellington
Ottawa ON K1A 0N4
Canada

Your file Votre référence
ISBN: 0-612-94025-X
Our file Notre référence
ISBN: 0-612-94025-X

The author has granted a non-exclusive licence allowing the National Library of Canada to reproduce, loan, distribute or sell copies of this thesis in microform, paper or electronic formats.

L'auteur a accordé une licence non exclusive permettant à la Bibliothèque nationale du Canada de reproduire, prêter, distribuer ou vendre des copies de cette thèse sous la forme de microfiche/film, de reproduction sur papier ou sur format électronique.

The author retains ownership of the copyright in this thesis. Neither the thesis nor substantial extracts from it may be printed or otherwise reproduced without the author's permission.

L'auteur conserve la propriété du droit d'auteur qui protège cette thèse. Ni la thèse ni des extraits substantiels de celle-ci ne doivent être imprimés ou aturement reproduits sans son autorisation.

In compliance with the Canadian Privacy Act some supporting forms may have been removed from this dissertation.

Conformément à la loi canadienne sur la protection de la vie privée, quelques formulaires secondaires ont été enlevés de ce manuscrit.

While these forms may be included in the document page count, their removal does not represent any loss of content from the dissertation.

Bien que ces formulaires aient inclus dans la pagination, il n'y aura aucun contenu manquant.

Canada

DALHOUSIE UNIVERSITY

To comply with the Canadian Privacy Act the National Library of Canada has requested that the following pages be removed from this copy of the thesis:

Preliminary Pages
- Examiners Signature Page (pii)
- Dalhousie Library Copyright Agreement (piii)

Appendices
- Copyright Releases (if applicable)

I dedicate this to the some of the people closest to me whom I love, and who happen to think that education is a worthwhile pursuit.

To my wife Mai, for all her sacrifices, and for being so understanding of all of the time and energy that this has taken.

To my father Robert, mother Patricia, and my sisters Suzanne (Gould), Elizabeth (Wojcik) and Sarah (Fadhil), for your encouragement.

And of course, this is also for my son Michael, because I want him to think education is a worthwhile pursuit, and because recently he has had to do without his dad on many occasions.

TABLE OF CONTENTS

LIST OF TABLES x

LIST OF FIGURES xi

ABSTRACT xvi

List of Abbreviations and Symbols Used xvii

Acknowledgments xviii

CHAPTER 1. Introduction 1

1.1 Objectives and scope of this thesis 1
1.2 Organization of this thesis 2
1.3 Introduction to denudation of rifted margins 3
1.3.1 Tectonic models 3
1.3.2 Surface process models 5
1.3.3 Empirical studies of onshore denudation at rifted margins 7
1.4 Introduction to geologic settings described in this thesis 8
1.4.1 The Fundy Basin and Nova Scotia rifted margin, 45 °N Latitude 8
1.4.2 The Canadian Arctic archipelago and western Greenland, 75°- 85 °N Latitude 11
1.4.2.1 The Sverdrup Basin 11
1.4.2.2 The Nares Strait - Kane Basin - Smith Sound region 14
1.4.2.1.1 The Nares Strait Controversy 15

CHAPTER 2. Introduction to low temperature thermochronology using apatite 16

2.1 FT Dating 16
2.1.1 FT fundamentals 16
2.1.2 FT ages 19
2.1.3 The radial plot and age component analysis 21
2.1.4 Track annealing and track length studies 24
2.1.5 Effects of composition 24
2.1.6 Apatite FT modelling 27
2.1.7 Geological applications 29
2.1.7.1 Provenance studies 29
2.1.7.2 Denudation of orogenic belts 30
2.1.7.3 Thermal analysis of sedimentary basins 31
2.1.7.4 Evolution of rifted continental margins 31
2.1.7.5 Denudation of the onshore of rifted margins 32

2.1.8 Analytical procedures for FT analysis 32
2.2 Apatite (U-Th)/He dating 35
2.2.1 Radiogenic ^{4}He accumulation 36
2.2.2 Age equation 37
2.2.3 Correction for α-emission 37
2.2.4 Helium diffusion in apatite 41
2.2.5 (U-Th)/He thermochronology 43
2.2.6 (U-Th)/He modelling 43
2.2.7 Geological applications 44
2.2.8 Analytical procedures for (U-Th)/He analysis 45

CHAPTER 3. Post-Paleocene cooling in the southern Canadian Atlantic region: Evidence from apatite fission track models 48

3.1 Abstract 48
3.2 Introduction 48
3.3 Regional geological framework 51
3.4 Sampling strategy 54
3.5 Apatite fission track dating 55
3.5.1 Analytical procedures 58
3.6 Discussion of FT data 58
3.6.1 Digby D-1 drillhole 58
3.6.2 Permian-Triassic (PT) outcrop samples 63
3.7 Apatite FT thermal history modelling 66
3.7.1 Digby D-1 model input parameters 67
3.7.2 PT outcrop sample model input parameters 68
3.7.3 FT model results 69
3.8 Discussion and geological interpretation of model results 73
3.9 Conclusions 80
3.10 Acknowledgements 81
3.11 References cited 81

CHAPTER 4. Apatite (U-Th)/He dating constraints on fission track thermal history models of the southern Canadian Atlantic margin 89

4.1 Abstract 89
4.2 Introduction 90
4.2.1 Regional geology 91
4.2.2 Description of samples 92
4.2.2 Apatite (U-Th)/He dating and FT thermal models 95
4.3 Discussion of results 97
4.4 Apatite (U-Th)/He constrained FT thermal models 100
4.5 Conclusions 108

4.6 Acknowledgements 109
4.7 References cited 109
Appendix 1. Analytical procedures for (U-Th)/He analysis 115

CHAPTER 5. Cooling of the Sverdrup Basin during Tertiary basin inversion: implications for hydrocarbon exploration 117

5.1 Abstract 117
5.2 Introduction 118
5.2.1 Regional geology 120
5.2.2 Previous thermal history investigations 123
5.3 Methodology 125
5.3.1 Sample details 125
5.3.2 Apatite fission-track data 128
5.3.3 Modelling procedures 128
5.3.4 Vitrinite reflectance data 133
5.4 Interpretation of thermal history 134
5.4.1 Well samples 134
5.4.1.1 Depot Point L-24, Axel Heiberg Island 134
5.4.1.2 Fosheim N-27 well, Ellesmere Island 134
5.4.1.3 Taleman J-34 well, Ellesmere Island 141
5.4.1.4 Neil O-15 well, Ellesmere Island 141
5.4.1.5 Mid Fiord J-53 well, Axel Heiberg Island 142
5.4.1.6 Sherwood P-37 well, Axel Heiberg Island 142
5.4.2 Outcrop samples 143
5.4.2.1 Fire Bay, Emma Fiord 143
5.4.2.2 Hare Fiord, Chapman Glacier 146
5.4.2.3 Mount Schuchert, Blue Mountains 150
5.4.2.4 Fosheim Anticline, Ellesmere Island 152
5.4.2.5 Mount Bridgeman, Sawtooth Range 154
5.4.2.6 Contact halo suite 158
5.5 Discussion 158
5.5.1 Time of cooling 158
5.5.2 Regional cooling patterns 159
5.5.3 Implications for hydrocarbon maturation 165
5.6 Summary 166
5.7 Acknowledgements 166
5.8 References cited 167

CHAPTER 6. Insights into the thermal history of the Nares Strait, Kane Basin and Smith Sound region in Canada and Greenland from apatite fission track and (U-Th)/He dating 174

6.1 Abstract 174
6.2 Introduction 175
6.2.1 Regional geology 178
6.2.1.1 The Nares Strait Controversy 179
6.2.2 Apatite fission track and (U-Th)/He dating 180
6.2.3 Previous thermal history investigations 182
6.3 Sampling strategy 184
6.4 Discussion of data 189
6.5 Interpretation and geological significance of results 190
6.5.1 Paleozoic-Mesozoic FT-aged samples 190
6.5.1.1 Mesozoic denudation rates 201
6.5.2 Paleogene FT-aged samples 203
6.5.2.2 Does the Wegener Fault exist? 207
6.6 Conclusions 207
6.7 Acknowledgements 208
6.8 References cited 209
Appendix:1 Analytical procedures 216
6.4.1 FT dating 216
6.4.2 (U-Th)/He dating 216

CHAPTER 7. Apatite fission track and (U-Th)/He thermal history modelling of the Nares Strait, Kane Basin, and Smith Sound region in Canada and Greenland 218

7.1 Abstract 218
7.2 Introduction 219
7.3 Thermal history modelling using apatite 220
7.3.1 FT inverse modelling 220
7.3.2 (U-Th)/He forward modelling 221
7.3.3 Calibration of the Laslett et al. (1987) annealing model 222
7.4 Regional geology 227
7.5 Discussion of data and model input parameters 230
7.5.1 Samples with Paleozoic and Mesozoic FT ages 230
7.5.2 Samples with Paleocene FT ages 231
7.5.3 (U-Th)/He forward models 231
7.6 Quantitative apatite compositions 231
7.7 Model results 236
7.7.1 Samples with Paleozoic and Mesozoic FT ages 236
7.7.2 Samples with Paleocene FT ages 243
7.8 Discussion and geological significance of model results 249
7.9 Conclusions 251
7.10 Acknowledgements 252
7.11 References cited 252

CHAPTER 8. Summary and geologic overview 258

8.1. Discussion of methodology 258
8.2. Discussion of regional denudation of basin margins 260
8.2.1. Low-temperature thermal history of the Nova Scotia margin 260
8.2.1.1 History of rifting 260
8.2.1.2 Late Cretaceous heating 262
8.2.2. Low-temperature thermal history of the Sverdrup Basin 263
8.2.3. Low-temperature thermal history of eastern Ellesmere Island and western Greenland 264
8.2.4. Low-temperature thermal history of Nares Strait 265
8.3. Scientific contributions of this work 266

REFERENCES CITED 268

APPENDIX A. Sample preparation 295
A.1. Mineral separation techniques used to obtain apatite 295
A.2. Preparation of apatite grainmounts for fission track analysis 297

APPENDIX B. Apatite FT model inversion control parameters used and resulting model temperature history summaries for the Digby D-1 well and Permian-Triassic outcrop samples 303

APPENDIX C. Apatite FT model inversion control parameters used and resulting model temperature history summaries for the (U-Th)/He constrained thermal models for the southern Canadian Atlantic margin 339

APPENDIX D. Apatite FT model inversion control parameters used and resulting model temperature history summaries for the eastern Ellesmere Island, Nares Strait, Kane Basin and western Greenland outcrop samples 357

APPENDIX E. Apatite compositional data for the Nares Strait, Kane Basin region of Ellesmere Island and western Greenland 406

APPENDIX F. Letters of permission for the use of copyrighted materials 419

LIST OF TABLES

Table 2.1. The isotopic abundances, half-lives and decay constants of ^{238}U, ^{235}U, ^{232}Th and ^{147}Sm 36

Table 3.1. A summary of the locations and lithologies of the samples in the southern Atlantic margin 56

Table 3.2. A summary of the apatite FT age and TL data. 60

Table 4.1. A summary of the samples and (U-Th)/He data 102

Table 5.1. Apatite fission track age and length data for well samples 130

Table 5.2. Vitrinite reflectance data from well samples 136

Table 5.3. Vitrinite reflectance data from outcrop samples 147

Table 5.4. Apatite fission track age and length data for outcrop samples 149

Table 6.1. Samples collected during the Nares Strait Geocruise 2001 187

Table 6.2. A summary of the FT age and TL data. 192

Table 6.3. A summary of the (U-Th)/He data 195

Table 7.1. Average compositional analyses of selected apatite samples 233

LIST OF FIGURES

Figure 1.1. Schematic illustration of the evolution of a rifted continental margin 4

Figure 1.2. Conceptual illustration of lithospheric necking 6

Figure 1.3. Geologic map and schematic cross section of the Fundy Basin region 10

Figure 1.4. Map of the Canadian Arctic Archipelago. 12

Figure 1.5. Schematic relationship between depth of burial, hydrocarbon maturity, maximum temperature, vitrinite reflectance, and apatite FT annealing 14

Figure 2.1. The ion spike model for the formation of fission tracks 18

Figure 2.2. The steps involved in the external method 22

Figure 2.3. Example of a radial plot of FT age data 23

Figure 2.4. Schematic illustration of the apatite FT PAZ and an exhumed PAZ 26

Figure 2.5. Diagrammatic illustration of the relationship between subsidence of a basin margin and denudation of the sediment source region 33

Figure 2.6. FT age-length plots (boomerangs) for 5 data sets obtained from the onshore part of rifted continental margins 34

Figure 2.7. The decay schemes for ^{238}U to stable ^{206}Pb and ^{235}U to stable ^{207}Pb. 38

Figure 2.8. The decay scheme for ^{232}Th to stable ^{208}Pb. 39

Figure 2.9. The F_t correction as a function of grain radius for a hexagonal prism 40

Figure 2.10. A comparison of the FT PAZ and helium PRZ in apatite 42

Figure 2.11. Schematic illustration of the (U-Th)/He quadropole mass spectrometer sample line 47

Figure 3.1. Map of the study area in southern Atlantic margin 50

Figure 3.2. Schematic cross section of the central part of the study area 52

Figure 3.3. A cross-section of the Digby D-1 drillhole and summary figures of AFT

age and mean confined track length vs. depth. 57

Figure 3.4. Confined TL histograms and statistics for the Digby D-1 drillhole. 61

Figure 3.5. Radial plots of the AFT age data from the Digby D-1 drillhole. 62

Figure 3.6. Confined TL histograms and statistics for eight PT outcrop samples 64

Figure 3.7. Radial plots of the AFT age data for eight PT outcrop samples 65

Figure 3.8. Cooling only t-T models for 2 Digby D-1 well samples 70

Figure 3.9. One heat pulse time-temperature models for the Digby D-1 drillhole 71

Figure 3.10. One heat pulse models obtained for the Martin Head, McCumber Point, Rainy Cove, and Partridge Island samples 72

Figure 3.11. Exponential mean t-T paths for 8 samples from the Digby D-1 well, and geothermal gradients 74

Figure 3.12. Long-term eustatic Mesozoic and Cenozoic sea level curve 75

Figure 3.13. Zonally averaged mean annual surface temperature as a function of latitude for Campanian time and the present day 77

Figure 3.14. Temperature change as a function of time for depths of 0.5 to 5 km that would result from an instantaneous change in surface temperature of -20 °C. 79

Figure 4.1. Map of the study area showing sample locations and selected lithologic and stratigraphic elements 93

Figure 4.2. Schematic cross-section A-A' of the central part of the study area 94

Figure 4.3. Inverse FT thermal models and modelled /measured TL distributions for an empirically determined Durango apatite standard length distribution 99

Figure 4.4. Thermal history models for the Gays River Pb-Zn deposit in southern Nova Scotia, and for the Digby D-1 well 105

Figure 4.5. Apatite FT inverse thermal models and (U-Th)/He forward model results 107

Figure 5.1. Simplified geology of the northern Canadian Arctic archipelago 119

Figure 5.2. North-south cross section from Fig. 5.1(a) area 126

Figure 5.3. Summary of compositions from detrital apatite grains from sandstone samples, Fosheim Peninsula. 131

Figure 5.4. Well profiles showing apatite fission-track data, vitrinite reflectance measurements, and stratigraphy.. 138-140

Figure 5.5. Geology and samples locations from Emma Fiord, Ellesmere Island 145

Figure 5.6. Geology of the Lake Hazen fault zone between Hare Fiord and Chapman Glacier, Ellesmere Island 151

Figure 5.7. Geology of the Blue Mountains, Ellesmere Island 153

Figure 5.8. Geology of the Fosheim Anticline, Fosheim Peninsula, Ellesmere Island . 155

Figure 5.9. Geology of the northern Sawtooth Range 157

Figure 5.10. Summary of fission-track data from outcrop and shallow well samples . 161

Figure 5.11. Summary of ages estimated for the onset of track retention from 10 outcrop samples from northern Ellesmere Island 162

Figure 5.12. Geographic distribution of cooling in the Sverdrup Basin 163

Figure 6.1. Generalized map of the Innuitian Orogen of Arctic Canada and western Greenland 177

Figure 6.2. Clastic sediment supply curve for the Sverdrup Basin 181

Figure 6.3. Simplified geologic map of the Cape Back area 185

Figure 6.4. FT age vs mean TL for outcrop samples from eastern Ellesmere and Devon Islands, western Greenland and the Sverdrup Basin 198

Figure 6.5. Radial plots (left) and TL histograms (right) of the FT data for samples from the Leffert Glacier and Makinson Inlet on eastern Ellesmere Island 199

Figure 6.6. Radial plots (left) and TL histograms (right) of the FT data for samples from the Wolstenholme Fjord/Thule region of Greenland 200

Figure 6.7. Radial plots (left) and TL histograms (right) of the FT data for samples from Cape Faraday and Orne Island, eastern Ellesmere Island, and the Carey Øer 202

Figure 6.8. FT age vs. elevation (top) and mean TL vs. elevation (bottom) for samples from Devon Island, Kap Trautwine, and Rensselaer Bugt 204

Figure 6.9. Radial plots (left) and TL histograms (right) of the FT data for samples from south of Cape Baird, north of Cape Back, and Cape Lawrence 206

Figure 7.1. Induced and spontaneous track length distributions in Durango apatite standard 224

Figure 7.2. Inverse FT thermal models and modelled /measured TL distributions for Durango apatite standard 226

Figure 7.3. Generalized map of the Innuitian Orogen of Arctic Canada and western Greenland 228

Figure 7.4. A plot of measured apatite FT age vs. confined TL for the samples from the Nares Strait - Kane Basin - Smith Sound region 229

Figure 7.5. Summary ternary plots of Cl-F-OH compositions for apatite 234

Figure 7.6. Chondrite-normalized REE compositions determined by ICP-MS. 237

Figure 7.7. Apatite FT inverse and (U-Th)/He forward thermal models for samples from the Inglefield Uplift 238

Figure 7.8. Apatite FT inverse and (U-Th)/He forward thermal models for volcanic samples from Manson Øer, Thule and Dundas Mountain 241

Figure 7.9. Apatite FT inverse thermal models for samples from Herbert Ø, Haklyut Ø and Kap Trautwine 242

Figure 7.10. Apatite FT inverse and (U-Th)/He forward thermal models for samples from Talbot Inlet and Carey Øer 244

Figure 7.11. Apatite FT inverse and (U-Th)/He forward thermal models for Archean gneiss samples from southeastern Devon Island 245

Figure 7.12. Apatite FT inverse and (U-Th)/He forward thermal models for Upper Paleocene-aged samples from the Pavy Formation 247

Figure 7.13. Apatite FT inverse and (U-Th)/He forward thermal models for samples from the Cambrian Archer Fiord Formation (left) and Upper Paleocene Mount Lawson Formation, Ellesmere Island 248

Figure 7.14. Exponential mean t-T histories for closely spaced samples with substantially different elevations 250

Figure A.1. A Frantz® magnetic barrier laboratory separator equipped with a constant current amplifier 296

Figure A.2. Epoxy grainmounts on Teflon-coated bakeware 298

Figure A.3. A Struers® Planopol-V semi-automatic polisher equipped with a PDM-Force sample holder. 300

Figure A.4. Two irradiation capsules that are used to compress a stack of fission track samples 302

ABSTRACT

Apatite fission track (FT) and (U-Th)/He thermochronology and vitrinite reflectance (R_o) are used to study cooling and inferred denudation in 3 areas; 1) the Triassic - Early Jurassic Fundy Basin, a failed rift subsequently exhumed as part of the onshore southern Canadian Atlantic margin; 2) the Late Paleozoic - Mesozoic Sverdrup Basin, an inverted intracratonic failed rift that developed following the Ellesmerian Orogeny in the Canadian Arctic Archipelago; and 3) the Sverdrup Basin sediment source region around Nares Strait - Kane Basin - Smith Sound, an area affected by the Paleogene Eurekan Orogeny.

A limitation of the Laslett et al. (1987) FT annealing model is elucidated, and I demonstrate that low-temperature estimates from that model are inconsistent with measured (U-Th)/He ages. An initial model track length of 15 μm eliminates unrealistic late-stage FT model cooling and produces temperature histories compatible with (U-Th)/He data. The importance of measuring ^{147}Sm in (U-Th)/He-dated samples is also demonstrated. Up to 20% of the radiogenic ^{4}He in my samples was ^{147}Sm-derived. Failure to consider this ^{4}He source would cause considerable overestimation of (U-Th)/He ages.

(U-Th)/He data and FT models for the southern Canadian Atlantic margin demonstrate that following the onset of Atlantic rifting, the region experienced rapid Jurassic exhumational cooling. FT and R_o data from the Sverdrup Basin demonstrate substantial cooling from inversion during the Eurekan Orogeny. Many thrust faults drilled during hydrocarbon exploration in the basin in the 1970's were active during the Eurekan Orogeny, which post-dates primary hydrocarbon maturation and migration, and are therefore poor targets. (U-Th)/He data and FT models for the Kane Basin - Smith Sound region suggest the complex thermal history results from at least 3 tectonic influences; 1) Late Paleozoic - Early Mesozoic regional exhumation related to Sverdrup Basin development; 2) Late Cretaceous cooling of rift flanks following the onset of Labrador Sea - Baffin Bay rifting; and 3) Paleocene inversion related to Eurekan convergence between Ellesmere Island and Greenland. FT ages related to the orogeny from fault-bounded basins near Nares Strait are older than ages from thrust fault hanging walls in central Ellesmere Island, suggesting cooling progressed east-west.

LIST OF ABBREVIATIONS AND SYMBOLS USED

FT = fission track

TL = track length

PAZ = partial annealing zone

(U-Th)/He = uranium-thorium-helium

PRZ = partial retention zone

F_t = fraction of helium retained

Ma = millions of years before present

My = millions of years duration

ICP-MS = inductively coupled plasma - mass spectrometer

REE = rare earth element

μm = micrometres

SMB = South Mountain Batholith

t-T = time-temperature

ACKNOWLEDGEMENTS

Although I take complete responsibility for the contents of this thesis, I am grateful to a number of people who have helped me to see it to completion with scientific, technical and/or logistical support. The most important among these is my committee supervisor Marcos Zentilli. He not only assisted me with much of the science in this thesis, he is also a great facilitator. He helped me to become involved with the Nares Strait Geocruise, and he allowed the FT and (U-Th)/He work in this thesis to proceed at the expense of the Dalhousie Fission Track Laboratory. He is also unflaggingly optimistic. This work could not have been completed without his guidance and support. I also gratefully acknowledge the valuable contributions of my other committee members; Chris Beaumont, for his very insightful and perceptive suggestions and his willingness to thoroughly review numerous early versions of this manuscript; and Peter Reynolds, for his valuable discussions on the science, the thesis layout, and his pragmatic approach to getting the work done in a timely fashion.

I am also very grateful to Dennis Arne for allowing me to include his scientific research on the Sverdrup Basin in this thesis (Chapter 5), for helping me to become involved in the study of the low-temperature thermal history of the Arctic Archipelago, and for his insights on Late Cretaceous heating in the southern Canadian Atlantic margin. Ken Farley has provided many valuable insights on all aspects of (U-Th)/He dating, and has shown me a great deal of hospitality during my visits to his lab at Caltech. Lindsey Hedges also taught me a lot of the technical 'hands-on' (U-Th)/He dating procedures at Caltech, ran most of my ICP-MS analyses, and provided excellent company during long evenings of sample preparation.

I also gratefully acknowledge the contributions of several of the participants of the Nares Strait Geocruise, who provided me with scientific, logistical and financial support; in particular, Franz Tessensohn, Ruth Jackson and Christopher Harrison. Thanks also to Debra Wheeler, for her enthusiastic and capable assistance in mineral separation and sample preparation in the Fission Track Laboratory, and to Patricia Stoffyn, who provided excellent technical guidance during my apatite compositional analyses in the Microprobe Laboratory.

I also gratefully acknowledge the contributions of my thesis external examiner, Tony Hurford, for his constructive reviews of my thesis and my defence presentation, and to the other examining committee members, Marcos Zentilli, Peter Reynolds, Djordje Grujic, and Rebecca (Becky) Jamieson, for a final edit of the thesis.

Finally, I have to especially acknowledge my co-conspirator in the lab/office space, Milton Graves, for putting up with both good days and bad days for many years now.

CHAPTER 1. Introduction

1.1 Objectives and scope of this thesis

This thesis presents the results of three separate but related geological thermochronology studies using apatite fission track (FT) dating and FT-based inverse thermal modelling. Each study also incorporates a second thermochronometric technique that is used to extend the range of the study to higher (vitrinite reflectance) or lower (apatite (U-Th)/He dating) temperatures. These techniques are used to infer detailed thermal histories and develop thermal models for two regions where coupled basin - source region systems have evolved in the Canadian Arctic and the southern Canadian Atlantic margin. The geological settings for the Arctic studies are the Sverdrup Basin, an inverted post-orogenic basin and failed rift that developed during Late Paleozoic and Mesozoic time following the Ellesmerian Orogeny, and the exhumed onshore sediment source region around Nares Strait - Kane Basin - Smith Sound on the northeastern flank of the Sverdrup Basin. The Atlantic passive margin study focusses on the Fundy Basin region, a Triassic failed rift that subsequently formed part of the onshore of the present Atlantic margin.

The principal objective of this thesis is to demonstrate that the patterns of denudation of sediment source regions for the southern Canadian Atlantic rifted margin and the margin of the Sverdrup Basin in the Canadian Arctic Archipelago broadly conform to tectonic and surface process models that have been developed to describe the evolution of passive rifted margins. The primary assumption of this work is that the exhumation or denudational history of the onshore portion of these systems is intimately related to the burial and subsidence history within the offshore basins. Periods of peak basin subsidence correspond to periods of accelerated denudation of the onshore. However, unlike the offshore regions where the subsidence history is recorded in the sediment sequences, the direct geological evidence of exhumation onshore is lost through erosion.

The apatite FT and (U-Th)/He techniques are uniquely suited to the study of onshore denudation because they are sensitive to temperatures which correspond to those that exist in the upper few km of the crust and, therefore, have the potential to provide quantified

estimates of the spatial and temporal distribution of denudation. Using both of these techniques increases the range of temperatures over which thermal history information can be inferred beyond that of either technique individually. In addition, because the temperature sensitivities of the methods are based on independent kinetic mechanisms (He diffusion and track annealing) each method demonstrates consistency in the other, and thereby permits development of a quantitative intercalibration between them. In areas where the geological history is reasonably well understood refinements to the calibration of these complementary thermochronometric techniques are demonstrated.

1.2 Organization of this thesis

This thesis comprises an introduction, five papers (two published in scientific journals and three in preparation for publication), a summary discussion of the major results, and several appendices (containing compositional data and FT thermal model parameters). Chapter 1 is an introduction to the thesis. It describes the main objectives of the work, provides an introduction to the concept of denudation at continental margins, and provides a statement of the problem and an overview of the regional geologic framework for each of the study areas. Chapter 2 introduces apatite FT and (U-Th)/He methodology and serves to establish the capacity of these methods to infer the detailed thermal history of the study regions. Chapters 3 and 4 present the results of an apatite FT and (U-Th)/He study of the onshore region of the southern Canadian Atlantic margin. Chapter 3 presents apatite FT inverse thermal models for this region, and was published in Canadian Journal of Earth Sciences (Grist and Zentilli 2003). Chapter 4 presents (U-Th)/He dating and forward modelling constraints on the FT thermal models in Chapter 3. Chapters 5-7 present the results of two thermochronology studies set in the Canadian Arctic Archipelago and western Greenland. Chapter 5 is a study of the inversion of the Late Paleozoic - Mesozoic Sverdrup Basin using apatite FT and vitrinite reflectance and was published in Basin Research (Arne et al. 2002). Chapter 6 presents the results of an apatite FT and (U-Th)/He study of the northeast margin of the Sverdrup Basin in the Nares Strait - Kane Basin - Smith Sound region. Chapter 7 presents apatite FT inverse models that are constrained by (U-Th)/He

forward models for the Nares Strait - Kane Basin - Smith Sound region. Chapter 8 provides an overview and discussion of the main results of Chapters 3 - 7.

As detailed in the student contribution form at the beginning of this thesis, all of the written material herein (except Chapter 5) is the original work of A.M. Grist with assistance and guidance from M. Zentilli and others (who are acknowledged in individual chapters). Chapter 5 was written by D.C. Arne. A.M. Grist provided scientific input for that work, performed the inverse FT modelling, analyses of all surface samples, and provided assistance in manuscript and figure preparation.

1.3 Introduction to denudation of rifted margins

An overview of the development of numerical modelling of tectonic processes at convergent and divergent plate boundaries was recently given by Beaumont et al. (2000). The following summary is mainly derived from that work, and from van der Beek (1995).

Passive, or Atlantic-type, continental margins are formed fundamentally by the rifting and divergence of lithospheric fragments as a result of upward convection of the underlying mantle, and are one of the Earth's primary topographic features (Fig. 1.1). The principal result of rifting is subsidence and basin formation. However, exhumation and denudation of the onshore has also long been recognized as an integral part of the rifting process. Falvey (1974) first proposed that an unconformity (the breakup unconformity) present in the sedimentary record of the adjacent onshore flanks of rifted continental margins was caused by uplift and erosion of the flanks during mantle upwelling prior to the initiation of sea-floor spreading in the basin.

1.3.1 Tectonic models

Early models of lithospheric rifting were focussed on tectonic processes operating on a crustal-scale. McKenzie (1978) presented the first mathematical formulation which described the isostatic response to thinning and stretching of the lithosphere by pure shear. Subsequently, a number of refinements to the McKenzie (1978) model were incorporated to include the effects of lateral heat conduction to the basin flanks (Cochran 1983), the finite

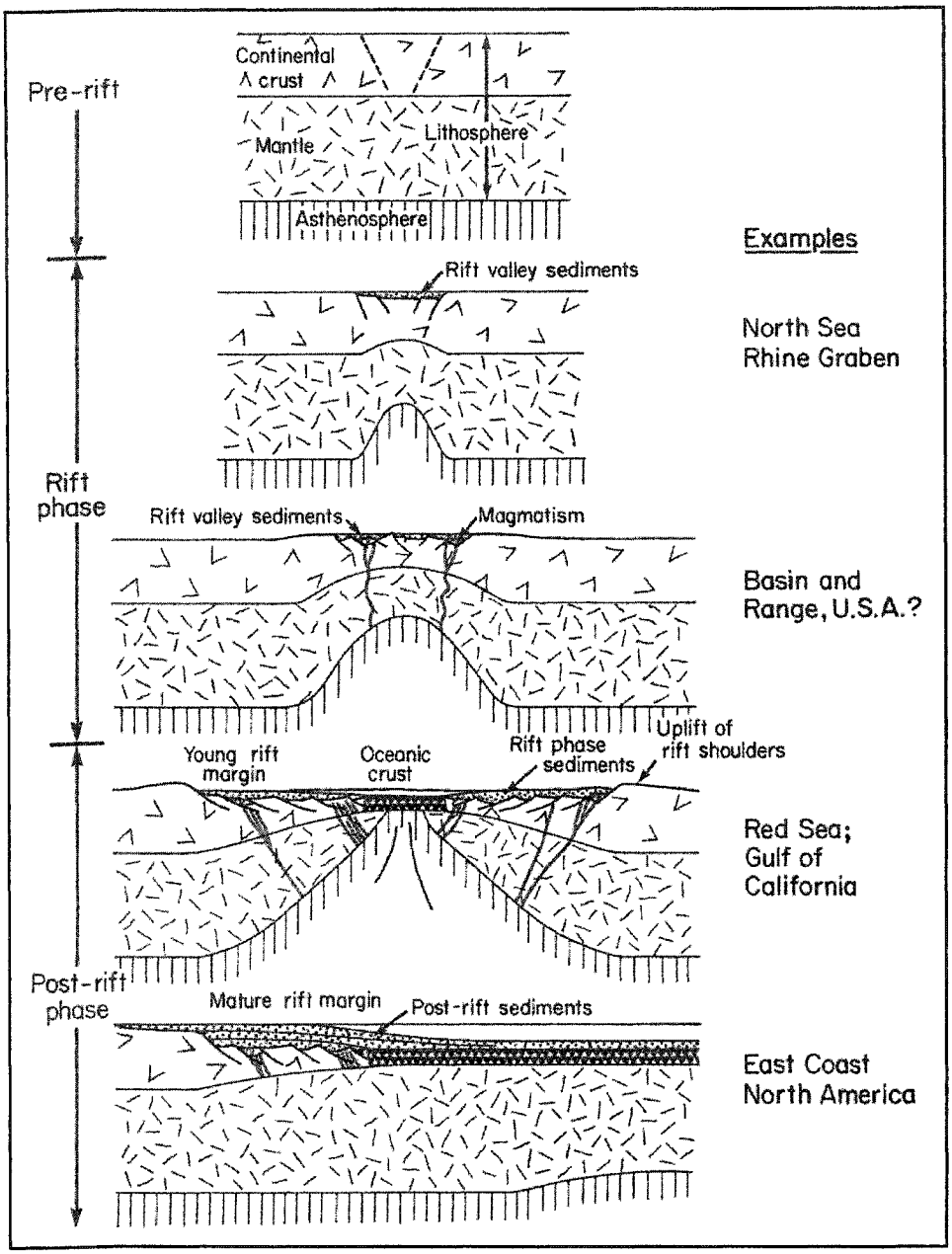

Figure 1.1. Schematic illustration of the evolution of a rifted continental margin (from Keen and Beaumont, 1990). Examples of each of the evolutionary stages are given at right. The transition from the rifting stage to the drifting (post-rift) stage is associated with the initial production of oceanic crust.

duration of rifting (Jarvis and McKenzie 1980), and depth-dependent extension (Royden and Keen 1980; Beaumont et al. 1982). Alternate kinematic models based on simple shear or a combination of simple and pure shear have also been developed (e.g. Wernicke 1985; Lister et al. 1986, 1991; Hegarty et al. 1988; Issler et al. 1989).

A number of possible mechanisms for causing rift flank uplift have been proposed based on the tectonic models. These include differential stretching between the crust and mantle (Royden and Keen 1980), lateral heat flow (Cochran 1983), magmatic underplating (White and McKenzie 1989), and the effects of secondary mantle convection (Buck 1986). Braun and Beaumont (1989) demonstrated that for an extensional model using a rheologically layered lithosphere, if the level of necking was sufficiently deep it would be below the depth of isostatic compensation for the basin, and an upward state of flexure would be induced in the rift flanks (Fig. 1.2). Weissel and Karner (1989) also propose a flexural isostatic response caused by mechanical unloading of the lithosphere. These latter two mechanisms are appealing in that they allow for observed persistence of uplifted rift flanks on time scales of >100 Ma; much longer than the time required for cooling of the lithosphere following rift-related heating (e.g. Braun and Beaumont 1989).

1.3.2 Surface process models

Although tectonic models are useful for describing the large-scale features of rifted margins, they do not adequately predict the detailed geomorphology that is observed. Features such as the great escarpments which are present in the margins of southern Africa, eastern South America, southeastern Australia, and elsewhere (e.g. Ollier 1985) are not well explained by these models, and the diverse topographic expressions of many passive margins of similar age suggest that in addition to tectonic processes, they also reflect a complex interplay of a variety of surface processes. These surface processes redistribute material through denudation of the uplifted regions and deposition in the basins, and thereby modify the gravitational forces and affect the fundamental tectonic processes and the syn- and post-rift tectonic and isostatic evolution of the margin (e.g. Beaumont et al. 2000). In order to better understand the detailed evolution of rifted margins, surface process models (and

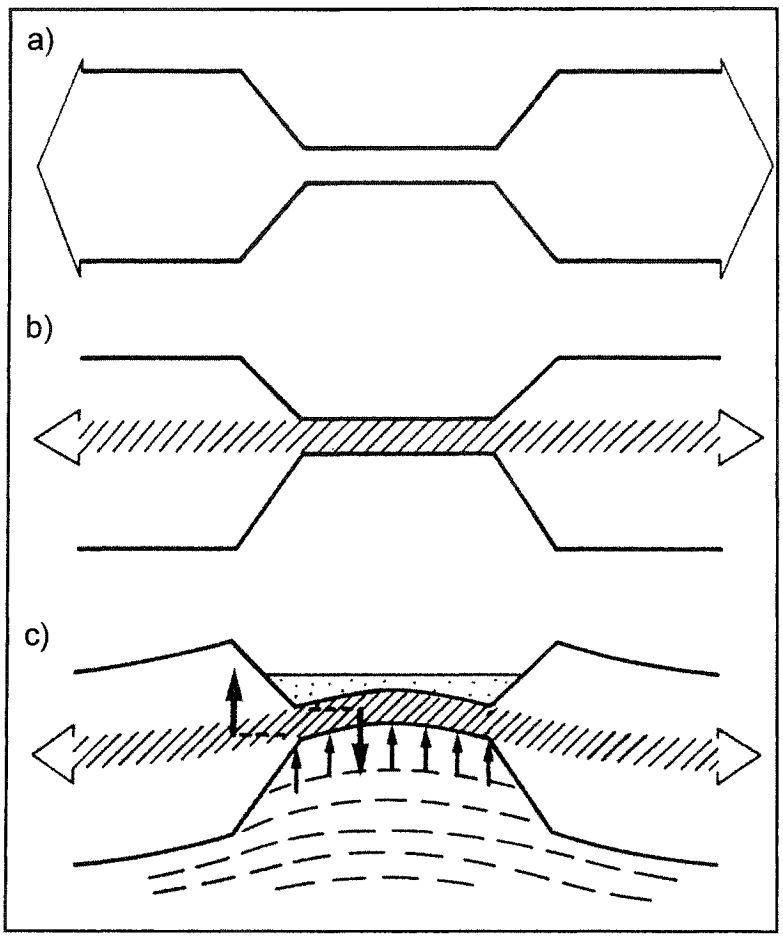

Figure 1.2. Conceptual illustration of lithospheric necking and isostatic adjustment (simplified from Braun and Beaumont 1989). a: Symmetric intrinsic necking of uniform lithosphere. b: Non-symmetric necking of a non-uniform lithosphere controlled by a strong layer (diagonally shaded band). c: If necking occurs below the depth of isostatic compensation, buoyancy forces from the underlying asthenosphere (dashed area) result in upward flexure and mechanical support of the rift flanks and overdeepening of the basin adjacent to the rift flanks. If the level of necking is shallow (not shown), the sense of the buoyancy is reversed, and downward flexure of the lithosphere results.

coupled tectonic-surface process models), which incorporate the lateral flux of mass in response to both tectonic uplift and the evolving geomorphology have been developed (e.g. Gilchrist et al. 1994; Kooi and Beaumont 1994, 1996; Tucker and Slingerland 1994; van der Beek et al. 2002; and others).

In regard to the erosion of rift flank uplift, the key components of these models are the antecedent (ancestral) drainage pattern and the position of the antecedent drainage divide, the mode of fluvial evolution, and the erodability of the material affecting the landscape response time. Two principal modes of landscape evolution as a result of drainage were identified by Kooi and Beaumont (1994), slow parallel retreat and rapid incision. Rapid incision allows high-capacity antecedent rivers draining large catchment areas to compete with the rapid uplift caused by rift flank tectonics and continue to drain as before. In areas of small rivers, the tectonic escarpment forms a new drainage divide, and the escarpment migrates away from the coast by slow parallel retreat (e.g. Beaumont et al. 2000). The rate of landscape evolution is also influenced by the erodability of the tectonically uplifted material. Denudational response times are rapid for sedimentary rocks that are easily eroded, and are much longer for crystalline rocks. The combination of lithologies that exhumed during rapid incision or slow retreat can also strongly influence the geomorphic evolution, producing complex features such as pinnacles and scarps with resistant caprocks.

1.3.3 Empirical studies of onshore denudation at rifted margins

A number of empirical studies have focussed on the post-rift denudational history of the onshore part of passive margins (e.g. Mathews 1975; Ollier 1985; Pazzaglia and Gardner 1994). Poag and Sevon (1989), Poag (1992), Pazzaglia and Brandon (1996), Pazzaglia and Gardner (2000), and others have inferred spatial and temporal patterns of denudation in the central Appalachians based on sediment yields in the central North Atlantic margin. These studies require an assumption about the spatial and temporal relationship between sediment yields in the basin and denudation rates in the source regions because the provenance of the sediments is ultimately unknown.

A number of thermochronology studies have also been done using apatite FT dating

to infer the denudation histories of the on-land part of rifted margins (e.g. Omar et al. 1989; Brown 1992; Gallagher et al. 1994, 1995; Menzies et al. 1997; Brown et al. 2002; and others). An advantage of this type of approach is that quantitative estimates of the geographical distribution of cooling and inferred denudation can be easily obtained. However, a limitation of thermochronology studies is that it is often difficult to distinguish between tectonic denudation associated with normal faulting and erosional denudation. The application of FT thermochronology to the study of denudation is discussed further in Chapter 2.

1.4 Introduction to geologic settings described in this thesis

The regional geology of the southern Canadian Atlantic margin is discussed in detail in Chapters 3 and 4 of this thesis. The geologic history of the Sverdrup Basin is discussed in Chapters 5 and 6. The geologic history of the eastern Arctic Nares Strait - Kane Basin - Smith Sound region is given in Chapters 6 and 7. A brief overview of the principal geological elements and a description of the problems related to the regional thermal history that are addressed in those chapters is given here.

1.4.1 The Fundy Basin and Nova Scotia rifted margin, 45 °N Latitude

Offshore Nova Scotia forms part of the present southern Canadian Atlantic margin, an active depositional basin from Late Triassic-Early Jurassic time to the present (e.g. Keen and Williams 1990). Early rifting of the margin was focussed between Nova Scotia and New Brunswick, and remnants of this failed rift comprise the Triassic Fundy Basin (Fig. 1.3; e.g. Wade et al. 1996; Olsen and Schlishe 1990). A major Late Triassic erosional unconformity in southwestern Nova Scotia marks the beginning of accumulation of Fundy Basin rift-related sequences. Post-Jurassic strata are largely absent in the onshore region, although limited Lower Cretaceous strata consist of small, unconsolidated deposits of kaolinitic clay and quartzose sand preserved from erosion in depressions and sinkholes in central Nova Scotia, which are collectively called the Chaswood Formation (Stea et al. 1997).

The traditional model for the evolution of the Nova Scotia margin therefore is one

of long-term peneplanation and an ancient landscape (e.g. Goldthwait 1924). Apatite FT studies of Paleozoic basement in Nova Scotia (Ravenhurst et al. 1990; Arne et al. 1990) and of Upper Paleozoic strata from the Maritimes Basin, Nova Scotia, Prince Edward Island, and beneath the Gulf of St. Lawrence (Ryan and Zentilli 1993; Grist et al. 1995) have confirmed that strata now at or near the surface were formerly buried by extensive Late Carboniferous to Early Permian cover to depths of at least 4-5 km. Recently, based on existing geological and geophysical data, Withjack et al. (1998) inferred a regional inversion of the Fundy Basin between ca. 185 Ma.and 150 Ma (Late Jurassic - Early Cretaceous). A thermal history of simple cooling following Triassic rifting was also inferred by Ravenhurst et al. (1990) based on apatite fission track data from southwestern Nova Scotia.

The presence of Lower Cretaceous strata however, implies a more complex thermal history than simple cooling, and at least 2 cycles of (pre- and post- Early Cretaceous) denudation. Coal compaction and vitrinite reflectance studies (Hacquebard 1984) of lignite contained in several of these deposits in Nova Scotia support this hypothesis, and indicate that these are erosional remnants of formerly more extensive strata. Hacquebard (1984) estimated that up to 700-800 m of Cretaceous sediments may have covered Nova Scotia onshore. Arne et al. (1990) suggested that basement rocks at Gays River in southwestern Nova Scotia also experienced heating to temperatures of 60-80 °C between about 100 and 50 Ma. The Arne et al. (1990) thermal model was constrained by Albian-Aptian-aged spores and lignite in Chaswood Formation sediments preserved from glacial erosion in karst depressions, indicating that the strata were at the surface at about 120-100 Ma. However, a lack of long confined apatite fission tracks, which would have accumulated if the samples had remained at the surface for 120 million years, implied that the rocks had experienced significant post-Albian heating. Evidence for similar heating (in terms of magnitude and timing) was also indicated by FT models for the offshore region in Scotian Basin strata, 300 km southeast of Gays River (Grist et al. 1992; Li et al. 1995).

Thus it is possible that elevated temperatures during Late Cretaceous - Early Tertiary time were a regional phenomenon, meriting a focussed study of Mesozoic and older rocks in order to investigate the timing, magnitude, and areal extent, and to assess possible causes,

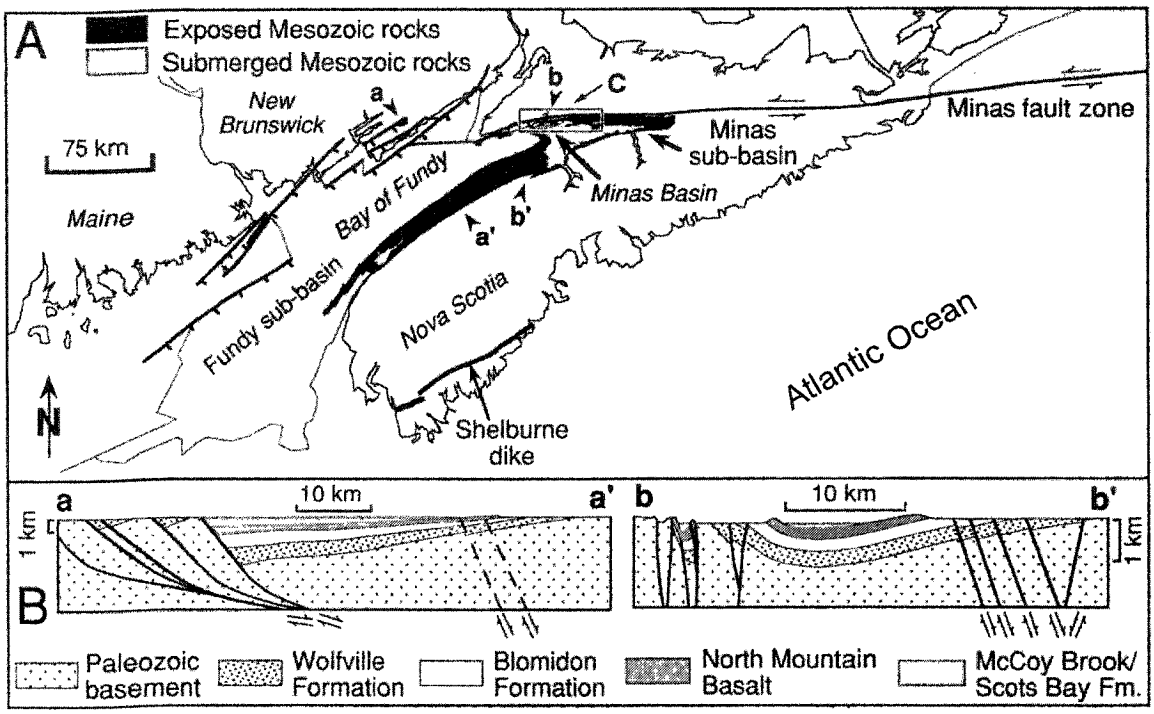

Figure 1.3. Geologic map and schematic cross sections of the Fundy Basin region showing the relationship of the main stratigraphic elements (simplified from Olsen and Schlishe 1990). Summaries of the geologic history of the basin and descriptions of the formations named below the cross sections are given in Chapter 3.

effects, and significance of elevated temperatures with respect to tectonic models. The recent emergence of the southern Canadian Atlantic margin as an area of intense hydrocarbon exploration and development activity has only increased the necessity for refined thermal history models for this region.

1.4.2 The Canadian Arctic Archipelago and Western Greenland, 75°- 85°N Latitude

1.4.2.1 The Sverdrup Basin

The Sverdrup Basin is a Late Carboniferous and Mesozoic failed continental rift basin in the northern Canadian Arctic Archipelago (Fig. 1.4). Sedimentation ended in latest Cretaceous and Paloegene time and the basin was inverted as a result of the relative tectonic movements between northwest Greenland and eastern Ellesmere Island (the Eurekan Orogeny). In many parts of the basin, >10 km thickness of Late Paleozoic and Mesozoic strata occur, however the basin's resource potential remains largely unknown because of its large size (ca. 1300 km long by up to 400 km wide) and relative inaccessibility.

The Sverdrup Basin received considerable attention as a frontier hydrocarbon province during the 1960s and 1970s. Over 175 exploratory and delineation wells were drilled, resulting in the discovery of 1 oil field and 18 gas fields (e.g. Embry et al. 1991, Fig. 20A.1), mainly in the central and western regions. However, a number of major structures were found to contain only trace hydrocarbons, leading Waylett and Embry (1992) to suggest that hydrocarbons had leaked from breached structural traps. Several regional studies of thermal maturity using organic indicators and conodonts have been carried out in the basin (e.g. Henao-Londoño, 1977; Powell, 1978; Utting et al., 1989). These studies have provided only general constraints on the timing of maximum burial temperatures and peak hydrocarbon generation relative to the development of structural traps formed during either the mid-Paleozoic Ellesmerian or Early Cenozoic Eurekan Orogeny.

Evaluation of thermal histories in inverted sedimentary basins is complicated by the regional loss of section during inversion, as well as locally on structural culminations such as the hangingwalls of thrust faults and the cores of anticlines (Green et al. 1995). Exhumational cooling also typically marks the cessation of hydrocarbon generation and

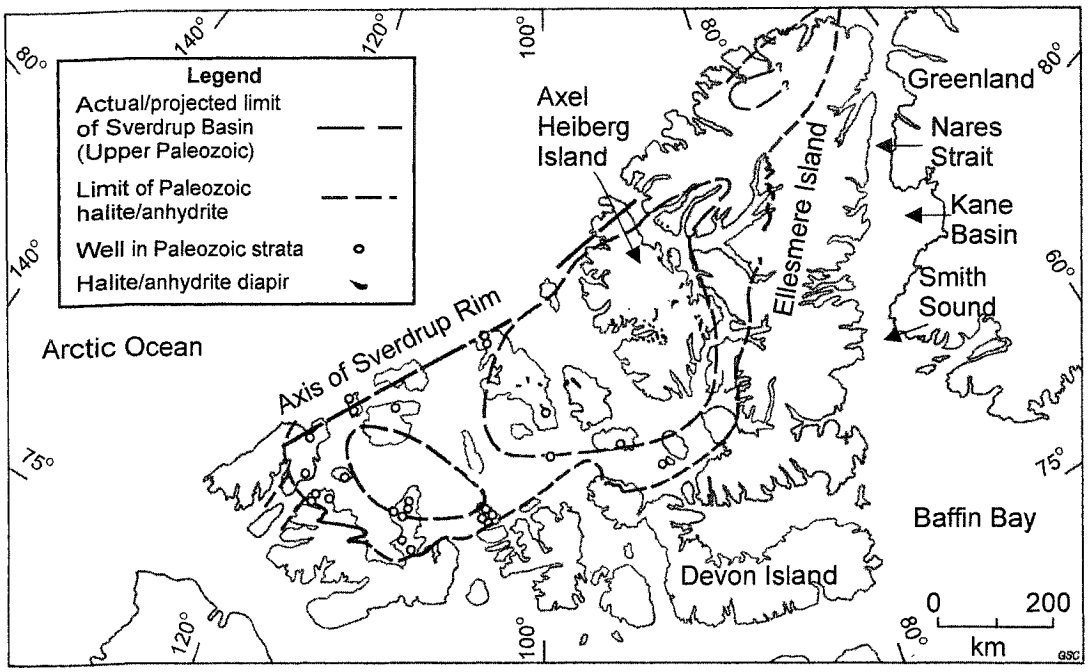

Figure 1.4. Map of the Canadian Arctic Archipelago (simplified and modified from Davies and Nassichuk 1991) showing the locations of the Sverdrup Basin (Chapter 5) and the Nares Strait - Kane Basin - Smith Sound region (Chapters 6 and 7).

primary migration. Thus the timing of generation and migration relative to the formation of structural traps is of critical importance to the evaluation of hydrocarbon potential, and has important implications for future exploration in the region. Apatite FT thermochronology is well-suited to the study of cooling in this environment because the temperatures at which tracks are annealed roughly correspond to the liquid oil window (Fig. 1.5).

1.4.2.2 The Nares Strait - Kane Basin - Smith Sound region

A number of apatite FT studies have demonstrated that the thermal history related to denudation and exhumation of the onshore part of rifted margins is intimately related to the thermal history from burial subsidence of the offshore margin. Studies have shown that sediment supply for the Sverdrup Basin was mainly from the south and east (e.g. Trettin 1991a). Widespread conglomeratic redbeds were deposited during rift-related subsidence in Namurian time (ca. 327-314 Ma; e.g. Davies and Nassichuk 1991). The other principal clastic units have mid-Permian ages (ca. 280-260 Ma). During Triassic to Late Cretaceous time clastic sedimentation was more-or-less continuous, although the rate of sediment supply varied markedly. Periods of high sedimentation have been inferred based on the presence of thick progradational deltaic facies deposits. Embry (1982) and Balkwill (1978) suggested that high sedimentation reflected epeirogenic exhumation at times when large river systems existed on the craton and flowed north and west into the basin.

The Nares Strait - Kane Basin - Smith Sound study examines the complex thermal history of the basin sediment source regions in northeastern Arctic Canada and western Greenland (Fig. 1.4) using apatite FT and (U-Th)/He thermochronology to investigate several possible thermal history elements:

(1) Late Paleozoic to Mesozoic cooling, principally a result of exhumation of the sediment source regions flanking the Sverdrup Basin;

(2) Cooling from rift flank uplift and normal faulting related to the beginning of the Late Cretaceous development of the Baffin Bay – Labrador Sea Rift at ca. 85 Ma; (anomaly 34; Srivastava 1978; Tessensohn and Piepjohn 2000);

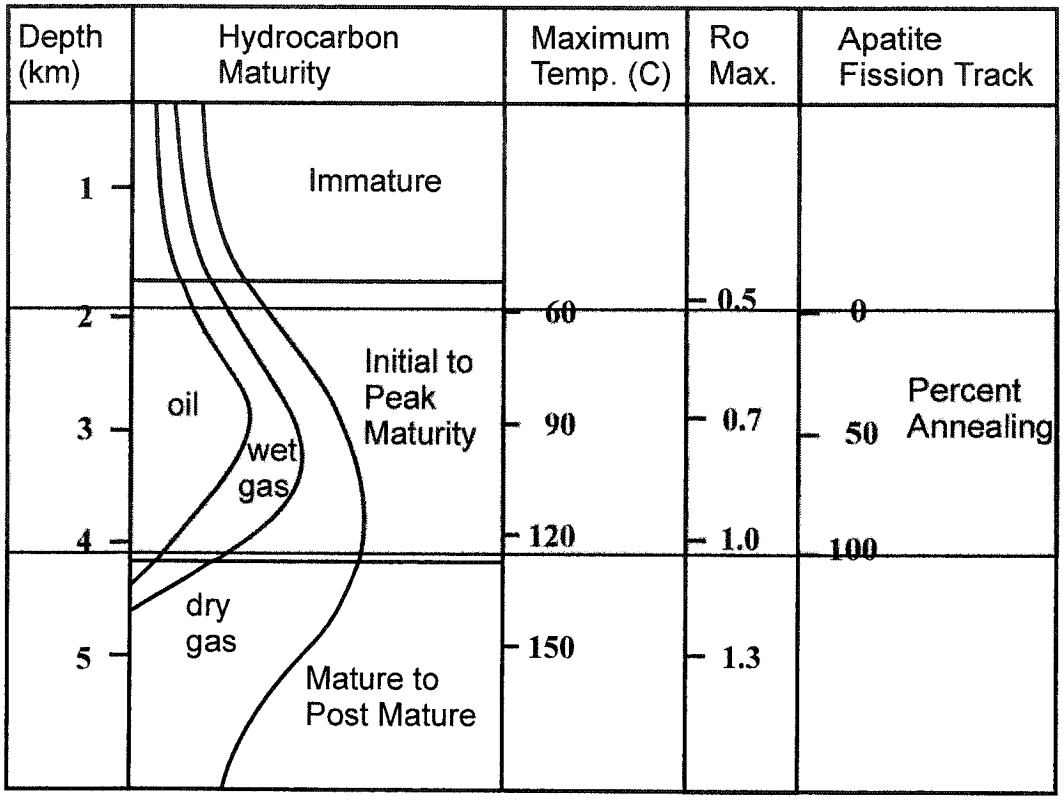

Figure 1.5. Schematic relationship between depth of burial, hydrocarbon maturity, maximum temperature, vitrinite reflectance, and apatite FT annealing (modified from Gleadow et al. 1983). The range of temperatures associated with FT annealing roughly coincides with the 'liquid oil window'. Like vitrinite reflectance, FT can indicate thermal maturity in hydrocarbon-prone strata. Unlike vitrinite reflectance, FT can provide an estimate of the timing of maturation relative to the development of structural traps.

(3) Cooling from exhumation of thrust hanging walls related to Eurekan compression;

(4) Post-Eurekan denudational cooling of the Paleogene clastic units.

1.4.2.2.1 The Nares Strait Controversy

Nares Strait offsets the Paleocene spreading ridge axis in northern Baffin Bay from the eastern flank of the Lomonosov Ridge, a 1700 km long sliver of continental crust which rifted from the Kara - Barents Sea shelves during Late Paleocene time (e.g. Sweeney et al. 1982; Kristoffersen 1990). Nares Strait therefore occupies a similar tectonic setting at the northern end of Baffin Bay to the Ungava Transform in Davis Strait (which offsets spreading centers in the Labrador Sea from those in Baffin Bay by several hundred kilometers), and its linear nature suggests it is also fault controlled. The Nares Strait controversy is an enduring geological debate about a postulated plate tectonic boundary between North America and Greenland first proposed by Alfred Wegener, who inferred that ca. 200 km of sinistral offset along Nares Strait was needed to account for the drift of Greenland from North America during the opening of Baffin Bay (i.e., Wegener 1929).

Story et al. (1998) suggested that tholeiitic volcanism and rifting in northern Baffin Bay were initiated by the development of the Iceland mantle plume at about 62 Ma. The offset of the rift axis from Labrador Sea to Baffin Bay along the Ungava Transform was also accompanied by an episode of substantial basaltic volcanism (the North Atlantic igneous province) on both the Baffin Island and the Greenland continental margins at about 55 Ma (e.g. Riisager et al. 2003; Story et al. 1998). Thus, if Nares Strait was also a continental rift transform active during Paleocene rifting in northern Baffin Bay, the thermal effects of basaltic volcanism may be discernable using low-temperature thermochronometric methods.

CHAPTER 2. Introduction to low temperature thermochronology using apatite

Radiometric dating methods are based on the gradual depletion of a radioactive (parent) substance, and the corresponding accumulation of a (daughter) substance or radiation damage through time in a closed system. If the decay rate is known and we make an assumption about the initial system condition (e.g. initial concentration of daughter is 0) we can measure parent/daughter ratios to determine the time that has elapsed since the system became closed.

Most of the decay of radioactive ^{238}U is by the initial emission of a helium nucleus (an α particle) as part of a chain of decays through intermediate radioisotopes that eventually produces stable ^{206}Pb, and a variety of dating methods have been developed based on this uranium series decay, including the U-Th/He method (see section 2.2 below). A very small proportion of ^{238}U (ca. 1 in 1-2 million) however, decays by spontaneous fission. The fission track (FT) dating technique is based on this spontaneous fission decay of ^{238}U.

2.1 FT Dating

2.1.1 FT fundamentals

A fission track is formed from the spontaneous fission decay of a single atom. The fission decay of U isotopes creates two (usually unequal) fission fragments, typically short-lived radioisotopes (such as ^{140}Xe and ^{94}Sr from the decay of ^{236}U), with atomic masses of ca. 85-105 and 130-150 (e.g. von Gunten 1969). As these two fragments are driven apart by Coulomb repulsion they interact with the surrounding lattice, gradually losing kinetic energy until they come to a stop. The mathematics which describe the track forming process resulting from this many-body, predominantly electronic interaction of nuclear fragments and a molecular lattice are governed by the laws of quantum mechanics, and are not easily determined or proved.

The most commonly invoked mechanism for the formation of fission tracks is the ion spike model (Fleischer et al. 1965, 1975). Although this model does account for many of the observed characteristics of fission tracks, such as that they only occur in insulating solids,

it does not explain observed discontinuities in track structure (e.g. Dartyge et al. 1978, 1981). Chadderton (1988) ascribed this intermittent character of tracks to discontinuities in the enclosing lattice, especially in layered minerals, but also emphasized that the current lack of knowledge of the fine structure of unetched fission tracks and the lack of an accurate crystallographic model for the enclosing lattice were limiting factors to progress in the development of a comprehensive model for the mechanism of track formation.

A diagram illustrating the ion spike explosion formation of a fission track is shown in Figure 2.1. Following a fission event the two highly-charged fission fragments are driven apart by mutual Coulomb repulsion. Their repulsion velocity exceeds the electron orbital velocity, so they lose all of their electrons. As they separate they strip electrons from the surrounding medium, which gradually causes them to lose kinetic energy and finally stop, leaving a trail of positively-charged ions. In a crystalline insulating solid mutual repulsion of the positively charged ions forces them a short distance into the crystal lattice, resulting in a linear defect that is stable at low temperatures. Newly formed fission tracks in apatite are typically 16-17 μm long and a few tens of angstroms wide.

Fission tracks were first observed by Silk and Barnes (1959) who observed unetched tracks, and also observed track fading using scanning electron microscopy. Price and Walker (1962, 1963) discovered that tracks could be enlarged by chemical etching and thereby observed using an optical microscope, and subsequently proposed a dating technique based on the assumption that the number of fission tracks accumulated in a substance depends only on the initial concentration of ^{238}U, and its rate of decay by spontaneous fission.

Beginning in the 1960s many geological and non-geological applications of FT research were developed including research in the areas of anthropology, geochemistry, geochronology, geothermometry, paleobotany, nuclear physics, paleontology, environmental monitoring, plate tectonics, hydrocarbon exploration, and others. Much of this work has been summarized by Fleischer et al. (1975) and Wagner and Van den Haute (1992). The geological applications, such as geochronology, geothermometry, exhumation studies, hydrocarbon exploration, and others are based primarily on the dating method, and on subsequent improvements in the understanding of track fading and track length distributions.

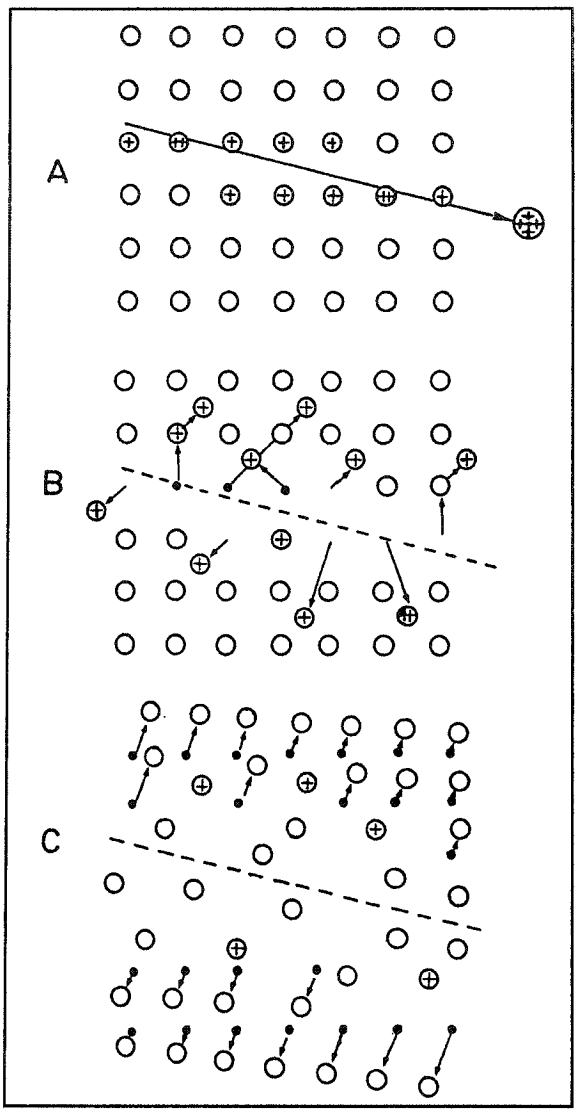

Figure 2.1. The ion spike model for the formation of fission tracks within a crystal lattice (Fleischer et al. 1975). a) Following a decay by spontaneous fission, highly positively charged nuclear fragments are forced explosively apart by mutual repulsion. b) As they pass through the crystal lattice they strip electrons causing positive ionization of lattice molecules. Coulomb repulsion of these positive ions displaces them a small distance into the surrounding lattice forming a single track that is typically 15-20 μm long and a few tens of angstroms wide. c) The stressed region of the track relaxes elastically straining the surrounding lattice. The charge imbalance along the fission track is preferentially attacked by etchants, and thus a track can be made visible by chemical etching.

2.1.2 FT ages

FT dating is based on the measured density of spontaneous tracks (i.e., naturally occurring tracks produced during spontaneous fission of trace amounts of ^{238}U). In monotonically cooling systems track densities provide a measure of age with respect to the closure temperature of the system (Dodson 1973). The FT age of a mineral or glass grain can be calculated absolutely using the fundamental age equation (e.g. Hurford 1986);

$$t=\frac{1}{\lambda_d}\ln[1+\frac{\lambda_d \Phi \sigma I g \rho_s}{\lambda_f \rho_i}] \qquad 2.1$$

where λ_d = $1.5513x10^{-10}y^{-1}$, the total decay constant for ^{238}U (Hurford 1990); λ_f = approximately $7\text{-}8x10^{-17}y^{-1}$, the spontaneous fission decay constant for ^{238}U (Friedlander et al. 1981; Roberts et al. 1968); $I = 7.2527x10^{-3}$, $^{235}U/^{238}U$ isotope abundance ratio (Hurford 1990); $\sigma = 580.2x10^{-24}cm^2$, the thermal neutron cross section for ^{235}U (Hurford 1990); Φ = the thermal neutron fluence; g = the geometry factor (0.5 for the external detector method); ρ_s = the spontaneous track density; ρ_i = the induced track density.

Fleischer et al. (1975), Hurford and Green (1982, 1983) and others have noted that the large uncertainties in the estimates of the spontaneous fission decay constant for ^{238}U, and the inherent uncertainties in determination of the absolute neutron flux and the thermal neutron capture cross section are prohibitive obstacles to the determination of FT ages using absolute calibration techniques. Fleischer and Hart (1972), Fleischer et al. (1975) and Hurford and Green (1982, 1983) proposed an alternative approach to the calculation of FT ages whereby track densities in samples having unknown ages are compared to those in age standards using a ζ (zeta) factor. The ζ factor is defined such that it is an empirically measurable quantity that represents the net total of the effects of the neutron flux, the thermal capture cross section, the $^{235}U/^{238}U$ isotope abundance ratio, and the ^{238}U spontaneous fission decay constant;

$$\zeta=\frac{\Phi \sigma I}{\lambda_f \rho_d} \qquad 2.2$$

where ρ_d = the induced track density of a standard glass with known uranium content. When ζ in equation 2.2 is substituted into equation 2.1, the fundamental age equation becomes;

$$t=\frac{1}{\lambda_d}\ln[1+\zeta\lambda_d g\frac{\rho_s}{\rho_i}] \qquad 2.3$$

Rearranging equation 2.3 and solving it for ζ using age standards gives;

$$\zeta=\frac{(e\rho^{\lambda_D t_{std}}-1)}{\lambda_D(\rho_s/\rho_i)_{std}g\rho_d} \qquad 2.4$$

where t_{std} = the age of the standard; $(\rho_s/\rho_i)_{std}$ = the spontaneous/induced track ratio of the standard. The modified age equation then becomes;

$$t=\frac{1}{\lambda_D}\ln[1+\lambda_D\zeta g\frac{\rho_s}{\rho_i}\rho_d] \qquad 2.5$$

where ζ = the individual mean zeta value.

The error in the modified age equation is given by;

$$\sigma_{(t)}=t\sqrt{\frac{1}{n_s}+\frac{1}{n_i}+\frac{1}{n_d}+[\frac{\sigma_{(\zeta)}}{\zeta}]^2} \qquad 2.6$$

and the error in the zeta factor is given by;

$$\sigma_{(\zeta)}=t\sqrt{\frac{1}{n_s}+\frac{1}{n_i}+\frac{1}{n_d}+[\frac{\sigma(t_{std})}{t_{std}}]^2} \qquad 2.7$$

where n_s, n_i and n_d are the numbers of spontaneous, induced and dosimeter glass tracks counted, respectively.

Several methods have been developed for the determination FT ages (e.g. Fleischer et al. 1975; Wagner and Van den Haute 1992). All ages reported in this thesis were determined using the external detector method, (Fleischer et al. 1964; Hurford and Green 1982). For this method (illustrated in Fig. 2.2) a thin sheet of low-uranium muscovite is attached to the polished surface of each grainmount to detect neutron-induced fission. The number of induced tracks in the mica provides an estimate of the uranium concentration of the mineral grain (the parent). The number of spontaneous tracks in the mineral provides an estimate of the concentration of the daughter. Induced tracks are counted in approximately the same area of the same grains as the spontaneous tracks, and individual ratios of ρ_s/ρ_i and single grain age estimates are thereby obtained. Typically, 10-40 grains and grain track images are counted. An aggregate sample age is calculated using of any three statistical methods (e.g. Gallagher et al. 1998).

If the data have a Poissonian distribution, as determined using a χ^2 test, then the spontaneous and induced counts are pooled, resulting in a single ratio ρ_s/ρ_i. If the data are non-Poissonian, a mean age that is simply the arithmetic mean of the individual ρ_s/ρ_i ratios may be used in the age calculation. Galbraith and Laslett (1993) proposed the central age calculation which uses the weighted mean of the log normal distribution of the single grain ages. For samples that pass the χ^2 test, central age is the same as the pooled age. For samples that fail the χ^2 test, the central age calculation is less sensitive to age outliers, and thus may provide better age estimate than the mean age.

2.1.3 The radial plot and age component analysis

The radial plot (Galbraith 1990; Galbraith and Laslett 1993) is simply a graphical method of presenting FT age data that allows a comparison of the spread in FT ages and takes into account the differences in the precision between each counted grain. A sample radial plot is shown in Fig. 2.3. In this plot the uncertainty for each grain age (2 std. dev.) is a line segment of equal length, and the sample fails the χ^2 test if any of these do not overlap the central age. The utility of these plots is that they allow the easy identification of age outliers that may not be readily apparent from the count statistics. Brandon (1992), Galbraith

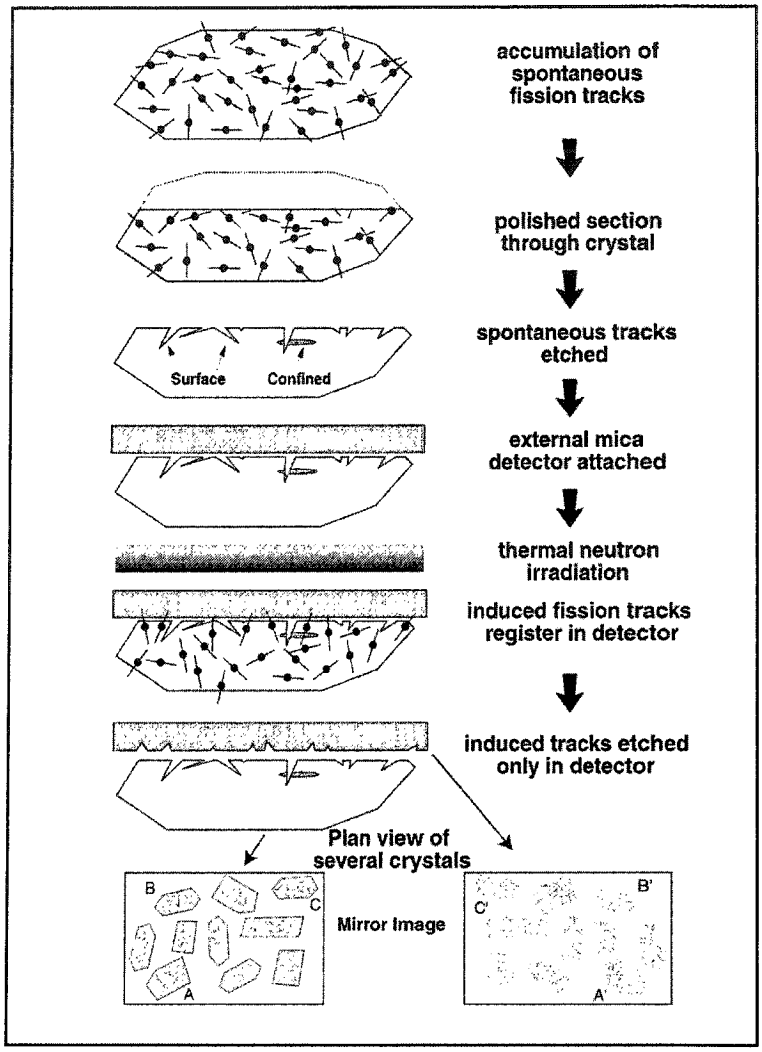

Figure 2.2. The steps involved in the external method (from Hurford and Carter 1991). A crystal containing latent spontaneous tracks is mounted, polished on an internal surface, and etched to reveal them. Etched tracks either intersect the polished surface or another track or a crack that in turn intersects the polished surface. A uranium-free detector (i.e., Muscovite mica) is placed in intimate contact with this surface, and the grainmount is irradiated with low-energy thermal neutrons, inducing fission in ^{235}U. Some fission fragments cross the interface between the mineral and the mica, producing a mirror image of the original grain. The mica is then etched to reveal the induced tracks.

and Laslett (1993), and others have developed methods for discrimination of component populations in samples containing mixtures of grains having different FT ages.

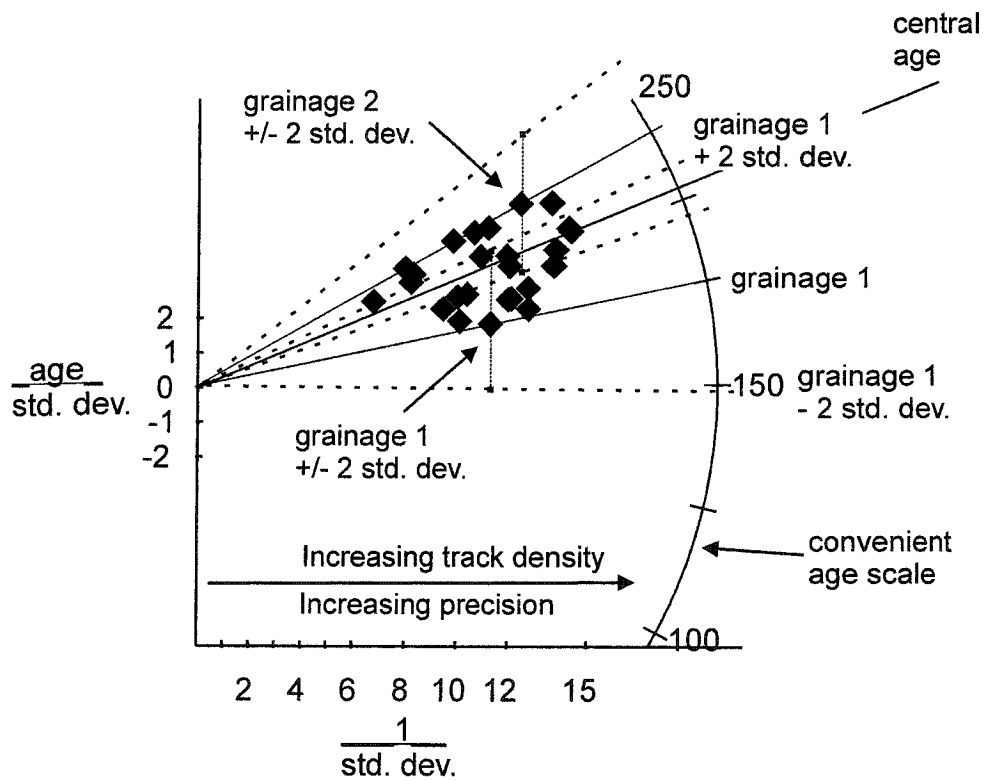

Figure 2.3. Example of a radial plot of FT age data. The y-axis is a standardized estimate of the age (i.e., age/(std. dev.)) and the x-axis is a standardized estimate of precision (i.e., 1/(std. dev.)). A suitable radial age scale is chosen to display the grain ages, which plot along a line drawn through the '0' on the y-axis.

2.1.4 Track annealing and track length studies

Track length (TL) reduction by annealing of fission damage is an incremental and irreversible process that is dominantly thermally activated. In apatite, annealing of fission damage begins to be significant at temperatures of ca. 60 °C over geologic time periods and is essentially complete at ca. 100 - 150 °C (depending on composition). Between 60° and ca.130 °C etchable tracks are retained, but are progressively shortened in response to the highest temperatures experienced. Because tracks are formed continuously through time, the TL distributions are indicative of the integrated thermal history below ca. 130°C. Assuming a geothermal gradient of 30 °C/km, this would be equivalent to burial of 4-5 km. The probability of a track intersecting a polished surface and contributing to the age is proportional to its length however, and therefore FT ages in systems with complex thermal histories may not represent a geologically significant event in time. This temperature-dependent behavior between 60° and ca.130 °C (referred to as the partial annealing zone or PAZ) allows the apatite FT method to be used as a low-temperature thermochronometer. Green et al. (1986) characterized the annealing behaviour of fission tracks in the Durango apatite standard within the PAZ by measuring TL distributions in samples heated from 20 minutes to 500 days at temperatures between 95 and 400 °C. A number of apatite FT annealing models have been developed based on empirical extrapolations of the Green et al. (1986) annealing data to geologic time.

2.1.5 Effects of composition

Although it is widely accepted that observed variable annealing behaviour of fission tracks in apatite as a function of temperature is an effect of composition, controversy remains within the FT community about whether chlorine content is the only significant influence as suggested by Green et al. (1985), Green (1996), and others, or whether the annealing rate is a more complex function of composition (e.g. Carlson et al. 1999). The development of a rigorous model which quantitatively describes variable annealing behaviour as a function of temperature for apatites of different composition has been complicated by effects related to crystallographic anisotropy of both annealing and etching.

Figure 2.4. A: Schematic illustration of the apatite FT PAZ (A) and an exhumed PAZ (B). A: At sufficiently elevated temperatures no tracks are retained. At intermediate temperatures both ages and lengths are reduced in proportion to the temperature. At low temperatures no age or length reduction occurs, resulting in old FT ages and long mean lengths. B: Following a period of (rapid) cooling a new temperature equilibrium and present PAZ are established. Rocks formerly in the PAZ still have reduced ages and mean lengths, although no further age or length reduction occurs above the present PAZ. Rocks formerly in the zone of total annealing will start to accumulate tracks that are not annealed (above the present PAZ), but the FT age of these rocks will be younger, and reflect the time of cooling (modified after Naeser et al. 1989).

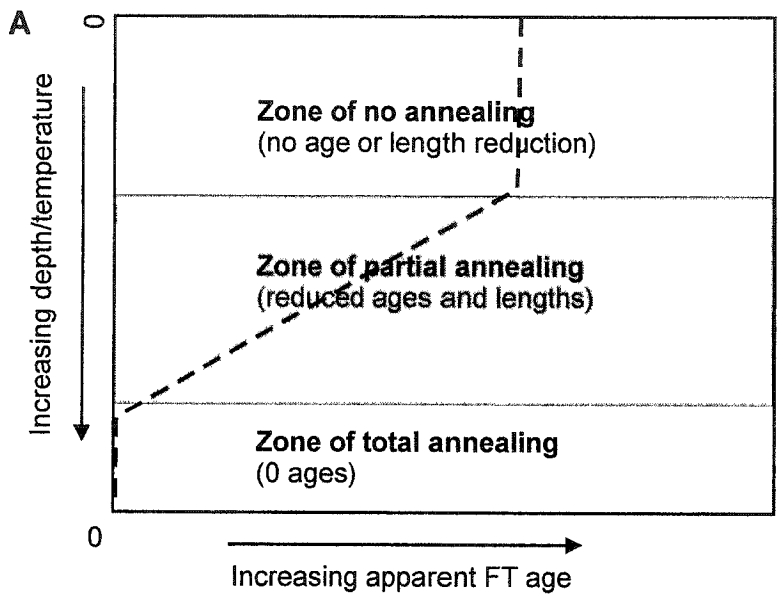
A
0
Increasing depth/temperature
Zone of no annealing
(no age or length reduction)
Zone of partial annealing
(reduced ages and lengths)
Zone of total annealing
(0 ages)
0
Increasing apparent FT age

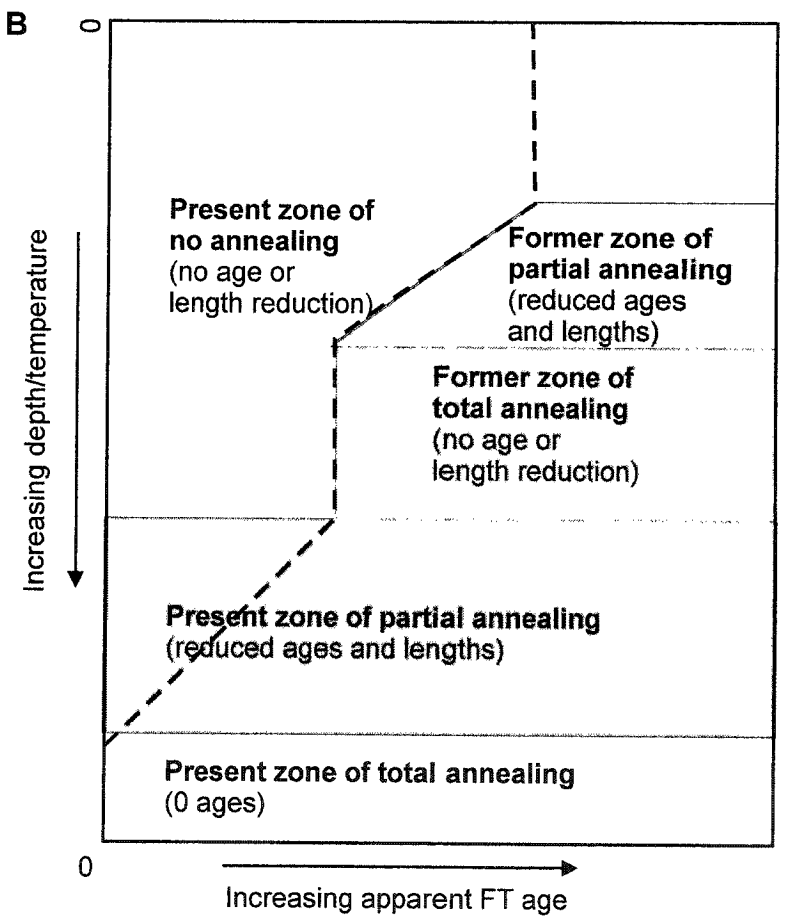
B
0
Increasing depth/temperature
Present zone of
no annealing
(no age or
length reduction)
Former zone of
partial annealing
(reduced ages
and lengths)
Former zone of
total annealing
(no age or
length reduction)
Present zone of partial annealing
(reduced ages and lengths)
Present zone of total annealing
(0 ages)
0
Increasing apparent FT age

Donelick (1991) demonstrated that annealing behaviour as a function of temperature is influenced by the crystallographic orientation of the individual tracks. At high degrees of annealing tracks oriented at a high angle to the c-axis are considerably more annealed than tracks oriented near the c-axis. Apatite also exhibits considerable track etch anisotropy. Etch pits are longer parallel to the crystallographic c-axis than they are parallel to the a-axis, and etch anisotropy also varies as a function of composition. Ravenhurst et al. (2003) demonstrated that for a variety of apatite compositions, the temperature-dependent annealing behaviour is superimposed on etching effects, and although the relationship between the two influences remains unclear, fluorapatites appear to be the most easily annealed, and chlorapatites the most retentive.

2.1.6 Apatite FT modelling

The most widely used apatite annealing model is the Laslett et al. (1987) fanning-Arrhenius model, based on the Durango standard (F apatite with 0.4 wt% Cl). Annealing models have also been developed for apatites of different compositions, such as the Crowley et al. (1991) fluorapatite model, and based on kinetic behaviour (Carlson 1990). Ketcham et al. (1999) developed a multi-compositional kinetic model for apatite annealing that is also based on etch pit characteristics. These models have been incorporated into a number of software packages that use Monte-Carlo type search techniques to evolve thermal history simulations to predict apatite FT age and length distributions (e.g. Gallagher 1995; Willett 1997).

Thermal history modelling for this thesis was done using AFTINV (Willett 1997) modified to run on a personal computer (Issler 1996a). AFTINV uses a Monte Carlo search technique to evolve a thermal history. Component sets of unannealed fission tracks are introduced at discrete time intervals and annealed in response to subsequent temperatures as the thermal history is evolved, resulting in an integrated TL distribution and an apparent age. Predicted TL distributions and ages are compared to the measured data using a goodness-of-fit statistic. A solution set of the best-fitting histories is maintained as the algorithm repeats iteratively until all solutions in the set fit the data to the desired confidence

level (in this instance 95%). User-input constraints on heating, cooling and rate bounds based on independent geological data are used to limit the search space to geologically reasonable solutions.

The Laslett et al. (1987) annealing model has been shown to under-predict annealing at low temperatures when applied over geologic timescales (Vrolijk et al. 1992; Corrigan 1993). Although it is generally accepted that apatite fission tracks may undergo some shortening at temperatures below the lower limit of the PAZ (i.e., 60 °C; e.g. Bertel et al. 1977; Green 1988), such shortening is generally considered of minor importance. Laslett et al. (1987), Green et al.(1989) and others have suggested that at temperatures below 50 °C tracks are mostly retained at their initial lengths. However, Donelick et al. (1990) demonstrated that in induced track populations reduction of the initial mean length by as much as 0.5 μm occurred within a few days at room temperature.

Greater differences are seen between the mean TL and length distributions of spontaneous tracks in the supposedly unannealed Durango and Fish Canyon Tuff FT age standards relative to corresponding (artificially-induced) unannealed length distributions. The mean spontaneous TL of the Durango standard is reduced by 1.5-2 μm. Unannealed tracks in apatite (i.e., >16 μm), which are abundant in the induced population are relatively uncommon in most fossil populations, even though the Laslett et al. (1987) model predicts that they should be stable at temperatures up to 50 °C, corresponding to a burial depth of ca. 2 km in a typical geothermal gradient. As a result of failing to consider this low temperature annealing, many apatite FT modelling studies include a late-stage of 30-40 °C cooling that is an artefact required to reconcile the thermal model with the observed lack of unannealed tracks.

Several authors have taken the approach of introducing a reduction of the initial mean length to 14.5 μm (e.g. Gunnell et al. 2003) or 15.5 μm (e.g. Grist and Zentilli 2003; Chapter 3 of this thesis). Although this approach does not provide insights into the mechanisms responsible for low-temperature annealing, it does essentially eliminate late-stage cooling, which appears to reconcile the low-temperature part of FT thermal models with independent geological and geomorphological constraints (Grist and Zentilli 2003; Gunnell et al. 2003).

However, renormalizing the low-temperature behaviour of fission track annealing also introduces a (lesser) change in model temperature history estimates in the upper part of the PAZ. The approach of using a reduced initial track length for the Laslett et al. (1987) annealing model was criticized by Green (2004) on the basis that the modified annealing model should be independently validated using other thermochronometric techniques.

Apatite (U-Th)/He dating offers an opportunity to refine the low-temperature part of FT thermal models because the temperature range of the PRZ is lower than the FT PAZ. Temperatures of ca. 50 °C, which are often seen in the late stages of FT thermal models are high enough to cause significant He diffusion, so (U-Th)/He ages allow us to distinguish whether such late stage cooling is real, or whether low-temperature track annealing needs to be considered. The use of (U-Th)/He forward modelling (described in section 2.2.6) to calibrate the low-temperature part of the Laslett et al. (1987) annealing model is described in Chapters 4 and 7 of this thesis.

2.1.7 Geological applications

In addition to the direct dating of the ages of rocks, a number of applications of the apatite FT method have been developed. Useful reviews of many of these applications are given in Wagner and Van den Haute (1992) and Gallagher et al. (1998). Dumitru (2000) described applications to Quaternary geochronology studies. Some of the principal applications related to basin thermal history analysis and denudation of basin sediment source regions are described below.

2.1.7.1 Provenance studies

Although zircon FT analysis is better suited for sedimentary provenance studies because of its higher closure temperatures, apatite FT studies have also been used to infer the provenance of detrital grains in samples that have experienced relatively little post-depositional heating (e.g. Hurford and Carter 1991). If enough individual grain ages are analyzed, separate age populations can be identified using age component analysis (e.g. Brandon 1992). If the length data are uniquely linked to particular FT single grain ages it is

also possible to identify and model separate elements of thermal history of samples with multiple sources (e.g. Lonergan and Johnson 1998). In practice however, the unique identification of a particular length population with a corresponding grain age population is difficult to achieve. Additional discussion of sedimentary provenance of samples using apatite FT analysis is given in Chapters 5 and 6.

2.1.7.2. Denudation in orogenic belts

In orogenic belts formed as a result of continental collision, apatite FT analysis provides information on cooling that can be inferred to be linked to tectonic and erosional denudation. In a large number of studies detailed cooling histories have been obtained by the application of apatite and zircon FT analysis in conjunction with other radiometric techniques to co-existing minerals within the same samples (e.g. Harrison et al. 1979; Zeitler et al. 1982; Parrish 1983; Hurford 1986; Hunzicker et al. 1992; and others). Detailed summaries of this application of FT dating are also given in Wagner and Van den Haute (1992) and Gallagher et al. (1998).

Wagner and Van den Haute (1992) inferred that in many instances a cooling rate can be obtained directly from the slope of apatite FT age-elevation profiles, i.e.,

$$\text{cooling rate} = \text{elevation difference} / \text{FT age difference} \qquad 2.8$$

Gallagher et al. (1998) demonstrated that in many instances this simplified interpretation of the relationship between cooling , elevation and FT age may not be valid. Complications arise from a number of circumstances which include: samples that do not move vertically through isotherms; samples that experience non-erosional cooling (e.g. tectonic denudation); samples not totally annealed prior to exhumational cooling (inheritance effects or an exhumed PAZ); or samples that are not rapidly cooled and are partially annealed. The relationship between denudation, elevation and FT age in non-orogenic settings is discussed further in Chapter 6.

2.1.7.3. Thermal analysis of sedimentary basins

One of the most widespread applications of apatite FT dating is in the study of the thermal history of sedimentary basins. Overviews of this application of FT dating are given by Naeser et al. (1989) and Gallagher et al. (1998). In addition to provenance information that can be derived (discussed above) the method is useful in the study of basin thermal histories mainly because the range of temperatures over which apatite FT annealing occurs roughly corresponds to the peak temperature for the generation of liquid hydrocarbons (liquid oil window) over geologic time-scales (e.g. Gleadow et al. 1983; Green et al. 1989), and it can be used therefore as an indicator of thermal maturation. Unlike conventional maturation indices however, that can only assess the combined effects of time and temperature to the overall maturity, FT dating can be used to at least partially separate the relative contributions of these two influences, and often can be used to infer the time of maturation. Arne et al. (1998) demonstrated that information on the timing of hydrocarbon maturation relative to the development of suitable traps in an inverted basin can be crucial to the success or failure of exploration.

Arne and Zentilli (1994) presented a review of studies which combined apatite FT dating and vitrinite reflectance and were able to demonstrate a range of heating times and temperatures over which the two maturation indices could be correlated. A number of such studies have been done combining FT dating of apatite and/or zircon with organic maturation indices to obtain detailed thermal history information over a broad range of temperatures (e.g. Feinstein et al. 1989; Grist et al. 1995; Arne et al. 2002).

2.1.7.4 Evolution of rifted continental margins

Rifted continental margins represent a special class of sedimentary basins. Crustal thinning and subsidence are a result of the tectonic and thermal effects of rifting and associated magmatism. A number of studies have been done using FT dating of well samples to assess thermal maturation of offshore strata (e.g. Grist et al. 1992; Li et al. 1995).

2.1.7.5 Denudation of the onshore of rifted margins

A number of apatite FT studies have demonstrated that the thermal history of denudation and exhumation of the onshore part of rifted margins is intimately related to the burial and subsidence of the offshore part of the margin (e.g. Moore et al. 1986; Bohannon et al. 1989; Dumitru et al. 1991; Gallagher et al. 1994; 1995; Brown 1992; Menzies et al. 1997; Brown et al. 1990, 2000; and others). This situation is shown diagrammatically in Fig. 2.5. These studies have shown that although rift-related heating is associated with the development of the offshore part of the margin, at shallow crustal levels (i.e., <10 km) the thermal history of rocks in the onshore is dominated by vertical movements through an invariant geothermal regime. The main aspects of this application of apatite FT dating were recently summarized by Gallagher and Brown (1997) and Gallagher et al. (1998).

An approach commonly used in the interpretation of FT data is to present it in the form of a plot of age vs. mean TL (Fig. 2.6). The use of such figures has been described in detail by Brown el al. (1994), Gallagher and Brown (1997), Gallagher et al. (1998), and others. On these plots FT age and mean TL data often form a coherent pattern, commonly referred to as a boomerang, that is more or less well developed. The longest mean track lengths correspond to the youngest and the oldest FT ages. At intermediate FT ages, lengths are reduced. The coherent pattern of ages and lengths in a boomerang plot is another way of representing the exhumed PAZ shown in Fig. 2.4 (e.g. Fitzgerald et al. 1995; Dumitru 2000). Rocks formerly in the zone of total annealing have long mean lengths and young FT ages, representing rapid denudation from temperatures above ca. 130 °C. Rocks that were above the former PAZ have experienced very little annealing and have long mean lengths, but older FT ages. Rocks from the former PAZ have intermediate ages and reduced mean lengths.

2.1.8 Analytical procedures for FT analysis

Apatite is obtained from samples using the techniques described in Appendix 1. Aliquots of the apatite separates are mounted in Araldite® epoxy using the Naeser (1976) method. A description of this technique as it is done at the Dalhousie University Fission Track Laboratory is given in Appendix 2. If sufficient material is obtained, two mounts are

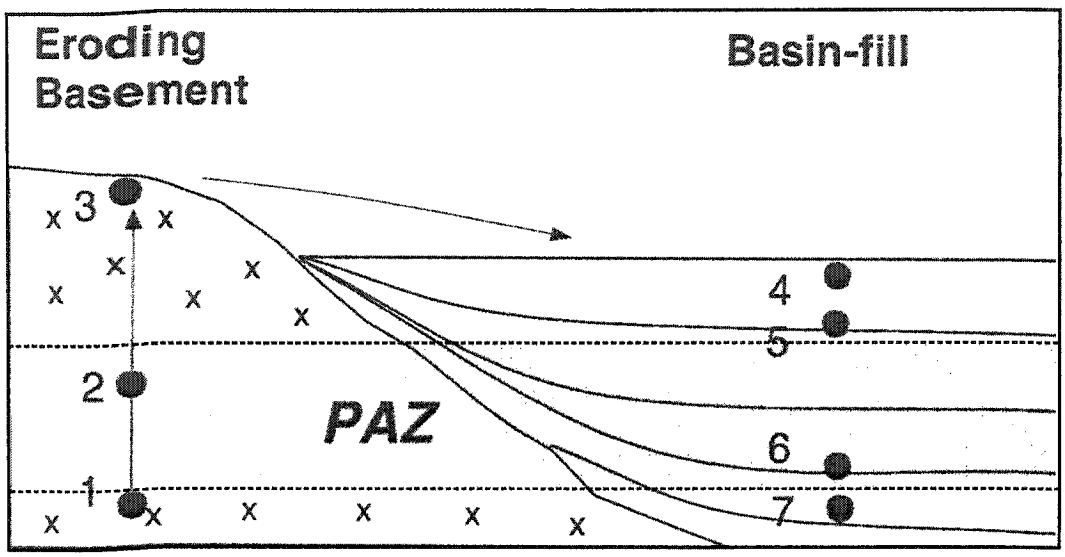

Figure 2.5. Diagrammatic illustration of the relationship between subsidence of a basin margin and denudation of the sediment source region (from Rohrmann 1995). Samples 1-3 experience denudation and FT ages increase as they cool through the PAZ. Sample 4 has experienced little post-depositional heating and yields information on sediment provenance. Samples 5-7 have FT ages that decrease to 0 Ma as they are progressively heated by burial and subsidence.

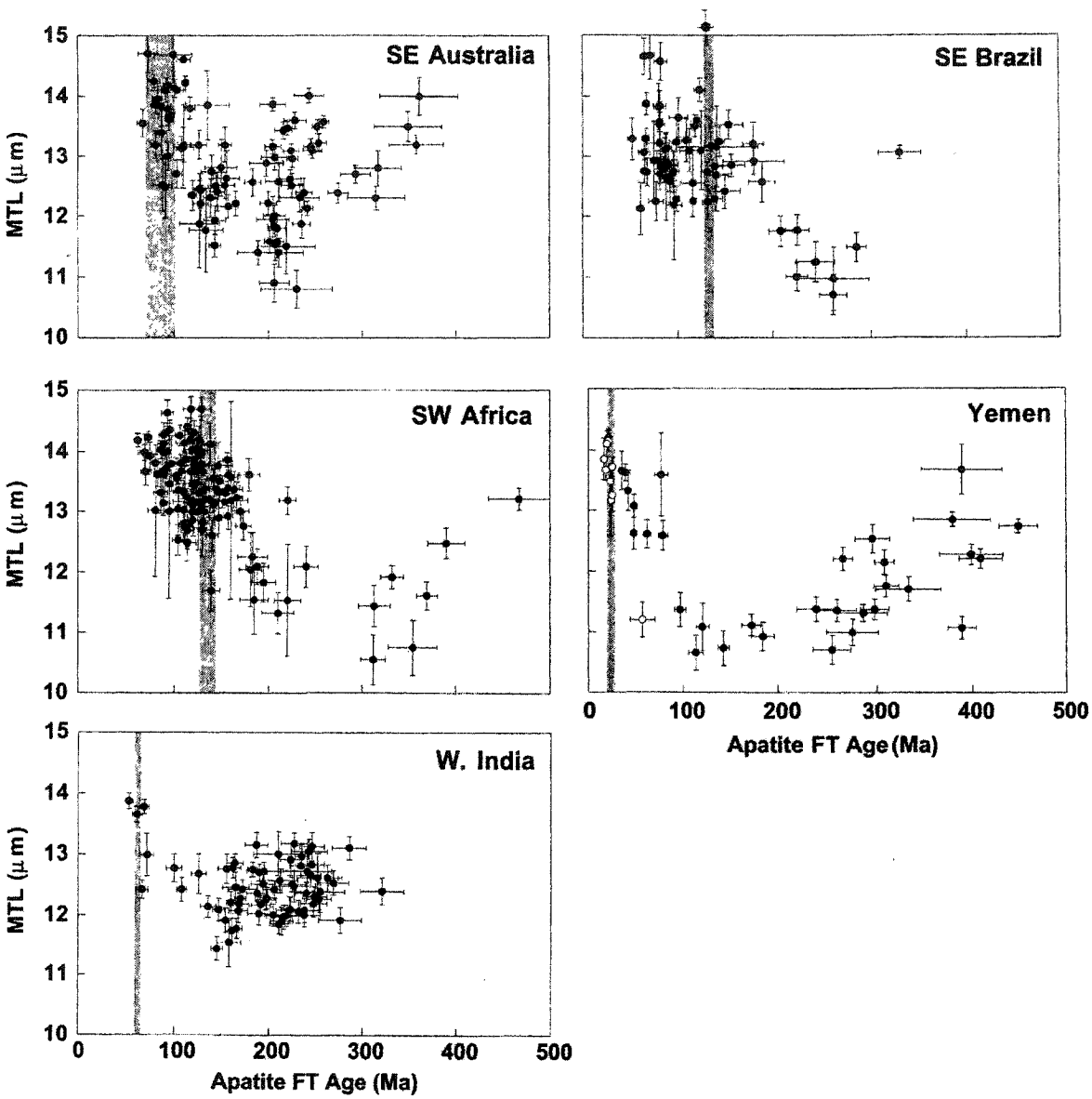

Figure 2.6. FT age-length plots (boomerangs) for 5 data sets obtained from the onshore part of rifted continental margins (from Gallagher et al. (1998) and references therein). The grey bars represent the time of onset of rifting and breakup at each of the margins. The data from the Yemen margin show a distinct boomerang pattern. The other data sets show combinations of patterns from more complex thermal histories and/or partial boomerangs.

made for each sample. After the apatite grains have been exposed and polished to reveal internal surfaces, one grainmount for each sample is etched in 5M HNO_3 for 20 seconds at 24 °C to reveal spontaneous fission tracks. If the track density of the etched mount is sufficiently high, the second mount is also etched. If the spontaneous track density is quite low, the second is not etched. Instead, it is irradiated under vacuum with heavy fission fragments from a collimated ^{252}Cf source. The fission fragments penetrate about 8-10 μm into the surface of the grains and form etchable pathways that increase the amount of confined tracks that are revealed by etching. The samples are irradiated this way until a ^{252}Cf induced track density of 3 - 4 x10^6 tracks/cm^2 is obtained. This density typically results in a 5-fold increase in the number of confined tracks revealed by etching.

Samples are irradiated at the Dalhousie University Slowpoke reactor in the presence of glass neutron dosimeters (CN1 or CN5) of known characteristics. The thermal-neutron fluence obtained is ca. 9 x 10^{15} neutrons/cm^2. Micas are etched at room temperature in 48% HF for 22 minutes. Spontaneous and induced track densities (tracks/cm^2) are counted at 1000x magnification (100x dry objective, 10x oculars 1x drawing tube) on a Zeiss® Axioplan microscope equipped with an Autoscan® AS3000 stage. Ages are calculated using a weighted mean zeta calibration factor (Fleischer et al. 1975; Hurford and Green 1983), determined using the Fish Canyon Tuff and Durango apatite age standards. TL distributions of horizontal, confined tracks (in crystallographic planes parallel to the c-axis) are also measured at 1000x magnification using a digitizing pad interfaced with a personal computer. The precision of each measured length is ± 0.20 μm.

2.2 Apatite (U-Th)/He dating

The (U-Th)/He method was one of the earliest techniques developed for the dating of geologic materials (e.g. Rutherford 1905; Strutt 1905), but was often considered unreliable owing to the ease with which radiogenic He could be lost from the host mineral resulting in too-young ages. With the advent of apparently more reliable radiometric methods such as K-Ar, interest in helium systematics faded. Recently the technique has experienced a renaissance after its potential as a low temperature thermochronometer was suggested by

Zeitler et al. (1987).

2.2.1 Radiogenic ^{4}He accumulation

The (U-Th)/He method is based on accumulation (ingrowth) of α-particles, (radiogenic ^{4}He nuclei) through the series decay of ^{238}U , ^{235}U, ^{232}Th, as well as by decay of ^{147}Sm. Isotopic abundances, half lives and decay constants for these isotopes are given in Table 2.1. Radioactive ^{147}Sm has a very long half-life (Table 2.1) and decays by emission of a single ^{4}He nucleus to stable ^{143}Nd. In almost all minerals therefore, the contribution of ^{4}He from ^{147}Sm is negligible, so that radiogenic helium can be said to accumulate from the decay of ^{238}U, ^{235}U and ^{232}Th.

Element	Isotopic abundance	Half life	Decay constant
^{238}U	99.274	4.468×10^{9} y	1.55125×10^{-10} y^{-1}
^{235}U	0.720	7.038×10^{8} y	9.8485×10^{-10} y^{-1}
^{232}Th	100	1.401×10^{10} y	4.9475×10^{-11} y^{-1}
^{147}Sm	100	1.06×10^{11} y	6.54×10^{-12} y^{-1}

Table 2.1. The isotopic abundances, half-lives and decay constants of ^{238}U, ^{235}U, ^{232}Th and ^{147}Sm (data from Lederer et al. (1967) and Steiger and Jäger (1977)).

The decay series for these three isotopes are shown in Figs. 2.7 and 2.8. In these figures decay by α-particle emission (the ejection of 2 protons and 2 neutrons, decreasing both the atomic and neutron numbers by 2) is shown by the arrows pointing down and left. Decay by β-particle emission (the ejection of an electron which converts a neutron to a proton, decreasing the neutron number by one and increasing the atomic number by one) is shown by arrows that point up and left. From these figures it can be seen that the decay of a single molecule of ^{238}U ultimately produces one atom of ^{206}Pb through the emission of 8 ^{4}He nuclei and 6 β-particles (electrons). Similarly, the decay of a single ^{235}U molecule

ultimately produces a molecule of ^{207}Pb through the emission of 7 ^{4}He nuclei and 4 β-particles, and the decay of a molecule of ^{232}Th produces ^{207}Pb through the series emission of 6 ^{4}He nuclei and 4 β-particles.

2.2.2 Age equation

The equation that describes the accumulation of radiogenic ^{4}He in a mineral as a function of time is:

$$He = 8(^{238}U(e^{\lambda_{238}t}-1)) + 7(^{235}U(e^{\lambda_{235}t}-1)) + 6(^{232}Th(e^{\lambda_{232}t}-1)) \qquad 2.9$$

where He is the total accumulation of ^{4}He; ^{238}U, ^{235}U and ^{232}Th are the present-day amounts of these isotopes, t is the age, and λ_{238}, λ_{235} and λ_{232} are the respective decay constants. This equation assumes secular equilibrium among all the daughters in the decay chain. The effects of secular disequilibrium are negligible for minerals older than about 1 Ma (Farley et al. 2002). Equation 2.9 also assumes no initial ^{4}He is present in the mineral grain.

2.2.3 Correction for α-emission

The energies associated with the ejection of an α-particle from U and Th are in the MeV range, and the associated stopping distances for these particle are on the order of 20 μm in apatite (e.g. Ziegler 1977; Farley et al. 1996). Near grain boundaries a predictable fraction of the ^{4}He that is produced is ejected from the host grain and lost to the system. Farley et al. (1996) developed a quantitative model for the correction of measured (U-Th)/He ages to account α-ejection from the host grain (F_t correction). F_t represents the fraction of ^{4}He that is retained in the host grain. The controlling factor in determining the magnitude of the F_t correction is the grain radius, and the correction is slightly greater at any grain radius for Th than for U because of the higher emission energy for the ^{232}Th series decay. Figure 2.9 shows F_t as a function of grain radius for a hexagonal prism geometry (i.e., apatite) from Farley (2002). Below an F_t of about 0.65 (grain radius of ca. 70 μm) the magnitude of the correction

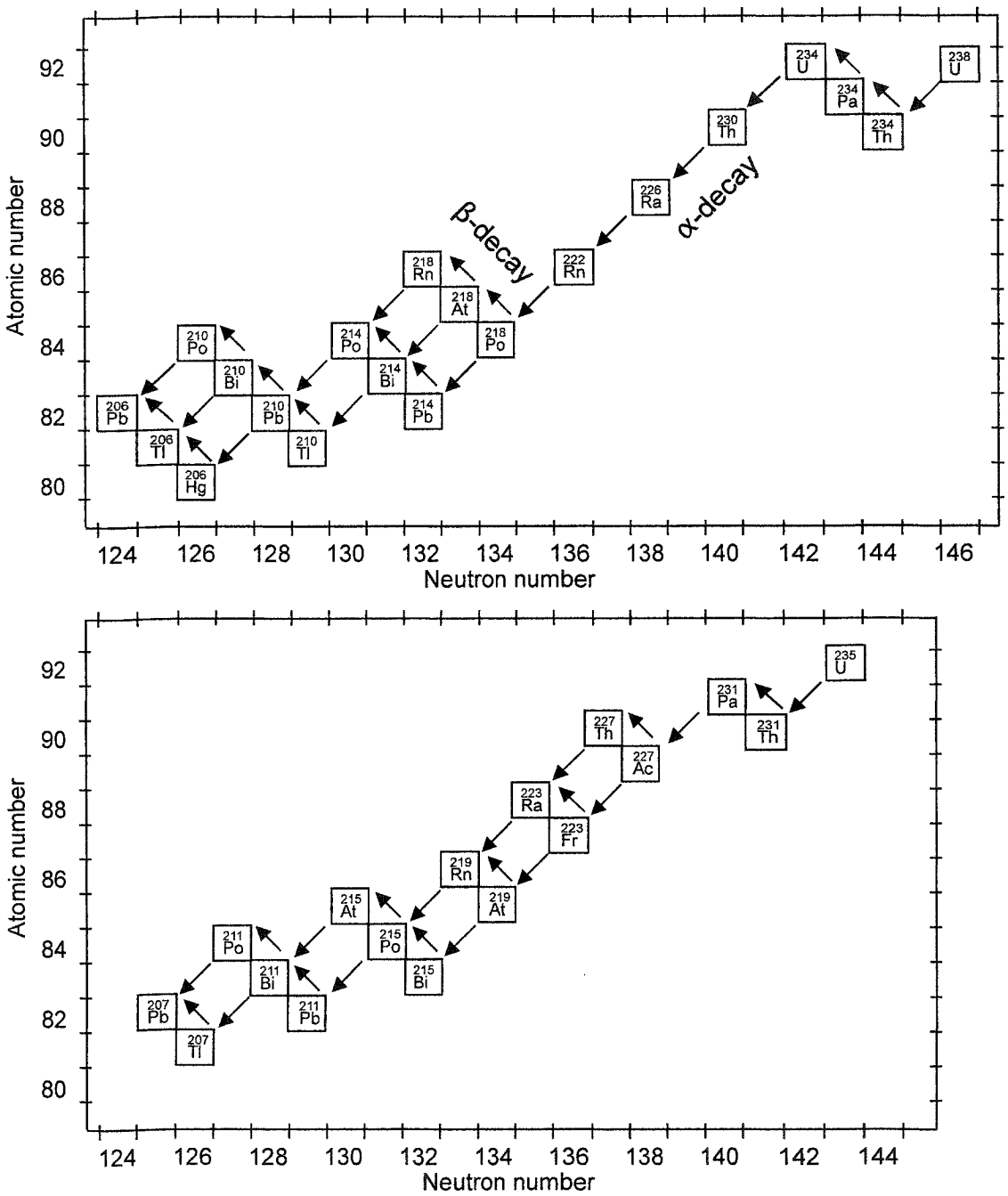

Figure 2.7. The decay schemes for ^{238}U to stable ^{206}Pb (top) and ^{235}U to stable ^{207}Pb (bottom). The decay of 1 atom of ^{238}U ultimately produces 8 ^{4}He nuclei. The decay of ^{235}U ultimately produces 7 ^{4}He nuclei (from Faure 1986).

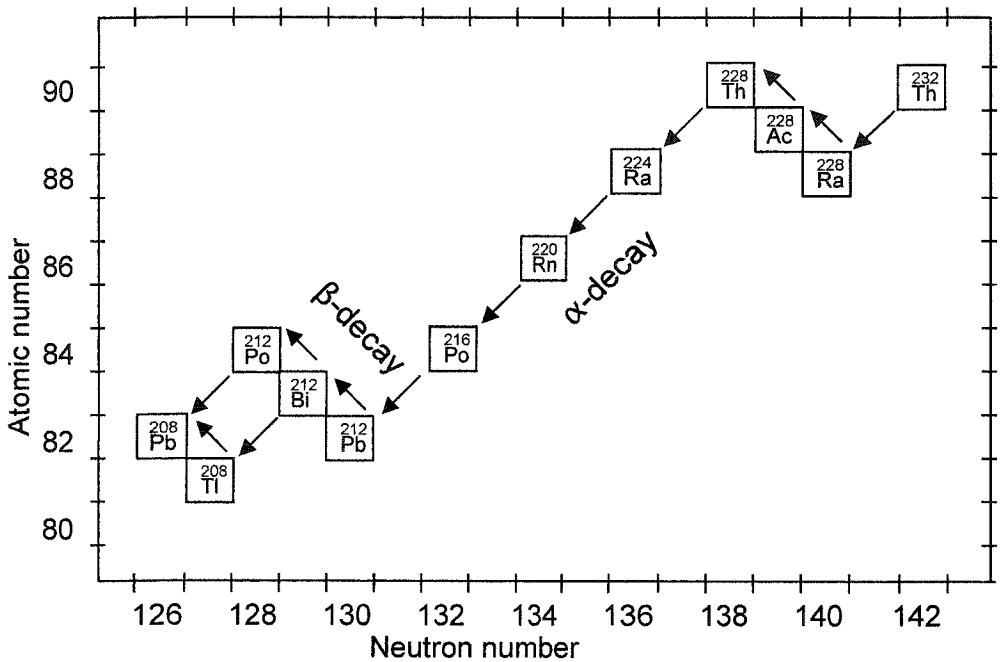

Figure 2.8. The decay scheme for ^{232}Th to stable ^{208}Pb. The decay of 1 atom of ^{232}Th ultimately produces 6 ^{4}He nuclei (from Faure 1986).

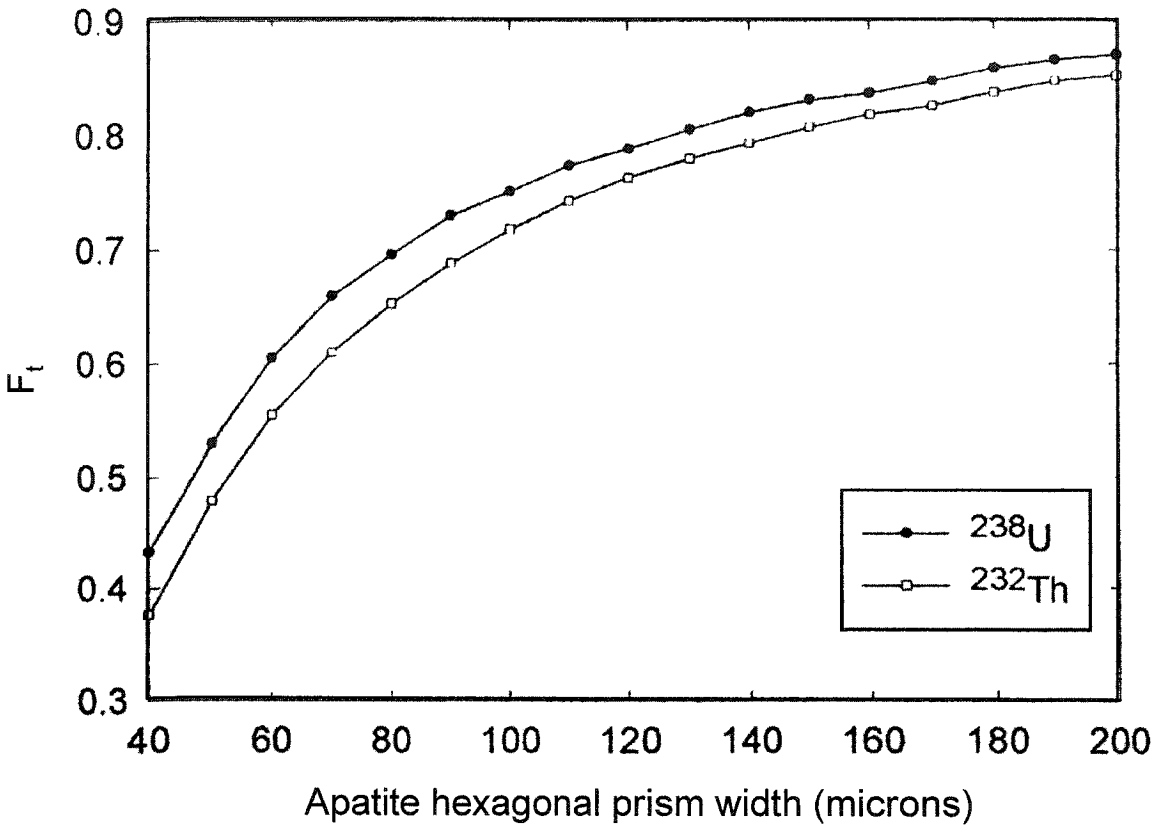

Figure 2.9. The F_t or 'total fraction of α-particles retained' correction as a function of grain radius for a hexagonal prism geometry. The value of F_t is greater for ^{238}U because it has a lower emission energy than ^{232}Th. The ^{235}U curve plots on the ^{232}Th plot (from Farley 2002).

increases rapidly with decreasing grain-size.

2.2.4 Helium diffusion in apatite

The behavior of radiogenic He in a crystal lattice is governed by laws of diffusion (e.g. Wolf et al. 1998; Reiners and Farley 1999; Farley 2000; Reiners et al. 2002) which are highly temperature-dependent. Helium diffusion as a function of time and temperature obeys an Arrhenius relationship so that the rate of loss of helium by diffusion is given by

$$\frac{D_t}{a^2} = \frac{D_o}{a^2} e^{\frac{-E_a}{RT_t}} \qquad 2.10$$

where D_t = the rate of diffusion at a given temperature; a = the frequency factor, an expression of the smallest diffusion domain; D_o= rate of diffusion at infinite temperature; E_a = the activation energy; R = the gas constant; and T_t = temperature as a function of time, i.e., thermal history.

Laboratory diffusion measurements indicate that radiogenic helium is retained in apatite at surface temperatures, but becomes mobile at only slightly elevated temperatures (Zeitler et al. 1987). More recent studies (Lippolt et al. 1994; Wolf et al. 1996; Wolf et al. 1998; Farley 2000) have demonstrated that diffusive loss of He from apatite becomes significant at temperatures as low as 40 °C, and is essentially complete at temperatures of 85-90 °C over geologic time-scales. Farley (2000) and Reiners and Farley (2001) inferred that apatite is crystallographically isotropic with respect to helium diffusion, and that diffusivity scales with the inverse square of the grain radius, which suggests the physical grain is the diffusion domain. Farley (2000) suggested an effective closure temperature of ca. 70 °C for monotonically cooled apatites with a grain radius of 100 μm. The progressive diffusive loss of radiogenic He between 40 - 90 °C results in a helium partial retention zone (PRZ) analogous to the PAZ. Thus apatite FT and (U-Th)/He dating are two independently calibrated low-temperature thermochronometers that may be used to constrain heating and cooling through temperatures of 40 to 130 °C with essentially no overlap (Fig. 2.10).

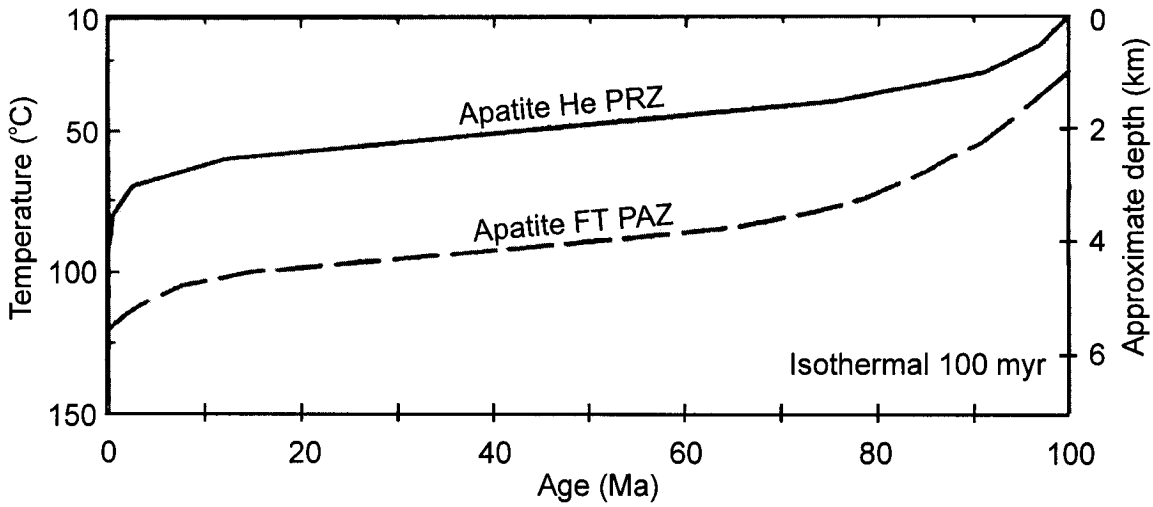

Figure 2.10. A comparison of the FT PAZ and the He PRZ in apatite calculated using 100 My of isothermal heating at the indicated temperatures (modified from Wolf et al. 1998, and Farley 2002). The scaling of depth to temperature assumes a constant geothermal gradient of 20 °C/km and a constant surface temperature of 10 °C.

2.2.5 (U-Th)/He thermochronology

All diffusive loss of radiogenic ^{4}He occurs at the grain boundary. Apatite grains which have experienced temperatures of ca. 40 - <90 °C over geologic time-scales can be expected to have heterogeneous ^{4}He concentration profiles, with the highest helium concentrations in the core of the grains and the lowest at the rims. Because the concentration gradient is a sensitive function of the thermal history (e.g. Farley 2002), apatite (U-Th)/He - based thermochronology, using step-heating techniques to determine ^{4}He concentration profiles in single grains has the potential to yield detailed cooling history information over temperatures within the PRZ (e.g. Shuster and Farley 2003). However, these studies have only recently come under investigation, and to date there are no published geological applications of this methodology. An alternative approach to (U-Th)/He thermochronology involves the use of multiple aliquots of a single sample over a range of grain-sizes. Farley (2000) suggested closure temperature correlates with grain size. Coarser grain fractions have slightly higher closure temperatures than do the finer grains, and thus systematic differences in the ages of the various size fractions can be used to infer information on cooling rates, especially for samples that have a protracted history within the helium PRZ.

2.2.6 (U-Th)/He modelling

Like all other thermochronometric techniques, the interpretation of (U-Th)/He ages in the simplest circumstances is in terms of monotonic cooling through the closure temperature (Dodson 1973). However, because apatite (U-Th)/He ages are sensitive to such low temperatures, the processes that dominate the exposure of rocks at the Earth's surface such as tectonic and erosional denudation are likely to yield more complex thermal histories. A method for exploring the low-temperature thermal history of samples by predicting (U-Th)/He ages was demonstrated by Wolf et al. (1998). Ages are calculated using iterative forward modelling of the ingrowth and diffusion of radiogenic ^{4}He over a number of isothermal time-steps (Wolf et al. 1998; Equation 5). The (U-Th)/He age in terms of the amount of helium present (^4He) and the rate of ingrowth (P) is described by:

$$\frac{^4He}{P} = t' = \frac{a^2}{D}\left(\frac{1}{15} - \sum_{n=1}^{\infty}\frac{6}{\pi^4 n^4}\exp\left[-n^2\pi^2\frac{D}{a^2}t\right]\right) + \frac{^4He^*}{P}\sum_{n=1}^{\infty}\frac{6}{\pi^2 n^2}\exp\left[-n^2\pi^2\frac{D}{a^2}t\right] \quad 2.11$$

where t' is the (U-Th)/He age, t is the time over which isothermal production and diffusion occur, and $^4He^*$ is the initial helium concentration, and P is the rate of production.

Forward thermal history modelling of (U-Th)/He age data in this thesis was done using the program "Age Calculation.vi", (proprietary code of Ken Farley) that uses the LabVIEW® software platform. Input parameters for "Age Calculation.vi" are a series of times/temperatures, the measured grain radius (for calculating the α-ejection correction), the diffusion grainsize, activation energy, time-step duration, and the U and Th contents. Further discussion of the input constraints is given in Chapters 4 and 7 of this thesis.

2.2.7 Geological applications

Reviews of many of the current and potential future applications of (U-Th)/He thermochronology are given by Farley (2002) and Ehlers and Farley (2003). Because (U-Th)/He thermochronometry is relatively new, however, many of the various possible applications have not yet been fully explored and it is difficult to say how it will ultimately come to be used. One important aspect of the method is that the rate of ^{4}He ingrowth from multiple parent isotopes is relatively rapid. Also, analytical precision can be quite high, with typical 2σ errors on the order of 6% (e.g. Farley 2002), and as a result, fairly high-precision ages can be obtained even on very young (i.e., <1 Ma) samples (e.g. Spotila et al. 2001). Another aspect that distinguishes apatite (U-Th)/He dating from other techniques is the sensitivity that results from low He diffusion temperatures. The method is sensitive to lesser amounts of denudational cooling than apatite FT dating, and can be used to infer a more detailed thermal history in the upper few km of the crust (e.g. Stockli et al. 2000). Studies that combine (U-Th)/He thermochronometry with other techniques such as apatite or zircon FT or K-feldspar ^{40}Ar/^{39}Ar dating are becoming increasingly common, and can be used to

infer detailed thermal histories over a wide range of temperatures (e.g. Armstrong et al. 2003; this study).

2.2.8 Analytical procedures for (U-Th)/He analysis

Analytical (U-Th)/He dating was done at Ken Farley's noble gas laboratory at Caltech, Pasadena, California. The procedures used in this study (described below) have also been described in Appendix 1 of Farley (2002). Individual samples consisting of between 1 and 4 inclusion-free grains (Tables 4.1 and 6.3) were selected for (U-Th)/He analysis using a stereo binocular microscope equipped with a transmitted light source and a rotating stage. Only grains that appeared completely dark when viewed with the stage rotated to extinction (in crossed polarized light) were selected. Prior to analysis, sample grains were measured using a microscope equipped with an ocular graticule and stage micrometer to calculate α-ejection corrections.

Two slightly different analytical procedures were used for He extraction (Fig. 2.11). Most of the samples from the Nova Scotia margin were heated using a conventional resistance furnace. Heating of all of the samples from the Nares Strait - Kane Basin - Smith Sound region and two of the Nova Scotia margin samples was done using a Nd-YAG laser following the method of House et al. (2000). For furnace heating, sample grains were placed in stainless steel crucibles that were then spot-welded shut to trap the grains but allow the free exchange of evolved gases. Individual crucibles were heated to ca. 950 °C for 20 minutes to completely outgas the grains. For Nd-YAG laser heating sample grains were placed in platinum microtubes, that were then pinched closed and loaded into a laser planchet. Individual microtubes were heated using a Nd-YAG laser to temperatures of ca. 1050°C for 5 minutes to outgas the grains.

Evolved gases were spiked with approximately 0.4 pmol of ^{3}He and adsorbed on an activated charcoal bead cooled to 16 K using a cryogenic trap. Purification to remove all gases other than He was done by heating the trap to 37 K and venting the released gas. $^{4}He/^{3}He$ ratios were measured in a quadrupole mass spectrometer (QMS). Completeness of gas extraction was verified for each sample by performing a re-extraction heating following

each He analysis. Sample blanks were also measured between sample analyses to verify the linearity of QMS detector memory and ion consumption effects. Ratios were referenced to multiple determinations of a known volume of ^{4}He standard processed in the same way as the samples, and appropriate discrimination corrections were made to the measured $^{4}He/^{3}He$ ratios.

Following degassing the steel crucibles were opened to retrieve the heated grains. Pt microtubes were not opened. Samples were placed in 100 ml of concentrated HNO_3 to dissolve the apatite grains. Solutions were spiked with a 25 ml calibrated ^{230}Th and ^{235}U solution and diluted to 250 ml with ultrapure water. The spiked samples were analyzed as 0.5 ml aliquots of ca. 1-5 ppb U-Th solutions by isotope dilution using a Finnigan Element2 ICP-MS with a Teflon micro-flow nebulizer and double-pass spray chamber. U and Th blanks by this method are 1 ± 0.1 pg and 2 ± 1 pg, respectively. Estimated uncertainty of measured sample U-Th are on the order of 1-2% (2σ).

The raw age data were corrected according to the method of Farley et al. (1996) to account for ejection from the host grain of a portion of the He produced by α-decay of uranium and thorium isotopes owing to the large stopping distances for the emitted He nuclei (ca. 12-34 μm in apatite). Based on statistical analysis of multiple (U-Th)/He age determinations for the Fish Canyon and Durango apatite standards, overall analytical uncertainty in the individual corrected sample ages is on the order of 6-8% at the 2σ confidence level. Aliquots of the laboratory apatite standard 97MR22, (average laser multi-grain age of 4.50 ± 0.24 Ma; House et al. 2000) were also analyzed.

During the ICP-MS analyses it was discovered that many of the Nares Strait - Kane Basin - Smith Sound samples had very high light REE contents, in particular, Sm was up to 1150 ppm. One of the principal Sm isotopes (^{147}Sm) is radioactive and decays by emission of a single He nucleus to ^{143}Nd, ($t_{1/2} = 1.06 \times 10^{11}$ yr), so that for some samples over 20% of the He nuclei were from ^{147}Sm decay. An additional correction was therefore applied to the (U-Th)/He age data to account for the contribution of ^{147}Sm-derived He nuclei.

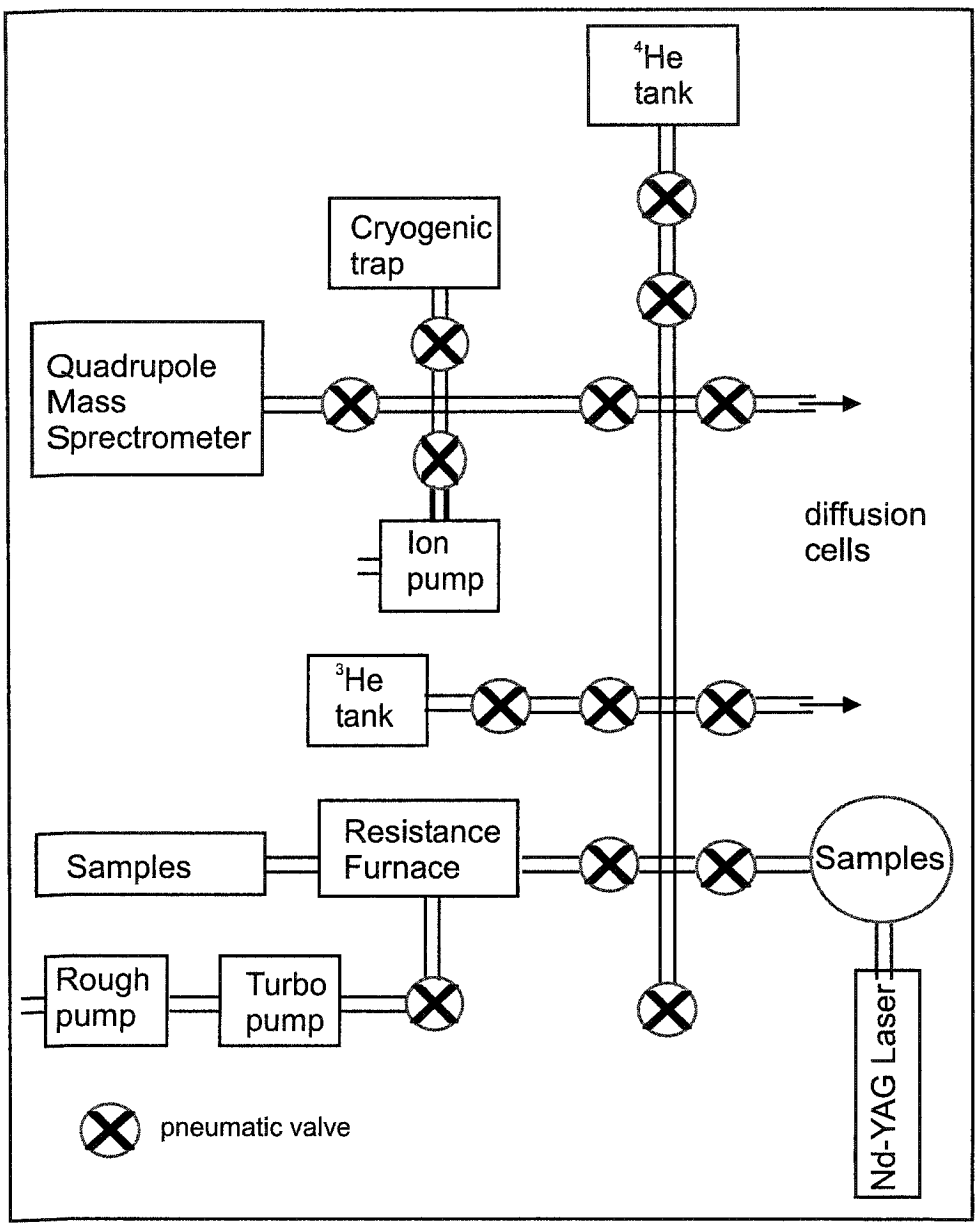

Figure 2.11. Schematic illustration of the He quadrupole mass spectrometer sample line.

CHAPTER 3. Post-Paleocene cooling in the southern Canadian Atlantic region: Evidence from apatite fission track models [1]

A.M. Grist and M. Zentilli

3.1 Abstract

The traditional view of the geomorphic evolution of the southern Canadian Atlantic margin is one of gradual exhumation and peneplanation following Triassic-Jurassic rifting. Thermal modelling of apatite fission track data from pre-Carboniferous granitic basement in Nova Scotia, and from Permian and Triassic sandstones from Nova Scotia, New Brunswick, and Prince Edward Island, suggests a more complex thermal evolution of the onshore part of the margin. Models clearly indicate significantly elevated regional paleotemperatures during Jurassic time, and as much as 30 °C of post-Paleocene cooling. Model-predicted paleo-geothermal gradients for granitic samples from the Digby D-1 well are normal, ranging from 15 to 20 °C/km. Post-Paleocene cooling may be attributable to the combined effects of 13 °C of exhumational cooling from erosion of ca. 700 m of post-Aptian sediments caused by decreased eustatic sea levels, and 8-17 °C of cooling from the propagation to depth of a 10-20 °C decrease in paleo-mean annual surface temperatures between Late Cretaceous time and the present. The combined effects of burial heating related to increased eustatic sea level and the propagation to depth of higher paleo-mean annual surface temperatures in the Late Cretaceous may also explain elevated vitrinite reflectance levels in Cretaceous lignites and in Jurassic strata in the Fundy Basin of Nova Scotia. These models demonstrate that the traditional view comprising solely passive peneplanation and slow exhumation of the margin since Early Jurassic time is not tenable.

---

[1] Grist, A.M. and Zentilli, M. 2003. Post-Paleocene cooling in the southern Canadian Atlantic region: Evidence from apatite fission track models, Canadian Journal of Earth Sciences, **40**, no. 9, 1279-1297.

3.2 Introduction

Apatite fission track (FT) studies of Paleozoic basement in Nova Scotia (Ravenhurst et al. 1990; Arne et al. 1990) and of upper Paleozoic strata from the Maritimes Basin, Nova Scotia, Prince Edward Island, and beneath the Gulf of St. Lawrence (Ryan and Zentilli 1993; Grist et al. 1995) have inferred that strata now at or near the surface were formerly buried by extensive Late Carboniferous to Early Permian cover to depths of at least 4-5 km. The thermal effects of this burial resulted in ubiquitous regional resetting of apatite FT parameters consistent with regional surface vitrinite reflectance levels in the upper Paleozoic strata (Fig. 3.1) of 0.5 % *Ro* to >1.0 % *Ro* (e.g. Hacquebard and Donaldson 1970).

The style and timing of exhumation and erosion of the cover has been addressed by several authors. Ravenhurst et al. (1990) proposed simple linear cooling from approximately 100 °C in Triassic time to the present for Carboniferous-aged marine sandstones from the southern flank of the Maritimes Basin in central Nova Scotia and the South Mountain Batholith (SMB), southwestern Nova Scotia (including 2 samples that were re-analyzed for this study). This interpretation supports a Davisian-type model (Davis 1922) of long-term (post-Triassic) peneplanation of Nova Scotia (e.g. Goldthwait 1924) and implies that except for Neogene glaciation, the present distribution and exposure of crystalline and cover rocks have slowly evolved since the Triassic.

Arne et al. (1990) suggested that basement rocks beneath the Lower Carboniferous unconformity at Gays River in the Shubenacadie Basin (Fig. 3.1) experienced heating to temperatures of 60-80 °C between about 100 and 50 Ma. The Arne et al. (1990) thermal model was constrained by Albian-Aptian-aged spores and lignite in sediments preserved from glacial erosion in karst depressions in Mississippian limestone at Gays River (Davies et al. 1984; Akande and Zentilli 1983), indicating that the strata were at the surface at about 120-100 Ma. However, a lack of long confined apatite fission tracks, which would have accumulated if the samples had remained at the surface for 120 million years, implied that the rocks had experienced significant post-Albian heating.

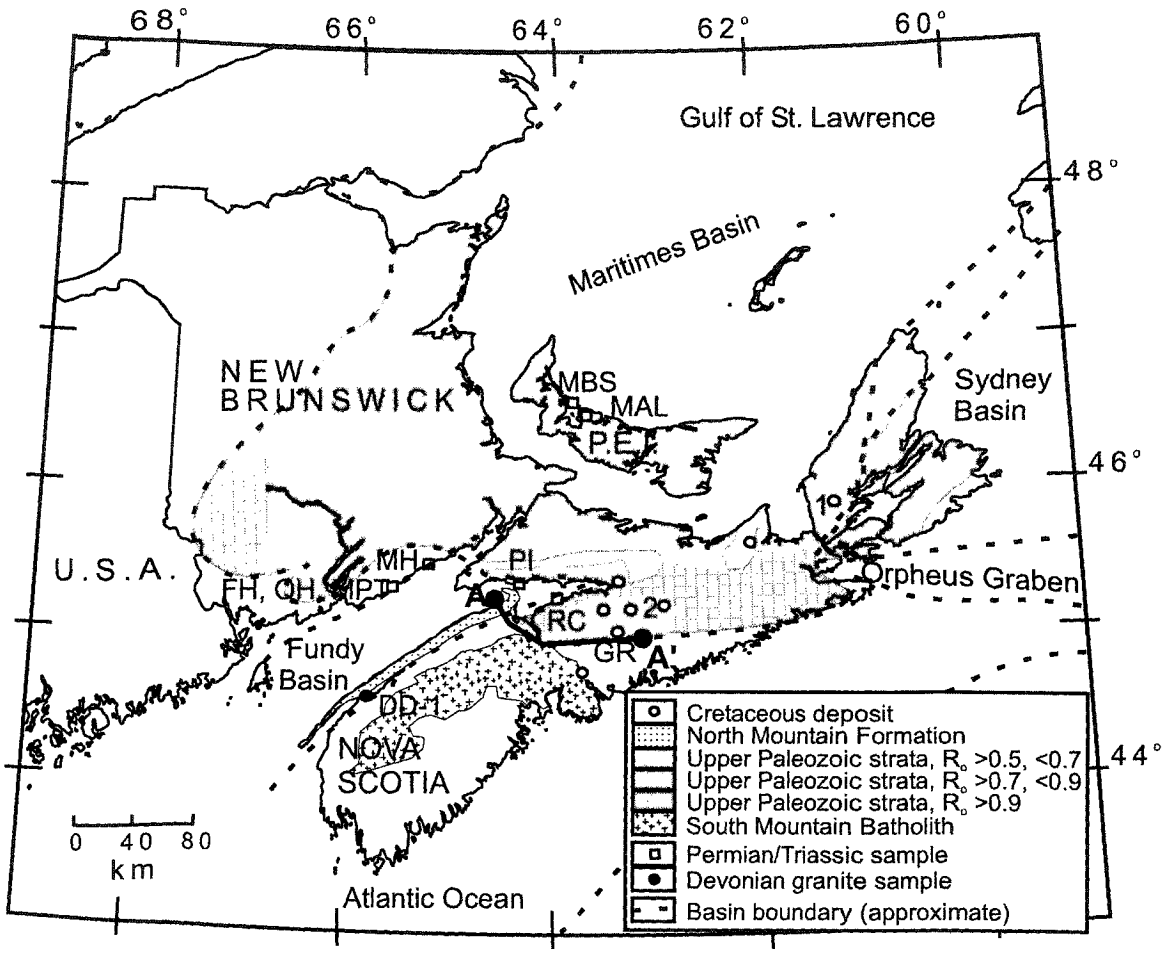

Figure 3.1. Map of the study area showing sample locations, some stratigraphic elements, and areas of iso-reflectance within the Maritimes Basin. Abbreviations used are: DD-1 = Digby D-1 drillhole; FH = Fownes Head; QH = Quaco Head; MPT = McCumber Point; MH = Martin Head; PI = Partridge Island; RC = Rainy Cove; GR = Gays River; MBS = Malpeque Bay Sill; MAL = Malpeque; 1 = Diogenes Brook; 2 = Dickey Brook. Iso-reflectance contours are modified from Hacquebard and Donaldson (1970).

Evidence for similar heating (in terms of magnitude and timing) was also indicated by apatite FT models for the offshore region in Scotian Basin strata, 300 km southeast of Gays River (Grist et al. 1992; Li et al. 1995). Thus it is possible that elevated temperatures during Late Cretaceous - Early Tertiary time were a regional phenomenon, meriting a focussed study of Mesozoic and older rocks in order to investigate the timing, magnitude, and areal extent, and to assess possible causes, effects, and significance of elevated temperatures with respect to tectonic models. The recent emergence of the southern Canadian Atlantic margin as an area of intense hydrocarbon exploration and development activity has only increased the necessity for refined thermal history models for this region.

3.3 Regional geological framework

The study area lies within the southern Canadian Appalachians. Basement rocks have been affected by both the Devonian Acadian and Late Permian Appalachian Orogenies, and are also partially overlain and overprinted by rift assemblages related to the Mesozoic and Cenozoic development of the Atlantic passive margin. The complex regional geology was summarized in Williams (1995).

In southern New Brunswick, basement rocks are upper Precambrian sedimentary and volcanic rocks and overlying Cambrian and Ordovician shales and sandstones (van de Poll 1995). Crystalline basement in southern Nova Scotia, and beneath the Scotian and Fundy Basins, consists of metamorphosed Late Cambrian to Early Devonian-aged siliciclastic sequences of the Meguma Zone (Schenk 1995*a*, 1995*b*). These rocks were folded and metamorphosed during the Devonian Acadian orogeny, and in Nova Scotia were intruded by the SMB, an extensive granodioritic intrusion, at ca. 380-370 Ma (Reynolds et al. 1981; Clarke et al. 1993). Considerable erosion followed the emplacement of the SMB, and by the Early Carboniferous (ca. 350 Ma), Horton Group terrestrial clastics and Windsor Group marine carbonates and evaporites (Gibling 1995) were being deposited nonconformably on the granodiorite, or Meguma metasediments (Figs. 3.1, 3.2).

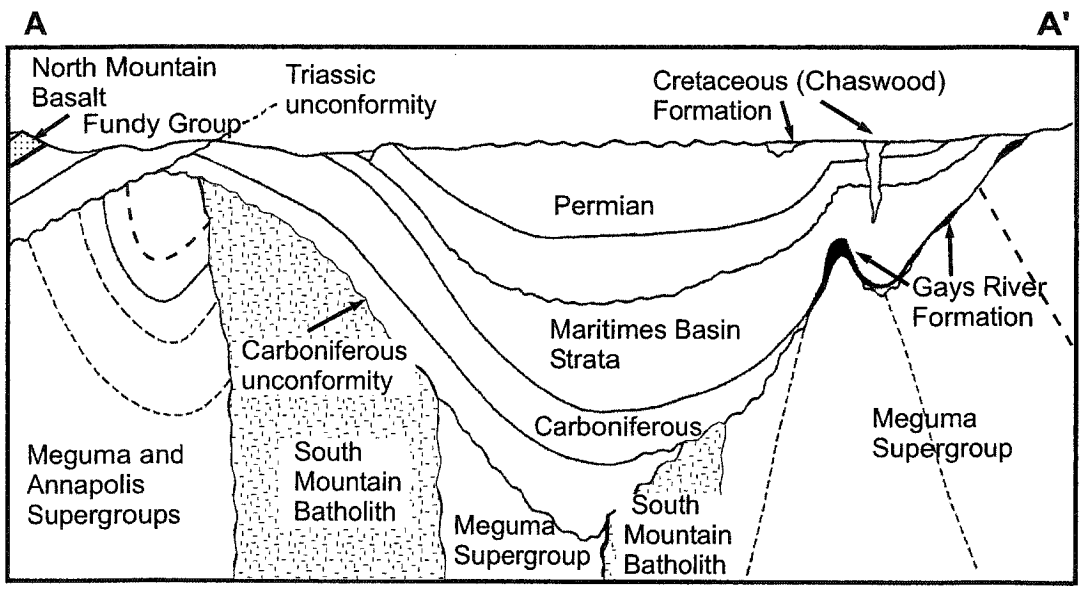

Figure 3.2. Schematic cross-section A-A' of the central part of the study area showing the stratigraphic relationships of the principal structural elements referred to in the text (substantial vertical exaggeration). The approximate location of the A-A' cross section is shown in Fig. 3.1 (modified from Moore et al. 2000).

The Carboniferous to Permian Maritimes Basin (composite Fundy Basin of Bradley 1982) is a complex of erosional remnants of upper Paleozoic strata. Northeast of Prince Edward Island, sediment thickness exceeds 12,000 m (Sanford and Grant 1990). The basin is flanked by platformal areas in western New Brunswick, southern Nova Scotia, and western Newfoundland with relatively thin, mildly deformed upper Paleozoic strata (e.g. Bradley 1982). The youngest basin strata are Lower Permian (Artinskian) redbeds found on Prince Edward Island (van de Poll 1995) including the Malpeque sample area (Fig. 3.1). Previous apatite FT studies have inferred that basin inversion led to erosion of at least 4-5 km of sediments by the Late Triassic (Ryan and Zentilli 1993; Grist et al. 1995), and a similar conclusion was reached for the Sydney Basin (Gibling et al. 2002).

A major Late Triassic erosional unconformity in southwestern Nova Scotia marks the beginning of accumulation of Atlantic rift-related sequences. Early rifting was focussed between Nova Scotia and New Brunswick, and remnants of this failed rift comprise the Triassic Fundy Basin (Fig. 3.1). The Triassic and Early Jurassic Newark Supergroup (e.g. Greenough 1995; Wade et al. 1996) comprise continental red clastics and tholeiitic basalts deposited in the faulted half-graben of the Fundy Basin. These strata thicken northward to >9000 m under the Bay of Fundy, and Triassic-Jurassic mafic dikes occur beyond the boundaries of the graben in New Brunswick and in Malpeque Bay, Prince Edward Island. In New Brunswick, the Triassic Fundy Group is exposed in three small but relatively thick successions on the north coast of the Bay of Fundy (Nadon and Middleton 1985). In Nova Scotia, the stratigraphically equivalent Wolfville and Blomidon Formations exist in a 200 km long by up to 20 km wide belt along the northwestern coastal part of the province (Wade et al. 1996; Hubert and Mertz 1984; and others). Offshore Nova Scotia forms part of the present Atlantic passive margin, an active depositional basin from the Late Triassic - Early Jurassic to the present (e.g. Keen and Williams 1990).

Several igneous provinces and cycles of intra-plate magmatic activity related to successive stages of rifting of the Atlantic margin have been recognized in New England and Atlantic Canada (McHone and Butler 1984). The Malpeque Bay Sill is included in the Coastal New England Province (e.g. Greenough 1995), which was active close to the

Permian-Triassic time boundary. The gently northwest dipping basalt flows of the North Mountain Formation are included in the Eastern North America Dolerite Province (e.g. Greenough 1995) and were extruded during the Early Jurassic cycle. In the Nova Scotia offshore rift margin, the extrusion of the North Mountain basalt has been inferred to coincide tectonically with the regional breakup unconformity (Wade and MacLean 1990), though elsewhere the eastern North America such rocks are precursors to the development of initial Atlantic Ocean crust (McHone et al. 1987). The North Mountain Formation has been paleontologically assigned a Hettangian (200-197 Ma, earliest Jurassic) stratigraphic age (Olsen et al. 1987). K-Ar radiometric ages ranging from 191± 2 Ma (Hayatsu 1979; Hodych and Hayatsu 1988) to 202 Ma (Wark and Clarke 1980) and a U-Pb zircon age of 202 ± 1 Ma (Hodych and Dunning 1992) confirm that the North Mountain basalt was extruded very close in time to the Triassic-Jurassic boundary (using the timescale of Okulitch 1999).

Only limited post-Jurassic strata occur on land in Nova Scotia and consist of small, unconsolidated deposits of Lower Cretaceous kaolinitic clay and quartzose sand preserved from erosion in depressions and sinkholes in central Nova Scotia, collectively called the Chaswood Formation (Stea et al. 1997). Lithologically similar sands also occur in southern New Brunswick (Lockhart 1984). Coal compaction and vitrinite reflectance studies (Hacquebard 1984) of lignite contained in deposits at Gays River, Dickey Brook, and Diogenes Brook indicate that these are erosional remnants of formerly more extensive strata. Hacquebard (1984) estimated that up to 700-800 m of Cretaceous sediments may have covered Nova Scotia onshore. An average vitrinite reflectance (*Ro*) value of 0.44 ± 0.03% was cited by Davies et al. (1984) for lignite at Gays River.

3.4 Sampling strategy

A summary of the samples is given in Table 3.1, and their locations are shown on Fig. 3.1. The principal objective in sample selection was to determine whether the apatite FT age and track length (TL) parameters would (*i*) reflect cooling from the thermal effects of Triassic rifting of the Fundy Basin, thereby supporting widespread post-Early Jurassic regional peneplanation, or (*ii*) reflect elevated Late Cretaceous/Early Tertiary temperatures

of a similar magnitude to those detected in previous apatite FT studies, indicating that elevated temperatures were regionally extensive, thereby refuting the peneplanation model.

Outcrop samples were obtained from sandstones of the Triassic Fundy Group in Nova Scotia and New Brunswick. These rocks represent the earliest deposits in the Fundy graben above the Triassic unconformity. An additional three samples were obtained from youngest Permian units within the strata of the Maritimes Basin from near the Triassic Malpeque Bay Sill, Prince Edward Island.

The Digby D-1 drill hole (Chatterjee and Dostal 2002), cored granodiorite of the SMB to a depth of >1400 m on the southeast flank of the Fundy Basin in Nova Scotia (latitude 44°29′0.85″N, longitude 63°43′19.7″W), below the Triassic unconformity. It was assumed that apatite fission tracks here were totally annealed by burial heating prior to inversion of the Maritimes Basin. They may also have been influenced by the thermal effects of rifting. Uncertainties related to provenance are not a factor because these samples are granodiorites and the emplacement age is known. Two of the D-1 samples previously reported by Ravenhurst et al. (1990) are included in Table 3.2. However, technical difficulties arising from high U content and a non-standardized grain etch used in the earlier analyses necessitated remounting, re-irradiating, and re-analyzing the separates to standardize the data.

3.5 Apatite fission track dating

Reviews of apatite FT dating, its application to geological problems, and the development of apatite FT thermal models have been provided by Wagner and Van den Haute (1992), Gallagher et al. (1998), Gleadow and Brown (2000), and others. Only a few (specifically) relevant details are discussed here.

Apatite FT thermochronology is based on the measured density and length distribution of linear tracks of crystal damage produced during spontaneous fission of trace amounts of ^{238}U in apatite. In monotonically cooling systems, track densities provide a measure of age with respect to closure temperature. Complete annealing of apatite fission tracks occurs at temperatures of 100°-150 °C over geologic time periods. Track length reduction by annealing of fission damage is an incremental and irreversible process that is dominantly thermally

Sample number and location		Stratigraphic age and lithology
Digby D-1 well samples		
OSNS-21	D-1 (60.2-60.6 m)	Devonian granodiorite
OSNS-22	D-1 (249.5-250 m)	Devonian granodiorite
OSNS-24	D-1 (620-624 m)	Devonian granodiorite
OSNS-26	D-1 (848.8-849.3 m)	Devonian granodiorite
OSNS-28	D-1 (1004 m)	Devonian granodiorite
OSNS-30	D-1 (1197 m)	Devonian granodiorite
OSNS-29	D-1 (1315 m)	Devonian granodiorite
OSNS-27	D-1 (1437-1437.9 m)	Devonian granodiorite
PT outcrop samples		
FT-010 Martin Head, N.B.		Fundy Group Triassic sandstone
FT-011 Quaco Head, N.B.		Fundy Group Middle Triassic (Ladinian?) sandstone
FT-012 Quaco Head, N.B.		Fundy Group Middle Triassic (Ladinian?) sandstone
FT-013 McCumber Point, N.B.		Fundy Group Triassic sandstone
FT-014 Fownes Head, N.B.		Fundy Group Late Triassic (Carnian?) sandstone
FT-019 Malpeque Bay, P.E.I.		Lower Permian sandstone in contact with dike
FT-020 Malpeque Bay, P.E.I.		Lower Permian sandstone in contact with dike
FT-021 Malpeque P.E.I.		Lower Permian sandstone
FT-045 Rainy Cove, N.S.		Fundy Group Triassic sandstone
FT-046 Partridge Island, N.S.		Fundy Group Triassic sandstone

Table 3.1. A summary of the locations and lithologies of the samples.

activated. Tracks are formed continuously through time and the TL distributions are indicative of the integrated thermal history below the closure temperature. However, the probability of a track intersecting a polished surface and contributing to the age is proportional to its length, and therefore apatite FT ages in systems with complicated thermal histories may not represent a geologically significant event in time.

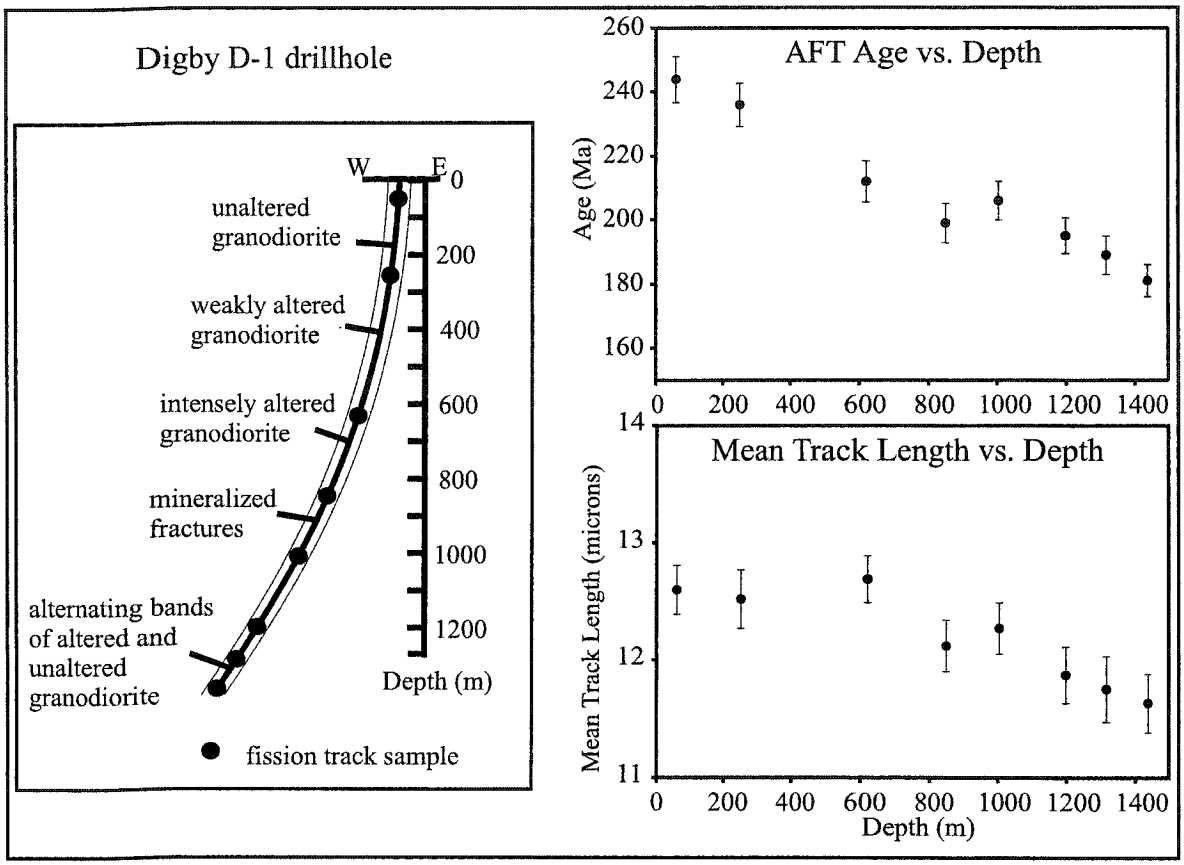

Figure 3.3. A cross-section of the Digby D-1 drillhole (modified from Chatterjee and Dostal, 2002) and summary figures of apatite FT age and mean confined track length vs. depth for the Digby samples.

3.5.1 Analytical procedures

Samples were mounted in epoxy and polished to expose internal grain surfaces. Spontaneous tracks were revealed by etching in 5M HNO_3 for 20 s at 24 °C. Apatite FT ages were determined using the external detector method (Fleischer et al. 1964; Hurford and Green 1982). A thin sheet of low-uranium muscovite was attached to the polished surface of each grainmount to detect neutron-induced fission. Samples were irradiated at the Dalhousie University Slowpoke reactor in the presence of glass neutron dosimeters (CN1 or CN5) of known characteristics. The thermal-neutron fluence obtained was approximately 9 x 10^{15} neutrons/cm^2. The cadmium ratio for Au is 4.3 at the site. Micas were etched at room temperature in 48% HF for 22 min. Spontaneous and induced track densities (tracks/cm^2) were counted at 1000x magnification (100x dry objective, 10x oculars 1x drawing tube) on a Zeiss® Axioplan microscope equipped with an Autoscan® AS3000 stage. Ages were calculated using a weighted mean zeta calibration factor (Fleischer et al. 1975; Hurford and Green 1983), determined using the Fish Canyon Tuff and Durango apatite age standards. TL distributions of horizontal, confined tracks (in crystallographic planes parallel to the *c*-axis) were also measured at 1000x magnification using a digitizing pad interfaced with a personal computer. The precision of each measured length is ± 0.20 μm.

3.6 Discussion of FT data

3.6.1 Digby D-1 drillhole

Apatite FT data are presented in Table 3.2. Summary figures of the age and length data as a function of depth, TL histograms, and radial plots (Galbraith 1990) of the age data are shown in Figs. 3.3-3.5. Spontaneous track densities were very high, resulting in counts of up to 7800 fossil tracks and measurements of up to 216 confined tracks per sample. Both ages and mean track lengths decrease with increasing depth, but not to the same extent.

Table 3.2. A summary of the FT age and TL data. Samples with χ^2 probability <.05 fail the χ^2 test at the 95% confidence level. Ages reported are the central age (Galbraith and Laslett 1993). Abbreviations are as follows: N_s, N_i, N_d = the number of spontaneous (fossil), induced, and flux dosimeter (CN-5 or CN-1) tracks counted; Rho $_s$, Rho_i, Rho_d = density ($x10^5/cm^2$) of spontaneous (fossil), induced, and dosimeter (CN-5 or CN-1) tracks; SE = standard error. Age error estimates are at the 2σ confidence level. Analyses by A.M. Grist using a zeta of 353.5 ± 7.1 (CN-5) or 10,540 ± 180 (CN-1).

*Ravenhurst et al. (1990) reported ages of 219 ± 12 Ma and 170 ± 9 Ma and mean confined track lengths of 13.32 ± 0.11 μm (n = 101 lengths) and 12.68 ± 0.14 μm (n = 100 lengths) for the OSNS-21 and OSNS-27 samples respectively (1σ errors).

		Age Data									Length Data		
Sample No.	Sample Location	Grains Counted	N_s	N_i	Rho_s	Rho_i	χ^2 Prob.	N_d	Rho_d	Age (Ma)	No. of Lengths	Mean (μm)	SE (μm)
OSNS-21*	D-1 (60.2-60.6 m)	18	6553	5059	50.6	39.1	.8096	8100	10.88	**244 ± 14.4**	181	12.60	0.22
OSNS-22	D-1 (249.5-250 m)	21	7800	6229	41.9	33.5	.3052	8100	10.88	**236 ± 13.4**	184	12.52	0.25
OSNS-24	D-1 (620-624 m)	16	5326	4745	41.2	36.7	.9988	8100	10.88	**212 ± 13.8**	216	12.69	0.20
OSNS-26	D-1 (848.8-849.3 m)	17	4523	4308	45.0	42.8	.8368	8100	10.88	**199 ± 12.4**	179	12.12	0.22
OSNS-28	D-1 (1004 m)	18	5955	5462	45.5	41.7	.4348	8100	10.88	**206 ± 12.2**	176	12.27	0.22
OSNS-30	D-1 (1197 m)	20	6661	6475	41.6	40.4	.1516	8100	10.88	**195 ± 11.2**	186	11.87	0.24
OSNS-29	D-1 (1315 m)	13	4212	4228	47.4	47.6	.5047	8100	10.88	**189 ± 12.0**	153	11.75	0.28
OSNS-27*	D-1 (1437-1437.9 m)	20	7707	8061	42.5	44.6	.0826	8100	10.88	**181 ± 10.0**	178	11.63	0.25
FT-010	Martin Head	22	1169	1047	15.0	13.4	.9947	8000	35.1	**203 ± 20**	155	13.26	0.16
FT-011	Quaco Head-1	19	2130	1684	39.4	31.6	.4828	8000	35.1	**230 ± 17**	157	13.44	0.20
FT-012	Quaco Head-2	19	2818	2051	42.7	31.1	.0048	8000	35.1	**256 ± 28**	161	13.60	0.19
FT-013	McCumber Point	32	1042	916	9.65	8.48	.1354	8000	35.1	**207 ± 20**	110	13.39	0.19
FT-014	Fownes Head	20	956	901	12.5	11.8	.1305	8000	35.1	**193 ± 20**	110	13.24	0.25
FT-019	Malpeque Bay Sill-1	28	1238	1101	12.3	10.0	.9989	8000	35.1	**223 ± 21**	113	12.59	0.23
FT-021	Malpeque	28	1438	1058	13.1	9.60	.9079	8000	35.1	**247 ± 22**	126	12.94	0.23
FT-045	Rainy Cove	27	2299	1746	24.6	18.2	.1303	8000	35.1	**239 ± 18**	136	12.81	0.24
FT-046	Partridge Island	27	1549	1345	18.5	16.1	.1740	8000	35.1	**210 ± 18**	124	13.06	0.26

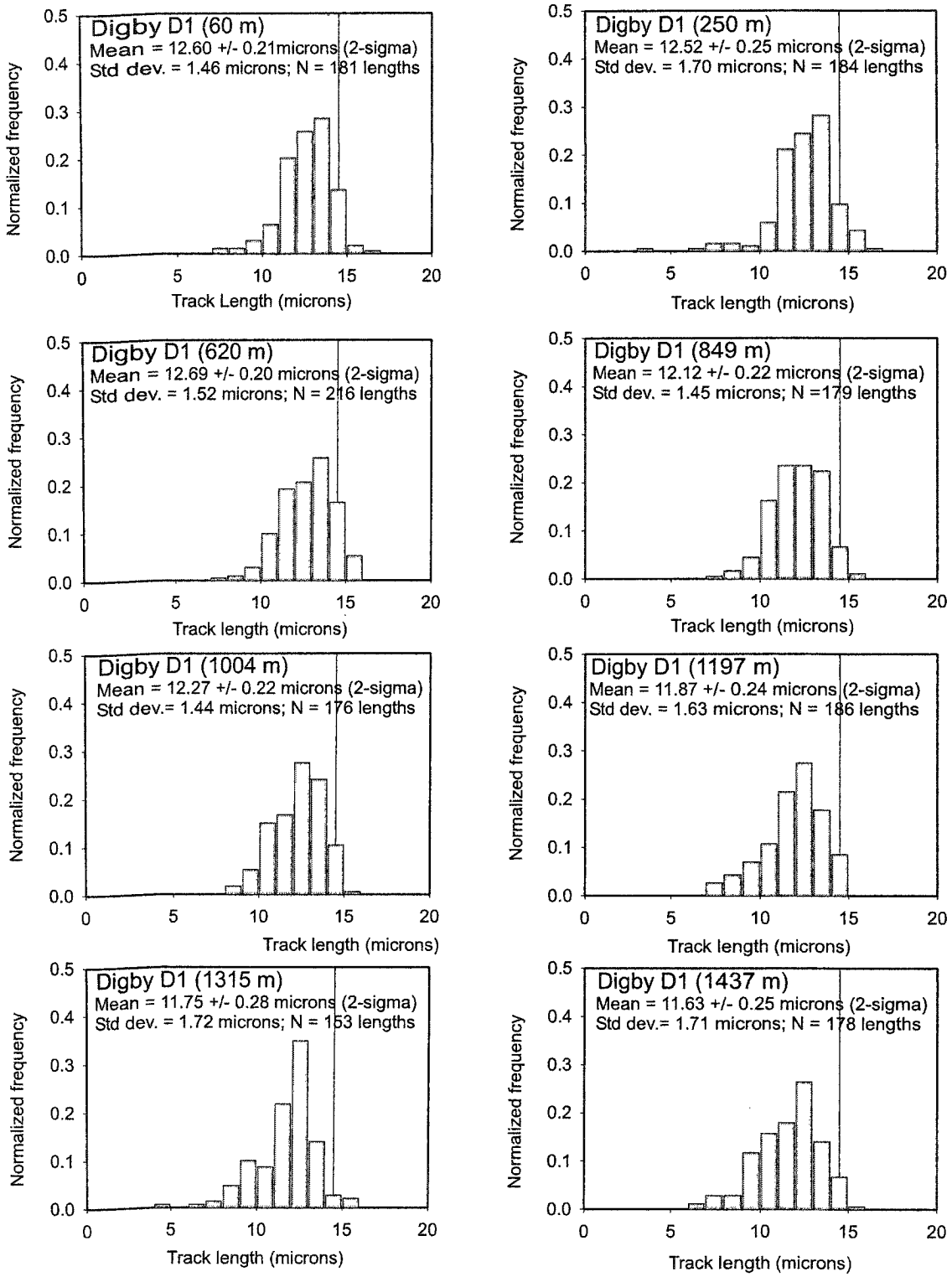

Figure 3.4. Confined TL histograms and statistics for the Digby D-1 drillhole. A reference line at 14.5 μm is shown on each histogram for comparative purposes.

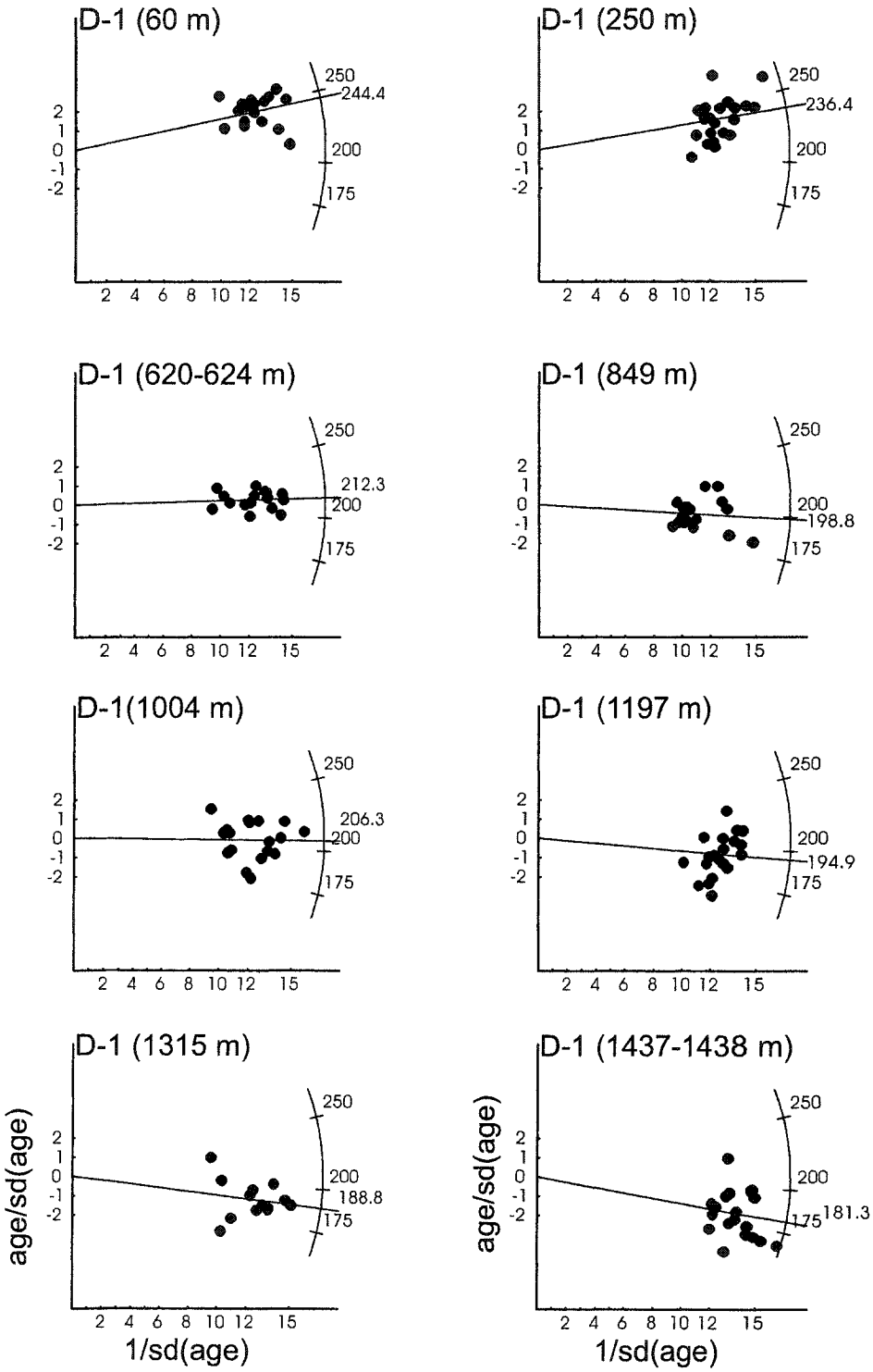

Figure 3.5. Radial plots of the FT age data from the Digby D-1 drillhole.

The length distributions in Fig. 3.4 are different from those that result from various styles of simple cooling (i.e., Gleadow and Brown 2000), which produces a length distribution with a principal peak centred at 14-15 μm (indicated in Fig. 3.4) and varying amounts of skewness and kurtosis. In contrast, the D-1 data display distributions with broad peaks centred between 11 and 13.5 μm and a distinct lack of tracks >15 μm, implying relatively recent annealing. The relative lack of abundant long tracks (especially in the near surface samples) is similar to the Arne et al. (1990) observations from the Gays River samples and precludes the hypothesis that the present surface has evolved as a result of simple cooling over the past 200 Ma.

3.6.2 Permian-Triassic (PT) outcrop samples

The FT data from the outcrop samples are presented in Table 3.2. Summary TL histograms and radial plots of eight of these samples are shown in Figs. 3.6 and 3.7. Grain morphologies and track etch pit characteristics indicate some samples contain a range of compositions while others are relatively homogenous. Apatite FT ages are Triassic, though individual grain ages within some samples range from mid-Paleozoic to Lower Cretaceous. Spontaneous track densities are also high, therefore some significance can be attributed to the old and young individual grain ages. The Late Jurassic and Early Cretaceous grain ages indicate enough post-Triassic heating to partially anneal the fission tracks in these grains. In contrast, mid-Paleozoic grain ages imply that post-Triassic heating was insufficient to completely anneal the fission tracks in all grains. Samples with mixed individual grain ages (i.e., the FT-012 Quaco Head sample) probably have a significant range in apatite compositions resulting in variable annealing response (see the next section).

Mean track lengths range from 12.4 to 13.6 μm, and confined length histograms are typically moderately peaked. There is a lack of tracks >15 μm similar to that seen in the Digby data, implying that some of the annealing is relatively recent. However, with the exception of the samples collected near the Malpeque Bay Sill (FT-019 and FT-020) the histograms do not indicate as high a degree of annealing as do the Digby data.

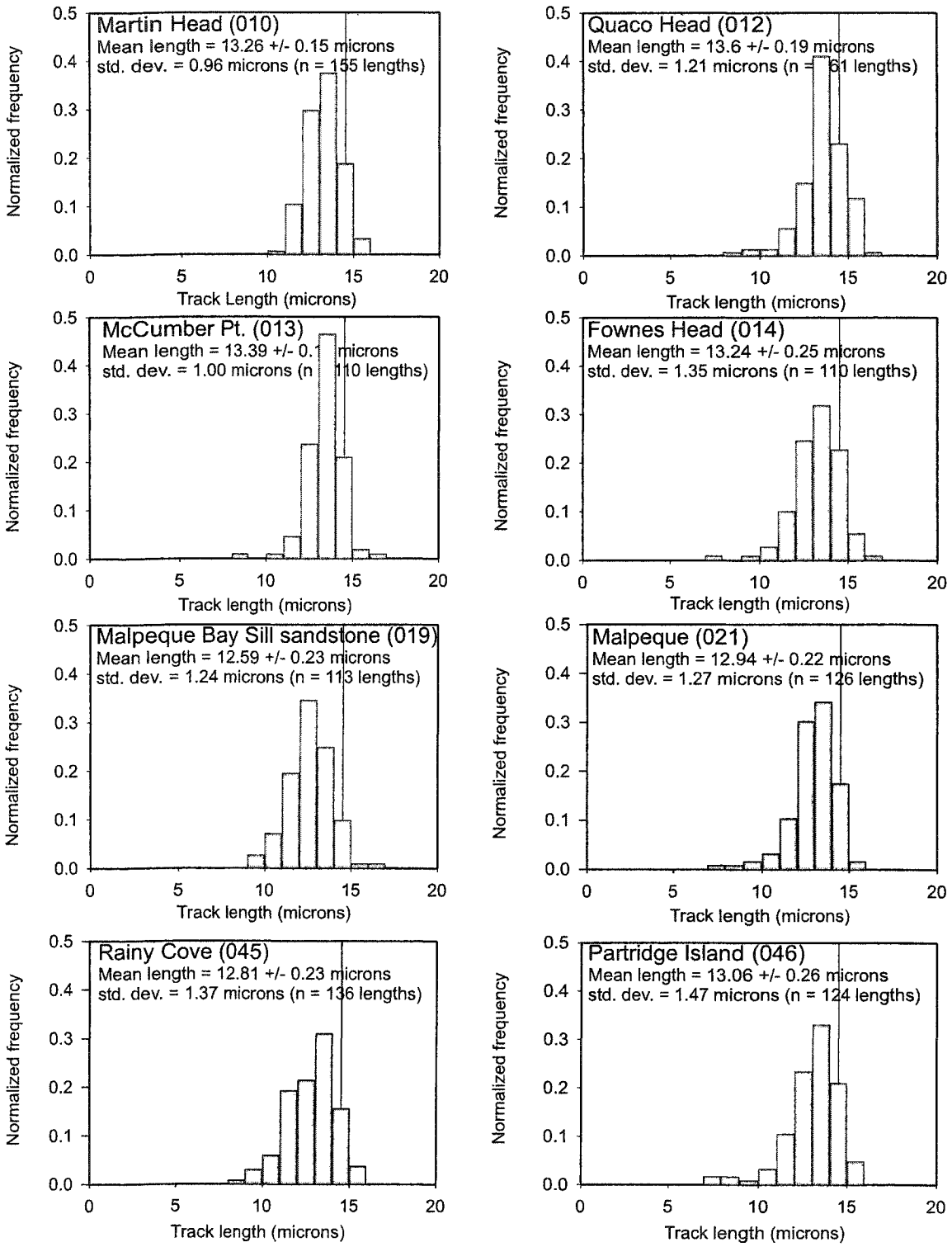

Figure 3.6. Confined TL histograms and statistics for eight PT outcrop samples (one sample each from Quaco Head and the Malpeque Bay sandstone are omitted). A reference line at 14.5 μm is shown on each histogram for comparative purposes.

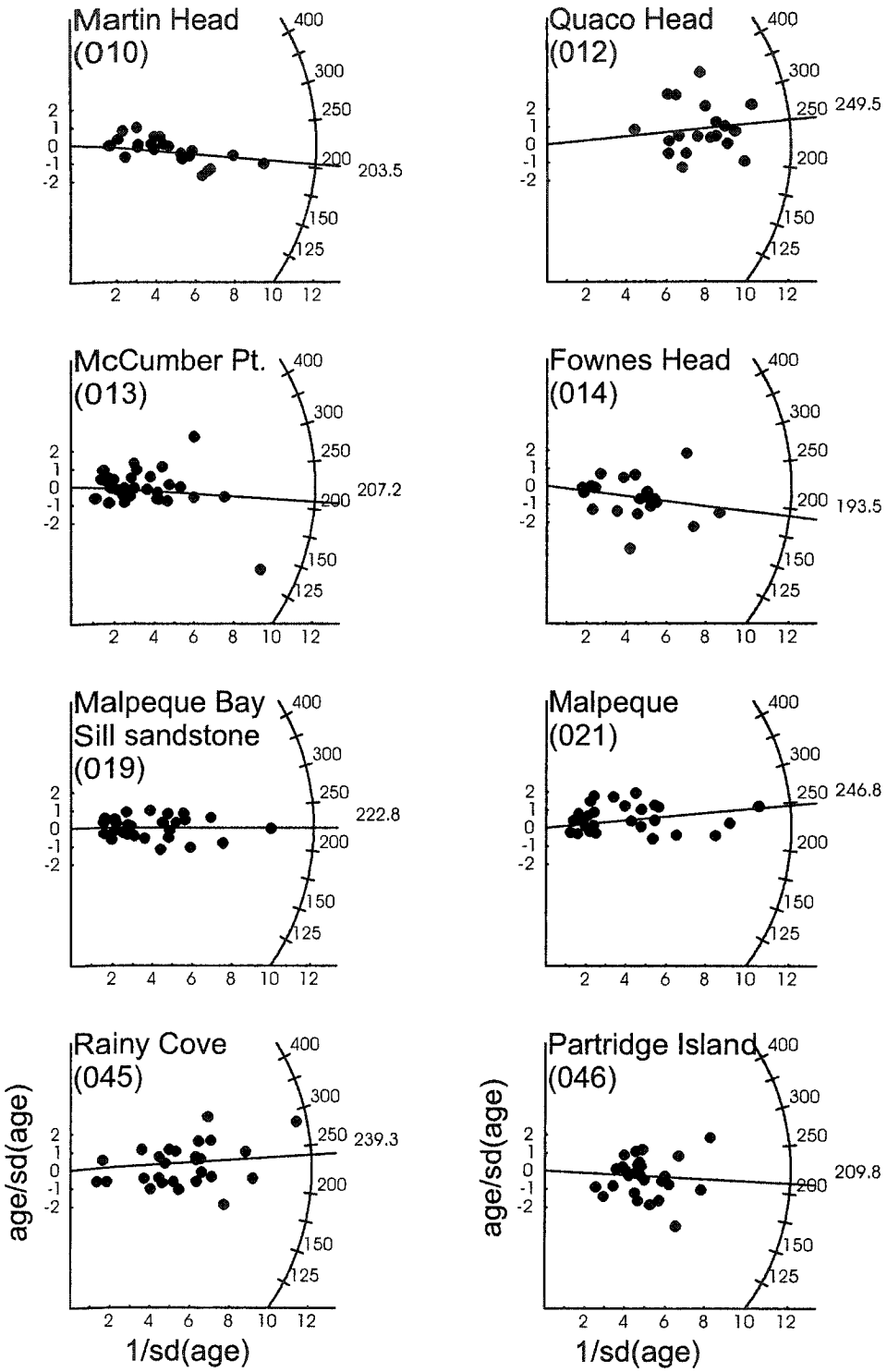

Figure 3.7. Radial plots of the FT age data for the eight outcrop samples shown in Fig. 3.6.

3.7 Apatite FT thermal history modelling

The range of temperatures over which fission tracks are shortened but not totally annealed, resulting in a reduction of the fission track age and a broadening of the TL distribution, is called the partial annealing zone (PAZ). Green et al. (1986) characterized the annealing behaviour of fission tracks in apatite within the PAZ by measuring TL distributions in samples heated from 20 minutes to 500 days at temperatures between 95 and 400 °C. Apatite FT annealing models have been developed based on empirical extrapolations of the Green et al. annealing data to geologic time. The most widely used is the Laslett et al. (1987) fanning-Arrhenius model, which has been incorporated into a number of modelling software packages developed using Monte Carlo type search techniques to evolve thermal history simulations to predict apatite FT age and length distributions (e.g. Gallagher 1995; Willett 1997).

Although it is widely accepted that observed variable annealing behaviour of fission tracks in apatite as a function of temperature is an effect of composition, controversy remains within the fission track community about whether chlorine content is the only significant influence as suggested by Green et al. (1985), Green (1996), and others, or whether the annealing rate is a more complex function of composition (e.g. Carlson et al. 1999). Notwithstanding, only the Laslett et al. (1987) annealing model based on the Durango apatite standard (an F-rich apatite with 0.4 wt% Cl) is widely accepted and, according to Green (1996) it is the only published model that should be used to interpret data.

A database of 55 SMB apatite analyses done at Dalhousie University using a JEOL 733 Superprobe indicates it is a near end-member fluorapatite. Fluorine ranged from 1.60 to 3.67 wt% (average = 2.36 wt.%). Chlorine is mostly below the detection limit (average 0.07 wt.%). The Digby area SMB samples may reasonably be modelled based on the Durango (fluorapatite) annealing model; however, because Cl content of SMB apatites is less than Durango, temperatures predicted by the model may overestimate actual temperatures by a few degrees. Compositional analyses of the PT outcrop samples have not been done, but analyses of similar apatites from the Sydney Basin area of the Maritimes Basin demonstrate that they do not have chlorine-rich compositions (Gibling et al. 2002).

Thermal history modelling was done using the FORTRAN program AFTINV (Willett 1997) modified to run on a personal computer (Issler 1996) which produces synthetic FT age and TL data as follows. Component sets of unannealed (i.e., 16.15 μm) fission tracks are introduced at discrete (user input) time intervals. Lengths are annealed in response to subsequent temperatures as the thermal history evolves, resulting in an integrated TL distribution and an apparent age. Predicted TL distributions and ages are compared to the measured data using a goodness-of-fit statistic. A solution set of the best-fitting histories is maintained as the algorithm repeats iteratively until all solutions in the set fit the data to the desired confidence level (in this instance 95%). User-input constraints on heating, cooling, and rate bounds based on independent geological data help limit the search space to geologically reasonable solutions.

For the models presented here 10 My time-steps were used and populations of tracks were introduced at 5 My intervals. An initial reduction in mean length to 15.5 μm was also introduced to minimize the effects of observed underprediction of low-temperature annealing seen in the Laslett et al. (1987) model (e.g. Vrolijk et al. 1992).

3.7.1 Digby D-1 model input parameters

Apatite FT modelling of the Digby D-1 data follows a modified form of the approach by Arne et al. (1990). The oldest model times used were 350 Ma to reflect erosional uplift and cooling following emplacement of the SMB. Vitrinite reflectance levels in overlying Horton Group strata (ca. 340 Ma) reached sufficiently high levels to indicate complete annealing of apatite fission tracks during a thermal maximum associated with regional burial of the northern Appalachians at ca. 300 Ma (Bradley 1982).

In contrast to the Arne et al. (1990) model, which indicates continuous regional cooling from 300 Ma until Aptian/Albian time, we suggest the regional Triassic unconformity indicates that exhumation and cooling ceased during Early Triassic time. The stratigraphy indicates heating in Middle to Late Triassic time in the Fundy Basin region (stratigraphically above the Digby D-1 drillhole). The age of the base of the Wolfville Formation (the oldest unit above the unconformity) is ca. 240 Ma, and this sits directly on Pennsylvanian to Early

Permian strata (Wade et al. 1996). Regional heating likely culminated with the extrusion of the North Mountain Formation basalts during Hettangian time (Early Jurassic, ca. 200 Ma). For our model, therefore, Triassic heating was inferred from 240 to 200 Ma.

Between 200 and 30 Ma, two different thermal models were attempted. In the first, cooling-only histories were assumed (i.e., the peneplanation model). For the second model cooling was required to 120 Ma to allow for Aptian sedimentation. Although the Upper Cretaceous deposits present at Gays River and elsewhere in Nova Scotia (e.g. Fig. 3.1) are not regionally extensive, they are likely erosional remnants and thus imply that at least locally, near-surface temperatures prevailed at that time. From 100 to 30 Ma, one heat pulse was allowed.

Development of the Antarctic ice sheet in Late Eocene to Early Oligocene time dramatically cooled regional climates and decreased global eustatic sea levels. During Eocene to Miocene time sediment fluxes into the north and middle Atlantic continental margin increased dramatically (e.g. Poag and Sevon 1989; Roden 1991; Poag 1992), resulting in a change from carbonate to siliciclastic deposition in the continental shelf and slope in the western North Atlantic region (e.g. Miller et al. 1998). These offshore changes were accompanied by relative uplift and cooling of sediment source areas. Therefore, the model was required to find cooling-only solutions from 30 Ma to the present. Present-day temperatures of 10°-30 °C (for the 60.7 m sample) to 25°-50 °C (for the 1437 m sample) were specified.

3.7.2 PT outcrop sample model input parameters

Although modelling was attempted for all samples from this group, obvious compositional heterogeneity in some limits their usefulness. Only samples that appeared to be dominated by a single composition (based on grain morphology and etch pit characteristics) and whose radial plots and chi-square (χ^2) values suggest a single age population are included here.

The Martin Head, McCumber Point, Rainy Cove, and Partridge Island samples were all modelled with the same heating and cooling constraints because of their similar

stratigraphic positions. The oldest model time used was 300 Ma. A depositional age of 240 Ma (Anisian) was used. The model was constrained to find cooling-only solutions prior to deposition, and heating-only solutions, to reflect regional heating during Middle Triassic to Late Triassic - Early Jurassic time, to 200 Ma. From 200 Ma to the present the heating and cooling constraints were the same as those used for the Digby D-1 samples. Present-day surface temperatures of 10°-25 °C were specified.

3.7.3 FT model results

Figures 3.8-3.10 summarize the time-Temperature (t-T) models. Each panel in Figs. 3.8-3.10 shows the exponential mean t-T history and the upper and lower bounding solution envelopes. The solution envelopes indicate the total range temperatures explored at each time-step by the 250 successful model solutions; however, they are not themselves solutions. The mean t-T history is the exponential mean of all 250 solutions at each temperature step.

Fig. 3.8 shows typical cooling-only models for surface and near-surface samples. Although most of the cooling-only models converged successfully, the resulting t-T histories are incompatible with the regional geology. As mentioned above, the presence of scattered Aptian/Albian-aged deposits implies that near-surface temperatures prevailed, at least locally, at that time. The cooling-only models shown in Fig. 3.8, however, require temperatures of approximately 50-60 °C between 120 and 100 Ma, indicating burial beneath ca. 2 km of Triassic-Jurassic strata. These models demonstrate that long-term peneplanation is inconsistent with the geology.

Figures 3.9 and 3.10 show the one-heat-pulse models, which also converged successfully. Despite the differences between our model constraints and those of Arne et al. (1990), predicted t-T histories during Late Cretaceous to Early Tertiary time are similar. Though not explicitly required by the input constraints, our models also suggest significant post-Aptian heating. This result was expected owing to the relative lack of abundant long tracks that would have accumulated if the samples had remained at the surface for the last 120 my. Predicted time of peak post-Aptian temperatures is approximately 60 Ma for most samples. The models also all predict significant post-Paleocene cooling (about 25-30 °C).

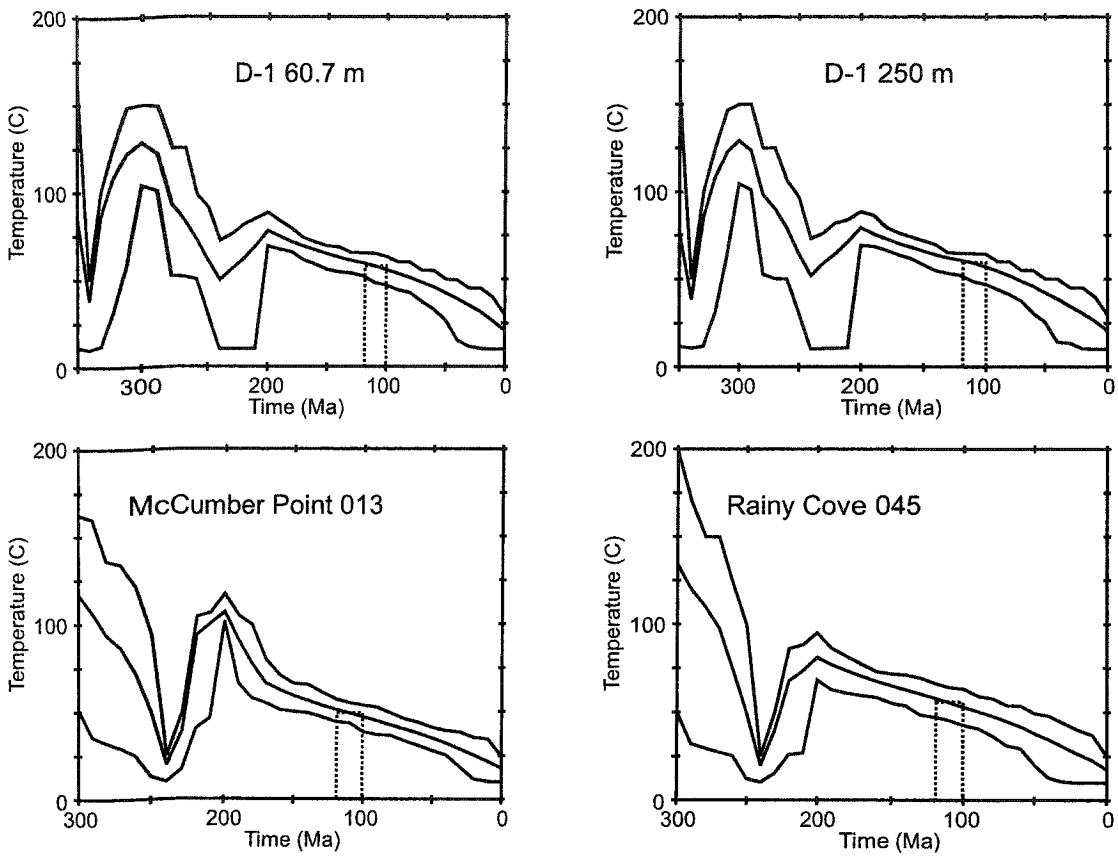

Figure 3.8. Cooling-only t-T models for 2 Digby D-1 well samples (60.7 m and 250 m) and 2 PT outcrop samples (McCumber Point and Rainy Cove). Each panel shows the exponential mean t-T history and the upper and lower bounding solution envelopes. The envelopes indicate the range of acceptable temperatures at each time-step for all 250 t-T paths in the solution set, but they are not themselves solutions. The mean t-T path is the locus of points defined by the exponential mean of all 250 t-T paths at each time-step. These models predict temperatures of ca. 50-60 °C during Aptian/Albian time (dotted lines) and are therefore incompatible with the regional geology.

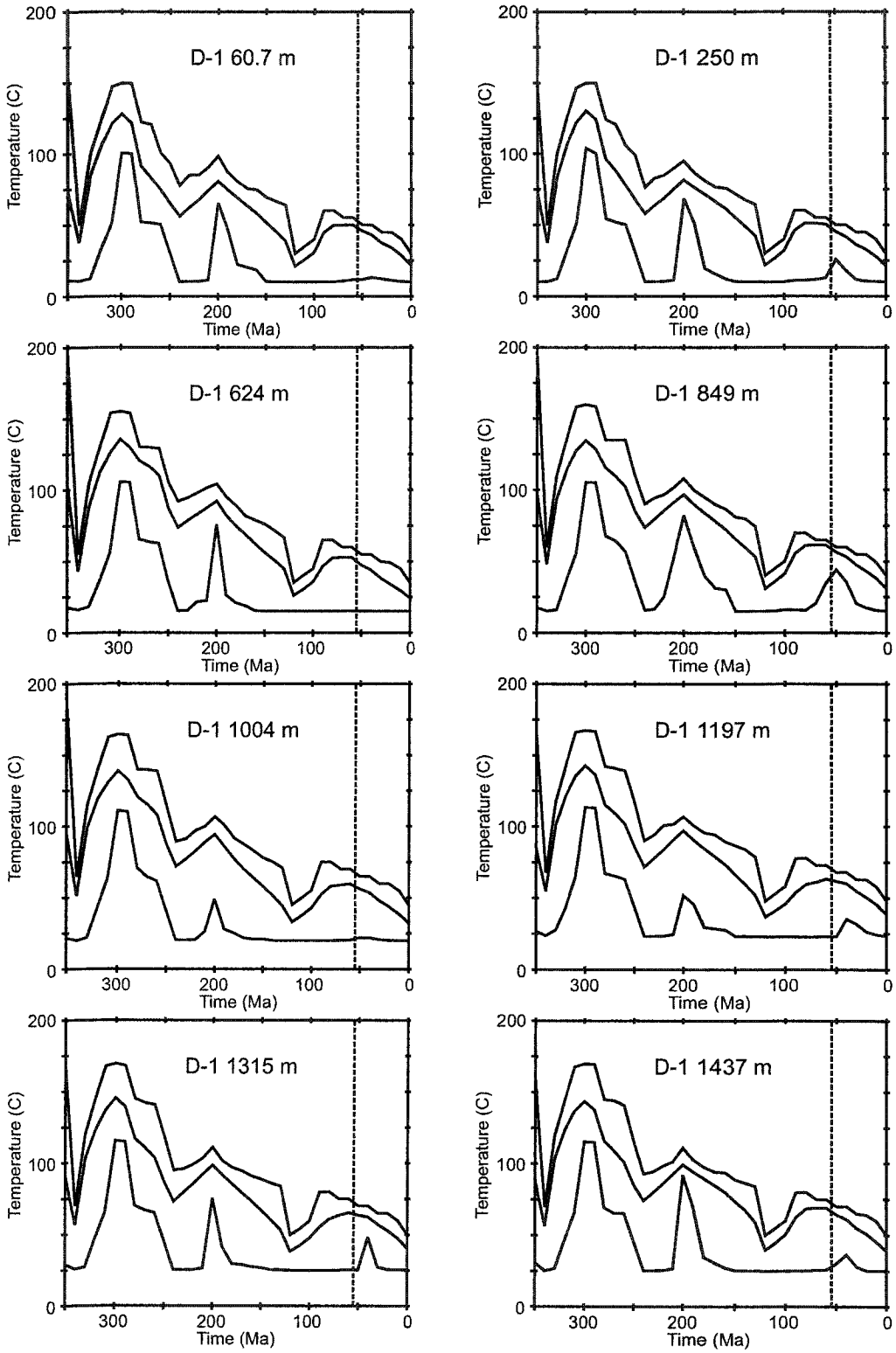

Figure 3.9. One heat pulse t-T models for the Digby D-1 drillhole samples between 60.7 m and 1437 m (see Fig. 3.8 caption for details). The dashed reference lines at 55 Ma indicate the end of the Paleocene Epoch.

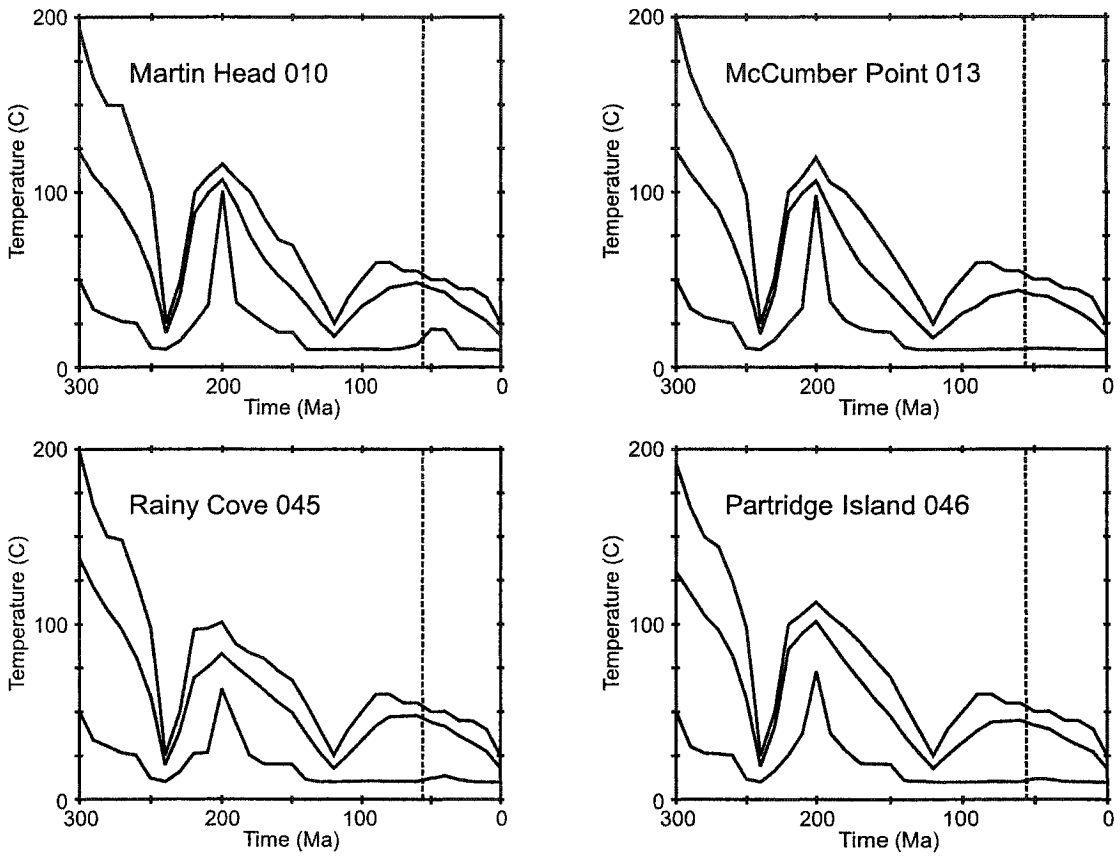

Figure 3.10. One heat pulse models obtained for the Martin Head (upper left), McCumber Point (upper right), Rainy Cove (lower left), and Partridge Island (lower right), Triassic red bed samples (see Fig. 3.8 and 3.9 captions for details).

Paleogeothermal gradients can be estimated by comparing the mean t-T paths for the samples from the Digby D-1 well (Fig. 3.11). Figure 3.11 also shows geothermal gradients (°C/km) estimated for the 5 sample pairs having >1 km difference in depth (i.e., 1437 m and 60.7 m; 1437 m and 250 m, etc.). Gradients of ca. 15 °C/km are indicated since 250 Ma; however, gradients appear to decrease slightly from 150 to 75 Ma. There is, however, also increased scatter in the estimates and a corresponding crossing of temperature paths in the upper panel, likely indicating that the annealing characteristics of the samples differ slightly. Although the model results lack the necessary accuracy to calculate gradients at all model times, there is also no suggestion of unusually high gradients. There is close agreement between FT model-based predictions for the present-day geothermal gradient of 13-18 °C/km (Fig. 3.11) and the measured gradient of 16-18 °C/km determined from borehole logs (Elliott et al. 1977).

3.8 Discussion and geological interpretation of model results

The FT thermal history models in Figs. 3.9 and 3.10 indicate as much as 30 °C of post-Paleocene cooling. This cooling can be interpreted in terms of decreased eustatic sea level and changes in mean annual surface temperatures (T_s) during this time. Figure 3.12 shows the long-term Mesozoic and Cenozoic eustatic sea level curve of Haq et al. (1987). The Haq et al. (1987) curve assumes an ice-free world, hence present-day long-term eustatic sea level is approximately 50 m and not 0 m. Development of the Antarctic ice sheet has contributed an additional 50 m decrease in eustatic sea level. Mesozoic-Cenozoic sea levels are inferred to have been highest from 100 to 35 Ma, representing >100 m increase from Early Cretaceous levels, and as much as 250 m above present day. Large portions of the margin were submerged, resulting in observed and inferred sediment deposition and burial heating in both onshore and offshore regions (e.g. Bond 1976). The Cenozoic eustatic sea level curve of Miller et al. (1998) for the New Jersey coastal plain and continental shelf is similar in shape to the Haq et al. (1987) curve, but their estimated long-term decrease since Early Cenozoic time is somewhat less (150-200 m since 65 Ma).

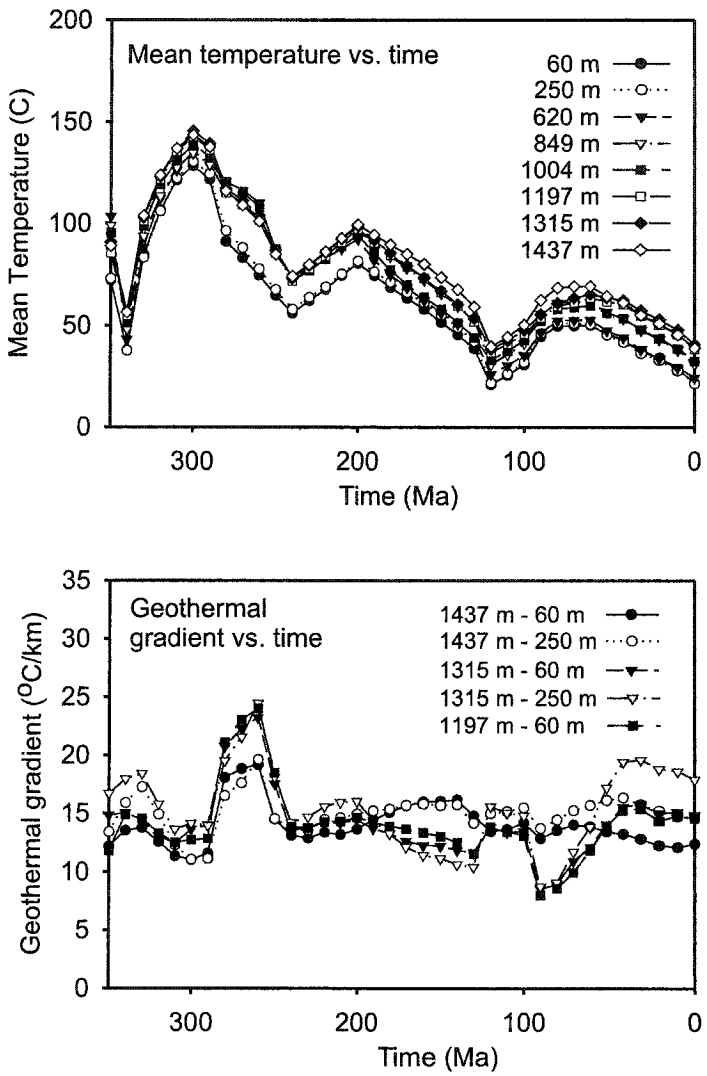

Figure 3.11. Exponential mean t-T paths (top) for 8 samples from the Digby D-1 well, and geothermal gradients (bottom) for the 5 sample pairs having >1 km difference in depth (i.e., 1437 m and 60.7 m; 1437 m and 250 m etc.).

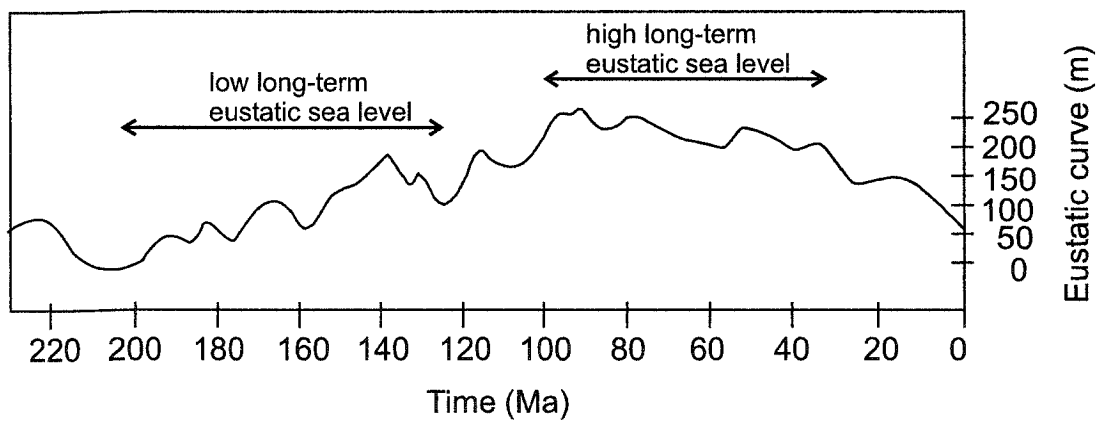

Figure 3.12. Long-term eustatic Mesozoic and Cenozoic sea level curve (from Haq et al. 1987). Long-term eustatic sea level increased throughout much of the Mesozoic. The highest long-term eustatic sea levels, ca. 250 m higher than present day and about 100 m higher than the Valanginian-Barremian eustatic sea level, occurred between Late Cretaceous and Eocene time (100-35 Ma). Note that Haq et al. (1987) assume an ice-free world, and hence present-day long-term eustatic sea level is ca. 50 m rather than 0 m.

As a result of the subsequent decrease in eustatic sea level, the depositional surface rebounded isostatically and much of this sediment was exhumed and eroded. Assuming a purely isostatic response to unloading, the maximum thickness of sediment that can be exhumed and eroded as a result of uplift can be calculated approximately as follows;

$$\Delta t_s = \Delta sl\left(\frac{\rho_s}{\rho_m - \rho_s}\right) \qquad 3.1$$

(e.g. Einsele; 2000) where Δt_s is the sediment thickness eroded; Δsl is the change in sea level; and ρ_m and ρ_s are the mantle and sediment densities (~3.3 and 2.4 g/cm^3, respectively). Equation 3.1 assumes that the sediment surface is initially at sea level. From Equation 3.1, a 250 m decrease in eustatic sea level would produce erosion of 667 m of sediment for samples currently at sea level. Assuming a geothermal gradient of 20°/km, the amount of cooling that would result from decreased eustatic sea levels is about 13°.

Geological evidence and variations in global isotopic and faunal distributions with time reveal that paleo-T_s has also varied substantially (e.g. Frakes 1979; Barrera and Johnson 1999). Frakes et al. (1992) proposed a scheme for dividing Phanerozoic time into a series of warm and cool modes. According to Frakes et al.(1992), cool modes occurred from Middle Jurassic to Early Cretaceous time (ca. 183-105 Ma), and from Early Eocene to the present (ca. 55-0 Ma). During Early Cretaceous to Early Eocene time (ca. 105-55 Ma), however, Earth was in a warm mode.

Figure 3.13 shows paleo-T_s as a function of latitude obtained from palaeoclimatology models for Campanian time and the present (from DeConto et al. 1999) as well as the range of model predictions of T_s for the Cretaceous (from Barron 1983). Globally averaged T_s in the Late Cretaceous was thought to be about 6 °C higher than at present. As shown in Fig. 3.13, it was also a time of more equable temperatures (e.g. Barron 1983; Valdes et al. 1996), and thus effects of changing T_s were more pronounced at moderate to high latitudes (e.g. Nova Scotia) than in equatorial regions. Horizontal lines on the Fig. 3.13 indicate that the

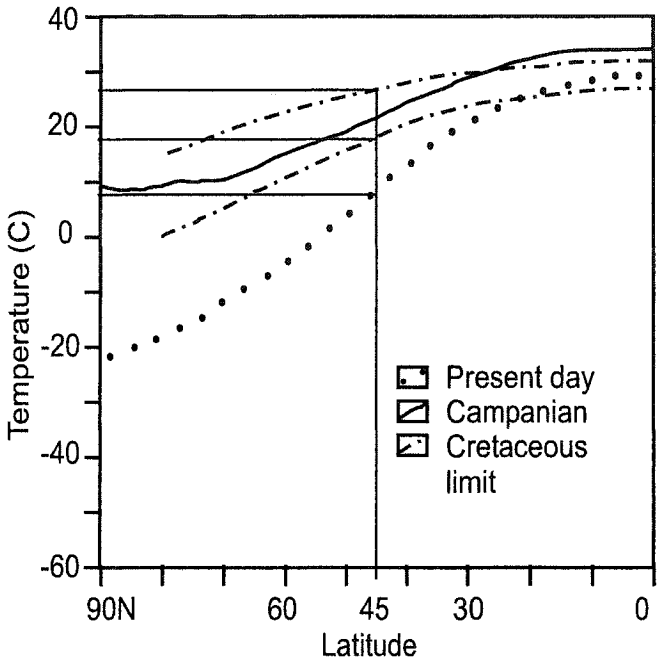

Figure 3.13. Zonally averaged mean annual surface temperature as a function of latitude for Campanian time and the present day (modified from DeConto et al. 1999), as well as minimum and maximum estimates for the Cretaceous (modified from Barron 1983). The horizontal lines indicate a range of ca. 10-20 °C decrease in estimated mean annual T_s from Cretaceous time to the present at 45°N latitude.

decrease in T_s at latitude 45°N between Cretaceous time and the present is approximately 10-20 °C. Karstification and deep lateritic weathering of Late Aptian and younger age documented in Atlantic Canada (Davies et al. 1984) provide supporting evidence for periods of significantly increased T_s in this region.

Long-term decreased T_s can produce a comparable amount of cooling at depth. Heat-flow calculations and case histories show that a change in T_s acting over 1-10 My can penetrate kilometres deep into the crust (Beck 1977; O'Sullivan and Brown 1998). Figure 3.14 shows this effect for a decrease in T_s of 20 °C.

From Figs. 3.13 and 3.14 we can see that at a depth of 2-3 km (i.e., approximately the depth of the deepest Digby samples under 667 m of additional sediment), a decrease in T_s of 10-20 °C would cause an 8-17 °C decrease within 5 My (Fig. 3.14). Combining this 8-17 °C decrease with 13 °C of cooling on exhumation gives a total post-Paleocene cooling of 21-30 °C, a amount similar to that predicted by the FT models.

The interpretation of the FT models in terms of the combined effects of changes in eustatic sea level and the propagation to depth of changes in paleo-surface temperatures may also explain the model-predicted temperature increase between Aptian and Paleocene time. From Fig. 3.12 it is also apparent that from 200 to 100 Ma, eustatic sea level increased substantially. Additionally, there was an increase in T_s between about 120 and 100 Ma to about 55 Ma, corresponding to the transition from the Middle Jurassic to Early Cretaceous cool mode to the Late Cretaceous to Early Eocene warm mode (e.g. Frakes and Francis 1988; Frakes et al. 1992; Barker 2000). The increased temperatures that would have resulted from the combined effects of burial heating related to increased eustatic sea level, and the propagation to depth of higher paleo-T_s, would likely have been sufficient to produce some annealing of existing tracks in the apatite grains.

There is also some geological evidence to suggest increased temperatures during Late Cretaceous time. Hacquebard (1984) estimated that 770 m of sediment must have covered Nova Scotia based on vitrinite reflectance levels in Cretaceous lignites at Dickey Brook and Diogenes Brook (Fig. 3.1), and Davies et al. (1984) observed similar maturation levels for Cretaceous lignite at Gays River. In the Fundy Basin, Cretaceous-aged and younger deposits

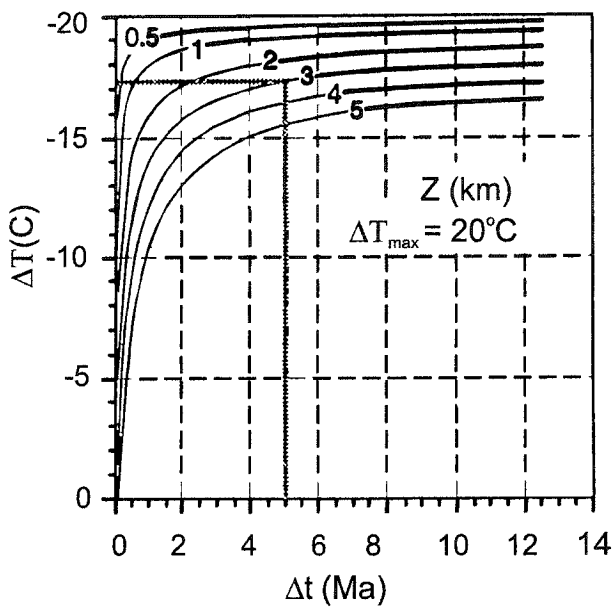

Figure 3.14. Temperature change as a function of time for depths of 0.5 to 5 km that would result from an instantaneous change in surface temperature of -20 °C. The plot shows that this results in a -17 °C change at a depth of 3 km after 5 My (from O'Sullivan and Brown 1996).

are absent, yet vitrinite reflectance values for Jurassic strata above the lavas are close to 1% R_o (Wade et al. 1996), implying either high paleogeothermal gradients or substantial post-Jurassic burial for which there are no extant strata. Wade et al. (1996) inferred from seismic data that ca. 2 km of erosion of the youngest (Jurassic) sediments overlying the North Mountain basalt has occurred, although the time of erosion is unclear.

The fact that near-surface rocks have experienced as much as 30 °C of post-Paleocene cooling has implications for petroleum systems in the region. Our FT models imply that generation of oil and gas from post-Triassic-Jurassic rocks in the Fundy Basin, or from suitably buried older rocks, could have occurred as late as the Paleocene. The depositional sites of the clastic rocks (potential reservoirs) eroded since the Cretaceous probably reflect the exhumation history of the on-land areas of Atlantic Canada, and a record of that erosional phase may be found in the Cenozoic stratigraphic record offshore.

3.9 Conclusions

1) Apatite FT thermal models demonstrate that elevated temperatures during Jurassic time and Late Cretaceous - Early Tertiary time in the southern Canadian Atlantic region were significant and widespread. FT models predict ca. 25-30 °C of post-Paleocene cooling. Interpretation of model results within a regional geological context demonstrates that the traditional view of passive peneplanation and slow exhumation of the Nova Scotia margin since the Jurassic is not tenable.
2) The model predictions can be explained by the combined effects of decreased eustatic sea levels resulting in the erosion of approximately 700 m of sediments, causing 13 °C of exhumational cooling, and the propagation to depth of 10-20 °C decrease in paleo-mean annual surface temperatures.
3) Elevated vitrinite reflectance levels in Cretaceous lignites, and in Jurassic strata in the Fundy Basin of Nova Scotia, offer support for the interpretation of the FT models in terms of the combined effects of limited burial heating and exhumational cooling related to changes in eustatic sea level and the propagation to depth of changes in pale-surface temperatures.

3.10 Acknowledgements

We are thankful to many people for assistance with this research. In particular, to Dave Brown for discussions on Fundy Basin stratigraphy and for supplying several outcrop samples; to Chris Beaumont, who insisted we consider the apatite FT models in terms of eustatic sea level and climate variations; and to Dennis Arne for promoting further discussion on the post-Aptian heating observed at Gays River. A.K. Chatterjee supplied the Digby samples. Ralph Stea enlightened us about onshore Cretaceous geology of Nova Scotia. Thanks to Ann Blythe, Richard Ketcham, and Larry Heaman for providing critical reviews of this manuscript, and also to Mike Steckler, Dennis Arne, Paul Green, and Ian Duddy, who reviewed previous versions. Mai Nguyen helped draft some of the figures. Funds to support this work were supplied by the Dalhousie Fission Track Laboratory and a Natural Sciences Engineering Research Council Research Grant to M. Zentilli (A-9036).

3.11 References cited

Akande, S.O. and Zentilli, M. 1983. Genesis of the lead-zinc mineralization at Gays River, Nova Scotia, Canada. In International Conference on Mississippi Valley Type Lead-Zinc Deposits, Proceedings Volume. Edited by G. Kisvarsanyi, S.K. Grant, W.P. Pratt, and J.W. Koenig. University of Missouri, Rolla, Missouri, pp. 546-557.

Arne, D.C., Duddy, I.R., and Sangster, D.F. 1990. Thermochronologic constraints on ore formation at the Gays River Pb-Zn deposit, Nova Scotia, Canada, from apatite fission track analysis. Canadian Journal of Earth Sciences, **27**: 1013-1022.

Barker, C.E. 2000. A paleolatitude approach to assessing surface temperature history for use in burial heating models. International Journal of Coal Geology, **43**, 1-4: 121-135.

Barrera, E., and Johnson, C.C. (Editors) 1999. Evolution of the Cretaceous ocean-climate system. Geological Society of America Special Paper 332.

Barron, E.J. 1983. A warm, equable Cretaceous: The nature of the problem. Earth Science Reviews, **19**: 305-338.

Beck, A.E. 1977. Climatically perturbed temperature gradients and their effect on regional and continental heat-flow means. Tectonophysics, **41**: 17-39.

Bond, G. 1976. Evidence for continental subsidence in North America during the Late Cretaceous global submergence. Geology, **4**: 557-560.

Bradley, D.C. 1982. Subsidence in Late Paleozoic basins in the northern Appalachians. Tectonics, **1**, 1: 107-123.

Brown, R.W., Gallagher, K., and Duane, M.J. 1994. A quantitative assessment of the effects of magmatism on the thermal history of the Karoo sedimentary sequence. African Journal of Earth Sciences, **18**: 227-243.

Carlson, W.D., Donelick. R.A., and Ketcham, R.A. 1999. Variability of apatite fission-track annealing kinetics: 1. Experimental results. American Mineralogist, **84**: 1213-1223.

Chatterjee, A.K. and Dostal, J. 2002. Deep drill hole in the Devonian South Mountain Batholith, Nova Scotia: a potential for hidden mineral deposits within the batholith. Atlantic Geology, **38**, 1-10.

Clarke, D.B., MacDonald, M.A., Reynolds, P.H., and Longstaffe, F.J. 1993. Leucogranites from the eastern part of the South Mountain Batholith, Nova Scotia. Journal of Petrology, **34**: 653-679.

Davies, E.H., Akande, S.O., and Zentilli, M. 1984. Early Cretaceous deposits in the Gays River Lead-zinc mine, Nova Scotia: evidence from $^{40}Ar/^{39}Ar$ mineral ages. In Current Research, part A. Geological Survey of Canada, Paper 84-1A, pp. 353-358.

Davis, W.M. 1922. Peneplains and the geographic cycle. Geological Society of America Bulletin, **33.3**: 587-598.

DeConto, R.M., Hay, W.W., Thompson, S.L., and Bergengren, J. 1999. Late Cretaceous climate and vegetation interactions; cold continental interior paradox. In Evolution of the Cretaceous ocean-climate system. Edited by E. Berrara and C. Johnson. Geological Society of America Special Paper 332, pp. 391-406.

Einsele, G. 2000. Sedimentary basins: Evolution, facies, and sediment budget. 2nd ed. Springer, New York.

Elliott, B.E., Bernius, G.R., and Killean, P.G. 1997. Borehole geophysical logs South Mountain Batholith at Digby and the Wedgeport granite Nova Scotia. Geological Survey of Canada, Open File Report, 3352.

Fleischer, R.L., Price, P.B., and Walker, R.M., 1964. Fission track ages of zircons. Journal of Geophysical Research, **69**: 4885.

Fleischer, R.L., Price, P.B., and Walker, R.M. 1975. Nuclear Tracks in Solids: Principles and Applications. University of California Press, Berkeley, California.

Frakes, L.A. 1979. Climates throughout geologic time. Elsevier, Amsterdam.

Frakes, L.A., and Francis, J.E. 1988. A guide to Phanerozoic cold polar climates from high-latitude ice-rafting in the Cretaceous. Nature, **333**, 9: 547-549.

Frakes, L.A., Francis, J.E., and Syktus, J.I. 1992. Climate modes of the Phanerozoic; the history of the Earth's climate over the past 600 million years. Cambridge University Press, Cambridge.

Galbraith, R.F. 1990. The radial plot: graphical assessment of spread in ages. Nuclear Tracks and Radiation Measurements, **17**, 3: 207-214.

Galbraith, R.F., and Laslett, G.M. 1993. Statistical models for mixed fission track ages. Nuclear Tracks and Radiation Measurements, **21**: 459-470.

Gallagher, K. 1995. Evolving temperature histories from apatite fission-track data. Earth and Planetary Science Letters, **136**, 421-435.

Gallagher, K., and Brown, R.W. 1997. The onshore record of passive margin evolution. Journal of the Geological Society, London, **154**: 451-457.

Gallagher, K., Brown, R.W., and Johnson, C. 1998. Fission track analysis and its applications to geological problems. Annual Review of Planetary Science Letters. **26**: 519-572.

Gibling, M.R. 1995. Upper Paleozoic rocks, Nova Scotia. In Geology of the Appalachian-Caledonian Orogen in Canada and Greenland. Edited by H. Williams. Geological Survey of Canada, Geology of Canada, no. 6, pp. 493-523.

Gibling, M.R., Langenburg, W., Kalkrueth, W.D., Waldron, J.W.F., Courtney, R., Paul, J., and Grist, A.M. 2002. Deformation of Upper Carboniferous coal measures in the Sydney Basin: evidence for late Alleghanian tectonism in Atlantic Canada. Canadian Journal of Earth Sciences, **39**: 79-93.

Gleadow, A.J.W., and Brown, R.W. 2000. Fission-track thermochronology and the long-

term denudational response to tectonics. In Geomorphology and Global Tectonics. Edited by M.A. Summerfield. J. Wiley and Sons, New York, pp. 57-75.

Goldthwait, J.W. 1924. Physiography of Nova Scotia. Geological Survey of Canada, Memoir 140.

Green, P.F. 1996. The importance of compositional influence on fission track annealing in apatite. In International Workshop on Fission Track Dating. Gent, Belgium, 1996, Abstracts, p. 43.

Green, P.F., Duddy, I.R., Gleadow, A.J.W., Tingate, P.R., and Laslett, G.M. 1985. Fission-track annealing in apatite: Track length measurements and the form of the Arrhenius plot. Nuclear Tracks **10**: 323-328.

Green, P.F., Duddy, I.R., Gleadow, A.J.W., Tingate, P.R., and Laslett, G.M. 1986. Thermal annealing of fission tracks in apatite 1. A qualitative description: Chemical Geology, **59**: 237-253.

Greenough, J.D. 1995. Mesozoic rocks. In Geology of the Appalachian-Caledonian Orogen in Canada and Greenland. Edited by H.Williams. Geological Survey of Canada, Geology of Canada, no. 6, pp. 567-600.

Grist, A.M., Reynolds, P.H., Zentilli, M., and Beaumont, C. 1992. The Scotian Basin offshore Nova Scotia: thermal history and provenance of sandstones, from apatite fission track analysis 40Ar/39Ar data. Canadian Journal of Earth Sciences, **29**: 909-924.

Grist, A.M., Ryan, R.J., and Zentilli, M. 1995. The thermal evolution and timing of hydrocarbon generation in the Maritimes Basin of eastern Canada: evidence from apatite fission track data. Bulletin of Canadian Petroleum Geology, **43**, 2: 145-155.

Hacquebard, P.A. 1984. Composition, rank and depth of burial of two Nova Scotia lignite deposits. In Current Research, part A. Geological Survey of Canada, Paper 84-1A, pp. 11-15.

Hacquebard, P.A., and Donaldson, J.R. 1970. Coal metamorphism and hydrocarbon potential in the Upper Paleozoic of the Atlantic Provinces, Canada. Canadian Journal of Earth Sciences, **7**: 1139-1158.

Haq, B.U., Hardenbol, J., and Vail, P.R. 1987. Chronology of fluctuating sea levels since the Triassic. Science, **235**: 1156-1166.

Hayatsu, A. 1979. K-Ar isochron age of the North Mountain Basalt, Nova Scotia. Canadian Journal of Earth Sciences, **16**: 973-975.

Hodych, J.P., and Dunning, G.R. 1992. Did the Manicouagan impact crater trigger end-of-Triassic mass extinction? Geology, **20**: 51-54.

Hodych, J.P., and Hayatsu, A. 1988. Paleomagnetism and K-Ar isochron dates of Early Jurassic basaltic flows and dikes of Atlantic Canada. Canadian Journal of Earth Sciences, **25**: 1972-1988.

Hubert, J.F., and Mertz, K.A. 1984. Eolian sandstones in Upper Triassic-Lower Jurassic red beds of the Fundy Basin, Nova Scotia. Journal of Sedimentary Petrology, **54**: 798-810.

Hurford, A.J., and Green, P.F. 1982. A users' guide to fission track dating calibration. Earth and Planetary Science Letters, **59**: 343-354.

Hurford, A.J., and Green, P.F. 1983. The zeta age calibration of fission track dating. Chemical Geology (Isotope Geoscience Section), **1**: 285-317.

Issler, D.I. 1996. An inverse model for extracting thermal histories from apatite fission track data: Instructions and software for the Windows95 environment. Geological Survey of Canada, Open File Report, 2325.

Keen, M.J., and Williams, H. (Editors) 1990. Geology of the continental margin of eastern Canada. Geological Survey of Canada, Geology of Canada, no. 2.

Laslett, G.M., Green, P.F., Duddy, I.R., and Gleadow, A.J.W. 1987. Thermal annealing of fission tracks in apatite: 2. A quantitative analysis. Chemical Geology (Isotope Geoscience Section), **65**: 1-13.

Li, G., Ravenhurst, C.E., and Zentilli, M. 1995. Implications of apatite fission track analysis for the thermal history of the Scotian Basin, offshore Nova Scotia, Canada. Bulletin of Canadian Petroleum Geology, **43**: 127-144.

Lockhart, A.W. 1984. Sussex silica and aggregate; New Brunswick Department of Natural Resources and Energy, Assessment File No. 473023.

McHone, J.G., and Butler, J.R. 1984. Mesozoic igneous provinces of New England and the

opening of the North Atlantic Ocean. Geological Society of America Bulletin, **95**: 757-765.

McHone, J.G., Ross, M.E., and Greenough, J.D. 1987. Mesozoic dyke swarms of Eastern North America; In Mafic Dyke Swarms. Edited by H.C. Halls and W.F. Fahrig. Geological Association of Canada, Special Paper 34, pp. 279-288.

Miller, K.G., Mountain, G.S., Browning, J.V., Kominz, M., Sugarman, P.J., Christie-Blick, N., Katz, M.E., and Wright, J.D. 1998. Cenozoic global sea level, sequences, and the New Jersey transect: Results from coastal plain and continental slope drilling. Reviews of Geophysics, **36**, 4: 569-601.

Moore, R.G., Ferguson, S.A., Boehner, R.C., and Kennedy, C.M. 2000. Preliminary map of the Wolfville/Windsor Area, Kings and Hants Counties, Nova Scotia (21H/01 and Parts of 21A/16C and D). Scale 1:50,000.

Nadon, G.C., and Middleton, G.V. 1985. The stratigraphy and sedimentology of the Fundy Group (Triassic) of the St. Martins area, New Brunswick. Canadian Journal of Earth Sciences, **22**: 1183-1203.

Okulitch, A.V. 1999. Geologic time scale. Geological Society of Canada, Open File 3040 (National Earth Science Series, Geological Atlas) - Revised.

Olsen, P.E., Shubin, N.H., and Anders, M.H. 1987. New Early Jurassic tetrapod assemblages constrain Triassic-Jurassic tetrapod extinction event. Science, **237**: 1025-1029.

O'Sullivan, P.B., and Brown, R.W. 1998. Effects of surface cooling on apatite fission-track data: evidence for Miocene climatic change, North Slope, Alaska. In Advances in Fission Track Geochronology. Edited by P. Van den haute and F. De Corte. Kluwer, Dordrecht, pp. 255-267.

Poag, C.W. 1992. U.S. middle Atlantic continental rise: Provenance, dispersal, and deposition of Jurassic to Quaternary sediments. In Geologic Evolution of Atlantic Continental Rises. Edited by C.W. Poag and P.C. de Graciansky. Van Nostrand Reinhold, New York, pp. 217-263.

Poag, C.W., and Sevon, W.D. 1989. A record of Appalachian denudation in postrift Mesozoic and Cenozoic sedimentary deposits of the U.S. middle Atlantic continental

margin. Geomorphology, **2**: 119-157.

Ravenhurst, C.E., Donelick, R., Zentilli, M., Reynolds, P., and Beaumont, C. 1990. A fission track pilot study of the thermal effects of rifting on the onshore Nova Scotian margin, Canada. Nuclear Tracks and Radiation Measurement, **17**, 3: 373-378.

Reynolds, P.H.R., Zentilli, M., and Muecke, G.K. 1981. K-Ar and $^{40}Ar/^{39}Ar$ geochronology of granitoid rocks from southern Nova Scotia: Its bearing on the geological evolution of the Meguma Zone of the Appalachians. Canadian Journal of Earth Sciences, **18**: 386-394.

Roden, M. K. 1991. Apatite fission-track thermochronology of the southern Appalachian basin: Maryland, West Virginia, and Virginia. Journal of Geology, **99**: 41-53.

Ryan, R.J., and Zentilli, M. 1993. Allocyclic and thermochronological constraints on the evolution of the Maritimes Basin of eastern Canada, Atlantic Geology, **29**: 187-197.

Sanford, B.V., and Grant, A.C. 1990. Bedrock geological mapping and basin studies in the Gulf of St. Lawrence; In Current Research, Part B; Geological Survey of Canada, Paper 90-1B, pp. 33-42.

Schenk, P.E. 1995a. Meguma Zone. In Geology of the Appalachian-Caledonian Orogen in Canada and Greenland. Edited by H.Williams. Geological Survey of Canada, Geology of Canada, no. 6, pp. 261-277.

Schenk, P.E. 1995b. Annapolis Belt. In Geology of the Appalachian-Caledonian Orogen in Canada and Greenland. Edited by H.Williams. Geological Survey of Canada, Geology of Canada, no. 6, pp. 367-383.

Stea, R. R., Finck, P. W., and Fensome, R. A. 1997. Lithostratigraphy of Early Cretaceous and Quaternary unconsolidated sediments in the Musquodoboit and Shubenacadie Valleys, Nova Scotia, Canada. In Nova Scotia Department of Natural Resources, Mineral Resources Division. Report of Activities, 1996, Report 97-1, pp. 163-173.

Valdes, P.J., Sellwood, B.W., and Price, G.D. 1996. Evaluating concepts of Cretaceous equability. Palaeoclimates, **2**: 139-158.

van de Poll, H.W. 1995. Upper Paleozoic rocks: New Brunswick, Prince Edward Island, and Iles de la Madeleine. In Geology of the Appalachian-Caledonian Orogen in Canada and

Greenland. Edited by H.Williams. Geological Survey of Canada, Geology of Canada, no. 6, pp. 455-492.

Vrolijk, P., Donelick, R.A., Queng, J., and Cloos, M. 1992. Testing models of fission track annealing in apatite in a simple thermal setting: site 800, leg 129. In (R.L. Larson and Y. Lancelot, Editors) Proceedings of the Ocean Drilling Program, Scientific Results, **129**: pp. 169-176.

Wade, J.A., and McLean, B.C. 1990. The geology of the southeastern margin of Canada. In Geology of the Continental Margin of Eastern Canada. Edited by M.J. Keen and G.L. Williams. Geological Survey of Canada, Geology of Canada, no. 2, pp. 167-238.

Wade, J.A., Brown, D.E., Traverse, A., and Fensome, R.A. 1996. The Triassic-Jurassic Fundy Basin, eastern Canada. Atlantic Geology, **32**: 189-231.

Wagner, G.A., and Van den Haute, P. 1992. Fission track dating. Kluwer Academic Publishers, Dordrecht.

Wark, J.M., and Clarke, D.B. 1980. Geochemical discriminators and the palaeotectonic environment of the North Mountain basalt, Nova Scotia. Canadian Journal of Earth Sciences, **17**: 1740-1745.

Willett, S.D. 1997. Inverse modeling of annealing of fission tracks in apatite 1: A controlled random search method. American Journal of Science, **297**: 939-969.

Williams, H. (Editor) 1995. Geology of the Appalachian-Caledonian Orogen in Canada and Greenland. Geological Survey of Canada, Geology of Canada, no. 6.

CHAPTER 4. Apatite (U-Th)/He dating constraints on fission track thermal history models of the southern Canadian Atlantic margin

A.M. Grist and M. Zentilli.

4.1 Abstract:

Apatite (U-Th)/He ages have been determined for 6 samples obtained from granodiorite of the Devonian South Mountain Batholith in Nova Scotia, a Permian sandstone from the Maritimes Basin in Prince Edward Island, and Triassic sandstones from the Fundy Basin in New Brunswick. Late Triassic to Middle Jurassic (U-Th)/He ages are significantly younger than the respective emplacement age of the granodiorite or the stratigraphic ages of the sandstones, and are also somewhat younger than corresponding fission track (FT) ages reported for several of these same samples by Ravenhurst et al. (1990) and Grist and Zentilli (2003). The (U-Th)/He ages are used to refine the FT thermal history models proposed by Ravenhurst et al. (1990), Grist and Zentilli (2003) and others for the southern Canadian Atlantic margin.

Forward modelling of the (U-Th)/He age data for the Fundy Basin sandstones in New Brunswick shows that the ages are consistent with a proposed thermal maximum at ca. 200 Ma inferred by Grist and Zentilli (2003) that was associated with burial heating after the onset of rifting in the basin. The (U-Th)/He ages are also consistent with proposed elevated temperatures in that region during Late Cretaceous to Paleocene time, however temperature estimates are somewhat less than was initially suggested based on the FT models alone. The difference in the temperature estimates is likely caused by an artefact of the Laslett et al. (1987) annealing model which results in the systematic under-prediction of low-temperature FT annealing.

(U-Th)/He age data for a sandstone from the Maritimes Basin and a granodiorite from the SMB from the Digby D-1 well, located very near the Triassic breakup unconformity of the Fundy Basin, are also consistent with elevated temperatures at ca. 200 Ma. FT models for SMB samples obtained ca. 50 km southwest of the Triassic unconformity do not,

however, suggest a thermal maximum at 200 Ma, but appear to reflect protracted cooling of the Atlantic margin from ca. 300 Ma to 120 Ma. The models may indicate an increased rate of cooling after the onset of rifting in the Fundy Basin or the Atlantic margin. The (U-Th)/He data in this region are also consistent with slightly elevated temperatures during Late Cretaceous to Paleocene time.

4.2. Introduction

The purpose of this study is to determine the regional trends of apatite (U-Th)/He ages in several of the principal tectono-stratigraphic elements of the southern Canadian Atlantic margin (Fig. 1). The (U-Th)/He age data are used to test and refine FT thermal models for this region (Arne et al. 1990; Ravenhurst et al. 1990; Grist et al. 1992; Li et al. 1995; Grist et al. 1995; Grist and Zentilli 2003). He diffusion in apatite is sensitive to lower temperatures than FT annealing, and (U-Th)/He dating can be done using the same samples. Thus the method is uniquely suited to refine temperature estimates for the low-temperature parts of FT models that are not well constrained by the Laslett et al. (1987) annealing model.

Previous apatite FT time-temperature models for samples obtained from close to the margins of the Fundy Basin in southern New Brunswick, southwestern Nova Scotia, and in Prince Edward Island (Grist and Zentilli 2003), suggest a thermal history below ca. 120 °C that is dominated by thermal effects of Triassic continental rifting and subsequent burial heating in the basin, followed by cooling to Late Cretaceous time. Ravenhurst et al. (1990) reached a similar conclusion, that apatite FT data for some areas in southern Nova Scotia reflect cooling following Fundy Basin and/or Atlantic rift-related igneous activity between ca. 230-220 Ma and 195-185 Ma, whereas in other areas (e.g. the Maritimes Basin) FT data reflect slow cooling following a regional burial maximum at ca 320-300 Ma (Grist et al. 1995).

The Grist and Zentilli (2003) models and earlier apatite FT models by Arne et al. (1990), Grist et al. (1992) and Li et al. (1995) also indicate widespread elevated Late Cretaceous/Paleocene temperatures in the southern Canadian Atlantic margin. Rocks now at the surface in southwestern Nova Scotia, and in hydrocarbon exploration wells in the

Scotian Basin, offshore Nova Scotia (Fig. 4.1), were inferred to have experienced temperatures during Late Cretaceous to Paleocene time that were as much as 30 °C higher than they are at present, indicating significant regional post-Paleocene cooling of ca. 30 °C has occurred. These models are consistent with the occurrence of numerous limited Cretaceous-aged (Albian/Aptian) deposits that have recently been recognized in Nova Scotia (e.g. Stea et al. 1997).

4.2.1. Regional geology

Basement rocks in the southern Canadian Atlantic margin have been affected by both the Devonian Acadian and Late Permian Appalachian Orogenies, and are also partially overlain and overprinted by rift assemblages related to the Mesozoic and Cenozoic development of the Atlantic passive margin. The South Mountain Batholith (SMB) is an extensive granodioritic complex that intruded metasediments of the Meguma Zone (Schenk 1995a, 1995b) during Devonian time (ca. 380-370 Ma; Reynolds et al. 1981; Clarke et al. 1993). Considerable erosion followed emplacement of the SMB, and by the Early Carboniferous (ca. 350 Ma), terrestrial clastics and marine carbonates and evaporites were being deposited nonconformably on the exhumed granodiorite, or Meguma metasediments (Figs. 4.1, 4.2).

The Carboniferous to Permian Maritimes Basin (composite Fundy Basin of Bradley 1982) is a complex of erosional remnants of upper Paleozoic strata. Northeast of Prince Edward Island, sediment thickness of this succession exceeds 12,000 m (Sanford and Grant 1990). The basin is flanked by platformal areas in western New Brunswick, southern Nova Scotia, and western Newfoundland with relatively thin, mildly deformed upper Paleozoic strata (e.g. Bradley 1982). The youngest basin strata are Lower Permian (Artinskian) redbeds found on Prince Edward Island (van de Poll 1995) including the Malpeque sample area (Fig. 4.1).

The Triassic Fundy Basin, located between southern New Brunswick and western Nova Scotia, is a Late Triassic failed rift basin in the southern Canadian Atlantic margin (Fig. 4.1) which was subsequently shortened, likely as a result of ridge-push following the

onset of sea-floor spreading in the present Atlantic margin, and partially tectonically inverted beginning in Early Jurassic time (e.g. Withjack et al. 1995). Strata consist of continental red clastics and tholeiitic basalts of the Triassic and Early Jurassic Newark Supergroup (e.g. Greenough 1995; Wade et al. 1996). These were deposited in a faulted half-graben and thicken northward to >9000 m under the Bay of Fundy. In New Brunswick, the Fundy Group is exposed in three small but relatively thick successions on the north coast of the Bay of Fundy (Nadon and Middleton 1985). In Nova Scotia, the stratigraphically equivalent Wolfville and Blomidon Formations exist in a 200 km long by up to 20 km wide belt along the northwestern coastal part of the province (Wade et al. 1996; Hubert and Mertz 1984; and others).

Withjack et al. (1995, 1998) suggested that following the transition from rifting to drifting in the present southern Canadian Atlantic margin in Early Jurassic time, the Fundy Basin and its margins experienced inversion and exhumation in excess of 1.5 km. Post-Jurassic strata are largely absent in the onshore region of the southern Canadian Atlantic margin. Small, unconsolidated deposits of Lower Cretaceous kaolinitic clay and quartzose sand occur in several locations in Nova Scotia and New Brunswick. These are collectively referred to as the Chaswood Formation (Stea et al. 1997). Previous maturation studies by Akande and Zentilli (1983), Hacquebard (1984) and Davies et al. (1984) have suggested that these are only erosional remnants, and Hacquebard (1984) suggested that elevated vitrinite reflectance levels were consistent with the erosion of 700-800 m of overlying Cretaceous sediments from two such deposits in Nova Scotia. It has been recently suggested however, that much of the organic material in these deposits is charcoal that was likely produced by forest fires (Martin Gibling, pers. comm.). If any of this material was analysed during the previous studies, anomalously high maturities and an overestimation of the amount of erosion would result.

4.2.2 Description of samples

Four of the samples dated here were originally collected as part of a regional apatite FT study (Grist and Zentilli 2003). Samples for that study were obtained from sandstones of

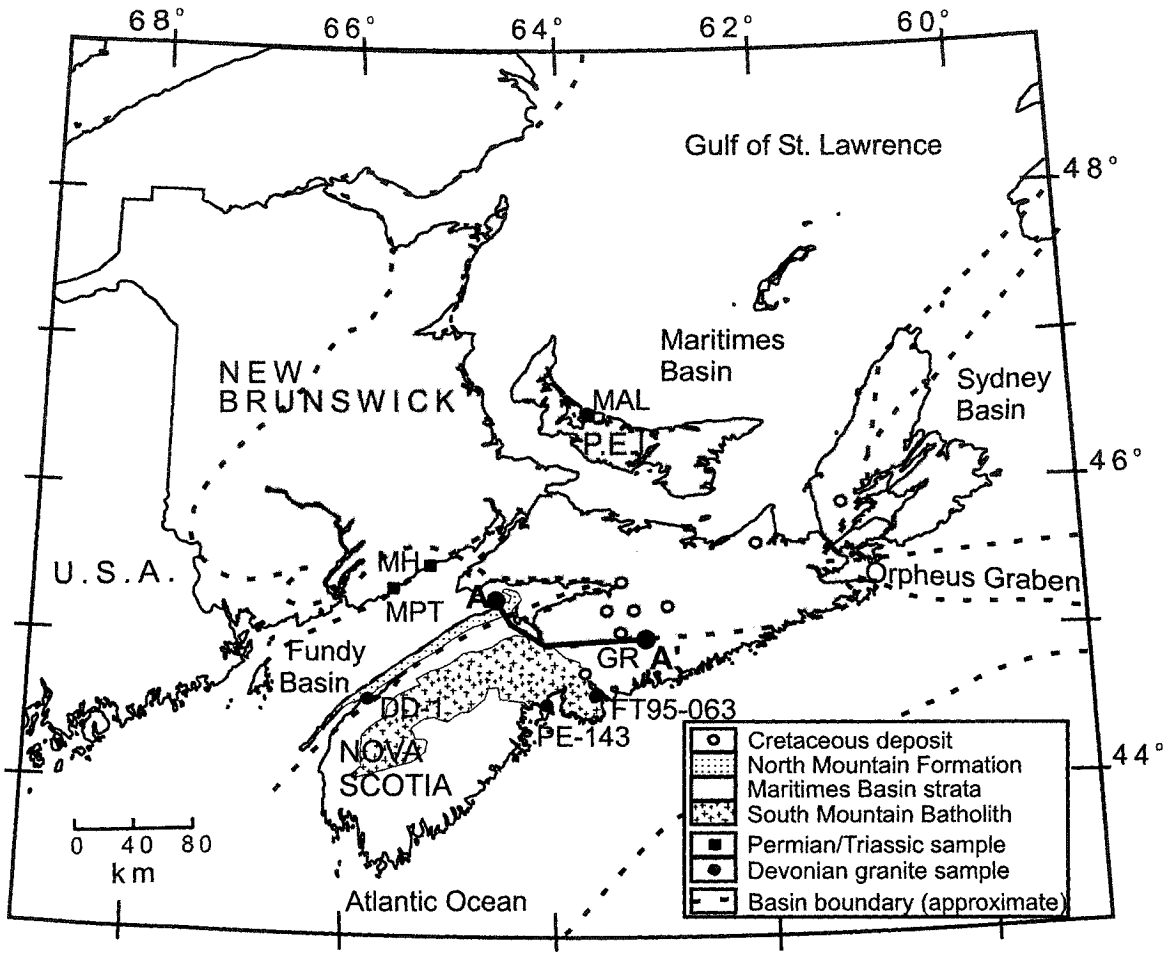

Figure 4.1. Map of the study area showing sample locations and selected lithologic and stratigraphic elements. Abbreviations used are: DD-1 = Digby D-1 drillhole; MPT = McCumber Point; MH = Martin Head; GR = Gays River; MAL = Malpeque.

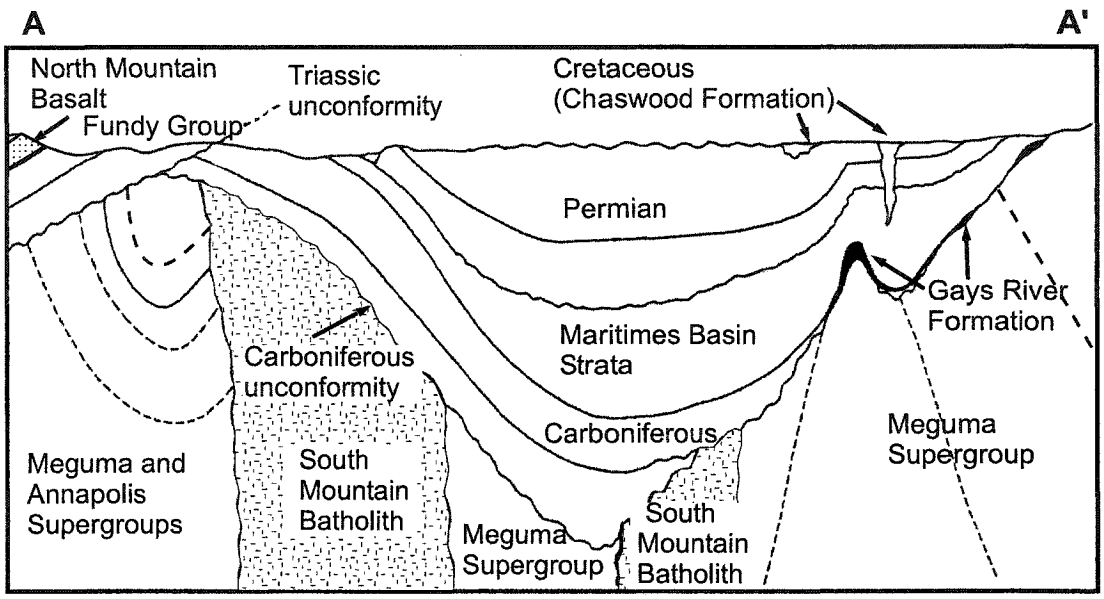

Figure 4.2. Schematic cross-section A-A' of the central part of the study area showing the stratigraphic relationships of the principal structural elements referred to in the text (substantial vertical exaggeration). The approximate location of the A-A' cross section is shown in Fig. 4.1 (modified from Moore et al. 2000).

the Triassic Fundy Group in Nova Scotia and New Brunswick, the earliest deposits in the Fundy graben above the Triassic unconformity, as well from Permian units within the strata of the Maritimes Basin from near the Triassic Malpeque Bay Sill, Prince Edward Island. Samples were also obtained from the Digby D-1 drill hole (Chatterjee and Dostal 2002) which cored granodiorite of the SMB to a depth of >1400 m on the southeast flank of the Fundy Basin in Nova Scotia (latitude 44°29′0.85″N, longitude 63°43′19.7″W), just below the Triassic unconformity. However, most of the apatite in the samples was found to contain ubiquitous microscopic inclusions of zircon and other refractory mineral phases that render it unsuitable for (U-Th)/He dating. For the present study an additional 2 outcrop samples from the SMB were selected from the southeastern part of the batholith, one each from Mahone Bay, and Halifax, Nova Scotia. FT data for the D-1 sample were reported by Ravenhurst et al. (1990). Age data for the Mahone Bay sample were originally obtained by Grist (1986), (also in Ravenhurst et al. 1990). Because a non-standard etch was used in the original analyses however, additional grainmounts of those samples were made and re-analyzed for the present study to ensure that the data were comparable. The locations of the samples are shown on Fig. 4.1.

4.2.3 Apatite (U-Th)/He dating and FT thermal models

Apatite (U-Th)/He dating provides an opportunity to refine the low temperature part of FT thermal models that are not well-constrained by FT annealing studies. Late-stage temperatures of ca. 50 °C in the Grist and Zentilli (2003) and Arne et al. (1990) models for the southern Canadian Atlantic margin are high enough to cause significant He diffusion. (U-Th)/He ages will allow us to refine estimates of the maximum Late Cretaceous temperatures experienced by the samples.

The (U-Th)/He method was one of the first techniques developed for the dating of geologic materials (e.g. Rutherford 1905; Strutt 1905), but was often considered unreliable owing to the ease with which radiogenic He could be lost from the host mineral resulting in too-young ages. The technique experienced a renaissance recently after its potential as a low temperature thermochronometer was suggested by Zeitler et al. (1987).

The behaviour of radiogenic He in a crystal lattice is governed by laws of diffusion (e.g. Wolf et al. 1998; Reiners and Farley 1999; Farley 2000; Reiners et al. 2002) which are highly temperature dependent. Wolf et al. (1998) demonstrated that diffusive loss of He from apatite becomes significant at temperatures as low as 40 °C, and is essentially complete at temperatures of 80-85 °C over geologic time-scales.The progressive diffusive loss of radiogenic He between 40 and 80 °C results in a He partial retention zone (PRZ), and the use of (U-Th)/He thermochronometry based on ^{4}He concentration profiles to constrain low-temperature cooling histories has recently been demonstrated by Reiners et al. (2003), Ehlers and Farley (2003), Shuster and Farley (2003), and others.

Similarly, track length (TL) reduction by annealing of fission damage is an incremental and irreversible process that is dominantly thermally activated. In apatite etchable tracks are retained between 60 and 130 °C over geologic time periods, but are progressively shortened in response to the highest temperatures experienced. Tracks are formed continuously through time, and therefore TL distributions are indicative of the integrated thermal history below the closure temperature, and apparent FT ages in systems with complex thermal histories may not represent geologically significant events. However, it is the temperature-dependent behavior between 60° and ca.130°C (referred to as the partial annealing zone or PAZ) that allows the apatite FT method to be used as a low-temperature thermochronometer.

FT annealing models (e.g. Laslett et al. 1987; Carlson 1990; Crowley et al. 1991) have been developed based on extrapolations of empirical laboratory annealing data (e.g. Green 1986; Crowley et al. 1991) to geologic time. The most widely used is the Laslett et al. (1987) fanning-Arrhenius model, which has been incorporated into a number of modelling software packages developed using Monte Carlo search techniques to evolve thermal history simulations to predict FT age and length distributions (e.g. Gallagher 1995; Willett 1997).

The Laslett et al. (1987) annealing model is known to under-predict fission track annealing at low temperatures over geologic time (e.g. Donelick et al. 1990; Vrolijk et al. 1992). As discussed in Grist and Zentilli (2004; Chapter 7 of this thesis), under-prediction of low-temperature annealing results in late-stage cooling in FT models that is required to

account for the low numbers of unannealed fission tracks observed in most samples. This late-stage cooling has significant implications with respect to (U-Th)/He ages that would be predicted based on the FT models because apatite He diffusion is sensitive to lower temperatures than FT annealing. An example of the effects of under-prediction of low-temperature annealing for the Durango apatite standard is shown in Fig. 4.3 (simplified from Grist and Zentili 2004).

The accepted FT age of Durango apatite is 31.4 ± 1.2 Ma (e.g. Wagner and Van den Haute 1992), and it has a measured (U-Th)/He age of 32.1 ± 1.2 Ma (e.g. House et al. 2000). The left panels of Fig. 4.3 show thermal models for Durango based on the empirically determined length distributions shown in the right panels. The lower left panel of Fig. 4.3 shows the thermal history model obtained using an initial (unannealed) track length of 16.1 μm. This model predicts temperatures of ca. 50-70 °C from 25 to 5 Ma, and significant cooling after ca. 4 Ma. These temperatures would cause significant He diffusion, and result in a (U-Th)/He age of only 17.3 Ma (The method used to calculate (U-Th)/He ages is described in Section 4.4). The upper left panel shows the same model except that an initial TL of 15 μm was used. This model does not display late-stage cooling, and predicts a (U-Th)/He age of 29.1 Ma.

4.3 Discussion of results

The (U-Th)/He age data are shown in Table 4.1. Typical analytical uncertainty of the corrected ages is approximately 8% at the 2σ level. A total of 13 analyses were obtained from the 6 samples, however one of the sandstone samples (FT91013a) outgassed during He extraction in a manner that typically indicates U-rich inclusions (Ken Farley, pers. comm.). One of the granodiorite samples (D-1) was also flagged as possibly having inclusions during grain selection. These two samples produced the oldest (U-Th)/He ages, however it is likely that both of these samples are affected by 'parentless' He from the inclusions and that these ages are not geologically meaningful.

Corrected (U-Th)/He ages for the Fundy Basin sandstone samples are 196 ± 16 Ma and 175 ± 14 Ma, for the Martin Head and McCumber Point samples, respectively (average

of 2 analyses each). These ages are similar to, or slightly less than, corresponding pooled FT ages for these same samples of 203 ± 20 Ma, (Martin Head) and 207 ± 20 Ma (McCumber). The (U-Th)/He ages likely reflect the thermal effects of Fundy Basin rifting and subsidence, between ca. 230-200 Ma, and are consistent with the inference of Grist and Zentilli (2003) that the low-temperature thermal history is dominated by rift-related burial heating during Triassic to earliest Jurassic time. The (U-Th)/He ages also demonstrate that cooling, likely as a result of exhumation, to temperatures below the PRZ, occurred very soon after this in Early to Middle Jurassic time. The average corrected (U-Th)/He age for the (Permian) sandstone from Maritimes Basin strata at Malpeque is 161 ± 13 Ma, which is younger than the corresponding FT age of 247 ± 22 Ma. The (U-Th/He) age is also consistent with exhumational cooling following the thermal effects of Triassic Fundy Basin or Early Jurassic Atlantic rifting.

The corrected (U-Th)/He age for the granodiorite sample from the D-1 well is 210 ± 17 Ma, which is slightly younger than the measured FT age of 244 ± 14 Ma, and somewhat older than (U-Th)/He ages of the samples from within the basin. The location of the Digby D-1 drillhole, stratigraphically below the Triassic breakup unconformity and near the margin of the Fundy Basin, suggests that the thermal history was affected by Triassic rifting. It is likely that the granodiorite at this location experienced cooling as result of flank uplift prior to rifting and only negligible (i.e., <1 km) burial prior to regional Early to Middle Jurassic exhumation. It is also possible however, that this sample is slightly affected by parentless He (as discussed above). None of the other samples from the Digby D-1 well were judged suitable for (U-Th)/He dating owing to the presence of ubiquitous zircon inclusions, and it is possible that this remaining single grain sample also contained an inclusion.

Corrected (U-Th)/He ages for the SMB granodiorite samples from Halifax and Mahone Bay are 207 ± 16 and 193 ± 15 Ma, respectively (average of 2 analyses each). These ages are similar to, or slightly less than, corresponding FT ages of 220 ± 12 Ma (Halifax), and 217 ± 13 Ma (Mahone Bay). Grist (1986) and Ravenhurst et al. (1990) interpreted FT data from the Halifax sample as likely a result of exhumational cooling from a regional burial maximum at ca. 320-300 Ma. This interpretation was also suggested by Arne et al. (1990)

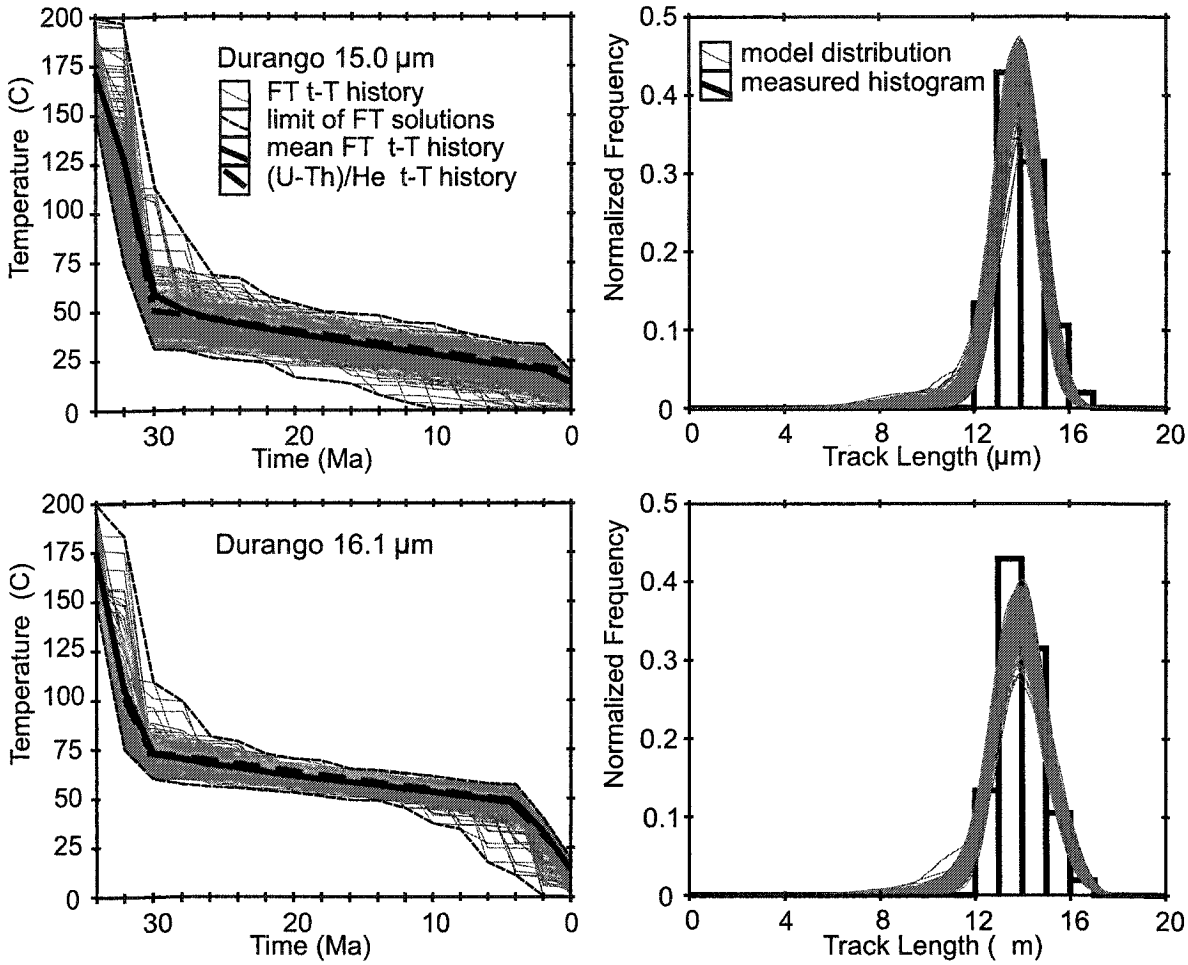

Figure 4.3. Inverse FT thermal models (left) and modelled /measured TL distributions (right) for an empirically determined Durango apatite standard length distribution. Each left panel shows 250 FT model t-T histories that pass the goodness-of-fit test (thin grey lines), the exponential mean of the 250 histories (thick black line), the upper and lower solution-bounding envelopes (thin dashed lines), and the (U-Th)/He forward model (thick dashed line). Note that the solution-bounding envelopes are not themselves solutions. The models in the upper panels were done using an initial TL of 15 µm. The models in the lower panels were done using an initial TL of 16.1 µm.

for samples obtained from basement rocks that have experienced a similar thermal history at nearby Gays River. The (U-Th)/He ages for theses samples suggest that it is likely that they underwent a period of more rapid cooling (similar to the D-1 well sample) from rift-flank uplift related to incipient rifting of the Atlantic margin in this region at ca. 190 Ma (e.g. Wade and MacLean 1990) because the they are slightly older than the age of the oldest oceanic crust.

4.4 Apatite (U-Th)/He constrained FT thermal models

A detailed description of the apatite FT Monte-Carlo inverse modelling procedures and input parameters used for the SMB and the Maritimes and Fundy Basin samples is given in Grist and Zentilli (2003), and only a brief summary is presented here. Fission tracks in apatite throughout the southern Canadian Atlantic region were likely completely annealed during heating associated with regional burial at ca. 320-300 Ma (e.g. Bradley 1982). As discussed above, Ravenhurst et al. (1990) interpreted FT data from a Halifax sample as likely a result of exhumational cooling from this regional burial maximum. Arne et al. (1990) also suggested continuous regional cooling of metasedimentary basement host rocks at the Gays River Pb-Zn deposit in southeastern Nova Scotia, from 300 Ma until Aptian/Albian time. Grist and Zentilli (2003) inferred that exhumation and cooling ended during Early Triassic time in the Fundy Basin region.

The Arne et al. (1990) model for Gays River included post-Albian heating to 60-80 °C. The presence of Aptian - Early Albian sediments implied that samples there were at the surface at approximately 120-100 Ma, but an insufficient proportion of long (i.e., >14 μm) fission tracks were observed for the data to be consistent with a thermal history with no post-Aptian heating. Grist and Zentilli (2003) also inferred elevated Late Cretaceous - Paleogene temperatures for samples now at or near the surface, but suggested these were likely ca. 20° less than the Arne et al. (1990) model. Grist and Zentilli (2003) incorporated an initial TL reduction to 15.5 μm to account for the under-prediction of low-temperature annealing of the Laslett et al. (1987) model, and consequently their maximum temperature estimates for surface samples during the Late Cretaceous were only ca. 50 °C.

Table 4.1: A summary of the samples and the (U-Th)/He data. 'Ft' is the grain size factor for the alpha ejection correction. Other abbreviations are; ppm = parts per million, nmol/g = nanomols per gram; r = grain radius; l = grain length. Raw ages were corrected according to the method of Farley et al. (1996) to account for ejection of a portion of the He produced by alpha decay (Analyses by A.M.G. and Lindsey Hedges). Overall errors to corrected ages are estimated to be 8% at the 2σ level.

* = He extraction by laser heating.

Sample number	grains	U (ppm)	Th (ppm)	He (nmol/g)	mass µg	Ft	mean r (µm)	mean l (µm)	re-extract (y/n)	Raw age (Ma)	**Corrected age ± 2σ (Ma)**
FT95-063 Halifax, N.S., Devonian SMB granodiorite											
FT95-063(a)	2	48.0	6.8	41.2	7.1	0.72	42.9	237.1	n	150.5	**208.5 ± 16.7**
FT95-063(b)	1	74.2	6.6	71.1	12.1	0.83	80.0	234.3	n	169.6	**204.6 ± 16.4**
D-1 well (60.2-60.6 m) Digby, N.S., Devonian SMB granodiorite											
D160.7(a)	1	27.6	1.9	27.0	11.2	0.83	80.0	217.1	n	173.6	**210.2 ± 16.8**
D160.7(b)	1	43.5	2.5	51.6	7.4	0.80	68.6	194.3	n	210.7	**263.4 ± 21.1**
PE-143 Mahone Bay, N.S., Devonian SMB granodiorite											
PE-143(a)	1	62.9	4.9	58.2	8.1	0.81	74.3	182.8	n	164.1	**202.9 ± 16.2**
PE-143(b)	1	56.7	3.6	47.0	8.6	0.81	74.3	194.3	n	147.9	**182.4 ± 14.6**
FT010 Martin Head, N.B., Fundy Group Triassic sandstone											
FT010(a)*	3	41.4	86.2	51.8	7.8	0.70	42.9	268.6	n	152.8	**218.7 ± 17.5**
FT010(b)*	3	26.8	31.1	23.9	9.5	0.73	51.4	222.8	n	127.4	**172.7 ± 13.8**
FT013 McCumber Point, N.B., Fundy Group Triassic sandstone											
FT013(a)	5	1.9	7.2	4.0	47.7	0.83	73.1	336.0	n	204.2	**246.3 ± 19.7**
FT013(b)	5	1.6	7.9	2.9	29.1	0.80	60.0	288.0	n	149.9	**187.4 ± 15.0**
FT013(c)	3	3.8	9.7	4.1	11.5	0.76	49.5	173.3	n	123.0	**162.3 ± 13.0**
FT021 Malpeque P.E.I., Maritimes Basin Lower Permian sandstone											
FT021(a)	5	2.7	11.6	3.6	25.7	0.78	54.8	317.1	n	121.5	**155.6 ± 12.4**
FT021(b)	2	2.4	9.5	3.0	5.0	0.71	44.3	154.3	y	118.8	**166.3 ± 13.3**
Standard											
mr22std-1*	4	19.8	10.76	0.4	20.31	0.76	53.57	325.7	n	3.28	**4.3 ± 0.3**
mr22std-2*	4	14.63	7.21	0.34	51.34	0.82	75	422.12	n	3.85	**4.7 ± 0.4**

Forward diffusion modelling of (U-Th)/He ages presented here has been done using proprietary software "Age Calculation.vi" written by K. Farley. The program calculates an apparent (U-Th)/He age based on net radiogenic He accumulation (a balance between ingrowth and diffusive loss) as described by Equation 2.11 in Chapter 2 (Equation 5 in Wolf et al. 1998). Input parameters for the age calculation are the measured grain radius, the diffusion grainsize, the activation energy (33 kcal/mol; e.g. Farley 2000) and the U and Th contents. Calculated ages were corrected to account for ejection from the host grain of a portion of the He produced by alpha decay.

Initially, thermal histories that approximated the exponential mean thermal history solution obtained from the FT inverse models shown in Figs 3.8 to 3.10 of Grist and Zentilli (2003), and the Arne et al. (1990) model t-T history (Arne et al. 1990, Fig. 7) were used as input for the (U-Th)/He age calculation. FT models from Arne et al. (1990) (top) and a representative model from Grist and Zentilli (2003) (bottom) are shown in Fig. 4.4. The thick dashed line on each panel shows the input thermal history for the (U-Th)/He age calculation.

Calculated (U-Th)/He ages based on the previous FT models are generally significantly less than the measured ages presented here. Using the minimum heating estimates shown in the top panel of Fig. 4.4 (i.e., heating to 60 °C at 75 Ma, immediately followed by cooling to the present day) results in a calculated (U-Th)/He age of 111 Ma. The Grist and Zentilli (2003) FT thermal model similarly predicts (U-Th)/He ages that are too young. The exponential mean thermal history shown in the model for the Digby D-1 well sample predicts (U-Th)/He age of only 117 Ma, compared with the measured (U-Th)/He age of 210 Ma for this sample. The FT models for the Triassic Fundy Basin samples from Grist and Zentilli (2003; Fig. 3.10) fit the (U-Th)/He data better because they predict lower post-Albian temperatures, however the calculated (U-Th)/He ages are also younger than measured ages. Based on the exponential mean thermal histories of those samples, the predicted (U-Th)/He ages are ca. 131-142 Ma, as opposed to the average measured (U-Th)/He ages of 175 and 196 Ma for the MPT013 and MH010 samples.

The (U-Th)/He data presented here imply that maximum post-Jurassic temperatures experienced by any of the dated samples was <50 °C, which suggests that the observed lack

of unannealed tracks is at least partly a result of low-temperature annealing. This an important result with respect to the previous FT-based thermal models for this region by Ravenhurst et al. (1990) and Arne et al. (1992) because the elevated Late Cretaceous temperatures predicted by those models to account for the lack of long tracks are likely too high. Although Grist and Zentilli (2003) used a reduced initial track length (15.5 μm), the maximum Late Cretaceous temperatures of ca. 50 °C for surface samples in those FT models would also cause some He diffusion.

Based on the preceding discussion, new FT models have been obtained for the samples dated here. The input temperature parameters and heating and cooling constraints for the samples that were modelled by Grist and Zentilli (2003) are slightly modified. The most important change is that maximum post-Albian temperatures were constrained to be less than 50 °C. An initial TL reduction to 15 μm (rather than 15.5 μm) was also used, and temperatures when samples were presumed to be at the surface and at the present day were specified to be 0-20 °C. For the FT95-063 and PE-143 samples the temperature constraints used were those used by Arne et al. (1990), but with the same modifications described for the Fundy Basin samples.

Summary time-temperature plots of the (U-Th)/He-constrained FT thermal models are shown in Fig. 4.5. Each panel shows 250 model t-T solutions (thin grey lines) as well as the exponential mean t-T history(thick solid line) and the t-T history used for the (U-Th)/He age calculation (thick dashed line). In most cases a much better match between the (U-Th)/He age predicted by the FT exponential mean thermal history and the measured (U-Th)/He age was obtained.

The calculated (U-Th)/He ages from the FT models for the Triassic Fundy Basin sandstone samples (Fig. 4.5, top) are similar to the measured ages for these samples (within 2σ errors). The mean thermal histories for these samples are consistent with Late Triassic

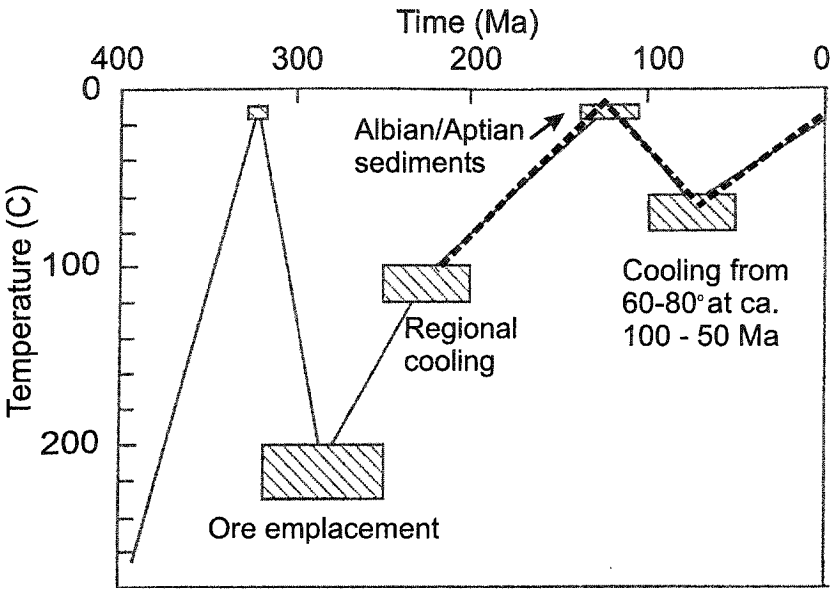

Modelled (U-Th)/He age = 111 Ma.

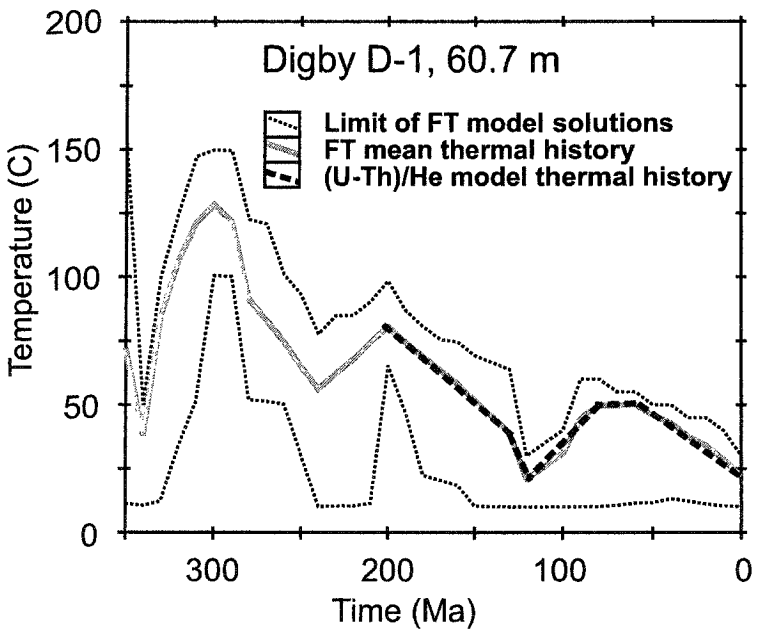

Measured (U-Th)/He age = 210 Ma; Modelled (U-Th)/He age = 117 Ma.

Figure 4.4. Thermal history models for the Gays River Pb-Zn deposit in southern Nova Scotia (simplified from Arne et al. 1990) and for the Digby D-1 well in southwestern Nova Scotia (from Grist and Zentilli 2003) (the temperature scale of the Arne et al. (1990) model is inverted). Also shown on each panel is the time-temperature history that was used as input for the (U-Th)/He age calculation (thick dashed line). Both models are too hot after Albian time to be compatible with measured (U-Th)/He ages.

Figure 4.5. Apatite FT inverse thermal models and (U-Th)/He forward model results for the Triassic Fundy Basin (top) and Permian Maritimes Basin (centre left) samples; and for the SMB samples from (Digby D-1) beneath the Triassic unconformity near the margin of the Fundy Basin (centre right), and from outcrop in the southeastern part of the batholith at Halifax and Mahone Bay (bottom).

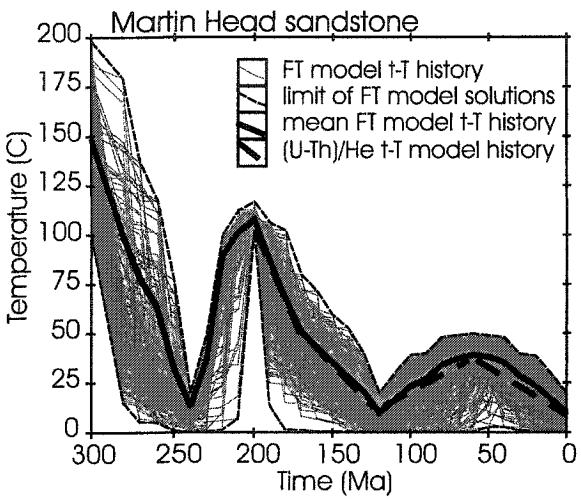

Observed (U-Th)/He ages = 218.7 Ma, 172.7 Ma.
Modelled (U-Th)/He age = 161.5 Ma.

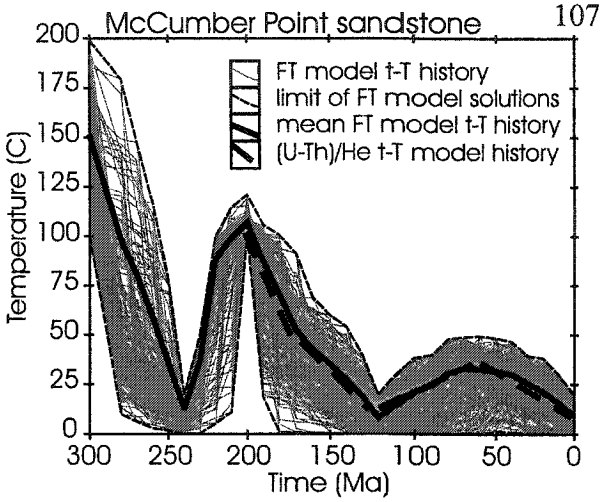

Observed (U-Th)/He ages = 162.3 Ma, 187.4 Ma.
Modelled (U-Th)/He age = 161.5 Ma.

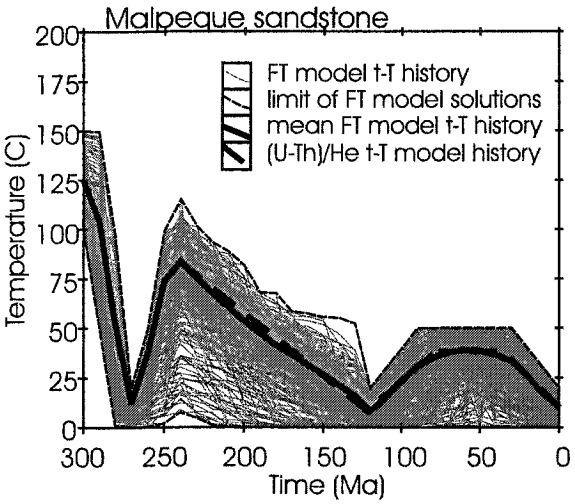

Observed (U-Th)/He ages = 155.6 Ma, 166.3 Ma.
Modelled (U-Th)/He age = 166 Ma.

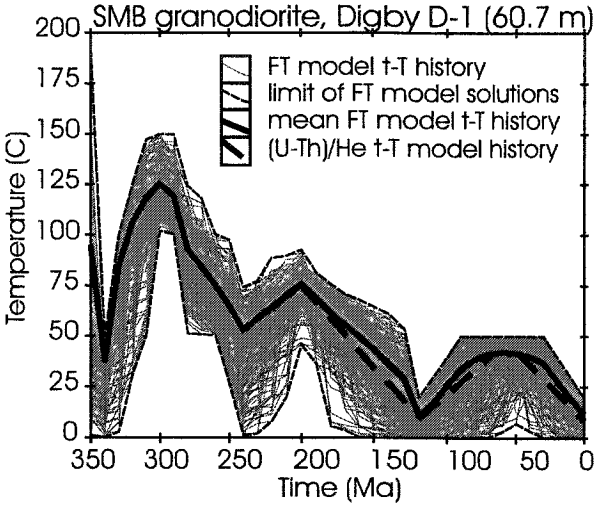

Observed (U-Th)/He age = 210.2 Ma.
Modelled (U-Th)/He age = 166 Ma.

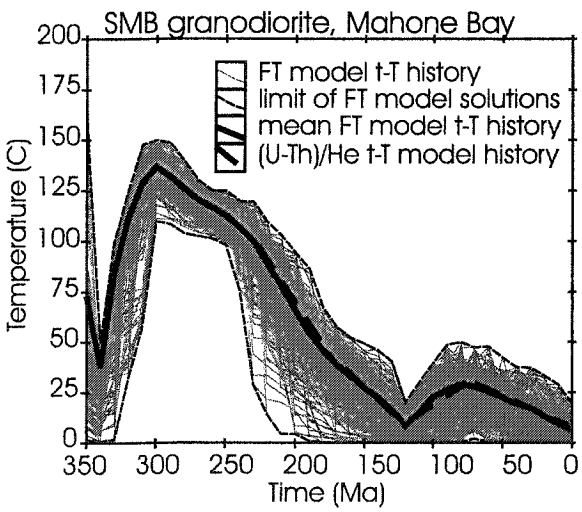

Observed (U-Th)/He ages = 202.9 Ma, 182.4 Ma.
Modelled (U-Th)/He age = 187.8 Ma

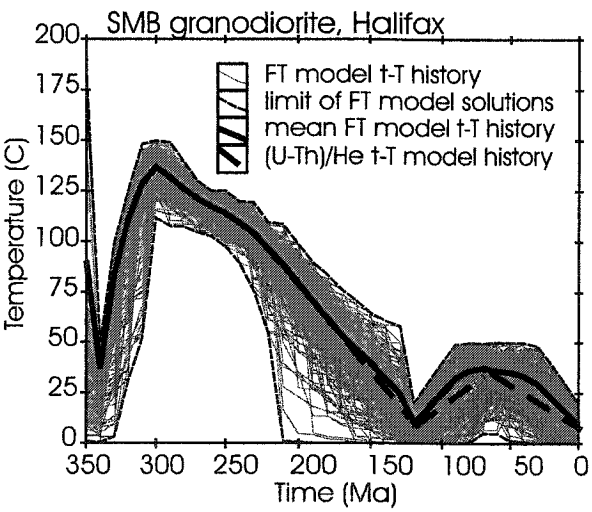

Observed (U-Th)/He ages = 208.5 Ma, 204.6 Ma.
Modelled (U-Th)/He age = 171.6 Ma.

burial heating, followed by rapid cooling that was likely from exhumation during Early Jurassic time caused by inversion of the Fundy Basin (Withjack et al. 1995).

The Permian sandstone from Malpeque was not previously modelled by Grist and Zentilli (2003). This model (Fig. 4.5, centre left) was not required to heat following the Triassic breakup unconformity because it is not from within the Fundy Basin. As suggested above this sample indicates a lower rate of cooling than do the Fundy Basin samples. The FT thermal model for the Digby D-1 well sample (Fig. 4.5, centre right) is less than satisfactory. The (U-Th)/He age predicted by the FT mean thermal history is significantly younger than the measured (U-Th)/He age. The FT thermal models for both the Malpeque and the Digby D-1 samples also appear to suggest higher post-Albian temperatures than are permitted by the (U-Th)/He age data. In the Digby D-1 sample, this may be related to the presence of a U-rich inclusion and parentless He, as discussed above.

The FT thermal models for the granodiorite samples from Halifax and Mahone Bay (Fig. 4.5 bottom) do not appear to suggest any significant thermal effects from Triassic rifting. These models do suggest a period of rapid cooling during Early Jurassic time, likely as a result of exhumation of the margin following the onset of Atlantic rifting (e.g. Ravenhurst et al. 1990).

4.5. Conclusions

Modelling of apatite (U-Th)/He ages using time-temperature histories from FT thermal models by Grist and Zentilli (2003), and an earlier FT model by Arne et al. (1990), demonstrates that the models are generally not consistent with measured (U-Th)/He ages. The (U-Th)/He data require that maximum post-Jurassic temperatures of the samples never exceeded 50 °C, which is somewhat less than was suggested based on the previous FT models. The earlier models did not take sufficiently into account the under-prediction of low-temperature annealing of the Laslett et al. (1987) annealing model. (U-Th)/He ages predicted using FT thermal models that include an initial mean track length reduction to 15 μm and post-Jurassic temperatures limited to <50 °C are similar to the measured (U-Th)/He data.

Thermal models for sandstones from the Fundy Basin are consistent with a thermal

maximum at ca. 200 Ma associated with burial heating after the onset of rifting in the basin as previously proposed by Grist and Zentilli (2003). Thermal models for granodiorite samples obtained ca. 50 km southwest of the Fundy Basin appear to reflect protracted cooling of the Atlantic margin from ca. 300 Ma to 120 Ma, as inferred by Arne et al. (1990) and Ravenhurst et al. (1990). The models also suggest there may have been an increased rate of cooling after the onset of rifting in the Fundy Basin or the Atlantic margin.

4.6 Acknowledgements

A. Grist is very grateful to Ken Farley at Caltech for the insights he has offered into many aspects of (U-Th)/He dating, and for the use of his (U-Th)/He age-modelling software Thanks also to Lindsey Hedges at Caltech for her patient instruction and assistance in grain selection and sample preparation, as well as for performing the ICP-MS work. Chris Beaumont provided helpful discussion and reviewed early versions of this manuscript.

4.7 References cited:

Akande. S.O., and Zentilli, M. 1983. Genesis of the lead-zinc mineralization at Gays River, Nova Scotia, Canada. In International Conference on Mississippi Valley Type Lead-Zinc Deposits, Proceedings Volume. Edited by G. Kisvarsanyi, S.K. Grant, W.P. Pratt, and J.W. Koenig. University of Missouri, Rolla, Missouri, 546-557.

Arne, D.C., Duddy, I.R., and Sangster, D.F. 1990. Thermochronologic constraints on ore formation at the Gays River Pb-Zn deposit, Nova Scotia, Canada, from apatite fission track analysis. Canadian Journal of Earth Sciences, **27**: 1013-1022.

Bradley, D.C. 1982. Subsidence in Late Paleozoic basins in the northern Appalachians. Tectonics, **1**, 1: 107-123.

Carlson, W.D. 1990. Mechanisms and kinetics of apatite fission-track annealing. American Mineralogist, **75**, 1120-1139.

Clarke, D.B., MacDonald, M.A., Reynolds, P.H., and Longstaffe, F.J. 1993. Leucogranites from the eastern part of the South Mountain Batholith, Nova Scotia. Journal of Petrology, **34**: 653-679.

Crowley, K.D., Cameron, M. And Schaefer, R.L. 1991. Experimental studies of annealing of etched tracks in flluorapatite. Geochimica et Cosmochimica Acta, **55**, 1449-1465.

Davies, E.H., Akande, S.O., and Zentilli, M. 1984. Early Cretaceous deposits in the Gays River Lead-zinc mine, Nova Scotia: evidence from $^{40}Ar/^{39}Ar$ mineral ages. In Current Research, part A. Geological Survey of Canada, Paper 84-1A, 353-358.

Davis, W.M. 1922. Peneplains and the geographic cycle. Geological Society of America Bulletin, **33.3**: 587-598.

Donelick, R.A., Roden, M.K., Mooers, J.D., Carpenter, B.S., and Miller, D.S. 1990. Etchable length reduction of induced fission tracks in apatite at room temperature (~23°C): Crystallographic orientation effects and "initial" mean lengths. Nuclear Tracks and Radiation Measurements, **17**, no. 3, 261-265.

Ehlers, T.A. and Farley, K.A. 2003. Apatite (U-Th)/He thermochronometry: methods and applications to problems in tectonic and surface processes. Earth and Planetary Science Letters, **206**, 1-14.

Farley, K.A. 2000. Helium diffusion in apatite: General behavior as illustrated by Durango fluorapatite. Journal of Geophysical Research, **105**, 2903-2914.

Farley, K.A., Wolfe, R.A., and Silver, L.T. 1996. The effects of long alpha-stopping distances on (U-Th)/He ages. Geochimica et Cosmochimica Acta, **60**, no. 21, 4223-4229.

Gallagher, K. 1995. Evolving temperature histories from apatite fission-track data. Earth and Planetary Science Letters, **136**, 421-435.

Goldthwait, J.W. 1924. Physiography of Nova Scotia. Geological Survey of Canada, Memoir 140.

Green, P.F., Duddy, I.R., Gleadow, A.J.W., Tingate, P.R., and Laslett, G.M. 1986. Thermal annealing of fission tracks in apatite 1. A qualitative description: Chemical Geology, **59**: 237-253.

Greenough, J.D. 1995. Mesozoic rocks. In Geology of the Appalachian-Caledonian Orogen in Canada and Greenland. Edited by H.Williams. Geological Survey of Canada, Geology of Canada, no. 6, 567-600.

Grist, A.M. 1986. Low temperature geochronology of the South Mountain Batholith, Nova Scotia, using 40Ar/39Ar and fission track dating techniques, unpublished B.Sc. Thesis, Dalhousie University, Halifax Nova Scotia, 74p.

Grist, A.M., Reynolds, P.H., Zentilli, M., and Beaumont, C. 1992. The Scotian Basin offshore Nova Scotia: thermal history and provenance of sandstones, from apatite fission track analysis 40Ar/39Ar data. Canadian Journal of Earth Sciences, **29**: 909-924.

Grist, A.M., Ryan, R.J. and Zentilli. 1995. The thermal evolution and timing of hydrocarbon generation in the Maritimes Basin of eastern Canada: Evidence from apatite fission track data. Bulletin of Canadian Petroleum Geology, **43**, no. 2, 145-155.

Grist, A.M. and Zentilli, M. 2003. Post-Paleocene cooling in the southern Canadian Atlantic region: evidence from apatite fission track models, Canadian Journal of Earth Sciences, **40**, no. 9, 1279-1297.

Grist, A.M. and Zentilli, M. 2004. Apatite Fission Track and (U-Th)/He thermal history modelling of the Nares Strait, Kane Basin Region in Canada and Greenland (in prep.)

Hacquebard, P.A. 1984. Composition, rank and depth of burial of two Nova Scotia lignite deposits. In Current Research, part A. Geological Survey of Canada, Paper 84-1A, 11-15.

House, M.A., Farley, K.A. and Stockli, D. 2000. Helium chronometry of apatite and titanite using Nd-YAG laser heating. Earth and Planetary Science Letters, **183**, 365-368.

Hubert, J.F., and Mertz, K.A. 1984. Eolian sandstones in Upper Triassic-Lower Jurassic red beds of the Fundy Basin, Nova Scotia. Journal of Sedimentary Petrology, **54**: 798-810.

Laslett, G.M., Green, P.F., Duddy, I.R., and Gleadow, A.J.W. 1987. Thermal annealing of fission tracks in apatite: 2. A quantitative analysis. Chemical Geology (Isotope Geoscience Section), **65**: 1-13.

Li, G., Ravenhurst, C.E., and Zentilli, M. 1995. Implications of apatite fission track analysis for the thermal history of the Scotian Basin, offshore Nova Scotia, Canada. Bulletin of Canadian Petroleum Geology, **43**: 127-144.

Moore, R.G., Ferguson, S.A., Boehner, R.C., and Kennedy, C.M. 2000. Preliminary map of the Wolfville/Windsor Area, Kings and Hants Counties, Nova Scotia (21H/01 and Parts of 21A/16C and D). Scale 1:50,000.

Nadon, G.C., and Middleton, G.V. 1985. The stratigraphy and sedimentology of the Fundy Group (Triassic) of the St. Martins area, New Brunswick. Canadian Journal of Earth Sciences, **22**: 1183-1203.

Ravenhurst, C.E., Donelick, R., Zentilli, M., Reynolds, P., and Beaumont, C. 1990. A fission track pilot study of the thermal effects of rifting on the onshore Nova Scotian margin, Canada. Nuclear Tracks and Radiation Measurement, **17**, 3: 373-378.

Reiners, P.W., Farley, K.A., and Hickes, H.J. 2002. He diffusion and (U-Th)/He thermochronometry of zircon: Initial results from Fish Canyon Tuff and Golde Butte: Tectonophysics, **349**, 297-308.

Reiners, P.W. and Farley, K.A. 1999. Helium diffusion and (U-Th)/He thermochronometry of titanite. Geochimica et Cosmochimica Acta, **63**, 3485-3859.

Reiners, P.W., Spell, T.L., Nicolescu, S., and Zanetti, K. 2003. Zircon (U-Th)/He thermochronometry: He diffusion and comparisons with $^{40}Ar/^{39}Ar$ dating. Geochimica et Cosmochimica Acta, **68**, 1857-1887.

Reynolds, P.H.R., Zentilli, M., and Muecke, G.K. 1981. K-Ar and $^{40}Ar/^{39}Ar$ geochronology of granitoid rocks from southern Nova Scotia: Its bearing on the geological evolution of the Meguma Zone of the Appalachians. Canadian Journal of Earth Sciences, **18**: 386-394.

Rutherford, E. 1905. Present problems in radioactivity. Popular Science Monthly, May, 1-34.

Sanford, B.V., and Grant, A.C. 1990. Bedrock geological mapping and basin studies in the Gulf of St. Lawrence; In Current Research, Part B; Geological Survey of Canada, Paper 90-1B, 33-42.

Schenk, P.E. 1995a. Meguma Zone. In Geology of the Appalachian-Caledonian Orogen in Canada and Greenland. Edited by H.Williams. Geological Survey of Canada, Geology of Canada, no. 6, 261-277.

Schenk, P.E. 1995b. Annapolis Belt. In Geology of the Appalachian-Caledonian Orogen in

Canada and Greenland. Edited by H.Williams. Geological Survey of Canada, Geology of Canada, no. 6, 367-383.

Shuster, D.L. and Farley, K.A. 2003. $^{4}He/^{3}He$ thermochronometry. Earth and Planetary Science Letters, **217**, 1-17.

Stea, R. R., Finck, P. W., and Fensome, R. A. 1997. Lithostratigraphy of Early Cretaceous and Quaternary unconsolidated sediments in the Musquodoboit and Shubenacadie Valleys, Nova Scotia, Canada. In Nova Scotia Department of Natural Resources, Mineral Resources Division. Report of Activities, 1996, Report 97-1, 163-173.

Strutt, R.J. 1905. On the radioactive minerals. Proceedings of the Royal Society, **A76**, 88-101.

van de Poll, H.W. 1995. Upper Paleozoic rocks: New Brunswick, Prince Edward Island, and Iles de la Madeleine. In Geology of the Appalachian-Caledonian Orogen in Canada and Greenland. Edited by H.Williams. Geological Survey of Canada, Geology of Canada, no. 6, 455-492.

Vrolijk, P., Donelick, R.A., Queng, J., and Cloos, M. 1992. Testing models of fission track annealing in apatite in a simple thermal setting: site 800, leg 129. In (R.L. Larson and Y. Lancelot, Editors) Proceedings of the Ocean Drilling Program, Scientific Results, **129**: pp. 169-176.

Wade, J.A., and McLean, B.C. 1990. The geology of the southeastern margin of Canada. In Geology of the Continental Margin of Eastern Canada. Edited by M.J. Keen and G.L. Williams. Geological Survey of Canada, Geology of Canada, no. 2, pp. 167-238.

Wade, J.A., Brown, D.E., Traverse, A., and Fensome, R.A. 1996. The Triassic-Jurassic Fundy Basin, eastern Canada. Atlantic Geology, **32**: 189-231.

Wagner, G.A., and Van den Haute, P. 1992. Fission track dating. Kluwer Academic Publishers, Dordrecht.

Willett, S.D. 1997. Inverse modeling of annealing of fission tracks in apatite 1: A controlled random search method. American Journal of Science, **297**: 939-969.

Withjack, M.O., Olsen, P.E. and Schlische, R.W. 1995. Tectonic evolution of the Fundy rift basin, Canada: Evidence of extension and shortening during passive margin

development. Tectonics, **14**, no. 2, 390-405.

Withjack, M.O., Schlische, R.W. and Olsen, P.E. 1998. Diachronous rifting, drifting, and inversion on the passive margin of central eastern North America: an analog for other passive margins. American Association of Petroleum Geologists Bulletin, **82**, no. 5A, 817-835.

Wolf, R.A., Farley, K.A., and Kass, D.M. 1998. Modeling of the temperature sensitivity of the apatite (U-Th)/He thermochronometer. Chemical Geology, **148**, 105-114.

Zeitler, P.K., Herczeg, A.L., McDougall, I., and Honda, M. 1987. U-Th-He dating of apatite: A potential thermochronometer. Geochimica et Cosmochimica Acta, **51**, 2865-2868.

Appendix 1. Analytical procedures for (U-Th)/He analysis

Apatite mineral separates were obtained using conventional heavy liquid and magnetic separation techniques. Individual samples consisting of between 1 and 5 inclusion-free grains (Table 4.1) were selected for (U-Th)/He analysis using a stereo binocular microscope equipped with a transmitted light source and a rotating stage. Only grains that appeared completely dark when viewed with the stage rotated to extinction (in crossed polarized light) were selected. Prior to analysis, sample grains were measured using a microscope equipped with an ocular graticule and stage micrometer to calculate alpha ejection corrections. Two slightly different analytical procedures were used for He extraction. Most samples were heated using a conventional furnace. The extraction for the FT010 and MR22STD samples was done using a Nd-YAG laser.

For furnace heating, sample grains were placed in stainless steel crucibles that were spot welded shut. Individual crucibles were heated to temperatures of ca. 900 °C to completely out gas the grains. For laser heating sample grains were placed in platinum microtubes, that were then pinched closed and loaded into a laser planchet. Helium extraction was done using a Nd-YAG laser following the method of House et al. (2000). Individual microtubes were heated to temperatures of ca. 1050 °C. Completeness of gas extraction was verified for each crucible/microtube by performing a re-extraction heating following each He analysis. Evolved gases were spiked with approximately 0.4 pmol of ^{3}He and adsorbed on activated charcoal cooled to 16 K using a cryogenic trap. Purification to remove contaminant gases was done by heating the trap to 37 K, thereby releasing only helium. $^{4}He/^{3}He$ ratios were measured in a quadrupole mass spectrometer (QMS). Ratios were referenced to multiple determinations of a known volume of ^{4}He standard processed in the same way as the samples, and appropriate discrimination corrections were made to the measured $^{4}He/^{3}He$ ratios.

Following degassing, furnace sample grains were retrieved from the crucibles and dissolved in 100 ml of concentrated HNO_3. Pt microtubes were placed directly in acid to dissolve the contained apatite grains. Solutions were spiked with a 25 ml calibrated ^{230}Th and ^{235}U solution and diluted to 250 ml with ultrapure water. The spiked samples were analysed

as 0.5 ml aliquots of ca. 1-5 ppb U-Th solutions by isotope dilution using a Finnigan Element2 ICP-MS with a teflon micro-flow nebulizer and double-pass spray chamber. U and Th blanks by this method are 1 ± 0.1 pg and 2 ± 1 pg, respectively. Estimated uncertainty of measured sample U-Th are on the order of 1-2% (2σ).

The raw age data were corrected according to the method of Farley et al. (1996) to account for ejection from the host grain of a portion of the He produced by alpha decay of uranium and thorium isotopes owing to the large stopping distances for the emitted He nuclei (ca. 12-34 μm in apatite). Based on statistical analysis of multiple (U-Th)/He age determinations for the Fish Canyon and Durango apatite standards, overall analytical uncertainty in the individual corrected sample ages is on the order of 6-8% at the 2σ confidence level. Aliquots of the laboratory apatite standard 97MR22, (average laser multigrain age of 4.50 ± 0.24 Ma; House et al. 2000) were also analyzed (see Table 4.1).

CHAPTER 5. Cooling of the Sverdrup Basin during Tertiary basin inversion: implications for hydrocarbon exploration[2]

D.C. Arne, **A.M. Grist**, M. Zentilli, M. Collins, A. Embry, and T. Gentzis

5.1 Abstract

The regional thermal history of the northeastern Sverdrup Basin, Canadian Arctic Archipelago, has been assessed using apatite fission track thermochronology and vitrinite reflectance data. Fission track data for 27 samples from six wells through the Mesozoic section on Axel Heiberg and Ellesmere Islands reveal significant Palaeocene cooling associated with basin inversion during the Eurekan Orogeny. Fission track data for 29 outcrop samples, ranging in stratigraphic age from Cambrian to Tertiary, also reveal significant Palaeocene cooling. Vitrinite reflectance data from carbonaceous shales and coal seams in well and outcrop samples are consistent with these conclusions. The degree of Palaeocene cooling observed is greatest for well and outcrop samples in the cores of anticlines, such as the Fosheim anticline or the hanging walls of thrust faults, such as the Lake Hazen fault system, and the East Cape and Vesle Fiord thrust faults. Palaeocene cooling is largely attributed to the denudation of structures during the Eurekan Orogeny.

At one locality on northwestern Ellesmere Island, which is on the northern flank of the Sverdrup Basin, the underlying Franklinian basement rocks yield Early Cretaceous fission track ages with relatively long mean track lengths. This indicates that this part of the basin was uplifted at this time and that subsequent sedimentation and subsidence in the Cretaceous and early Tertiary were modest. This locality thus appears to be on the rift shoulder, which developed along the flank of the Amerasia Basin in the Lower Cretaceous.

At a locality on western Axel Heiberg Island, which is downflank from the rift shoulder, the Upper Jurassic Awingak sandstone has a Late Cretaceous fission track age.

---

[2] Arne, D.C., Grist, A.M., Zentilli, M., Collins, M., Embry, A., and Gentzis, T. 2002. Cooling of the Sverdrup Basin during Tertiary basin inversion: implications for hydrocarbon exploration, Basin Research, **14**, 183-205.

This is best explained by heating above the total annealing temperature for fission tracks in apatite by extensive Lower Cretaceous intrusions and subsequent heat dissipation and cooling in the Late Cretaceous followed by further substantial cooling due to Tertiary denudation.

These results indicate that maximum burial temperatures occurred in the presently exposed Mesozoic section prior to basin inversion during the Eurekan Orogeny. It can therefore be inferred that peak hydrocarbon generation and primary migration predated the formation of structural traps during the Tertiary at shallow depths within the northern Sverdrup Basin.

5.2 Introduction

The evaluation of thermal histories in inverted sedimentary basins is complicated by the loss of stratigraphic section during denudation on a regional scale, as well as locally on structural culminations such as the hanging walls of thrust faults and the cores of anticlines (Green et al. 1995). Denudational cooling typically marks the cessation of hydrocarbon generation and primary migration; thus the timing of cooling relative to the formation of structural traps is of critical importance to the evaluation of hydrocarbon potential.

The Sverdrup Basin, Canadian Arctic Archipelago, received considerable attention as a frontier hydrocarbon province during the 1960s and 1970s. Several gas fields were discovered, mainly in the central and western portions of the basin (Fig. 5.1a). However, a number of major structures were found to contain only trace hydrocarbons, leading Waylett and Embry (1992) to suggest that hydrocarbons had leaked from breached structural traps. Several regional studies of thermal maturity using organic indicators and conodonts have been carried out in the basin (e.g. Henao-Londoño 1977; Powell 1978; Utting et al. 1989). These studies have provided only general constraints on the timing of maximum burial temperatures and peak hydrocarbon generation relative to the development of structural traps formed during either the mid-Palaeozoic Ellesmerian or Early Cenozoic Eurekan Orogeny. The timing of hydrocarbon generation and primary migration relative to deformation therefore has important implications for future exploration in the region.

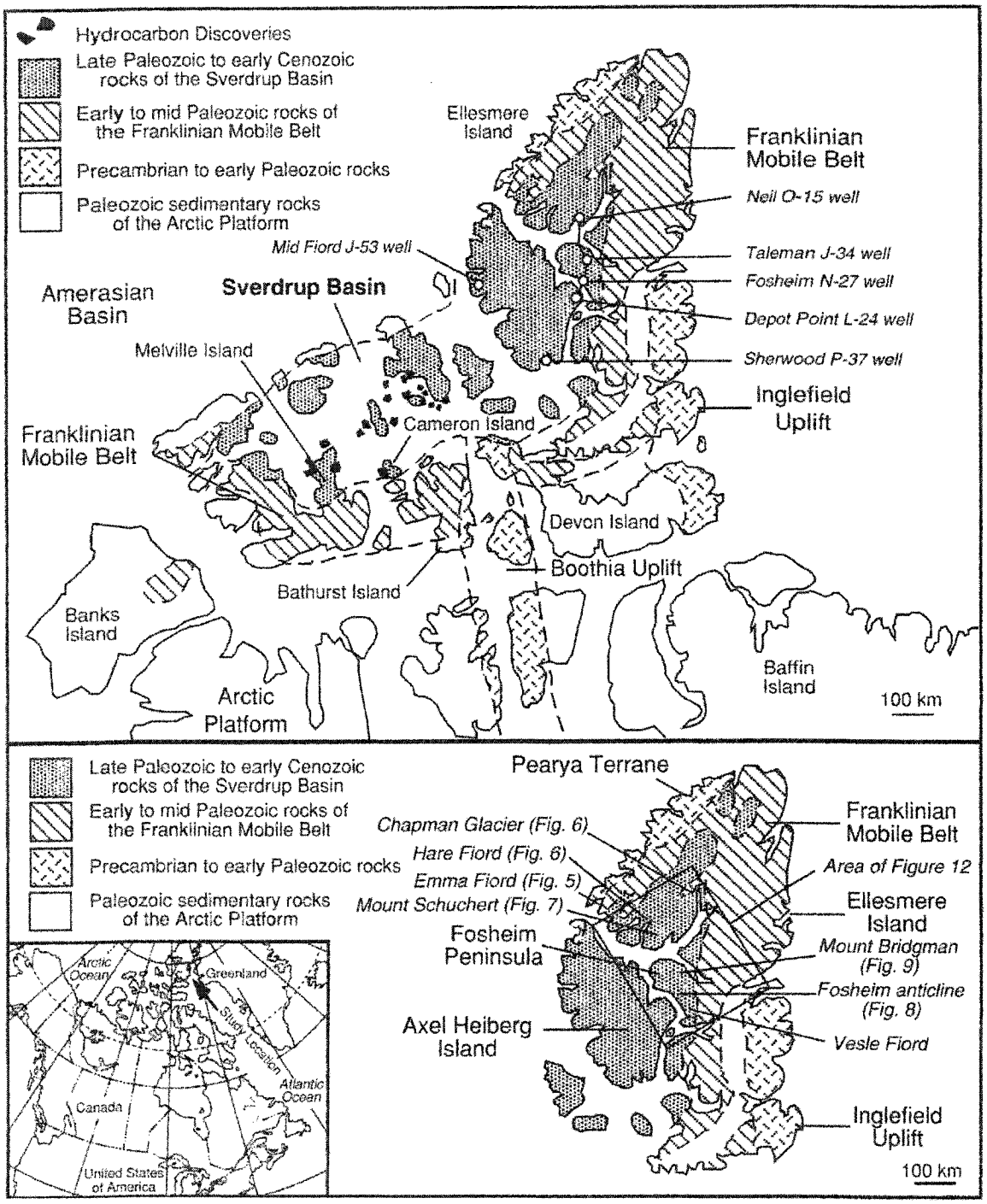

Figure 5.1. Simplified geology of the northern Canadian Arctic Archipelago. (top) Locations of wells studied and hydrocarbon discoveries. (bottom) Locations of outcrop sections discussed in the text. Modified from Trettin (1991a).

This study represents the first regional examination of thermal history in the Canadian Arctic Archipelago using apatite fission track data. New vitrinite reflectance data are also presented, and these were used as a guide to sampling wells for fission track analysis, as well as an aid in the interpretation of fission track data from outcrop sections. As described by Arne and Zentilli (1994), the integration of the two thermal history techniques is particularly useful in deformed sedimentary basins because a reflectance value of $0.8 \pm 0.1\%$ equates to total annealing of fission tracks in most apatite grains. Apatite fission track and vitrinite reflectance data are presented from six well sections, as well as six measured outcrop sections. The results of this study reveal the extent of Tertiary cooling associated with the Eurekan Orogeny in the northeastern Sverdrup Basin and adjacent Franklinian Mobile Belt. They also provide constraints on the timing of maximum temperatures in the exposed Mesozoic section of the eastern Sverdrup Basin relative to Eurekan deformation.

5.2.1 Regional geology

The Franklinian Mobile Belt and Sverdrup Basin (Fig. 5.1a) comprise part of the Innutian Tectonic Province (Trettin 1991a). Lower Palaeozoic rocks of the Franklinian Mobile Belt were progressively deformed beginning in the late Silurian to early Devonian, probably in response to docking of the late Proterozoic to late Silurian Pearya Terrane onto northern Ellesmere Island outboard of a yet to be identified continental land mass (Trettin 1991b). During this time, a foreland basin developed in front of the southwesterly advancing orogen and accumulated at least 4 km of sediment derived from the north and east (Embry 1991a). Deformation culminated in the Ellesmerian Orogeny during the latest Devonian to early Carboniferous and resulted in recumbent and overturned folds in the lower Palaeozoic strata of the orogen, as well as broader, more open folds in the foreland (Trettin 1991b). The Sverdrup Basin subsequently developed over the site of the former orogenic belt. This resulted in a series of broadly parallel, Ellesmerian fold belts trending east-west along the southern margin of the preserved Sverdrup Basin and northeast - southwest along the eastern and northeastern margins. Regional thermal maturity trends, discussed in more detail in the following section, suggest the removal of a considerable thickness of lower and mid-

Palaeozoic strata prior to the initiation of Sverdrup Basin deposition in late Early Carboniferous.

Rifting in the Sverdrup Basin began in mid-Carboniferous and was accompanied by deposition of carbonates, evaporites, redbeds, marine shales with minor chert, and extrusion of basalt unconformably on the underlying Franklinian rocks (Davies and Nassichuk 1991). A discordance occurring within the lower Permian strata (Melville Disturbance) may be related to transcurrent fault movement during extension to form pull-apart basins (Davies and Nassichuk 1991). A period of non-deposition and, locally, denudation of the underlying upper Palaeozoic succession occurred near the Permian-Triassic boundary prior to the deposition of a thick Mesozoic sequence in a series of transgressive-regressive cycles (Embry 1991b, 1993). Sediment was sourced mainly from the south and east at this time with a rapid influx of clastic sediment during the early Triassic, indicating substantial denudation of the source regions.

Sedimentation in the Sverdrup Basin proceeded more or less continuously through the Triassic to the Early Cretaceous and included the deposition of potential hydrocarbon source rocks such as the Schei Point Group (Powell 1978) and mobilization of the underlying Carboniferous evaporites into diapirs (Davies and Nassichuk 1991). A second phase of mafic magmatism affected the region during the Early Cretaceous and was interpreted by Embry and Osadetz (1988) to be related to major volcanic activity associated with the Alpha Hot Spot which was centred in the oceanic Amerasian Basin to the west. Sills are most common on northwestern Axel Heiberg Island and gradually become less common to the south and east.

Terrestrial sediment of the Eureka Sound Group was deposited beginning in the Late Cretaceous and continuing through to the mid-Tertiary. It is considered to be conformable with the underlying Mesozoic succession in the centre of the Sverdrup Basin (Miall 1991). However a significant unconformity occurs within the group near the Cretaceous-Tertiary boundary, and numerous minor breaks in sedimentation have also been postulated to occur within the group (Ricketts 1994; Harrison et al. 1999). The depositional environment was dominantly fluvial and involved the formation of numerous coal seams, but the precise

controls on sedimentation are controversial, particularly regarding the importance of basement arches (Miall 1986, 1991; Ricketts and Stephenson 1994; Ricketts 1994; Harrison et al. 1999). Burial curves suggest that Mesozoic source rocks in the southwestern Sverdrup Basin reached the oil window during Late Cretaceous to early Tertiary burial (Embry et al. 1991b).

The Eurekan Orogeny deformed early Tertiary and older strata of the Sverdrup Basin, mainly during the early to middle Tertiary (Okulitch and Trettin 1991; Harrison et al. 1999). Both the nature and timing of this orogeny are uncertain (De Paor et al. 1989). Kinematic models based on sea-floor magnetic data suggest that Ellesmere Island and Greenland converged between 56 and 35 Ma (Roest and Srivastava 1989), and this convergence adequately explains the dominant structural grain on Ellesmere and Axel Heiberg Islands (Oakey 1994). The widespread uplift in the latest Cretaceous and the initiation of substantial subsidence following the K-T boundary indicates a tectonic realm of increasing compression (Stephenson et al. 1994). Thrust faulting is interpreted to have begun by late Palaeocene (Arne et al. 1998; Harrison et al. 1999), but the main period of deformation occurred during the middle Eocene, as evidenced by deposition of syn-tectonic conglomerates in a series of intermontane basins (Ricketts and Stephenson 1994).

Eighteen oil and gas fields were discovered in the central and southwestern portions of the Sverdrup Basin (Fig. 5.1a) following the drilling of 176 exploration wells. All but one of these fields occur in Mesozoic clastic strata on the crests of anticlinal structures, many of which are salt-cored. The main source rocks for the hydrocarbons are interpreted to be bituminous shales in the middle to upper Triassic Schei Point Group (Brooks et al. 1992). No significant hydrocarbon discoveries have been made in upper Palaeozoic rocks of the Sverdrup Basin and a single producing oil field, Bent Horn, occurs in Devonian carbonate rocks on Cameron Island. The only notable hydrocarbon show in the eastern Sverdrup Basin occurs within the Jurassic section encountered in Romulus C-42 on Fosheim Peninsula, Ellesmere Island. Evidence of oil staining in many large, barren, structural traps, coupled with reservoirs filled to well under the spill point, led Waylett and Embry (1992) to suggest that many anticlines had been breached by faulting. Peak hydrocarbon generation prior to the

Eurekan Orogeny could also be a factor in these observations.

5.2.2 Previous thermal history investigations

The earliest regional studies of thermal maturity in the Franklinian Mobile Belt and the Sverdrup Basin were by Henao-Londoño (1977) and Powell (1978). Both studies noted that Devonian strata in portions of the Franklinian Mobile Belt and Carboniferous to Permian strata along the southern margin of the Sverdrup Basin ranged from immature to mature, particularly on Cameron Island, eastern Melville Island and western Bathurst Island. Distinct breaks in maturity across a major regional unconformity at the base of the Sverdrup Basin succession in areas such as Melville Island led Powell (1978) to conclude that hydrocarbon generation in lower to mid-Palaeozoic strata preceded the Ellesmerian Orogeny. Similarly, Powell (1978) inferred that hydrocarbon generation in the Sverdrup Basin preceded the Eurekan Orogeny.

Utting et al. (1989) described the thermal maturity of surface and subsurface samples from Upper Carboniferous and Permian rocks along the southern and eastern margins of the Sverdrup Basin (Fig. 5.1) using thermal alteration indices (TAI), conodont alteration indices (CAI) and vitrinite reflectance (R_o) determinations. The lowest maturities in outcropping Upper Carboniferous rocks (CAI = 1-1.5; TAI = 2) occur along the southern margin of the Sverdrup Basin, on Melville Island. Outcropping Permian samples also have CAI values of 1.5 or less in this region, and this belt of low maturity extends to the east and north to central Ellesmere Island. Maturity levels in outcrop samples increase from central to northern Ellesmere Island where maximum CAI values of 4.5 and TAI values up to 4 are reported. Similar high maturity values occur on the northwest extremity of Axel Heiberg Island (Fig. 5.1b). The presence of upper Palaeozoic rocks showing high maturities at surface along the margins of the northern Sverdrup Basin indicates appreciable post-Permian heating followed by later exhumation, although it is not clear from these maturity data when cooling from peak temperatures occurred.

Detailed thermal maturity studies using organic indicators have focussed on the western Sverdrup Basin in the vicinity of known hydrocarbon fields. On Melville Island (Fig.

5.1a), hydrocarbons in the Hecla and Drake fields are hosted by uppermost Triassic sandstones (Embry and Johannessen 1992). Vitrinite reflectance profiles in petroleum exploration wells from northern Melville Island are continuous through the upper Palaeozoic to Upper Cretaceous section (Gentzis and Goodarzi 1991, 1992a, b), indicating that maximum temperatures in the southern Sverdrup Basin were attained during late Mesozoic or early Cenozoic burial.

In a simple conceptual model of thermal evolution in a sedimentary basin, geotherms, as indicated by isoreflectance contours, would be expected to be sub-parallel to depositional contacts, assuming constant burial, heat flow and thermal conductivities across the basin. Isoreflectance contours in the upper Palaeozoic to upper Mesozoic Sverdrup Basin succession are typically oblique to structural contours (Gentzis and Goodarzi 1991, 1993), indicating that regional thermal maturity variations are related to either differential burial, heat flow or thermal conductivities. Furthermore, this variability suggests maximum thermal maturities were attained following deposition of upper Mesozoic sediments in the Sverdrup Basin.

Gentzis et al. (1996) reported graptolite reflectance values from lower Palaeozoic rocks from the southern and eastern margins of the Sverdrup Basin. Maximum reflectance values up to 4.7% are related to deep, synorogenic burial during the Ellesmerian Orogeny. Prominent offsets in bitumen reflectance profiles across a major unconformity at the base of the Carboniferous strata further indicate that maximum burial temperatures in the lower to mid-Palaeozoic (pre-Ellesmerian) strata of the Franklinian Mobile Belt on Melville Island were attained prior to the onset of Sverdrup Basin sedimentation (Gentzis and Goodarzi 1992b).

In a preliminary analysis of thermal histories across the Vesle Fiord Thrust in the northeastern Sverdrup Basin using apatite fission track and vitrinite reflectance data, Arne et al. (1998) concluded that maximum palaeotemperatures in the Mesozoic section exposed in the hanging wall of the fault predated thrusting. Modelling of the data using the techniques described in Willett (1997) further indicated Late Palaeocene initiation of cooling, very shortly after deposition of footwall sediments of the Strand Bay Formation.

The preliminary results from the Vesle Fiord region favour the initiation of tectonism in the Sverdrup Basin prior to the Eocene timing inferred from kinematic models (Roest and Srivastava 1989). Furthermore, the thermal history data indicate that the thermal maximum and by inference, peak conditions for hydrocarbon generation, were attained prior to thrusting, at least within the strata presently exposed. Therefore, peak hydrocarbon generation in the Vesle Fiord area appears to predate the development of Eurekan structures that have been a favoured target for hydrocarbon exploration in the northeast Sverdrup Basin. This interpretation would down-grade Eurekan-age structural traps at shallow levels as potential reservoirs, but data from elsewhere in the Sverdrup Basin are required to confirm this conclusion given the implications for further exploration in the region.

5.3 Methodology

5.3.1 Sample details

Six wells from Axel Heiberg and Ellesmere Islands; Mid Fiord J-53, Sherwood P-37, Depot Point L-24, Fosheim N–27, Taleman J-34 and Neil O-15, were analysed in the course of this investigation. With the exception of Mid Fiord J-53, the wells form a north-south profile parallel to the eastern margin of the Sverdrup Basin (Fig. 5.1). Although aligned sub-parallel to the structural grain of both the Ellesmerian and Eurekan Orogens (Oakey 1994), a cross section based on four of these wells indicates that the well transect cuts obliquely across structural culminations and depressions displaying at least two kilometres of stratigraphic relief (Fig. 5.2). Additional stratigraphic data from Halcyon O-16 and Romulus C-42 are also provided in this cross section. The Depot Point L-24 and Fosheim N–27 wells are located on structural highs on the southern portion of the section. Eureka Sound Group sediments are preserved on Fosheim Peninsula where they overlie a continuous Mesozoic sequence intersected by the Romulus C-42, Taleman J-34 and Halcyon O-16 wells. A truncated Mesozoic succession is again intersected by the Neil O-15 well on northern Ellesmere Island. The positions of major mafic sills of probable Cretaceous age are also shown on the section, as are the positions of inferred thrust faults.

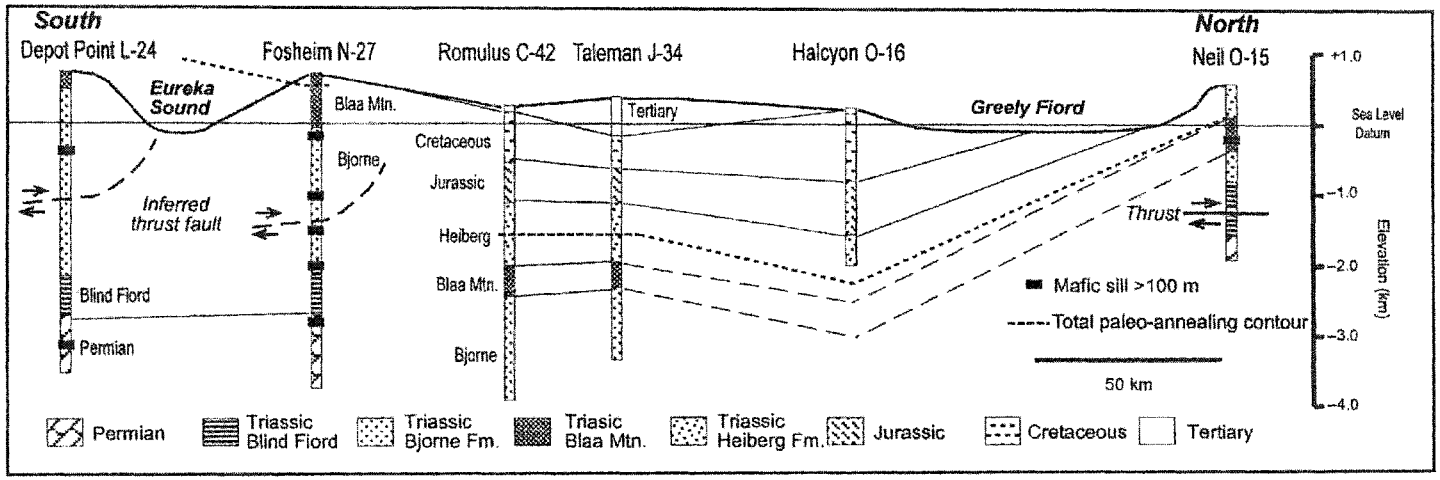

Figure 5.2. North-south cross section from Fig. 5.1(a) showing an interpreted stratigraphic section through Fosheim Peninsula.

Samples of cuttings (~1 kg) were composited over approximately 100 m intervals where either sandy lithologies or mafic sills were intersected by drilling. One drill core was sampled close to the interval over which cuttings were collected in Taleman J-34. These two samples, FT94-85 and FT94-8, give similar apatite fission track ages and mean track lengths (Table 5.1), consistent with minimal downhole contamination by cuttings, at least in this instance. Where possible, sampling was concentrated over the position of the 0.8% iso-reflectance contour in order to maximize the information obtained from the fission track data (Arne and Zentilli 1994).

Outcrop sections were collected from seven localities (Fig. 5.1) during the summer of 1994. Data from one of these localities, Vesle Fiord, have been presented previously (Arne et al. 1998). Field localities were selected to assess breaks in thermal history across a number of Eurekan structures, but were constrained by logistical support available from Otto Fiord (northern Ellesmere Island) and Eureka (Fosheim Peninsula).

Samples were collected from clastic sedimentary rocks and mafic sills for fission track thermochronology, and from fresh exposures of carbonaceous shale and coal for vitrinite reflectance. Where possible, samples for fission track and vitrinite analysis were collected as close together as possible. Sampling of the Mesozoic section at Fosheim anticline, Mount Bridgman and Mount Schuchert was linked to stratigraphic sections measured previously by the Geological Survey of Canada.

Estimated present-day temperatures of all well samples are presented in Table 5.1. These were calculated from geothermal gradients and depth to permafrost provided by J.A. Majorowicz (pers. comm., 1993) using corrected, deep bottom-hole temperatures (BHT) collected during exploration drilling. As all wells examined yielded data from greater than 1 km in depth, the estimated gradients are considered to be reliable. Present-day geothermal gradients calculated using shallow BHT data from onshore wells in the Arctic have been shown to be unreliable, as they are affected by recent surface temperature changes due to relative sea level fluctuations and submergence/emergence of coastal areas (Jones et al. 1989).

5.3.2 Apatite fission track data

Apatite concentrates obtained using conventional heavy mineral separation techniques were analysed by the external detector method at Dalhousie University. Thermal neutron irradiations for apatite were performed in the Dalhousie University Slowpoke-2 reactor (Cd ratio for Au of 4.3). Fission track ages were determined using the zeta calibration method, as recommended by Hurford (1990). The statistical spread in fission track age between individual apatite grains is reflected in the χ^2 statistic, with values greater than .05 indicating a single population of ages. Central ages (Galbraith and Laslett 1993) were calculated for those samples failing the χ^2 test. Horizontal confined track lengths were measured using the procedure described in Gleadow et al. (1986). Samples with low spontaneous track densities were irradiated with ^{252}Cf at Rensselaer Polytechnic Institute, New York, to increase the number of etched confined track lengths for measurement (Donelick et al. 1992). An asterisk in the data tables indicates samples treated in this way.

Eight age standards were included with the irradiations used for this study. A weighted mean age of 26.4 ± 2.3 Ma was obtained from four separate samples of Fish Canyon Tuff. This age compares favourably with a reference age of 27.95 ± 0.18 Ma (Renne et al. 1994). Four separate Durango apatite samples gave a weighted mean age of 31.5 ± 2.8 Ma, in close agreement with the reference age of 31.4 ± 0.5 Ma (Green 1985). The uncertainties associated with these replicate analyses of age standards also give an estimate of analytical precision (9%), although this should be taken as a minimum, given the good quality of the age standards. Replicate track length measurements were also made for two samples, FT94-007 and FT94-075 (Table 5.1). The repeat measurements are in close agreement, indicating good precision for the track length data.

5.3.3 Modelling procedures

The modelling approach used is based on the annealing data of Laslett et al. (1987) for Durango apatite, described using the mathematical fit of Crowley et al. (1991). The program (AFTINV32) uses the algorithm described by Willett (1997) with modifications by Issler (1996). Modelling of apatite fission track data from samples that show a significant

Table 5.1. Apatite fission track age and length data for well samples.

*Second aliquot irradiated with ^{252}Cf for tack length measurements. Samples with χ^2 probability of >.05 pass the χ^2 test at the 95% confidence level. Ages for these samples are calculated using pooled statistics. Ages of samples that fail the χ^2 test are calculated using the central age equation (Galbraith and Laslett 1993). ρ_d, ρ_s and ρ_i are the density of dosimeter glass (CN-5 or CN-1) fossil and induced tracks ($x10^5/cm^2$). Numbers of tracks counted or measured is shown in parentheses. A zeta of 363 ± 6 (CN-5 glass) was used. Age error estimates are at the 2σ confidence level. Analyses by D.C. Arne. Present day temperatures (T) were estimated from the following depths to the base of the permafrost and corrected geothermal gradients provided by J.A. Majorowicz: Taleman J-34 - 716 m, 28 °C/km; Fosheim N–27 - 252 m, 24 °C/km; Depot Point L-24 - 372 m, 35 °C/km; Mid Fiord J-53 - 332 m, 27 °C/km; Sherwood P-37 - 250 m, 24 °C/km; Neil O-15 - 373 m, 21 °C/km.

Sample number	Depth (m)	Rock unit	Stratigraphic age (Ma)	Grains counted	ρ_d (n_d)	ρ_s (n_s)	ρ_i (n_i)	χ^2 Prob.	Fission track Age (Ma)	Mean length (μm)	Std. Dev. (μm)	Present day T (°C)
Taleman J-34 well												
FT94-5	1248–1339	Deer Bay	140–130	21	1.133 (2213)	31.3 (606)	24.6 (476)	0.712	256 ± 34	10.6 ± 0.4 (100)	1.9	14
FT94-7	2404–2495	Heiberg	215–180	29	1.133 (2213)	4.40 (312)	19.8 (1406)	0	49 ± 11	11.6 ± 0.5 (70)	2.2	49
										11.8 ± 0.6 (51)	2.0	
FT94-85*	2988–3006	Bjorne	245–241	8	1.122 (2185)	2.08 (36)	11.5 (200)	0.598	36 ± 13	11.0 ± 1.0 (28)	2.5	64
FT94-8	2952–3043	Bjorne	245–241	19	1.133 (2213)	5.52 (162)	27.5 (808)	0.115	41 ± 7	11.4 ± 1.6 (14)	3.0	64
FT94-9	3439–3530	Bjorne	245–241	27	1.133 (2213)	2.21(115)	15.3 (795)	0.173	30 ± 6	11.6 ± 1.2 (17)	2.4	78
Fosheim N-27 well												
FT94-61*	700–791	Bjorne	245–241	14	1.105 (2111)	7.05 (151)	20.3 (434)	0.949	69 ± 14	13.7 ± 0.5 (48)	1.8	12
FT94-62	1278–1369	Bjorne	245–241	22	1.105 (2111)	7.55 (473)	30.9 (1934)	0.705	49 ± 6	13.7 ± 0.3 (58)	1.0	25
FT94-63*	1993–2069	Bjorne	245–241	30	1.105 (2111)	5.34 (404)	20.9 (1584)	0.987	51 ± 6	13.1 ± 0.3 (100)	1.3	43
FT94-64*	2252–2343	Bjorne	245–241	19	1.105 (2111)	3.86 (167)	20.3 (878)	0	44 ± 12	13.3 ± 0.4 (53)	1.3	49
FT94-65*	2617–2678	Mafic sill	144–65	30	1.105 (2111)	0.417 (41)	1.58 (155)	0.949	52 ± 19	13.1 ± 0.3 (100)	1.3	57
FT94-66*	2800–2891	Bjorne	245–241	30	1.105 (2111)	0.763 (69)	3.70 (335)	0.943	40 ± 11	12.7 ± 0.3 (100)	1.6	62
FT94-67*	3408–3500	Mafic sill	144–65	30	1.105 (2111)	0.339 (30)	2.07 (183)	0.353	32 ± 13	13.0 ± 0.7 (31)	1.8	77
Depot point L-24 well												
FT94-68*	502–593	Murray Harb.	240–230	20	1.105 (2111)	6.04 (217)	20.9 (939)	0.001	58 ± 14	13.8 ± 0.3 (96)	1.4	0
FT94-69	1126–1217	Bjorne	245–241	29	1.105 (2111)	7.31 (217)	27.9 (829)	0.921	51 ± 8	12.7 ± 0.4 (46)	1.5	19
FT94-70*	1522–1613	Bjorne	245–241	20	1.105 (2111)	7.11 (341)	26.9 (1275)	0.951	52 ± 7	12.53 ± 0.4 (83)	1.7	29
FT94-71	1978–2069	Bjorne	245–241	14	1.105 (2111)	6.40 (213)	21.0 (700)	0.889	59 ± 10	13.90 ± 0.6 (11)	1.0	37
FT94-72	3597–3682	Mafic sill	144–65	14	1.105 (2111)	0.362 (9)	6.44 (160)	0.529	11 ± 7	no lengths		76
Mid Fiord J-53 well												
FT94-73*	426–517	Awingak	145–135	30	1.105 (2111)	4.30 (337)	11.3 (884)	0	86 ± 20	12.3 ± 0.5 (100)	2.3	3
FT94-75*	1970–1983	Heiberg	215–180	23	1.122 (2185)	4.25 (162)	26.0 (991)	0.127	33 ± 6	11.6 ± 1.1 (29)	2.8	44
										11.8 ± 0.8 (36)	2.5	
Sherwood P-37 well												
FT94-76	30–122	Deer Bay	140–130	19	1.122 (2185)	3.57 (110)	17.2 (530)	0.586	42 ± 9	12.9 ± 1.5 (8)	1.9	0
FT94-78*	1339–1400	Mafic sill	144–65	35	1.122 (2185)	0.586 (59)	2.82 (284)	0.92	42 ± 12	13.8 ± 0.7 (39)	2.1	27
FT94-79*	1917–2039	Mafic sill	144–65	40	1.122 (2185)	0.585 (50)	3.81 (326)	0.978	31 ± 10	13.4 ± 0.7 (35)	1.9	42
FT94-80*	2252–2343	Heiberg	215–180	26	1.122 (2185)	3.30 (269)	18.8 (1528)	0.017	37 ± 7	13.4 ± 0.3 (100)	1.4	49
Neil O-15 well												
FT94-81*	274–365	Heiberg	215–180	17	1.122 (2185)	7.47 (259)	23.0 (797)	0	90 ± 28	13.2 ± 0.6 (51)	2.2	0
FT94-82	822–898	Mafic sill	144–65	40	1.122 (2185)	0.712 (95)	3.36 (448)	0.655	43 ± 10	13.4 ± 0.8 (32)	2.2	18
FT94-83*	1506–1582	Bjorne	245–241	20	1.122 (2185)	5.18 (229)	22.8 (1006)	0.604	46 ± 7	12.7 ± 0.5 (74)	2.1	25
FT94-84*	2343–2435	Permian	300–250	28	1.122 (2185)	6.25 (336)	31.6 (1700)	0.691	40 ± 5	13.1 ± 0.4 (65)	1.8	43

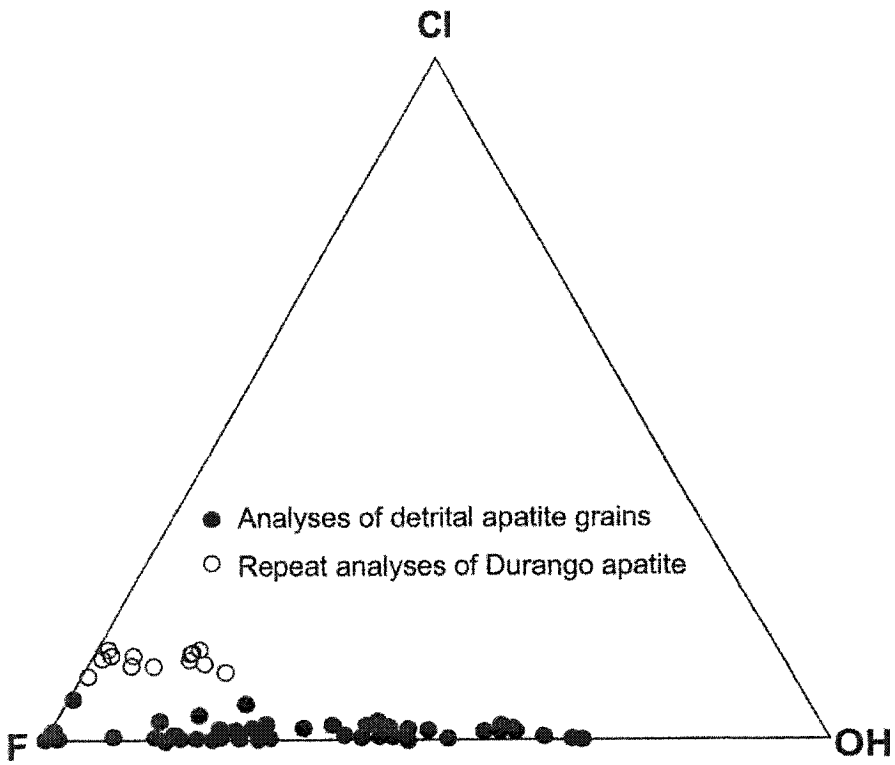

Figure 5.3. Summary of compositions of detrital apatite grains from sandstone samples, Fosheim Peninsula.

spread in fission track age from individual apatite grains within the samples, as indicated by a χ^2 probability of less than .05, has not been attempted. Such a spread may either indicate variations in cooling history from different detrital source areas or differential partial annealing of apatite grains having varying chemistry (Green et al. 1986; O'Sullivan and Parrish 1995). In such circumstances use of a mono-compositional annealing model is inappropriate.

Those samples for which fission track data have been modelled are inferred to have been totally annealed following deposition and to have cooled rapidly enough, that differential annealing due to possible compositional variations has not been significant. Microprobe analysis of 46 individual apatite grains from four samples representative of the late Palaeozoic and Mesozoic units sampled for this study using a JEOL 733 Superprobe at Dalhousie University indicate that they range from fluorapatite to hydroxyapatite in composition (Fig. 5.3), similar to data previously reported by Arne et al. (1998). OH was calculated from excess oxygen assuming stoichiometry. The spread in composition of Durango apatite from the F-Cl axis towards hydroxyapatite indicates the level of uncertainty associated with the calculation of OH by this approach. Regardless, analyses of the detrital apatite grains reveals more spread in OH compositions than shown by the Durango data, suggesting the presence of significant OH in the samples. Although no compositional data are available from lower Palaeozoic units, these results suggest that the Durango annealing model can be used to approximate rapid cooling of most samples following total annealing of fission tracks, assuming that OH has not had a significant effect on annealing behaviour.

Model runs for samples inferred to have cooled rapidly during the early Tertiary were constrained to allow cooling only from a maximum temperature of 150 °C in order to allow for the onset of track retention during cooling at rates of up to 10 °C/My (Willett 1997). Although thermal histories other than simple cooling might be permitted by the data, it was not the purpose of the modelling to explore these possibilities, but rather to constrain the onset of track retention during simple cooling. Other explicit constraints on the modelling include the present-day temperature of the samples and the time at which the modelling runs commenced. For the present purposes, models were run for 150 My to allow for the

possibility of slow cooling histories. Each modelling run accumulated 250 acceptable solutions based on a fit of fission track age and the track length data at a .05% level of confidence (Willett 1997). The retention age represents the oldest fission tracks in the sample that survive during cooling.

5.3.4 Vitrinite reflectance data

Polished mounts for vitrinite reflectance determination were made using samples from fresh coal seams and carbonaceous shales interbedded with clastic units from either outcrop or hydrocarbon exploration well cuttings. Reflectance measurements for all samples (cuttings and outcrop) were made under oil immersion using a Zeiss MPM II reflected light microscope equipped with UV excitation. All reported values are random measurements.

The vitrinite reflectance data presented in this study are from three sources. The Geological Survey of Canada (GSC) provided the bulk of the well data, whereas data from the outcrop samples were supplied by Global Geoenergy Research Ltd. (GGRL) and data from Taleman-J34 are by T. Gentzis. In order to assess possible systematic variations in R_o from two of the sources, five well samples from the Mid-Fiord J-53, Depot Point L-24 and Fosheim N–27 wells were analysed by GGRL for direct comparison with data provided by the GSC (Table 5.2). In one instance (Fosheim N–27, 701 m), the data provided by GGRL are lower by ~0.7% compared to nearby data supplied by the GSC. In four cases, the data are comparable. Although no systematic variation is obvious, this comparison highlights the subjective nature of grain selection for reflectance determinations.

The reproducibility of R_o data from GGRL was also assessed by the inclusion of a blind duplicate with the samples submitted for analysis. The R_o values obtained, 0.46% and 0.41%, are compatible within one standard deviation, indicating satisfactory precision for the data. In the following comparison of R_o and fission track data from well and outcrop samples, the thermal history interpretations were found to be generally compatible, with a few notable exceptions. These exceptions will be addressed individually in the following sections.

5.4 Interpretation of thermal history

5.4.1 Well samples

The depth at which fission tracks in apatite are inferred to have been totally annealed prior to Palaeocene cooling is illustrated in Fig. 5.2. This line also coincides broadly with R_o values of ~0.8% used to guide sampling (Arne and Zentilli 1994). A R_o value of ~0.8% corresponds to a temperature of ~125 °C for a heating time of 10 My (Burnham and Sweeney 1989). In Fig. 5.4, detailed fission track and vitrinite reflectance data for the six wells are plotted against depth along with the simplified stratigraphy for each well. Fission track analytical data for the well samples are presented in Table 5.1. All uncertainties are plotted or quoted at 2σ. Vitrinite reflectance data for all well samples are given in Table 5.2.

5.4.1.1 Depot Point L-24 well, Axel Heiberg Island

Vitrinite reflectance values in this well typically exceed 0.8% (Fig. 5.4a), suggesting that fission tracks in detrital apatite grains would have been totally annealed at some time following deposition of the sediments. This is supported by fission track ages from the four shallowest samples in the well. These range between 51 ± 8 Ma and 59 ± 10 Ma and are significantly younger than the respective Mesozoic stratigraphic ages of the samples (Table 5.1). The deepest sample, FT94-72, has a much younger age compared to the other samples in the well and this can be explained, at least in part, by its present-day temperature of 76 °C. The four shallowest samples give similar fission track ages over nearly 1.5 km of section, indicating rapid cooling during the early Tertiary.

Reflectance data from the Permian Van Hauen and Hare Fiord Formations range from 2.81 to 3.95% at depths greater than 3.5 km in the Depot Point L-24 well. Such high values are likely to indicate the great depth of burial of the upper Palaeozoic strata as well as the significant intrusion of diabase sills and dikes in the Depot Point area.

5.4.1.2 Fosheim N–27 well, Ellesmere Island

As in the case of the Depot Point L-24 well, vitrinite reflectance values from Fosheim N–27 typically exceed 0.8% (Fig. 5.4b), again suggesting that fission tracks in detrital apatite

Table 5.2. Vitrinite reflectance data from well samples.

*P.K. Mukhopadhyay analyst. All remaining data from the GSC, except for Taleman J-34 (T. Gentzis-analyst). Note that only samples with more than five analyses have been plotted in Fig. 5.4.

Taleman J-34 Well			Mid-Fiord J-53 Well			Fosheim N–27 Well		
Depth (m)	R_o(%)	n	Depth (m)	R_o(%)	n	Depth (m)	R_o(%)	n
100	0.49	50	473*	1.18	30	29	0.62	9
110	0.49	50	1131	1.27	3	305	0.84	5
145	0.53	50	1271	1.16	3	427	0.85	14
175	0.52	50	1387	1.06	6	488	0.87	17
190	0.55	50	1433	0.95	2	668	1.02	14
215	0.57	50	1509*	1.02	14	677	1.20	10
330	0.58	50	1591	1.46	9	685	1.07	6
355	0.56	50	1740	1.47	16	701*	0.38	16
375	0.56	50	1982*	2.46	20	3051	1.86	5
415	0.57	50				3810	1.82	18
430	0.56	50				3870	1.90	3
450	0.54	50						
505	0.56	50	Depot Point L-24 well			Neil 0-15 well		
545	0.57	50	Depth (m)	R_o(%)	n	Depth (m)	R_o(%)	n
565	0.55	50						
605	0.57	50	229	0.99	15	100	1.06	36
630	0.50	50	329	1.44	8		1.13	16
755	0.57	50	503*	1.10	12	381	0.51	4
815	0.59	50	716	1.09	10	511	0.56	2
875	0.55	50	1268	1.81	2	744	0.46	3
915	0.52	50	1493	1.40	4	1064	0.54	2
985	0.52	50	2316	1.72	4	1094	0.74	5
1015	0.51	50	2675	0.66	2	1141	0.67	4
1020	0.51	50	3414	2.81	8	1220	0.88	4

Taleman J-34 Well			Depot point L-24 well			Neil 0-15 well		
Depth (m)	R_o(%)	n	Depth (m)	R_o(%)	n	Depth (m)	R_o(%)	n
1135	0.58	50	3551	3.80	17	1585	1.61	7
1445	0.57	50	3719	3.51	11	1676	1.74	12
1475	0.56	50	3801	3.44	22	1957	0.85	2
1585	0.55	50	3871	3.95	30			
1605	0.60	50	3962	3.23	13			
1680	0.62	50						
1775	0.62	50						
1825	0.62	50						
2335	0.62	50						

Figure 5.4. Well profiles showing apatite fission track data, vitrinite reflectance measurements, and stratigraphy. (a) Depot Point L-24 well. (b) Fosheim N–27 well. (c) Taleman J-34 well. (d) Neil O-15 well. (e) Mid Fiord J-53 well. (f) Sherwood P-37 well.

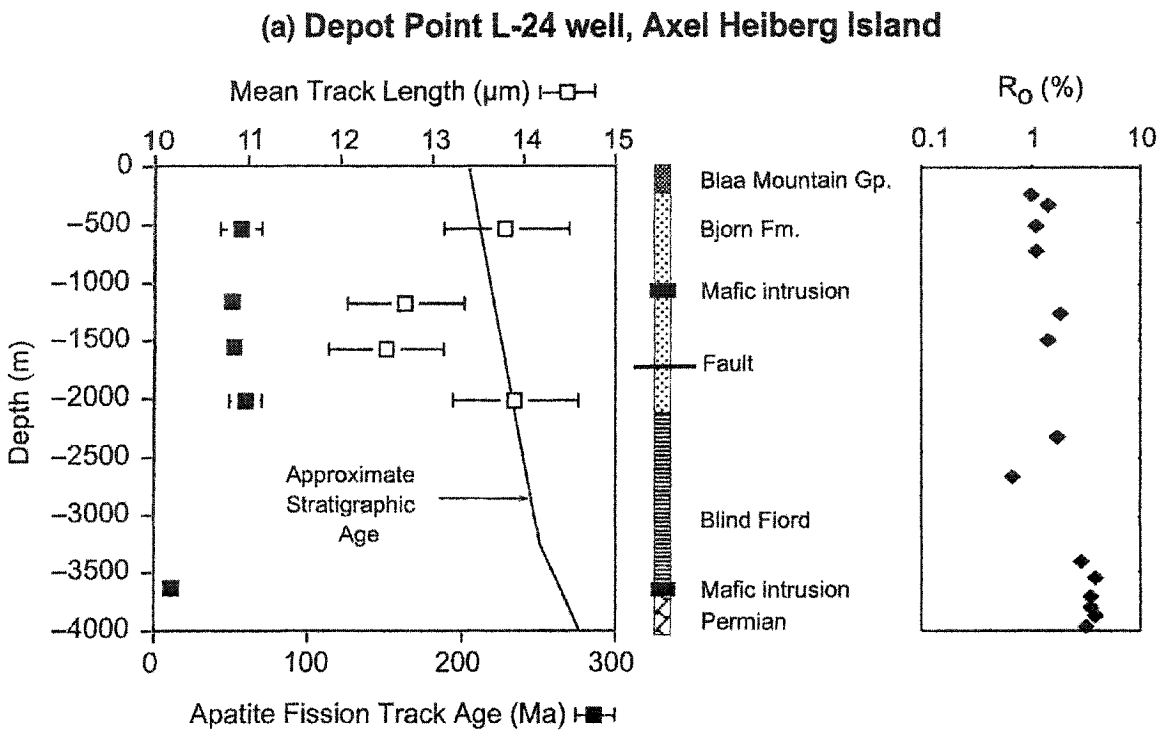
(a) Depot Point L-24 well, Axel Heiberg Island
Mean Track Length (μm)
10
11
12
13
14
15
0
−500
−1000
−1500
−2000
−2500
−3000
−3500
−4000
Depth (m)
Approximate
Stratigraphic
Age
0
100
200
300
Apatite Fission Track Age (Ma)
Blaa Mountain Gp.
Bjorn Fm.
Mafic intrusion
Fault
Blind Fiord
Mafic intrusion
Permian
R_O (%)
0.1
1
10

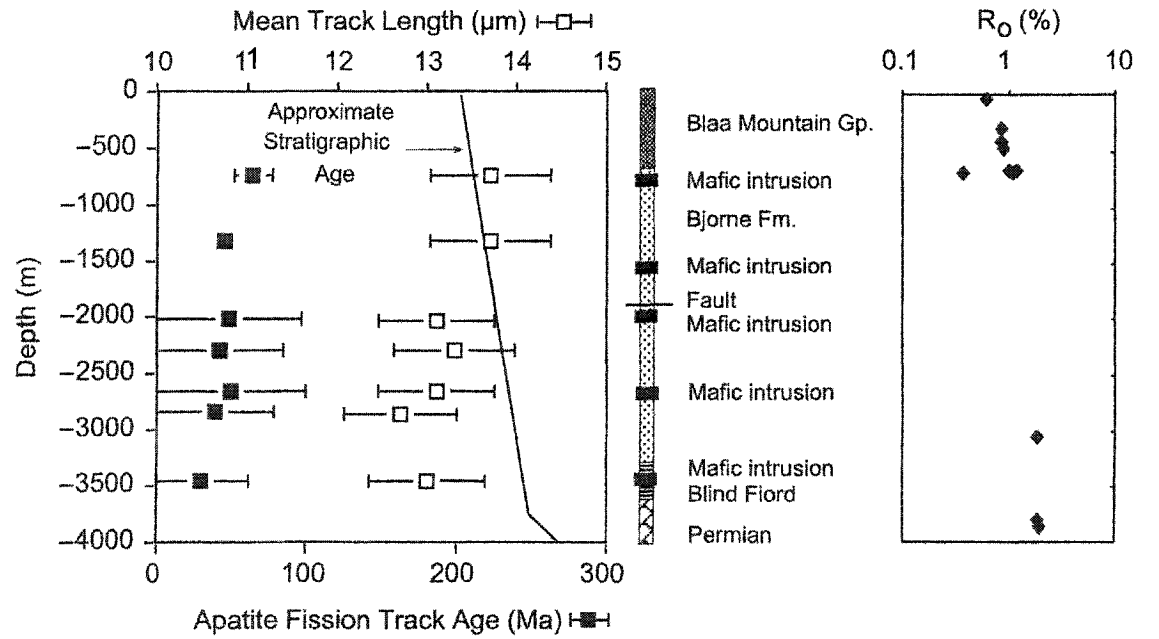
(b) Fosheim N-27 well, Ellesmere Island
Mean Track Length (μm)
10
11
12
13
14
15
0
−500
−1000
−1500
−2000
−2500
−3000
−3500
−4000
Depth (m)
Approximate
Stratigraphic
Age
0
100
200
300
Apatite Fission Track Age (Ma)
Blaa Mountain Gp.
Mafic intrusion
Bjorne Fm.
Mafic intrusion
Fault
Mafic intrusion
Mafic intrusion
Mafic intrusion
Blind Fiord
Permian
R_O (%)
0.1
1
10

Figure 5.4 (continued.)

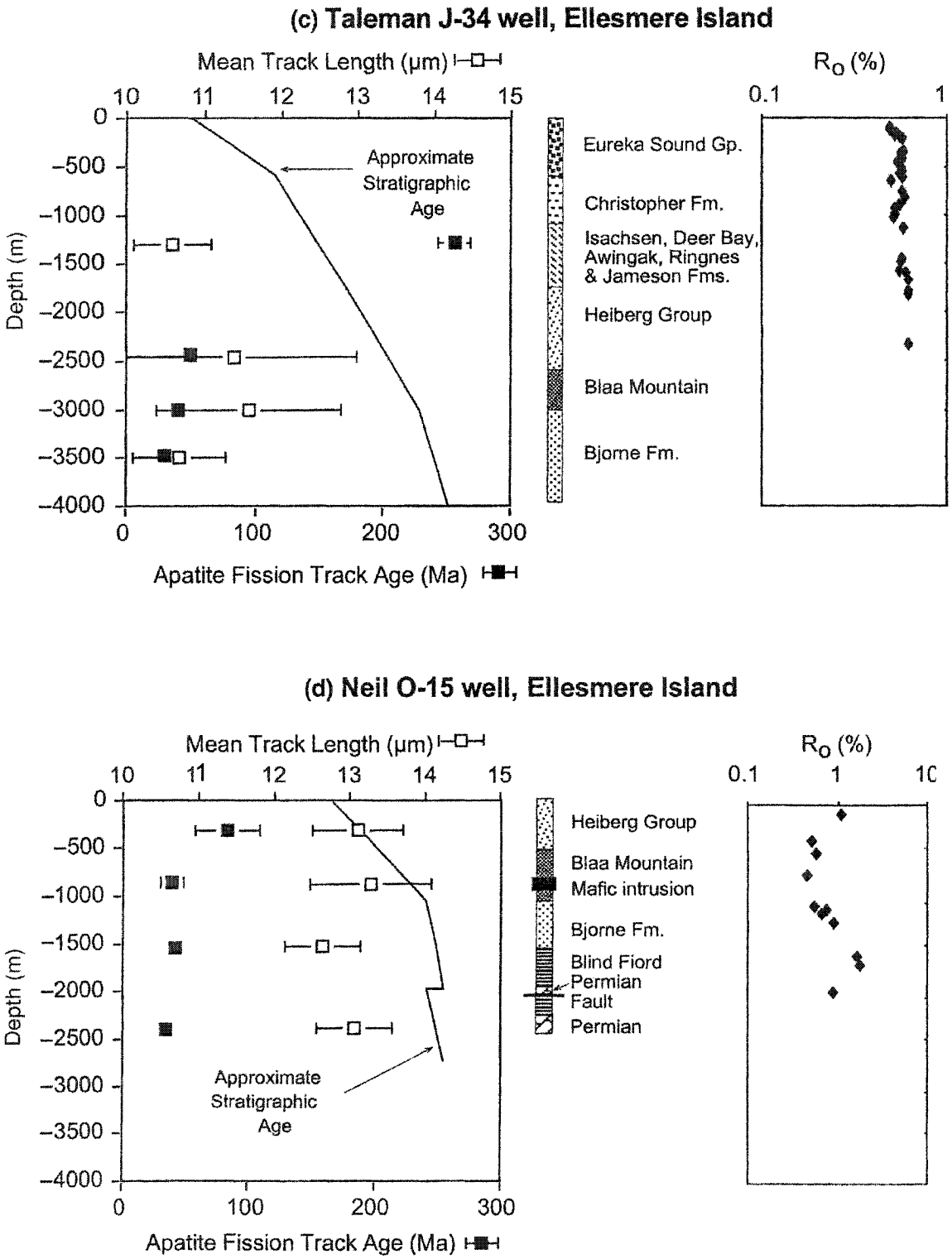

Figure 5.4 (continued.)

(e) Mid Fiord J-53 well, Axel Heiberg Island

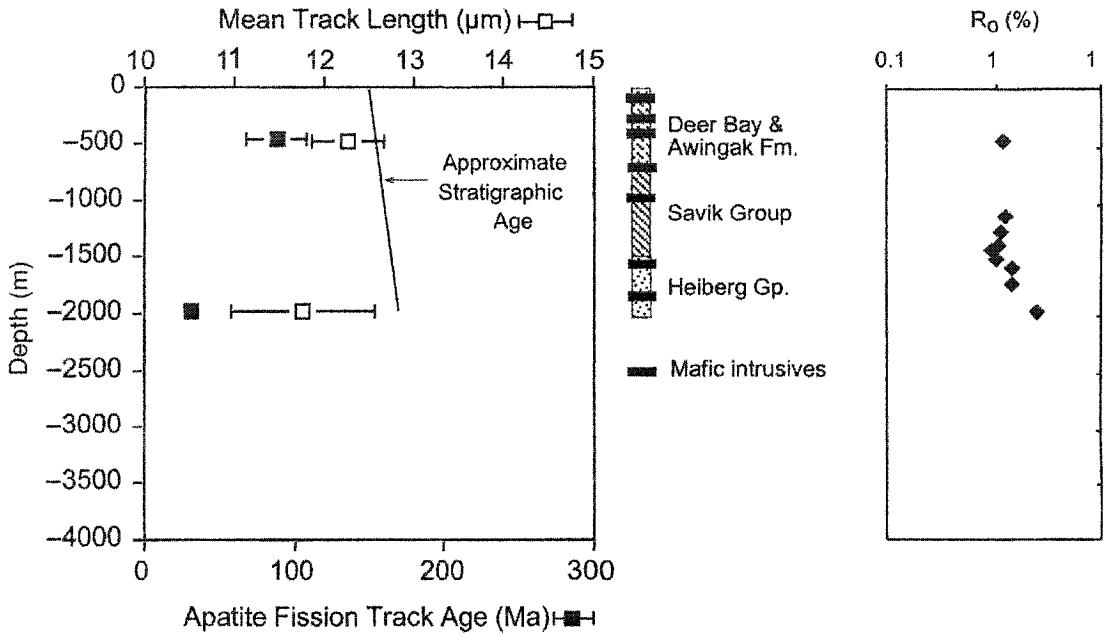

(f) Sherwood P-37 well, Axel Heiberg Island

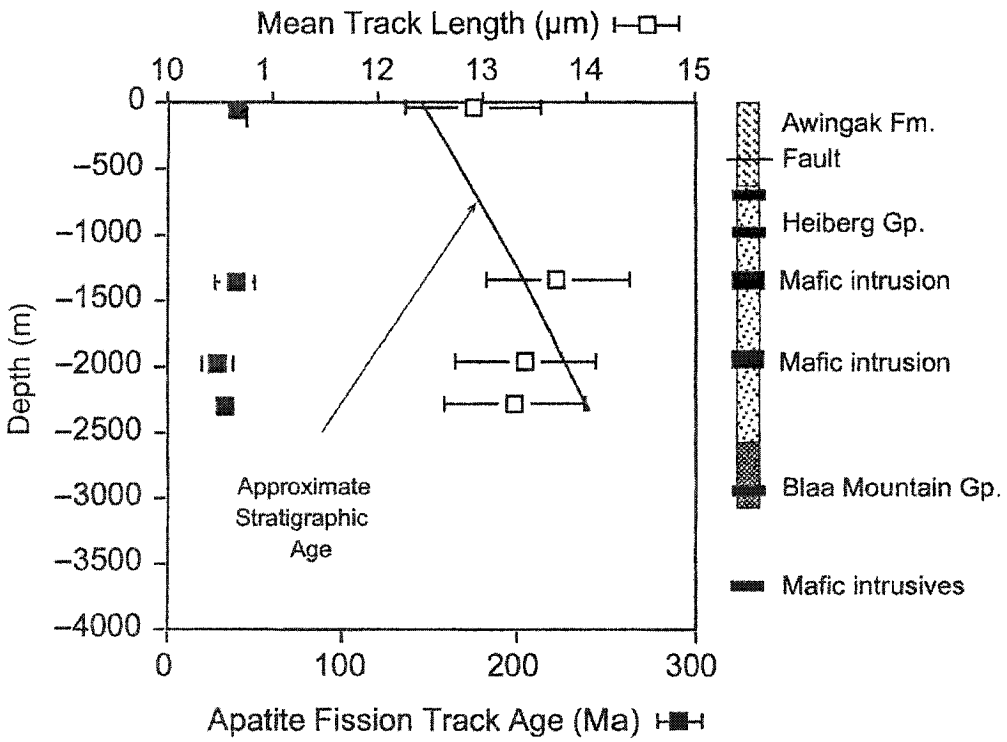

grains would have been totally annealed at some time following deposition of the sediments. This interpretation is supported by fission track ages ranging between 69 ± 14 Ma and 32 ± 13 Ma that are significantly younger than the stratigraphic age of the sediments or the inferred emplacement age of mafic sills. Mean track lengths decrease progressively from 13.7 ± 0.5 μm at the top of the well, to 12.7 ± 0.3 μm at a depth of 2.85 km. The similarity in both fission track age and mean track length over a depth interval of ~3 km is consistent with rapid cooling of the succession during the early Tertiary.

5.4.1.3 Taleman J-34 well, Ellesmere Island

Vitrinite reflectance data are less than 0.7% to a depth of 2.3 km in this well (Fig. 5.4c), suggesting that fission tracks in detrital apatite grains over this interval were not totally annealed at any time during burial. The shallowest sample, FT94-5, gives an age of 256 ± 34 Ma that is significantly older than the stratigraphic age of the sample, consistent with this interpretation. This sample also has a relatively short mean track length and a broad track length distribution indicating a significant degree of post-depositional partial annealing. The remaining four samples, FT94-7, 8, 9 and 85, all from depths greater than 2.4 km, give ages significantly less than their respective stratigraphic ages. Broad track length distributions and relatively short mean track lengths around 11 μm for these samples suggest partial track annealing followed by rapid cooling.

5.4.1.4 Neil O-15 well, Ellesmere Island

The fission track profile for Neil O-15 is similar to those of the Depot Point L-24 and Fosheim N–27 wells. Fission track ages are significantly less than the respective stratigraphic or magmatic emplacement ages of the samples, suggesting partial to total annealing of fission tracks following deposition. This conclusion is supported by sparse vitrinite reflectance data from the well, which are typically greater than 0.8%. However, individual apatite grains in the shallowest sample, FT94-81, show a significant spread in fission track age, with some grains giving ages significantly older than the stratigraphic age of the sample. In addition, the track length distribution for this sample is distinctly bimodal, consistent with a high degree

of partial track annealing in the sample prior to cooling. The age data therefore define a break-in-slope between 400 and 800 m, consistent with rapid cooling of the profile in the Tertiary (Fig. 5.4d).

5.4.1.5 Mid Fiord J-53 Well, Axel Heiberg Island

The two samples from the well give fission track ages significantly younger than their respective stratigraphic ages, consistent with R_o values greater than 0.8% (Fig. 5.4e). The shallowest sample, FT94-73, has a relatively broad track length distribution and contains a few apatite grains giving significantly older fission track ages than the central age population, indicating partial track annealing prior to final cooling. The vitrinite data, however, suggest that fission tracks in apatite from this sample of Upper Jurassic Awingak Formation were totally annealed following burial; this likely occurred during the intrusion of Lower Cretaceous sills in this area. The Late Cretaceous fission track age for sample FT94-73 is best interpreted as reflecting heat dissipation and cooling in the Late Cretaceous despite further subsidence, followed by significant Tertiary cooling.

The deeper of the two samples, FT94-75, gives a fission track age of 33 ± 6 Ma that is consistent with total annealing of fission tracks due to burial and sill intrusion prior to Tertiary cooling. A vitrinite sample from a core at the bottom of the well (1982 m) gives a relatively high R_o value of 2.46% compared to other samples in the well. The 50 m thick sill that occurs 75 m above the sample and the possibility of a sill below the bottom hole sample could account for such a high reflectance.

5.4.1.6 Sherwood P-37 well, Axel Heiberg Island

No vitrinite reflectance data are available for the Sherwood P-37 well, but the apatite fission track data indicate total annealing of fission tracks. Relatively consistent fission track ages and mean track lengths over a depth range of ~2 km indicate rapid cooling of the sequence during the early Tertiary (Fig. 5.4f). Such an interpretation is consistent with data from the Depot Point L-24 and Fosheim N–27 wells to the north. It is interesting to note that fission tracks in apatite from the Deer Bay and Awingak Formations on Axel Heiberg Island

were totally annealed following deposition. This is in contrast to the partially annealed samples of the Deer Bay and Awingak Formations from localities on Ellesmere Island (Taleman J-34, Hare Fiord/Chapman Glacier and Mt. Bridgman). This indicates either deeper burial due to substantial Cretaceous and early Tertiary sedimentation on Axel Heiberg Island, or a higher palaeogeothermal gradient compared with the Ellesmere localities, as suggested for the Mid Fiord J-53 well previously.

5.4.2 Outcrop samples

5.4.2.1 Fire Bay, Emma Fiord

A fault-bounded inlier of Eureka Sound Group occurs at Fire Bay on the south side of Emma Fiord (Fig. 5.5). At this locality the Eureka Sound Group consists of upper Palaeocene to lower Eocene Iceberg Bay Formation (coal member) overlain with angular unconformity by middle Eocene Buchanan Lake Formation (Ricketts and Stephenson 1994; Ricketts 1994). The coal member contains fining upward sequences up to 10 m thick and locally capped by coal beds up to several metres thick. Bedding dips moderately to the southeast towards the contact with lower Palaeozoic rocks, but bedding dips and grainsize fines to the northwest close to Emma Fiord, suggesting the presence of an anticline or faulting. The overlying Buchanan Lake Formation varies from moderately northwest dipping to sub-horizontal beds. It consists of a thick sequence of polymictic conglomerate interbedded with cross-bedded quartz sandstone indicative of high-energy sedimentation in a fluvial system. The surrounding pre-Cenozoic strata comprise Palaeozoic sedimentary and volcanic rocks of the Ordovician to Silurian Mount Rawlinson and Kulutingwak assemblages, Silurian Lands Lokk Formation and Carboniferous Emma Fiord Formation (Fig. 5.5). Mafic dykes of presumed Late Cretaceous age are common in lower Palaeozoic units and are locally found along the contact with the Iceberg Bay Formation. Clasts of Palaeozoic material occur within both units of the Eureka Sound Group and in addition, clasts of coal occur in the Buchanan Lake Formation.

Although the northeast bounding fault separating the Eureka Sound Group from Palaeozoic rocks (hereafter referred to as the Fire Bay fault) is not well exposed, the outcrop

pattern of the coal member suggests that it underlies the Mount Rawlinson and Kulutingwak assemblages, indicating reverse movement. Such an interpretation is consistent with the presence of a pronounced angular unconformity in the Eureka Sound Group suggesting folding of the coal member prior to deposition of the Buchanan Lake Formation. It is also supported by evidence of overturning of coal member beds in close proximity to the fault, and the presence of coal clasts in the Buchanan Lake Formation presumably derived from the underlying coal member.

R_o values from coal beds within the coal member range from 0.24% to 0.29%, indicating minimal post- depositional heating of the Eureka Sound Group (Table 5.3). This conclusion is further supported by apatite fission track data from both the Iceberg Bay and Buchanan Lake Formations that are significantly older than the Tertiary stratigraphic ages of the samples. Palaeozoic samples in the hanging wall of the Fire Bay fault give similar Mesozoic fission track ages, consistent with the local derivation of sediment during Eureka Sound deposition. Mean track lengths from the Eureka Sound samples are 0.5 to 1.0 μm less than those from the Palaeozoic samples (Table 5.4), suggesting minor post-depositional heating (i.e. < 50 °C) of the Eureka Sound samples. Modelling of the fission track data from a sample from the Mount Rawlinson and Kulutingwak assemblages (FT94-101) indicates prolonged cooling of the lower Palaeozoic succession. The onset of track retention in this sample is inferred to be at approximately 140 Ma, followed by gradual cooling to present-day temperatures, although this age should be taken as a minimum estimate for the initiation of cooling. Modelling indicates that this locality, which is on the northern flank of the Sverdrup Basin, was exhumed in earliest Cretaceous during initiation of volcanism. Subsequent Cretaceous and Tertiary sedimentation in this area was apparently modest such that fission tracks in apatite from the Franklinian basement rocks did not undergo significant annealing. These data are compatible with this locality being on the rifted flank of the Amerasia Basin, which opened in Early Cretaceous.

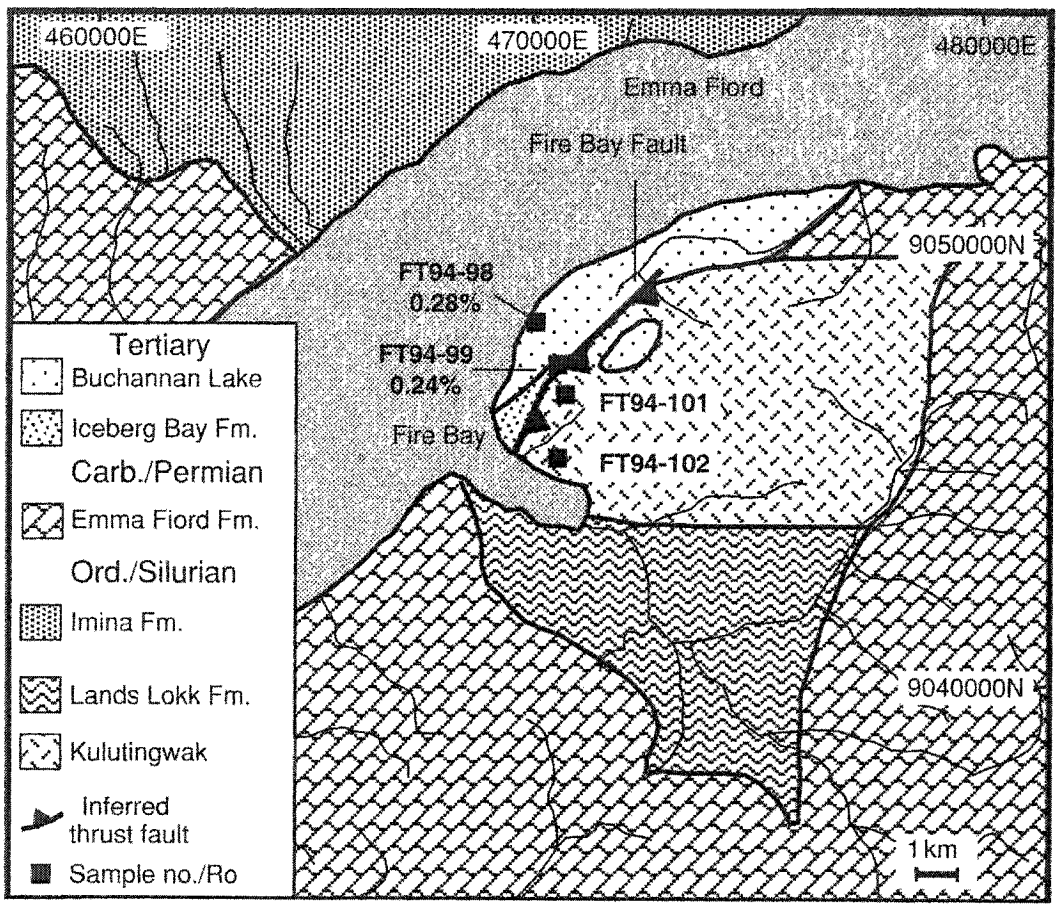

Figure 5.5. Geology and samples locations from Emma Fiord, Ellesmere Island (see Fig. 5.1 for location). Modified from Okulitch (1988).

5.4.2.2 Hare Fiord/Chapman Glacier

Samples were collected at two localities across faults from the Lake Hazen fault zone (Okulitch and Trettin 1991) to determine the timing of the most recent cooling across this structure. Samples were collected from Palaeozoic strata in the hanging wall of thrust faults at the eastern end of Hare Fiord and near Chapman Glacier, and in Mesozoic strata in the footwall of the eastern continuation of the faults directly east of Chapman Glacier (Fig. 5.6). Syntectonic sediments in the footwall of one of the en echelon faults comprising the Lake Hazen fault zone indicate an Eocene to Oligocene timing for denudation of the hanging wall (Miall 1991).

The Cambrian Grantland Formation is thrust over a succession of Carboniferous-Permian strata between Hare Fiord and Chapman Glacier, which in turn are thrust over Mesozoic strata. The Rollrock Fault is a splay off the Lake Hazen fault zone that terminates at Tanquary Fiord. All five samples from the hanging wall of the Lake Hazen fault zone give fission track ages in the range 44 to 53 Ma and mean track lengths around 14 μm, indicating rapid cooling during the early Tertiary.

The footwall succession to the east of Chapman Glacier consists of Upper Triassic to Lower Cretaceous strata dipping moderately to the northeast, obliquely toward the thrust fault. No detrital apatite was recovered from the Heiberg Formation. Vitrinite from a section of Savik Group (Jurassic) containing dark brown, petroliferous shale and siltstone gives a R_o value of 0.63% (Table 5.3). Apatite in a massive sandstone from the Jurassic Awingak Formation directly overlying the Savik Group gives a central age of 57 ± 11 Ma, with a mean track length of 12.1 μm (Table 5.4). A bimodal track length distribution in this sample suggests partial annealing of fission tracks prior to final cooling in the Tertiary, which is consistent with a R_o of 0.63% for the Savik Group sample. Apatite grains from a sample of Lower Cretaceous Isachsen Formation, also from the eastern edge of the Chapman Glacier (Fig. 5.6), show a significant spread in fission track age, for which a central age of 281 ± 64 Ma has been calculated. Fission tracks in this sample have clearly been less annealed than the underlying Awingak sample prior to Tertiary cooling, and suggest preservation of a partially annealed profile in the footwall of the Lake Hazen fault zone. The transition from

Sample no.	Stratigraphic Unit	Location	R_o (%)	S.D (%)	n
DA94-33	Eureka Sound Group	Fire Bay, Emma Fiord	0.29	0.04	51
DA94-34	Eureka Sound Group	Fire Bay, Emma Fiord	0.28	0.02	51
DA94-35	Eureka Sound Group	Fire Bay, Emma Fiord	0.24	0.03	29
DA94-45	Blaa Mountain Group	Mt. Schuchert, Blue Mountains	0.96	0.11	37
DA94-51	Ringes Formation	Mt. Schuchert, Blue Mountains	2.17	0.24	35
DA94-58	Savik Group	Chapman Glacier, Tanquary Fiord	0.63	0.07	51
DA94-62	Upper Heiberg Formation	Fosheim Anticline	0.70	0.03	50
DA94-65	Awingak Formation	Fosheim Anticline	0.41	0.04	52
DA94-67	Isachsen Formation	Fosheim Anticline	0.50	0.03	50
DA94-70	Hassel Formation	Fosheim Anticline	0.42	0.07	53
DA94-73	Expedition Formation	Fosheim Anticline	0.46	0.03	51
DA94-75	Christopher Formation	Vesle Fiord, Sawtooth Range	0.54	0.08	51
DA94-77	Lower Kanguk Formation	Vesle Fiord, Sawtooth Range	0.34	0.05	35
DA94-79	Strand Bay Formation	Vesle Fiord, Sawtooth Range	0.48	0.02	50
DA94-81	Strand Bay Formation	Vesle Fiord, Sawtooth Range	0.53	0.03	50
DA94-83	Strand Bay Formation	Vesle Fiord, Sawtooth Range	0.46	0.03	50
DA94-94	Blaa Mountain Group	Mt. Bridgman, Sawtooth Range	0.34	0.02	33
DA94-96	Blaa Mountain Group	Mt. Bridgman, Sawtooth Range	0.48	0.05	45
DA94-98	Upper Heiberg Formation	Mt. Bridgman, Sawtooth Range	0.37	0.03	51
DA94-101	Strand Bay Formation	Mt. Bridgman, Sawtooth Range	0.47	0.05	50
DA94-103	Strand Bay Formation	Mt. Bridgman, Sawtooth Range	0.48	0.03	50
DA94-116	Expedition Formation*	Fosheim Anticline	0.41	0.03	50

*Blind duplicate sample of DA94-73.

Table 5.3. Vitrinite reflectance data from outcrop samples.

Table 5.4. Apatite fission track age and length data for outcrop samples.

*Second aliquot irradiated with ^{252}Cf for tack length measurements. Samples with χ^2 probability of >.05 pass the χ^2 test at the 95% confidence level. Ages for these samples are calculated using pooled statistics. Ages of samples that fail the χ^2 test are calculated using the central age equation (Galbraith and Laslett 1993). ρ_d, ρ_s and ρ_i are the density of dosimeter glass (CN-5 or CN-1) fossil and induced tracks ($x10^5/cm^2$). Numbers of tracks counted or measured are shown in parentheses. Ages of samples marked with a cross (†) were calculated using a zeta factor of 105.4 ± 1.8 (CN-1 glass). All other ages use a zeta of 345.3 ± 12 (CN-5 glass). Error estimates are at the 2σ confidence level. Analyses by A.M. Grist.

Sample onset number	Rock unit	Stratigraphic age (Ma)	Grains counted	ρ_d (n_d)	ρ_s (n_s)	ρ_i (n_i)	Chi squared prob.	Fission track age (Ma)	Mean length (μm)	Std. Dev. (μm)	Modelled onset age (Ma)
FT94-098*	Buchanan Lake Fm.	57–39	9	9.99 (7200)	6.89 (154)	8.29 (183)	0.5005	144 ± 33	12.4 ± 0.8 (33)	2.2	
FT94-099*	Iceberg Bay Fm.	57–50	13	9.99 (7200)	4.06 (255)	7.43 (467)	0.011	96 ± 22	12.7 ± 0.3 (138)	1.9	
FT94-101	Rawlinson Fm.	460–410	22	9.99 (7200)	14.1 (1080)	20.6 (1577)	0.1664	117 ± 13	13.4 ± 0.3 (117)	1.7	
FT94-102	Rawlinson Fm.	460–410	19	9.99 (7200)	10.8 (251)	13.2 (307)	0.9735	140 ± 26	13.2 ± 0.6 (44)	2.1	
FT94-103*	Borup Fm.	320–310	24	9.99 (7200)	6.22 (255)	22.2 (911)	0.0507	48 ± 8	13.8 ± 0.3 (126)	1.6	66 ± 6
FT94-104*	Grant Land Fm.	530–520	14	11.4 (3200)	4.24 (163)	16.7 (643)	0.456	50 ± 9	13.7 ± 0.3 (66)	1.3	65 ± 6
FT94-105	Blaa Mountain Gp.	240–220	18	9.99 (7200)	6.18 (168)	24.4 (663)	0.3063	44 ± 8	13.7 ± 0.7 (11)	1.1	
FT94-107	Blind Fiord Fm.	245–240	26	9.99 (7200)	9.39 (187)	35.2 (702)	0.9963	46 ± 8	13.7 ± 0.6 (15)	1.2	
FT94-108	Blind Fiord Fm.	245–240	26	9.99 (7200)	5.20 (294)	20.6 (1164)	0.9999	43 ± 7	13.5 ± 0.3 (113)	1.4	63 ± 4
FT94-109	Hoyle Bay Fm.	230–225	27	11.4 (3200)	9.33 (616)	33.9 (2235)	0.8907	54 ± 6	13.8 ± 0.3 (106)	1.3	70 ± 3
FT94-110*	Mafic sill	144–65	25	11.4 (3200)	1.33 (87)	4.50 (293)	0.9987	58 ± 15	13.4 ± 0.3 (92)	1.8	80 ± 9
FT94-113	Heiberg Fm.	215–180	19	11.4 (3200)	20.0 (882)	9.79 (431)	0	331 ± 74	10.2 ± 0.8 (63)	3	
FT94-114	Isachsen Fm.	128–110	9	11.4 (3200)	13.1 (164)	8.90 (111)	0.1896	283 ± 73	11.6 ± 1.1 (10)	1.7	
FT94-117	Borup Fm.	320–310	15	11.4 (3200)	4.14 (98)	15.1 (358)	0.7003	53 ± 13	14.1 ± 0.5 (21)	1.1	
FT94-118	Grant Land Fm.	530–520	28	11.4 (3200)	5.08 (534)	21.8 (2293)	0.9152	46 ± 5	13.9 ± 0.3 (110)	1.5	62 ± 3
FT94-120*	Awingak Fm.	145–135	16	11.4 (3200)	7.49 (161)	25.7 (553)	0.6159	57 ± 11	13.1 ± 0.4 (121)	1.9	
FT94-121	Isachsen Fm.	128–110	25	11.4 (3200)	4.17 (595)	2.78 (397)	0	281 ± 64	10.9 ± 0.4 (134)	2.4	
FT94-126†	Christopher Fm.	112–97	26	35.6 (9000)	7.06 (408)	11.5 (666)	0.9308	114 ± 15	12.3 ± 0.3 (141)	1.8	
FT94-129	Mokka Fiord Fm.	60–45	24	10.6 (8000)	4.61 (349)	6.66 (504)	0.0887	125 ± 20	12.8 ± 0.4 (58)	1.6	
FT94-143	Bjorne Fm.	245–241	24	10.6 (8000)	26.2 (3848)	28.2 (4145)	0	131 ± 24	12.7 ± 0.4 (150)	2.2	
FT94-144	Pat Bay Fm.	227–225	2	10.2 (6000)	8.86 (33)	8.59 (32)	0.8901	179 ± 89	12.0 ± 1.3 (7)	1.6	
FT94-145	Awingak Fm.	215–180	9	10.2 (6000)	28.6 (428)	20.9 (314)	0	254 ± 76	12.6 ± 0.4 (94)	1.7	
FT94-146*	Christopher Fm.	112–97	16	10.2 (6000)	6.50 (109)	11.1 (186)	0.9096	102 ± 26	13.0 ± 0.3 (85)	1.4	
FT94-147*	Mount Lawson Fm.	61–57	25	10.2 (6000)	2.00 (117)	3.57 (209)	0.9655	98 ± 24	12.7 ± 0.3 (127)	1.8	
FT94-153	Bjorne Fm.	245–241	25	10.7 (8600)	7.02 (597)	23.0 (1957)	0.5733	56 ± 7	13.7 ± 0.3 (116)	1.5	72 ± 2
FT94-154	Bjorne Fm.	245–241	27	10.7 (8600)	10.7 (646)	24.0 (1453)	0	82 ± 17	12.6 ± 0.4 (132)	2.5	
FT94-157	Bjorne Fm.	245–241	22	10.7 (8600)	7.84 (520)	20.8 (1382)	0.0007	70 ± 10	12.9 ± 0.4 (121)	2.2	
FT94-158	Bjorne Fm.	245–241	26	10.7 (8600)	8.99 (748)	19.8 (1646)	0.102	83 ± 10	12.6 ± 0.4 (131)	2.2	
FT94-159	Bjorne Fm.	245–241	28	10.7 (8600)	9.85 (743)	21.8 (1645)	0.7543	83 ± 10	12.9 ± 0.4 (122)	2.3	

total to partially annealed samples probably occurs in either the Jurassic Savik Group or the Upper Triassic to Lower Jurassic Heiberg Formation.

5.4.2.3 Mount Schuchert, Blue Mountains

A well exposed profile through the Mesozoic succession in the northern Sverdrup Basin occurs on the southern flank of the Blue Mountains near Mount Schuchert (Fig. 5.1b). The sequence dips moderately toward the southeast where it is exposed on the northern limb of a northeast-trending syncline in the hanging wall of a major thrust fault (Fig. 5.7) and ranges in age from Triassic in the northwest to Lower Cretaceous in the southeast. Mafic sills are common within the succession. A section was sampled in detail to constrain the fission track profile through the Mesozoic sequence prior to Tertiary cooling.

Four samples distributed through the Mesozoic stratigraphic section and one mafic sill of inferred Cretaceous age gave indistinguishable apatite fission track ages ranging from 43 ± 7 Ma to 58 ± 15 Ma, with mean track lengths between 13.3 and 13.8 μm. These data, as well as the lack of variation in age through a section 1.8 km thick, suggest that fission tracks in the section were totally annealed prior to cooling in the Tertiary. Vitrinite from a sample of Triassic Murray Harbour Formation in the same section gives a R_0 value of 0.96% (Table 5.3), consistent with total annealing of fission tracks in the samples at some time after deposition. Modelling fission track data in three of these samples, FT94-108, FT94-109 and FT94-110, indicates that track retention commenced in the latest Cretaceous or Palaeocene for these samples.

A sample of sandstone (FT94-113) from the top of the Heiberg Formation (Lower Jurassic) and a sample of Lower Cretaceous Isachsen Formation (FT94-114) give central ages of 331 ± 74 Ma and 283 ± 73 Ma, respectively (Table 5.4). Both samples have relatively short mean track lengths and broad track length distributions. Single grain fission track ages significantly older than the respective stratigraphic ages of the samples coupled with mixed track length distributions are consistent with partial annealing of these samples prior to cooling. A sample of vitrinite from the Jurassic Ringnes Formation gives a R_0 value of 2.17%

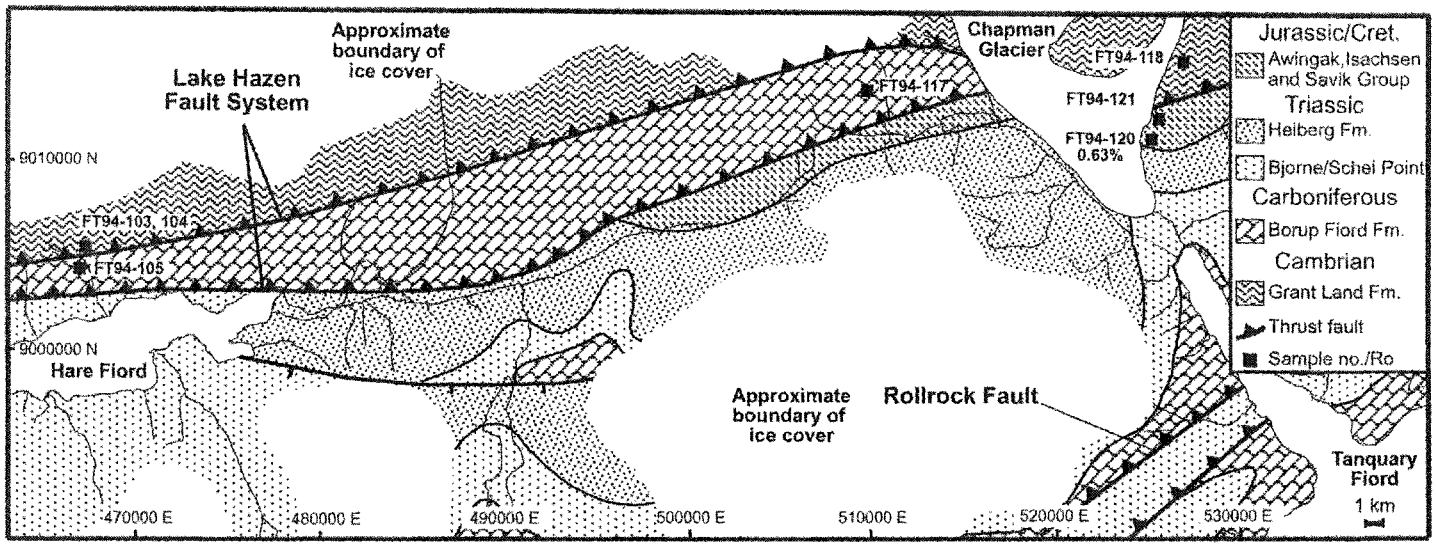

Figure 5.6. Geology of the Lake Hazen fault zone between Hare Fiord and Chapman Glacier, Ellesmere Island (see Fig. 5.1 for location), modified from Okulitch (1988). Fission track sample localities and vitrinite reflectance data are also given.

(Table 5.3) that is clearly inconsistent with the fission track data from this part of the section. The reflectance data are therefore either due to reworked organic material in the unit, to weathering and oxidation of pyrite in the sequence at surface, or to the local thermal effects of Cretaceous magmatism.

A totally to partially annealed fission track profile is therefore preserved at the surface at Mount Schuchert. Based on the available sample distribution, the transition from samples in which fission tracks in apatite were totally annealed prior to cooling, to those samples in which fission tracks were only partially annealed, occurs somewhere within the Heiberg Formation or the upper part of the Blaa Mountain Group. This estimate is broadly similar to that inferred for the Chapman Glacier region.

5.4.2.4 Fosheim Anticline, Ellesmere Island

The Fosheim anticline exposes a continuous stratigraphic section from Triassic Blaa Mountain Group in its core to Tertiary Eureka Sound Group on its northern flank (Fig. 5.8). Approximately 3 km of relatively undisturbed section outcrops in this region, although the northeastern flank of the anticline is disrupted by a series of north- to northwest-trending faults and a series of minor folds. Tertiary sediments on Fosheim Peninsula are Campanian to early Eocene in age and a major unconformity separates the Tertiary strata from the underlying, very thin Upper Cretaceous strata (Ricketts 1994).

Four coal samples from the Jurassic to Tertiary succession give vitrinite reflectance values ranging from 0.41 to 0.50%, whereas a sample of Upper Triassic/Lower Jurassic Heiberg Formation coal gives a value of 0.70% (Table 5.3). These vitrinite reflectance data suggest that fission tracks in apatite through the sequence would not have been totally annealed following deposition (Arne and Zentilli 1994). This conclusion is supported by fission track data from a sample of sandstone from the Christopher Formation and a sample

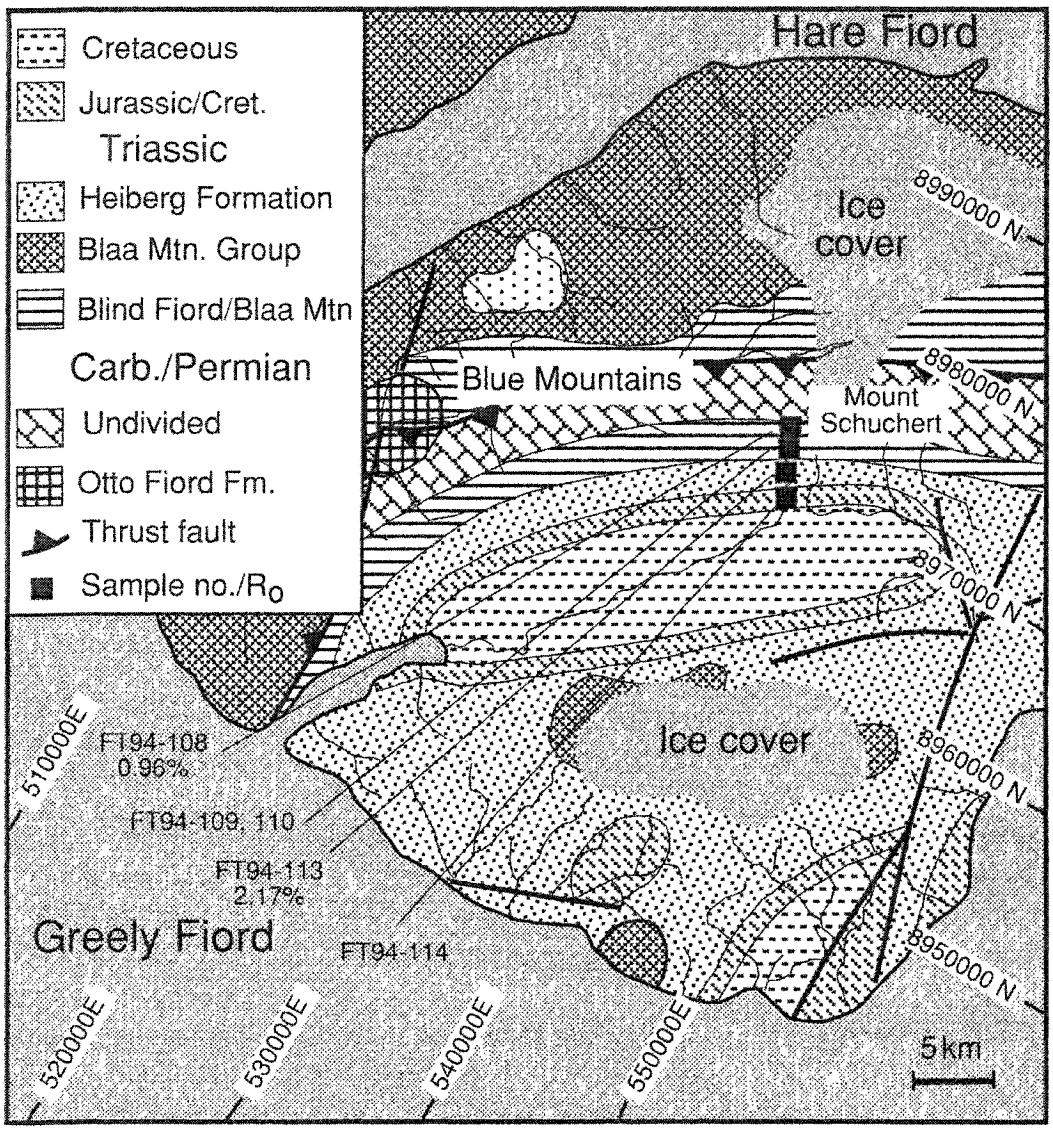

Figure 5.7. Geology of the Blue Mountains, Ellesmere Island (see Fig. 5.1 for location), modified from Okulitch (1988). Also shown are fission track sample locations and vitrinite reflectance values.

of Iceberg Bay Formation giving ages of 114 ± 15 Ma and 125 ± 20 Ma, respectively (Table 5.4). In the case of the Christopher Formation sample, the fission track age is indistinguishable from the stratigraphic age, probably due to the incorporation of volcanic material (Embry 1991b), whereas the apatite in the sample of Iceberg Bay sandstone is clearly dominated by a detrital age component. Thus neither sample shows clear evidence for significant post-depositional heating.

5.4.2.5 Mount Bridgman, Sawtooth Range

The Sawtooth Range is the topographic manifestation of the Vesle Fiord and East Cape thrust faults, a major fault system on the eastern margin of the Sverdrup Basin that juxtaposes Permian carbonate rocks over Tertiary Eureka Sound Group (De Paor et al. 1989). Three localities were sampled along the Sawtooth Range; two profiles in the Mount Bridgman region sampled the footwall and hanging wall of the East Cape Thrust (Fig. 5.9), and a continuous profile near Vesle Fiord sampled both the footwall and hanging wall of the Vesle Fiord thrust fault. Results from the profile across the Vesle Fiord thrust fault are reported in Arne et al. (1998).

The Eureka Sound Group dips west towards the thrust fault in the Vesle Fiord region, sub-parallel to the fault plane (Arne et al. 1998). A syncline cored by Eureka Sound Group occurs in the footwall of the East Cape thrust fault in the northern Sawtooth Range near Mount Bridgman (Fig. 5.9). The western limb of this syncline is in turn truncated by the East Cape thrust fault which has carried west-dipping Permian to Triassic sediments over a steep to moderately east-dipping Triassic to Tertiary succession.

The most common unit of the Eureka Sound Group exposed in the footwalls of both the Vesle Fiord and East Cape thrust faults is the Strand Bay Formation of Ricketts (1994) which is mid-Palaeocene in age. Thus thrusting had to occur during the mid-Palaeocene or later. The Palaeocene timing for the onset of cooling inferred from modelling of apatite fission track data from the hanging wall of the Vesle Fiord thrust fault is consistent with this constraint (Arne et al. 1998).

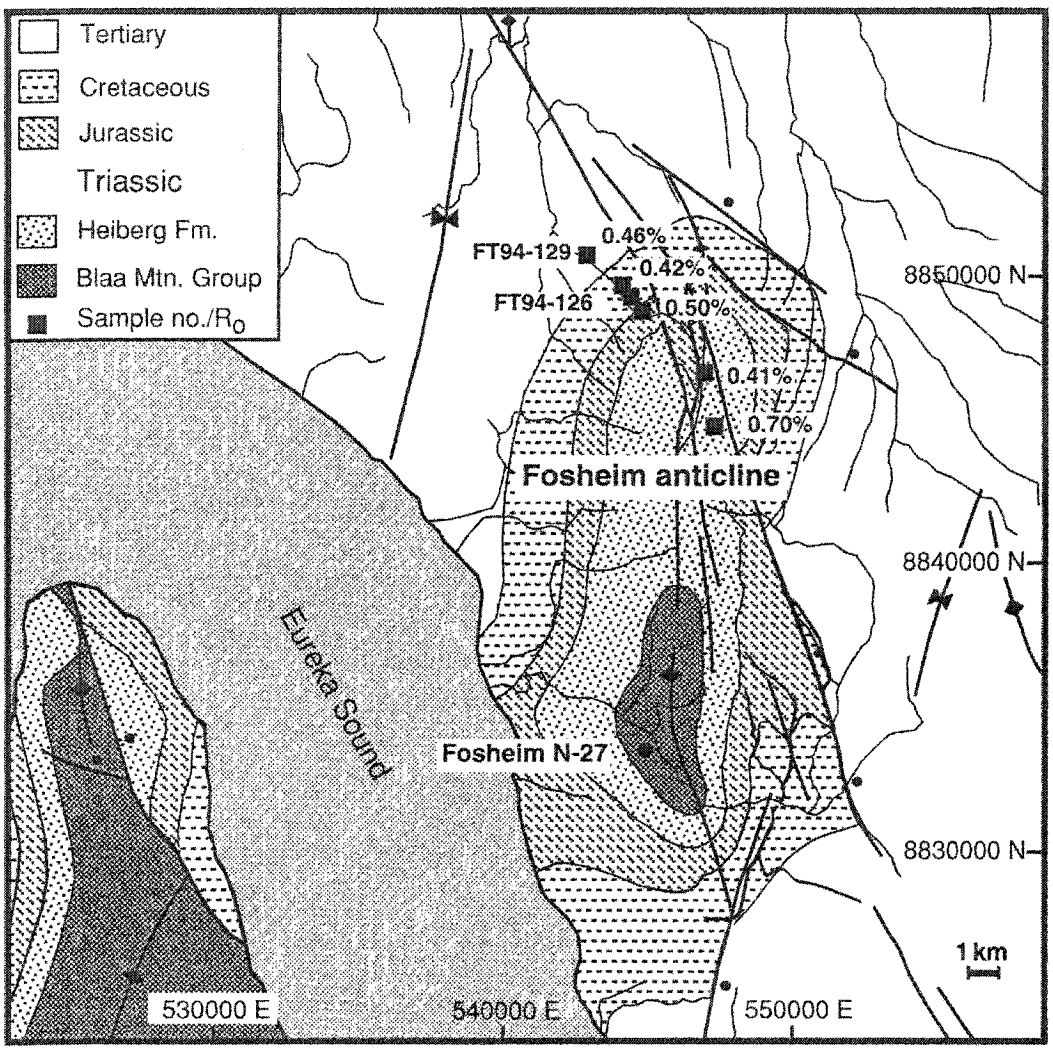

Figure 5.8. Geology of the Fosheim Anticline, Fosheim Peninsula, Ellesmere Island (see Fig. 5.1 for location), simplified after Thorsteinsson (1972a). Fission track sample localities and vitrinite reflectance data are also shown.

Samples FT94-143 to 147 were collected on the western limb of the syncline forming the footwall of the East Cape thrust fault from a stratigraphic sequence ranging in age from Triassic to Tertiary (Fig. 5.9). Vitrinite from samples of Lower Triassic carbonaceous shales and Upper Triassic to Tertiary coal samples give reflectance values between 0.34 and 0.48%, and show no consistent variation over ~2 km of section (Table 5.3). These data indicate that the footwall sequence was never heated to temperatures sufficient to totally anneal fission tracks in detrital apatite grains, consistent with the data presented in Table 5.4.

Sample FT94-143 from the Triassic Bjorne Formation gives a central fission track age of 134 ± 24 Ma, significantly younger than the stratigraphic age of the sample. However, individual apatite grains in this sample show a significant spread in fission track age, as indicated by a χ^2 probability <.05, with some individual grains giving fission track ages indistinguishable from the stratigraphic age. Along with the broad track length distribution for this sample (2.2 μm), the fission track age data indicate significant partial annealing of fission tracks in the sample prior to cooling. Samples from higher in the sequence, FT94-144 to 147, give fission track ages similar to their respective stratigraphic ages, consistent with their having undergone only partial track annealing prior to Palaeocene cooling.

Apatite was not obtained from the Permian section west of Mount Bridgman. However, two samples of Triassic Bjorne Formation gave fission track ages significantly younger than the stratigraphic age of the samples (Table 5.4), indicating appreciable post-depositional annealing of fission tracks. The stratigraphically lower of the two, sample FT94-153, gives a pooled fission track age of 56 ± 7 Ma and a mean length of 13.7 ± 0.3 μm, consistent with this sample having been totally annealed prior to rapid cooling during the early Tertiary. By contrast, individual apatite grains in sample FT94-154 give a significant spread in fission track age, and the mean track length is significantly shorter than that obtained from sample FT94-153. These differences, along with the broad spread about the mean in the track length distribution, indicates that fission tracks in apatite from sample FT94-154 were not completely annealed prior to cooling in the early Tertiary.

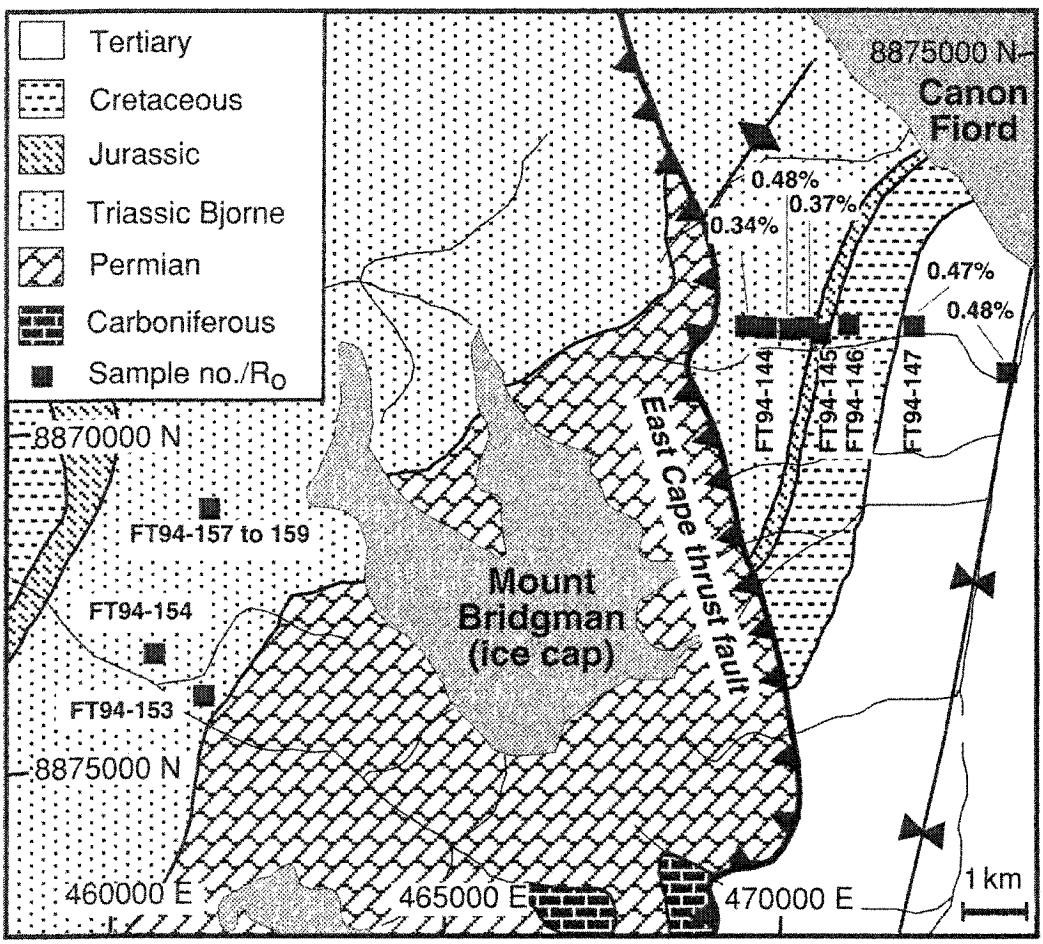

Figure 5.9. Geology of the northern Sawtooth Range (see Fig. 5.1 for location), simplified after Thorsteinsson (1972b). Fission track sample localities and vitrinite reflectance data are also shown.

5.4.2.6 Contact halo suite

A suite of three samples of Bjorne Formation sandstone were collected at distances of 0.9, 4.5 and 45 m from the contact of a mafic dyke ~23 m thick inferred to be of Cretaceous age (Fig. 5.9). These samples were analysed in order to assess the thermal affects associated with Cretaceous magmatism at ca. 115 to 95 Ma (Embry 1991b). Samples FT94-157 to 159 (in order of increasing distance from the contact) give fission track ages between 70 and 83 Ma, and are in general similar to data obtained from sample FT94-154 collected several kilometres away from the dyke. There is therefore no direct evidence for Cretaceous heating associated with dyke emplacement preserved in the samples, as the fission track data in all samples are dominated by Tertiary cooling.

5.5 Discussion

5.5.1 Time of cooling

The fission track data from outcrop and shallow well samples are summarized in Fig. 5.10, a plot of mean confined track length against fission track age. Samples in which fission tracks were totally annealed prior to cooling rapidly during the early Tertiary have mean track lengths of ~14 μm and form a tight grouping in this figure. Samples with older fission track ages and shorter mean track lengths are interpreted to have undergone partial track annealing to various degrees prior to Tertiary cooling (Green 1986). Also apparent on this figure are two samples with fission track ages of ~130 Ma and mean track lengths around 13 μm that were obtained from Emma Fiord on Ellesmere Island. These samples appear to have cooled during the Mesozoic and to have undergone minimal subsequent heating, consistent with R_o data from Tertiary rocks at Emma Fiord.

The cooling history of ten of these samples has been modelled to constrain the onset of track retention, and thus provide a lower limit on the initiation of cooling (Fig. 5.11), as cooling may also have occurred prior to the onset of track retention. The histogram shown in Fig. 5.11 represents the results of 2500 acceptable cooling history paths for ten rapidly cooled outcrop samples, including data from Arne et al. (1998), and displays a symmetrical distribution of retention ages about a weighted mean of 66 ± 3 Ma. This timing, calculated

from samples over a large area of the northern Sverdrup Basin, overlaps a 61 ± 3 Ma age inferred for cooling of the hanging wall of the Vesle Fiord thrust fault (Arne et al. 1998), suggesting that the initiation of cooling during the Palaeocene was of regional extent. As the onset of track retention ages indicates the time at which fission tracks first began to accumulate in the sample during cooling, the modelling provides only a lower limit on the onset of cooling in the samples. Cooling may have been initiated as early as the Late Cretaceous and was thus well in progress during deposition of the Eureka Sound Group.

5.5.2 Regional cooling patterns

Both the apatite fission track and vitrinite reflectance data from structural culminations, such as the Fosheim anticline, or from the hanging walls of major thrust faults, such as the Lake Hazen fault zone, Vesle Fiord fault and East Cape fault, clearly show evidence for significant cooling (Fig. 5.12). Outcrop and well samples in which fission tracks were totally annealed prior to the Palaeocene have cooled from above ~120 °C, the precise value depending on apatite composition and cooling rate. For these samples, the maximum temperature prior to cooling can be estimated from the vitrinite reflectance data using the distributed activation model of Burnham and Sweeney (1989) for a heating duration of 1 My. No R_o data are available from the Sherwood P-37 well, and the data from the Neil O-15 well are generally of poor quality (i.e. few measurements). However, based on the fission track data alone, strata from below a depth of 500 m in Neil O-15 have cooled from temperatures greater than 120 °C. R_o data from depths greater than 500 m in Fosheim N–27 suggest maximum temperatures of between 130 and 185 °C, consistent with evidence from the fission track data for temperatures in excess of ~120 °C. The R_o data suggest that the Mesozoic sequence in Depot Point L-24 has been heated to maximum temperatures in the range 140-175 °C. Even Mesozoic rocks from Taleman J-34, which was drilled off-structure, have been heated to temperatures of 80 to 105 °C based on the R_o data, although the fission track data suggest slightly higher temperatures. Vitrinite reflectance data from the Mid Fiord J-53 well from western Axel Heiberg Island suggest maximum temperatures of 150 to 205 °C prior to Late Cretaceous-Tertiary cooling, possibly due to Cretaceous magmatism.

Comparison of estimated maximum palaeotemperatures with present-day temperatures suggests 145 to 175 °C of cooling in Depot Point L-24, 125 to 165 °C of cooling in Mid Fiord J-53, ~120 °C of cooling in Fosheim N–27, 100 °C of cooling in Neil O-15, and ~65 °C of cooling in Taleman J-34. The cooling indicated for these wells is a cumulative effect and includes ~15 °C of cooling in mean seawater temperatures from the Eocene to present-day (Miall 1991) in addition to cooling during the Eurekan Orogeny.

A distinct break in fission track age across the East Cape thrust fault indicates differential cooling across the structure, similar to that described for the Vesle Fiord fault in the southern Sawtooth Range (Arne et al. 1998). Modelling of the fission track data from sample FT94-153 suggests that track retention commenced in the Late Cretaceous, at 72 ± 2 Ma. This timing is significantly older than the stratigraphic age of the youngest sediments preserved in the core of the footwall syncline to the east (Middle Palaeocene to Lower Eocene). Therefore, cooling of the East Cape Fault hanging wall commenced during sedimentation onto the footwall, although there is no direct evidence for syntectonic deposition. The inferred onset of track retention is also significantly older than the 61 ± 3 Ma estimated for the hanging wall of the Vesle Fiord Fault by Arne et al. (1998), consistent with an eastward decrease in the time of thrusting.

Another break in fission track age occurs near Chapman Glacier where Cambrian and Carboniferous strata were thrust over a folded Triassic to Cretaceous succession across the Lake Hazen fault zone. Modelling of fission track data from three hanging wall samples from between Hare Fiord and Chapman Glacier gives consistent Palaeocene ages for the onset of track retention (Table 5.4), with a weighted mean of 62 ± 2 Ma. As fission tracks in the Palaeozoic samples were totally annealed prior to Tertiary cooling, any record of earlier cooling events related to the late Palaeozoic Ellesmerian Orogeny has been lost. Preservation of an annealing profile showing evidence for early Tertiary cooling in the Mesozoic footwall stratigraphic sequence of the Lake Hazen fault zone, as well as at Mount Schuchert, also indicates that maximum palaeotemperatures were attained in the Mesozoic sequence in these two areas immediately prior to the Eurekan Orogeny.

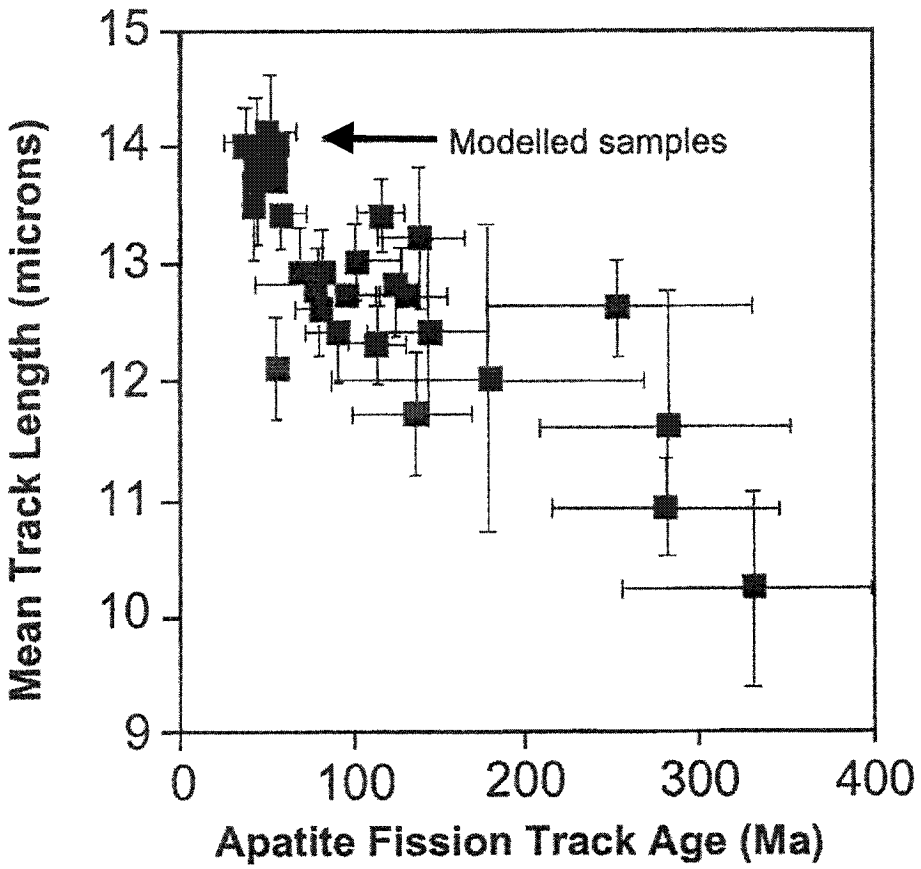

Figure 5.10. Summary of fission track data from outcrop and shallow well samples. Those samples used for modelling purposes are indicated by the arrow.

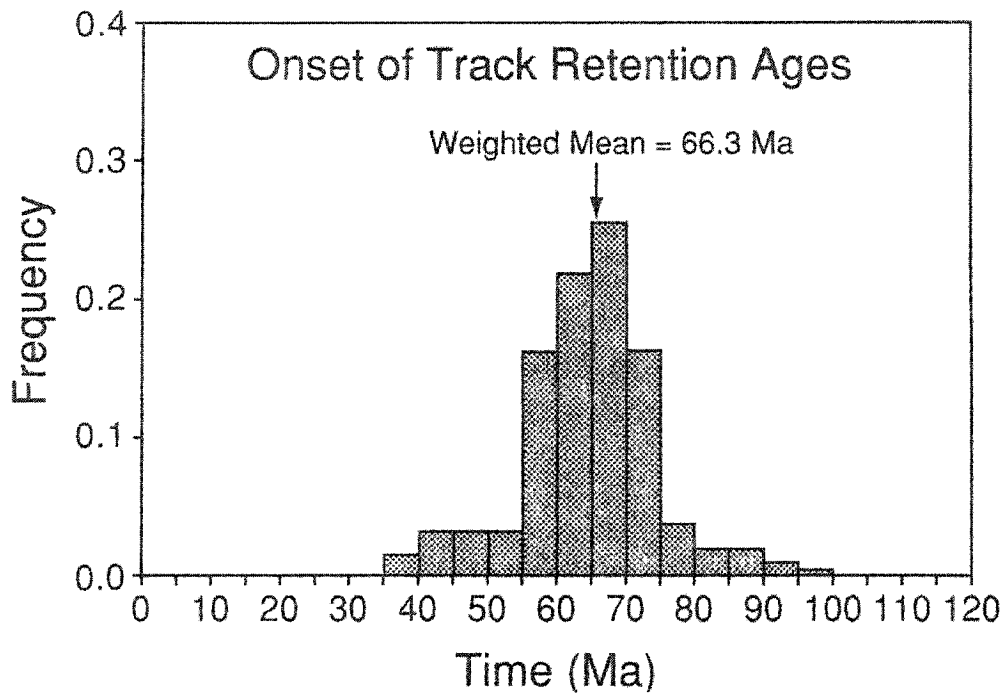

Figure 5.11. Summary of ages estimated for the onset of track retention from 10 outcrop samples from northern Ellesmere Island.

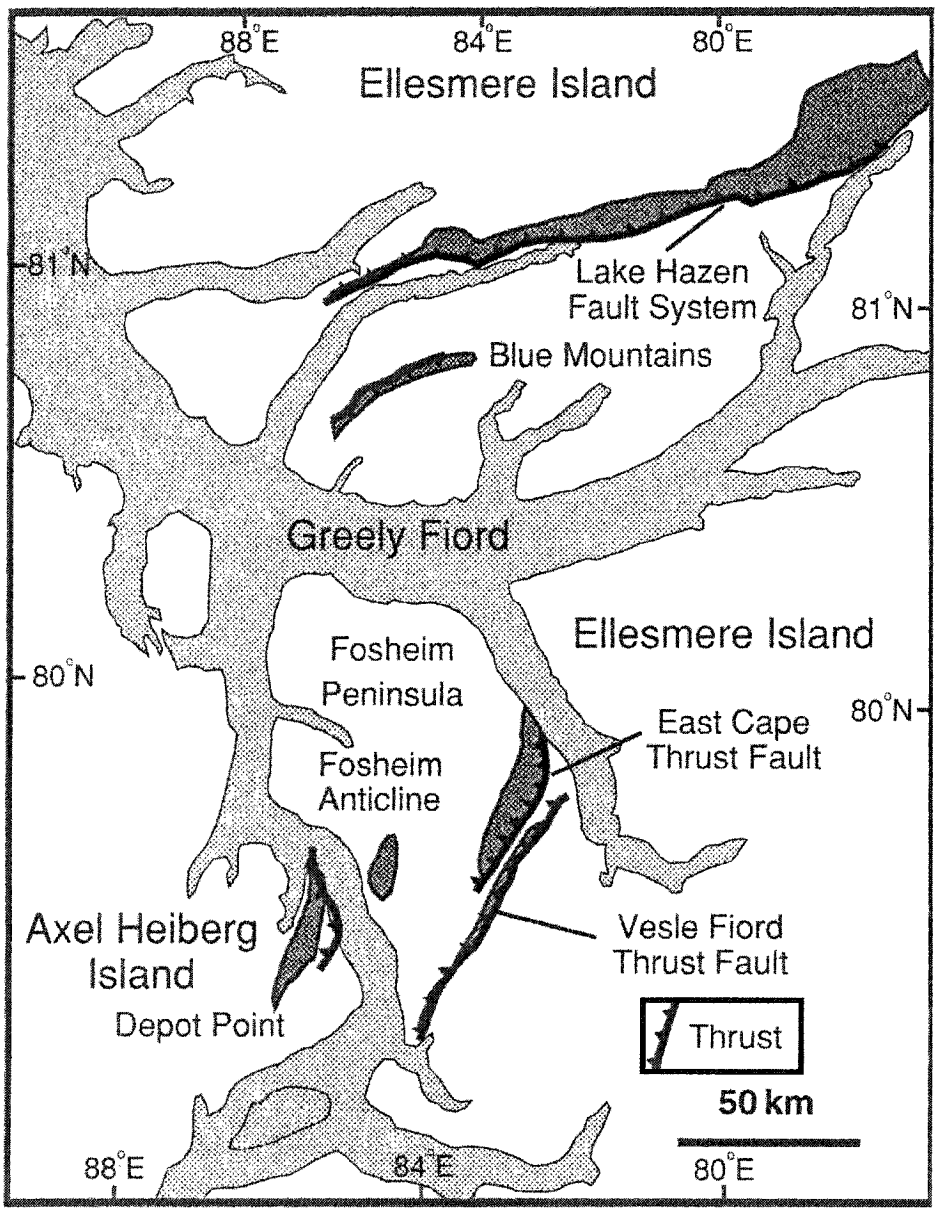

Figure 5.12. Geographic distribution of cooling in the Sverdrup Basin (see Fig. 5.1 for location). The shaded areas represent late Palaeozoic to early Mesozoic rocks in which detrital apatite grains are inferred to have been totally annealed prior to the onset of latest Cretaceous to early Tertiary cooling.

The significance of cooling of the hanging walls of thrust faults having stratigraphic offsets on the scale of kilometres has been discussed by Arne and Zentilli (1994), Arne et al. (1997, 1998), and Arne (2000). Several possibilities exist to explain differential cooling histories across thrust faults, including contrasts in geothermal gradients during or following thrusting due to juxtaposition of rocks having different thermal conductivities, or local variations in heat flow due to the effects of topographically driven groundwater flow. Alternatively, cooling variations may reflect denudational contrasts across the structure during or shortly after thrusting. In each instance, cooling occurs as a direct consequence of faulting, and thus timing constraints from fission track data can be inferred indirectly to reflect the time of thrusting (Arne 2000). Any lag between thrusting and cooling due to groundwater circulation and/or erosion is likely to fall within the uncertainties typically associated with fission track data (i.e. ± 10%).

Ultimately, the cooling of thrust plates is likely to occur in response to a combination of influences, the relative importance of which will vary depending on local relief, climate and changes in base level (Kooi and Beaumont 1996). Having stated this, it is difficult to envision that local contrasts in geothermal gradients would produce the regional effects observed in the northern Sverdrup Basin, especially where cooling has also occurred off major structures. Therefore, it seems likely that Mesozoic and Tertiary cooling is related to erosion that accompanied tectonic inversion of the Sverdrup Basin during the Eurekan Orogeny. As would be expected, denudation was greatest on structural culminations and the hanging walls of major thrust faults, but was superimposed upon a less significant, but broader scale denudation of the entire northern Sverdrup Basin. This interpretation is consistent with the conclusion of Ricketts and Stephenson (1994) that the Sverdrup Basin was tectonically active by the Palaeocene, even though Palaeocene sediments on eastern Fosheim Peninsula are interpreted to have been deposited in a low-energy depositional environment (Miall 1991).

These results contrast markedly with fission track results from Devonian rocks south of the Sverdrup Basin. Here, samples from wells on Melville, Cameron and Banks Islands (Fig. 5.1) show clear evidence for cooling during the early to middle Triassic (Arne et al.

1995). Cooling in these wells was probably due largely to denudation of the Franklinian Mobile Belt on the southern margin of the Sverdrup Basin and is consistent with a rapid influx of sediment into the Sverdrup Basin from the south during the early Triassic (Embry 1991b, 1993).

5.5.3 Implications for hydrocarbon maturation

Arne and Zentilli (1994) reviewed the use of integrated apatite fission track thermochronology and vitrinite reflectance data to constrain the timing of maximum burial temperatures in foreland basins relative to thrusting. A distinct break in R_o values across structures indicates that maximum temperatures and, by inference, peak hydrocarbon generation and primary migration predated deformation, assuming no later reactivation. Such a situation does not necessarily preclude maximum temperatures after deformation deeper in the section due to tectonic burial (Deming and Chapman 1989), but does diminish the likelihood that hydrocarbons were locally generated and structurally trapped at shallow depths.

Both the regional data, and detailed profiles across individual structures support the attainment of maximum temperatures in much of the exposed Mesozoic section of the northern Sverdrup Basin prior to the Eurekan Orogeny, particularly in the hanging walls of thrust faults. This conclusion has important implications for the hydrocarbon prospectivity of Eurekan structures, as it implies that hydrocarbon generation within potential Mesozoic source rocks such as the Blaa Mountain Gp., Jameson Bay Fm., Kanguk Fm. and Ringnes Fm. (Leith et al. 1992) predated the development of many of the structural traps presently found at shallow (i.e. < 3 km) levels. Significant hydrocarbon generation in the northeastern Sverdrup Basin may have occurred within the Mesozoic section associated with thrust stacking and tectonic burial of the succession. Support for this suggestion comes from the footwall of the East Cape thrust fault where R_o values are similar through several kilometres of section (Fig. 5.9), consistent with the attainment of maximum palaeo-temperatures following tilting of the sequence. In this regard, it is worthwhile to note that carbonaceous beds within the Tertiary Strand Bay Formation contain bituminite, suberinite and abundant

cutinite, and thus would make good source rocks for hydrocarbons (P. Mukhopadhyay, pers. comm., 1994). Future hydrocarbon exploration in the northeastern Sverdrup Basin should therefore focus on sub-thrust plays to test potential structural traps at depth.

5.6 Summary

Apatite fission track and vitrinite reflectance data in both outcrop and well samples from the eastern margin of the northern Sverdrup Basin indicate that the presently exposed and shallowly buried Mesozoic section began cooling from maximum burial temperatures during the Palaeocene, or possibly as early as the latest Cretaceous, and continued cooling through the Eocene. The extent of Tertiary cooling was greatest on structural culminations and the hanging walls of thrust faults, but also occurred off-structure (e.g. Taleman J-34), indicating that cooling was associated with tectonic inversion and regional denudation of the northern Sverdrup Basin during the Eurekan Orogeny. Maximum temperatures in the Mesozoic section predated thrusting, suggesting that peak hydrocarbon generation and primary migration preceded the formation of structural traps during the Eurekan Orogeny.

5.7 Acknowledgements

This study was funded by a Canadian Natural Sciences and Engineering Research Council Strategic Grant to M. Zentilli (STR0149876). Logistical support by the Polar Continental Shelf Program and the Geological Survey of Canada (GSC) is also gratefully acknowledged. In particular, we would like to thank Benoit Beauchamp of the GSC for his support. Guodong Li assisted with mineral separations and Dr. Dale Issler provided the AFTINV32 modelling software used in this study. Additional vitrinite reflectance data were supplied by P.K. Mukhopadhyay of Global Geoenergy Research Ltd. Halifax. R.L. Fleischer of Rensselaer Polytechnic Institute, Troy, kindly provided the ^{252}Cf irradiations. Casey Ravenhurst supplied the method of calculating OH in apatite. Paul Green kindly provided the vitrinite modelling software. Detailed reviews by Kerry Gallagher, Andrew Miall and Charlotte Cederbom for Basin Research were most appreciated.

5.8 References cited

Arne, D.C. 2000. Cooling of thrust sheets. 9th International Conference on Fission-track Dating and Thermochronology, Geological Society of Australia Abstract Series, **58**, 9-10.

Arne, D. and Zentilli, M. 1994. Apatite fission-track thermochronology integrated with vitrinite reflectance. In; Vitrinite Reflectance as a Maturity Parameter: Applications and Limitations Edited by P.K. Mukhopadhyay and W.G. Dow. American Chemical Society Symposium Series, **570**, pp. 249-268.

Arne, D.C., Embry, A., Zentilli, M. and Collins, M. 1995. Thermal and tectonic history of the Sverdrup Basin and Franklinian Mobile Belt, Canadian Arctic Archipelago. Geological Association of Cananada Mineraogical Association of Canada Abstract, **20**, 4.

Arne, D., Worley, B., Wilson, C.J.L., Chen, S., Luo, Z., Liu, S. and Dirks, P. 1997. Differential exhumation in response to episodic thrusting along the eastern margin of the Tibetan Plateau. Tectonophysics, **280**, 239-256.

Arne, D.C., Zentilli, M., Grist, A.M., and Collins, M. 1998. Constraints on the timing of thrusting during the Eurekan orogeny, Canadian Arctic Archipelago: an integrated approach to thermal history analysis. Canadian Journal of Earth Sciences, **35**, 1: 30-38.

Brooks, P.W., Embry, A.F., Goodarzi, F. and Stewart, R. 1992. Organic geochemistry and biological marker geochemistry of Schei Point Group (Triassic) and recovered oils from the Sverdrup Basin (Arctic Islands, Canada). Bulletin of Canadian Petroleum Geology, **40**, 173-187.

Burnham, A.K. and Sweeney,J.J. 1989. A chemical kinetic model of vitrinite reflectance maturation. Geochemica. Et Cosmochemica Acta, **53**, 2649-2657.

Crowley, K.D., Cameron, M. and Schaeffer, R.L. 1991. Experimental studies of annealing of etched fission tracks in fluorite. Geochimica et Cosmochimica Acta, 55, 1449-1465.

Davies, G.R. and Nassichuk, W.W. 1991. Carboniferous and Permian history of the

Sverdrup Basin, Arctic Islands. In Geology of the Innuitian Orogen and Arctic Platform of Canada and Greenland. Edited by H.P. Trettin. Geological Survey of Canada, Geology of Canada **3**, pp. 345-367.

De Paor, D.G., Bradley, D.C., Eisenstadt, G. and Phillips, S.M. 1989. The Arctic Eurekan Orogen: a most unusual fold-and-thrust belt. Geological Society of America Bulletin, **101**, 952-967.

Deming, D. and Chapman, D.S. 1989. Thermal histories and hydrocarbon generation: Example from Utah-Wyoming thrust belt. Geological Society of America Bulletin, **73**, 1455-1471.

Donelick, R.A., Bergman, S.C. and Talbot, J. 1992. 252Cf irradiation of apatite fission track samples improves spontaneous, confined, track-in-track (TINT) densities. 7th International Workshop on Fission-track Thermochronology, Philadelphia, Program with Abstracts, 80.

Embry, A.F. (1991a) Middie-Upper Devonian clastic wedge of the Arctic Islands.In Geology of the Innuitian Orogen and Arctic Platform of Canada and Greenland. Edited by H.P. Trettin. Geological Survey of Canada, Geology of Canada **3**, pp. 263-279.

Embry, A.F. (1991b) Mesozoic history of the Arctic Islands. In; Geology of the Innuitian Orogen and Arctic Platform of Canada and Greenland. Edited by H.P. Trettin. Geological Survey of Canada, Geology of Canada **3**, pp. 371-433.

Embry, A,F. 1993. Transgressive-regressive (T-R.) sequence stratigraphy of the Jurassic succession of the Sverdrup Basin, Canadian Arctic Archipelago. Canadian Journal of Earth Sciences, **30**, 301-320.

Embry, A.F. and Johannessen, E.P. 1992. T-R. sequence stratigraphy, facies analysis and reservoir distribution in the uppermost Triassic-Lower Jurassic succession, western Sverdrup basin, Arctic Canada. In; Arctic Geology and Petroleum Potential. Edited by T.O. Vorren, E. Bergsager, E. Dahl-Stamnes, E. Holter, B. Johansen, E. Lie and T.B. Lund, Norwegian Petroleum Society, Special Publication **2**, pp.121-146.

Embry, A.F. and Osadetz, K.G. 1988. Stratigraphy and tectonic significance of Cretaceous volcanism in Queen Elizabeth Islands, Canadian Arctic Archipelago. Canadian

Journal of Earth Sciences, **25**, 1209-1219.

Embry, A.F., Powell, T.G. and Mayr, U. 1991. Petroleum resources, Arctic Islands. In: Geology of the Innuitian Orogen and Arctic Platform of Canada and Greenland. Edited by H.P. Trettin. Geological Survey of Canada, Geology of Canada **3**, pp. 517-525.

Galbraith, R.F., and Laslett, G.M. 1993. Statistical models for mixed fission track ages. Nuclear Tracks and Radiation Measurements, **21**: 459-470.

Gentzis, T. and Goodarzi, F. 1991. Thermal maturity and hydrocarbon potential of the sedimentary succession from the Hecla field in Sverdrup Basin, Arctic Canada. International Journal of Coal Geology, **19**, 483-517.

Gentzis, T. and Goodarzi, F. 1992a. The source-rock potential and thermal maturity of the sedimentary succession in the Drake and Hecla hydrocarbon fields, Melville Island, Canadian Arctic Archipelago. In; Arctic Geology and Petroleum Potential. Edited by T.O. Vorren, E. Bergsager, E. Dahl-Stamnes, E. Holter, B. Johansen, E. Lie and T.B. Lund, Norwegian Petroleum Society, Special Publication **2**, pp. 159-171.

Gentzis, T. and Goodarzi, F. 1992b. Thermal maturity and source-rock potential in northwestern Melville Island, Arctic Canada. Energy Sources, **14**, 423-442.

Gentzis, T. and Goodarzi, F. 1993. Regional thermal maturity in the Franklinian Mobile Belt, Melville Island, Arctic Canada. Marine and Petroleum Geology, **10**, 215-230.

Gentzis, T., De Freitas, T.,Goodarzi, F., Melchin, M. and Lenz, A. 1996. Thermal maturity of Lower Paleozoic sedimentary successions in Arctic Canada. Bulletin of the American Association of Petroleum Geologists, **80**, 1065-1084.

Gleadow, A.J.W., Duddy, I.R., Green, P.F. and Lovering, J.F. 1986. Confined fission track lengths in apatite -a diagnostic tool for thermal history analysis. Contributions in Mineralogy and Petrology. **94**, 405-415.

Green, P.F. 1985. A comparison of zeta calibration baselines in zircon, sphene and apatite. Chemical Geology (Isotope Geoscience Section), **58**, 1-22.

Green, P.F. 1986. On the thermo-tectonic evolution of Northern England: Evidence from fission track analysis. Geology Magazine, **123**, 493-506.

Green, P.F., Duddy, I.R., Gleadow, A.J.W., Tingate, P.R., and Laslett, G.M. 1986. Thermal annealing of fission tracks in apatite 1. A qualitative description: Chemical Geology, **59**: 237-253.

Green, P.F., Duddy, I.R. and Bray, R.J. 1995. Applications of thermal history reconstruction in inverted basins. In; Basin Inversion, Edited by J.G. Buchanan and P.G. Buchanan, Geological Society Special Publishers, **88**, 149-165.

Harrison, J.C., Mayr, U., McNeil, D.H., Sweet, A.R., McIntyre, D.J., Eberle, J.J., Harrington, C.R., Chalmers, J.A., Dam. G., and Nøhr-Hansen, H. 1999. Correlation of Cenozoic sequences of the Canadian Arctic region and Greenland: implication for the tectonic history of northern North America. Bulletin of Canadian Petroleum Geology, **47**, 3: 223-254.

Henao-Londono, D. 1977. A preliminary geochemical evaluation of the Arctic Islands. Bulletin of Canadian Petroleum Geology, **25**, 1059-1084.

Hurford, A.J. 1990. Standardization of fission track dating calibration: recommendation by the Fission track Working Group of the I.U.G.S. Subcommission on Geochronology. Chemical Geology (Isotope Geoscience Section), **80**, 171-178.

Issler, D.R. 1996. Optimizing time step size for apatite fission track annealing models. Computers and Geosciences, **22**, no.1, 67-74.

Jones, F.W., Majorowicz, J.A. and Embry, A.F. 1989. A heat flow profile across the Sverdrup Basin, Canadian Arctic Islands. Geophysics, **54**, 171-180.

Kooi, H. and Beaumont, C. 1996. Large-scale geomorphology: Classical concepts reconciled and integrated with contemporary ideas via a surface process model. Journal of Geophysical Research, **101**, 3361-3386.

Laslett, G.M., Green, P.F., Duddy, I.R., and Gleadow, A.J.W. 1987. Thermal annealing of fission tracks in apatite: 2. A quantitative analysis. Chemical Geology (Isotope Geoscience Section), **65**: 1-13.

Leith, T.L., Weiss, H.M., Mork, A., Arhus, N., Elvebakk, G., Embry, A.F., Brooks, P.W., Stewart, K.R., Pchelina, T.M., Bro, E.G., Verba, M.L., Danyushevskaya, A. and , Borisov, A.V. 1992. Mesozoic hydrocarbon source-rocks of the Arctic region. In;

Arctic Geology and Petroleum Potential. Edited by T.O. Vorren, E. Bergsager, E. Dahl-Stamnes, E. Holter, B. Johansen, E. Lie and T.B. Lund, Norwegian Petroleum Society, Special Publication **2**, pp. 1-25.

Miall, A.D. 1986. The Eureka Sound Group (Upper-Cretaceous-Oligocene), Canadian Arctic Islands. Bulletin of Canadian Petroleum Geology. **34**: 240-270.

Miall, A.D. 1991. Late Cretaceous and Tertiary basin development and sedimentation, Arctic islands. In; Geology of the Innuitian Orogen and Arctic Platform of Canada and Greenland. Edited by H.P. Trettin. Geological Survey of Canada, Geology of Canada **3**, pp. 467-458.

Oakey 1994. A structural fabric defined by topographic lineaments: Correlation with Tertiary deformation of Ellesmere and Axel Heiberg Islands, Canadian Arctic. Journal of Geophysical Research, B, **99**, 20,311-20,321.

Okulitch, A.V. 1988. 1: 2,000,000 Geology of the Canadian Arctic Archipelago, Northwest Territories and North Greenland.In Geology of the Innuitian Orogen and Arctic Platform of Canada and Greenland. Edited by H.P. Trettin. Geological Survey of Canada, Geology of Canada **3**.

Okulitch, A.V. and Trettin, H.P. 1991. Late Cretaceous - Early Tertiary deformation, Arctic Islands, In; Geology of the Innuitian Orogen and Arctic Platform of Canada and Greenland. Edited by H.P. Trettin. Geological Survey of Canada, Geology of Canada **3**, 469-489.

O'Sullivan, P.O. and Parrish, R.R. 1995. The importance of apatite composition and single-grain ages when interpreting fission track data from plutonic rocks: a case study from the Coast Ranges, British Columbia. Earth and Planetary Science Letters, **132**, 213-224.

Powell, T.G. 1978. An assessment of the hydrocarbon potential of the Canadian Arctic Islands. Geological Survey of Canada, Paper 78-12.

Renne, P.R., Deino, A.L., Walter, R.C., Turrin, B.D., Swisher, C.C., Becker, T.A., Curtis, G.H., Sharp, W.D. and Jaouni, A.-R. 1994 Intercalibration of astronomical and radioisotopic time. Geology, **22**, 783-786.

Ricketts, B.D. 1994. Basin analysis, Eureka Sound Group, Axel Heiberg and Ellesmere Islands, Canadian Arctic Archipelago. Geological Survey of Canada, Memoir 439.

Ricketts, B.D. and Stephenson, R.A. 1994. The demise of the Sverdrup Basin: Late Cretaceous-Paleocene sequence stratigraphy and forward modelling. Journal of Sedimentary Research, B, **64**, 516-530.

Roest, W.R. and Srivastrava, S.P. 1989. Sea-floor spreading in the Labrador Sea: a new reconstruction. Geology, **17**, 1000-1003.

Stephenson, R.A., Boerstoel, J., Embry, A.F. and Ricketts, B.D. 1994. Subsidence analysis and tectonic modelling of the Sverdrup Basin. In; Proceedings of the 1992 International Conference on Arctic Margins, Edited by D.K. Thurston and K. Fujita, pp. 149-154. U.S. Department of the Interior, Minerals Management Service, MMS 94-0040.

Thorsteinsson, R. 1972a. 1:250,000 Geology of Eureka Sound, District of Franklin. Geological Survey of Canada Map 1300A.

Thorsteinsson, R. 1972b. 1:250,000 Geology of Cañon Fiord, District of Franklin. Geological Survey of Canada Map 1308A.

Trettin, H.P. 1991a. Tectonic Framework. In; Geology of the Innuitian Orogen and Arctic Platform of Canada and Greenland. Edited by H.P. Trettin. Geological Survey of Canada, Geology of Canada **3**, pp. 59-66.

Trettin, H.P. 1991b. Late Silurian-early Devonian deformation, metamorphism, and granitic plutonism, Northern Ellesmere and Axel Heiberg Islands. In; Geology of the Innuitian Orogen and Arctic Platform of Canada and Greenland. Edited by H.P. Trettin. Geological Survey of Canada, Geology of Canada **3**, pp. 293-341.

Utting, J., Goodarzi, F ., Dougherty, B.J. and Henderson, C.M. 1989. Thermal maturity of Carboniferous and Permian rocks of the Sverdrup Basin, Canadian Arctic Archipelago. Geological Survey of Canada, Paper 89-19.

Waylett, D.C. and Embry, A.F. 1992. Hydrocarbon loss from oil and gas fields of the Sverdrup Basin, Canadian Arctic Islands. In; Arctic Geology and Petroleum Potential. Edited by T.O. Vorren, E. Bergsager, E. Dahl-Stamnes, E. Holter, B.

Johansen, E. Lie and T.B. Lund, Norwegian Petroleum Society, Special Publication **2**, pp.195-204.

Willett, S.D. 1997. Inverse modeling of annealing of fission tracks in apatite 1: A controlled random search method. American Journal of Science, **297**: 939-969.

CHAPTER 6. Insights into the thermal history of the Nares Strait, Kane Basin and Smith Sound region in Canada and Greenland from apatite fission track and (U-Th)/He dating

A. M. Grist and M. Zentilli

6.1 Abstract:

Apatite fission track and (U-Th)/He data have been obtained for samples with Proterozoic to Neogene lithologic ages that were collected along the margin of Nares Strait, Kane Basin and Smith Sound in Ellesmere Island and Greenland, and also in Devon and Baffin Islands in the Canadian Arctic Archipelago. These data provide important insights into the complex thermal history of this region. In the sediment source region for the developing Sverdrup Basin to the west, fission track age-length relationships are consistent with at least 2 phases of exhumational cooling. Data from samples obtained proximal to the Sverdrup Basin margin reflect Late Paleozoic cooling likely related to uplift of rift flanks and widespread clastic sedimentation during the initial phase of rifting and thermal subsidence. Data from more distal samples reflect Early Mesozoic cooling that was likely related to epeirogenic denudation of the basin sediment source areas during periods of increased basin subsidence and high sediment supply from well developed river systems during Triassic time.

Several samples from the Wolstenholme Fjord - Thule region of Greenland, the Inglefield Uplift in Devon Island, and Talbot Inlet in Ellesmere Island have Early Jurassic fission track ages and broad or bimodal track length distributions. Late Cretaceous (U-Th)/He ages are evident in samples from Cape Faraday and from Orne Island, and Mansen and Carey Øer in northern Baffin Bay. These data likely reflect cooling from flank uplift and denudation in response to Late Cretaceous rifting in Baffin Bay. Relatively rapid denudation rates are indicated for southeastern Devon Island, which are consistent with a thick accumulation of presumed Upper Cretaceous strata immediately offshore in Lancaster Sound. Slower rates of denudation are indicated for Rensselaer Bugt, and Kap Trautwine, Greenland.

Most fission track and (U-Th)/He data for the Nares Strait region reflect the thermal

effects of Paleogene plate movements between Greenland and Ellesmere Island related to the Eurekan Orogeny including mafic volcanism, strike-slip or flank uplift exhumation, and minor thrust exhumation. However, the data suggest that only relatively minor strike-slip tectonism occurred along Nares Strait, indicating that deformation may have been partitioned into a number of thrust fault zones across a relatively wide belt.

6.2 Introduction

Recently, a number of apatite fission track (FT) thermochronology studies have demonstrated that the thermal history resulting from denudation and exhumation of the onshore part of rifted margins is intimately related to the thermal history from burial and subsidence of the offshore part of the margin (e.g. Moore et al. 1986; Dumitru et al. 1991; Gallagher et al. 1994, 1995; Brown 1992; Menzies et al. 1997; Brown et al. 2000; and others). The application of apatite FT thermochronology modelling to the onshore part of present-day passive margin settings was recently summarized by Gallagher and Brown (1997) and by Gallagher et al. (1998).

In a study of the low-temperature thermal history of the Late Paleozoic - Mesozoic Sverdrup Basin, in the Canadian Arctic Archipelago (Fig. 6.1), Arne et al. (1998, 2002) used apatite FT thermochronology and vitrinite reflectance to investigate cooling and inversion of the basin associated with the Paleogene collision between northern North America and northern Greenland (i.e., the Eurekan Orogeny). Studies have shown that sediment supply for the Sverdrup Basin was mainly from the south and east and, therefore, the region east of the basin margin was likely exhumed during periods of active basin subsidence (e.g. Trettin 1991a). The purpose of the present study is to examine the thermal history of the basin sediment source regions in the Nares Strait, Kane Basin, Smith Sound region of Arctic Canada and Greenland (Fig. 6.1) using apatite FT and (U-Th)/He thermochronology to investigate several possible thermal history elements:

(1) Late Paleozoic to Mesozoic cooling, principally a result of exhumation of the sediment source regions flanking the Sverdrup Basin;

(2) Cooling from rift flank uplift and normal faulting related to the beginning of the

Late Cretaceous development of the Baffin Bay – Labrador Sea Rift at ca. 85 Ma (anomaly 34; Srivastava 1978; Tessensohn and Piepjohn 2000);

(3) Thermal effects related to the Eurekan Orogeny, including rift-related volcanism or possible exhumational cooling during Paleocene transpression, and/or exhumation of thrust fault hanging walls during Eocene compression;

(4) Post-Eurekan denudational cooling of the Paleogene clastic units.

The size of the Sverdrup Basin (1300 km long and as much as 400 km wide) is of a similar magnitude to the rifted margins studied using the apatite FT method. The present study will follow a similar approach using apatite FT and (U-Th)/He thermochronology to study the onland part of this large, inverted, intracratonic failed rift basin.

The study region on the eastern margin of the Sverdrup Basin from Axel Heiberg to northern Ellesmere Island is a mountainous terrane produced by Eurekan thrusting, which uplifted the basin margin and caused basin inversion during Paleogene time. Eastern basin strata are considered less prospective owing to the thermally overmature conditions and the greater extent of thrust exhumation there; however this high level of exposure is amenable to the study of features for which the equivalents are deeply buried in the southwestern part of the basin.

Nares Strait, Kane Basin and Smith Sound between Ellesmere Island and Greenland (Fig. 6.1) extend northwards from the failed rift margin that progressively opened the Labrador Sea, Davis Strait, and Baffin Bay, and created the continental margins between eastern Arctic Canada and western Greenland during Late Cretaceous to Early Paleogene time. The presence of elevated Precambrian crystalline terranes around Baffin Bay (e.g. Trettin 1991b) is most likely the result of thermal perturbations after rifting, yet little is known about the timing of this uplift, nor why it is still elevated after modification by Tertiary drainage systems and Pleistocene glaciation. This study also examines those aspects of the low-temperature thermal history of the northern Baffin Bay rift flanks, and the cryptic plate tectonic boundary in Nares Strait between the North America and Greenland that was first proposed by Wegener (1929).

ARCTIC COASTAL PLAIN
- Neogene to Recent

SVERDRUP BASIN
- Carboniferous to Paleogene

CANADIAN SHIELD
- Thule, Borden basins — Mid-Proterozoic
- Archean and Paleoproterozoic

FRANKLINIAN MOBILE BELT
- Pearya — Mid-Proterozoic to Upper Silurian
- Deep-Water Province
- Sedimentary-Volcanic Subprovince — Cambrian to Devonian
- Sedimentary Subprovince — Lower Cambrian to Devonian
- Shelf Province — Lower Cambrian to Upper Silurian
- Arctic Platform — Cambrian to Devonian
- Boothia Uplift

Figure 6.1. Generalized map of the Innuitian Orogen of Arctic Canada and western Greenland showing the distribution of the main tectonic elements and geologic units, modified from Oakey et al. (2000). The approximate outline of the Sverdrup Basin outcrop is shown using a thick line. Sample locations are shown using closed circles.

6.2.1 Regional geology

The complex geology in the Canadian Arctic and western Greenland was summarized in Trettin (1991c). The region can be broadly considered to consist of 4 geologic terranes (Fig. 6.1). The oldest rocks (Archean to Proterozoic) are mainly gneisses, metasedimentary rocks, granitic intrusive rocks, dykes and sills of the Canadian Shield. Around southern Kane Basin and northern Baffin Bay, these outcrop over a wide area of southeastern Ellesmere Island (Inglefield Uplift), eastern Devon Island and western Greenland (Inglefield Land). The Neoproterozoic Franklin igneous event was a period of voluminous mafic magmatism throughout the northwest Canadian Shield which emplaced the Franklin dyke swarm at about 723 Ma (Heaman et al. 1992).

In the Nares Strait - Kane Basin - Smith Sound region, the shield rocks are unconformably overlain to the northwest by Cambrian to Devonian shelf carbonates and clastic rocks belonging to the Arctic Platform, Shelf, and Deep-Water Provinces, which form part of the Franklinian Mobile Belt. These rocks were strongly deformed, metamorphosed and intruded during the accretion of the Pearya Terrane from the northwest, which culminated in the Late Devonian-Early Carboniferous Ellesmerian Orogeny.

Beginning in mid-Carboniferous time the Sverdrup Basin, a complex successor basin and failed rift, formed in the core of the region affected by the former Ellesmerian Orogeny. Rift-related subsidence and sedimentation of conglomerate, carbonates and evaporites occurred intermittently during Carboniferous and Permian time. The earliest widespread clastic unit is the Borup Formation conglomeratic redbeds, deposited during Namurian time (ca. 327-314 Ma; e.g. Davies and Nassichuk 1991). The other principal clastic units, whose thickness varies considerably from place to place, range in age from Artkinsinian to Wordian (ca. 280-260 Ma). During Triassic to Late Cretaceous time clastic sedimentation was more-or-less continuous, although the rate of sediment supply varied markedly. Figure 6.2 is a sediment supply curve for the Sverdrup Basin during Mesozoic time (from Embry 1991). Periods of high sedimentation rates were inferred based on the presence of thick progradational deltaic facies deposits. Most sediment was derived from cratonic areas to the east and south, suggesting that the study region was undergoing protracted exhumation

during this time. Embry (1982) and Balkwill (1978) inferred that high sedimentation rates reflected epeirogenic denudation at times when large river systems existed on the craton and flowed north and west into the basin.

The Eureka Sound Group was originally defined by Troelson (1950) for widespread sandstone, shale and lignites that appear to postdate the last (Eurekan) orogeny. Subsequent investigations have revealed that formations of the Eureka Sound Group show strong variations from place to place within the Arctic Islands, and reflect a complex paleogeography that was continuously evolving in response to contemporaneous movements of the Eurekan Orogeny. Miall (1986) suggested the Eureka Sound Group represents the last pulse of clastic sedimentation of the Sverdrup Basin succession, and ranges in age from Maastrichtian to earliest Oligocene. Recently, Harrison et al. (1999) reorganized the diverse formations of the Eureka Sound Group into a number of regionally correlative depositional sequences that range in age from Lower Paleocene to Pleistocene.

The Eurekan Orogeny was originally defined by Thorsteinsson and Tozer (1970) to refer to a phase of compressive deformation that followed deposition of the Eureka Sound Group. However, as discussed above, Okulitch and Trettin (1991) and others have suggested that significant deformation occurred during deposition of the Eureka Sound Group. The relative movement between Greenland and Ellesmere Island was caused by the counterclockwise rotation of Greenland with respect to Ellesmere Island as a result of rifting in the Labrador Sea-Baffin Bay region (Kerr 1967). During Early Eocene time the North Atlantic Ocean began to open east of Greenland with the initiation of rifting activity there and in the Greenland Sea, and the relative motion between Greenland and Ellesmere Island became compressive in eastern Ellesmere Island (Srivastava 1985; Tessensohn and Piepjohn 2000). Both transpressive and compressive deformation related to the Eurekan Orogeny are now recognized, and the age of the orogeny is broadly considered to range from latest Cretaceous to Early Oligocene (Okulitch and Trettin 1991).

6.2.1.1 The Nares Strait controversy

The Nares Strait - Kane Basin - Smith Sound region between Ellesmere Island in the

Canadian Arctic, and Greenland (Fig. 6.1) offsets the Paleocene spreading ridge axis in northern Baffin Bay from the eastern flank of the Lomonosov Ridge, a 1700 km long sliver of continental crust which rifted from the Kara/Barents Sea shelves during late Paleocene time and subsequently subsided under the Arctic Ocean (e.g. Sweeney et al. 1982; Kristoffersen 1990).

There are three somewhat conflicting hypotheses regarding the postulated plate tectonic boundary between North America and Greenland. (1) Nares Strait is a major strike-slip fault (i.e., the Wegener Fault; Wegener 1929) with ca. 150 km of sinistral offset due to Late Cretaceous to Paleocene rifting that opened Baffin Bay. (2) Plate motion between the North American and Greenland Plates has been taken up by a broad band of deformation (e.g. Okulitch et al. 1990). (3) Nares Strait is not a major plate tectonic boundary, and the geology can be correlated across it (Dawes and Kerr 1982a, 1982b).

Nares Strait occupies a similar tectonic setting at the northern end of Baffin Bay to the Ungava Transform in Davis Strait (which offsets spreading centres in the Labrador Sea from those in Baffin Bay by several hundred kilometres), and its linear nature suggests it is also fault-controlled. If the strait was also a continental rift transform active during Paleocene rifting in northern Baffin Bay, the thermal effects of tholeiitic and\or basaltic volcanism may be discernable using low-temperature thermochronometric methods.

6.2.2 Apatite fission track and (U-Th)/He dating

FT analysis is based on the measured density and length distribution of linear tracks of crystal damage produced during spontaneous fission of trace amounts of ^{238}U. In monotonously cooling systems track densities provide a measure of age with respect to the closure temperature. Reviews of the method, its application to geological problems, and the development of FT thermal models have been provided by Wagner and Van den Haute (1992), Gallagher et al. (1998), Gleadow and Brown (2000), and others.

Track length (TL) reduction by annealing of fission damage is an incremental and irreversible process that is dominantly thermally activated. In apatite, annealing of fission damage begins to be significant at temperatures of ca. 60 °C over geologic time periods and

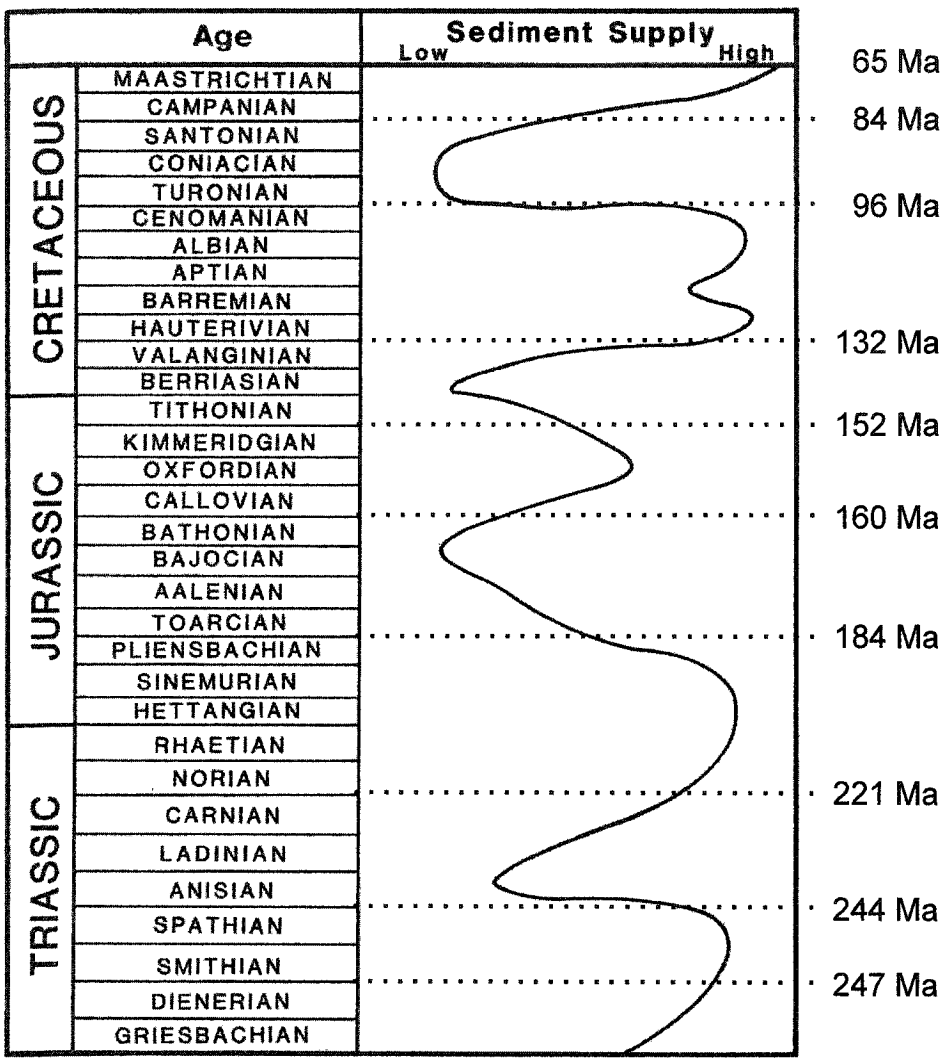

Figure 6.2. Clastic sediment supply curve for the Sverdrup Basin during Mesozoic time (modified from Embry 1991). Periods of high sediment supply were identified by Balkwill (1978) and Embry (1982) based on the presence of thick deltaic deposits in the basin, at which times large river systems were inferred to have existed on the craton to the south and east.

is essentially complete at ca. 100-150 °C (depending on composition). Between 60 and ca. 130 °C etchable tracks are retained, but are progressively shortened in response to the highest temperatures experienced. Because tracks are formed continuously through time, the TL distributions are indicative of the integrated thermal history below the closure temperature. Assuming a geothermal gradient of 30 °C/km, this would be equivalent to a burial depth of 4-5 km. It is this temperature-dependent behavior between 60 and ca.130 °C (the partial annealing zone or PAZ) that allows the apatite FT method to be used as a low-temperature thermochronometer. However, the probability of a track intersecting a polished surface and contributing to the age is proportional to its length, and therefore FT ages in systems with complex thermal histories may not represent a geologically significant event in time.

The (U-Th)/He method was one of the earliest techniques developed for the dating of geologic materials (e.g. Rutherford 1905; Strutt 1905), but was formerly considered unreliable owing to the ease with which radiogenic He could be lost from the host mineral resulting in too-young ages. With the advent of apparently more reliable radiometric methods such as K-Ar, interest in He systematics faded. Recently the technique has experienced a renaissance after its potential as a low temperature thermochronometer was suggested by Zeitler et al. (1987).

The behavior of radiogenic He in a crystal lattice is governed by laws of diffusion (e.g. Wolf et al. 1998; Reiners and Farley 1999; Farley 2000; Reiners et al. 2002) which are highly temperature-dependent. Wolf et al. (1998) demonstrated that diffusive loss of He from apatite becomes significant at temperatures as low as 40 °C, and is essentially complete at temperatures of 85-90 °C over geologic timescales. The progressive diffusive loss of radiogenic He between 40-90 °C results in a helium partial retention zone (PRZ) that is analogous to the PAZ. Thus apatite FT and (U-Th)/He dating are two independently calibrated low-temperature thermochronometers that may be used to constrain heating and cooling through temperatures of 40 to 130 °C with essentially no overlap.

6.2.3 Previous thermal history investigations

Arne et al. (2002) studied regional cooling and inversion in the Sverdrup Basin on

western Ellesmere and Axel Heiberg Islands using apatite FT dating and vitrinite reflectance. In that work and a previous study (Arne et al. 1998) the authors inferred that peak hydrocarbon generation and primary migration predated the formation of Eurekan structural traps, and hence these structures were likely to be poor prospective hydrocarbon exploration targets. Arne et al. (2002) also found that particularly for outcrop samples, apatite FT age and length trends are controlled by the distribution of Eurekan thrust faults. The youngest (Late Paleocene to Eocene) apatite FT ages and longest mean lengths occurred in the thrust hanging walls, indicating thrust-related exhumation. Arne et al. (1998) inferred from apatite FT models an average time of onset of cooling from exhumation of 66 ± 3 Ma for strata in the hanging walls of the Vesle Fiord Thrust and the East Cape Thrust, in central Ellesmere Island, and the Lake Hazen Fault system, north of Greely Fiord. In thrust footwalls and away from thrusts, samples had older ages and shorter mean lengths and were interpreted to have undergone partial annealing to various degrees prior to Cenozoic cooling.

A comprehensive review of existing radiometric age determinations for Cenozoic igneous rocks in the circum-Arctic region was provided by Harrison et al. (1999). The North Atlantic igneous province represents one of the most extensive magmatic events on Earth (e.g. Riisager, 2003). Story et al. (1998) and others have suggested that tholeiitic volcanism and rifting in northern Baffin Bay were initiated by the thermal effects of the proto-Icelandic mantle plume at about 62 Ma. The offset of the rift axis from Labrador Sea to Baffin Bay along the Ungava Transform was also accompanied by an episode of substantial basaltic volcanism on both the Baffin Island and the Greenland continental margins at about 55 Ma (e.g. Story et al. 1998; Riisager et al. 2003).

Early Paleocene volcanism was inferred by Estrada and Tessensohn (2004) for volcanogenic clasts obtained from the Upper Paleocene Pavy Formation at Cape Back, Ellesmere Island. Grist and Zentilli (2004) obtained apatite FT ages of 56-63 Ma for several samples from the Nares Strait region, and also interpreted these data in terms of Paleocene volcanism, strike-slip exhumation and minor thrusting that was contemporaneous with the Eurekan Orogeny. They inferred that the data were compatible with plate tectonic reconstructions based on magnetic anomalies, but that they did not refute or support

conclusions based on the reconstructions that require extensive Paleocene strike-slip motion. Data from the volcanic-derived Pavy Formation near Cape Back, and south of Cape Baird, suggest that the outcrops of the magnetic, fault-bounded Pavy Formation may be close to the locus of a now thrust-overridden Wegener Fault. (U-Th)/He data have been obtained in this study for some of these same samples, and for completeness the FT data for those samples are repeated here.

6.3 Sampling strategy

The location of samples is given in Table 6.1 and Fig. 6.1. Sampling was carried out from aboard the icebreaker C.C.G.S. Louis S. St. Laurent, and also from a fly camp in Inglefield Brednig, Greenland. The samples were obtained over a broad area of the eastern sediment source region of the Sverdrup Basin in the Nares Strait - Kane Basin - Smith Sound regions of Ellesmere Island and Greenland. In areas of known normal faults, we collected samples of crystalline rocks on both up- and down-faulted blocks, in order to ascertain any differences in thermal history that could help determine the age of faulting. On Ellesmere Island our strategy was to sample the hanging wall and footwall of regional thrust faults, such as the Rawlings Bay Thrust at Cape Lawrence, and the Mount Ross Fault at Cape Back (Fig. 6.3). In many locations Tertiary sediments, interpreted to have been deposited in a foreland basin setting (e.g. Piepjohn et al. 2000), are overridden by Eurekan thrusting and involved in complex deformation; a fact which suggests that thrusting was a protracted event. The Paleocene mafic sandstones of the Pavy Formation, sampled near Cape Baird on Judge Daly Promontory, and at Cape Back (Fig. 6.3) were considered to be particularly significant for our study. The apatite in these units has a simple pre-depositional thermal history (Estrada and Tessensohn 2004) because of its volcanic provenance, and hence should be a good indicator of the post-depositional thermal history.

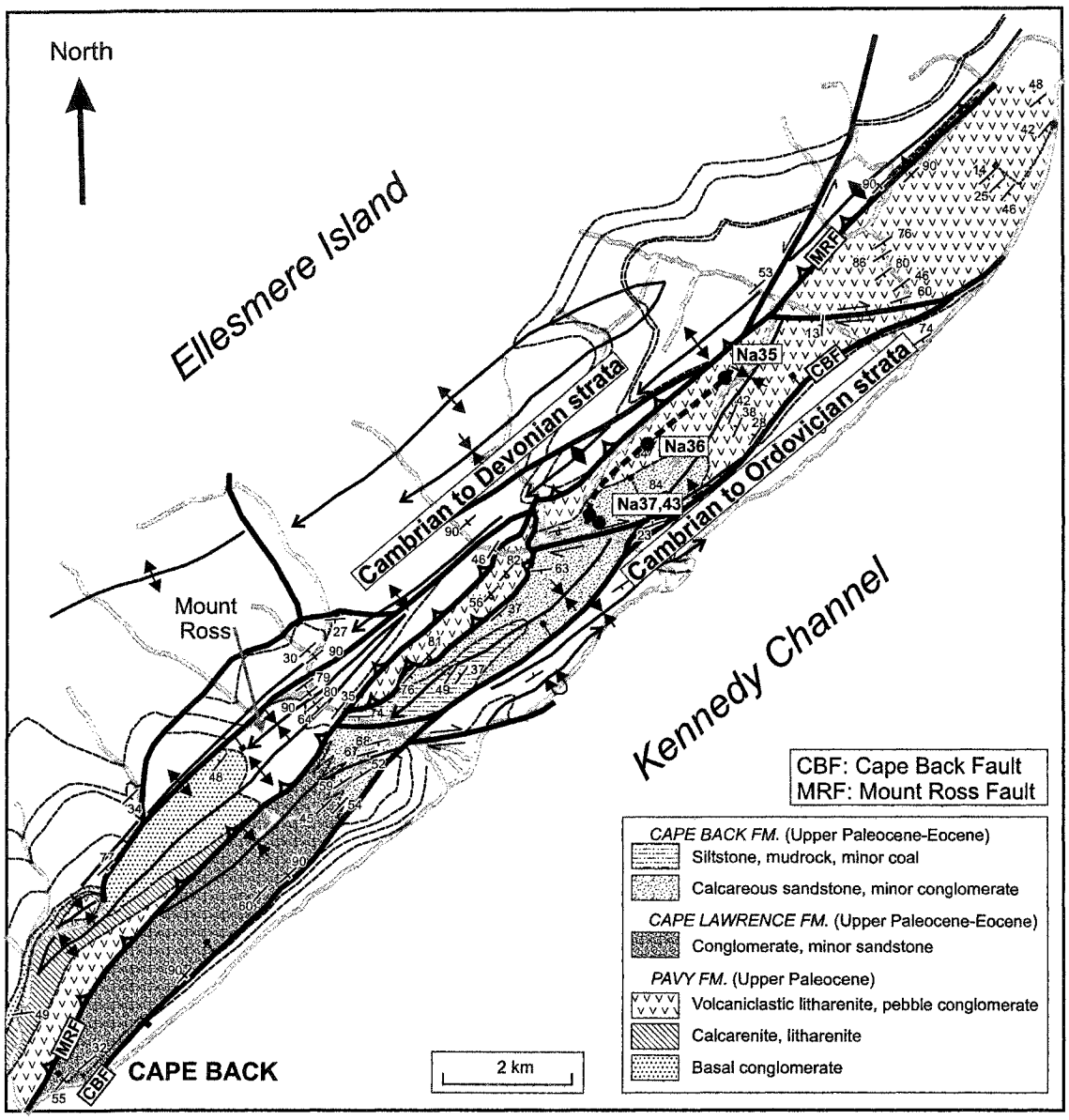

Figure 6.3. Simplified geologic map of the Cape Back area (see Fig. 6.1 for location); modified from C. Harrison (pers. com.). Sample locations are shown with black dots.

Table 6.1. Samples collected during the Nares Strait Geocruise 2001 (arranged by geographic distribution and tectonic element). Samples marked 'inc.' have not been analyzed; 'no ap' have insufficient apatite to permit analysis; 'poor' have pits, defects, inclusions, and/or high track densities that preclude analysis. Samples marked with a cross (†) were previously reported in Grist and Zentilli (2004).

Sample number Location and lithology	Latitude and Longitude	Elevation	status
Baffin Island:			
Na01 Iqaluit, gneiss	63° 45.0′N 68° 30.1′W	130 m	no ap
Na02 Iqaluit, gneiss	63° 44.9′N 68° 30.7′W	48 m	done
Inglefield Uplift, Devon Island - Philpotts Island			
Na03 Devon Island, gneiss	74° 31.9′N 82° 6.7′W	700 m	done
Na04 Devon Island, gneiss	74° 31.6′N 82° 7.5′W	444 m	done
Na05 Devon Island, gneiss	74° 31′N 82° 10.4′W	80 m	done
Na06 Philpotts Island, dyke	75° 5′N 79° 35′W	10 m	no ap
Na07 Philpotts Island, dyke	75° 0′N 79° 37′W	10 m	no ap
Inglefield Uplift, Ellesmere Island: Leffert Glacier - Buchanan Bay			
Na53 Pim Island, granite	78° 41.1′N 74° 17.6′W	441 m	no ap
Na54 Pim Island, granite	78° 41.0′N 74° 14.0′W	0 m	poor
Na55 Leffert Glacier, gneiss	78° 43.6′N 76° 06.3′W	661 m	done
Na56 Leffert Glacier, dyke	78° 43.6′N 75° 41.0′W	460 m	done
Inglefield Uplift, Ellesmere Island: Talbot Inlet			
Na57 Cape Faraday, dyke	77° 53.9′N 76° 38.8′W	3 m	done
Na58 Orne Island, dyke	77° 52.9′N 76° 19.1′W	10 m	done
Inglefield Uplift, Ellesmere Island: Makinson Inlet			
Na74 Bowman Island, granite	77° 14.9′N 80° 14.0′W	60 m	done
Ellesmere Island: west of Makinson Inlet			
Na66† Split Lake, Mount Lawson Fm., sandstone	77° 51.3′N 81° 37.0′W	398 m	done
Na70 Strathcona Fiord Fm, sandstone	77° 35.1′N 80° 41.8′W	500 m	done
Na71 Strathcona Fiord Fm., sandstone	77° 34.1′N 81° 54.6′W	457 m	done
Greenland: Wolstenholme Fjord - Thule			
Na59 Wolstenholme Ø, Thule Super Group, sandstone	76° 26.0′N 69° 54.8′W	351 m	inc.
Na60 Wolstenholme Ø, sill	76° 27.1′N 69° 55.0′W	43 m	no ap
Na61 Manson Øer, dyke	76° 37.9′N 69° 11.0′W	0 m	done
Na75 Thule, dyke	76° 27.6′N 69° 14.5′W	3 m	done
Na76 Carey Øer, dyke/gneiss	76° 44.3′N 73° 13.5′W	15 m	done
Na77 Dundas Mountain, sill top	76°32'N 68°50'W	222 m	done
Na78 Dundas Mountain, sill base	76°32'N 68°50'W	197 m	done
Greenland: Inglefield Brednig			
Na08 Herbert Ø, dyke	77° 25.2′N 70° 25.3′W	769 m	no ap

Table 6.1 (continued)

Na09 Herbert Ø, dyke	77° 24.3′N 71° 04.6′W	235 m	no ap
Na10 Herbert Ø, sill	77° 29.3′N 71° 07.5′W	0 m	done
Na11 Northumberland Ø, dyke	77° 21.7′N 71° 33.4′W	348 m	no ap
Na12 Northumberland Ø, dyke	77° 21.9′N 71° 31.4′W	286 m	done
Na18 Hakluyt Ø, dyke	77° 25.8′N 72° 38.3′W	409 m	done
Na63 Kap Trautwine, gneiss	77° 12.7′N 69° 45.3′W	665 m	done
Na64 Kap Trautwine, gneiss	77° 14.2′N 69° 53.1′W	0 m	done
Na65 Granville Fjord, gneiss	76° 59.0′N 69° 39.0′W	3 m	done
Na79 Olrich Fjord, dyke	77° 10′N 66° 20′W	425 m	no ap
Greenland: Inglefield Land			
Na19 Kap Alexander, sill	78° 10.0′N 72° 58.5′W	411 m	no ap
Na20 Rensselaer Bugt, gneiss	78° 20.6′N 70° 21.4′W	456 m	done
Na21 Rensselaer Bugt, gneiss	78° 20.7′N 70° 21.4′W	466 m	poor
Na22 Rensselaer Bugt, gneiss	78° 29.9′N 70° 31.5′W	391 m	poor
Na23 Rensselaer Bugt, gneiss	78° 34.5′N 70° 37.0′W	169 m	poor
Na24 Rensselaer Bugt, gneiss	78° 36.1′N 70° 41.7′W	0 m	done
Na25 Marshall Bugt, gneiss	78° 31.4′N 68° 22.4′W	592 m	poor
Na26 Marshall Bugt, amphibolite	78° 39.0′N 68° 58.3′W	357 m	poor
Na27 Marshall Bugt, gneiss	78° 39.4′N 68° 54.7′W	380 m	no ap
Greenland: Washington Land			
Na50 Cass Fjord, Bjornehiet Fm., sandstone			
	80° 25.6′N 64° 26.5′W	395 m	done
Ellesmere Island: Kennedy Channel - Nares Strait, Cape Lawrence			
Na32† Archer Fiord Fm., sandstone	80° 23.7′N 69° 43.4′W	1015 m	done
Ellesmere Island: Kennedy Channel - Nares Strait, Cape Back			
Na35† Pavy Fm., (volc.) sandstone	80° 59.8′N 66° 58.8′W	411 m	done
Na36† Pavy Fm., (volc.) sandstone	80° 59.5′N 67° 00.4′W	279 m	done
Na37† Cape Back Fm., sandstone	80° 59.4′N 67° 01.1′W	173 m	done
Na43† Cape Back Fm., sandstone	80° 59.4′N 66° 59.8′W	314 m	inc.
Ellesmere Island: Kennedy Channel - Nares Strait, south of Cape Baird:			
Na48† Pavy Fm., (volc.) sandstone	81° 28.3′N 65° 17.4′W	215 m	done
Na48b† Pavy Fm., (volc.) sandstone	81° 28.3′N 65° 17.4′W	215 m	done
Ellesmere Island: Kennedy Channel - Nares Strait, Cape de Fosse			
Na42† Eids Fm., sandstone	81° 14.6′N 65° 37.7′W	535 m	done

6.4 Discussion of data

Analytical procedures used at Dalhousie University to obtain FT ages (using the external detector method) and confined TL distributions have been described in Grist and Zentilli (2003) and elsewhere, and are also described in Appendix A1.1. FT age and length data are shown in Table 6.2 and Figs. 6.4-6.8. Only 2 of 33 FT samples failed the χ^2 statistical test, indicating that they were composed of more than 1 age population. One of these samples (Na37) had a clearly bimodal age population, and thus the central age of 171 Ma is not geologically meaningful. The other sample (Na42) marginally failed the χ^2 test owing to a few age outliers and, therefore, the measured age of 240 Ma is probably meaningful.

Procedures used to obtain (U-Th)/He ages at Caltech are given in Farley (2002), and elsewhere, and are also are given in Appendix A1.2. (U-Th)/He age data are shown in Table 6.3. The raw age data were corrected using the method of Farley et al. (1996) to account for ejection from the host grain of a portion of the He produced by alpha decay. Based on statistical analysis of multiple age determinations for the Fish Canyon and Durango apatite standards, overall analytical uncertainty in the individual corrected sample ages is on the order of 6-8% at the 2σ confidence level. Aliquots of the laboratory apatite standard 97MR22 (average laser multigrain age of 4.50 ± 0.24 Ma; House et al. 2000) were also analyzed.

During the ICP-MS analyses it was discovered that many of the samples had very high light REE contents; in particular, the samarium content of several samples was over 500 ppm (Table 6.3). One of the principal Sm isotopes (^{147}Sm) is radioactive and decays by emission of a single He nucleus to ^{143}Nd ($t_{1/2} = 1.06 \times 10^{11}$ yr), so that for some samples up to 15% of the He nuclei were from ^{147}Sm decay. An additional correction was therefore applied to the He age data to account for the contribution of ^{147}Sm-derived He nuclei.

One sample (Na57-1) did not outgas completely during initial heating, likely indicating that it contained a U-Th-Sm-bearing inclusion (K. Farley, pers. comm.) such as monazite or zircon. This type of inclusion contributes radiogenic He, but is not dissolved by HNO_3 prior to ICP-MS analysis, and thus is a source of 'parentless' He, which results in an anomalously old age (e.g. Lippolt et al. 1994; House et al. 1997; Farley 2002). The age for

that sample is not considered geologically meaningful. Additionally, the ages of several other pairs of samples did not reproduce within the 2σ error estimates (i.e., Na48-1, 2; Na61-1, 2; Na75-1, 2; Na76-1, 2; Na77-1, 2). It appears that in each of these pairs the younger (U-Th)/He age is more likely to be meaningful than the older age. In particular, for sample Na77-2 the apparent (U-Th)/He age (750 Ma) exceeds the Franklinian emplacement age of the Dundas Mountain sill. Similarly, the (U-Th)/He age of sample Na48-2 (111.8 Ma) exceeds the age of the Paleocene-aged volcanic protolith of the Pavy Formation. The (U-Th)/He age of sample Na48-1 (46.4 Ma) is indistinguishable from the other pair of Pavy Formation sample ages (Na35-1, 2). The older ages of the other sample pairs are also likely to be affected by parentless He. Most of the dated samples are particularly sensitive to parentless He from U-Th-Sm-bearing inclusions because they have very low U contents (<3 ppm), and low He yields. Alternatively, it is possible that excess He was implanted from adjacent U-Th-Sm-bearing grains (e.g. Farley et al. 1996).

6.5 Interpretation and geological significance of results

Figure 6.4 is a plot of apatite FT age vs. mean TL for the samples analyzed for the present study (filled circles) and from the Sverdrup Basin study of Arne et. (2002, Fig. 10; open circles). The use of such figures in the interpreting of apatite FT data has been described by Gallagher et al. (1998) and others. Several different aspects of the complex regional thermal history of the Sverdrup Basin and the Nares Strait - Kane Basin - Smith Sound part of the margin which are recorded by the apatite FT data (groups 1-5) are evident in this figure. These groups are discussed in detail in the following sections.

6.5.1 Paleozoic-Mesozoic FT-aged samples

The first group (1) consists of two widely spaced samples, one from near the margin of the continental ice sheet in Inglefield Land, Greenland, and the other from Iqaluit, Baffin Island. The FT data for these samples likely indicate slow exhumation of these shield rocks beginning in Late Proterozoic time, and they appear to be relatively unaffected by the subsequent tectonics related to the development of the Sverdrup Basin, rifting in Baffin Bay,

Table 6.2. A summary of the FT age and TL data. Samples with a χ^2 value >5 pass the χ^2 test at the 95% confidence level (i.e., appear to be one age population). The ages reported are the central age of Galbraith and Laslett (1993). Abbreviations are as follows: N_s, N_i, and N_d are the number of spontaneous, induced, and flux dosimeter (CN-5) tracks, respectively. Rho_s, Rho_i, and Rho_d are the density of spontaneous, induced, and dosimeter tracks, respectively ($x10^6/cm^2$). A value of 353.5 ± 7.1 (CN-5) was used for the zeta factor. Age and length error estimates are at the 1σ confidence level. For samples marked with an asterisk (*) a ^{252}Cf-irradiated grainmount was used to increase the number of measurable track lengths. Samples marked with a cross (†) were previously reported in Grist and Zentilli (2004) (Analyses by A.M.G.).

	Age data											
										Length data		
Sample Number	Grains counted	Rho_s	N_s	Rho_i	N_i	χ^2	Rho_d	N_d	Age ± error (Ma, 1-σ)	No. of tracks	Mean ± error (μm, 1-σ)	Std. Dev. (μm)
Baffin Island:												
Na02	18	8.40	8472	3.51	3540	73.8	1.157	5387	**472 ± 14.8**	157	**12.27 ± 0.15**	1.89
Devon Island Inglefield Uplift:												
Na03	33	1.16	3285	1.13	3198	32.7	1.157	5387	**207 ± 7.2**	136	**12.61 ± 0.15**	1.69
Na04*	32	0.384	1223	0.405	1289	87.0	1.157	5387	**191 ± 8.9**	162	**12.57 ± 0.12**	1.53
Na05*	31	0.431	1078	0.499	1247	98.0	1.157	5387	**174 ± 8.4**	198	**12.13 ± 0.12**	1.72
Ellesmere Island Inglefield Uplift: Leffert Glacier - Buchanan Bay												
Na-55	19	4.36	4668	3.27	3496	26.6	1.172	5234	**271 ± 8.9**	101	**11.67 ± 0.24**	2.36
Na56*	31	0.278	734	0.183	468	98.8	1.172	5234	**317 ± 20.3**	203	**13.33 ± 0.12**	1.75
Ellesmere Island Inglefield Uplift: Talbot Inlet												
Na57	29	0.155	495	0.191	613	97.9	1.133	5063	**160 ± 10.4**	97	**12.24 ± 0.19**	1.89
Na58	33	0.102	294	0.240	693	99.5	1.133	5063	**84.4 ± 6.2**	95	**13.12 ± 0.18**	1.78
Ellesmere Island Inglefield Uplift: Makinson Inlet												
Na74	27	0.637	1346	0.479	1013	100.	1.172	5234	**270 ± 13.**	148	**12.19 ± 0.18**	2.24
Ellesmere Island west of Inglefield Uplift: west of Makinson Inlet												
Na66*†	32	0.151	358	0.518	1227	99.8	1.172	5234	**60.2 ± 3.9**	132	**14.07 ± 0.12**	1.35
Na70	26	2.699	4837	1.968	3527	92.	1.172	5234	**278 ± 9.1**	104	**13.01 ± 0.14**	1.45
Na71	26	2.59	5510	1.63	3472	60.9	1.172	5234	**321 ± 10.4**	125	**12.58 ± 0.15**	1.66
Greenland Thule - Wolstenholme Fjord:												
Na59	not done											
Na61	28	0.222	664	0.215	644	98.9	1.133	5063	**203 ± 12.3**	140	**13.38 ± 0.13**	1.54
Na75*	32	0.170	396	0.174	405	100.	1.157	5387	**197 ± 14.7**	154	**12.53 ± 0.17**	2.08
Na76*	31	0.300	640	0.238	507	99.1	1.157	5387	**253 ± 16.2**	173	**11.26 ± 0.17**	2.17
Na77	31	0.241	536	0.234	522	99.3	1.157	5387	**207 ± 13.7**	170	**13.18 ± 0.12**	1.59

Table 6.2 (continued)

Na78*	31	0.323	1021	0.296	937	95.3	1.157	5387	**219 ± 11.2**	185	**13.06 ± 0.11**	1.47
Greenland Inglefield Brednig:												
Na10	30	0.560	792	0.472	668	100.	1.093	4885	**225 ± 13.1**	131	**13.11 ± 0.14**	1.58
Na12*	27	0.257	303	0.255	300	99.8	1.172	5234	**206 ± 17.5**	62	**12.79 ± 0.25**	1.94
Na18*	30	0.400	783	0.303	593	97.8	1.172	5234	**268 ± 16.**	156	**12.64 ± 0.16**	2.00
Na63	25	1.96	3957	1.45	2937	48.7	1.133	5063	**264 ± 9.1**	151	**12.81 ± 0.15**	1.84
Na64	28	1.62	3828	1.72	4077	3.06	1.133	5063	**189 ± 5.9**	158	**12.44 ± 0.14**	1.69
Na65	29	1.70	4603	1.86	5049	6.48	1.133	5063	**180 ± 5.7**	127	**12.14 ± 0.16**	1.84
Greenland Inglefield Land:												
Na20	17	2.55	3344	1.07	1398	1.00	1.133	5063	**462 ± 18.5**	142	**12.55 ± 0.14**	1.66
Na24	18	8.93	11623	6.11	7956	57.1	1.133	5063	**286 ± 8.1**	161	**12.59 ± 0.14**	1.83
Greenland Washington Land:												
Na50	23	3.351	3076	2.061	1892	81.	1.172	5234	**328 ± 12.5**	182	**12.31 ± 0.13**	1.78
Ellesmere Island Kennedy Channel - Nares Strait: Cape Lawrence												
Na32†	30	0.775	1667	2.521	5422	51.	1.172	5234	**63.4 ± 2.3**	160	**14.11 ± 0.12**	1.45
Ellesmere Island Kennedy Channel - Nares Strait: Cape Back												
Na35*†	25	0.231	390	0.780	1319	95.3	1.172	5234	**61.0 ± 3.8**	127	**14.33 ± 0.09**	0.98
Na36*†	32	0.373	687	1.23	2270	99.9	1.172	5234	**62.4 ± 3.1**	162	**14.10 ± 0.11**	1.33
Na37†	28	1.137	2029	1.011	1803	0	1.172	5234	**171 ± 23.**	139	**11.46 ± 0.15**	1.80
Ellesmere Island Kennedy Channel - Nares Strait: south of Cape Baird:												
Na48*†	31	0.154	354	0.544	1254	88.6	1.172	5234	**58.2 ± 3.8**	137	**14.00 ± 0.12**	1.34
Na48b*†	23	0.216	439	0.796	1616	98.4	1.172	5234	**56.0 ± 3.3**	155	**13.86 ± 0.12**	1.43
Ellesmere Island Kennedy Channel - Nares Strait: Cape de Fosse												
Na42†	25	4.23	4813	3.48	3962	0.013	1.133	5063	**240 ± 7.8**	126	**12.38 ± 0.14**	1.54

Table 6.3. A summary of the (U-Th)/He data. 'Ft' is the grain size factor for the alpha ejection correction. Raw ages were corrected according to the method of Farley et al. (1996) to account for ejection of a portion of the He produced by alpha decay. Because of high Sm contents, an additional age correction was applied to most samples to account for ^{147}Sm-derived He. Sm contents of the mr22std samples were negligible (Analyses by A.M.G. and Lindsey Hedges). Overall errors to corrected age errors are estimated to be 8% at the 2σ level.

Sample	No. of grains	U (ppm)	Th	Sm	He (nmol/g)	mass (μg)	Ft	mean radius (μm)	mean length (μm)	re-extract (y/n)	Raw age (Ma)	**Sm-Corrected age (Ma; 2σ)**
Devon Island Inglefield Uplift:												
Na03-1:	4	5.58	2.21	539.0	3	12.45	0.73	47.86	250.7	n	89.62	**110.2 ± 8.8**
Na03-2:	4	5.59	1.61	623.8	2.93	12.34	0.72	45	280.7	n	89.56	**109.3 ± 8.7**
Ellesmere Island Inglefield Uplift: Leffert Glacier - Buchanan Bay												
Na56-1:	4	2.43	7.47	516.7	4.51	21.79	0.73	48.57	432.84	n	195.55	**229.8 ± 18.4**
Na56-2:	4	2.83	7.91	534.7	4.68	26.25	0.76	52.85	432.84	n	181.02	**209.2 ± 16.7**
Na56-3:	3	2.13	6.47	404.0	6.02	56.66	0.83	80.95	528.55	n	296.8	**312.2 ± 25.0**
Ellesmere Island Inglefield Uplift: Talbot Inlet												
Na57-1:	4	2.00	7.11	353.7	2.02	24.55	0.77	62.85	289.27	y	100.66	**115.9 ± 9.3**
Na57-2:	4	9	28	353.7	1.26	33.8	0.78	66.43	359.98	n	53.3	**61.5 ± 4.9**
Na57-3:	2	2.1	7.16	358.4	1.45	35.66	0.84	87.14	437.12	n	69.96	**74.8 ± 6.0**
Na58-1:	4	1.88	5.88	379.2	1.39	26.64	0.78	65	293.56	n	77.77	**86.8 ± 6.9**
Na58-2:	4	2.2	6.88	410.8	1.6	12.93	0.73	52.85	214.28	n	76.54	**92.0 ± 7.4**
Ellesmere Island west of Inglefield Uplift: west of Makinson Inlet												
Na66-1:	4	1.21	30.88	66.17	2.1	26.99	0.76	58.57	357.84	n	45.51	**59.3 ± 4.7**
Na66-2:	4	2.27	48.26	44.86	3.55	43.5	0.8	70	392.12	n	47.85	**59.6 ± 4.8**
Na70-1:	4	66.67	45.18	228.3	69.62	11.15	0.73	49.28	209.99	n	163.18	**221.7 ± 17.7**
Greenland Thule - Wolstenholme Fjord:												
Na59-1:	3	8.63	8.08	146.9	7.2	12.49	0.76	58.09	231.42	n	124.39	**160.3 ± 12.8**
Na59-2:	2	48.66	5.74	206.1	41.38	8.23	0.78	58.57	197.13	n	149.87	**190.7 ± 15.3**
Na61-1:	4	2.18	7.71	363.8	2.52	24.86	0.76	55.71	381.41	n	115.1	**136.3 ± 10.9**

Table 6.3 (continued)

Na61-2:	4	2.49	8.45	406.4	2.13	19.49	0.75	52.85	316.27	n	87.02	**104.0 ± 8.3**
Na75-1:	4	2.36	7.66	506.9	3.23	15.02	0.72	45.71	334.27	n	141.31	**171.1 ± 13.7**
Na75-2:	4	2.19	6.64	523.1	1.75	9.33	0.69	43.57	227.13	n	85.33	**108.4 ± 8.7**
Na76-1:	4	2.02	5.35	470.5	1.5	17.85	0.72	45.0	413.55	n	83.78	**99.0 ± 7.9**
Na76-2:	4	1.99	6.05	438.6	3.71	17.89	0.73	46.43	379.27	n	197.05	**233.2 ± 18.7**
Na77-1:	3	2.54	8.6	414.3	2.72	6.72	0.68	40.95	245.7	n	108.77	**143.2 ± 11.5**
Na77-2:	3	2.25	7.39	380.8	13.78	8.12	0.71	46.66	231.42	n	607.14	**750.3 ± 60.0**
Ellesmere Island Kennedy Channel - Nares Strait: Cape Lawrence												
Na32-1:	3	9.71	4.42	211.1	2.65	5.94	0.69	41.9	208.56	n	45.08	**63.4 ± 5.1**
Na32-2:	3	12.08	2.4	155.5	4.15	10.52	0.75	55.24	217.13	n	59.97	**78.5 ± 6.3**
Na32-3:	1	20.53	3.71	91.6	5.44	11.16	0.83	85.71	282.84	n	46.59	**55.7 ± 4.5**
Ellesmere Island Kennedy Channel - Nares Strait: Cape Back												
Na35-1:	4	3.57	3.26	89.0	0.99	46.05	0.83	86.42	284.99	n	41.82	**49.1 ± 3.9**
Na35-2:	4	5.4	3.45	89.0	1.34	24.47	0.79	70.0	233.56	n	39.54	**48.9 ± 3.9**
Ellesmere Island Kennedy Channel - Nares Strait: south of Cape Baird:												
Na48-1:	3	1.71	3.81	246.2	0.62	44.96	0.84	91.42	354.27	n	43.33	**46.4 ± 3.7**
Na48-2:	4	1.37	0.82	45.0	0.78	27.21	0.79	64.28	308.56	n	91.62	**111.8 ± 8.9**
mr22std-1:	4	19.8	10.76	128.2	0.4	20.31	0.76	53.57	325.7	n	3.28	**4.3 ± 0.3**
mr22std-2:	4	14.63	7.21	104.0	0.34	51.34	0.82	75	422.12	n	3.85	**4.7 ± 0.4**

or the Eurekan Orogeny. No (U-Th)/He data were obtained for these samples.

The second group (2) form a loose cluster of ca. 300 Ma ages, with mean track lengths of ca. 13 μm. These samples are from areas proximal to the Sverdrup Basin, from the Inglefield Uplift at Makinson Inlet, and south of the Leffert Glacier, on Ellesmere Island. Representative FT age and TL data for this group are shown in Fig. 6.5. The FT data from this group are inferred to reflect denudational cooling related to uplift of rift flanks and clastic sedimentation in the Sverdrup Basin during early rifting and basin subsidence in Late Carboniferous to Early Permian time. The only (U-Th)/He-dated sample from this area (Na56) yielded Triassic ages of ca. 210-230 Ma, which were the oldest (U-Th)/He ages obtained in this study. These ages are inferred to reflect denudational cooling to temperatures below ca. 40 °C during Triassic time in this area.

The third group (3) forms a cluster of 200-220 Ma ages, with mean lengths of ca. 13 μm. These samples were obtained from areas distal from the Sverdrup Basin, in Wolstenholme Fjord, and Inglefield Brednig, in the southeastern part of the study area. Representative FT age and TL data for this group are shown in Fig. 6.6. These samples cooled during a period of increased subsidence and sediment supply within the basin beginning in Early Triassic time (Fig. 6.4), and are inferred to reflect denudation of this area as a source region for basin sediments.

Sm-corrected (U-Th)/He ages of separate aliquots of most samples in this group (Table 6.3) did not reproduce within 2σ analytical uncertainty. As discussed above, this is likely to be at least partly a result of parentless He, and the younger (Early Cretaceous) ages are more likely to be geologically meaningful. The youngest ages in this group are ca. 100 Ma, which suggests that in addition to Triassic denudational cooling, the samples also experienced accelerated cooling during a period of increased basin subsidence and sediment supply beginning in Early Cretaceous time (Fig. 6.4). Alternatively, accelerated Early Cretaceous cooling may have been related to the onset of rifting in the Amerasian Basin, (e.g. Embry and Dixon 1990). Partial diffusive loss of He as a result of heating may also partially account for the high degree of scatter in the (U-Th)/He ages of these samples.

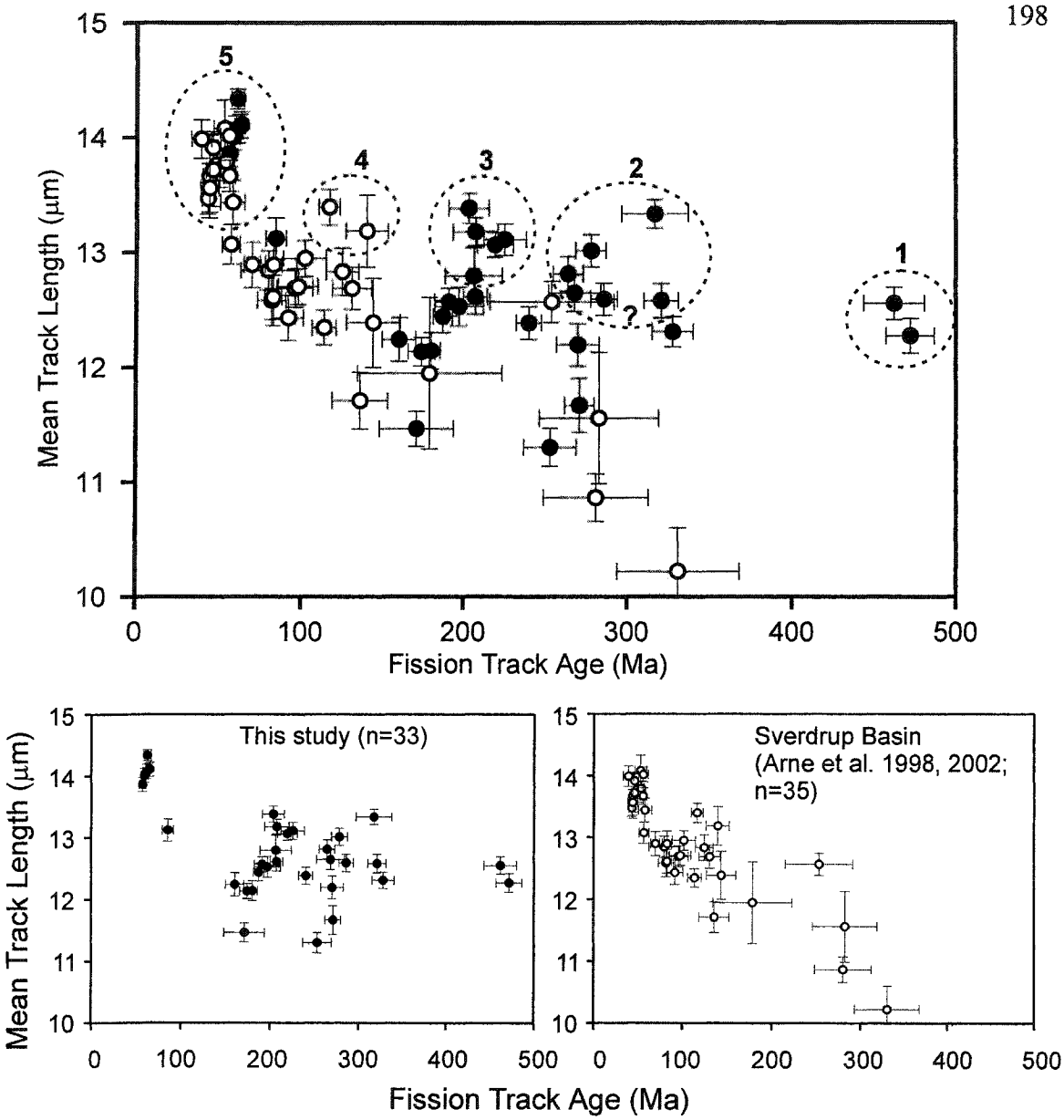

Figure 6.4. FT age vs mean TL for outcrop samples from eastern Ellesmere and Devon Islands, and western Greenland (this study) and the Sverdrup Basin, central Ellesmere and Axel Heiberg Islands (Arne et al. 2002). Periods of cooling and inferred exhumation discussed in detail in the text are numbered 1-5. Shaded areas correspond to inferred intervals of high sediment influx into the basin (Balkwill 1978; Embry 1982) during the Mesozoic (Fig. 6.2), and to intervals of clastic deposition during the Late Paleozoic (e.g. Davies and Nassichuk 1991). The mean TL of one sample (FT94-120), incorrectly reported as 12.1 µm instead of 13.1 µm in Arne et al. (2002), Table 4 is corrected here (Analyses by A.M.G.).

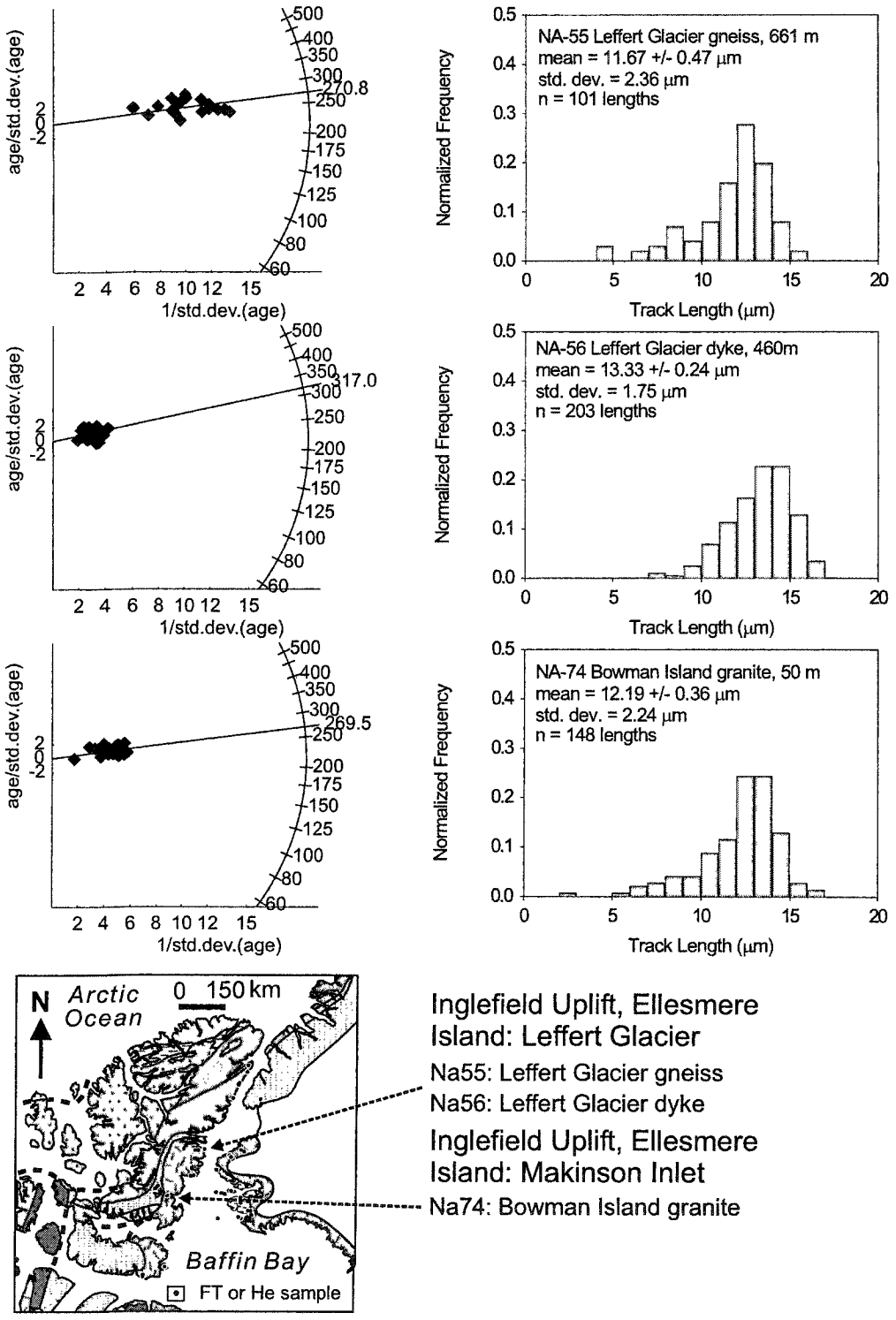

Figure 6.5. Radial plots (left) and TL histograms (right) of the FT data for samples from the Leffert Glacier and Makinson Inlet on eastern Ellesmere Island.

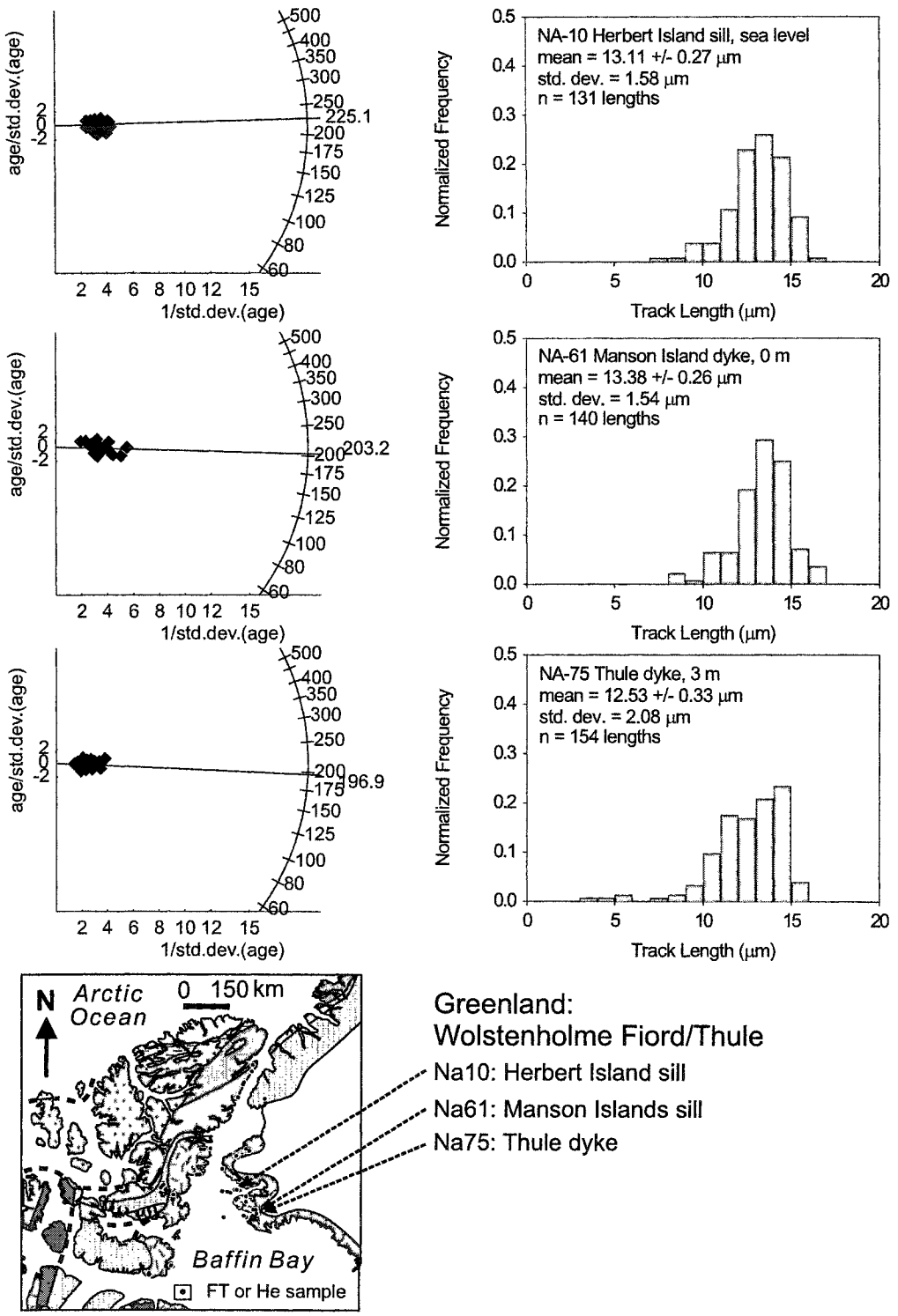

Figure 6.6. Radial plots (left) and TL histograms (right) of the FT data for samples from Wolstenholme Fjord/Thule region of Greenland.

The fourth group (4) comprises two samples from within the Sverdrup Basin with ages of ca. 100-130 Ma, and mean lengths of ca. 13 μm. These samples were inferred by Arne et al. (2002) to have cooled during Mesozoic time (e.g. Early Cretaceous) as a result of flank uplift related to the opening of the Arctic Ocean and the onset of rifting in the Amerasian Basin.

The FT data from some of the samples from Wolstenholme Fjord - Thule region of Greenland, and the Inglefield Uplift in Devon and Talbot Inlet in Ellesmere Island (Table 6.2) have broad or bimodal TL distributions. Younger (U-Th)/He ages are also evident for these samples, particularly in the data for the Cape Faraday and Orne Island, and Mansen and Carey Øer samples in northwestern Baffin Bay. These samples were likely affected by a combination of two or more thermal history events, and in particular, may have experienced cooling and inferred exhumation as a result of flank uplift from rifting in Baffin Bay in Late Cretaceous time. Representative FT age and TL data for this group are shown in Fig. 6.7.

The remaining samples (other than group 5 discussed below) which also have reduced mean track lengths and intermediate ages, likely have been affected by a combination of two or more thermal elements. In the Sverdrup Basin, these data may also reflect provenance ages that have been reduced by limited burial heating in the basin prior to inversion. In the basin sediment source region, these data may also reflect slow or episodic exhumation.

6.5.1.1 Mesozoic denudation rates

Studies have shown that in nonorogenic (i.e., slowly eroded) environments, crustal cooling is mainly result of vertical advection of mass through a near steady-state geotherm (e.g. Gallagher et al. 1994 1995, 1998; Brown et al. 1994, 2000). In such cases, the rate of cooling can be used to infer the rate of denudation. It therefore follows that provided certain requirements are met (i.e., samples do not occur across major structural breaks, differences in length are negligible and samples have similar compositions) the difference in FT ages of relatively closely spaced samples with substantial elevation contrasts can be used to obtain a rough estimate of the rate of denudation.

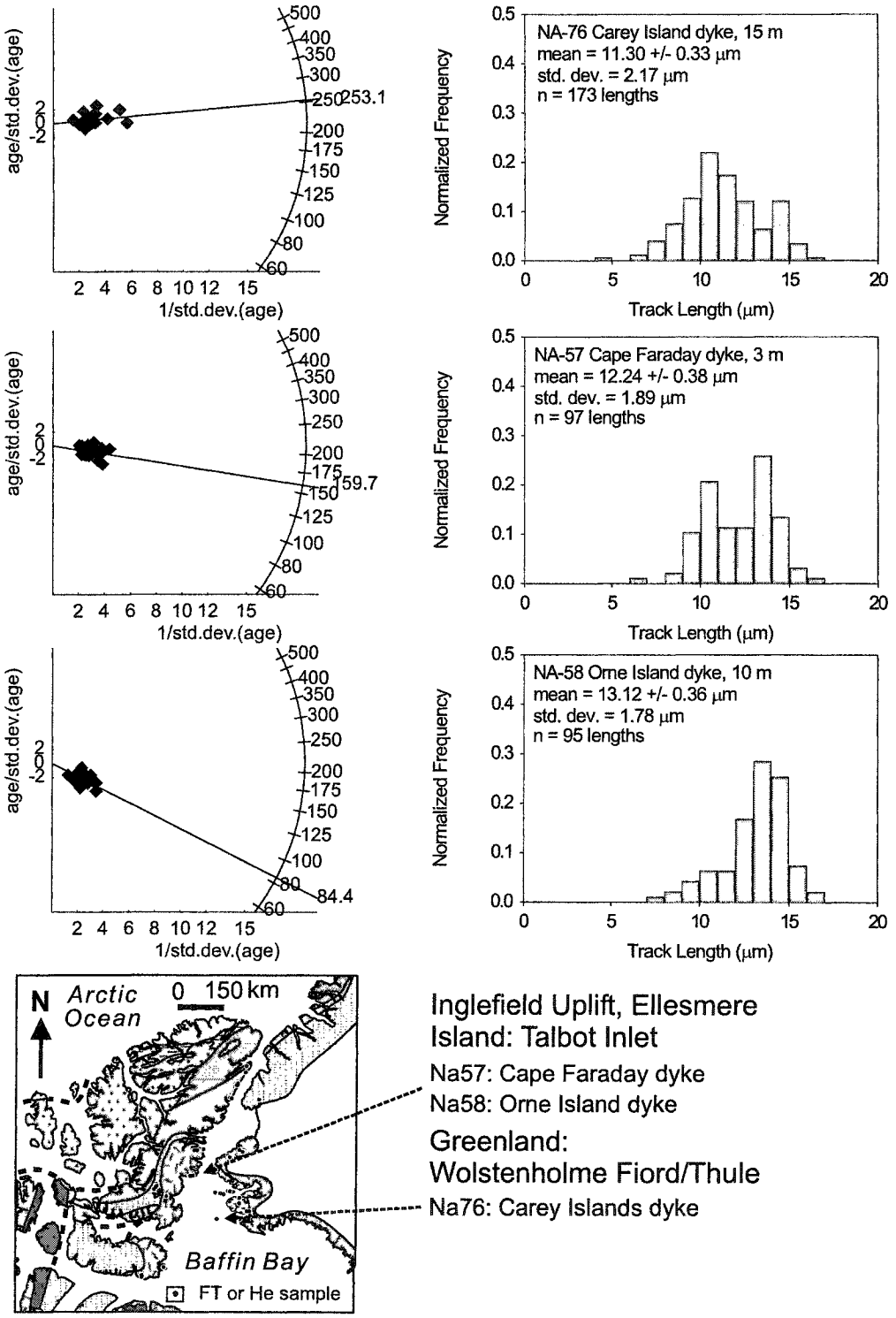

Figure 6.7. Radial plots (left) and TL histograms (right) of the FT data for samples from Cape Faraday and Orne Island, eastern Ellesmere Island, and the Carey Øer, Greenland.

Several groups of samples in this study whose FT age and length characteristics are dominated by Paleozoic or Mesozoic thermal history, and which were collected at different elevations, display a correlation of FT age with elevation (Fig. 6.8). At Kap Trautwine, FT ages decrease by 75 My (28%) over a 665 m decrease in elevation (mean TL decreases 3%). At Rensselaer Bugt, FT ages decrease by 176 My (38%) over a 456 m decrease in elevation (mean TL increases 0.5%). For these samples, denudation rates of ca. 8.9 m/My and 2.6 m/My, respectively, can be estimated. These rates are interpreted to reflect slow exhumation of these regions during Paleozoic and Mesozoic time. Although (U-Th)/He data from these areas are generally lacking, the few ages obtained also appear to reflect Late Paleozoic to Early Mesozoic regional cooling.

On southeastern Devon Island, FT ages decrease by 33 My (16%) over a 620 m decrease in elevation (mean TL decreases 4%) along a 3 km transect. For these samples a much higher denudation rate of 18.8 m/My is obtained, apparently suggesting rapid, Jurassic cooling and exhumation of the shield and overlying platform successions on this part of Devon Island. However, Sm-corrected (U-Th)/He ages of ca. 110 Ma obtained for one of these samples (Na03), may indicate that the samples experienced accelerated cooling during Late Cretaceous time. The offshore geology in Lancaster Sound and northern Baffin Bay, south and east of Devon Island, offer some support for this latter interpretation. Lancaster Sound is the principal channel for drainage in the eastern Canadian Arctic (e.g. Fortier and Morley 1956; Pelletier 1966), and likely represents a Tertiary river valley that was deepened and straightened by pre-Late Wisconsinan glaciation (Trettin 1991a). A thick succession of presumed Upper Cretaceous to Paleogene sedimentary strata occurs in eastern Lancaster Sound (maximum thickness of 4000 m; e.g. Harrison 2004), suggesting that southeastern Devon Island was likely to have been exhumed at this time.

6.5.2 Paleogene FT-aged samples

The fifth group (5) forms a cluster of ca. 40-60 Ma ages with mean lengths around 14 μm. The FT ages and length characteristics of these samples are dominated by the thermal effects of the Eurekan Orogeny. Representative FT age and TL data from the Nares Strait

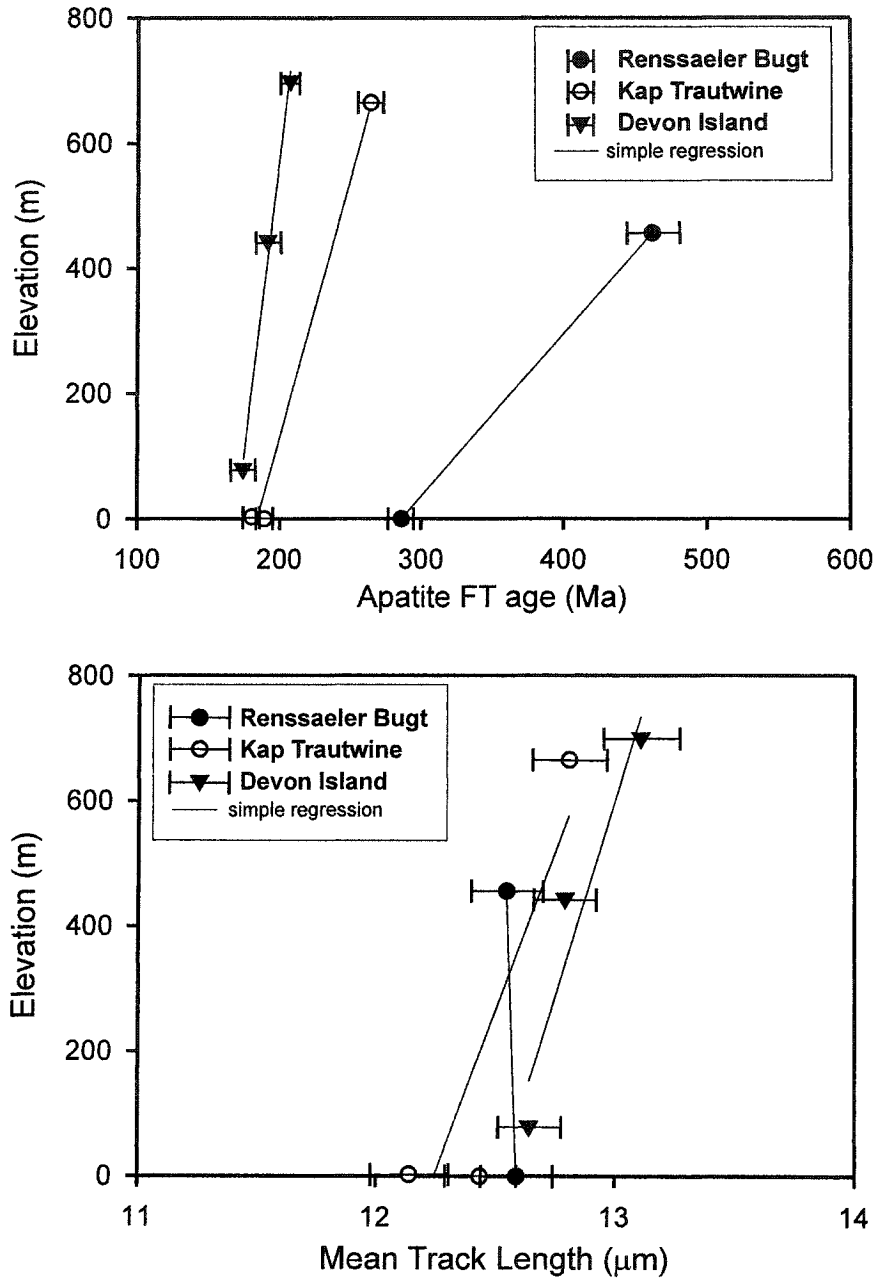

Figure 6.8. FT age vs. elevation (top) and mean TL vs. elevation (bottom) for samples from southeastern Devon Island, Kap Trautwine, and Rensselaer Bugt. From the age/elevation plot approximate rates of denudation (assuming isothermal cooling) can be calculated. The Devon Island samples yield a rate of ca. 18.9 m/My. The Kap Trautwine and Rensselaer Bugt samples appear to have been exhumed more slowly (8.9 m/My and 2.6 m/My, respectively).

region for this group are shown in Fig. 6.9 (modified from Grist and Zentilli 2004). Most of these samples (from the Pavy Formation, north of Cape Back (Fig. 6.3) and south of Cape Baird, and the Mount Lawson Formation, west of Makinson Inlet) were derived from volcanism which was contemporaneous with sedimentation and were inferred by Grist and Zentilli (2004) to have experienced minimal post-depositional heating.

The Sm-corrected (U-Th)/He ages of these samples are shown in Table 6.3. Three samples from the Pavy Formation gave an average age of 48 Ma (Early Eocene), which is significantly younger than the Early Paleocene FT ages. These data indicate that the Pavy Formation samples experienced sufficient post-depositional heating to cause some He diffusion, but negligible track annealing (i.e., ca. 50 °C) prior to cooling to below about 40 °C, likely as a result of exhumation by thrusting during Early Eocene time. The two Mount Lawson Formation samples gave (U-Th)/He ages of ca. 59 Ma (Late Paleocene) that are indistinguishable from the 60 Ma FT age, and which are interpreted as reflecting the provenance age of the volcanic source. This suggests that following deposition, these samples did not experience temperatures exceeding 40 °C.

The other sample (Cambrian Archer Fiord Formation), obtained from the overturned hanging wall succession of the Rawlings Bay thrust at Cape Lawrence, was inferred by Grist and Zentilli (2004) to have cooled from temperatures >130 °C during Early Paleocene time. The Sm-corrected (U-Th)/He age for this sample (Table 6.3) is Late Paleocene (56 Ma). Although the sample was obtained close to the upper plane of the thrust, these data suggest that cooling was initiated during an earlier phase of tectonism which predated the main phase of thrusting during post-Middle Eocene time (Piepjohn et al. 2000). Piepjohn et al. (2000) also tentatively identified transpressional structures that they suggested may have been related to sinistral displacements along Nares Strait at Cape Lawrence, and therefore cooling may have been initiated as a result of exhumation during this earlier phase of transpressive motion on the Rawlings Bay thrust. Alternatively, cooling may have been initiated by rift flank uplift during deposition of ca.1000 m of (Paleocene-aged) Cape Lawrence Formation conglomerate, which comprises the footwall succession of the Rawlings Bay thrust at Cape Lawrence. Within the Sverdrup Basin, Paleogene ages are obtained from samples obtained

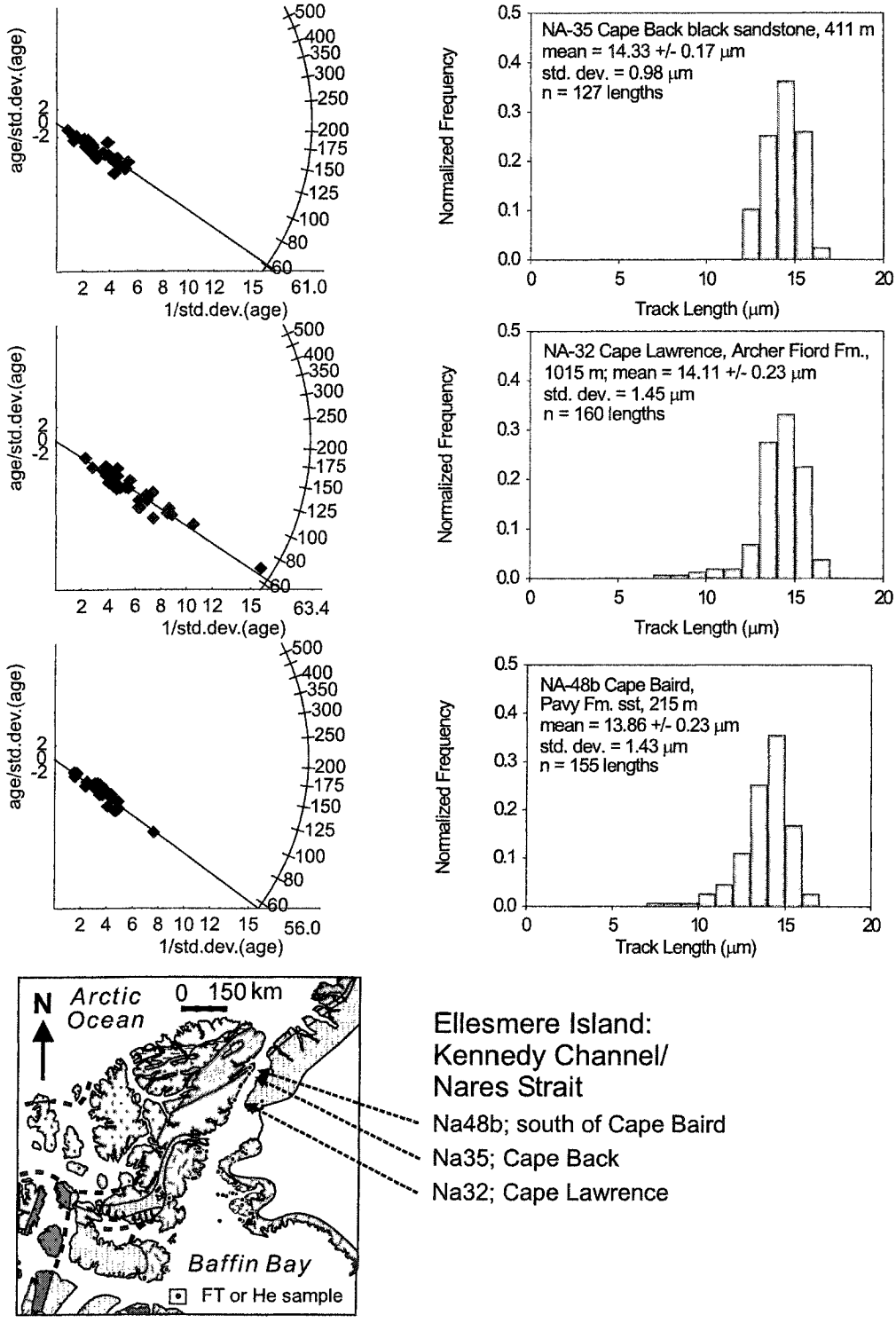

Figure 6.9. Radial plots (left) and TL histograms (right) of the FT data for samples from south of Cape Baird, north of Cape Back, and Cape Lawrence in the Nares Strait region of Ellesmere Island (modified from Grist and Zentilli 2004).

from the hanging walls of major thrusts. Arne et al. (1998, 2002) inferred that these samples were totally annealed by burial heating prior to Paleocene cooling as a result of thrusting during inversion.

6.5.2.1 Does the Wegener Fault exist?

FT and (U-Th)/He data for most samples from the Nares Strait region reflect Paleogene mafic volcanism, strike-slip and minor thrust exhumation that was contemporaneous with the inversion of the Sverdrup Basin during the Eurekan Orogeny. They are compatible with kinematic plate tectonic reconstructions that require extensive Paleocene strike-slip motion (e.g. Srivastava 1985), however they suggest only relatively minor strike-slip tectonism focused along the strait. Arne et al. (1998, 2002) inferred that the initiation of cooling in central Ellesmere Island also occurred in Early Paleocene time, during sinistral strike-slip relative displacements between Greenland and Ellesmere Island, and prior to the onset of Eocene convergence (e.g. Tessensohn and Piepjohn 2000).

Based on the data of Arne et al. (1998, 2002) and the apatite FT and (U-Th)/He data presented here, it is therefore likely that Eurekan strike-slip tectonism was partitioned into a number of discrete fault zones across Ellesmere Island rather than along a single transform offset in the Nares Strait region. From Fig. 6.4, it appears that the Paleocene (group 5) samples from the Nares Strait region are slightly older than similar samples from within the Sverdrup Basin, approximately 200 km west of the present study area. This suggests that cooling and inferred exhumation of hanging wall strata of the Lake Hazen fault zone at Hare Fiord, and from the Vesle Fiord Thrust in central Ellesmere Island, were more recent than near the coast. It is possible that strike-slip deformation was initially focused along the Nares Strait and progressed farther inland during Paleocene time, thus being partitioned into a relatively wide belt.

6.7 Conclusions

The apatite FT and (U-Th)/He data from south of the Kane Basin, in the Inglefield Uplift region of southeast Ellesmere Island and similar rocks in the Inglefield Brednig and

Inglefield Land, Greenland, provide important insights into the complex thermal history of the eastern Canadian Arctic Archipelago. The data are consistent with multiple phases of denudational cooling and exhumation related to the development of the Sverdrup Basin. An early phase corresponds to a period of subsidence and widespread clastic sedimentation likely as a result of uplift of rift flanks during Late Carboniferous to Early Permian time. A later phase corresponds to a period of increased subsidence and high sediment supply within the basin beginning in Early Triassic time.

Some samples from Wolstenholme Fjord - Thule region of Greenland, and the Inglefield Uplift in Devon Island and Talbot Inlet, Ellesmere Island, have much younger FT ages and broad or bimodal TL distributions. Younger (U-Th)/He ages are also evident in samples from Cape Faraday and from Orne Island, and Mansen and Carey Øer in northwestern Baffin Bay. These data likely reflect Late Cretaceous cooling of rift flanks in response to rifting in Baffin Bay. Relatively rapid denudation rates of ca. 20 m/My are indicated for southeastern Devon Island, and these are consistent with a thick accumulation of presumed Late Cretaceous strata immediately offshore in Lancaster Sound. Lower denudation rates of 2.6 m/My and 8.9 m/My are indicated for Rensselaer Bugt, and Kap Trautwine, Greenland, respectively.

In the Nares Strait region FT and (U-Th)/He data for the Nares Strait region reflect Paleogene relative plate movements between Greenland and Ellesmere Island, but suggest that only relatively minor strike-slip tectonism occurred along the strait. This may indicate that deformation was partitioned into a number of thrust fault zones across a relatively wide belt, instead of along a single transform (the Wegener Fault).

6.8 Acknowledgements

A. Grist and M. Zentilli are very grateful to Co-chief Scientists Franz Tessensohn and Ruth Jackson, and to Chris Harrison for allowing us the opportunity to participate in the Nares Strait Geocruise. Chris Harrison also provided invaluable insight into the complex regional geology. We are also appreciative of the combined efforts of Captain Stewart Klebert, Chief Officer Bob Strowbridge, and the crew of the C.C.G.S. Louis S. St. Laurent.

Helicopter pilots Harrison Macrae and Adrien Godin were very accommodating to our ambitious sampling plans. Henry Halls, Jason Anderson and Anna Jensen also kindly assisted us by collecting a few FT samples during their paleomagnetic and geodetic studies. Special thanks to Brian Atagootak and Jimmy Nungaq of Grise Fiord, who assisted us during sample collection. Many thanks to Ken Farley at Caltech for instruction on many aspects of (U-Th)/He dating, and also to Lindsey Hedges for her invaluable assistance in the (U-Th)/He laboratory, and for doing the ICP-MS analyses. Thanks to Chris Beaumont, Peter Reynolds and Ken Farley for critically reviewing early versions of this manuscript.

6.9 References cited

Arne, D.C., Zentilli, M., Grist, A.M., and Collins, M. 1998. Constraints on the timing of thrusting during the Eurekan orogeny, Canadian Arctic Archipelago: an integrated approach to thermal history analysis. Canadian Journal of Earth Sciences. **35**, 1: 30-38.

Arne, D.C., Grist, A.M., Zentilli, M., Collins, M., Embry, A., and Gentzis, T. 2002. Cooling of the Sverdrup Basin during Tertiary basin inversion: implications for hydrocarbon exploration. Basin Research, **14**: 183-205.

Balkwill, H.R. 1978. Evolution of the Sverdrup Basin, Arctic Canada. The American Association of Petroleum Geologists Bulletin, **62**, 1004-1028.

Brown, R.W. 1992. A fission track study of the sub-arial continental margins of southern Africa. Ph.D. thesis, University of Melbourne, 407 pp.

Brown, R.W., Gallagher, K. and Duane, M. 1994. A qualitative assessment of the effects of magmatism on the thermal history of the Karoo sedimentary sequence. Journal of African Earth Sciences, **18**, 227-243.

Brown, R.W., Gallagher, K., Gleadow, A.J.W., and Summerfield, M.A. 2000. Morphotectonic evolution of the south Atlantic margins of Africa and South America. In; Geomorphology and Global Tectonics. Edited by M.A. Summerfield. J. Wiley and Sons, New York, 255-281.

Davies, G.R. and Nassichuk, W.W. 1991. Carboniferous and Permian history of the

Sverdrup Basin, Arctic Islands; chapter 13 - in; Geology of the Innuition Orogen and Arctic Platform of Canada and Greenland, Edited by H.P. Trettin. Geological Survey of Canada, Geology of Canada **3**, 343-368 (also Geological Society of America, The Geology of North America, Vol. E).

Dawes, P.R. and Kerr, J.W. (editors) 1982a. Nares Strait and the Drift of Greenland: a Conflict in Plate Tectonics; Meddelelser om Grønland, Geoscience **8**, 392 p.

Dawes, P.R. and Kerr, J.W. 1982b. The case against major displacement along Nares strait; In; Nares Strait and the Drift of Greenland: a Conflict in Plate Tectonics, Edited by P.R. Dawes and J.W. Kerr, Meddelelser om Grønland, Geoscience **8**, 369-386.

Dumitru, T.A., Hill, K.C., Coyle, D.A., Duddy, I.R., Foster, D.A., Gleadow, A.J.W., Green, P.F., Kohn, B.P., Laslett, G.M., and O'Sullivan, A.J. 1991. Fission track thermochronology: Application to continental rifting of south-eastern Australia. Australian Petroleum Exploration Association Journal, **31**, 131-142.

Embry, A.F. 1982. The Upper Triassic - Lower Jurassic Heiberg deltaic complex of the Sverdrup Basin; in; Arctic Geology and Geophysics, Edited by A.F. Embry and H.R. Balkwill; Canadian Society of Petroleum Geologists, Memoir, **8**, 189-217.

Embry, A.F. 1991. Mesozoic history of the Arctic Islands; chapter 14 - in; Geology of the Innuition Orogen and Arctic Platform of Canada and Greenland, Edited by H.P. Trettin. Geological Survey of Canada, Geology of Canada **3**, 369-433 (also Geological Society of America, The Geology of North America, Vol. E).

Embry, A.F. and Dixon, J. 1990. The breakup unconformity of the Amerasia Basin, Arctic Ocean: Evidence from Arctic Canada. Geological Society of America Bulletin, **102**, 1526-1534.

Estrada, S. and Tessensohn, F. (2004) Late Palaeocene Nares Strait volcanic province: Evidence from volcanic pebbles, (in prep.) .

Farley, K.A. 2000. Helium diffusion in apatite: General behavior as illustrated by Durango fluorapatite. Journal of Geophysical Research, **105**, p. 2903-2914.

Farley, K.A. 2002. (U-Th)/He dating: Techniques, calibration and applications. In; Noble Gases in Geochemistry and Cosmochemistry, Edited by D. Porcelli, C.J. Ballentine

and R. Wieler. Reviews in Mineralogy and Geochemistry, **47**, pp. 819-844.

Farley, K.A., Wolf, R.A. and Silver, L.T. 1996. The effects of long alpha-stopping distances on (U-Th)/He ages. Geochimica et Cosmochimica Acta, **60**, no. 21, p. 4223-4229.

Fleischer, R.L., Price, P.B. and Walker, R.M. 1964. Fission track ages of zircons. Journal of Geophysical Research, **69**: 4885.

Fleischer, R.L., Price, P.B. and Walker, R.M. 1975. Nuclear Tracks in Solids: Principles and Applications. University of California Press, Berkeley, California.

Fortier, Y.O. and Morley, L.W. 1956. Geological unity of the Arctic Islands. Royal Society of Canada Transactions, **50**, 3-12.

Galbraith, R.F. 1990. The radial plot: graphical assessment of spread in ages. Nuclear Tracks and Radiation Measurements, **17**, 3: 207-214.

Galbraith, R.F. and Laslett, G.M. 1993. Statistical models for mixed fission track ages. Nuclear Tracks and Radiation Measurements, **21**: 459-470.

Gallagher, K. 1995. Evolving temperature histories from apatite fission-track data.Earth and Planetary Science Letters, **136**, 421-435.

Gallagher, K. and Brown, R.W. 1997. The onshore record of passive margin evolution. Journal of the Geological Society, London, **154**: 451-457.

Gallagher, K., Hawkesworth, C. and Montovani, M. 1994. The denudation history of the onshore continental margin of S.E. Brazil inferred from fission track data. Journal of Geophysical Research, **99**, 18117-18145.

Gallagher, K., Hawkesworth, C. and Montovani, M. 1995. Denudation, fission track analysis and the long-term evolution of passive margin topography: application to the S.E. Brazilian margin. Journal of South American Earth Sciences, **8**, 65-77.

Gallagher, K., Brown, R.W. and Johnson, C. 1998. Fission track analysis and its applications to geological problems. Annual Review of Planetary Science Letters. **26**: 519-572.

Gleadow, A.J.W. and Brown, R.W. 2000. Fission-track thermochronology and the long-term denudational response to tectonics. In; Geomorphology and Global Tectonics. Edited by M.A. Summerfield. J. Wiley and Sons, New York, 57-75.

Grist, A.M. and Zentilli, M. 2004 (submitted). The Thermal History of the Nares Strait,

Region in Canada: Insights from Apatite Fission Tracks. Geologishes Jahrbuch

Harrison, J.C. (2004; In prep.) Geological map of the Nares Strait region, explanatory notes. Geologishes Jahrbuch.

Harrison, J.C., Mayr, U., McNeil, D.H., Sweet, A.R., McIntyre, D.J., Eberle, J.J., Harrington, C.R., Chalmers, J.A., Dam. G., and Nøhr-Hansen, H. 1999. Correlation of Cenozoic sequences of the Canadian Arctic region and Greenland: implication for the tectonic history of northern North America. Bulletin of Canadian Petroleum Geology, **47**, 3: 223-254.

Heaman, l., LeCheminant, A.N. and Rainbird, R.H. 1992. Nature and timing of Franklin igneous events, Canada: Implications for a Late Proterozoic mantle plume and the break-up of Laurentia. Earth and Planetary Science Letters, **109**, 117-131.

House, M.A., Wernicke, B.P., Farley, K.A., and Dumitru, T. 1997. Cenozoic thermal evolution of the central Sierra Nevada from apatite (U-Th)/He ages. Nature, **396**, 66-69.

House, M.A., Farley, K.A. and Stockli, D. 2000. Helium chronometry of apatite and titanite using Nd-YAG laser heating. Earth and Planetary Science Letters, **183**, 365-368.

Hurford, A.J. and Green, P.F. 1982. A users' guide to fission track dating calibration. Earth and Planetary Science Letters, **59**: 343-354.

Hurford, A.J. and Green, P.F. 1983. The zeta age calibration of fission track dating. Chemical Geology (Isotope Geoscience Section), **1**: 285-317.

Kerr, J.W. 1967. Nares submarine rift valley and the relative rotation of north Greenland: Bulletin of Canadian Petroleum Geology, **15**, 483-520.

Kristoffersen, Y. 1990. Eurasia Basin. In; The Arctic Ocean Region: The Geology of North America, Edited by L, A. Grantz, L. Johnson, and F.J. Sweeney, Geological Society of America, Boulder, 365-379.

Lippolt, H.J., Leitz, M., Wernicke, R.S., and Hagedorn,B. 1994. (U+Th)/He dating of apatite; Experience with samples from different geochemical environments. Chemical Geology (Isotope Geoscience Section), **112**, 179-191.

Menzies, M.A., Gallagher, K., Hurford, A.J., and Yelland, A. 1997. Red Sea and Gulf of

Aden rifted margins, Yemen: denudational histories and margin evolution. Geochimica et Cosmochemica, Acta, **61**, 2511-2527.

Miall, A.D. 1986. The Eureka Sound Group (Upper-Cretaceous-Oligocene), Canadian Arctic Islands. Bulletin of Canadian Petroleum Geology. **34**: 240-270.

Moore, M.E., Gleasdow, A.J.W. and Lovering, J.F. 1986. Thermal evolution of rifted continental margins: new evidence from fission tracks in basement apatites from southeastern Australia. Earth and Planetary Science Letters, **78**, 255-270.

Oakey, G.N., Hearty, B., Forsberg, R., and Jackson, H.R. 2000. Gravity anomaly of the Innuitian region, Canadian and Greenland Arctic. Geological Survey of Canada Open File 3934d, scale 1:1,500,000.

Okulitch, A.V. and Trettin, H.P. 1991. Late Cretaceous - Early Tertiary deformation, Arctic Islands, chapter 17 - in; Geology of the Innuition Orogen and Arctic Platform of Canada and Greenland, Edited by H.P. Trettin. Geological Survey of Canada, Geology of Canada **3**, 469-489 (also Geological Society of America, The Geology of North America, Vol. E).

Okulitch, A.V., Dawes, P.R., Higgins, A.K., Soper, N.J., and Christie, R.L. 1990. Towards a Nares Strait solution: Structural studies on southeastern Ellesmere Island and northwestern Greenland. Marine Geology, **93**, 369-384.

Pelletier, B.R. 1966. Development of submarine physiography in the Canadian Arctic and its relation to crustal movements; In; Continental Drift, Edited by G.D. Garland, The Royal Society of Canada, Special Publication no. 9, 77-101.

Piepjohn, K., Tessensohn, F., Harrison, C., and Mayr, U. 2000. Involvement of a Tertiary foreland basin in the Eurekan foldbelt deformation, NW coast of Kane Basin, Ellesmere Island, Canada. Polarforschung **68**: 101-110.

Reiners, P.W., Farley, K.A. and Hickes, H.J. 2002. He diffusion and (U-Th)/He thermochronometry of zircon: Initial results from Fish Canyon Tuff and Golde Butte: Tectonophysics, **349**, 297-308.

Reiners, P.W. and Farley, K.A. 1999. Helium diffusion and (U-Th)/He thermochronometry of titanite. Geochimica et Cosmochimica Acta, **63**, 3485-3859.

Riisager, J., Riisager, P. and Pederson, A.K. 2003. Paleomagnetism of large igneous provinces: case-study from West Greenland, North Atlantic igneous province; Earth and Planetary Science Letters, **214**, 409-425.

Rutherford, E. 1905. Present problems in radioactivity. Popular Science Monthly, May, 1-34.

Srivastava, S.P. 1978. Evolution of the Labrador Sea and its bearing on the early evolution of the North Atlantic. Geophysical Journal of the Royal Astronomical Society, **52**, 313-357.

Srivastava, S.P. 1985. Evolution of the Eurasian Basin and its implications to the motion of Greenland along Nares Strait, Tectonophysics, **114**, 29-53.

Story, M., Duncan, R.A., Pederson, A.K., Larsen, L.M., and Larsen, H.C. 1998. $^{40}Ar/^{39}Ar$ geochronology of the West Greenland Tertiary volcanic province; Earth and Planetary Science Letters, **160**, 569-586.

Strutt, R.J. 1905. On the radioactive minerals. Proceedings of the Royal Society, **A7,** 88-101.

Sweeney, J.F., Weber, R.R. and Blasco, S.M. 1982. Continental ridges in the Arctic Ocean: LOREX constraints; Tectonophysics, **89**, 217-238.

Tessensohn, F. and Piepjohn, K. 2000. Eocene compressive deformation in Arctic Canada, North Greenland and Svalbard and its plate tectonc causes. Polarforschung **68**: 121-124.

Thorsteinsson, R. and Tozer, E.T. 1970. Geology of the Arctic Archipelago. In; Geology and Economic Minerals of Canada. Edited by R.J.W. Douglas. Geological Survey of Canada Economic Geology Report no. 1, 547-590.

Trettin, H.P. 1991a. Tectonic framework. chapter 4 In; Geology of the Innuitian Orogen and Arctic Platform of Canada and Greenland. Edited by H.P. Trettin. Geological Survey of Canada, Geology of Canada **3**, 59-66 (also Geological Society of America, The Geology of North America, Vol. E).

Trettin, H.P. 1991b. Summary and remaining problems. In; Geology of the Innuitian Orogen and Arctic Platform of Canada and Greenland. Edited by H.P. Trettin. Geological Survey of Canada, Geology of Canada **3**, 547-543 (also Geological Society of America, The Geology of North America, Vol. E).

Trettin, H.P. 1991c (Editor). Geology of the Innuitian Orogen and Arctic Platform of Canada and Greenland. Geological Survey of Canada, Geology of Canada, No. 3 (also Geological Society of America, The Geology of North America, Vol. E).

Troelson, J.C. 1950. Contributions to the geology of north-west Greenland, Ellesmere Island and Axel Heiberg Island. Meddelelser om Grønland, **149**, no. 7, 85 p.

Wagner, G.A. and Van den Haute, P. 1992. Fission track dating. Kluwer Academic Publishers, Dordrecht.

Wegener, A.L. 1929. Die Enstehung der Kontinente und Ozeane, Friedich Vieweg & Sohn, Braunschweig, 1929.(The Origin of Continents and Oceans, Translated in 1966 by John Biram from 4th revised edition).

Wolf, R.A., Farley, K.A. and Kass, D.M. 1998. Modeling of the temperature sensitivity of the apatite (U-Th)/He thermochronometer. Chemical Geology, **148**, 105-114.

Zeitler, P.K., Herczeg, A.L., McDougall, I., and Honda, M. 1987. U-Th-He dating of apatite: A potential thermochronometer. Geochimica et Cosmochimica Acta, **51**, 2865-2868.

Appendix 1. Analytical procedures:

A1.1 FT dating:

Apatite mineral separates were obtained using conventional heavy liquid and magnetic separation techniques. Aliquots of individual separates for FT dating were mounted in epoxy and polished to expose internal grain surfaces. Spontaneous tracks were revealed by etching in 5M HNO_3 for 20 seconds at 24 °C. FT ages were determined using the external detector method (Fleischer et al. 1964, Hurford and Green 1982). A thin sheet of low-uranium muscovite was attached to the polished surface of each grainmount to detect neutron-induced fission. Samples were irradiated at the Dalhousie University Slowpoke reactor in the presence of glass neutron dosimeters (CN5) of known characteristics. The thermal-neutron fluence obtained was ca. $9 \times 10^{15}/cm^2$. The cadmium ratio for Au is 4.3 at the site. Micas were etched at room temperature in 48% HF for 22 minutes. Spontaneous and induced track densities (tracks/cm^2) were counted at 1000X magnification (100X dry objective, 10X oculars) on a Zeiss® Axioplan microscope equipped with an Autoscan® AS3000 stage. Ages were calculated using a weighted mean zeta calibration factor (Fleischer et al. 1975, Hurford and Green 1983), determined using the Fish Canyon Tuff and Durango apatite age standards. Length distributions of horizontal, confined tracks (in crystallographic planes parallel to the c-axis) were also measured at 1000X magnification using a digitizing pad interfaced with a personal computer. The precision of each measured length is ± 0.20 μm. Where sufficient apatite was obtained, 2 grainmounts were made for each sample. For samples with relatively low spontaneous track densities the second grainmount was exposed to a source of heavy fission fragments (^{252}Cf) to greatly increase the number of etchant pathways and thereby, the number of confined tracks revealed by etching.

A1.2 (U-Th)/He dating:

Individual samples consisting of between 1 and 4 inclusion-free grains (Table 6.3) were selected for (U-Th)/He analysis using a stereo binocular microscope equipped with a transmitted light source and a rotating stage. Only grains that appeared completely dark when viewed with the stage rotated to extinction (in crossed polarized light) were selected. Prior

to analysis, sample grains were measured using a microscope equipped with an ocular graticule and stage micrometer to calculate alpha ejection corrections. For(U-Th)/He analysis sample grains were placed in platinum microtubes, that were then pinched closed and loaded into a laser planchet. He extraction was done using a Nd-YAG laser following the method of House et al. (2000). Individual microtubes were heated to temperatures of ca. 1050 °C to completely out gas the grains. Evolved gases were spiked with approximately 0.4 pmol of ^{3}He and adsorbed on activated charcoal cooled to 16 K using a cryogenic trap. Purification to remove contaminant gases was done by heating the trap to 37 K, thereby releasing only He. $^{4}He/^{3}He$ ratios were measured in a quadrupole mass spectrometer. Completeness of gas extraction was verified for each sample by performing a re-extraction heating following each He analysis. Ratios were referenced to multiple determinations of a known volume of ^{4}He standard processed in the same way as the samples, and appropriate discrimination corrections were made to the measured $^{4}He/^{3}He$ ratios.

Following degassing the Pt microtubes were placed in 100 ml of concentrated HNO_3 to dissolve the apatite grains. Solutions were spiked with a 25 ml calibrated ^{230}Th and ^{235}U solution and diluted to 250 ml with ultrapure water. The spiked samples were analyzed as 0.5 ml aliquots of ca. 1-5 ppb U-Th solutions by isotope dilution on a Finnigan Element2 ICP-MS with a teflon micro-flow nebulizer and double-pass spray chamber. U and Th blanks by this method are 1 ± 0.1 pg and 2 ± 1 pg, respectively. Estimated uncertainty of measured sample U-Th are on the order of 1-2% (2σ).

CHAPTER 7. Apatite fission track and (U-Th)/He thermal history modelling of the Nares Strait, Kane Basin, Smith Sound region in Canada and Greenland

A.M. Grist and M. Zentilli

7.1 Abstract

This paper presents a simple method of calibrating apatite fission track (FT) inverse model thermal history predictions using diffusion-based forward modelling of (U-Th)/He ages from the same samples. FT inverse and (U-Th)/He forward thermal models have been obtained for samples from several areas in the Nares Strait, Kane Basin, Smith Sound region of the eastern Canadian Arctic and western Greenland. The (U-Th)/He ages predicted by the FT model thermal histories demonstrate that it is crucial to consider the effects of low temperature track annealing in FT models. If FT modelling is done using an initial mean track length (TL) of 16.15 μm, the Laslett et al. (1987) annealing model is too retentive, and the temperatures required to produce measured length distributions are too high to be compatible with measured (U-Th)/He ages. Thermal histories that are compatible with both FT and (U-Th)/He data are obtained using the Laslett et al. (1987) annealing model with an initial mean TL of 15 μm.

FT and (U-Th)/He models for samples from the Ingelfield Uplift region of eastern Ellesmere Island are consistent with a history of cooling from temperatures of >130 °C beginning in Late Paleozoic time, likely as a result of exhumation of the uplifted rift flanks following the initiation of rifting in the Sverdrup Basin in central Ellesmere Island. Thermal history models for samples from the Wolstenholme Fjord - Inglefield Brednig region in western Greenland are consistent with a history of monotonic cooling beginning in Mesozoic time, that was likely caused by denudation of this area during periods of increased sediment input into the Sverdrup Basin in Mesozoic time (Embry 1991; Grist and Zentilli 2004). Thermal models for samples from the Inglefield Uplift region on southern Devon Island show evidence of a period of heating and elevated temperatures during Late Cretaceous time, and an accelerated rate of cooling from Paleocene time to the present. Thermal models for

other samples obtained from islands and coastal regions of Baffin Bay, in Inglefield Brednig, Greenland, and Talbot Inlet, Ellesmere Island, are also consistent with Late Cretaceous rift-related heating.

In the Nares Strait region, (U-Th)/He forward models for samples from the volcanogenic sandstones of the Pavy Formation are consistent with very limited post-depositional heating to temperatures that were too low to cause significant track annealing (<50 °C), likely during Early Eocene time. However, the inverse fission track model for a sample from the Archer Fiord Formation in the hanging wall of the Rawlings Bay thrust at Cape Lawrence clearly indicates that a major phase of cooling during Eurekan tectonic movement occurred during Late Paleocene time, and only minor (i.e., <2 km) Eocene thrusting is evident.

7.2 Introduction

The objective of the present study is to develop quantitative thermal history models using inverse thermal modelling of apatite FT age and length data and forward modelling of (U-Th)/He age data for samples from the Nares Strait, Kane Basin, Smith Sound region of eastern Arctic Canada and western Greenland (Grist and Zentilli 2004a, b). Using these two thermochronometric techniques together in modelling geologic thermal histories offers a number of advantages. Although the systematics of FT annealing and He diffusion differ, both of these temperature-dependent systems operate over similar ranges (ca. 60-130 °C for apatite FT, and 40-80 °C for apatite (U-Th)/He), and thus they provide complementary data. They also use the same mineral, which provides the opportunity to use data from one technique as an independent test of the model predictions of the other.

We have taken the approach of using measured and forward modelled apatite (U-Th)/He ages to test FT model predictions and constrain the part of the thermal history that is not well characterised using the Laslett et al. (1987) FT annealing model. We first suggest a simple calibration of the Laslett et al. annealing model using diffusion-based forward modelling of (U-Th)/He ages for the Durango apatite standard. We then present calibrated FT inverse models for data from Grist and Zentilli (2004a, b), who inferred that multiple

episodes of cooling of Archean to Paleozoic samples in the Nares Strait, Kane Basin, Smith Sound region were related to Late Paleozoic exhumation of parts of the area during clastic sedimentation in the Sverdrup Basin, northwest of the study area, and to periods of increased subsidence and sediment supply to the basin during Mesozoic time. Thermal models are also presented for several samples that were inferred to have cooled as a result of flank uplift during the onset of Late Cretaceous rifting in Baffin Bay, and for samples affected by Paleogene tectonics related to the Eurekan Orogeny.

7.3 Thermal history modelling using apatite

7.3.1 FT inverse modelling

FT analysis is based on the measured density and length distribution of linear tracks of crystal damage produced during spontaneous fission of trace amounts of ^{238}U (e.g. Wagner and Van den Haute 1992; Gallagher et al. 1998). In simple, rapidly-cooled systems track densities provide a measure of age with respect to the Dodson (1973) concept of a closure temperature of approximately 100 °C.

Gradual TL reduction by annealing of fission damage is an irreversible process that is dominantly thermally activated. In apatite etchable tracks are retained between 60 and 130 °C, but are progressively shortened in response to the highest temperatures experienced. Tracks are formed continuously through time, and length distributions are therefore indicative of the integrated thermal history below the closure temperature. It is this temperature-dependent behaviour between ca. 60 and 130 °C (referred to as the partial annealing zone or PAZ) that allows the apatite FT method to be used as a low-temperature thermochronometer. However, in systems with complex thermal histories apparent FT ages may not represent a geologically significant event in time because the probability of a track intersecting a polished surface and thus contributing to the age is proportional to its length.

Green et al. (1986) characterized the annealing behaviour of fission tracks in Durango apatite within the PAZ by measuring TL distributions in samples heated from 20 minutes to 500 days at temperatures between 95 and 400 °C. FT annealing models have been developed based on empirical extrapolations of the Green et al. (1986) annealing data to geologic time.

The most widely used is the Laslett et al. (1987) fanning-Arrhenius model, which has been incorporated into a number of modelling software packages developed using Monte-Carlo type search techniques to evolve thermal history simulations to predict FT age and length distributions (e.g. Gallagher 1995; Willett 1997).

For this study inverse thermal history modelling of FT age and TL distributions was done using the FORTRAN program AFTINV (Willett 1997) modified to run on a personal computer (Issler 1996a), which produces synthetic FT age and TL data as follows. Component sets of unannealed (i.e., 16.15 μm) fission tracks are introduced at discrete (user-input) time intervals. Lengths are annealed in response to subsequent temperatures as the thermal history evolves, resulting in an integrated TL distribution and an apparent age. Predicted TL distributions and ages are compared to the measured data using a goodness-of-fit statistic. A solution set of the best-fitting histories is maintained as the algorithm repeats iteratively until all solutions in the set fit the data to the desired confidence level (in this instance 95%). User-input constraints on heating, cooling, and rate bounds based on independent geological data help limit the search space to geologically reasonable solutions.

7.3.2 (U-Th)/He forward modelling

The (U-Th)/He method, based on accumulation of radiogenic He (ingrowth) through U-series and Th-series decay, was one of the earliest techniques developed for the dating of geologic materials (e.g. Rutherford 1905; Strutt 1905). It was often considered unreliable owing to the ease with which radiogenic He could be lost from the host mineral resulting in underestimated ages, and with the advent of apparently more reliable radiometric methods such as K-Ar, interest in He systematics faded. Recently the technique has experienced a renaissance after its potential as a low temperature thermochronometer was suggested by Zeitler et al. (1987). The use of (U-Th)/He thermochronometry based on ^{4}He concentration profiles to constrain low-temperature cooling histories has recently been demonstrated by Reiners et al. (2003), Ehlers and Farley (2003), Shuster and Farley (2003), and others.

The behaviour of radiogenic He in a crystal lattice is governed by laws of diffusion (e.g. Wolf et al. 1998; Reiners and Farley 1999; Farley 2000; Reiners et al. 2002) which are

highly temperature-dependent. Wolf et al. (1998) demonstrated that diffusive loss of He from apatite becomes significant at temperatures as low as 40 °C, and is essentially complete at temperatures of 80-85 °C over geologic time-scales. The progressive diffusive loss of radiogenic He between 40-80 °C results in a He partial retention zone (PRZ) that is analogous to the PAZ. Thus apatite FT and (U-Th)/He dating are independent low-temperature thermochronometers that may be used to constrain heating and cooling through temperatures of 40 to 130 °C with essentially no overlap.

Forward diffusion modelling of (U-Th)/He ages was done using proprietary software "Age Calculation.vi" written by K. Farley. The program calculates an apparent (U-Th)/He age based on net radiogenic He accumulation (a balance between ingrowth and diffusive loss) as described by Equation 11 in Chapter 2 (Equation 5 in Wolf et al. 1998). Input parameters for the age calculation are the measured grain radius, the diffusion grainsize, the activation energy (33 kcal/mol; Farley 2000) and the U and Th contents. Calculated ages were corrected to account for ejection from the host grain of a portion of the He produced by alpha decay.

7.3.3 Calibration of the Laslett et al. (1987) annealing model

The Laslett et al. (1987) annealing model under-predicts annealing at low temperatures when applied over geologic timescales (Vrolijk et al. 1992). Although it is generally accepted that apatite fission tracks may undergo some shortening at temperatures below the lower limit of the PAZ (i.e., 60 °C; e.g. Bertel et al. 1977; Green 1988), such shortening is generally considered of minor importance. Laslett et al. (1987), Green et al.(1989) and others have suggested that at temperatures below 50 °C tracks are mostly retained at their initial lengths. However, Donelick et al. (1990) demonstrated that in induced track populations reduction of the initial mean length by as much as 0.5 μm occurred within a few days at room temperature.

Greater differences are seen between the mean TL and length distributions of spontaneous tracks in the supposedly unannealed Durango and Fish Canyon Tuff FT age standards relative to corresponding (artificially-induced) unannealed length distributions (e.g.

Fig. 7.1). The mean spontaneous TL of the Durango standard is reduced by 1.5-2 μm. Unannealed tracks in apatite (i.e., >16 μm), which are abundant in the induced population are relatively uncommon in most fossil populations, even though the Laslett et al. (1987) model predicts that they should be stable at temperatures up to 50 °C, corresponding to a burial depth of ca. 2 km in a typical geothermal gradient. As a result of failing to consider this low temperature annealing, many apatite FT modelling studies include a late-stage of 30-40 °C cooling that is an artefact required to reconcile the thermal model with the observed lack of unannealed tracks.

Apatite (U-Th)/He dating offers an opportunity to refine the low temperature part of FT thermal models because the temperature range of the PRZ is lower than the FT PAZ. Temperatures of ca. 50 °C, which are often seen in the late stages of FT thermal models are high enough to cause significant He diffusion, so (U-Th)/He ages allow us to distinguish whether such late stage cooling is real, or whether low-temperature track annealing needs to be considered.

Figure 7.2 shows an example of the under-prediction of low-temperature annealing for the Durango apatite standard using the Laslett et al. (1987) annealing model. The accepted age of Durango apatite is 31.4 ± 1.2 Ma (e.g. Wagner and Van den Haute 1992) and it has a measured (U-Th)/He age of 32.1 ± 1.2 Ma (e.g. House et al. 2000). The top panel shows a FT time-temperature (t-T) history (left) and measured and modelled length distributions for Durango obtained using an initial mean TL of 15 μm. The middle and lower panels show the same model, except that initial lengths of 15.5 μm, and 16.1 μm, respectively, were used. It is apparent from the t-T histories in the lower panels that the FT inverse model is forced to invoke late-stage cooling of as much as 35-40 °C after 4 Ma. in order to match the observed length distribution. However, if an initial length of 16.15 μm is used (lower panel) the high model temperatures cause significant He diffusion, and the predicted (U-Th)/He age is only 17.3 Ma. An initial TL of 15.5 μm produces a better result, with a predicted (U-Th)/He age of 26.8 Ma, however some late cooling is still evident. Using an initial TL of 15 μm in the FT inverse model gives a 29.1 Ma (U-Th)/He age, which is closer to the expected age, and essentially eliminates unrealistic late-stage cooling.

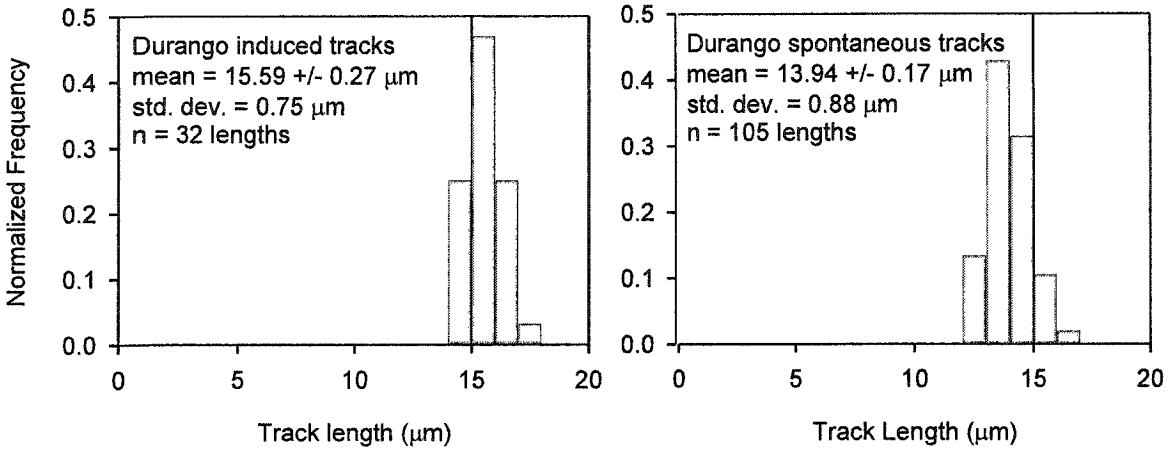

Figure 7.1. Induced (left) and spontaneous (right) track length distributions in the Durango apatite standard. A 1.65 μm difference in the mean lengths exists between the supposedly unannealed fossil and the induced distributions. A reference line is shown at 15 μm.

Figure 7.2. Inverse fission track thermal models (left) and modelled /measured track length distributions (right) for the Durango apatite standard spontaneous track length distribution in Fig. 7.1. Each model shows 250 t-T histories that pass the goodness-of-fit test (thin grey lines), the exponential mean of the 250 histories (thick black line), the upper and lower solution bounding envelopes (thin dashed lines), and the (U-Th)/He forward model (thick dashed line). Note that the solution bounding envelopes are not themselves solutions.The models were done using an initial length of 15 μm (top), 15.5 μm (middle) and 16.15.μm (bottom).

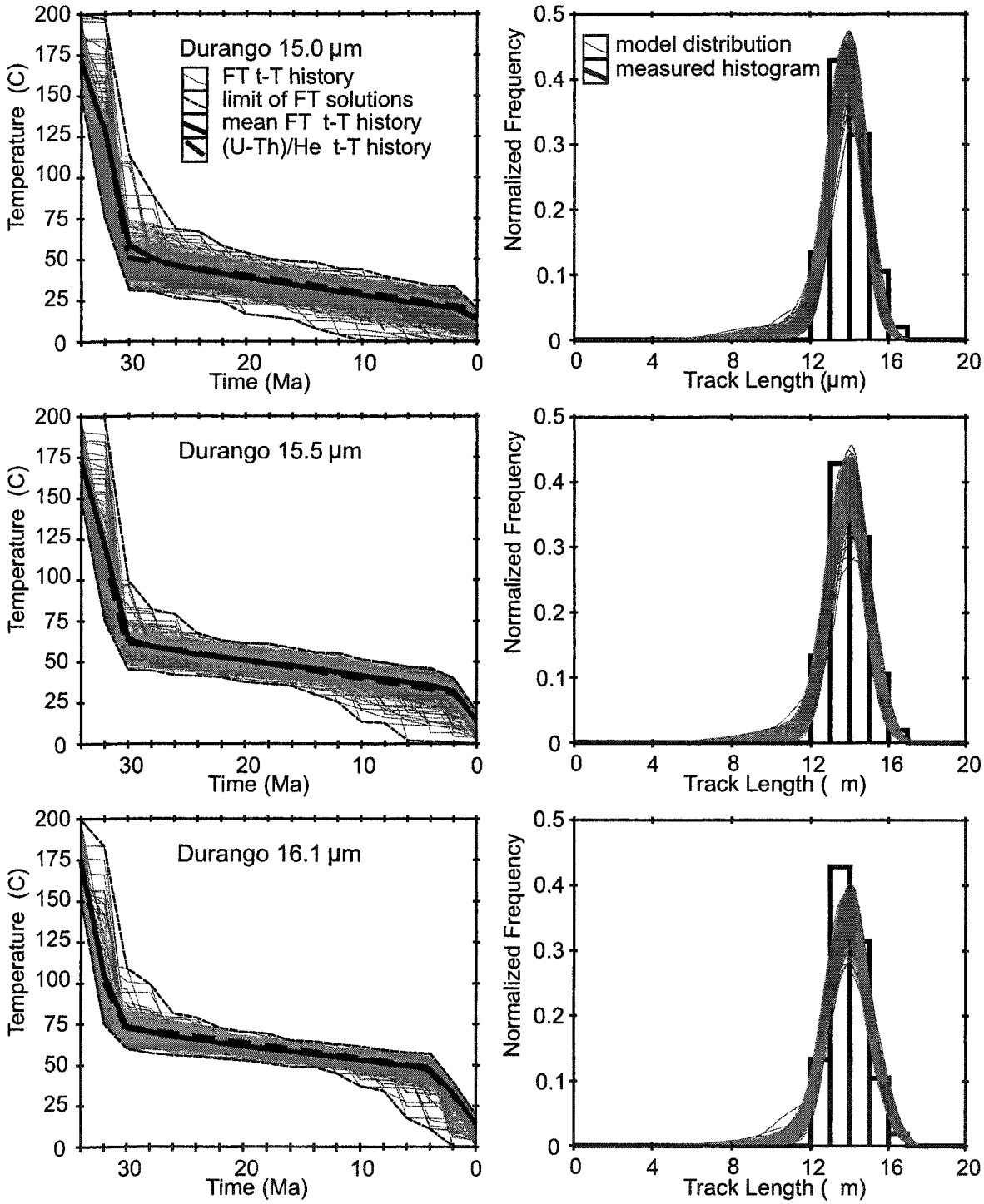
Durango 15.0 µm
FT t-T history
limit of FT solutions
mean FT t-T history
(U-Th)/He t-T history
Temperature (C)
Time (Ma)
model distribution
measured histogram
Normalized Frequency
Track Length (µm)
Durango 15.5 µm
Track Length (m)
Durango 16.1 µm

7.4 Regional geology

The complex regional geology of the Innuitian Orogen and the Arctic Platform was summarized in Trettin (991). A brief introduction to the regional geology of the present study area in eastern Ellesmere Island and northwestern Greenland is also given by Grist and Zentilli (2004). The study region lies to the east of the Sverdrup Basin, a large post-orogenic intracratonic basin and failed rift which formed at the site of the mid-Paleozoic Ellesmerian Orogeny. Initial rifting, subsidence and sedimentation of the Sverdrup Basin occurred during mid to Late Carboniferous time. The earliest widespread clastic unit is the conglomeratic redbeds of the (Namurian) Borup Formation (e.g. Davies and Nassichuk 1991). The main phase of basin development however, occurred during protracted subsidence and sedimentation from Early Triassic to Late Cretaceous time (e.g. Embry 1991). During this time sediment supply to the basin, which was mainly from the east and south (i.e., the present study area) varied considerably (e.g. Embry 1991). Based on the development of thick deltaic facies deposits in the central Sverdrup Basin, Balkwill (1978) and Embry (1982) inferred five main intervals of high sediment input during Mesozoic time. Grist and Zentilli (2004) inferred that apatite FT and (U-Th)/He data from samples obtained proximal to the basin reflected cooling of uplifted basin flanks during intervals of Late Carboniferous and Late Permian clastic sedimentation. Samples from more distal areas around Inglefield Brednig in Greenland reflected exhumational cooling of the craton during times when large river systems that drained into the basin would have existed in this region.

Beginning in latest Cretaceous to Paleogene time rifting and sea floor spreading initiated in northern Baffin Bay, which caused a counterclockwise rotation of Greenland with respect to Ellesmere Island (Trettin 1991). Following the cessation of sea floor spreading in Baffin Bay during Paleocene time and the onset of spreading in the Norwegian Sea east of Greenland, the motion of Greenland relative to Ellesmere Island became convergent (e.g. Kerr 1967; Srivastava 1985; Roest and Srivastrava 1989; Tessensohn and Piepjohn 2000). These events produced an inversion of the Sverdrup Basin (Arne et al. 2002) and its eastern margin during the Paleogene Eurekan Orogeny (e.g. Thorsteinsson and Tozer 1970; Okulitch and Trettin 1991).

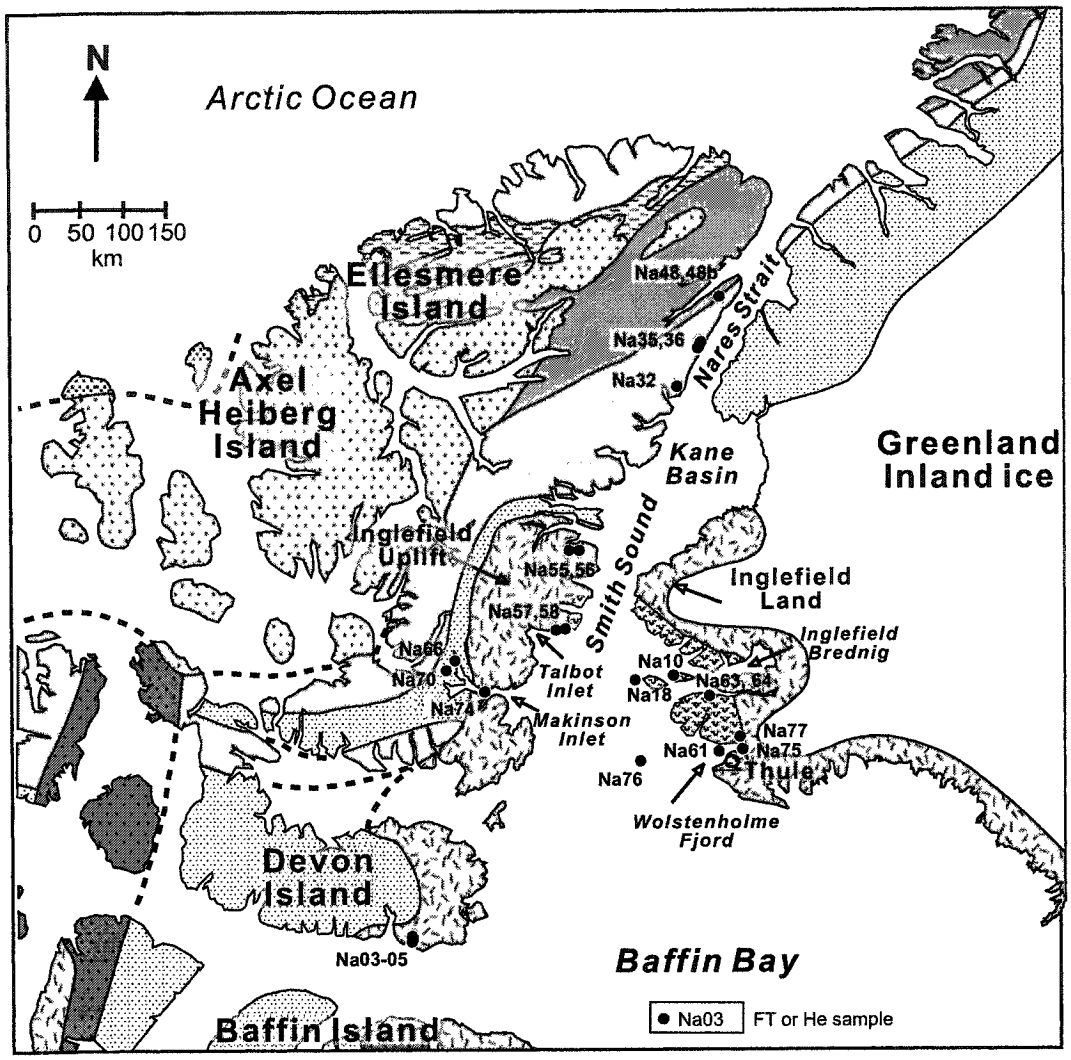

ARCTIC COASTAL PLAIN
Neogene to Recent

SVERDRUP BASIN
Carboniferous to Paleogene

CANADIAN SHIELD
Thule, Borden basins
Mid-Proterozoic
Archean and Paleoproterozoic

FRANKLINIAN MOBILE BELT
Pearya Mid-Proterozoic to Upper Silurian
Deep-Water Province
Sedimentary-Volcanic Subprovince
Cambrian to Devonian
Sedimentary Subprovince
Lower Cambrian to Devonian
Shelf Province
Lower Cambrian to Upper Silurian
Arctic Platform
Cambrian to Devonian
Boothia Uplift

Figure 7.3. Generalized map of the Innuitian Orogen of Arctic Canada and western Greenland showing the distribution of the main tectonic elements and geologic units (modified from Oakey et al. 2000). Apatite FT and/or (U-Th)/He sample locations are shown using closed circles.

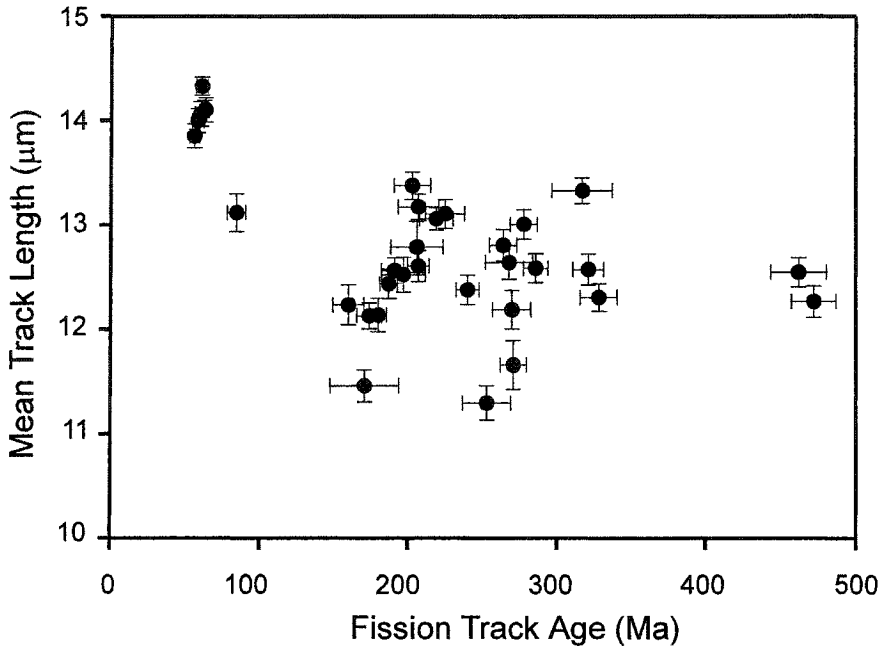

Figure 7.4. A plot of measured apatite FT age vs. confined TL for the samples from the Nares Strait - Kane Basin - Smith Sound region of eastern Ellesmere Island and western Greenland (simplified from Grist and Zentilli 2004). Most of the samples with Paleozoic and Mesozoic FT ages were interpreted in terms of the denudational cooling of the sediment source regions for the Sverdrup Basin (Fig. 7.3). Samples in the upper left of the figure reflect basaltic volcanism and post-tectonic cooling related to the Eurekan Orogeny.

7.5 Discussion of data and model input parameters

The FT age and TL data for the Nares Strait - Kane Basin - Smith Sound region are shown in Fig. 7.4 (simplified from Grist and Zentilli, 2004). The data for these samples can be considered to consist of three groups. The two samples at the right of Fig. 7.4 are from Archean shield lithologies at widely spaced locations near Iqaluit, on southern Baffin Island, and from near the margin of the continental ice sheet in Inglefield Land, Greenland. These data apparently reflect slow exhumation of these areas beginning in Late Proterozoic time, and were relatively unaffected by subsequent tectonics related to the development of the Sverdrup Basin, or the Paleogene Eurekan Orogeny. As discussed in Section 7.4, the majority of the samples (in the central part of Fig. 7.4) have Late Paleozoic - Mesozoic FT ages, and these data were interpreted by Grist and Zentilli (2004) as reflecting at least two phases of exhumational cooling of the sediment source areas of the Sverdrup Basin. An early phase of exhumation was likely related to erosion of rift flanks following the onset of rifting and widespread clastic sedimentation during Late Carboniferous to Early Permian time. A later phase of exhumation was likely related to epeirogenic denudation of the sediment source regions of the Sverdrup Basin during Early Triassic time. The existence of extensive river systems was inferred by Balkwill (1978) and Embry (1982) based on the presence of thick deltaic facies deposits in the basin during periods of active Mesozoic subsidence. The third group of samples have ca. 60 Ma FT ages, and 14 μm mean track lengths. The data for these samples reflect basaltic volcanism and tectonic exhumation related to the Eurekan Orogeny.

7.5.1 Samples with Paleozoic and Mesozoic FT ages

Most samples with Paleozoic and Mesozoic FT ages were modelled using a cooling-only constraint because we wished to characterize the style of cooling (although thermal histories other than simple cooling might be permitted by the data for some of the samples). Heating was permitted between 140 and 40 Ma for the models of the samples from Talbot Inlet, Mansen Øer and Carey Øer in northern Baffin Bay, to allow for the possible thermal effects from rifting in Baffin Bay or from the Eurekan Orogeny. A maximum time of either

380 or 180 Ma was used in the models, and populations of tracks were introduced at 2 My intervals. All models were forced to find cooling solutions from 40 Ma to the present.

7.5.2 Samples with Paleocene FT ages

A sample from the Cambrian Archer Fiord Formation at Cape Lawrence was modelled using cooling-only from 100 Ma. Samples from the Upper Paleocene Pavy and Mount Lawson Formations were assigned depositional ages of 60 Ma. Temperatures at deposition were assumed to be 0-5 °C. Populations of tracks were introduced at 1 My intervals. The model was forced to find heating solutions to 50 Ma, and cooling solutions with a heat pulse allowed from 50 Ma to 35 Ma to reflect burial during Late Paleocene transpression, or Eocene thrusting. The model was forced to find cooling-only solutions from 35 Ma to the present because tectonic activity in the Nares Strait region likely ended in Early Oligocene time (e.g. Tessensohn and Piepjohn 2000). For all models a present-day temperature of 0-5 °C was used, and an initial TL reduction to 15.0 μm was introduced to account for under-prediction of low temperature annealing of the Laslett et al. (1987) model.

7.5.3 (U-Th)/He forward models

For samples from which both FT and (U-Th)/He data were obtained, t-T histories that approximated the exponential mean thermal history solutions from the FT inverse models were used as input to predict the (U-Th)/He ages. If considerable mismatch resulted between the (U-Th)/He age predicted by the mean thermal history of the FT inverse model and the measured (U-Th)/He age (i.e., the Dundas Mountain Sill and Pavy Formation samples) alternate (U-Th)/He forward models were explored. An initial diffusion grainsize radius of 31.6 μm and 0.5 My time steps were used for all models.

7.6 Quantitative apatite compositions

Ideally, thermal modelling using the Laslett et al. (1987) annealing model for Durango apatite, a near end-member fluorapatite (e.g. Fig. 7.5a), should only be undertaken for apatite with the same, or very similar composition. However, though it is widely accepted that

variability of the temperature-dependence of FT annealing is related to composition, controversy remains within the FT community concerning whether chlorine content is the only significant influence as suggested by Green et al. (1985), Green (1996) and others, or whether annealing as a function of temperature has a more complex relationship to composition (e.g. Carlson et al. 1999).

Apatite compositions have been measured for FT-counted grains from 11 of the dated samples using a Jeol JXA 8200 Superprobe at Dalhousie University. Data acquisition was done using a wavelength dispersive system (WDS) with a 5 μm beam diameter, 15.0 kV accelerating voltage, and 2.0 $x10^{-8}$ A current settings. Average compositions are shown in Table 7.1. Ternary plots of F-Cl-OH for the samples are shown in Fig. 7.5. In these plots OH was calculated from excess oxygen assuming stoichiometry.

From Figure 7.5 it is evident that several of the dyke samples from Ellesmere Island (Na56, Na57, Na58) and the sample from the Thule dyke in Greenland (Na75) have fluorapatite compositions that are similar to Durango. The Pavy Formation (Na35, Na48) and Mount Lawson Formation (Na66) volcanogenic sandstones, and the Devon Island gneiss (Na03) have fluorapatite-hydroxyapatite compositions, and little or no Cl. These compositions are very similar to that of the apatite from the Sverdrup Basin (Fig. 5.3). The Carey Øer sample (Na76) has similar Cl content to Durango, but higher OH. In contrast, the samples from the Archer Fiord Formation (Na32) at Cape Lawrence, Ellesmere Island, and Dundas Mountain sill (Na-77) in Greenland are more compositionally heterogeneous with respect to F-Cl-OH, and have some grains that are substantially more Cl-rich than Durango.

From Table 7.1, it is evident that other significant compositional differences exist between the dated samples and Durango, but it is not known what effect (if any) these have on the annealing characteristics. Whereas Durango apatite has no Fe or Mg, all of the dyke/sill samples (i.e., Na56 - Na58, Na75 - Na77) have significant Fe contents. The Ellesmere Island dykes also have significant Mg, but among the Greenland dyke/sill samples, only the Thule dyke (Na75) has appreciable Mg. The Pavy Formation and Mount Lawson Formation volcanogenic sandstones (Na48 and Na66) also have significant Sr contents.Grist and Zentilli (2004) reported that many of the dyke/sill samples also had very high light rare earth element

Sample	No. of grains	O	F	Na	Mg	P	S	Cl	Ca	Mn	Sr	Fe	La	Ce	Total
Dur.	23	37.92	3.48	0.13	0	17.74	0.1	0.38	39.07	0.01	0	0.02	0.25	0.46	99.58
Na03	41	40.47	3.56	0	0	17.96	0	0.03	39.91	0	na	0.04	0.14	0.59	102.72
Na32	28	38.82	3.08	0.03	0	17.54	0.02	0.18	39.5	0.07	0	0.04	0.04	0.25	99.6
Na35*	29	34.88	2.99	0.01	0	16.71	0	0.01	37.21	0.01	na	0.01	0.01	0.05	92.74
Na48	29	39.62	1.99	0.02	0	17.48	0.04	0.01	39.01	0	0.6	0.01	0.02	0.2	99.01
Na56	30	38.85	3.6	0	0.14	17.82	0	0.12	39.3	0.05	0.02	0.31	0	0.14	100.37
Na57	24	38.58	3.16	0	0.11	17.91	0.01	0.17	39.43	0.05	0.03	0.28	0	0.12	99.87
Na58	27	38.48	3.71	0	0.13	18.15	0.01	0.11	39.39	0.05	0.02	0.37	0	0.1	100.53
Na66	30	39.3	2.27	0.05	0.02	17.37	0.04	0.02	39.18	0.02	0.6	0.04	0.04	0.21	99.16
Na75	30	38.28	3.52	0	0.13	18.14	0	0.16	39.03	0.04	0.03	0.33	0	0.13	99.8
Na76*	35	41.94	2.94	0	0.06	18.32	0	0.44	39.9	0.07	na	0.39	0	0.16	104.22
Na77	30	38.79	2.38	0	0.07	17.98	0.01	0.53	39.23	0.04	0.05	0.22	0.01	0.22	99.53

Table 7.1. Average compositions of selected apatite samples (wt %). A detection limit of 0.01% (100 ppm) was assumed for all elements (na = not analyzed).

*The low and high totals for samples Na35 and Na76 were caused by uneven carbon-coating of those samples prior to microprobe analyses.

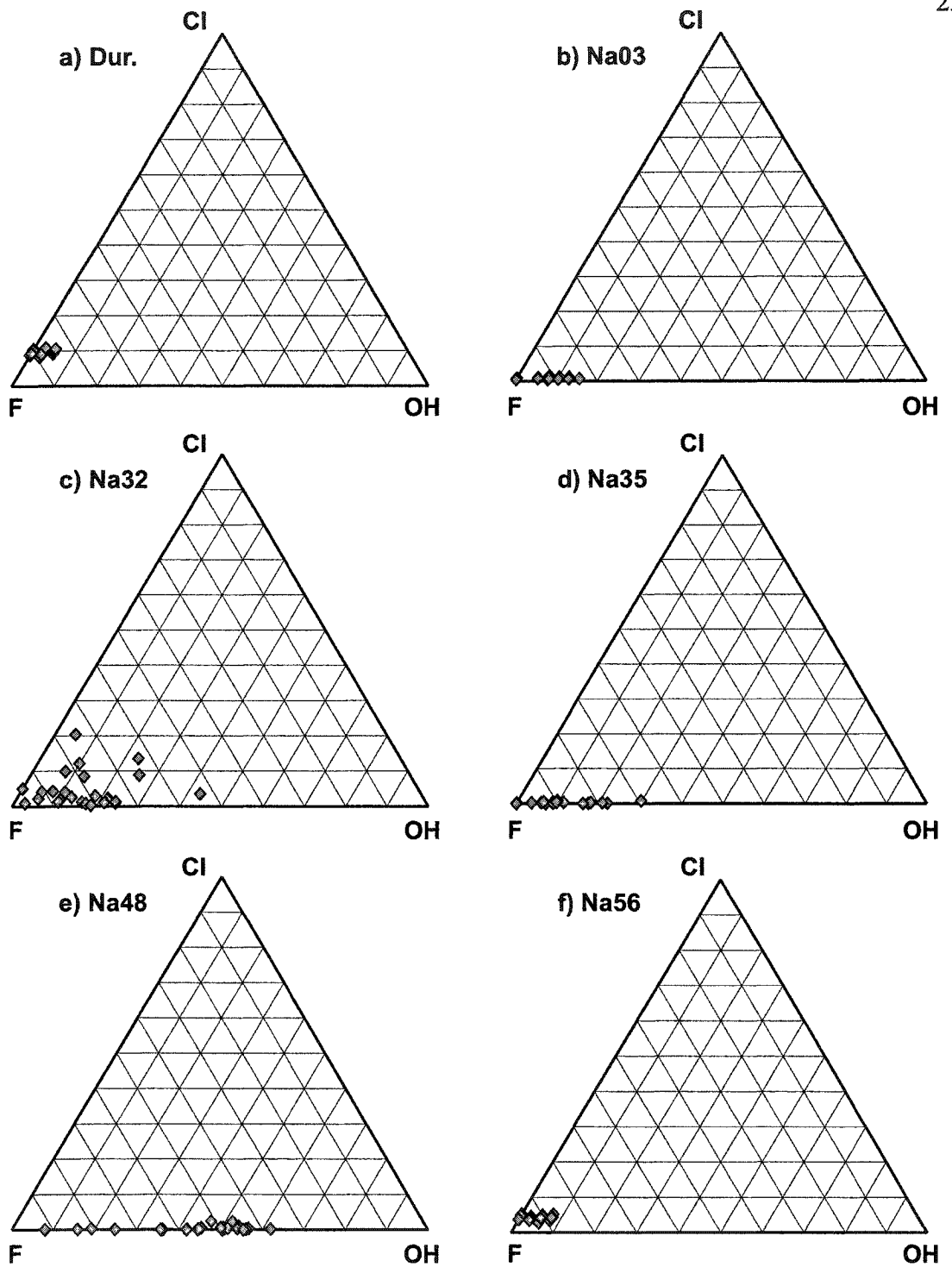

Figure 7.5. Summary ternary plots of Cl-F-OH compositions (wt. %) for apatite from 11 samples from the Nares Strait, Kane Basin, Smith Sound region as well as for the Durango apatite standard (Dur.).

Figure 7.5 (continued)

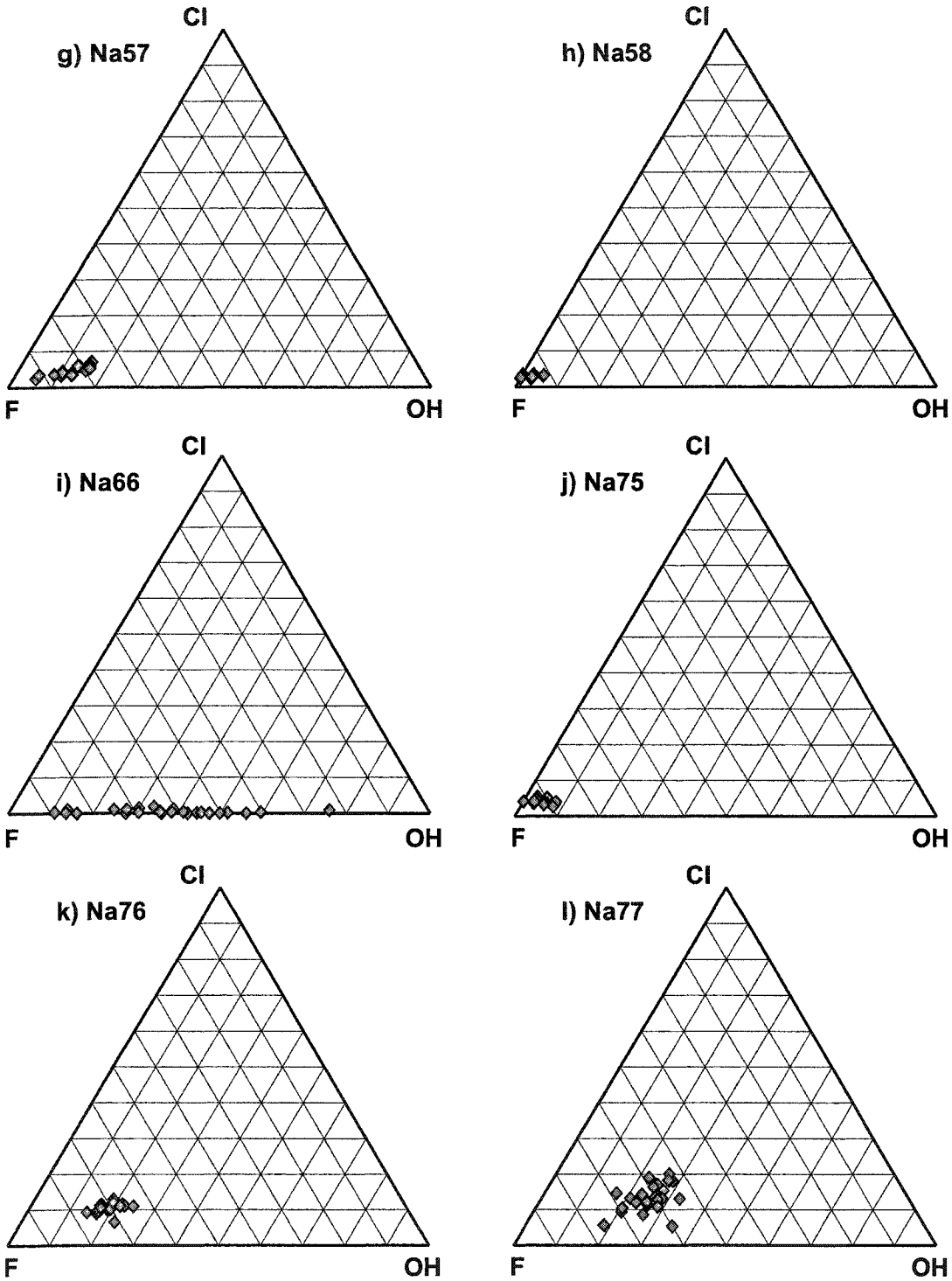

(REE) contents. Figure 7.6 shows chondrite-normalized REE compositions for the (U-Th)/He-dated samples, determined by ICP-MS analyses at Caltech. (Differences between values for Sr, La and Ce from the microprobe and the ICP-MS analyses are likely a result of the greater ICP-MS sensitivity.) All dyke/sill samples from Ellesmere Island and Greenland (left) and the Devon Island gneiss (Na03; upper right) are light-REE enriched with a negative Eu anomaly. The volcanogenic sandstone samples (lower right) are also light-REE enriched, but have no Eu anomaly. Other sandstone samples (upper right) have a negative Eu anomaly, but are not light-REE enriched.

The compositional heterogeneity displayed by the dated samples suggests that attempting to characterize compositional-based track annealing behaviour of individual samples would be prohibitive. Therefore, as a first approximation all of the samples were modelled using the Durango annealing model, with the assumption that the various other compositional differences do not have a significant effect on the annealing behaviour.

7.7 Model results

Model thermal histories for samples with Paleozoic and Mesozoic FT ages are shown in Figures 7.7-7.11, and for samples with Paleocene FT ages in Figures 7.12 and 7.13. Each model shows a solution set of 250 thermal histories, the exponential mean thermal history of the solution set and the solution envelope (see caption of Fig. 7.2 for details). If (U-Th)/He forward thermal models were obtained, these are shown with a thick dashed line. The measured (U-Th)/He ages (from Grist and Zentilli 2004) and modelled (U-Th)/He ages for these samples are indicated beneath the model.

7.7.1 Samples with Paleozoic and Mesozoic FT ages

Fig. 7.7 shows FT inverse and (U-Th)/He forward thermal models for samples from the Inglefield Uplift region in southeast Ellesmere Island. The two upper models are from samples obtained approximately 30 km (left) and 20 km (right) inland from the coast along the Leffert Glacier, from Archean granitic gneiss and a large Franklinian dyke, respectively. The two lower models are for samples obtained approximately 200 km farther south, from

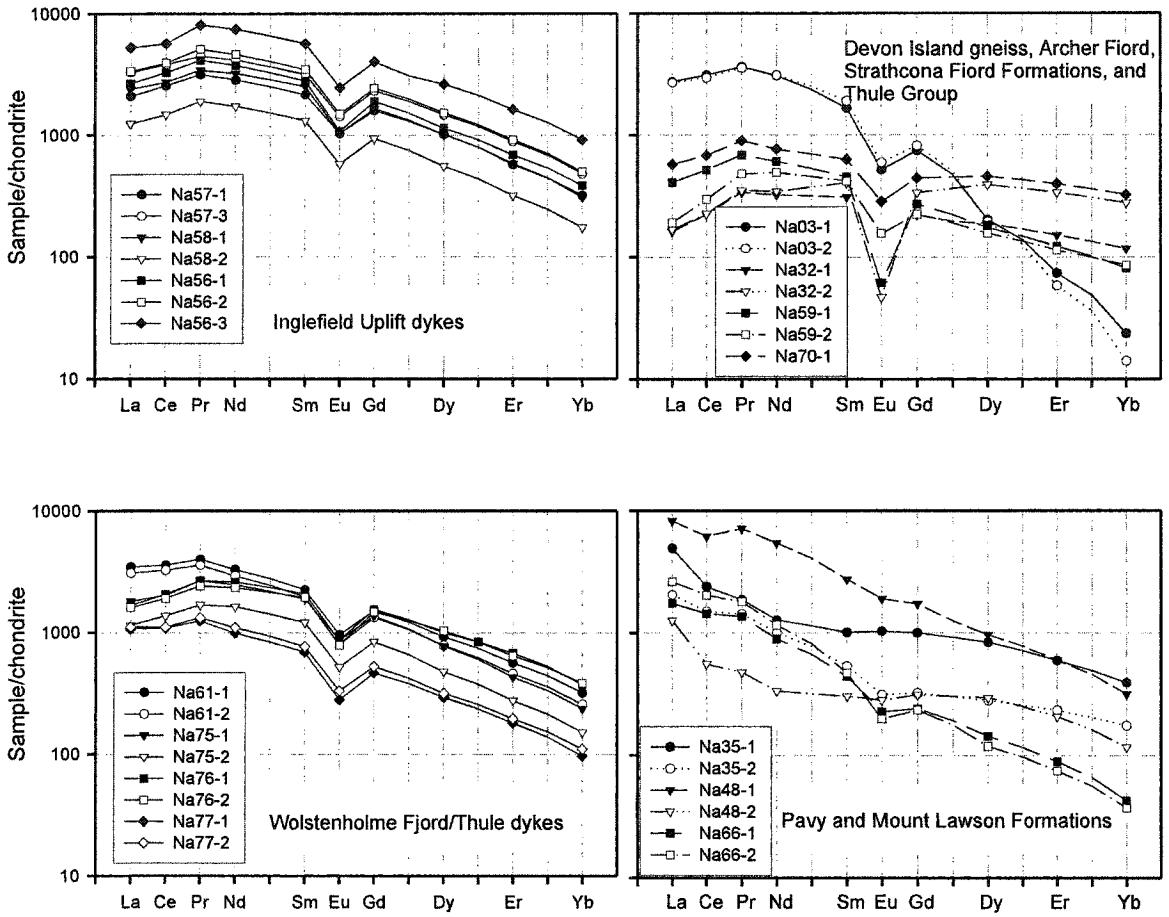

Figure 7.6. Chondrite-normalized REE compositions of apatite determined by ICP-MS. Left: volcanic dykes from the Inglefield Uplift in Ellesmere Island (top) and the Wolstenholme Fjord - Thule region in Greenland (bottom). Right: Sandstones from the Pavy and Mount Lawson Formations (top) and a Devon Island gneiss, and sandstones from the Archer Fiord and Strathcona Fiord Formations, Ellesmere Island, and Thule Group, Wolstenholme Ø, Greenland.

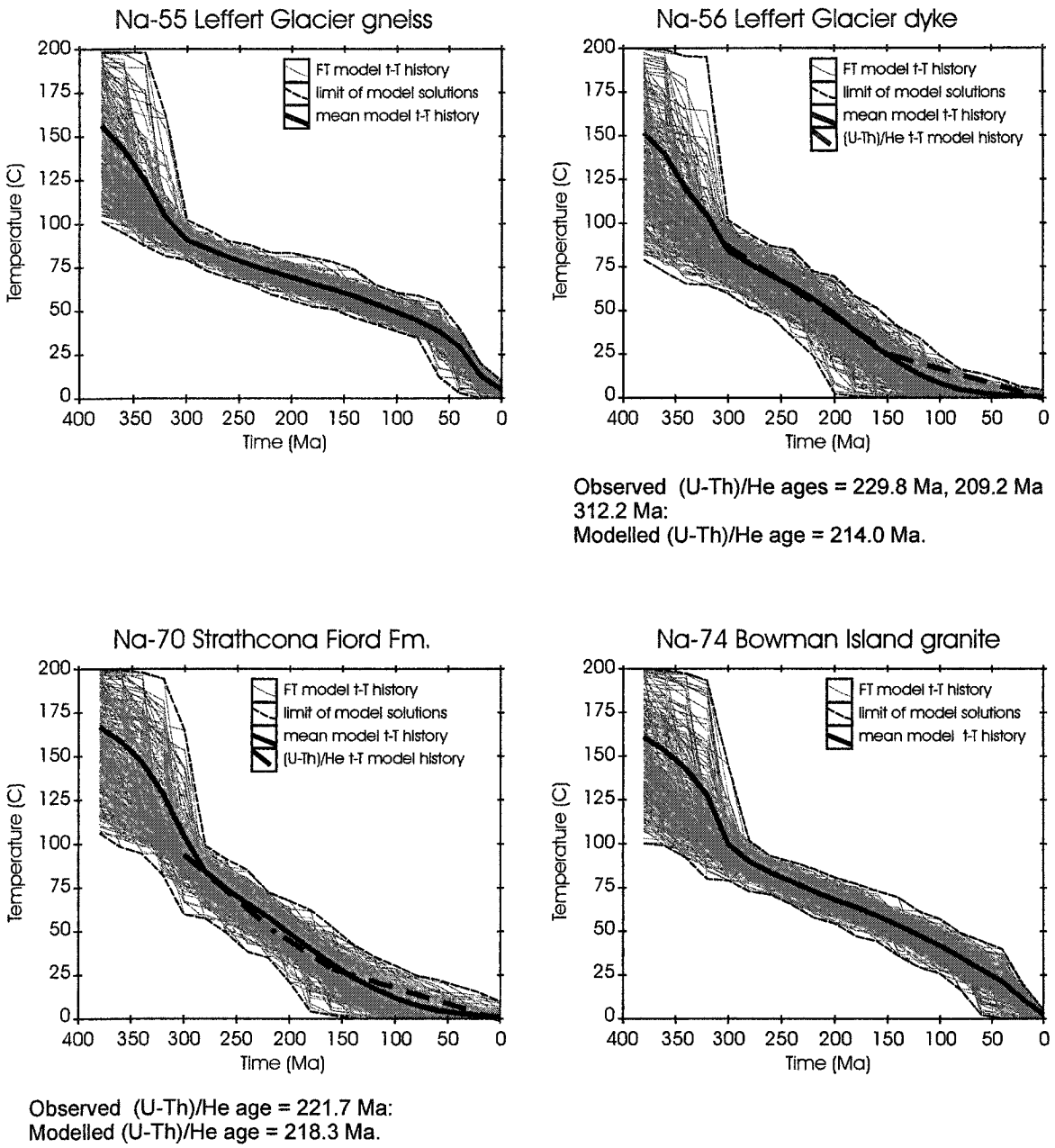

Figure 7.7. Apatite FT inverse and (U-Th)/He forward thermal models for samples from the Inglefield Uplift, in southeastern Ellesmere Island (see Fig. 7.2 caption for details).

the Devonian Strathcona Fiord sandstone west of Makinson Inlet (left) and from Archean granite on Bowman Island in the mouth of Makinson Inlet (right).

The FT models for the Leffert Glacier dyke and Strathcona Fiord sandstone samples indicate monotonic cooling of these samples through the PAZ between ca. 350 and 200 Ma. These histories are consistent with the interpretation of simple denudational cooling related to early rifting in the Sverdrup Basin to the west (Grist and Zentilli 2004), and they appear to be essentially unaffected by thermal effects related to rifting in Baffin Bay or the Eurekan Orogeny. There is good agreement between the FT model and the (U-Th)/He measured and modelled ages of 210-230 Ma, which suggests that the (U-Th)/He data are also consistent with this interpretation.

The FT models for the Bowman Island granite and Leffert Glacier gneiss samples, (which have negatively skewed TL distributions, substantial components of short tracks and reduced mean lengths) are less simple than those of the Leffert Glacier dyke and Strathcona Fiord Formation samples. Although these models also suggest initial cooling through the PAZ at about 350-300 Ma, predicted temperatures are somewhat higher throughout the cooling history and increased cooling in Late Cretaceous to Paleogene time is indicated, possibly related either to tectonic activity in Baffin Bay or to minor exhumation during Eurekan compression.

FT inverse and (U-Th)/He forward thermal models for volcanic samples from Manson Øer, Thule, and Dundas Mountain in the Wolstenholme Fjord region of Greenland are shown in Fig. 7.8. These models indicate that initial cooling of these samples through the PAZ began at ca. 250-200 Ma, which is consistent with the interpretation by Grist and Zentilli (2004) that this region underwent exhumational cooling during a period of increased sediment supply into the Sverdrup Basin in Early Triassic time.

(U-Th)/He forward model ages for these samples are generally consistent with this interpretation, however there is considerable scatter in the measured (U-Th)/He ages for this group (Grist and Zentilli 2004) that may reflect additional exhumational cooling during Early Cretaceous time. The FT model for the Manson Øer sample predicts a (U-Th)/He age of 144 Ma, which is older than the measured (U-Th)/He ages of 104 and 136.3 Ma. The FT model

for this sample is not well defined during this time because most of the FT thermal histories suggest temperatures beneath the PAZ. The predicted (U-Th)/He age of 139 Ma for the Dundas Mountain sample (Fig. 7.8) is similar to the observed age of 143.2 Ma. (The 750 Ma (U-Th)/He age of this sample is affected by parentless He, and not meaningful.) The apatite in this sample also has high Cl content (Fig. 7.5l) suggesting that the FT model may under-predict actual temperatures slightly.

FT inverse models for samples from Herbert Ø, Haklyut Ø, and Kap Trautwine, in the Inglefield Brednig region of Greenland (Fig. 7.9) are similar to those from Wolstenholme Fjord, although cooling of the samples obtained from high elevations on Haklyut Ø and Kap Trautwine began earlier (e.g. Late Carboniferous) than it did for samples obtained from sea level. The model for the sample from sea level at Kap Trautwine also suggests a period of accelerated cooling during Late Cretaceous to Paleogene time (similar to that seen in the models for the Leffert Glacier gneiss and Bowman Island granite samples in Fig. 7.7), that is not evident in the sample from 665 m elevation, likely because it had already cooled to temperatures below the PAZ by this time. Paleogeothermal gradient estimates based on the difference between the exponential mean thermal histories of closely spaced samples with substantially different elevations (e.g. Kap Trautwine) are discussed in section 7.9.

FT inverse and (U-Th)/He forward model histories for three Franklinian dykes sampled near sea level at Cape Faraday, and Orne Island in the Inglefield Uplift region of Ellesmere Island and one from Carey Øer, Baffin Bay are shown in Fig. 7.10. The inverse model for the Cape Faraday sample (upper left panel) suggests a period of slightly elevated temperatures during Late Cretaceous time, and an accelerated rate of cooling from Paleocene time to the present. The t-T history for the dyke sample from Orne Island (Fig. 7.10, upper right) indicates temperatures were high enough to completely anneal the apatite fission tracks prior to rapid cooling through the PAZ between about Late Cretaceous to Paleocene time. The Late Cretaceous (U-Th)/He forward model age of 58.2 Ma is consistent with this interpretation. Because these samples were obtained from the margin of Baffin Bay, it is likely that the heating (possibly from burial during subsidence) was related to the onset of rifting in Baffin Bay during Late Cretaceous time, although the models do not rule out heating related

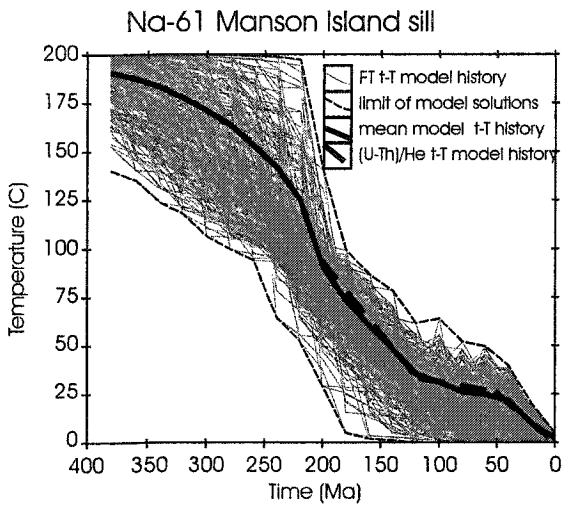

Observed (U-Th)/He ages = 136.3 Ma, 104.0 Ma:
Modelled (U-Th)/He age = 144.3 Ma.

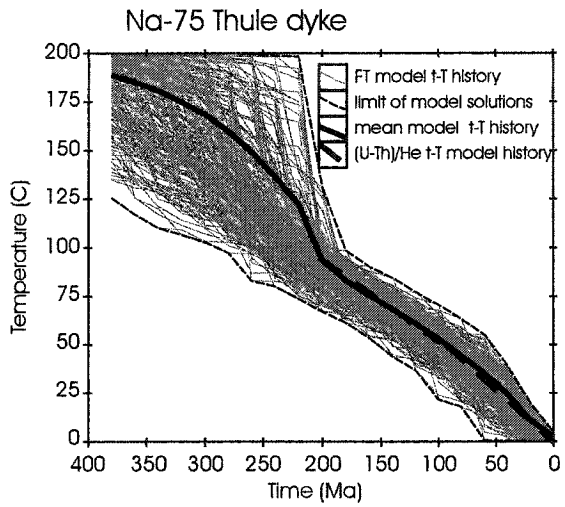

Observed (U-Th)/He ages = 171.1 Ma, 108.4 Ma:
Modelled (U-Th)/He age = 101.9 Ma.

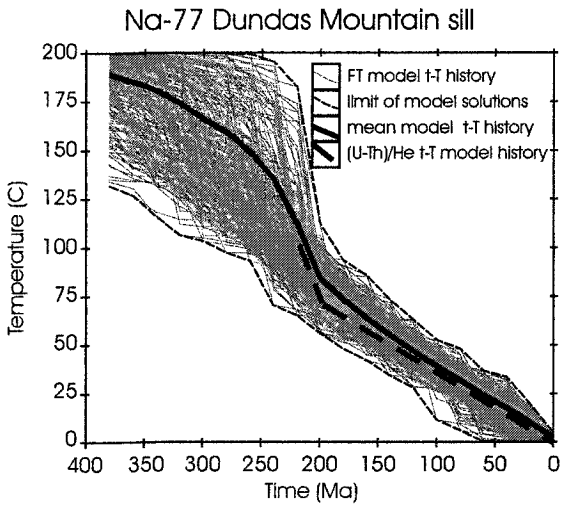

Observed (U-Th)/He ages = 143.2 Ma, 750.3 Ma:
Modelled (U-Th)/He age = 139.1 Ma.

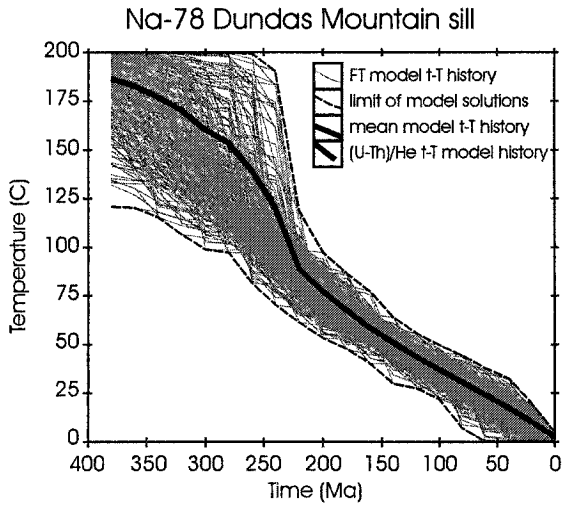

Figure 7.8. Apatite FT inverse and (U-Th)/He forward thermal models for volcanic samples from Manson Øer, Thule and Dundas Mountain, in the Inglefield Brednig region of Greenland (see Fig. 7.2 caption for details).

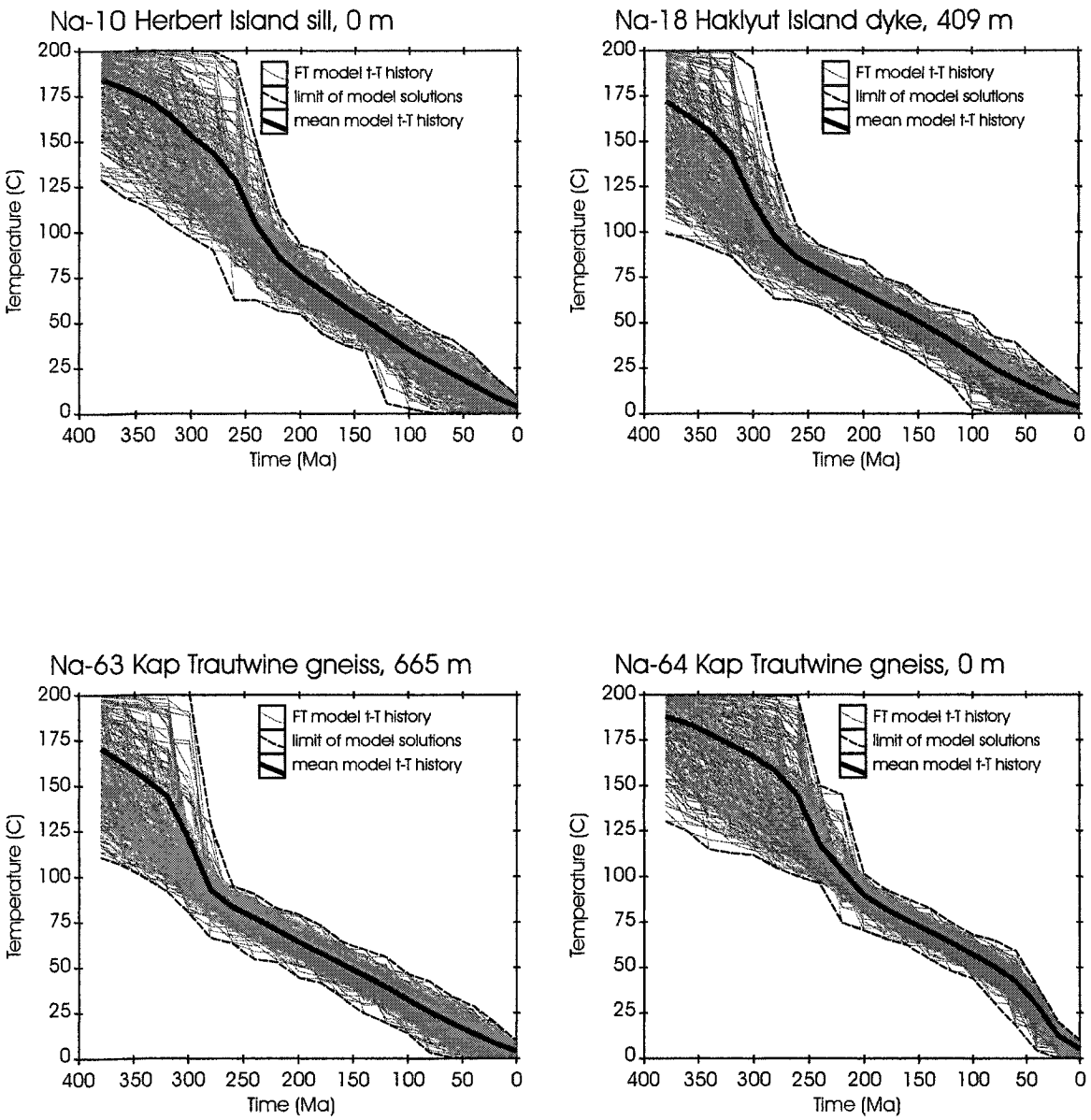

Figure 7.9. Apatite FT inverse thermal models for samples from Herbert Ø, Haklyut Ø and Kap Trautwine, in Inglefield Brednig, Greenland (see Fig. 7.2 caption for details).

to Eurekan compression.

The exponential mean t-T history for the sample from Carey Øer, like those of the Devon Island and Cape Faraday samples, shows pronounced Late Cretaceous heating which is reflected in the bimodal TL distributions of these samples (Grist and Zentilli 2004). The location of the Carey Øer in northwestern Baffin Bay suggests that heating was likely related to the onset of rifting in Baffin Bay. The FT t-T history indicates Late Cretaceous temperatures of ca. 75 °C, however these temperatures should have been sufficient to completely reset the (U-Th)/He age, resulting in the forward modelled age of ca. 70 Ma. The Sm-corrected (U-Th)/He ages are somewhat older, but there is considerable scatter (99 Ma and 233 Ma). The reason for this apparent discrepancy is unknown.

Fig. 7.11 shows FT inverse models for 3 Archean gneiss samples from a ca. 3 km transect down a steep slope on Devon Island. The upper-left panel (sample Na-03) also has (U-Th)/He forward model results. The exponential mean model t-T histories indicate initial cooling through the PAZ occurred at about 250 Ma, probably reflecting regional exhumation of the flanks of the Sverdrup Basin as discussed above. Like the samples shown in Fig. 7.10, the models for these samples also all suggest a period of elevated temperatures during Late Cretaceous time, followed by an accelerated rate of cooling to the present. This is most evident in the sample from near sea level (Na-05). There is close agreement between the (U-Th)/He forward model age (110.5 Ma) predicted from the FT exponential mean thermal history and the measured (U-Th)/He ages (110.2, 109.3 Ma) for sample Na-03. These models suggest that at about the time of the onset of rifting in Baffin Bay this area of Devon Island also experienced some heating (and possibly subsidence) prior to cooling that may have been from isostatic flank uplift. This interpretation is consistent with the offshore geology in Lancaster Sound and northern Baffin Bay, south and east of eastern Devon Island (e.g. Harrison 2004) where a succession (maximum thickness exceeding 4000 m) of presumed Upper Cretaceous to Paleogene sedimentary strata occurs.

7.7.2 Samples with Paleocene FT ages

Model thermal histories for samples having Paleocene FT ages are shown in Figs. 7.12

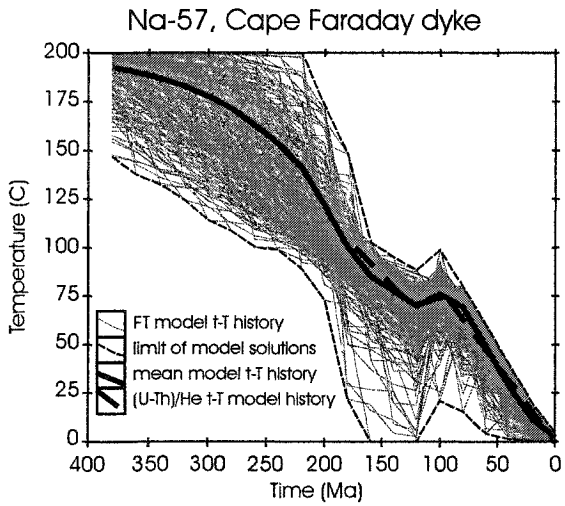

Observed (U-Th)/He ages = 115.9 Ma, 61.5 Ma:
Modelled (U-Th)/He age = 69.7 Ma.

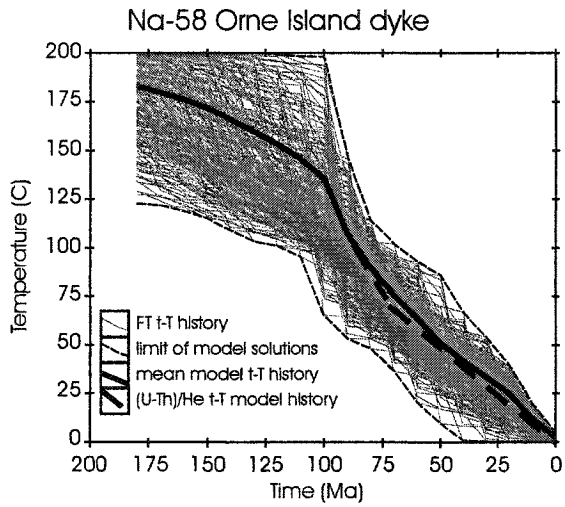

Observed (U-Th)/He ages = 86.8 Ma, 92.0 Ma:
Modelled (U-Th)/He age = 58.2 Ma.

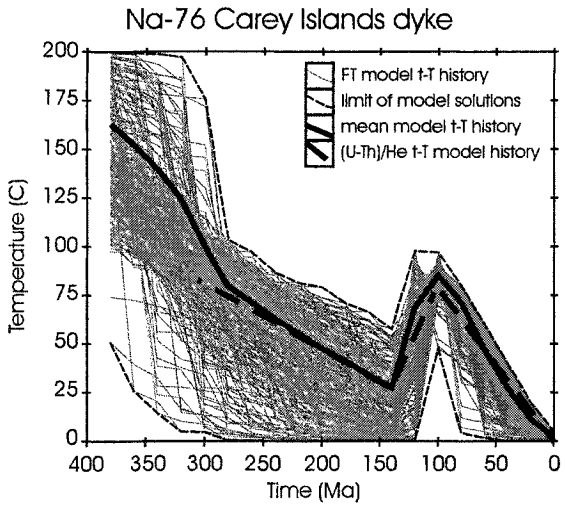

Observed (U-Th)/He ages = 99.0 Ma, 233.2 Ma:
Modelled (U-Th)/He age = 70 .1 Ma

Figure 7.10. Apatite FT inverse and (U-Th)/He forward thermal models for samples from Talbot Inlet, in the Inglefield Uplift area of southeastern Ellesmere Island and Carey Øer, Greenland (see Fig. 7.2 caption for details). Note reduced age scale for Na58.

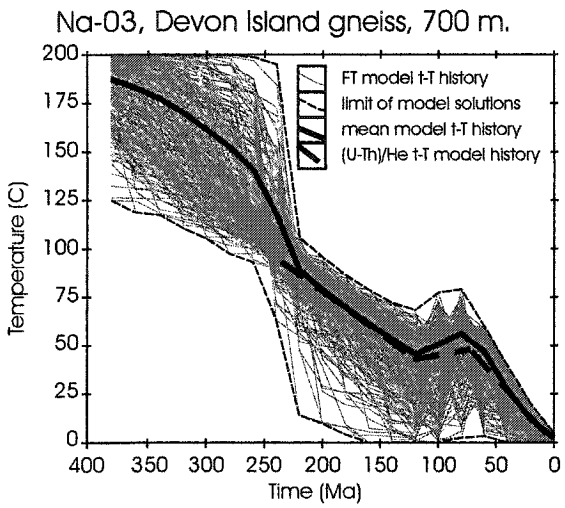

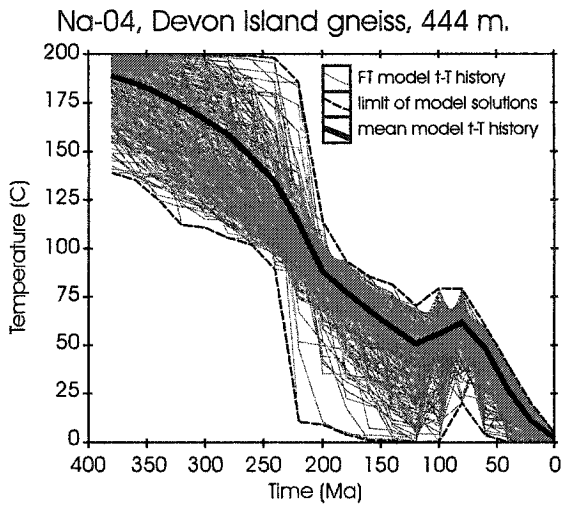

Observed (U-Th)/He ages = 110.2 Ma, 109.3 Ma:
Modelled (U-Th)/He age = 110.5 Ma.

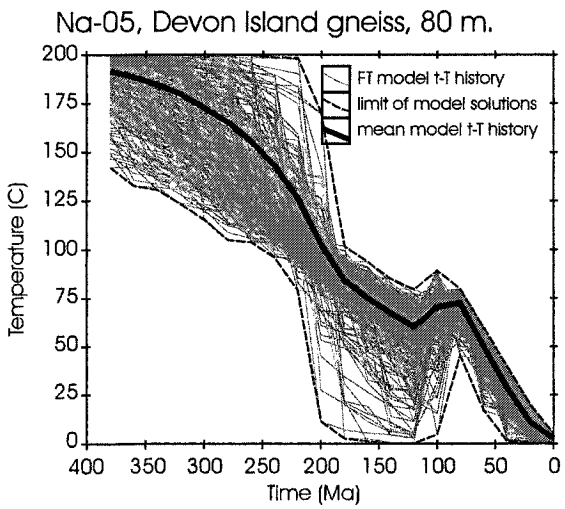

Figure 7.11. Apatite FT inverse and (U-Th)/He forward thermal models for Archean gneiss samples from southeastern Devon Island (see Fig. 7.2 caption for details).

and 7.13. The Pavy Formation samples (and the Mount Lawson Formation sample discussed below) are not as well suited to FT thermal history modelling as the sample from the Archer Fiord Formation. This is because the FT age and TL characteristics of these samples are typical of volcanic distributions that have retained cooling age characteristics of the volcanic protolith (ca. 61-59 Ma). Maximum post-depositional temperatures were likely < 55-60 °C, and were insufficient to cause substantial FT annealing.

Fig. 7.12 shows models for the Pavy Formation samples (note reduced age scale). These models converged after only a few hundred to ca. 1000 iterations and appear not to have fully explored all the possible t-T histories. On initial inspection there is considerable mismatch between the FT inverse models and the (U-Th)/He forward model ages. Peak post-depositional temperatures required to model the (U-Th)/He ages are higher than those predicted by the FT inverse models for Na-35 and Na-48, however the same (U-Th)/He forward models are compatible with the FT inverse models of samples Na-36 and Na-48b (i.e., they are within the bounds of acceptable FT modal thermal histories). (U-Th)/He forward model ages likely give a better indication of maximum post-depositional temperatures. Because geothermal gradients were likely higher during Upper Paleocene time (i.e., during active rifting) these results indicate that only minor burial of the strata of the Pavy Formation could have occurred prior to the onset of Eocene thrusting.

Fig. 7.13 shows a model for the Archer Fiord Formation sample from the hanging wall of the Rawlings Bay thrust at Cape Lawrence (left) and for the Mount Lawson Formation at Split Lake, west of Makinson Inlet (right). There is close agreement between the exponential mean FT thermal histories and the predicted (U-Th)/He ages for both of these samples. The FT inverse model for the Archer Fiord Formation sample indicates rapid cooling through the PAZ and the upper part of the PRZ from 65 Ma to 55 Ma and a reduced rate of cooling from about 50 Ma to the present. These results support the interpretation that the FT age and TL and (U-Th)/He age characteristics are dominated by the effects of Paleocene tectonic activity, and relatively unaffected by subsequent Eocene thrusting.

The results for the Mount Lawson Formation (Fig. 7.13) are similar to those for the Pavy Formation, although there is better agreement between the FT inverse model and the (U-

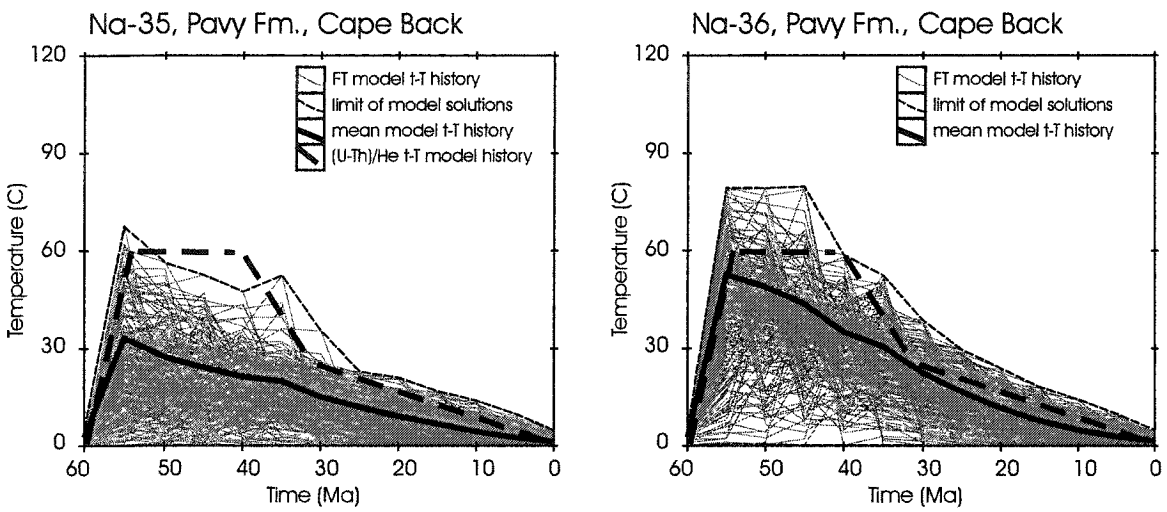

Observed (U-Th)/He ages = 49.1 Ma, 48.9 Ma:
Modelled (U-Th)/He age = 49.0 Ma.

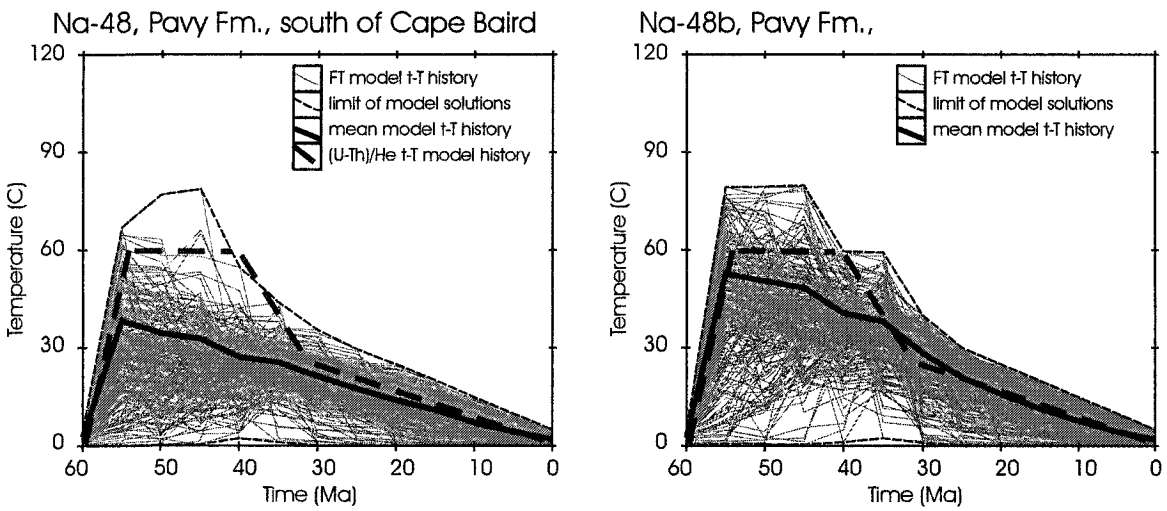

Observed (U-Th)/He ages = 46.4 Ma, 111.8 Ma:
Modelled (U-Th)/He age = 49.0 Ma.

Figure 7.12. Apatite FT inverse and (U-Th)/He forward thermal models for Upper Paleocene-aged samples from the Pavy Formation, north of Cape Back, and south of Cape Baird, Ellesmere Island (see Fig. 7.2 caption for details).

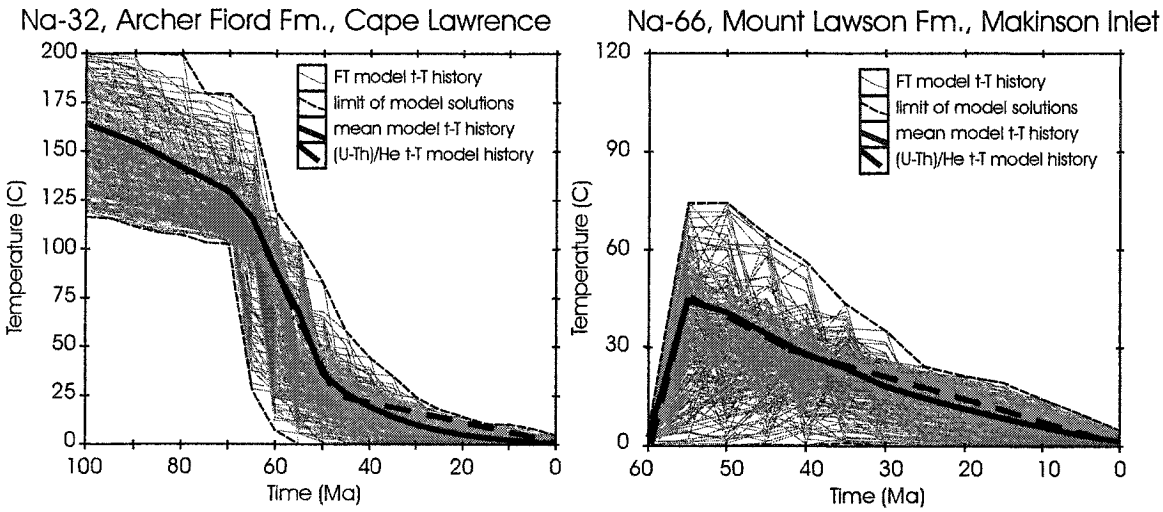

Observed (U-Th)/He ages = 63.4 Ma, 78.5 Ma, 55.7 Ma: Modelled (U-Th)/He age = 56.6 Ma.

Observed (U-Th)/He ages = 59.3 Ma, 59.6 Ma: Modelled (U-Th)/He age = 58.5 Ma.

Figure 7.13. Apatite FT inverse and (U-Th)/He forward thermal models for samples from the Cambrian Archer Fiord Formation (left) and Upper Paleocene Mount Lawson Formation, Ellesmere Island (see Fig. 7.2 caption for details).

Th)/He forward model for this sample. Both models are consistent with maximum post-depositional temperatures of only ca. 45 °C, and limited burial. These models imply that only minor Eocene exhumation (ca. 1-2 km) likely occurred in the hanging walls of major thrusts at Cape Back, Cape Lawrence, south of Cape Baird, or west of Makinson Inlet.

7.8 Discussion and geological significance of model results

Previous Sverdrup Basin studies have inferred that increased influx of sediments beginning in Triassic time was associated with substantial denudation of the sediment source regions to the south and east (Balkwill 1978; Embry 1982). The models presented here confirm that extensive regional denudation occurred in the eastern Canadian Arctic and western Greenland during Late Paleozoic and Mesozoic time. This was likely related to exhumation of the sediment source regions of the Sverdrup Basin prior to widespread inversion of the basin and its eastern margin during Late Cretaceous to Paleogene time. Many of the apatite compositions in Figure 7.5. also appear to be similar to those of apatite from the Sverdrup Basin (Fig. 5.3).

As suggested above, paleogeothermal gradients can be estimated from closely spaced samples with substantially different elevations, such as the two from Kap Trautwine (665 m), and the three from southern Devon Island (620 m). Fig. 7.14 shows model exponential mean thermal histories for these groups of samples and paleogeothermal gradients calculated by subtracting the model temperatures at each time step, and extrapolating the difference to 1 km. Paleogeothermal gradients for the Kap Trautwine samples after 200 Ma are 36-38 °C. Paleogeothermal gradients for the Devon Island samples between 200 and 100 Ma are 22-26 °C. Time-temperature paths for both groups of samples converge at recent times. This may be an effect of the propagation to depth of substantial surface cooling (e.g. O'Sullivan and Brown 1998; Grist and Zentilli 2003). The upward spikes in geothermal gradients prior to 220 Ma are modelling artefacts that occur at times when one (or both) of the samples from each pair are at temperatures above the PAZ.

Cooling rates (°C/My) can also be ascertained directly from the model t-T plots. The high elevation Kap Trautwine sample, for example (Fig. 7.14) indicates cooling of ca. 75 °C

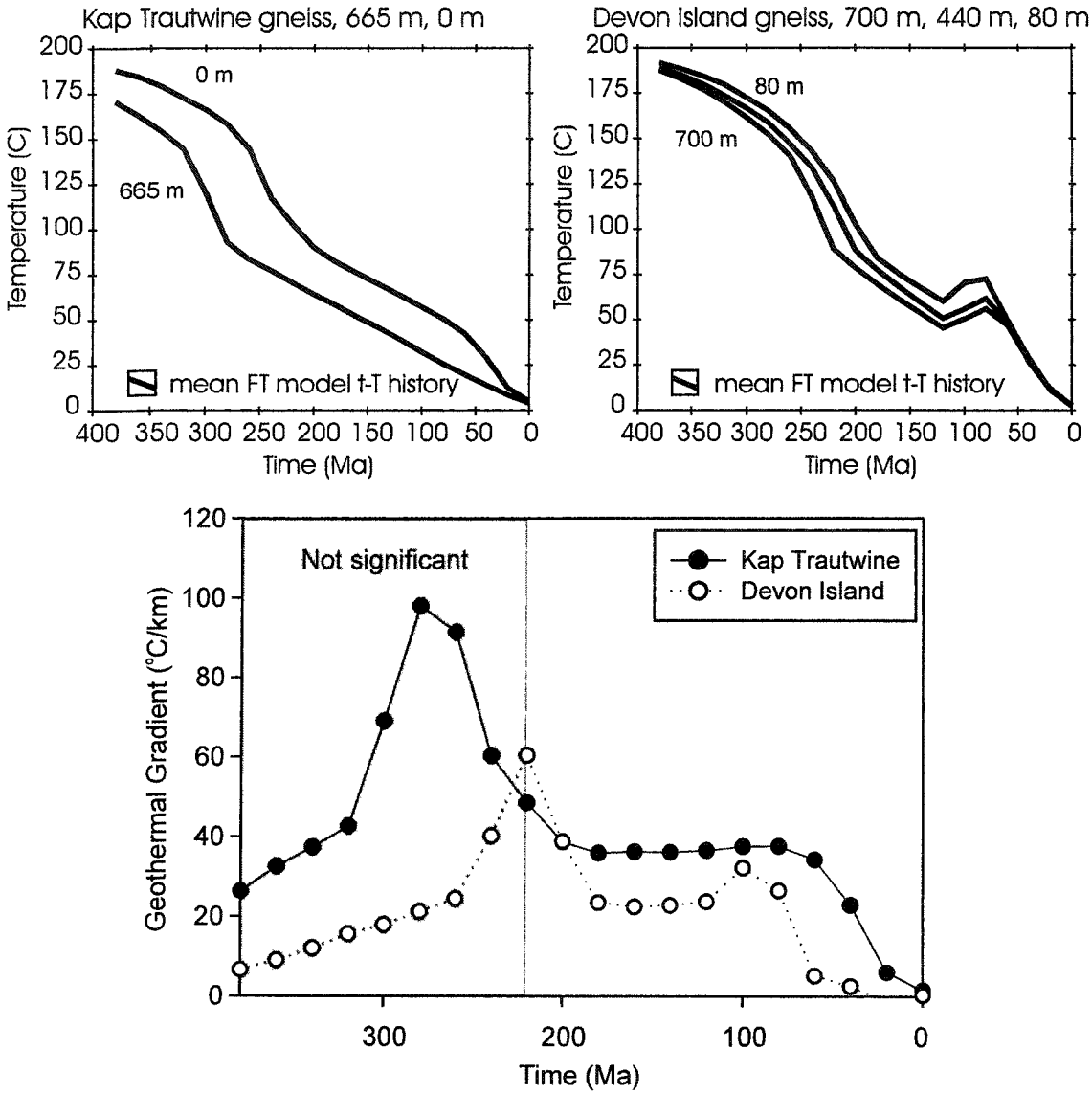

Figure 7.14. Exponential mean t-T histories for closely spaced samples with substantially different elevations from Kap Trautwine, Greenland (upper left), and south Devon Island (upper right). The differences in the t-T histories are used to estimate paleogeothermal gradients (lower panel). After 200 Ma, a geothermal gradient of 36-38 °C/km is indicated for the Kap Trautwine samples, and 22–26 °C/km is indicated for the Devon Island samples. The apparent upward spikes in the paleogeothermal gradients before 220 Ma (shaded grey) are modelling artefacts that occur at times when one (or both) of the samples from each pair are at temperatures above the PAZ.

from 225 Ma to the present, or 0.3 °C/My. The Devon Island samples suggest a somewhat higher cooling rate of 0.5 °C/My. Gallagher et al. (1994, 1995, 1998), Brown et al. (1994, 2000) and others have shown that in many circumstances cooling in a nonorogenic setting is mainly a result of advection of mass through a steady-state geothermal regime. Based on that assumption, denudation rates can be calculated by dividing the cooling rates by the geothermal gradient. For the Kap Trautwine samples an average denudation rate of 9 m/My is obtained. The Devon Island samples suggest an average denudation rate of 21 m/My. These estimates compare favourably to the average rates of denudation inferred by Grist and Zentilli (2004) based on differences between the FT ages of samples obtained from high and low elevations on Kap Trautwine and Devon Island of ca. 8.9 m/My and 18.8 m/My, respectively.

7.9 Conclusions:

Calibrated data models are a powerful tool for the elucidation of realistic thermal histories. The comparison of apatite FT-based thermal model predictions to (U-Th)/He data from the same samples gives an indication of the accuracy and limitations of these models that otherwise would be difficult to obtain. Forward modelling of (U-Th)/He ages demonstrate that it is crucial to consider the effects of low temperature annealing in the FT thermal models. A reduction of the initial TL eliminates the need for late-stage cooling that is a common artefact of apatite fission track modelling using the Laslett et al. (1987) model. Thermal histories compatible with both fission track and (U-Th)/He data are obtained using the Laslett et al. annealing model with reduced initial TL of 15 μm.

FT and (U-Th)/He thermal models suggest that the thermal history below ca. 130 °C in much of the Inglefield Uplift region in eastern Ellesmere and Devon Islands, and the Wolstenholme Fjord - Inglefield Brednig region in western Greenland is dominated by Late Paleozoic or Mesozoic denudational cooling related to exhumation of the sediment source regions for the Sverdrup Basin in Central Ellesmere and Axel Heiberg and the western Arctic Islands. Models for samples from southern Devon Island also show evidence of elevated temperatures during Late Cretaceous time, and accelerated cooling from Paleocene time to the present. Thermal models for other samples obtained from islands and coastal regions of

northern Baffin Bay and Talbot Inlet, Ellesmere Island, are also consistent with Late Cretaceous rift-related heating. (U-Th)/He forward models for samples from the Pavy Formation in the Nares Strait region are consistent with limited post-depositional heating, likely before Eocene time. The inverse model for a sample from the Archer Fiord Formation in the hanging wall of the Rawlings Bay thrust at Cape Lawrence indicates that cooling during Eurekan tectonic movement occurred during Late Paleocene time there, and only minor (i.e., <2 km) Eocene thrusting is evident.

7.10 Acknowledgements

A. Grist is very grateful to Ken Farley at Caltech for the insights he has offered into many aspects of (U-Th)/He dating, and for the use of his (U-Th)/He age- modelling software. Thanks to Patricia Stoffyn for her assistance and expertise on the microprobe. Thanks also to Chris Beaumont and Peter Reynolds for their helpful reviews of early versions of this manuscript.

7.11 References cited:

Arne, D.C., Grist, A.M., Zentilli, M., Collins, M., Embry, A., and Gentzis, T. 2002. Cooling of the Sverdrup Basin during Tertiary basin inversion: implications for hydrocarbon exploration. Basin Research, **14**: 183-205.

Balkwill, H.R. 1978. Evolution of the Sverdrup Basin, Arctic Canada. The American Association of Petroleum Geologists Bulletin, **62**, 1004-1028.

Bertel, E., Mark, T.D. and Pahl, M. 1977. A new method for the measurement of the mean etchable fission track length and of extremely high fission track densities in minerals. Nuclear Track Detection, **1**, 123-126.

Brown, R.W., Gallagher, K., and Duane, M.J. 1994. A quantitative assessment of the effects of magmatism on the thermal history of the Karoo sedimentary sequence. African Journal of Earth Sciences, **18**: 227-243.

Brown, R.W., Gallagher, K., Gleadow, A.J.W., and Summerfield, M.A. 2000. Morphotectonic evolution of the south Atlantic margins of Africa and South America.

In Geomorphology and Global Tectonics. Edited by M.A. Summerfield. J. Wiley and Sons, New York, 255-281.

Carlson, W.D., Donelick, R.A. and Ketcham, R.A. 1999. Variability of apatite fission track annealing kinetics: 1. Experimental results. American Mineralogist, **84**, 1213-1223.

Davies, G.R. and Nassichuk, W.W. 1991. Carboniferous and Permian history of the Sverdrup Basin, Arctic Islands. In Geology of the Innuitian Orogen and Arctic Platform of Canada and Greenland. Edited by H.P. Trettin. Geological Survey of Canada, Geology of Canada **3**, pp. 345-367.

Dodson, M.H. 1973. Closure temperature in cooling geochronological and petrological systems. Contributions in Mineralogy and Petrology, **40**, 259-274.

Donelick, R.A., Roden, M.K., Mooers, J.D., Carpenter, B.S., and Miller, D.S. 1990. Etchable length reduction of induced fission tracks in apatite at room temperature (~23 °C): Crystallographic orientation effects and "initial" mean lengths. Nuclear Tracks and Radiation Measurements, **17**, no. 3, 261-265.

Ehlers, T.A. and Farley, K.A. 2003. Apatite (U-Th)/He thermochronometry: methods and applications to problems in tectonic and surface processes. Earth and Planetary Science Letters, **206**, 1-14.

Embry, A.F. 1982. The Upper Triassic - Lower Jurassic Heiberg deltaic complex of the Sverdrup Basin; In; Arctic Geology and Geophysics, Edited by A.F. Embry and H.R. Balkwill, Canadian Society of Petroleum Geologists, Memoir, **8**, 189-217.

Embry. A.F. 1991. Mesozoic history of the Arctic Islands In: Geology of the Innuitian Orogen and Arctic Platform of Canada and Greenland. Edited by H.P. Trettin. Geological Survey of Canada, Geology of Canada **3**, pp. 371-433.

Farley, K.A. 2000. Helium diffusion in apatite: General behavior as illustrated by Durango fluorapatite. Journal of Geophysical Research, **105**, p. 2903-2914.

Farley, K.A., Wolf, R.A. and Silver, L.T. 1996. The effects of long alpha-stopping distances on (U-Th)/He ages. Geochimica et Cosmochimica Acta, **60**, no. 21, p. 4223-4229.

Gallagher, K. 1995. Evolving temperature histories from apatite fission-track data. Earth and Planetary Science Letters, **136**, 421-435.

Gallagher, K., Hawkesworth, C. and Montovani, M. 1994. The denudation history of the onshore continental margin of S.E. Brazil inferred from fission track data. Journal of Geophysical Research, **99**, 18117-18145.

Gallagher, K., Hawkesworth, C. and Montovani, M. 1995. Denudation, fission track analysis and the long-term evolution of passive margin topography: application to the S.E. Brazilian margin. Journal of South American Earth Sciences, **8**, 65-77.

Gallagher, K., Brown, R.W. and Johnson, C. 1998. Fission track analysis and its applications to geological problems. Annual Review of Planetary Science Letters. **26**: 519-572.

Green, P.F. 1988. The relationship between track shortening and fission track age reduction in apatite: combined influences of inherent instability, annealing anisotropy, length bias and system calibration. Earth and Planetary Science Letters, **89**, 335-352.

Green, P.F. 1996. The importance of compositional influence on fission track annealing in apatite. In International Workshop on Fission Track Dating. Gent, Belgium, (1996), Abstracts, p. 43.

Green, P.F., Duddy, I.R., Gleadow, A.J.W., Tingate, P.R., and Laslett, G.M.1985. Fission-track annealing in apatite: Track length measurements and the form of the Arrhenius plot. Nuclear Tracks **10**: 323-328.

Green, P.F., Duddy, I.R., Gleadow, A.J.W., Tingate, P.R., and Laslett, G.M. 1986. Thermal annealing of fission tracks in apatite 1. A qualitative description: Chemical Geology, **59**: 237-253.

Green, P.F., Duddy, I.R., Laslett, G.M., Hegarty, K.A., Gleadow, A.J.W., and Lovering, J.F. 1989. Thermal annealing of fission tracks in apatite 4. Quantitative modelling techniques and extension to geological timescales Chemical Geology (Isotope Geoscience Section), **79**:155-182.

Grist, A.M. and Zentilli, M. 2003. Post-Paleocene cooling in the southern Canadian Atlantic region: evidence from apatite fission track models. Canadian Journal of Earth Sciences, **40**, no. 9, 1279-1297.

Grist, A.M. and Zentilli, M.2004, in prep. Insights on the Thermal History of the Nares Strait, Kane Basin Region in Canada and Greenland from Apatite Fission Track and (U-

Th)/He dating, Canadian Journal of Earth Sciences, submitted.

House, M.A., Farley, K.A. and Stockli, D. 2000. Helium chronometry of apatite and titanite using Nd-YAG laser heating. Earth and Planetary Science Letters, **183**, 365-368.

Issler, D.I. 1996. An inverse model for extracting thermal histories from apatite fission track data: Instructions and software for the Windows95 environment. Geological Survey of Canada, Open File Report, 2325.

Kerr, J.W. 1967. Nares submarine rift valley and the relative rotation of north Greenland: Bulletin of Canadian Petroleum Geology, **15**, 483-520.

Laslett, G.M., Green, P.F., Duddy, I.R., and Gleadow, A.J.W. 1987. Thermal annealing of fission tracks in apatite: 2. A quantitative analysis. Chemical Geology (Isotope Geoscience Section), **65**: 1-13.

Oakey, G.N., Hearty, B., Forsberg, R., and Jackson, H.R. 2000. Gravity anomaly of the Innuitian region, Canadian and Greenland Arctic. Geological Survey of Canada Open File 3934d, scale 1:1,500,000.

Okulitch, A.V. and Trettin, H.P. 1991. Late Cretaceous - Early Tertiary deformation, Arctic Islands, In Geology of the Innuitian Orogen and Arctic Platform of Canada and Greenland. Edited by H.P. Trettin. Geological Survey of Canada, Geology of Canada **3**, 469-489.

O'Sullivan, P.B. and Brown, R.W. 1998. Effects of surface cooling on apatite fission-track data: evidence for Miocene climatic change, North Slope, Alaska. In: Advances in fissin track geochronology, Edited by P. Van den Haute and F. De Corte, Kluwer, Dordrecht, The Netherlands, pp. 255-267.

Reiners, P.W., Spell, T.L., Nicolescu, S., and Zanetti, K. 2003. Zircon (U-Th)/He thermochronometry: He diffusion and comparisons with $^{40}Ar/^{39}Ar$ dating. Geochimica et Cosmochimica Acta, **68**, 1857-1887.

Reiners, P.W., Farley, K.A. and Hickes, H.J. 2002. He diffusion and (U-Th)/He thermochronometry of zircon: Initial results from Fish Canyon Tuff and Golde Butte. Tectonophysics, **349**, 297-308.

Reiners, P.W. and Farley, K.A. 1999. Helium diffusion and (U-Th)/He thermochronometry

of titanite. Geochimica et Cosmochimica Acta, **63**, 3485-3859.

Roest, W.R. and Srivastrava, S.P. 1989. Sea-floor spreading in the Labrador Sea: a new reconstruction. Geology, **17**, 1000-1003.

Rutherford, E. 1905. Present problems in radioactivity. Popular Science Monthly, May, 1-34.

Shuster, D.L. and Farley, K.A. 2003. $^{4}He/^{3}He$ thermochronometry. Earth and Planetary Science Letters, **217**, 1-17.

Srivastava, S.P. 1985. Evolution of the Eurasian Basin and its implications to the motion of Greenland along Nares Strait, Tectonophysics, **114**, 29-53.

Strutt, R.J. 1905. On the radioactive minerals. Proceedings of the Royal Society, **A7**, 88-101.

Tessensohn, F. and Piepjohn, K. 2000. Eocene compressive deformation in Arctic Canada, North Greenland and Svalbard and its plate tectonc causes. Polarforschung **68**: 121-124.

Thorsteinsson, R. and Tozer, E.T. 1970. Geology of the Arctic Archipelago. In: Geology and Economic Minerals of Canada. Edited by R.J.W. Douglas. Geological Survey of Canada Economic Geology Report no. 1, 547-590.

Trettin, H.P. 1991a (Editor). Geology of the Innuitian Orogen and Arctic Platform of Canada and Greenland. Geological Survey of Canada, Geology of Canada **3**.

Trettin, H.P. 1991b. Tectonic Framework. In; Geology of the Innuitian Orogen and Arctic Platform of Canada and Greenland. Edited by H.P. Trettin. Geological Survey of Canada, Geology of Canada **3**, pp. 59-66.

Vrolijk, P., Donelick, R.A., Queng, J., and Cloos, M. 1992. Testing models of fission track annealing in apatite in a simple thermal setting: site 800, leg 129. In (R.L. Larson and Y. Lancelot, Editors) Proceedings of the Ocean Drilling Program, Scientific Results, **129**: pp. 169-176.

Wagner, G.A. and Van den Haute, P. 1992. Fission track dating. Kluwer, Dordrecht, The Netherlands, 285 p.

Willett, S.D. 1997. Inverse modeling of annealing of fission tracks in apatite 1: A controlled random search method. American Journal of Science, **297**: 939-969.

Wolf, R.A., Farley, K.A. and Kass, D.M. 1998. Modeling of the temperature sensitivity of the

apatite (U-Th)/He thermochronometer. Chemical Geology, **148**, 105-114.

Zeitler, P.K., Herczeg, A.L., McDougall, I., and Honda, M. 1987. U-Th-He dating of apatite: A potential thermochronometer. Geochimica et Cosmochimica Acta, **51**, 2865-2868.

CHAPTER 8. Summary and geologic overview

8.1. Discussion of methodology

Apatite fission track (FT) and (U-Th)/He dating are currently the methods best suited to the study of cooling in the uppermost part of the crust. Distributions of confined track lengths and radiogenic He concentration gradients within individual apatite grains contain valuable information on the thermal history in the temperature range of ca. 40-130 °C, corresponding to burial depths of >1 - 5 km in typical geothermal gradients. Fission tracks are formed at an initial length of > 16 μm and shortened in response to the highest temperatures they subsequently experience. Similarly, radiogenic He is produced continuously through time throughout an apatite crystal, and diffuses in response to the highest temperatures experienced. Therefore, during heating maximum temperature information may be recorded by grains, but little (or no) information is preserved about increasing temperature as a function of time. In cooling environments however, track length distributions and radiogenic He concentration gradients preserve detailed information about the shape of the time-temperature path (i.e., cooling rates). In denudational environments such as the onshore margin of sedimentary basins, and inverted basins overlying strata are absent, and the thermal imprint left as a result of burial beneath the eroded strata may provide the only direct indication of regional patterns of denudation. This makes the apatite FT and (U-Th)/He methods particularly well-suited to the study of these environments.

Studies such as this one, which combine both of these independent low-temperature thermochronometers, are particularly significant not only because they expand the range of temperatures that may be addressed by either technique individually, but also because each method can be used to test the other and thereby permit the development of quantitative intercalibration. This study has demonstrated significant under-prediction of low-temperature annealing by the Laslett et al. (1987) track annealing model. In geological applications where only the apatite FT method is used to investigate thermal histories (e.g. Chapter 3), even if under-prediction of low-temperature annealing is acknowledged, it is very difficult to distinguish between late-stage cooling that is forced by the model and geologically

significant cooling. The model artefact is especially significant in polar regions, where present-day temperatures are within a few degrees of 0 °C, and therefore model estimates of late-stage cooling would be greater.

Using measured apatite (U-Th)/He ages for the Durango apatite age standard to calibrate our FT inverse thermal models, I have shown that late-stage cooling that results from under-prediction of low-temperature annealing can be essentially eliminated by the introduction of an initial reduction of the mean confined TL from 16 to 15 μm. Is this, however, an acceptable modelling approach? In considering this question, it is important to first keep in mind that this is a relatively minor correction to the FT annealing model, which affects only the lowest part of the ca. 60-130 °C temperature sensitivity 'window'. However, apatite FT thermal history models are invariably presented showing temperatures as low as 0 °C, even though the method is relatively insensitive to temperatures below ca. 60 °C, and the elevated late-stage temperatures caused by the model artefact do have important implications for more temperature-sensitive systems such as apatite (U-Th)/He dating. Low-temperature annealing, therefore, needs to addressed.

Aesthetically, it is not entirely satisfying to introduce a 'fudge factor' (the term is itself pejorative) to the annealing model, and it tends to undermine confidence in the overall model. Richard Ketcham (pers. comm.) considers the introduction of an initial mean length reduction in the Laslett et al. (1987) an unacceptable compromise, and like others has pursued alternate annealing models (e.g. Ketcham et al. 1999). The important question is whether or not the thermal histories that are obtained through the use of an initial length reduction are more realistic, as I suggested in Chapter 7.

This is a difficult statement to prove. In order to do so I would need to have *a priori* knowledge of the actual geologic thermal history of a sample which, with the possible exception of extraterrestrial material, is a circumstance that is difficult to imagine. The thermal history obtained for the Durango age standard (Fig. 7.2), whose thermal history is assumed to be simple, and whose age has been independently confirmed by multiple dating methods, appears to be more realistic. Without the correction I am not able to reproduce the (presumably reliable) measured (U-Th)/He age. By applying the correction I am able to

reproduce both the FT and the (U-Th)/He ages, and by being able to satisfy more criteria, the model thermal histories are more realistic. There are more built-in assumptions concerning the sample model thermal histories because they are for the most part not simple (see Appendices B, C, and D) and compositions also vary. However, at the very least they are not affected by under-prediction of low-temperature annealing.

8.2. Discussion of regional denudation of basin margins

In this study I have examined denudation from basin inversion in the Fundy and Sverdrup Basins, and the response of wide scale isostatic exhumation of sediment source regions related to basin subsidence in the southern Atlantic passive margin, Lancaster Sound, and the Sverdrup Basin. I have suggested that denudation of the onshore region flanking the Sverdrup Basin occurred across a distance of >300 km from the basin margin. Denudation of the onshore in the southern Atlantic rifted margin, and also of southern Devon Island in response to subsidence in Lancaster Sound, occurs across a distance of >100 km from the margin. In the following sections I address the questions of how are regional patterns of denudation in these areas are similar and different; and also how denudation of the sediment source regions compares with the tectonic and surface process models that were discussed in Chapter 1.

8.2.1. Low-temperature thermal history of the Nova Scotia margin

8.2.1.1 History of rifting

Early evolution of the southern Canadian Atlantic margin occurred during two phases of rifting. During the initial phase in Triassic time, a series of northeast-southwest trending half-grabens developed extending from the Blake Plateau east of Florida, to the Bay of Fundy and Orpheus Graben in Nova Scotia, and on the conjugate African margin from Senegal to Morocco. Numerous rift basins developed above the half grabens, which dip southeast on the North American side and northwest on the African side. The northern boundary of this system occurs at the northern limit of the Fundy Rift Basin, the Orpheus Basin and, where it is truncated by large strike-slip faults, including the Cobequid-Chedabucto Fault Zone in

Nova Scotia and the Headlands Fault in New Brunswick. This system straddled the equator to about 10 °N latitude, and may have been similar in many respects to the present day East African Rift system. During this time much of this region likely experienced elevated heat flow as a result of fluid flow along faults, volcanism, and from burial subsidence heating in the rift basins. Apatite FT thermal models for the Fundy Basin samples (Chapter 3) are consistent with this interpretation.

In Early Jurassic time the mid-Atlantic ridge developed off of the southeastern United States, and propagated northwards east of Nova Scotia. Subsidence of the half grabens and Triassic rift basins ended, and widespread subsidence of the offshore basins of the Atlantic began. The thermal models constrained by (U-Th)/He data for Mahone Bay and Halifax (Chapter 4) reflect cooling at this time, likely related to erosion of uplifted rift flanks associated with the onset of rifting in the Scotian Basin, offshore Nova Scotia. Cooling also began in the early rift basins as a result of regional exhumation and the shedding of sediments into the developing offshore.

It is unlikely that the Nova Scotia margin contained major southeasterly-flowing rivers during this time, because the province is only ca. 100 km wide. Therefore, based on the discussion presented in Section 1.3, onshore erosion of the uplifted rift flanks in this part of the margin likely initially occurred by a process of parallel retreat rather than by rapid incision. It is noteworthy that apatite (U-Th)/He ages for this region (Chapter 4) are only slightly younger than corresponding FT ages (Chapter 3). This similarity of ages suggests a short landscape response time, and that rift flank erosion was relatively rapid, and likely complete by Middle Jurassic time. This suggests that the rocks that were formerly above the presently-exposed bedrock in Nova Scotia were rather easily eroded. The similarity of FT and (U-Th)/He ages also implies that during Cretaceous time only minor erosion of the Nova Scotia margin occurred. This supports the interpretation of Grist et al. (1992; Fig. 9), who inferred that during deposition of the Cretaceous Missisauga Formation in the Scotian Basin, sediment was derived via a major river system that existed northeast of Nova Scotia, at the present-day location of the Laurentian Channel, and which drained a catchment that included much of the area of the present-day Gulf of St. Lawrence. As suggested in Chapter 3,

additional cooling in this region may have also resulted from decreased mean annual surface temperatures from Middle Jurassic to Early Cretaceous time.

8.2.1.2 Late Cretaceous heating

Part of the focus of Chapter 3 was to investigate a proposed period of elevated temperatures in the southern Canadian Atlantic margin during Cretaceous time that had been inferred based on several previous FT studies from the region (e.g. Arne et al. 1990; Grist et al. 1992; Li et al. 1995). Limited Early Cretaceous strata are also known to occur in the region (the Chaswood Formation; Stea et al. 1997), and elevated vitrinite reflectance levels from this strata in lignite preserved from erosion in Karst sinkholes provide additional evidence of burial heating (e.g. Hacquebard 1984; Arne et al. 1990). However, as discussed in Chapter 4, some of the 'lignite' may have been contaminated by charcoal, and therefore estimates of maturity obtained by vitrinite reflectance may too high. The FT inverse models presented are also compatible with proposed elevated temperatures during Late Cretaceous time, but they are not deterministic. Deposition of the Chaswood Formation during Lower Cretaceous time however, provides necessary geologic support for the interpretation based on these models.

The purpose of apatite (U-Th)/He dating of some of these same samples from the southern Canadian Atlantic margin (Chapter 4) was two-fold. I wanted to improve the FT inverse models by providing additional temperature constraints for the lower part of the PAZ, as discussed above. I also wanted to attempt to date post-Albian cooling following heating that may have resulted from a combination of limited burial heating beneath the Cretaceous Chaswood Formation, and the propagation to depth of increased paleomean annual surface temperatures. The Digby D-1 drillhole samples appeared to be very well suited to this purpose because they were obtained from depths between ca. 60 and 1400 m. Even very minor heating of the deeper samples could be expected to bring them up to temperatures associated with significant helium diffusion. Unfortunately, S-type granites are notoriously poorly suited for (U–Th)/He dating because the apatite grains commonly contain ubiquitous mineral inclusions that render them undatable (K. Farley, pers. comm). The South Mountain

Batholith samples also contain abundant inclusions, and none of the deeper samples from the Digby D-1 drillhole contained inclusion-free apatite. The objective of dating elevated Late Cretaceous temperatures directly was therefore not achieved.

Although the existence of widespread Aptian/Albian deposits preserved onshore strongly suggests that the region underwent at least some burial, much of the evidence concerning significantly elevated post-Albian temperatures in the Southern Atlantic margin remains controversial. The FT models of Grist et al. (1992) and Li et al. (1995), which suggest a period of elevated Late Cretaceous temperatures in the offshore region, are likely not affected by under-prediction of low-temperature annealing because those well samples were obtained at depths where temperatures are currently within the PAZ. Significant erosional unconformities have also recently been identified in Paleocene strata offshore (Banquereau Formation; A. MacRae, pers. comm.), suggesting a period of denudational cooling at this time similar to that proposed for the onshore region (Chapter 3). However, (U-Th)/He age data for the near-surface and surface samples (Chapter 4) indicates that post-Albian temperatures in the onshore region never exceeded ca. 50 °C. Also, it has been recently recognized that many of the Cretaceous deposits contain abundant charcoal (M. Gibling, pers. comm.) that was presumably derived from forest fires. The presence of charcoal in the Chaswood Formation, which would yield high reflectance values, is not discussed in earlier studies (e.g. Hacquebard 1984) and therefore it is difficult to know if it was considered during reflectance measurements.

8.2.2. Low-temperature thermal history of the Sverdrup Basin

The Sverdrup Basin is a post-orogenic basin and a failed rifted continental margin that became inverted during Late Cretaceous to Paleogene time as a result of transpression and convergence between the eastern Canadian Arctic Archipelago and western Greenland. Apatite FT ages and length distributions for outcrop samples obtained from thrust hanging wall strata and the cores of anticlines in central Ellesmere Island clearly reflect cooling from temperatures above the PAZ during inversion. In contrast, many of the FT ages of samples obtained from thrust footwalls, and off-structure, fail the χ^2 test, indicating that they are

composed of more than one age population. Radial plots for these samples show that they contain a mixture of FT ages, and corresponding length distributions are broad and flat, or bimodal (e.g., Arne et al. 1998, Fig. 2). Low vitrinite reflectance levels in these samples (Chapter 5) suggest that it is unlikely that the pattern of ages and lengths is a result of differential annealing characteristics of apatite having different compositions, but is more likely related to mixed provenance of the detrital grains. The preservation of provenance ages suggests that these samples were heated to temperatures high enough to cause only relatively minor annealing following deposition in the basin, and have experienced limited denudation from inversion.

The discontinuity of the pattern of ages and lengths across thrusts indicates that exhumation of the hanging wall strata occurred mainly as a result of thrusting. Maximum temperatures in the hanging wall strata predated thrusting, suggesting that peak hydrocarbon generation and primary migration preceded the formation of these structural traps during the Eurekan Orogeny. Stratigraphic traps at depth in footwall section would present much better potential exploration targets.

8.2.3. Low-temperature thermal history of eastern Ellesmere Island and western Greenland

Apatite FT and (U-Th)/He data for the eastern Ellesmere Island - western Greenland (Chapter 6) reveal a complex low-temperature regional thermal history which has been influenced by several tectonic events. The oldest FT ages obtained (Fig. 6.4) are as old as any of the samples from shield areas on the flanks of rifted margins shown in Fig. 2.6, reflecting protracted denudational cooling, likely since Late Proterozoic time for these samples.

Most of the samples from this region have been influenced by denudational cooling related to the development of the Sverdrup Basin in the central Canadian Arctic Archipelago in two stages, during Late Carboniferous to Permian time and Early Triassic to Late Cretaceous time. Data from samples obtained proximal to the basin (from west of Makinson Inlet and along the Leffert Glacier) reflect Late Paleozoic denudation during deposition of clastic units, likely as a result of flank uplift during the early phase of rifting in the Sverdrup

Basin. More distal samples from Wolstenholme Fjord and Inglefield Brednig region of Greenland indicate Triassic denudation that likely reflects a much broader regional denudation that accompanied the main phase of Mesozoic basin development and subsidence.

FT thermal models for several of the samples obtained near sea-level from coastal exposures of northern Baffin Bay, Carey Øer, and Devon Island (Figs. 7.9 and 7.10) show evidence of increased temperatures during the Late Cretaceous, followed by accelerated Paleogene cooling. These samples likely experienced increased heat flow during the northward propagation of the Labrador Sea - Baffin Bay rift system, followed by exhumational cooling, possibly related to readjustment of offshore structural blocks from the incipient collision of Greenland and Ellesmere Island.

8.2.4. Low-temperature thermal history of Nares Strait

One of the important results of this study is that apatite FT data for samples from Cape Lawrence, Cape Back, and south of Cape Baird, along northern Nares Strait preserve Late Paleocene ages (58.2 to 63.4 Ma). Corresponding (U-Th)/He ages for these samples are Late Paleocene - Early Eocene (46.4 to >60 Ma). These data indicate that only relatively minor Eocene cooling occurred in this region. Piepjohn et al. (2000) and others, based on thrust deformation within the Late Paleocene - Early Eocene Cape Lawrence and Cape Back Formations, have suggested the main phase of deformation occurred during Eocene time. The FT and (U-Th)/He data, however, show that thrust deformation of strata currently exposed at the surface resulted in only minimal cooling during compression, and was relatively insignificant in the regional thermal evolution. An earlier phase of mafic volcanism, apparently related to continental rifting, and potentially the development of strike-slip offset between western Greenland and eastern Ellesmere Island, had a greater influence.

This interpretation is consistent with the conclusions of Tessensohn and Piepjohn (2000), Srivastava (1985) and others, based plate tectonic reconstructions, that a rift transform existed in Nares Strait during Paleogene time, but the data neither support nor refute extensive strike-slip motion at this time. The data from the Pavy Formation near Cape

Back and south of Cape Baird are consistent with mafic continental rift volcanism (Estrada and Tessensohn 2004) and minor thrusting, and the fault-bounded Pavy Formation may be close to the locus of a now thrust-overridden Wegener Fault.

Arne et al. (2002; i.e., Chapter 5) found that the geographic distribution of surface rocks in which detrital apatite was inferred to have been completely reset was restricted to the hanging walls of major thrust faults. Apatite FT ages of samples obtained from thrust fault hanging walls in central Ellesmere Island, such as at Vesle Fiord (Arne et al. 1998) and the Lake Hazen Fault zone (Chapter 5), are also somewhat younger than FT and (U-Th)/He ages of samples from thrust hanging walls in the Nares Strait area (Chapter 6). This suggests that Ellesmere Island may not have acted as a rigid plate during Eocene compression, and that deformation that was initially taken up in the strait region progressed inland during Eocene time.

8.3 Scientific contributions of this work

This thesis makes significant scientific contributions in two main areas, methodological and geological. With respect to methodology, the first contribution is by elucidating an important limitation of apatite fission track (FT) modelling as it is routinely used in numerous laboratories and academic institutions throughout the world. Several apatite FT studies have used geological and geomorphological constraints to infer that using the Laslett et al. (1987) annealing model with an initial mean length of 16 μm results in improbable time-temperature histories at temperatures below ca. 60 °C (e.g. Grist and Zentilli 2003 (this thesis); Gunnell et al. 2003). In Chapters 4 and 7 I demonstrated that the low-temperature estimates from that annealing model are also inconsistent with apatite (U-Th)/He age data. This discrepancy is not too surprising given the relative insensitivity of the FT method to temperatures at which (U-Th)/He ages are very sensitive. The use of an initial mean track length of 15 μm essentially eliminates unrealistic late-stage cooling in FT models and produces temperature histories that are compatible with (U-Th)/He data, however, further research is needed in order to test the validity of scaling the initial mean track length on temperature estimates in the upper part of the apatite partial annealing zone.

A second scientific contribution of this thesis work with respect to methodology is in demonstrating the importance of measuring ^{147}Sm in all samples dated by the (U-Th)/He method. A substantial proportion of the of the radiogenic ^{4}He in some of my samples (up to 20%), especially in the Franklinian dykes and Archean gneisses, was derived from ^{147}Sm. Failure to consider this source of radiogenic ^{4}He would have resulted in considerable overestimation of the (U-Th)/He ages of those samples.

This work has also made a number of significant geological contributions to understanding the low-temperature thermal history of both the southern Canadian Atlantic margin, and the northeastern Canadian Arctic Archipelago. In the southern Canadian Atlantic margin I have obtained the first apatite (U-Th)/He data, which when taken together with apatite FT models demonstrate that following the onset of Atlantic rifting, the region experienced rapid exhumational cooling during Jurassic time.

In the Sverdrup Basin, we have demonstrated that apatite FT data from both well and surface samples are consistent with substantial exhumational cooling during inversion that occurred during the Eurekan Orogeny. We also effectively demonstrated that many of the major thrust faults that were drilled during the peak period of hydrocarbon exploration in the Sverdrup Basin in the 1970's were active during the Eurekan Orogeny, and post-date primary oil maturation and migration, and are therefore likely to be poor targets.

In the Nares Strait - Kane Basin - Smith Sound region, I have shown that the complex thermal history can be considered to be a result of at least three tectonic influences; regional exhumation of the area as a sediment source for the developing Sverdrup Basin during Late Paleozoic to Early Mesozoic time; cooling of rift flanks following the onset of Late Cretaceous rifting in the Labrador Sea and Baffin Bay rift system; and inversion of the region as a result of the convergence of Ellesmere Island and Greenland during the Eurekan Orogeny. Finally, I have shown that Paleogene FT ages related to the Eurekan Orogeny in fault-bounded basins in the Nares Strait region are older than corresponding ages in thrust fault hanging walls and structural culminations in central Ellesmere Island, suggesting that cooling occurred earlier in the strait region and progressed westward.

References Cited

Akande, S.O. and Zentilli, M. 1983. Genesis of the lead-zinc mineralization at Gays River, Nova Scotia, Canada. In International Conference on Mississippi Valley Type Lead-Zinc Deposits, Proceedings Volume. Edited by G. Kisvarsanyi, S.K. Grant, W.P. Pratt, and J.W. Koenig. University of Missouri, Rolla, Missouri, pp. 546-557.

Armstrong, P.A., Ehlers, T.A., Chapman, D.S., Farley, K.A., and Kamp, P.A. 2003. Exhumation of the central Wasatch Mountains, Utah: 1. Patterns and timing of exhumation deduced from low-temperature thermochronology data. Journal of Geophysical Research, **108**, B3, 2172, doi:10.1029/2001JB001708.

Arne, D.C. 2000. Cooling of thrust sheets. 9th International Conference on Fission-track Dating and Thermochronology, Geological Society of Australia Abstract Series, **58**, 9-10.

Arne, D. and Zentilli, M. 1994. Apatite fission-track thermochronology integrated with vitrinite reflectance. In: Vitrinite Reflectance as a Maturity Parameter: Applications and Limitations Edited by P.K. Mukhopadhyay and W.G. Dow. American Chemical Society Symposium Series, **570**, pp. 249-268.

Arne, D.C., Duddy, I.R., and Sangster, D.F. 1990. Thermochronologic constraints on ore formation at the Gays River Pb-Zn deposit, Nova Scotia, Canada, from apatite fission track analysis. Canadian Journal of Earth Sciences, **27**: 1013-1022.

Arne, D.C., Embry, A., Zentilli, M. and Collins, M. 1995. Thermal and tectonic history of the Sverdrup Basin and Franklinian Mobile Belt, Canadian Arctic Archipelago. Geological Association of Cananada Mineraogical Association of Canada Abstract, **20**, 4.

Arne, D., Worley, B., Wilson, C.J.L., Chen, S., Luo, Z., Liu, S. and Dirks, P. 1997. Differential exhumation in response to episodic thrusting along the eastern margin of the Tibetan Plateau. Tectonophysics, **280**, 239-256.

Arne, D.C., Zentilli, M., Grist, A.M., and Collins, M. 1998. Constraints on the timing of thrusting during the Eurekan orogeny, Canadian Arctic Archipelago: an integrated approach to thermal history analysis. Canadian Journal of Earth Sciences, **35**, 1: 30-

38.

Arne, D.C., Grist, A.M., Zentilli, M., Collins, M., Embry, A., and Gentzis, T. 2002. Cooling of the Sverdrup Basin during Tertiary basin inversion: implications for hydrocarbon exploration. Basin Research, **14**: 183-205.

Balkwill, H.R. 1978. Evolution of the Sverdrup Basin, Arctic Canada. The American Association of Petroleum Geologists Bulletin, **62**, 1004-1028.

Barker, C.E. 2000. A paleolatitude approach to assessing surface temperature history for use in burial heating models. International Journal of Coal Geology, **43**, 1-4: 121-135.

Barrera, E., and Johnson, C.C. (Editors) 1999. Evolution of the Cretaceous ocean-climate system. Geological Society of America Special Paper 332.

Barron, E.J. 1983. A warm, equable Cretaceous: The nature of the problem. Earth Science Reviews, **19**: 305-338.

Beaumont, C., Keen, C.E. and Boutillier, R. 1982. On the evolution of rifted continental margins: Comparisons of models and observations for the Nova Scotia margin. Geophysical Journal of the Royal Astronomical Society, **70**, 667-715.

Beaumont, C., Kooi, H. and Willett, S.D. 2000. Coupled tectonic-surface process models with applications to rifted margins and collisional orogens. In: Geomorphology and Global Tectonics. Edited by M.A. Summerfield, John Wiley and Sons, New York, 29-55.

Beck, A.E. 1977. Climatically perturbed temperature gradients and their effect on regional and continental heat-flow means. Tectonophysics, **41**: 17-39.

Bertel, E., Mark, T.D. and Pahl, M. 1977. A new method for the measurement of the mean etchable fission track length and of extremely high fission track densities in minerals. Nuclear Track Detection, **1**, 123-126.

Bohannon, R.G., Naeser, C.N., Schmidt, D.L., and Zimmerman, R.A. 1989. The timing and uplift, vaocanism and rifting perpheral to the Red Sea: A case for passive rifting?. Journal of Geophysical Research, **94**, 1683-1701.

Bond, G. 1976. Evidence for continental subsidence in North America during the Late Cretaceous global submergence. Geology, **4**: 557-560.

Bradley, D.C. 1982. Subsidence in Late Paleozoic basins in the northern Appalachians. Tectonics, **1**, 1: 107-123.

Brandon, M.T. 1992. Decomposition of fission-track grain-age distributions. American Journal of Science, **292**, 535-564.

Braun, J. and Beaumont, C. 1989. A physical explanation for the relation between flank uplifts and the breakup unconformity at rifted continental margins. Geology, **17**, 760-764.

Brooks, P.W., Embry, A.F., Goodarzi, F. and Stewart, R. 1992. Organic geochemistry and biological marker geochemistry of Schei Point Group (Triassic) and recovered oils from the Sverdrup Basin (Arctic Islands, Canada). Bulletin of Canadian Petroleum Geology, **40**, 173-187.

Brown, R.W. 1992. A fission track study of the sub-arial continental margins of southern Africa. Ph.D. thesis, University of Melbourne, 407 pp.

Brown, R.W., Gallagher, K., and Duane, M.J. 1994. A quantitative assessment of the effects of magmatism on the thermal history of the Karoo sedimentary sequence. African Journal of Earth Sciences, **18**: 227-243.

Brown, R.W., Gallagher, K., Gleadow, A.J.W., and Summerfield, M.A. 2000. Morphotectonic evolution of the south Atlantic margins of Africa and South America. In; Geomorphology and Global Tectonics. Edited by M.A. Summerfield. J. Wiley and Sons, New York, 255-281.

Brown, R.W., Rust, D.J., Summerfield, M.A., Gleadow, A.J.W., and De Wit, M.C.J, 1990. An early Cretaceous phase of accelerated erosion on the south-western margin of Africa: Evidence from apatite fission track analysis and the offshore sedimentary record. Nuclear Tracks and Radiation Measurements, **17**, no. 3, 339-350.

Brown, R.W., Summerfield, M.A. and Gleadow, A.J.W. 2002. Denudational history along a transect across the Drakensberg Escarpment of southern Africa derived from apatite fission track thermochronology. Journal of Geophysical Research, **107**, b12, 2350, doi:10.1029/2001JB000745.

Buck, W.R. 1986. Small-scale convection induced by passive rifting: the cause for uplift of rift shoulders. Earth and Planetary Science Letters, **77**, 362-372.

Burnham, A.K. and Sweeney,J.J. 1989. A chemical kinetic model of vitrinite reflectance maturation. Geochemica. Et Cosmochemica Acta, **53**, 2649-2657.

Carlson, W.D. 1990. Mechanisms and kinetics of apatite fission-track annealing. American Mineralogist, **75**, 1120-1139.

Carlson, W.D., Donelick. R.A., and Ketcham, R.A. 1999. Variability of apatite fission-track annealing kinetics: 1. Experimental results. American Mineralogist, **84**: 1213-1223.

Chadderton, L.T. 1988. On the anatomy of a fission track. Nuclear Tracks and Radiation Measurements, **15**, 11-29.

Chatterjee, A.K. and Dostal, J. 2002. Deep drill hole in the Devonian South Mountain Batholith, Nova Scotia: a potential for hidden mineral deposits within the batholith. Atlantic Geology, **38**, 1-10.

Clarke, D.B., MacDonald, M.A., Reynolds, P.H., and Longstaffe, F.J. 1993. Leucogranites from the eastern part of the South Mountain Batholith, Nova Scotia. Journal of Petrology, **34**: 653-679.

Cochran, J.R. 1983. Effects of finite extension times on the development of sedimentary basins. Earth and Planetary Science Letters, **66**, 289-302.

Corrigan, J.D. 1993. Apatite fission track analysis of Oligocene strata in South Texas, USA: Testing annealing models, Chemical Geology, **104**, 227-249.

Crowley, K.D., Cameron, M. and Schaeffer, R.L. 1991. Experimental studies of annealing of etched fission tracks in fluorite. Geochimica et Cosmochimica Acta, 55, 1449-1465.

Dartyge, E., Duraud, J.P. and Langevin, Y. 1978. Thermal annealing of ion tracks in muscovite, labradorite and olivine, Nuclear Tracks and Radiation Measurements, Supplement, Proceedings of the 9th conference on Solid State Nuclear Track Detectors, Munchen, 395-399.

Dartyge, E., Duraud, J.P., Langevin, Y., and Maurette, M. 1981. New model of nuclear particle tracks in dielectric minerals. Physics Reviews, **B23**, 5213-5229.

Davies, E.H., Akande, S.O., and Zentilli, M. 1984. Early Cretaceous deposits in the Gays River Lead-zinc mine, Nova Scotia: evidence from $^{40}Ar/^{39}Ar$ mineral ages. In Current Research, part A. Geological Survey of Canada, Paper 84-1A, pp. 353-358.

Davies, G.R. and Nassichuk, W.W. 1991. Carboniferous and Permian history of the Sverdrup Basin, Arctic Islands. In Geology of the Innuitian Orogen and Arctic Platform of Canada and Greenland. Edited by H.P. Trettin. Geological Survey of Canada, Geology of Canada **3**, pp. 345-367.

Davis, W.M. 1922. Peneplains and the geographic cycle. Geological Society of America Bulletin, **33.3**: 587-598.

Dawes, P.R. and Kerr, J.W. (eds.) 1982a. Nares Strait and the Drift of Greenland: a Conflict in Plate Tectonics; Meddelelser om Grønland, Geoscience **8**, 392 p.

Dawes, P.R. and Kerr, J.W. 1982b. The case against major displacement along Nares strait; In; Nares Strait and the Drift of Greenland: a Conflict in Plate Tectonics, Edited by P.R. Dawes and J.W. Kerr, Meddelelser om Grønland, Geoscience **8**, 369-386.

De Paor, D.G., Bradley, D.C., Eisenstadt, G. and Phillips, S.M. 1989. The Arctic Eurekan Orogen: a most unusual fold-and-thrust belt. Geological Society of America Bulletin, **101**, 952-967.

DeConto, R.M., Hay, W.W., Thompson, S.L., and Bergengren, J. 1999. Late Cretaceous climate and vegetation interactions; cold continental interior paradox. In; Evolution of the Cretaceous ocean-climate system. Edited by E. Berrara and C. Johnson. Geological Society of America Special Paper 332, pp. 391-406.

Deming, D. and Chapman, D.S. 1989. Thermal histories and hydrocarbon generation: Example from Utah-Wyoming thrust belt. Geological Society of America Bulletin, **73**, 1455-1471.

Dodson, M.H. 1973. Closure temperature in cooling geochronological and petrological systems. Contributions in Mineralogy and Petrology, **40**, 259-274.

Donelick, R.A. 1991. Crystallographic orientation dependence of mean etchable fission track length in apatite: an empirical model and experimental observations. American Mineralogist, **76**, 83-91.

Donelick, R.A., Bergman, S.C. and Talbot, J. 1992. 252Cf irradiation of apatite fission track samples improves spontaneous, confined, track-in-track (TINT) densities. 7th International Workshop on Fission-track Thermochronology, Philadelphia, Program with Abstracts, 80.

Donelick, R.A., Roden, M.K., Mooers, J.D., Carpenter, B.S., and Miller, D.S. 1990. Etchable length reduction of induced fission tracks in apatite at room temperature (~23°C): Crystallographic orientation effects and "initial" mean lengths. Nuclear Tracks and Radiation Measurements, **17**, no. 3, 261-265.

Dumitru, T.A. 2000. Fission-track geochronology. In; Quaternary Geochronology: Applications to Quaternary Geology and Paleoseismology, Edited by J.S. Noller, J.M. Sowers and W.R. Lettis. Geological Society of America Special Publication, 131-155.

Dumitru, T.A., Hill, K.C., Coyle, D.A., Duddy, I.R., Foster, D.A., Gleadow, A.J.W., Green, P.F., Kohn, B.P., Laslett, G.M., and O'Sullivan, A.J. 1991. Fission track thermochronology: Application to continental rifting of south-eastern Australia. Australian Petroleum Exploration Association Journal, **31**, 131-142.

Ehlers, T.A. and Farley, K.A. 2003. Apatite (U-Th)/He thermochronometry: methods and applications to problems in tectonic and surface processes. Earth and Planetary Science Letters, **206**, 1-14.

Einsele, G. 2000. Sedimentary basins: Evolution, facies, and sediment budget. 2nd ed. Springer, New York.

Elliott, B.E., Bernius, G.R., and Killean, P.G. 1997. Borehole geophysical logs South Mountain Batholith at Digby and the Wedgeport granite Nova Scotia. Geological Survey of Canada, Open File Report, 3352.

Embry, A.F. 1982. The Upper Triassic - Lower Jurassic Heiberg deltaic complex of the Sverdrup Basin; In; Arctic Geology and Geophysics, Edited by A.F. Embry and H.R. Balkwill, Canadian Society of Petroleum Geologists, Memoir, **8**, 189-217.

Embry, A.F. (1991a) Middie-Upper Devonian clastic wedge of the Arctic Islands. In Geology of the Innuitian Orogen and Arctic Platform of Canada and Greenland. Edited by

H.P. Trettin. Geological Survey of Canada, Geology of Canada **3**, pp. 263-279.

Embry, A.F. (1991b) Mesozoic history of the Arctic Islands. In; Geology of the Innuitian Orogen and Arctic Platform of Canada and Greenland. Edited by H.P. Trettin. Geological Survey of Canada, Geology of Canada **3**, pp. 371-433.

Embry, A,F. 1993. Transgressive-regressive (T-R.) sequence stratigraphy of the Jurassic succession of the Sverdrup Basin, Canadian Arctic Archipelago. Canadian Journal of Earth Sciences, **30**, 301-320.

Embry, A.F. and Dixon, J. 1990. The breakup unconformity of the Amerasia Basin, Arctic Ocean: Evidence from Arctic Canada. Geological Society of America Bulletin, **102**, 1526-1534.

Embry, A.F. and Johannessen, E.P. 1992. T-R. sequence stratigraphy, facies analysis and reservoir distribution in the uppermost Triassic-Lower Jurassic succession, western Sverdrup basin, Arctic Canada. In; Arctic Geology and Petroleum Potential. Edited by T.O. Vorren, E. Bergsager, E. Dahl-Stamnes, E. Holter, B. Johansen, E. Lie and T.B. Lund, Norwegian Petroleum Society, Special Publication **2**, pp.121-146.

Embry, A.F. and Osadetz, K.G. 1988. Stratigraphy and tectonic significance of Cretaceous volcanism in Queen Elizabeth Islands, Canadian Arctic Archipelago. Canadian Journal of Earth Sciences, **25**, 1209-1219.

Embry, A.F., Powell, T.G. and Mayr, U. 1991. Petroleum resources, Arctic Islands. In; Geology of the Innuitian Orogen and Arctic Platform of Canada and Greenland. Edited by H.P. Trettin. Geological Survey of Canada, Geology of Canada **3**, pp. 517-525.

Estrada, S. and Tessensohn, F. (in press) Late Palaeocene Nares Strait volcanic province: Evidence from volcanic pebbles. need rest of this ref.

Falvey D.A. 1974. The development of continental margins in plate tectonic theory. Australian Petroleum Exploration Association Journal, **14**, 95-106.

Farley, K.A. 2000. Helium diffusion in apatite: General behavior as illustrated by Durango fluorapatite. Journal of Geophysical Research, **105**, B2, 2903-2914.

Farley, K.A. 2002. (U-Th)/He dating: Techniques, calibration and applications. In; Noble

Gases in Geochemistry and Cosmochemistry, Edited by D. Porcelli, C.J. Ballentine and R. Wieler. Reviews in Mineralogy and Geochemistry, **47**, pp. 819-844.

Farley, K.A., Wolfe, R.A., and Silver, L.T. 1996. The effects of long alpha-stopping distances on (U-Th)/He ages. Geochimica et Cosmochimica Acta, **60**, no. 21, 4223-4229.

Farley, K.A., Kohn, B.P. and Pillans, B. 2002. The effects of secular disequilibrium on (U-Th)/He systematics and dating of Quaternary volcanic zircon and apatite. Earth and Planetary Science Letters, **201**, 117-125.

Faure, G. 1986. Principles of isotope geology, 2nd edition, J. Wiley and Sons, New York.

Feinstein, S., Kohn, B.P. and Eyal, M. 1989. Significance of combined vitrinite reflectance and fission-track studies in evaluating thermal history of sedimentary basins: An example from Southern Israel. In; Thermal history of sedimentary basins, Edited by N.D. Naeser and T.H. McCulloh, Springer-Verlag, New York, pp.157-180.

Fitzgerald, P.G., Sorkhabi, R.B., Redfield, T.F., and Stump, E. 1995. Uplift and denudation of the central Alaska Range: A case study in the use of apatite fission track thermochronology to determine absolute uplift parameters. Journal of Geophysical Research, **110**, B10, 20,175-20,191.

Fleischer, R.L. and Hart, H.R. 1972. Fission track dating: Techniques and problems. In: Calibration of Hominid Evolution. Edited by W.W. Bishop, J.A. Miller and S. Cole. Scottish Academic Press, Edinburgh, 135-170.

Fleischer, R.L., Price, P.B., and Walker, R.M., 1964. Fission track ages of zircons. Journal of Geophysical Research, **69**: 4885.

Fleischer, R.L., Price, B.P. and Walker, R.M. 1965. The ion explosion spike mechanism for formation of charged particle tracks. Journal of Applied Physics, **36**, 3645-3652.

Fleischer, R.L., Price, P.B., and Walker, R.M. 1975. Nuclear Tracks in Solids: Principles and Applications. University of California Press, Berkeley, California.

Fortier, Y.O. and Morley, L.W. 1956. Geological unity of the Arctic Islands. Royal Society of Canada Transactions, **50**, 3-12.

Frakes, L.A. 1979. Climates throughout geologic time. Elsevier, Amsterdam.

Frakes, L.A., and Francis, J.E. 1988. A guide to Phanerozoic cold polar climates from high-latitude ice-rafting in the Cretaceous. Nature, **333**, 9: 547-549.

Frakes, L.A., Francis, J.E., and Syktus, J.I. 1992. Climate modes of the Phanerozoic; the history of the Earth's climate over the past 600 million years. Cambridge University Press, Cambridge.

Friedlander, G., Kennedy, J.W., Macias, S.M., and Miller, J.M. 1981. Nuclear and Radiochemistry, J. Wiley and Sons, New York.

Galbraith, R.F. 1990. The radial plot: graphical assessment of spread in ages. Nuclear Tracks and Radiation Measurements, **17**, 3: 207-214.

Galbraith, R.F., and Laslett, G.M. 1993. Statistical models for mixed fission track ages. Nuclear Tracks and Radiation Measurements, **21**: 459-470.

Gallagher, K. 1995. Evolving temperature histories from apatite fission-track data. Earth and Planetary Science Letters, **136**, 421-435.

Gallagher, K., and Brown, R.W. 1997. The onshore record of passive margin evolution. Journal of the Geological Society, London, **154**: 451-457.

Gallagher, K., Hawkesworth, C. and Montovani, M. 1994. The denudation history of the onshore continental margin of S.E. Brazil inferred from fission track data. Journal of Geophysical Research, **99**, 18117-18145.

Gallagher, K., Hawkesworth, C. and Montovani, M. 1995. Denudation, fission track analysis and the long-term evolution of passive margin topography: application to the S.E. Brazilian margin. Journal of South American Earth Sciences, **8**, 65-77.

Gallagher, K., Brown, R.W., and Johnson, C. 1998. Fission track analysis and its applications to geological problems. Annual Review of Planetary Science Letters. **26**: 519-572.

Gentzis, T. and Goodarzi, F. 1991. Thermal maturity and hydrocarbon potential of the sedimentary succession from the Hecla field in Sverdrup Basin, Arctic Canada. International Journal of Coal Geology, **19**, 483-517.

Gentzis, T. and Goodarzi, F. 1992a. The source-rock potential and thermal maturity of the sedimentary succession in the Drake and Hecla hydrocarbon fields, Melville Island,

Canadian Arctic Archipelago. In; Arctic Geology and Petroleum Potential. Edited by T.O. Vorren, E. Bergsager, E. Dahl-Stamnes, E. Holter, B. Johansen, E. Lie and T.B. Lund, Norwegian Petroleum Society, Special Publication **2**, pp. 159-171.

Gentzis, T. and Goodarzi, F. 1992b. Thermal maturity and source-rock potential in northwestern Melville Island, Arctic Canada. Energy Sources, **14**, 423-442.

Gentzis, T. and Goodarzi, F. 1993. Regional thermal maturity in the Franklinian Mobile Belt, Melville Island, Arctic Canada. Marine and Petroleum Geology, **10**, 215-230.

Gentzis, T., De Freitas, T.,Goodarzi, F., Melchin, M. and Lenz, A. 1996. Thermal maturity of Lower Paleozoic sedimentary successions in Arctic Canada. Bulletin of the American Association of Petroleum Geologists, **80**, 1065-1084.

Gibling, M.R. 1995. Upper Paleozoic rocks, Nova Scotia. In; Geology of the Appalachian-Caledonian Orogen in Canada and Greenland. Edited by H. Williams. Geological Survey of Canada, Geology of Canada, no. 6, pp. 493-523.

Gibling, M.R., Langenburg, W., Kalkrueth, W.D., Waldron, J.W.F., Courtney, R., Paul, J., and Grist, A.M. 2002. Deformation of Upper Carboniferous coal measures in the Sydney Basin: evidence for late Alleghanian tectonism in Atlantic Canada. Canadian Journal of Earth Sciences, **39**: 79-93.

Gilchrist, A.R., Kooi, H. and Beaumont, C. 1994. Post-Gondwana geomorphic evolution of south-western Africa: implications for the controls on landscape development from observations and numerical experiments. Journal of Geophysical Research, **99**, 12211-12228.

Gleadow, A.J.W., and Brown, R.W. 2000. Fission-track thermochronology and the long-term denudational response to tectonics. In; Geomorphology and Global Tectonics. Edited by M.A. Summerfield. J. Wiley and Sons, New York, pp. 57-75.

Gleadow, A.J.W., Duddy, I.R., Green, P.F. and Lovering, J.F. 1986. Confined fission track lengths in apatite -a diagnostic tool for thermal history analysis. Contributions in Mineralogy and Petrology. **94**, 405-415.

Gleadow, A.J.W., Duddy, I.R. and Lovering, J.F. 1983. Fission track analysis: A new tool for the evaluation of thermal histories and hydrocarbon potential. Australian

Petroleum Exploration Journal, **23**:1, 93-102.

Goldthwait, J.W. 1924. Physiography of Nova Scotia. Geological Survey of Canada, Memoir 140.

Green, P.F. 1985. A comparison of zeta calibration baselines in zircon, sphene and apatite. Chemical Geology (Isotope Geoscience Section), **58**, 1-22.

Green, P.F. 1986. On the thermo-tectonic evolution of Northern England: Evidence from fission track analysis. Geology Magazine, **123**, 493-506.

Green, P.F. 1988. The relationship between track shortening and fission track age reduction in apatite: combined influences of inherent instability, annealing anisotropy, length bias and system calibration. Earth and Planetary Science Letters, **89**, 335-352.

Green, P.F. 1996. The importance of compositional influence on fission track annealing in apatite. In; International Workshop on Fission Track Dating. Gent, Belgium, 1996, Abstracts, p. 43.

Green, P.F. 1996. The importance of validating annealing models. In; 10th International Conference on Fission Track Dating and Thermochronology, Amsterdam, The Netherlands, August 9-13, 2004, Abstracts, p. 53.

Green, P.F., Duddy, I.R. and Bray, R.J. 1995. Applications of thermal history reconstruction in inverted basins. In; Basin Inversion, Edited by J.G. Buchanan and P.G. Buchanan, Geological Society Special Publishers, **88**, 149-165.

Green, P.F., Duddy, I.R., Gleadow, A.J.W. and Lovering, J.F. 1989. Apatite fission-track analysis as a paleotemperature indicator for hydrocarbon exploration. In; Thermal history of sedimentary basins, Edited by N.D. Naeser and T.H. McCulloh, Springer-Verlag, New York, pp.181-195.

Green, P.F., Duddy, I.R., Gleadow, A.J.W., Tingate, P.R., and Laslett, G.M. 1985. Fission-track annealing in apatite: Track length measurements and the form of the Arrhenius plot. Nuclear Tracks **10**: 323-328.

Green, P.F., Duddy, I.R., Gleadow, A.J.W., Tingate, P.R., and Laslett, G.M. 1986. Thermal annealing of fission tracks in apatite 1. A qualitative description: Chemical Geology, **59**: 237-253.

Green, P.F., Duddy, I.R., Laslett, G.M., Hegarty, K.A., Gleadow, A.J.W., and Lovering, J.F. 1989. Thermal annealing of fission tracks in apatite 4. Quantitative modelling techniques and extension to geological timescales Chemical Geology (Isotope Geoscience Section), **79**:155-182.

Greenough, J.D. 1995. Mesozoic rocks. In; Geology of the Appalachian-Caledonian Orogen in Canada and Greenland. Edited by H.Williams. Geological Survey of Canada, Geology of Canada, no. 6, pp. 567-600.

Grist, A.M. 1986. Low temperature geochronology of the South Mountain Batholith, Nova Scotia, using 40Ar/39Ar and fission track dating techniques, unpublished B.Sc. Thesis, Dalhousie University, Halifax Nova Scotia, 74p.

Grist, A.M. and Ravenhurst, C.E. 1992. Mineral separation techniques used at Dalhousie University, Appendix 2 in; Mineralogical Association of Canada, short course handbook on low temperature thermochronology. Edited by M. Zentilli and P.H. Reynolds, 203-209.

Grist, A.M. and Zentilli, M. 2003. Post-Paleocene cooling in the southern Canadian Atlantic region: evidence from apatite fission track models, Canadian Journal of Earth Sciences, **40**, no. 9, 1279-1297.

Grist, A.M. and Zentilli, M. 2004 (submitted). The Thermal History of the Nares Strait, Kane Basin Region in Canada and Greenland: Insights from Apatite Fission Tracks. Geologishes Jahrbuch

Grist, A.M. and Zentilli, M. 2004a.(in prep.) Insights on the Thermal History of the Nares Strait, Kane Basin Region in Canada and Greenland from Apatite Fission Track and (U-Th)/He dating, Canadian Journal of Earth Sciences.

Grist, A.M. and Zentilli, M. 2004b.(in prep.) Apatite fission track and (U-Th)/He thermal history modelling of the Nares Strait, Kane Basin, Smith Sound region in Canada and Greenland, Canadian Journal of Earth Sciences.

Grist, A.M., Reynolds, P.H., Zentilli, M., and Beaumont, C. 1992. The Scotian Basin offshore Nova Scotia: thermal history and provenance of sandstones, from apatite fission track analysis 40Ar/39Ar data. Canadian Journal of Earth Sciences, **29**: 909-

924.

Grist, A.M., Ryan, R.J., and Zentilli, M. 1995. The thermal evolution and timing of hydrocarbon generation in the Maritimes Basin of eastern Canada: Evidence from apatite fission track data. Bulletin of Canadian Petroleum Geology, **43**, 2: 145-155.

Gunnell, Y., Gallagher, K., Carter, A., Widdowson, M., and Hurford, A.J. 2003. Denudation history of the continental margin of western peninsular India since the early Mesozoic - reconciling apatite fission track data with geomorphology, Earth and Planetary Science Letters, **215**, 187-201.

Hacquebard, P.A. 1984. Composition, rank and depth of burial of two Nova Scotia lignite deposits. In; Current Research, part A. Geological Survey of Canada, Paper 84-1A, pp. 11-15.

Hacquebard, P.A., and Donaldson, J.R. 1970. Coal metamorphism and hydrocarbon potential in the Upper Paleozoic of the Atlantic Provinces, Canada. Canadian Journal of Earth Sciences, **7**: 1139-1158.

Haq, B.U., Hardenbol, J., and Vail, P.R. 1987. Chronology of fluctuating sea levels since the Triassic. Science, **235**: 1156-1166.

Harrison, J.C. (2004, In prep.) Geological map of the Nares Strait region, explanatory notes. Geologishes Jahrbuch.

Harrison, J.C., Mayr, U., McNeil, D.H., Sweet, A.R., McIntyre, D.J., Eberle, J.J., Harrington, C.R., Chalmers, J.A., Dam. G., and Nøhr-Hansen, H. 1999. Correlation of Cenozoic sequences of the Canadian Arctic region and Greenland: implication for the tectonic history of northern North America. Bulletin of Canadian Petroleum Geology, **47**, 3: 223-254.

Harrison, T.M., Armstrong, R.L., Naeser, C.W., and Herakal, J.E.1979. Geochronology and thermal history of the Coast Plutonic Complex, near Prince Rupert, British Columbia. Canadian Journal of Earth Sciences, **16**, 400-410.

Hayatsu, A. 1979. K-Ar isochron age of the North Mountain Basalt, Nova Scotia. Canadian Journal of Earth Sciences, **16**: 973-975.

Heaman, l., LeCheminant, A.N. and Rainbird, R.H. 1992. Nature and timing of Franklin

igneous events, Canada: Implications for a Late Proterozoic mantle plume and the break-up of Laurentia. Earth and Planetary Science Letters, **109**, 117-131.

Hegarty, K.A., Weissel, J.K. and Mutter, J.C. 1988. Subsidence history of Australia's: Constraints on basin models. Australian Association of Petroleum Geologists Bulletin, **72**, 615-633.

Henao-Londoño, D. 1977. A preliminary geochemical evaluation of the Arctic Islands. Bulletin of Canadian Petroleum Geology, **25**, 1059-1084.

Hodych, J.P., and Dunning, G.R. 1992. Did the Manicouagan impact crater trigger end-of-Triassic mass extinction? Geology, **20**: 51-54.

Hodych, J.P., and Hayatsu, A. 1988. Paleomagnetism and K-Ar isochron dates of Early Jurassic basaltic flows and dikes of Atlantic Canada. Canadian Journal of Earth Sciences, **25**: 1972-1988.

House, M.A., Wernicke. B.P., Farley, K.A., and Dumitru, T. 1997. Cenozoic thermal evolution of the central Sierra Nevada from apatite (U-Th)/He ages. Nature, **396**, 66-69.

House, M.A., Farley, K.A. and Stockli, D. 2000. Helium chronometry of apatite and titanite using Nd-YAG laser heating. Earth and Planetary Science Letters, **183**, 365-368.

Hubert, J.F., and Mertz, K.A. 1984. Eolian sandstones in Upper Triassic-Lower Jurassic red beds of the Fundy Basin, Nova Scotia. Journal of Sedimentary Petrology, **54**: 798-810.

Hunzicker, J.C., Desmons, J. And Hurford, A.J. 1992. Thirty-two years of geochronological work in the Central and Western Alps: a review on seven maps. Mémoires de Géologie (Lausanne), **13**, 59 pp.

Hurford, A.J. 1986a. Cooling and uplift patterns in the Lepontine Alps, south central Switzerland, and an age of vertical movement on the Insubric fault line. Contributions in Mineralogy and Petrology, **92**, 413-427.

Hurford, A.J. 1986b. Application of the fission track dating method to young sediments: Principles, methodology and exampless. In: Dating Young Sediments. Edited by A.J. Hurford, E. Jäger and J.A.M. Ten Cate. Proceedings of the workshop Beijing,

People's Republic of China, September, 1985, 199-233.

Hurford, A.J. 1990. Standardization of fission track dating calibration: recommendation by the Fission track Working Group of the I.U.G.S. Subcommission on Geochronology. Chemical Geology (Isotope Geoscience Section), **80**, 171-178.

Hurford, A.J. and Carter, A. 1991. The role of fission-track dating in the discrimination of provenance. Geological Society Special Publication, **57**, 67-78.

Hurford, A.J., and Green, P.F. 1982. A users' guide to fission track dating calibration. Earth and Planetary Science Letters, **59**: 343-354.

Hurford, A.J., and Green, P.F. 1983. The zeta age calibration of fission track dating. Chemical Geology (Isotope Geoscience Section), **1**: 285-317.

Issler, D.I. 1996a. An inverse model for extracting thermal histories from apatite fission track data: Instructions and software for the Windows95 environment. Geological Survey of Canada, Open File Report, 2325.

Issler, D.R. 1996b. Optimizing time step size for apatite fission track annealing models. Computers and Geosciences, **22**, no.1, 67-74.

Issler, D.R., McQueen, H. and Beaumont, C. 1989. Thermal and isostatic consequences of simple shear extension of the continental lithosphere. Earth and Planetary Science Letters, **91**, 341-358.

Jarvis, G.T. and McKenzie, D.P. 1980. Sedimentary basin formation with finite extension rates. Earth and Planetary Science Letters, **48**, 42-52.

Jones, F.W., Majorowicz, J.A. and Embry, A.F. 1989. A heat flow profile across the Sverdrup Basin, Canadian Arctic Islands. Geophysics, **54**, 171-180.

Keen, C.E. and Beaumont, C. 1990. Geodynamics of rifted continental margins. Chapter 9 in; Geology of the Continental Margin of Eastern Canada. Edited by M.J. Keen and H. Williams. Geological Survey of Canada, Geology of Canada **2**, 393-472.

Keen, M.J., and Williams, H. (Editors) 1990. Geology of the Continental Margin of Eastern Canada. Geological Survey of Canada, Geology of Canada, no. 2.

Kerr, J.W. 1967. Nares submarine rift valley and the relative rotation of north Greenland: Bulletin of Canadian Petroleum Geology, **15**, 483-520.

Ketcham, R.A., Donelick, R.A., and Carlson, W.D. 1999. Variability of apatite fission-track annealing kinetics: III. Extrapolation to geologic time scales. American Mineralogist, **84**, 1235-1255.

Kooi, H. and Beaumont, C. 1994. Escarpment evolution on high-elevation rifted margins: insights derived from a surface process model that combines diffusion, advection and reactivation. Journal of Geophysical Research, **99**, 12191-12209.

Kooi, H. and Beaumont, C. 1996. Large-scale geomorphology: Classical concepts reconciled and integrated with contemporary ideas via a surface process model. Journal of Geophysical Research, **101**, 3361-3386.

Kristoffersen, Y. 1990. Eurasia Basin; In: The Arctic Ocean Region. Edited by A. Grantz, L. Johnson, and F.J. Sweeney, Geological Society of America, The Geology of North America, **L**, 365-378.

Laslett, G.M., Green, P.F., Duddy, I.R., and Gleadow, A.J.W. 1987. Thermal annealing of fission tracks in apatite: 2. A quantitative analysis. Chemical Geology (Isotope Geoscience Section), **65**: 1-13.

Lederer, M., Hollander, J.M. and Perlmann, I. 1967. Table of Isotopes. J. Wiley and Sons, New York.

Leith, T.L., Weiss, H.M., Mork, A., Arhus, N., Elvebakk, G., Embry, A.F., Brooks, P.W., Stewart, K.R., Pchelina, T.M., Bro, E.G., Verba, M.L., Danyushevskaya, A. and , Borisov, A.V. 1992. Mesozoic hydrocarbon source-rocks of the Arctic region. In: Arctic Geology and Petroleum Potential. Edited by T.O. Vorren, E. Bergsager, E. Dahl-Stamnes, E. Holter, B. Johansen, E. Lie and T.B. Lund, Norwegian Petroleum Society, Special Publication **2**, pp. 1-25.

Li, G., Ravenhurst, C.E., and Zentilli, M. 1995. Implications of apatite fission track analysis for the thermal history of the Scotian Basin, offshore Nova Scotia, Canada. Bulletin of Canadian Petroleum Geology, **43**: 127-144.

Lippolt, H.J., Leitz, M., Wernicke, R.S. and Hagedorn, B. 1994. (Uranium + thorium)/helium dating of apatite: experience with samples from different geochemical environments. Chemical Geology (Isotope Geoscience Section), **112**,

179-191.

Lister, G.A., Etheridge, M.A. and Symonds, P.A. 1986. Detachment faulting and the evolution of passive continental margins. Geology. **14**: 246-250.

Lister, G.A., Etheridge, M.A. and Symonds, P.A. 1991. Detachment models for the formation of passive continental margins. Tectonics, **10**, 1038-1064.

Lockhart, A.W. 1984. Sussex silica and aggregate; New Brunswick Department of Natural Resources and Energy, Assessment File No. 473023.

Lonergan, L. and Johnson, C. 1998. Reconstructing orogenic exhumation histories using synorogenic detrital zircons and apatites: an example from the Betic Cordillera, SE Spain. Basin Research, **10**, no. 3, 353-364.

Mathews, W.H. 1975. Cenozoic erosion and erosional surfaces of eastern North America. American Journal of Science, **275**, 818-824.

McHone, J.G., and Butler, J.R. 1984. Mesozoic igneous provinces of New England and the opening of the North Atlantic Ocean. Geological Society of America Bulletin, **95**: 757-765.

McHone, J.G., Ross, M.E., and Greenough, J.D. 1987. Mesozoic dyke swarms of Eastern North America; In; Mafic Dyke Swarms. Edited by H.C. Halls and W.F. Fahrig. Geological Association of Canada, Special Paper 34, pp. 279-288.

McKenzie, D. 1978. Some remarks on the development of sedimentary basins. Earth and Planetary Science Letters, **40**, 25-32.

Menzies, M.A., Gallagher, K., Hurford, A.J., and Yelland, A. 1997. Red Sea and Gulf of Aden rifted margins, Yemen: denudational histories and margin evolution. Geochemica et Cosmochemica, Acta, **61**, 2511-2527.

Miall, A.D. 1986. The Eureka Sound Group (Upper-Cretaceous-Oligocene), Canadian Arctic Islands. Bulletin of Canadian Petroleum Geology. **34**: 240-270.

Miall, A.D. 1991. Late Cretaceous and Tertiary basin development and sedimentation, Arctic islands. In; Geology of the Innuitian Orogen and Arctic Platform of Canada and Greenland. Edited by H.P. Trettin. Geological Survey of Canada, Geology of Canada **3**, pp. 467-458.

Miller, K.G., Mountain, G.S., Browning, J.V., Kominz, M., Sugarman, P.J., Christie-Blick, N., Katz, M.E., and Wright, J.D. 1998. Cenozoic global sea level, sequences, and the New Jersey transect: Results from coastal plain and continental slope drilling. Reviews of Geophysics, **36**, 4: 569-601.

Moore, R.G., Ferguson, S.A., Boehner, R.C., and Kennedy, C.M. 2000. Preliminary map of the Wolfville/Windsor Area, Kings and Hants Counties, Nova Scotia (21H/01 and Parts of 21A/16C and D). Scale 1:50,000.

Moore, M.E., Gleadow, A.J.W. and Lovering, J.F. 1986. Thermal evolution of rifted continental margins: new evidence from fission tracks in basement apatites from southeastern Australia. Earth and Planetary Science Letters, **78**, 255-270.

Nadon, G.C., and Middleton, G.V. 1985. The stratigraphy and sedimentology of the Fundy Group (Triassic) of the St. Martins area, New Brunswick. Canadian Journal of Earth Sciences, **22**: 1183-1203.

Naeser, C.W. 1976. Fission-track dating. U.S. Geological Survey Open-File Report 76-190, 65 pp.

Naeser, N.D., Naeser, C.W. and McCulloh. 1989. The application of fission-track dating to the depositional and thermal history of rocks in sedimentary basins. In; Thermal history of sedimentary basins, Edited by N.D. Naeser and T.H. McCulloh, Springer-Verlag, New York, pp.157-180.

Oakey 1994. A structural fabric defined by topographic lineaments: Correlation with Tertiary deformation of Ellesmere and Axel Heiberg Islands, Canadian Arctic. Journal of Geophysical Research, B, **99**, 20,311-20,321.

Oakey, G.N., Hearty, B., Forsberg, R., and Jackson, H.R. 2000. Gravity anomaly of the Innuitian region, Canadian and Greenland Arctic. Geological Survey of Canada Open File 3934d, scale 1:1,500,000.

Okulitch, A.V. 1988. 1: 2,000,000 Geology of the Canadian Arctic Archipelago, Northwest Territories and North Greenland. In: Geology of the Innuitian Orogen and Arctic Platform of Canada and Greenland. Edited by H.P. Trettin. Geological Survey of Canada, Geology of Canada **3**.

Okulitch, A.V. 1999. Geologic time scale. Geological Society of Canada, Open File 3040 (National Earth Science Series, Geological Atlas) - Revised.

Okulitch, A.V. and Trettin, H.P. 1991. Late Cretaceous - Early Tertiary deformation, Arctic Islands, In; Geology of the Innuitian Orogen and Arctic Platform of Canada and Greenland. Edited by H.P. Trettin. Geological Survey of Canada, Geology of Canada **3**, 469-489.

Okulitch, A.V., Dawes, P.R., Higgins, A.K., Soper, N.J., and Christie, R.L. 1990. Towards a Nares Strait solution: Structural studies on southeastern Ellesmere Island and northwestern Greenland. Marine Geology, **93**, 369-384.

Ollier, C.D. 1985. Morphotectonics of continental margins with great escarpments, In; Tectonic Geomorphology; Edited by: M. Morisawa and J.T. Hack, Allen and Unwin, Boston, pp. 3-25.

Olsen, P.E. and Schlishe, R.W. 1990. Transtensional arm of the early Mesozoic Fundy rift basin: Penecontemporaneous faulting and sedimentation. Geology, **18**, 695-698.

Olsen, P.E., Shubin, N.H., and Anders, M.H. 1987. New Early Jurassic tetrapod assemblages constrain Triassic-Jurassic tetrapod extinction event. Science, **237**: 1025-1029.

Omar, G.I., Steckler, M.S., Buck, W.R., and Kohn, B.P. 1989. Fission-track analysis of basement apatites at the western margin of the Gulf of Suez rift, Egypt: evidence for synchroneity of uplift and subsidence. Earth and Planetary Science Letters, 94, 316-328.

O'Sullivan, P.B., and Brown, R.W. 1998. Effects of surface cooling on apatite fission-track data: evidence for Miocene climatic change, North Slope, Alaska. In; Advances in Fission Track Geochronology. Edited by P. Van den Haute and F. De Corte. Kluwer, Dordrecht, pp. 255-267.

O'Sullivan, P.O. and Parrish, R.R. 1995. The importance of apatite composition and single-grain ages when interpreting fission track data from plutonic rocks: a case study from the Coast Ranges, British Columbia. Earth and Planetary Science Letters, **132**, 213-224.

Parrish, R.R. 1983. Cenozoic thermal evolution and tectonics of the Coast Mountains of

British Columbia 1, fission-track dating, apparent uplift rates, and patterns of uplift, Tectonics, **2**, 601-632.

Pazzaglia, F.J. and Brandon, M.T. 1996. Macrogeomorphic evolution of the post-Triassic Appalachian mountains determined by deconvolution of the offshore basin sedimentary record. Basin Research, **8**, 255-278.

Pazzaglia, F.J. and Gardner, T.W. 1994. Late Cenozoic flexural deformation of the middle U.S. Atlantic passive margin. Journal of Geophysical research, **99**, B6, 12,143-12,167.

Pazzaglia, F.J. and Gardner, T.W. 2000. Late Cenozoic landscape evolution of the U.S. Atlantic passive margin: insights into a North American Great Escarpment. In; Geomorphology and Global Tectonics. Edited by M.A. Summerfield, Wiley and Sons, New York, pp. 283-302.

Pelletier, B.R. 1966. Development of submarine physiography in the Canadian Arctic and its relation to crustal movements; in Continental Drift, G.D., Garland (ed.) The Royal Society of Canada, Special Publication no. 9, 77-101.

Piepjohn, K., Tessensohn, F., Harrison, C., and Mayr, U. 2000. Involvement of a Tertiary foreland basin in the Eurekan foldbelt deformation, NW coast of Kane Basin, Ellesmere Island, Canada. Polarforschung **68**: 101-110.

Poag, C.W. 1992. U.S. middle Atlantic continental rise: Provenance, dispersal, and deposition of Jurassic to Quaternary sediments. In; Geologic Evolution of Atlantic Continental Rises. Edited by C.W. Poag and P.C. de Graciansky. Van Nostrand Reinhold, New York, pp. 217-263.

Poag, C.W., and Sevon, W.D. 1989. A record of Appalachian denudation in postrift Mesozoic and Cenozoic sedimentary deposits of the U.S. middle Atlantic continental margin. Geomorphology, **2**: 119-157.

Powell, T.G. 1978. An assessment of the hydrocarbon potential of the Canadian Arctic Islands. Geological Survey of Canada, Paper 78-12.

Price, B.P. and Walker, R.M. 1962. Chemical etching of charged-particle tracks in solids. Journal of Applied Physics, **33**, 3407-3412.

Price, B.P. and Walker, R.M. 1963. Fossil tracks of charged particles and the age of minerals. Journal of Geophysical Research, **68**, 4847-4862.

Ravenhurst, C.E., Donelick, R., Zentilli, M., Reynolds, P., and Beaumont, C. 1990. A fission track pilot study of the thermal effects of rifting on the onshore Nova Scotian margin, Canada. Nuclear Tracks and Radiation Measurement, **17**, 3: 373-378.

Ravenhurst, C.E., Roden-Tice, M.K. and Miller, D.S. 2003. Thermal annealing of fission tracks in fluorapatite, chlorapatite, manganoapatite, and Durango apatite: experimental results. Canadian Journal of Earth Sciences, **40**, 995-1007.

Reiners, P.W. and Farley, K.A. 1999. Helium diffusion and (U-Th)/He thermochronometry of titanite. Geochimica et Cosmochimica Acta, **63**, 3485-3859.

Reiners, P.W. and Farley, K.A. 2001. Influence of crystal size on apatite (U-Th)/He thermochronology: an example from the Bighorn Mountains, Wyoming. Earth and Planetary Science Letters, **188**, 413-420.

Reiners, P.W., Farley, K.A., and Hickes, H.J. 2002. He diffusion and (U-Th)/He thermochronometry of zircon: Initial results from Fish Canyon Tuff and Golde Butte: Tectonophysics, **349**, 297-308.

Reiners, P.W., Spell, T.L., Nicolescu, S., and Zanetti, K. 2003. Zircon (U-Th)/He thermochronometry: He diffusion and comparisons with $^{40}Ar/^{39}Ar$ dating. Geochimica et Cosmochimica Acta, **68**, 1857-1887.

Renne, P.R., Deino, A.L., Walter, R.C., Turrin, B.D., Swisher, C.C., Becker, T.A., Curtis, G.H., Sharp, W.D. and Jaouni, A.-R. 1994 Intercalibration of astronomical and radioisotopic time. Geology, **22**, 783-786.

Reynolds, P.H.R., Zentilli, M., and Muecke, G.K. 1981. K-Ar and $^{40}Ar/^{39}Ar$ geochronology of granitoid rocks from southern Nova Scotia: Its bearing on the geological evolution of the Meguma Zone of the Appalachians. Canadian Journal of Earth Sciences, **18**: 386-394.

Ricketts, B.D. 1994. Basin analysis, Eureka Sound Group, Axel Heiberg and Ellesmere Islands, Canadian Arctic Archipelago. Geological Survey of Canada, Memoir 439.

Ricketts, B.D. and Stephenson, R.A. 1994. The demise of the Sverdrup Basin: Late

Cretaceous-Paleocene sequence stratigraphy and forward modelling. Journal of Sedimentary Research, B, **64**, 516-530.

Riisager, J., Riisager, P. and Pederson, A.K. 2003. Paleomagnetism of large igneous provinces: case-study from West Greenland, North Atlantic igneous province. Earth and Planetary Science Letters, **214**, 409-425.

Roberts, J.H., Gold, R. And Armani, R.J. 1968. Spontaneous fission decay-constant of 238U. Physical Reviews, **174**, 1482-1484.

Roden, M. K. 1991. Apatite fission-track thermochronology of the southern Appalachian basin: Maryland, West Virginia, and Virginia. Journal of Geology, **99**: 41-53.

Roest, W.R. and Srivastrava, S.P. 1989. Sea-floor spreading in the Labrador Sea: a new reconstruction. Geology, **17**, 1000-1003.

Rohrman, M.H.E.J. 1995. Thermal evolution of the Fennoscandian region from fission track thermochronology: an integrated approach. Ph.D. thesis, Proefschrift Vrije Universiteit Amsterdam, The Netherlands, 168 p.

Royden, L. and Keen, C.E. 1980. Rifting process and thermal evolution of the continental margin of eastern Canada determined from subsidence curves. Earth and Planetary Science Letters, **51**, 343-361.

Rutherford, E. 1905. Present problems in radioactivity. Popular Science Monthly, May, 1-34.

Ryan, R.J. and Zentilli, M. 1993. Allocyclic and thermochronological constraints on the evolution of the Maritimes Basin of eastern Canada, Atlantic Geology, **29**: 187-197.

Sanford, B.V. and Grant, A.C. 1990. Bedrock geological mapping and basin studies in the Gulf of St. Lawrence; In; Current Research, Part B; Geological Survey of Canada, Paper 90-1B, pp. 33-42.

Schenk, P.E. 1995a. Meguma Zone. In; Geology of the Appalachian-Caledonian Orogen in Canada and Greenland. Edited by H.Williams. Geological Survey of Canada, Geology of Canada, no. 6, pp. 261-277.

Schenk, P.E. 1995b. Annapolis Belt. In; Geology of the Appalachian-Caledonian Orogen in Canada and Greenland. Edited by H.Williams. Geological Survey of Canada, Geology of Canada, no. 6, pp. 367-383.

Shuster, D.L. and Farley, K.A. 2003. $^{4}He/^{3}He$ thermochronometry. Earth and Planetary Science Letters, **217**, 1-17.

Silk, E.C.H. and Barnes, R.S. 1959. Examination of fossil fission fragment tracks with an electron microscope. Philosophical Magazine, **4**, 970-972.

Spotila, J.A., Farley, K.A., Yule, J.D., and Reiners, P.W. 2001. Near-field convergence along the San Andreas fault zone in southern California, based on exhumation constrained by (U-Th)/He dating. Journal of Geophysical Research, **106**, 26731-26746.

Srivastava, S.P. 1978. Evolution of the Labrador Sea and its bearing on the early evolution of the North Atlantic. Geophysical Journal of the Royal Astronomical Society, **52**, 313-357.

Srivastava, S.P. 1985. Evolution of the Eurasian Basin and its implications to the motion of Greenland along Nares Strait, Tectonophysics, **114**, 29-53.

Stea, R. R., Finck, P. W., and Fensome, R. A. 1997. Lithostratigraphy of Early Cretaceous and Quaternary unconsolidated sediments in the Musquodoboit and Shubenacadie Valleys, Nova Scotia, Canada. In; Nova Scotia Department of Natural Resources, Mineral Resources Division. Report of Activities, 1996, Report 97-1, pp. 163-173.

Steiger, R.H. and Jäger, E. 1977. Subcommission on geochronology: convention on the use of dacay constants in geo- and cosmochronology. Earth and Planetary Science Letters, 36, 359-362.

Stephenson, R.A., Boerstoel, J., Embry, A.F. and Ricketts, B.D. 1994. Subsidence analysis and tectonic modelling of the Sverdrup Basin. In; Proceedings of the 1992 International Conference on Arctic Margins, Edited by D.K. Thurston and K. Fujita, pp. 149-154. U.S. Department of the Interior, Minerals Management Service, MMS 94-0040.

Stockli, D.F., Farley, K.A. and Dumitru. T.A. 2000. Calibration of the apatite (U-Th)/He thermochronometer on an exhumed fault block, White Mountains, California. Geology, **28**, no. 11, 983-986.

Story, M, Duncan, R.A., Pederson, A.K., Larsen, L.M., and Larsen, H.C. 1998. 40Ar/39Ar

geochronology of the West Greenland Tertiary volcanic province, Earth and Planetary Science Letters, **160**, 569-586.

Strutt, R.J. 1905. On the radioactive minerals. Proceedings of the Royal Society, **A76**, 88-101.

Sweeney, J.F., Weber, R.R. and Blasco, S.M. 1982. Continental ridges in the Arctic Ocean: LOREX constraints. Tectonophysics, **89**, 217-238.

Tessensohn, F., and Piepjohn, K. 2000. Eocene compressive deformation in Arctic Canada, North Greenland and Svalbard and its plate tectonc causes. Polarforschung **68**: 121-124.

Thorsteinsson, R. 1972a. 1:250,000 Geology of Eureka Sound, District of Franklin. Geological Survey of Canada Map 1300A.

Thorsteinsson, R. 1972b. 1:250,000 Geology of Cañon Fiord, District of Franklin. Geological Survey of Canada Map 1308A.

Thorsteinsson, R. and Tozer, E.T. 1970. Geology of the Arctic Archipelago. In; Geology and Economic Minerals of Canada. Edited by R.J.W. Douglas. Geological Survey of Canada Economic Geology Report no. 1, 547-590.

Trettin, H.P. 1991a. Tectonic Framework. In; Geology of the Innuitian Orogen and Arctic Platform of Canada and Greenland. Edited by H.P. Trettin. Geological Survey of Canada, Geology of Canada **3**, pp. 59-66.

Trettin, H.P. 1991b (Editor). Geology of the Innuitian Orogen and Arctic Platform of Canada and Greenland. Geological Survey of Canada, Geology of Canada **3**.

Trettin, H.P. 1991c. Late Silurian-early Devonian deformation, metamorphism, and granitic plutonism, Northern Ellesmere and Axel Heiberg Islands. In; Geology of the Innuitian Orogen and Arctic Platform of Canada and Greenland. Edited by H.P. Trettin. Geological Survey of Canada, Geology of Canada **3**, pp. 293-341.

Troelson, J.C. 1950. Contributions to the geology of north-west Greenland, Ellesmere Island and Axel Heiberg Island. Meddelelser om Grønland, **149**, no. 7, 85 p.

Tucker, G.E. and Sillingerland, R.L. 1994. Erosional dynamics, flexural isostasy, and long-lived escarpments: a numerical modeling study. Journal of Geophysical Research, **99**,

12229-12243.

Utting, J., Goodarzi, F ., Dougherty, B.J. and Henderson, C.M. 1989. Thermal maturity of Carboniferous and Permian rocks of the Sverdrup Basin, Canadian Arctic Archipelago. Geological Survey of Canada, Paper 89-19.

Valdes, P.J., Sellwood, B.W., and Price, G.D. 1996. Evaluating concepts of Cretaceous equability. Palaeoclimates, **2**: 139-158.

van de Poll, H.W. 1995. Upper Paleozoic rocks: New Brunswick, Prince Edward Island, and Iles de la Madeleine. In; Geology of the Appalachian-Caledonian Orogen in Canada and Greenland. Edited by H.Williams. Geological Survey of Canada, Geology of Canada, no. 6, pp. 455-492.

van der Beek, P.A. 1995. Tectonic evolution of continental rifts: inferences from numerical modelling and fission track thermochronology. Ph.D. thesis, Proefschrift Vrije Universiteit Amsterdam, The Netherlands, 232 p.

van der Beek, P.A., Summerfield, M.A., Braun, J., Brown, R.W., and Fleming, A. 2002. Modeling postbreakup landscape development and denudational history across the southeast African (Drakensberg Escarpment) margin. Journal of Geophysical Research, **107**, b12, 2351, doi:10.1029/2001JB000744.

von Gunten, H.R. 1969. Distribution of mass in spontaneous and neutron-induced fission, Actinides Reviews, **1**, 275-298.

Vrolijk, P., Donelick, R.A., Queng, J., and Cloos, M. 1992. Testing models of fission track annealing in apatite in a simple thermal setting: site 800, leg 129. In; Proceedings of the Ocean Drilling Program, Scientific Results, Edited by R.L. Larson and Y. Lancelot, **129**: pp. 169-176.

Wade, J.A., and McLean, B.C. 1990. The geology of the southeastern margin of Canada. In; Geology of the Continental Margin of Eastern Canada. Edited by M.J. Keen and G.L. Williams. Geological Survey of Canada, Geology of Canada, no. 2, pp. 167-238.

Wade, J.A., Brown, D.E., Traverse, A., and Fensome, R.A. 1996. The Triassic-Jurassic Fundy Basin, eastern Canada. Atlantic Geology, **32**: 189-231.

Wagner, G.A., and Van den Haute, P. 1992. Fission track dating. Kluwer Academic

Publishers, Dordrecht.

Wark, J.M., and Clarke, D.B. 1980. Geochemical discriminators and the palaeotectonic environment of the North Mountain basalt, Nova Scotia. Canadian Journal of Earth Sciences, **17**: 1740-1745.

Waylett, D.C. and Embry, A.F. 1992. Hydrocarbon loss from oil and gas fields of the Sverdrup Basin, Canadian Arctic Islands. In; Arctic Geology and Petroleum Potential. Edited by T.O. Vorren, E. Bergsager, E. Dahl-Stamnes, E. Holter, B. Johansen, E. Lie and T.B. Lund, Norwegian Petroleum Society, Special Publication **2**, pp.195-204.

Wegener, A.L. 1929. Die Enstehung der Kontinente und Ozeane, Friedich Vieweg & Sohn, Braunschweig, 1929.(The Origin of Continents and Oceans, Translated in 1966 by John Biram from 4th revised edition).

Weissel, J.K. and Karner, G.D. 1989. Flexural uplift of firt flanks dur to tectonic denudation ion the lithosphere during extension. Journal of Geophysical Research, **94**, 13919-13950.

Wernicke, B. 1985. Uniform-sense normal simple shear of the continental lithosphere. Canadian Journal of Earth Sciences, **22**, 108-125.

White, R. and McKenzie, D. 1989. Magmatism at rift zones: the generation of volcanic continental margins and flood basalts. Journal of Geophysical Research, **94**, 7685-7729.

Willett, S.D. 1997. Inverse modeling of annealing of fission tracks in apatite 1: A controlled random search method. American Journal of Science, **297**: 939-969.

Williams, H. (Editor) 1995. Geology of the Appalachian-Caledonian Orogen in Canada and Greenland. Geological Survey of Canada, Geology of Canada, no. 6.

Withjack, M.O., Olsen, P.E. and Schlische, R.W. 1995. Tectonic evolution of the Fundy rift basin, Canada: Evidence of extension and shortening during passive margin development. Tectonics, **14**, no. 2, 390-405.

Withjack, M.O., Schlische, R.W. and Olsen, P.E. 1998. Diachronous rifting, drifting, and inversion on the passive margin of central eastern North America: an analog for other

passive margins. American Association of Petroleum Geologists Bulletin, **82**, no. 5A, 817-835.

Wolf, R.A., Farley, K.A. and Silver, L.T. 1996. Helium diffusion and low temperature thermochronometry of apatite. Geochimica et Cosmochimica Acta, **60**, 4231-4240.

Wolf, R.A., Farley, K.A., and Kass, D.M. 1998. Modeling of the temperature sensitivity of the apatite (U-Th)/He thermochronometer. Chemical Geology, **148**, 105-114.

Zeitler, P.K., Herczeg, A.L., McDougall, I., and Honda, M. 1987. U-Th-He dating of apatite: A potential thermochronometer. Geochimica et Cosmochimica Acta, **51**, 2865-2868.

Zeitler, P.K., Johnson, N.M., Naeser, C.W., and Tahirkheli, R.A.K. 1982. Fission track evidence for Quaternary uplift of the Nanga Parbat region, Pakistan, Nature, **298**, 255-257.

Ziegler, J.F. 1977. Helium: Stopping powers and ranges in all elemental matter. Pergamon, New York.

APPENDIX A Sample preparation

A.1. Mineral separation techniques used to obtain apatite

Apatite is a non-magnetic mineral with a specific gravity of 3.15 - 3.20 g/cm^3. It is separated by a combination of heavy liquid and magnetic separation techniques. All mineral separation for apatite for this thesis was done at the Dalhousie University Fission Track Laboratory, and a description of the basic mineral separation techniques used there in 1992 is given in Grist and Ravenhurst, 1992. The techniques have subsequently evolved somewhat and are varied slightly from time to time according to the peculiarities of the samples being processed. A generalized description of current mineral separation techniques used at the Dalhousie University Fission Track Laboratory is given below.

Large samples are first reduced to 5-6 cm diameter (or less) pieces using a sledge hammer and a steel plate. These pieces are crushed using a Sturtevant® 2x6" steel jawcrusher with a plate spacing of about 8 mm. The crushed rock is pulverized using a Bico® UD rotary disk mill equipped with 20 cm diameter (8 inch) ceramic plates, with a plate spacing of 0.1 - 0.2 mm. The use of ceramic rather than steel plates is important both because ceramic is an insulator so that the plates do not get as hot during crushing, and because of the superior wear characteristics of ceramic compared to steel plates. The crushed sample is then sieved with a 0.5 mm (Tyler equivalent 30 mesh) nylon mesh cloth. If there is a substantial amount of the coarse fraction (i.e. more than a few tens of grams of >0.5 mm) it is re-pulverized.

Samples weighing less than ca. 1 kg are washed repeatedly with jets of water in order to remove clays and rock flour produced during crushing. After they have dried they are sieved with steel sieves at 0.25 mm (Tyler equivalent 60 mesh). Samples weighing more than ca. 1 kg are split into 3 fractions (i.e. heavy, medium and light) using a Wilfley® concentrating table. After they have dried the heavy and medium fractions are sieved at 0.25 mm. The <0.25 mm (-60 mesh) fractions are recombined.

A non-toxic, water soluble heavy liquid (sodium polytungstate; $Na_6(H_2W_{12}O_{40})\cdot H_20$) is used to separate the -60 mesh fractions at a specific gravity of about 2.82 - 2.84 g/cm^3. Density of the liquid is monitored using a glass hydrometer calibrated between 2.800 and 3.000 g/cm^3. Samples weighing ca. 600 g, or less are separated using glass separatory

funnels. A centrifuge with 6 x 250 ml cups is used for larger samples.

After they have dried, magnetite, pyrrhotite or illmenite-bearing grains are removed from the heavy fractions using a large steel magnet. A Frantz® magnetic barrier laboratory separator is used to remove most of the remaining Fe-bearing mineral phases such as garnets, biotite, hornblende, pyroxene etc (Figure A.1). Several passes through the Frantz® separator are usually required, using gradually increased electric current settings to remove progressively less magnetic grains.

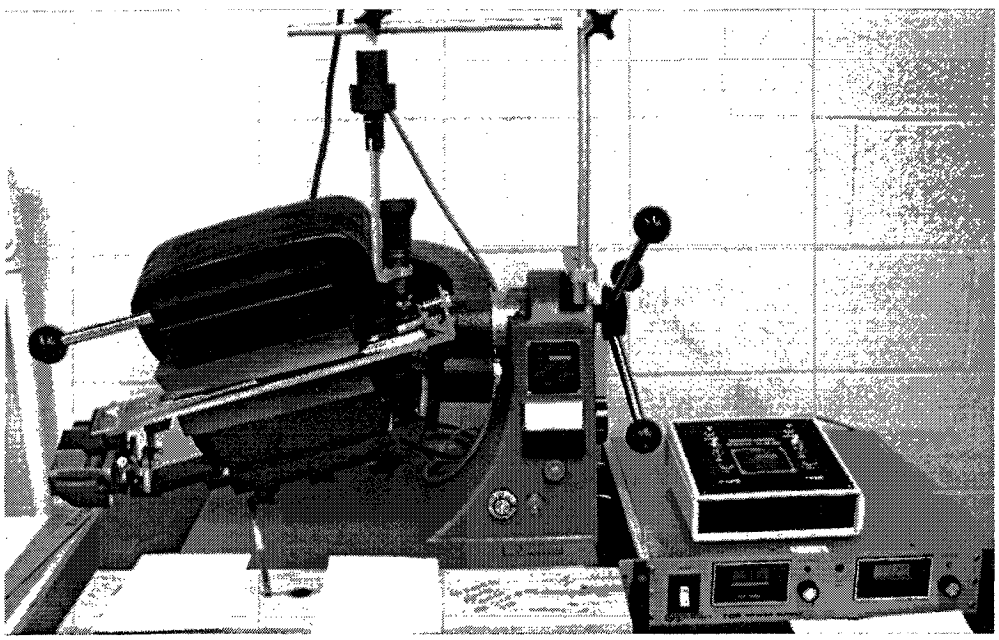

Figure A.1. A Frantz® magnetic barrier laboratory separator equipped with a constant current amplifier (lower right).

The toxic heavy liquid di-iodomethane (CH_2I_2) is used to separate the non-magnetic fractions at a specific gravity of about 3.30 g/cm^3. This step is required to remove relatively uranium-rich phases, especially zircons, as well as sulphide-bearing grains. A second separation using di-iodomethane diluted with acetone to a density of about 3.05 g/cm^3 is also usually performed in order to remove dolomite and grains with minor amounts of adhering sulphide in order to improve the purity of the final apatite separates. Purity of the final apatite

separates varies from <1% to essentially 100%, depending on the initial composition of the sample. Additional handpicking of the separates prior to preparation of grainmounts for fission track analysis is done as required.

A.2. Preparation of apatite grainmounts for fission track analysis

Apatite samples are mounted in Araldite® epoxy using the Naeser (1976) method. For each mount a 1-cm. diameter circle is drawn and labelled with the sample number using a fine-tipped marker on Teflon-coated bakeware (see Figure A.2). This circle serves as a 'target' for pouring the apatite grains and epoxy and it also diffuses into the epoxy as it cures, and can serve as a gauge for removing the correct amount of epoxy during subsequent grinding of the mount surface. Two glass microscope slides are taped about 2 cm apart on either side of the circle so that a third slide can be used to form a bridge over the circle. Aliquots consisting of up to about 1000 grains are gently poured out into the circle such that they form a single layer that is uniformly distributed. The epoxy is mixed in the correct ratio and after mixing it is left to sit for 5 minutes to remove any air bubbles that have formed. The stick used to stir the epoxy is used to drip about 6 drops into the centre of each circle. After removing any remaining air bubbles using a pin or a bit of tissue, a labelled microscope slide is placed so that it is centred on the epoxy and it forms a bridge between the other two glass slides. The epoxy spreads out under the glass slide, engulfing the apatite grains. The grainmounts are cured by letting them stand overnight, and then heating them in a 60 °C oven for 20 minutes. After the mounts have cooled, they are removed from the Teflon-coated cookware by flexing it slightly.

After removing the cured grainmounts from the Teflon bakeware the apatite grains are located just under the exposed surface. They must now be exposed and abraded to a depth of at least 20 μm to expose an internal surface that is then polished. The quality of the polish obtained is in part a function of the amount of experience of the person doing the work. Internal crystallographic imperfections also limit the quality of polish that is obtainable, and it is important not to over-polish the grains, which can cause relief on the mount and fracturing and chipping of the mineral grains.

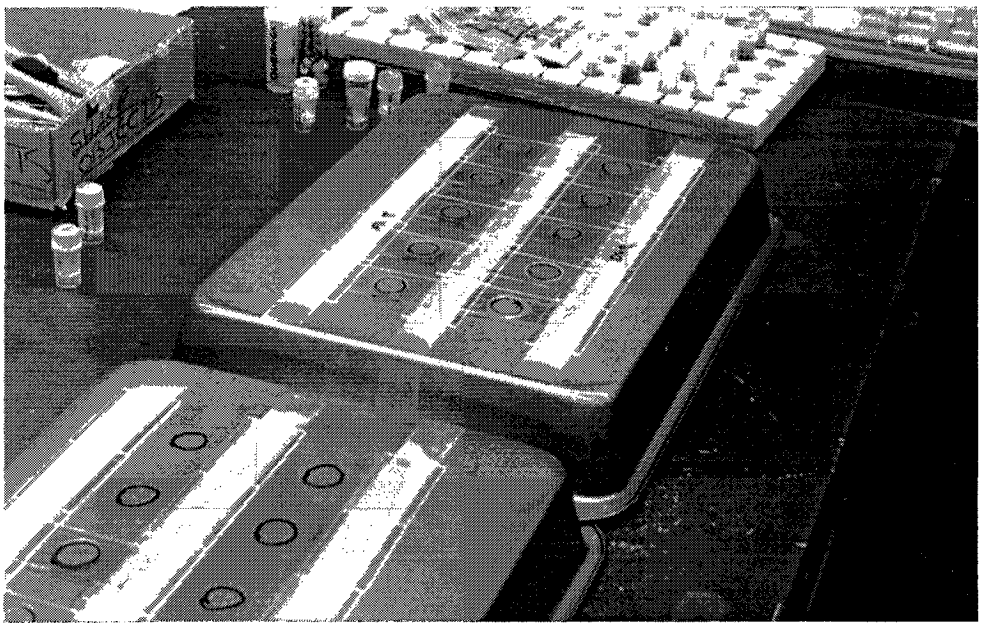

Figure A.2. Epoxy grainmounts on Teflon-coated bakeware (see text for description).

A 600-grit sandpaper is remove the thin layer of epoxy and expose an internal surface of the mineral grains. Each mount is placed on a specially machined Teflon block. The sandpaper is stuck down to a smooth surface using a piece of wetted paper towel. After adding about 25 ml of water to the sandpaper, the mount is turned against it by hand using light pressure 40 times, rotating the block 90 degrees every 10 turns in order to ensure a uniformly exposed mount surface. The ink circles should become quite faint but retain an even look during this process.

The remainder of the polishing is done on 30 cm polishing laps using a Struers® Planopol-V® semi-automatic polisher equipped with a PDM-Force® sample holder (see Figure A.3). The initial polish is done using a water-based slurry of 0.3 μm tin oxide on a cloth with a pile, such a Leco® flocked twill. In addition to removing the scratches from the mineral grains caused by the 600 grit sandpaper, this lap rapidly removes additional epoxy, and can cause considerable relief. Therefore, each mount is given only 20 turns. After this step, the mounts are checked using a microscope to ensure that the grains have been adequately exposed.

An oil-based 0-1 μm diamond slurry is used to obtain a flat polish of the exposed mineral grains. The mounts are polished for 15-20 minutes and then checked under the microscope to see if any polishing scratches remain. A extremely durable and flat cloth, such as the Struers® DP-Dur® (adhesive-backed silk) is required because the epoxy grainmounts have a small polishing area, and they toe-in to the turning wheel, causing considerable wear to the cloth. The wear is visible as shiny patches on the cloth. If the mounts start to degrade appreciably rather than take a polish, it usually indicates the cloth is worn, and a new one is required. The 0-1 μm diamonds impregnate the surface of the epoxy, effectively hardening it so that no more is removed, however the limit to this polish occurs when the edges of the grains start to chip appreciably.

The final polish is done the same as the initial polish using a water-based slurry of 0.3 μm tin oxide on the flocked twill cloth. The mount is turned against the lap 20 times, rotating 180 degrees after 10 turns. This polish removes all of the 0-1 μm diamonds produces a mount with a mirror surface and almost no relief. However, relief begins to develop rapidly after ca. 20 turns.

Apatite grainmounts are etched in 5M HNO_3 for 20 seconds at 24 °C to reveal spontaneous fission tracks. After etching, the mounts are quickly quenched by immersion in a large beaker of water, which is followed by a rinse under running water, and immersion in a second beaker of water, where they remain until all the mounts have been etched. If (as is often the case) several mounts are being etched at the same time it is important that mounts are not left in the first beaker for more than a few moments. The diluted HNO_3 that is introduced into this beaker during rinsing is capable of further etching the mounts, causing them to be over-etched.

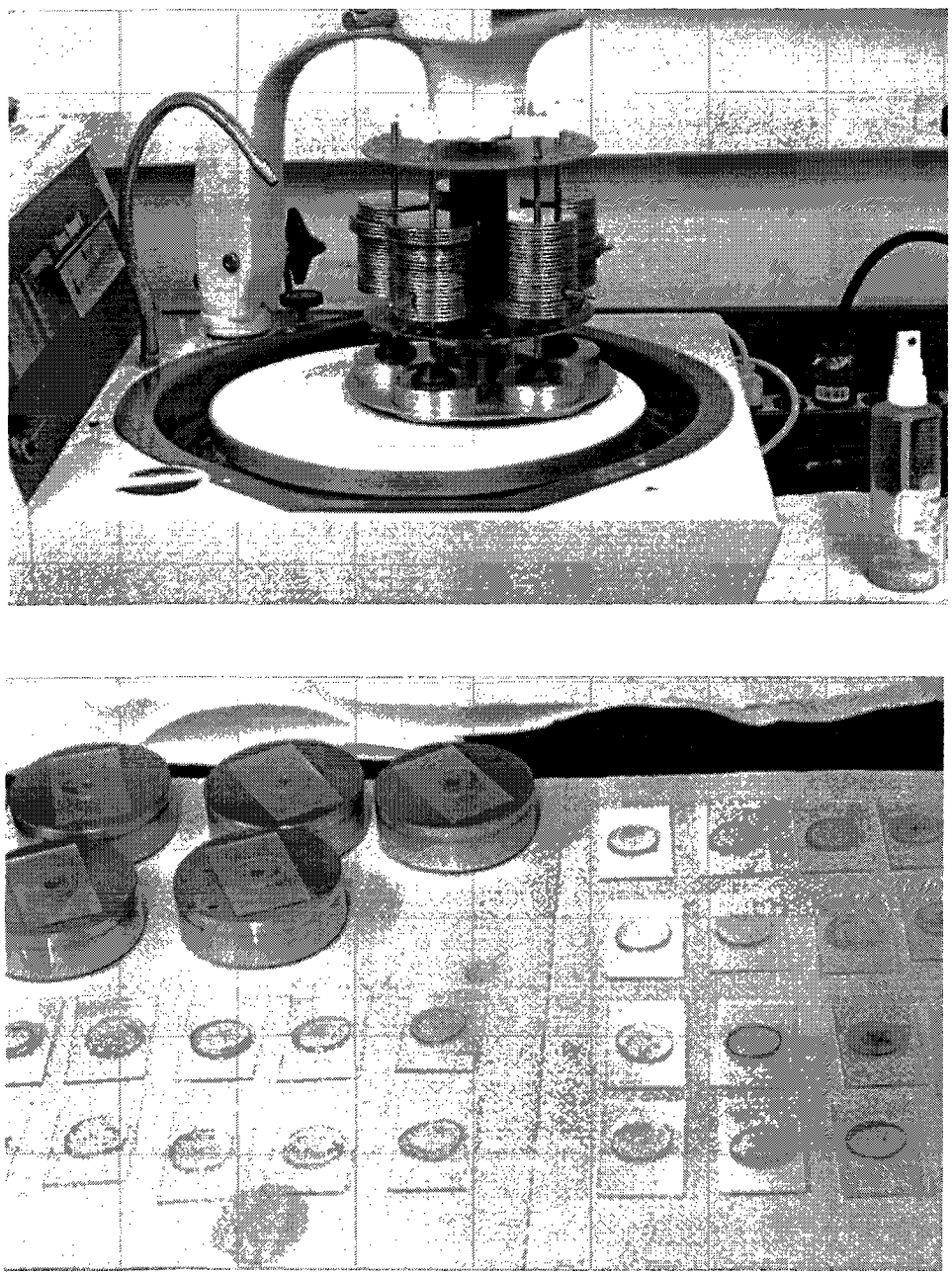

Figure A.3. top: A Struers® Planopol-V semi-automatic polisher equipped with a PDM-Force sample holder. bottom: Closeup view of the five aluminum mounting discs and a number of grainmount during the polishing process.

The water used to quench the etchant infiltrates the fission tracks. It can be essentially permanent in many of the tracks because of the very small amount of surface that is exposed to the air. The fluid-filled tracks have very little optical contrast to the host grain and are almost invisible. Small amounts of fluid in the ends of tracks can also make them look artificially shortened and cause length measurement errors. For this reason it is necessary to ensure that all of the water is removed from the tracks before an analysis is attempted. This is done by rinsing the mount with methanol, and then rubbing the mount 20-25 times with a methanol-soaked lint-free tissue (such as Kimwipe®). After a further rinse with methanol the grainmount is patted dry because impurities in the methanol will leave a residue if it is allowed to evaporate.

To prepare a mount for irradiation, first it is removed from the glass slide. This is done using a hot plate and a scalpel. The glass slide with attached grainmount is placed on the center of a hot plate heated to ca. 90 °C. A few drops of water are placed at the point of contact between the epoxy and the glass slide. Using pair of tweezers to hold the mount, a scalpel is rocked gently back and forth at the contact. After a few seconds the apatite starts to separate from the glass. The water is forced into the fissure by capillary action and helps the glass and epoxy to separate smoothly. If the grainmount warps during this process it is easily flattened again by clamping it between 2 glass slides with a fold-back binder clip and placing it on the hot plate for 1-2 minutes and allowing it to cool again before removing the clip.

A thin sheet of low-uranium muscovite is attached using adhesive tape to the polished surface of each grainmount to detect neutron-induced fission. To do this a commercially obtained block mica is first carefully cleaved (so as to avoid causing any stepped surfaces) to about 0.1 mm thin sheets, and then cut to the correct size using sharp scissors. Detector micas are also attached to dosimeter glasses and age standards. A piece of shrinkwrap is formed into a tube with one of the ends closed off using a hot wire cutter. The shrinkwrap is then placed around any appropriately sized metal tube and heated using a hot air gun to give it the shaped of an open ended cylinder. The samples, standards and glasses are stacked inside the cylinder and then the open end is sealed with the hot wire cutter and

the air gun is used to tighten the shrinkwrap around the stack to form a solid piece. This process helps to ensure flush contact between the grainmounts and the mica detectors.

To further ensure good contact, the stack is placed inside a specially designed irradiation capsule that fits snugly inside a polyvial (Figure A.4). The capsule contains two flat plastic discs. One of these has a threaded hole in the center and a plastic screw is used to force them apart, thereby decreasing the height of the open end of the capsule and applying significant pressure to the stack of grainmounts.

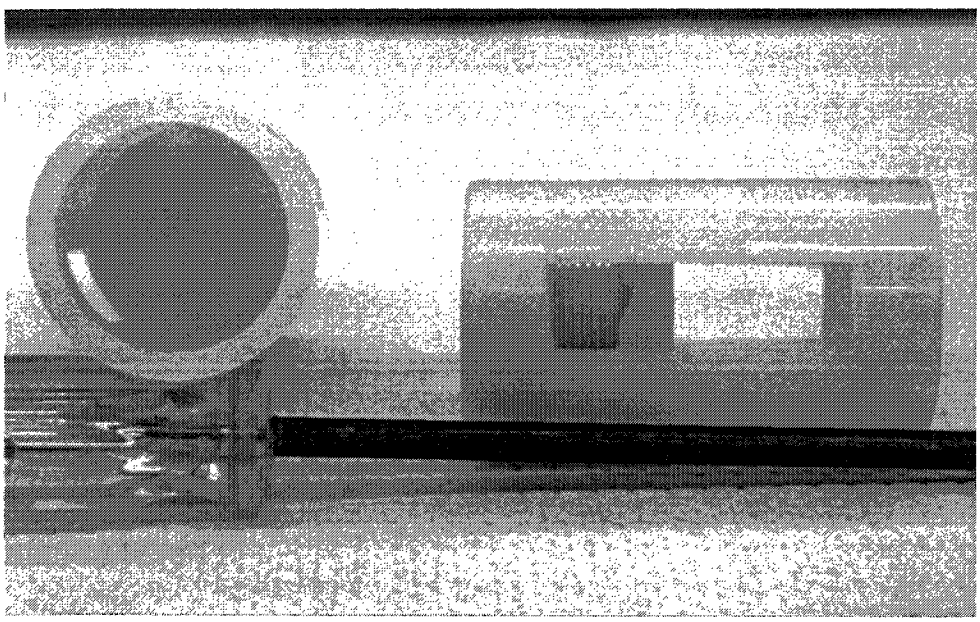

Figure A.4. Two irradiation capsules that are used to compress a stack of fission track samples in order to ensure flush contact between epoxy grainmounts and mica detectors.

Samples are irradiated at the Dalhousie University Slowpoke reactor in the presence of glass neutron dosimeters (CN1 or CN5) of known characteristics. The thermal-neutron fluence obtained is approximately 9×10^{15} neutrons/cm^2. The cadmium ratio for Au is 4.3 at the site. Micas are etched at room temperature in 48% HF for 22 min. Spontaneous and induced track densities (tracks/cm^2) are counted at 1000x magnification (100x dry objective, 10x oculars 1x drawing tube) on a Zeiss® Axioplan microscope equipped with an Autoscan® AS3000 stage.

APPENDIX B.

Apatite FT model inversion control parameters used and resulting model temperature history summaries for the Digby D-1 well and Permian-Triassic outcrop samples:

```
START DATE - MONTH:  4 DAY:  3 YEAR: 2003

START TIME: 16 HR/S    7 MIN    24 S
```

Digby D-1 60 m
model 1993-2 1 hp init 15.5 apt surf

```
LASLETT ET AL ANNEALING MODEL FOR DURANGO APATITE


 AFTINV32 v. 1.3 (AUGUST 3, 2000)
 32-bit Watcom F77 v. 10.6 compiled for Windows 95
 as a Windows NT windowed executable
 code optimized for an Intel Pentium processor
 Original source code developed by Sean Willett
 Source code modified by Dale Issler


  inversion control parameters:
 --------------------------------------------------
 ***MONTE CARLO RANDOM SEARCH METHOD USED***
 number of solutions (l) =          250
 number of timesteps (m) =           35
 number of parameters (m+1) =           36
 NUMERICAL ACCURACY (%), ACUR =        0.1000000
 timestep length (delsub) =  5.000
 obj fnct (2 = chi2; 3 = K-S; 4 = Kuiper) =            3
 convergence tolerance (tol95) =        0.0999941
 convergence tolerance (toler) =        0.0609323
 number of standard deviations to fit age 2.0
 measured age  =  244.00
 sigma of error in measured age  =   7.20
 number of tracks measured =          181
 intermediate output every           50 forward models
 random number generator seed =           13
 system number generator urand(iseed)
 expansion factor (alpha) = 1.300
 reposition factor for explicit bound (delta) = 0.0010
 original track length (xl0) 15.500
 initial mean radius of length ellipse (xl3e) =   0.000
 conventional mean data
 empirical model of age reduction
 track length reduction coefs.:
 -4.86999989   0.00016800 -28.12000084   0.00000000   0.34999999
2.70000005
 component variance coefs.:
  0.78990000   0.00303500  -0.00229830   0.00000000

     temperature bounds         rate bounds           delt
```

1	10.00	200.00	19.00	0.00	10.00
2	10.00	50.00	0.00	9.00	10.00
3	10.00	100.00	0.00	11.50	10.00
4	30.00	125.00	0.00	12.00	10.00
5	50.00	150.00	0.00	10.00	10.00
6	100.00	150.00	5.00	0.00	10.00
7	100.00	150.00	10.00	0.00	10.00
8	50.00	125.00	7.50	0.00	10.00
9	50.00	125.00	7.50	0.00	10.00
10	50.00	125.00	9.50	0.00	10.00
11	30.00	100.00	9.00	0.00	10.00
12	10.00	100.00	0.00	9.00	10.00
13	10.00	100.00	0.00	9.00	10.00
14	10.00	100.00	0.00	9.00	10.00
15	10.00	100.00	0.00	9.00	10.00
16	10.00	100.00	9.00	0.00	10.00
17	10.00	90.00	9.00	0.00	10.00
18	10.00	85.00	7.50	0.00	10.00
19	10.00	80.00	7.00	0.00	10.00
20	10.00	80.00	7.00	0.00	10.00
21	10.00	75.00	6.50	0.00	10.00
22	10.00	70.00	6.00	0.00	10.00
23	10.00	65.00	5.50	0.00	10.00
24	10.00	30.00	0.00	2.50	10.00
25	10.00	35.00	0.00	3.00	10.00
26	10.00	40.00	3.00	5.00	10.00
27	10.00	60.00	5.00	5.00	10.00
28	10.00	60.00	5.00	4.50	10.00
29	10.00	55.00	4.50	4.50	10.00
30	10.00	55.00	4.50	4.00	10.00
31	10.00	50.00	4.00	4.00	10.00
32	10.00	50.00	4.00	3.50	10.00
33	10.00	45.00	3.50	0.00	10.00
34	10.00	45.00	3.50	0.00	10.00
35	10.00	40.00	3.00	0.00	10.00
36	10.00	30.00			

HEATING/COOLING SELECTION SUMMARY:

REGION	TIME RANGE MA	# OF EVENTS HEATING	COOLING	NHP	NCP
1	350.0- 340.0	NO	MONOTONIC	0	-1
2	340.0- 300.0	MONOTONIC	NO	-1	0
3	300.0- 240.0	NO	MONOTONIC	0	-1
4	240.0- 200.0	MONOTONIC	NO	-1	0
5	200.0- 120.0	NO	MONOTONIC	0	-1
6	120.0- 100.0	MONOTONIC	NO	-1	0
7	100.0- 30.0	1	MONOTONIC	1	-1
8	30.0- 0.0	NO	MONOTONIC	0	-1

NUMBER OF FORWARD RANDOM TRIALS, ITER = 16189
max obj function = 0.099870
CONVERGENCE AT 0.05 SIGNIFICANCE LEVEL
number of forward models: 250
STOP DATES - MONTH: 4 DAY: 3 YEAR: 2003

STOP TIME : 16 HR/S 10 MIN 22 S

TOTAL EXECUTION TIME = 0.049438 HOURS OR 2.9663 MINUTES

MODEL RESULTS AT .05 SIGNIFICANCE LEVEL

TIME (MY)	TIME (MA)	EXP MEAN TEMPERATURE (DEG C)	MIN OBJ TEMPERATURE (DEG C)	LOWER TEMP BOUND	UPPER TEMP BOUND
0.00	350.00	72.05	51.35	11.27	154.95
10.00	340.00	37.80	44.24	10.57	49.92
20.00	330.00	84.68	80.05	12.23	99.97
30.00	320.00	106.40	110.41	33.42	124.92
40.00	310.00	121.16	116.85	51.35	147.35
50.00	300.00	128.22	125.49	100.42	149.79
60.00	290.00	121.60	106.05	100.01	149.47
70.00	280.00	91.06	85.79	51.84	122.36
80.00	270.00	82.96	77.00	51.36	120.55
90.00	260.00	74.53	70.14	50.14	100.79
100.00	250.00	64.76	62.69	30.28	92.92
110.00	240.00	56.01	56.44	10.09	77.55
120.00	230.00	62.07	63.14	10.31	84.77
130.00	220.00	67.63	67.92	10.38	84.87
140.00	210.00	74.40	70.29	11.35	90.32
150.00	200.00	80.46	75.84	65.24	98.31
160.00	190.00	74.39	70.41	46.76	86.79
170.00	180.00	68.73	65.96	22.33	80.42
180.00	170.00	63.32	63.02	20.28	75.42
190.00	160.00	57.96	59.56	18.34	74.52
200.00	150.00	51.46	57.26	10.26	69.20
210.00	140.00	45.35	50.36	10.15	66.43
220.00	130.00	38.69	48.59	10.05	63.77
230.00	120.00	21.05	26.48	10.00	29.96
240.00	110.00	25.57	29.05	10.00	34.86
250.00	100.00	30.78	33.40	10.01	39.97
260.00	90.00	44.62	54.99	10.08	59.97
270.00	80.00	49.70	59.23	10.10	59.96
280.00	70.00	49.77	48.66	10.65	55.00
290.00	60.00	50.02	48.16	11.48	55.00
300.00	50.00	45.84	45.79	11.63	49.99
310.00	40.00	42.79	41.97	13.14	49.99
320.00	30.00	37.36	41.76	12.20	44.98
330.00	20.00	34.06	36.45	11.12	44.93
340.00	10.00	28.71	31.61	10.37	39.94
350.00	0.00	21.81	29.74	10.07	29.99

START DATE - MONTH: 4 DAY: 3 YEAR: 2003

START TIME: 16 HR/S 15 MIN 5 S

Digby D-1 250 m
model 1993-2 1 hp init 15.5 apt surf

LASLETT ET AL ANNEALING MODEL FOR DURANGO APATITE

AFTINV32 v. 1.3 (AUGUST 3, 2000)
32-bit Watcom F77 v. 10.6 compiled for Windows 95
as a Windows NT windowed executable
code optimized for an Intel Pentium processor
Original source code developed by Sean Willett
Source code modified by Dale Issler

inversion control parameters:

MONTE CARLO RANDOM SEARCH METHOD USED
number of solutions (1) = 250
number of timesteps (m) = 35
number of parameters (m+1) = 36
NUMERICAL ACCURACY (%), ACUR = 0.1000000
timestep length (delsub) = 5.000
obj fnct (2 = chi2; 3 = K-S; 4 = Kuiper) = 3
convergence tolerance (tol95) = 0.0991837
convergence tolerance (toler) = 0.0604385
number of standard deviations to fit age 2.0
measured age = 236.00
sigma of error in measured age = 6.70
number of tracks measured = 184
intermediate output every 50 forward models
random number generator seed = 13
system number generator urand(iseed)
expansion factor (alpha) = 1.300
reposition factor for explicit bound (delta) = 0.0010
original track length (xl0) 15.500
initial mean radius of length ellipse (xl3e) = 0.000
conventional mean data
empirical model of age reduction
track length reduction coefs.:
-4.86999989 0.00016800 -28.12000084 0.00000000 0.34999999
2.70000005
component variance coefs.:
0.78990000 0.00303500 -0.00229830 0.00000000

	temperature bounds		rate bounds		delt
1	10.00	200.00	19.00	0.00	10.00
2	10.00	50.00	0.00	9.00	10.00
3	10.00	100.00	0.00	11.50	10.00
4	30.00	125.00	0.00	12.00	10.00
5	50.00	150.00	0.00	10.00	10.00
6	100.00	150.00	5.00	0.00	10.00
7	100.00	150.00	10.00	0.00	10.00
8	50.00	125.00	7.50	0.00	10.00
9	50.00	125.00	7.50	0.00	10.00

10	50.00	125.00	9.50	0.00	10.00
11	30.00	100.00	9.00	0.00	10.00
12	10.00	100.00	0.00	9.00	10.00
13	10.00	100.00	0.00	9.00	10.00
14	10.00	100.00	0.00	9.00	10.00
15	10.00	100.00	0.00	9.00	10.00
16	10.00	100.00	9.00	0.00	10.00
17	10.00	90.00	9.00	0.00	10.00
18	10.00	85.00	7.50	0.00	10.00
19	10.00	80.00	7.00	0.00	10.00
20	10.00	80.00	7.00	0.00	10.00
21	10.00	75.00	6.50	0.00	10.00
22	10.00	70.00	6.00	0.00	10.00
23	10.00	65.00	5.50	0.00	10.00
24	10.00	30.00	0.00	2.50	10.00
25	10.00	35.00	0.00	3.00	10.00
26	10.00	40.00	3.00	5.00	10.00
27	10.00	60.00	5.00	5.00	10.00
28	10.00	60.00	5.00	4.50	10.00
29	10.00	55.00	4.50	4.50	10.00
30	10.00	55.00	4.50	4.00	10.00
31	10.00	50.00	4.00	4.00	10.00
32	10.00	50.00	4.00	3.50	10.00
33	10.00	45.00	3.50	0.00	10.00
34	10.00	45.00	3.50	0.00	10.00
35	10.00	40.00	3.00	0.00	10.00
36	10.00	30.00			

HEATING/COOLING SELECTION SUMMARY:

REGION	TIME RANGE MA	# OF EVENTS HEATING	COOLING	NHP	NCP
1	350.0- 340.0	NO	MONOTONIC	0	-1
2	340.0- 300.0	MONOTONIC	NO	-1	0
3	300.0- 240.0	NO	MONOTONIC	0	-1
4	240.0- 200.0	MONOTONIC	NO	-1	0
5	200.0- 120.0	NO	MONOTONIC	0	-1
6	120.0- 100.0	MONOTONIC	NO	-1	0
7	100.0- 30.0	1	MONOTONIC	1	-1
8	30.0- 0.0	NO	MONOTONIC	0	-1

NUMBER OF FORWARD RANDOM TRIALS, ITER = 24827
max obj function = 0.099141
CONVERGENCE AT 0.05 SIGNIFICANCE LEVEL
number of forward models: 250
STOP DATES - MONTH: 4 DAY: 3 YEAR: 2003

STOP TIME : 16 HR/S 19 MIN 57 S

TOTAL EXECUTION TIME = 0.081257 HOURS OR 4.8754 MINUTES

MODEL RESULTS AT .05 SIGNIFICANCE LEVEL

TIME (MY)	TIME (MA)	EXP MEAN TEMPERATURE (DEG C)	MIN OBJ TEMPERATURE (DEG C)	LOWER TEMP BOUND	UPPER TEMP BOUND
0.00	350.00	72.91	42.45	10.34	147.76
10.00	340.00	37.58	36.98	10.22	49.89
20.00	330.00	83.17	93.48	12.23	99.80
30.00	320.00	105.99	116.18	31.95	124.92
40.00	310.00	122.19	117.42	51.21	146.47
50.00	300.00	130.30	137.83	103.76	149.89
60.00	290.00	124.32	137.04	100.25	149.84
70.00	280.00	96.31	111.86	54.27	124.24
80.00	270.00	87.97	97.29	51.86	120.79
90.00	260.00	77.64	65.54	50.14	106.14
100.00	250.00	67.46	64.92	30.28	99.01
110.00	240.00	57.84	15.35	10.19	76.40
120.00	230.00	63.72	22.96	10.31	82.73
130.00	220.00	68.88	56.25	10.38	84.79
140.00	210.00	75.22	58.71	11.35	89.63
150.00	200.00	81.52	75.67	68.38	94.83
160.00	190.00	76.25	75.48	51.36	86.79
170.00	180.00	71.27	73.78	19.39	80.96
180.00	170.00	66.26	66.73	15.59	76.43
190.00	160.00	61.18	66.63	12.06	75.68
200.00	150.00	54.92	63.89	10.26	71.48
210.00	140.00	48.90	57.19	10.15	67.32
220.00	130.00	42.22	52.37	10.05	64.16
230.00	120.00	21.79	11.58	10.00	29.96
240.00	110.00	26.34	17.04	10.00	34.86
250.00	100.00	31.95	29.49	10.01	39.97
260.00	90.00	46.04	40.58	10.99	59.97
270.00	80.00	51.20	46.02	11.13	59.96
280.00	70.00	50.99	54.05	11.59	55.00
290.00	60.00	50.49	54.85	12.82	55.00
300.00	50.00	45.21	48.76	25.77	49.99
310.00	40.00	41.63	47.66	18.01	49.97
320.00	30.00	36.32	43.75	11.78	44.95
330.00	20.00	32.87	42.85	10.43	44.91
340.00	10.00	27.87	17.34	10.27	39.94
350.00	0.00	21.41	16.61	10.05	29.84

START DATE - MONTH: 4 DAY: 3 YEAR: 2003

START TIME: 21 HR/S 22 MIN 15 S

Digby D-1 624 m
model 1993-2 1 hp init 15.5 apt surf

LASLETT ET AL ANNEALING MODEL FOR DURANGO APATITE

AFTINV32 v. 1.3 (AUGUST 3, 2000)
32-bit Watcom F77 v. 10.6 compiled for Windows 95
as a Windows NT windowed executable
code optimized for an Intel Pentium processor
Original source code developed by Sean Willett
Source code modified by Dale Issler

inversion control parameters:

MONTE CARLO RANDOM SEARCH METHOD USED
number of solutions (l) = 250
number of timesteps (m) = 35
number of parameters (m+1) = 36
NUMERICAL ACCURACY (%), ACUR = 0.1000000
timestep length (delsub) = 5.000
obj fnct (2 = chi2; 3 = K-S; 4 = Kuiper) = 3
convergence tolerance (tol95) = 0.0916123
convergence tolerance (toler) = 0.0558248
number of standard deviations to fit age 2.0
measured age = 212.00
sigma of error in measured age = 6.40
number of tracks measured = 216
intermediate output every 50 forward models
random number generator seed = 13
system number generator urand(iseed)
expansion factor (alpha) = 1.300
reposition factor for explicit bound (delta) = 0.0010
original track length (xl0) 15.500
initial mean radius of length ellipse (xl3e) = 0.000
conventional mean data
empirical model of age reduction
track length reduction coefs.:
-4.86999989 0.00016800 -28.12000084 0.00000000 0.34999999
2.70000005
component variance coefs.:
0.78990000 0.00303500 -0.00229830 0.00000000

	temperature bounds		rate bounds		delt
1	15.00	200.00	19.00	0.00	10.00
2	15.00	55.00	0.00	9.00	10.00
3	15.00	105.00	0.00	11.50	10.00
4	35.00	130.00	0.00	12.00	10.00
5	55.00	155.00	0.00	10.00	10.00
6	105.00	155.00	5.00	0.00	10.00
7	105.00	155.00	10.00	0.00	10.00
8	55.00	130.00	7.50	0.00	10.00
9	55.00	130.00	7.50	0.00	10.00

10	55.00	130.00	9.50	0.00	10.00
11	35.00	105.00	9.00	0.00	10.00
12	15.00	105.00	0.00	9.00	10.00
13	15.00	105.00	0.00	9.00	10.00
14	15.00	105.00	0.00	9.00	10.00
15	15.00	105.00	0.00	9.00	10.00
16	15.00	105.00	9.00	0.00	10.00
17	15.00	95.00	9.00	0.00	10.00
18	15.00	90.00	7.50	0.00	10.00
19	15.00	85.00	7.00	0.00	10.00
20	15.00	85.00	7.00	0.00	10.00
21	15.00	80.00	6.50	0.00	10.00
22	15.00	75.00	6.00	0.00	10.00
23	15.00	70.00	5.50	0.00	10.00
24	15.00	35.00	0.00	2.50	10.00
25	15.00	40.00	0.00	3.00	10.00
26	15.00	45.00	3.00	5.00	10.00
27	15.00	65.00	5.00	5.00	10.00
28	15.00	65.00	5.00	4.50	10.00
29	15.00	60.00	4.50	4.50	10.00
30	15.00	60.00	4.50	4.00	10.00
31	15.00	55.00	4.00	4.00	10.00
32	15.00	55.00	4.00	3.50	10.00
33	15.00	50.00	3.50	0.00	10.00
34	15.00	50.00	3.50	0.00	10.00
35	15.00	45.00	3.00	0.00	10.00
36	15.00	35.00			

HEATING/COOLING SELECTION SUMMARY:

REGION	TIME RANGE MA	# OF EVENTS HEATING	COOLING	NHP	NCP
1	350.0- 340.0	NO	MONOTONIC	0	-1
2	340.0- 300.0	MONOTONIC	NO	-1	0
3	300.0- 240.0	NO	MONOTONIC	0	-1
4	240.0- 200.0	MONOTONIC	NO	-1	0
5	200.0- 120.0	NO	MONOTONIC	0	-1
6	120.0- 100.0	MONOTONIC	NO	-1	0
7	100.0- 30.0	1	MONOTONIC	1	-1
8	30.0- 0.0	NO	MONOTONIC	0	-1

NUMBER OF FORWARD RANDOM TRIALS, ITER = 24955
max obj function = 0.091569
CONVERGENCE AT 0.05 SIGNIFICANCE LEVEL
number of forward models: 250
STOP DATES - MONTH: 4 DAY: 3 YEAR: 2003

STOP TIME : 21 HR/S 27 MIN 29 S

TOTAL EXECUTION TIME = 0.087261 HOURS OR 5.2357 MINUTES

MODEL RESULTS AT .05 SIGNIFICANCE LEVEL

TIME (MY)	TIME (MA)	EXP MEAN TEMPERATURE (DEG C)	MIN OBJ TEMPERATURE (DEG C)	LOWER TEMP BOUND	UPPER TEMP BOUND
0.00	350.00	103.30	41.70	17.68	196.27
10.00	340.00	43.09	34.24	15.99	54.90
20.00	330.00	88.06	86.50	18.05	104.83
30.00	320.00	112.13	109.05	35.54	129.91
40.00	310.00	126.02	121.37	55.85	153.69
50.00	300.00	135.47	139.75	105.39	154.89
60.00	290.00	129.71	134.90	105.24	153.76
70.00	280.00	120.28	129.36	65.37	129.99
80.00	270.00	116.11	129.10	63.59	129.75
90.00	260.00	109.90	127.82	62.48	128.99
100.00	250.00	86.91	92.92	35.54	104.88
110.00	240.00	73.56	79.18	15.45	91.98
120.00	230.00	78.62	80.72	15.48	94.45
130.00	220.00	82.92	82.48	21.58	97.88
140.00	210.00	87.43	82.52	22.36	101.41
150.00	200.00	92.10	83.15	75.80	104.01
160.00	190.00	81.88	77.92	26.26	94.97
170.00	180.00	74.68	77.66	20.85	88.96
180.00	170.00	68.64	74.01	18.82	81.60
190.00	160.00	62.19	68.77	15.32	78.71
200.00	150.00	55.99	62.49	15.09	75.90
210.00	140.00	50.72	40.42	15.08	71.48
220.00	130.00	44.71	35.12	15.04	66.46
230.00	120.00	25.90	27.10	15.00	34.98
240.00	110.00	30.35	29.87	15.00	39.96
250.00	100.00	35.40	33.08	15.00	44.72
260.00	90.00	46.33	21.82	15.01	64.85
270.00	80.00	52.31	46.17	15.01	64.99
280.00	70.00	52.67	52.17	15.02	59.98
290.00	60.00	52.64	54.30	15.25	59.99
300.00	50.00	47.37	48.56	15.04	54.99
310.00	40.00	43.90	45.94	15.03	54.99
320.00	30.00	38.18	41.98	15.02	49.98
330.00	20.00	33.76	35.37	15.01	48.95
340.00	10.00	29.44	33.84	15.00	44.77
350.00	0.00	24.24	27.45	15.00	34.84

START DATE - MONTH: 4 DAY: 3 YEAR: 2003

START TIME: 21 HR/S 46 MIN 5 S

Digby D-1 849 m
model 1993-2 1 hp init 15.5 apt surf

LASLETT ET AL ANNEALING MODEL FOR DURANGO APATITE

AFTINV32 v. 1.3 (AUGUST 3, 2000)
32-bit Watcom F77 v. 10.6 compiled for Windows 95
as a Windows NT windowed executable
code optimized for an Intel Pentium processor
Original source code developed by Sean Willett
Source code modified by Dale Issler

inversion control parameters:

MONTE CARLO RANDOM SEARCH METHOD USED
number of solutions (l) = 250
number of timesteps (m) = 35
number of parameters (m+1) = 36
NUMERICAL ACCURACY (%), ACUR = 0.1000000
timestep length (delsub) = 5.000
obj fnct (2 = chi2; 3 = K-S; 4 = Kuiper) = 3
convergence tolerance (tol95) = 0.1005456
convergence tolerance (toler) = 0.0612683
number of standard deviations to fit age 2.0
measured age = 199.00
sigma of error in measured age = 6.20
number of tracks measured = 179
intermediate output every 50 forward models
random number generator seed = 13
system number generator urand(iseed)
expansion factor (alpha) = 1.300
reposition factor for explicit bound (delta) = 0.0010
original track length (xl0) 15.500
initial mean radius of length ellipse (xl3e) = 0.000
conventional mean data
empirical model of age reduction
track length reduction coefs.:
-4.86999989 0.00016800 -28.12000084 0.00000000 0.34999999
2.70000005
component variance coefs.:
0.78990000 0.00303500 -0.00229830 0.00000000

	temperature bounds		rate bounds		delt
1	15.00	200.00	19.00	0.00	10.00
2	15.00	60.00	0.00	9.00	10.00
3	15.00	110.00	0.00	11.50	10.00
4	35.00	135.00	0.00	12.00	10.00
5	55.00	160.00	0.00	10.00	10.00
6	105.00	160.00	5.00	0.00	10.00
7	105.00	160.00	10.00	0.00	10.00
8	55.00	135.00	7.50	0.00	10.00
9	55.00	135.00	7.50	0.00	10.00

10	55.00	135.00	9.50	0.00	10.00
11	35.00	110.00	9.00	0.00	10.00
12	15.00	110.00	0.00	9.00	10.00
13	15.00	110.00	0.00	9.00	10.00
14	15.00	110.00	0.00	9.00	10.00
15	15.00	110.00	0.00	9.00	10.00
16	15.00	110.00	9.00	0.00	10.00
17	15.00	100.00	9.00	0.00	10.00
18	15.00	95.00	7.50	0.00	10.00
19	15.00	90.00	7.00	0.00	10.00
20	15.00	90.00	7.00	0.00	10.00
21	15.00	85.00	6.50	0.00	10.00
22	15.00	80.00	6.00	0.00	10.00
23	15.00	75.00	5.50	0.00	10.00
24	15.00	40.00	0.00	2.50	10.00
25	15.00	45.00	0.00	3.00	10.00
26	15.00	50.00	3.00	5.00	10.00
27	15.00	70.00	5.00	5.00	10.00
28	15.00	70.00	5.00	4.50	10.00
29	15.00	65.00	4.50	4.50	10.00
30	15.00	65.00	4.50	4.00	10.00
31	15.00	60.00	4.00	4.00	10.00
32	15.00	60.00	4.00	3.50	10.00
33	15.00	55.00	3.50	0.00	10.00
34	15.00	55.00	3.50	0.00	10.00
35	15.00	50.00	3.00	0.00	10.00
36	15.00	40.00			

HEATING/COOLING SELECTION SUMMARY:

REGION	TIME RANGE MA	# OF EVENTS HEATING	COOLING	NHP	NCP
1	350.0- 340.0	NO	MONOTONIC	0	-1
2	340.0- 300.0	MONOTONIC	NO	-1	0
3	300.0- 240.0	NO	MONOTONIC	0	-1
4	240.0- 200.0	MONOTONIC	NO	-1	0
5	200.0- 120.0	NO	MONOTONIC	0	-1
6	120.0- 100.0	MONOTONIC	NO	-1	0
7	100.0- 30.0	1	MONOTONIC	1	-1
8	30.0- 0.0	NO	MONOTONIC	0	-1

NUMBER OF FORWARD RANDOM TRIALS, ITER = 84639
max obj function = 0.100524
CONVERGENCE AT 0.05 SIGNIFICANCE LEVEL
number of forward models: 250
STOP DATES - MONTH: 4 DAY: 3 YEAR: 2003

STOP TIME : 22 HR/S 0 MIN 44 S

TOTAL EXECUTION TIME = 0.244274 HOURS OR 14.6564 MINUTES

MODEL RESULTS AT .05 SIGNIFICANCE LEVEL

TIME (MY)	TIME (MA)	EXP MEAN TEMPERATURE (DEG C)	MIN OBJ TEMPERATURE (DEG C)	LOWER TEMP BOUND	UPPER TEMP BOUND
0.00	350.00	98.78	61.48	17.54	196.82
10.00	340.00	48.07	55.46	15.23	59.96
20.00	330.00	93.54	59.34	15.99	109.70
30.00	320.00	113.37	63.17	36.78	134.88
40.00	310.00	127.44	65.75	55.52	158.11
50.00	300.00	134.50	143.42	105.09	159.82
60.00	290.00	128.59	138.25	105.04	158.43
70.00	280.00	115.51	134.50	67.73	135.00
80.00	270.00	109.51	130.52	64.38	135.00
90.00	260.00	102.08	125.10	56.94	135.00
100.00	250.00	84.90	106.70	36.00	109.85
110.00	240.00	73.68	76.82	15.86	90.10
120.00	230.00	79.31	78.18	16.39	94.35
130.00	220.00	85.51	79.42	25.04	96.65
140.00	210.00	91.20	83.00	52.61	101.45
150.00	200.00	96.58	88.23	82.05	107.81
160.00	190.00	89.84	86.35	59.99	99.71
170.00	180.00	83.68	85.89	39.55	94.71
180.00	170.00	78.10	79.60	31.10	89.70
190.00	160.00	72.17	67.38	29.93	86.34
200.00	150.00	65.65	63.31	15.07	80.91
210.00	140.00	59.57	62.09	15.05	79.66
220.00	130.00	52.97	40.23	15.02	74.33
230.00	120.00	30.71	28.39	15.01	39.93
240.00	110.00	35.70	31.28	15.12	44.83
250.00	100.00	41.23	46.13	16.00	49.94
260.00	90.00	55.56	58.05	15.87	69.84
270.00	80.00	61.15	64.51	15.58	69.73
280.00	70.00	61.40	64.91	20.59	65.00
290.00	60.00	61.25	64.92	34.73	65.00
300.00	50.00	56.48	59.26	43.97	59.99
310.00	40.00	53.22	55.93	35.60	59.99
320.00	30.00	47.56	53.33	20.46	54.91
330.00	20.00	43.06	45.15	17.37	54.82
340.00	10.00	37.96	45.02	15.61	49.45
350.00	0.00	30.88	35.28	15.05	39.94

START DATE - MONTH: 4 DAY: 3 YEAR: 2003

START TIME: 22 HR/S 15 MIN 11 S

Digby D-1 1004 m
model 1993-2 1 hp init 15.5 apt surf

LASLETT ET AL ANNEALING MODEL FOR DURANGO APATITE

AFTINV32 v. 1.3 (AUGUST 3, 2000)
32-bit Watcom F77 v. 10.6 compiled for Windows 95
as a Windows NT windowed executable
code optimized for an Intel Pentium processor
Original source code developed by Sean Willett
Source code modified by Dale Issler

inversion control parameters:

MONTE CARLO RANDOM SEARCH METHOD USED
number of solutions (l) = 250
number of timesteps (m) = 35
number of parameters (m+1) = 36
NUMERICAL ACCURACY (%), ACUR = 0.1000000
timestep length (delsub) = 5.000
obj fnct (2 = chi2; 3 = K-S; 4 = Kuiper) = 3
convergence tolerance (tol95) = 0.1013902
convergence tolerance (toler) = 0.0617830
number of standard deviations to fit age 2.0
measured age = 206.00
sigma of error in measured age = 6.10
number of tracks measured = 176
intermediate output every 50 forward models
random number generator seed = 13
system number generator urand(iseed)
expansion factor (alpha) = 1.300
reposition factor for explicit bound (delta) = 0.0010
original track length (xl0) 15.500
initial mean radius of length ellipse (xl3e) = 0.000
conventional mean data
empirical model of age reduction
track length reduction coefs.:
-4.86999989 0.00016800 -28.12000084 0.00000000 0.34999999
2.70000005
component variance coefs.:
0.78990000 0.00303500 -0.00229830 0.00000000

	temperature bounds		rate bounds		delt
1	20.00	200.00	19.00	0.00	10.00
2	20.00	65.00	0.00	9.00	10.00
3	20.00	115.00	0.00	11.50	10.00
4	40.00	140.00	0.00	12.00	10.00
5	60.00	165.00	0.00	10.00	10.00
6	110.00	165.00	5.00	0.00	10.00
7	110.00	165.00	10.00	0.00	10.00
8	60.00	140.00	7.50	0.00	10.00
9	60.00	140.00	7.50	0.00	10.00

10	60.00	140.00	9.50	0.00	10.00
11	40.00	115.00	9.00	0.00	10.00
12	20.00	115.00	0.00	9.00	10.00
13	20.00	115.00	0.00	9.00	10.00
14	20.00	115.00	0.00	9.00	10.00
15	20.00	115.00	0.00	9.00	10.00
16	20.00	115.00	9.00	0.00	10.00
17	20.00	105.00	9.00	0.00	10.00
18	20.00	100.00	7.50	0.00	10.00
19	20.00	95.00	7.00	0.00	10.00
20	20.00	95.00	7.00	0.00	10.00
21	20.00	90.00	6.50	0.00	10.00
22	20.00	85.00	6.00	0.00	10.00
23	20.00	80.00	5.50	0.00	10.00
24	20.00	45.00	0.00	2.50	10.00
25	20.00	50.00	0.00	3.00	10.00
26	20.00	55.00	3.00	5.00	10.00
27	20.00	75.00	5.00	5.00	10.00
28	20.00	75.00	5.00	4.50	10.00
29	20.00	70.00	4.50	4.50	10.00
30	20.00	70.00	4.50	4.00	10.00
31	20.00	65.00	4.00	4.00	10.00
32	20.00	65.00	4.00	3.50	10.00
33	20.00	60.00	3.50	0.00	10.00
34	20.00	60.00	3.50	0.00	10.00
35	20.00	55.00	3.00	0.00	10.00
36	20.00	45.00			

HEATING/COOLING SELECTION SUMMARY:

REGION	TIME RANGE MA	# OF EVENTS HEATING	COOLING	NHP	NCP
1	350.0- 340.0	NO	MONOTONIC	0	-1
2	340.0- 300.0	MONOTONIC	NO	-1	0
3	300.0- 240.0	NO	MONOTONIC	0	-1
4	240.0- 200.0	MONOTONIC	NO	-1	0
5	200.0- 120.0	NO	MONOTONIC	0	-1
6	120.0- 100.0	MONOTONIC	NO	-1	0
7	100.0- 30.0	1	MONOTONIC	1	-1
8	30.0- 0.0	NO	MONOTONIC	0	-1

NUMBER OF FORWARD RANDOM TRIALS, ITER = 15258
max obj function = 0.101247
CONVERGENCE AT 0.05 SIGNIFICANCE LEVEL
number of forward models: 250
STOP DATES - MONTH: 4 DAY: 3 YEAR: 2003

STOP TIME : 22 HR/S 17 MIN 42 S

TOTAL EXECUTION TIME = 0.042030 HOURS OR 2.5218 MINUTES

MODEL RESULTS AT .05 SIGNIFICANCE LEVEL

TIME (MY)	TIME (MA)	EXP MEAN TEMPERATURE (DEG C)	MIN OBJ TEMPERATURE (DEG C)	LOWER TEMP BOUND	UPPER TEMP BOUND
0.00	350.00	95.20	33.08	21.70	187.59
10.00	340.00	51.18	31.36	20.01	64.83
20.00	330.00	98.64	109.38	21.92	114.83
30.00	320.00	118.99	118.75	42.24	139.83
40.00	310.00	130.69	126.26	63.20	162.51
50.00	300.00	138.83	147.24	110.69	164.60
60.00	290.00	132.53	140.50	110.10	163.86
70.00	280.00	120.37	125.31	70.84	139.79
80.00	270.00	115.13	121.35	64.57	139.61
90.00	260.00	107.84	117.58	61.54	138.54
100.00	250.00	87.24	98.97	40.52	113.85
110.00	240.00	71.79	68.78	20.31	89.27
120.00	230.00	76.82	76.85	20.31	91.04
130.00	220.00	82.52	83.12	20.48	96.84
140.00	210.00	88.83	85.53	26.20	99.84
150.00	200.00	94.11	90.31	48.74	106.56
160.00	190.00	85.67	70.23	27.87	100.47
170.00	180.00	77.18	68.08	25.17	91.55
180.00	170.00	69.95	60.22	21.78	87.39
190.00	160.00	63.91	52.73	21.07	82.80
200.00	150.00	57.86	51.01	21.03	77.79
210.00	140.00	51.32	49.60	20.06	75.03
220.00	130.00	44.01	48.39	20.05	70.71
230.00	120.00	33.01	35.84	20.00	44.99
240.00	110.00	37.44	48.89	20.00	49.86
250.00	100.00	42.71	49.60	20.01	54.99
260.00	90.00	52.22	47.13	20.01	74.93
270.00	80.00	58.02	50.59	20.02	74.91
280.00	70.00	58.87	64.73	20.04	70.00
290.00	60.00	59.61	65.71	20.20	69.99
300.00	50.00	56.10	59.58	22.00	64.95
310.00	40.00	53.46	54.57	21.91	64.96
320.00	30.00	47.91	47.93	20.67	59.87
330.00	20.00	43.55	44.34	20.13	59.78
340.00	10.00	38.43	34.08	20.03	54.74
350.00	0.00	32.38	32.25	20.01	44.63

START DATE - MONTH: 4 DAY: 3 YEAR: 2003

START TIME: 22 HR/S 34 MIN 0 S

Digby D-1 1197 m
model 1993-2 1 hp init 15.5 apt surf

LASLETT ET AL ANNEALING MODEL FOR DURANGO APATITE

AFTINV32 v. 1.3 (AUGUST 3, 2000)
32-bit Watcom F77 v. 10.6 compiled for Windows 95
as a Windows NT windowed executable
code optimized for an Intel Pentium processor
Original source code developed by Sean Willett
Source code modified by Dale Issler

inversion control parameters:

MONTE CARLO RANDOM SEARCH METHOD USED
number of solutions (l) = 250
number of timesteps (m) = 35
number of parameters (m+1) = 36
NUMERICAL ACCURACY (%), ACUR = 0.1000000
timestep length (delsub) = 5.000
obj fnct (2 = chi2; 3 = K-S; 4 = Kuiper) = 3
convergence tolerance (tol95) = 0.0986543
convergence tolerance (toler) = 0.0601159
number of standard deviations to fit age 2.0
measured age = 195.00
sigma of error in measured age = 5.60
number of tracks measured = 186
intermediate output every 50 forward models
random number generator seed = 13
system number generator urand(iseed)
expansion factor (alpha) = 1.300
reposition factor for explicit bound (delta) = 0.0010
original track length (xl0) 15.500
initial mean radius of length ellipse (xl3e) = 0.000
conventional mean data
empirical model of age reduction
track length reduction coefs.:
-4.86999989 0.00016800 -28.12000084 0.00000000 0.34999999
2.70000005
component variance coefs.:
0.78990000 0.00303500 -0.00229830 0.00000000

	temperature bounds		rate bounds		delt
1	23.00	200.00	19.00	0.00	10.00
2	23.00	68.00	0.00	9.00	10.00
3	23.00	118.00	0.00	11.50	10.00
4	43.00	143.00	0.00	12.00	10.00
5	63.00	168.00	0.00	10.00	10.00
6	113.00	168.00	5.00	0.00	10.00
7	113.00	168.00	10.00	0.00	10.00
8	63.00	143.00	7.50	0.00	10.00
9	63.00	143.00	7.50	0.00	10.00

10	63.00	143.00	9.50	0.00	10.00
11	43.00	118.00	9.00	0.00	10.00
12	23.00	118.00	0.00	9.00	10.00
13	23.00	118.00	0.00	9.00	10.00
14	23.00	118.00	0.00	9.00	10.00
15	23.00	118.00	0.00	9.00	10.00
16	23.00	118.00	9.00	0.00	10.00
17	23.00	108.00	9.00	0.00	10.00
18	23.00	103.00	7.50	0.00	10.00
19	23.00	98.00	7.00	0.00	10.00
20	23.00	98.00	7.00	0.00	10.00
21	23.00	93.00	6.50	0.00	10.00
22	23.00	88.00	6.00	0.00	10.00
23	23.00	83.00	5.50	0.00	10.00
24	23.00	48.00	0.00	2.50	10.00
25	23.00	53.00	0.00	3.00	10.00
26	23.00	58.00	3.00	5.00	10.00
27	23.00	78.00	5.00	5.00	10.00
28	23.00	78.00	5.00	4.50	10.00
29	23.00	73.00	4.50	4.50	10.00
30	23.00	73.00	4.50	4.00	10.00
31	23.00	68.00	4.00	4.00	10.00
32	23.00	68.00	4.00	3.50	10.00
33	23.00	63.00	3.50	0.00	10.00
34	23.00	63.00	3.50	0.00	10.00
35	23.00	58.00	3.00	0.00	10.00
36	23.00	48.00			

HEATING/COOLING SELECTION SUMMARY:

REGION	TIME RANGE MA	# OF EVENTS HEATING	COOLING	NHP	NCP
1	350.0- 340.0	NO	MONOTONIC	0	-1
2	340.0- 300.0	MONOTONIC	NO	-1	0
3	300.0- 240.0	NO	MONOTONIC	0	-1
4	240.0- 200.0	MONOTONIC	NO	-1	0
5	200.0- 120.0	NO	MONOTONIC	0	-1
6	120.0- 100.0	MONOTONIC	NO	-1	0
7	100.0- 30.0	1	MONOTONIC	1	-1
8	30.0- 0.0	NO	MONOTONIC	0	-1

```
NUMBER OF FORWARD RANDOM TRIALS, ITER =     16849
  max obj function =        0.098601
 CONVERGENCE AT 0.05 SIGNIFICANCE LEVEL
 number of forward models:          250
STOP DATES - MONTH:  4 DAY:  3 YEAR: 2003

STOP TIME : 22 HR/S   36 MIN    48 S

 TOTAL EXECUTION TIME =  0.046799 HOURS OR    2.8079 MINUTES
```

MODEL RESULTS AT .05 SIGNIFICANCE LEVEL

TIME (MY)	TIME (MA)	EXP MEAN TEMPERATURE (DEG C)	MIN OBJ TEMPERATURE (DEG C)	LOWER TEMP BOUND	UPPER TEMP BOUND
0.00	350.00	85.45	42.78	26.86	167.67
10.00	340.00	54.76	42.25	23.71	67.71
20.00	330.00	101.21	95.14	27.69	117.97
30.00	320.00	121.50	131.86	43.32	142.78
40.00	310.00	135.39	137.10	64.33	166.22
50.00	300.00	142.69	141.05	113.32	167.46
60.00	290.00	136.19	127.11	113.03	166.86
70.00	280.00	115.06	125.39	67.13	142.28
80.00	270.00	109.14	122.77	65.44	140.88
90.00	260.00	101.83	115.95	63.14	139.20
100.00	250.00	85.74	56.18	43.25	116.85
110.00	240.00	71.75	52.72	23.31	90.15
120.00	230.00	77.74	66.24	23.31	94.04
130.00	220.00	83.85	69.57	23.43	100.71
140.00	210.00	90.66	72.44	24.52	101.50
150.00	200.00	97.12	94.33	51.74	106.82
160.00	190.00	90.58	91.69	45.69	100.68
170.00	180.00	84.51	90.13	29.62	95.57
180.00	170.00	78.85	70.47	28.62	94.21
190.00	160.00	73.13	66.54	27.66	89.23
200.00	150.00	66.27	60.80	23.28	86.65
210.00	140.00	59.57	51.65	23.17	83.92
220.00	130.00	51.82	43.75	23.06	78.54
230.00	120.00	36.81	37.31	23.00	47.88
240.00	110.00	40.84	44.12	23.00	52.82
250.00	100.00	45.68	50.61	23.01	57.99
260.00	90.00	53.72	33.80	23.01	77.58
270.00	80.00	59.42	26.83	23.01	77.91
280.00	70.00	61.05	24.36	23.04	72.88
290.00	60.00	63.47	62.06	23.15	72.99
300.00	50.00	61.66	65.41	23.17	67.95
310.00	40.00	60.12	67.27	35.19	67.97
320.00	30.00	54.84	56.16	31.86	62.95
330.00	20.00	50.37	52.60	26.32	62.93
340.00	10.00	45.50	48.40	24.42	57.82
350.00	0.00	38.36	43.76	23.29	47.97

START DATE - MONTH: 4 DAY: 3 YEAR: 2003

START TIME: 22 HR/S 47 MIN 23 S

Digby D-1 1315 m
model 1993-2 1 hp init 15.5 apt surf

LASLETT ET AL ANNEALING MODEL FOR DURANGO APATITE

AFTINV32 v. 1.3 (AUGUST 3, 2000)
32-bit Watcom F77 v. 10.6 compiled for Windows 95
as a Windows NT windowed executable
code optimized for an Intel Pentium processor
Original source code developed by Sean Willett
Source code modified by Dale Issler

inversion control parameters:

MONTE CARLO RANDOM SEARCH METHOD USED
number of solutions (l) = 250
number of timesteps (m) = 35
number of parameters (m+1) = 36
NUMERICAL ACCURACY (%), ACUR = 0.1000000
timestep length (delsub) = 5.000
obj fnct (2 = chi2; 3 = K-S; 4 = Kuiper) = 3
convergence tolerance (tol95) = 0.1086636
convergence tolerance (toler) = 0.0662151
number of standard deviations to fit age 2.0
measured age = 189.00
sigma of error in measured age = 6.00
number of tracks measured = 153
intermediate output every 50 forward models
random number generator seed = 13
system number generator urand(iseed)
expansion factor (alpha) = 1.300
reposition factor for explicit bound (delta) = 0.0010
original track length (xl0) 15.500
initial mean radius of length ellipse (xl3e) = 0.000
conventional mean data
empirical model of age reduction
track length reduction coefs.:
-4.86999989 0.00016800 -28.12000084 0.00000000 0.34999999
2.70000005
component variance coefs.:
0.78990000 0.00303500 -0.00229830 0.00000000

	temperature bounds		rate bounds		delt
1	25.00	200.00	19.00	0.00	10.00
2	25.00	70.00	0.00	9.00	10.00
3	25.00	120.00	0.00	11.50	10.00
4	45.00	145.00	0.00	12.00	10.00
5	65.00	170.00	0.00	10.00	10.00
6	115.00	170.00	5.00	0.00	10.00
7	115.00	170.00	10.00	0.00	10.00
8	65.00	145.00	7.50	0.00	10.00
9	65.00	145.00	7.50	0.00	10.00

10	65.00	145.00	9.50	0.00	10.00
11	45.00	120.00	9.00	0.00	10.00
12	25.00	120.00	0.00	9.00	10.00
13	25.00	120.00	0.00	9.00	10.00
14	25.00	120.00	0.00	9.00	10.00
15	25.00	120.00	0.00	9.00	10.00
16	25.00	120.00	9.00	0.00	10.00
17	25.00	110.00	9.00	0.00	10.00
18	25.00	105.00	7.50	0.00	10.00
19	25.00	100.00	7.00	0.00	10.00
20	25.00	100.00	7.00	0.00	10.00
21	25.00	95.00	6.50	0.00	10.00
22	25.00	90.00	6.00	0.00	10.00
23	25.00	85.00	5.50	0.00	10.00
24	25.00	50.00	0.00	2.50	10.00
25	25.00	55.00	0.00	3.00	10.00
26	25.00	60.00	3.00	5.00	10.00
27	25.00	80.00	5.00	5.00	10.00
28	25.00	80.00	5.00	4.50	10.00
29	25.00	75.00	4.50	4.50	10.00
30	25.00	75.00	4.50	4.00	10.00
31	25.00	70.00	4.00	4.00	10.00
32	25.00	70.00	4.00	3.50	10.00
33	25.00	65.00	3.50	0.00	10.00
34	25.00	65.00	3.50	0.00	10.00
35	25.00	60.00	3.00	0.00	10.00
36	25.00	50.00			

HEATING/COOLING SELECTION SUMMARY:

REGION	TIME RANGE MA	# OF EVENTS HEATING	COOLING	NHP	NCP
1	350.0- 340.0	NO	MONOTONIC	0	-1
2	340.0- 300.0	MONOTONIC	NO	-1	0
3	300.0- 240.0	NO	MONOTONIC	0	-1
4	240.0- 200.0	MONOTONIC	NO	-1	0
5	200.0- 120.0	NO	MONOTONIC	0	-1
6	120.0- 100.0	MONOTONIC	NO	-1	0
7	100.0- 30.0	1	MONOTONIC	1	-1
8	30.0- 0.0	NO	MONOTONIC	0	-1

NUMBER OF FORWARD RANDOM TRIALS, ITER = 25694
max obj function = 0.108598
CONVERGENCE AT 0.05 SIGNIFICANCE LEVEL
number of forward models: 250
STOP DATES - MONTH: 4 DAY: 3 YEAR: 2003

STOP TIME : 22 HR/S 50 MIN 54 S

TOTAL EXECUTION TIME = 0.058699 HOURS OR 3.5219 MINUTES

MODEL RESULTS AT .05 SIGNIFICANCE LEVEL

TIME (MY)	TIME (MA)	EXP MEAN TEMPERATURE (DEG C)	MIN OBJ TEMPERATURE (DEG C)	LOWER TEMP BOUND	UPPER TEMP BOUND
0.00	350.00	90.67	43.41	29.09	168.52
10.00	340.00	56.68	36.95	25.71	69.94
20.00	330.00	102.76	111.41	27.22	119.97
30.00	320.00	122.80	138.53	46.88	144.91
40.00	310.00	136.72	141.04	65.05	167.63
50.00	300.00	145.36	142.84	115.65	169.46
60.00	290.00	139.18	140.99	115.03	168.09
70.00	280.00	117.07	76.73	70.02	144.93
80.00	270.00	110.93	75.16	66.94	142.15
90.00	260.00	103.69	72.06	65.14	140.55
100.00	250.00	86.74	60.71	45.52	118.85
110.00	240.00	73.00	30.26	25.31	95.04
120.00	230.00	79.36	30.95	25.35	95.94
130.00	220.00	85.47	50.93	25.43	99.10
140.00	210.00	92.19	85.38	26.52	103.50
150.00	200.00	98.58	108.49	75.39	110.98
160.00	190.00	91.59	84.13	41.56	101.59
170.00	180.00	85.41	80.92	29.62	96.98
180.00	170.00	79.17	78.49	28.97	94.55
190.00	160.00	73.35	68.50	27.58	90.92
200.00	150.00	66.78	59.30	26.78	88.65
210.00	140.00	60.21	52.80	25.41	85.92
220.00	130.00	53.31	27.32	25.36	83.77
230.00	120.00	38.39	25.08	25.00	49.88
240.00	110.00	42.38	25.14	25.00	54.10
250.00	100.00	47.70	25.16	25.01	59.61
260.00	90.00	55.33	25.26	25.01	79.58
270.00	80.00	60.85	26.73	25.02	79.91
280.00	70.00	63.46	52.79	25.04	74.88
290.00	60.00	65.22	52.87	25.36	74.98
300.00	50.00	63.50	55.07	25.17	69.99
310.00	40.00	62.28	62.40	48.18	69.96
320.00	30.00	57.17	64.93	27.33	65.00
330.00	20.00	52.88	64.93	25.53	64.93
340.00	10.00	47.66	59.82	25.47	59.93
350.00	0.00	40.45	46.66	25.29	49.97

START DATE - MONTH: 4 DAY: 3 YEAR: 2003

START TIME: 22 HR/S 54 MIN 20 S

Digby D-1 1437 m
model 1993-2 1 hp init 15.5 apt surf

LASLETT ET AL ANNEALING MODEL FOR DURANGO APATITE

AFTINV32 v. 1.3 (AUGUST 3, 2000)
32-bit Watcom F77 v. 10.6 compiled for Windows 95
as a Windows NT windowed executable
code optimized for an Intel Pentium processor
Original source code developed by Sean Willett
Source code modified by Dale Issler

inversion control parameters:

MONTE CARLO RANDOM SEARCH METHOD USED
number of solutions (l) = 250
number of timesteps (m) = 35
number of parameters (m+1) = 36
NUMERICAL ACCURACY (%), ACUR = 0.1000000
timestep length (delsub) = 5.000
obj fnct (2 = chi2; 3 = K-S; 4 = Kuiper) = 3
convergence tolerance (tol95) = 0.1008247
convergence tolerance (toler) = 0.0614384
number of standard deviations to fit age 2.0
measured age = 181.00
sigma of error in measured age = 5.00
number of tracks measured = 178
intermediate output every 50 forward models
random number generator seed = 13
system number generator urand(iseed)
expansion factor (alpha) = 1.300
reposition factor for explicit bound (delta) = 0.0010
original track length (xl0) 15.500
initial mean radius of length ellipse (xl3e) = 0.000
conventional mean data
empirical model of age reduction
track length reduction coefs.:
-4.86999989 0.00016800 -28.12000084 0.00000000 0.34999999
2.70000005
component variance coefs.:
0.78990000 0.00303500 -0.00229830 0.00000000

	temperature bounds		rate bounds		delt
1	25.00	200.00	19.00	0.00	10.00
2	25.00	70.00	0.00	9.00	10.00
3	25.00	120.00	0.00	11.50	10.00
4	45.00	145.00	0.00	12.00	10.00
5	65.00	170.00	0.00	10.00	10.00
6	115.00	170.00	5.00	0.00	10.00
7	115.00	170.00	10.00	0.00	10.00
8	65.00	145.00	7.50	0.00	10.00
9	65.00	145.00	7.50	0.00	10.00

10	65.00	145.00	9.50	0.00	10.00
11	45.00	120.00	9.00	0.00	10.00
12	25.00	120.00	0.00	9.00	10.00
13	25.00	120.00	0.00	9.00	10.00
14	25.00	120.00	0.00	9.00	10.00
15	25.00	120.00	0.00	9.00	10.00
16	25.00	120.00	9.00	0.00	10.00
17	25.00	110.00	9.00	0.00	10.00
18	25.00	105.00	7.50	0.00	10.00
19	25.00	100.00	7.00	0.00	10.00
20	25.00	100.00	7.00	0.00	10.00
21	25.00	95.00	6.50	0.00	10.00
22	25.00	90.00	6.00	0.00	10.00
23	25.00	85.00	5.50	0.00	10.00
24	25.00	50.00	0.00	2.50	10.00
25	25.00	55.00	0.00	3.00	10.00
26	25.00	60.00	3.00	5.00	10.00
27	25.00	80.00	5.00	5.00	10.00
28	25.00	80.00	5.00	4.50	10.00
29	25.00	75.00	4.50	4.50	10.00
30	25.00	75.00	4.50	4.00	10.00
31	25.00	70.00	4.00	4.00	10.00
32	25.00	70.00	4.00	3.50	10.00
33	25.00	65.00	3.50	0.00	10.00
34	25.00	65.00	3.50	0.00	10.00
35	25.00	60.00	3.00	0.00	10.00
36	25.00	50.00			

HEATING/COOLING SELECTION SUMMARY:

REGION	TIME RANGE MA	# OF EVENTS HEATING	COOLING	NHP	NCP
1	350.0- 340.0	NO	MONOTONIC	0	-1
2	340.0- 300.0	MONOTONIC	NO	-1	0
3	300.0- 240.0	NO	MONOTONIC	0	-1
4	240.0- 200.0	MONOTONIC	NO	-1	0
5	200.0- 120.0	NO	MONOTONIC	0	-1
6	120.0- 100.0	MONOTONIC	NO	-1	0
7	100.0- 30.0	1	MONOTONIC	1	-1
8	30.0- 0.0	NO	MONOTONIC	0	-1

```
NUMBER OF FORWARD RANDOM TRIALS, ITER =     32097
  max obj function =        0.100774
 CONVERGENCE AT 0.05 SIGNIFICANCE LEVEL
 number of forward models:          250
STOP DATES - MONTH:  4 DAY:  3 YEAR: 2003

STOP TIME : 22 HR/S   59 MIN    24 S

 TOTAL EXECUTION TIME =  0.084455 HOURS OR    5.0673 MINUTES
```

MODEL RESULTS AT .05 SIGNIFICANCE LEVEL

TIME (MY)	TIME (MA)	EXP MEAN TEMPERATURE (DEG C)	MIN OBJ TEMPERATURE (DEG C)	LOWER TEMP BOUND	UPPER TEMP BOUND
0.00	350.00	88.84	74.95	30.86	161.65
10.00	340.00	56.45	60.20	25.05	69.59
20.00	330.00	103.63	115.74	26.60	119.94
30.00	320.00	123.70	142.86	46.88	144.75
40.00	310.00	136.78	148.59	65.28	167.63
50.00	300.00	143.42	151.72	115.32	169.76
60.00	290.00	137.54	146.58	115.01	169.36
70.00	280.00	115.89	127.98	69.13	144.81
80.00	270.00	108.85	118.95	65.33	144.00
90.00	260.00	100.91	106.86	65.14	140.55
100.00	250.00	84.73	90.59	45.25	115.27
110.00	240.00	74.08	73.13	25.31	92.94
120.00	230.00	79.83	83.16	25.35	94.39
130.00	220.00	86.06	84.40	25.43	98.42
140.00	210.00	92.57	90.06	26.52	101.35
150.00	200.00	99.26	95.97	92.05	110.98
160.00	190.00	94.31	92.38	69.75	102.85
170.00	180.00	89.51	90.79	34.55	97.57
180.00	170.00	84.89	89.58	30.70	94.30
190.00	160.00	79.95	67.20	27.11	93.68
200.00	150.00	73.53	64.87	25.28	88.65
210.00	140.00	67.59	58.19	25.15	86.42
220.00	130.00	59.06	54.24	25.06	84.03
230.00	120.00	39.59	42.96	25.00	49.96
240.00	110.00	44.35	45.18	25.00	54.82
250.00	100.00	50.32	49.62	25.02	59.90
260.00	90.00	62.34	68.97	25.07	79.62
270.00	80.00	68.37	78.29	25.11	79.99
280.00	70.00	69.10	69.11	25.55	74.98
290.00	60.00	69.13	65.96	25.70	75.00
300.00	50.00	64.34	62.99	30.23	69.99
310.00	40.00	61.02	60.24	36.33	69.99
320.00	30.00	55.00	46.15	27.95	64.98
330.00	20.00	50.92	44.22	25.21	64.05
340.00	10.00	45.37	43.24	25.20	59.81
350.00	0.00	38.87	35.65	25.08	49.94

START DATE - MONTH: 4 DAY: 4 YEAR: 2003

START TIME: 14 HR/S 46 MIN 44 S

Martin Head 010
model 1993-2 1 hp init 15.5 apt surf

LASLETT ET AL ANNEALING MODEL FOR DURANGO APATITE

AFTINV32 v. 1.3 (AUGUST 3, 2000)
32-bit Watcom F77 v. 10.6 compiled for Windows 95
as a Windows NT windowed executable
code optimized for an Intel Pentium processor
Original source code developed by Sean Willett
Source code modified by Dale Issler

inversion control parameters:

MONTE CARLO RANDOM SEARCH METHOD USED
number of solutions (l) = 250
number of timesteps (m) = 30
number of parameters (m+1) = 31
NUMERICAL ACCURACY (%), ACUR = 0.1000000
timestep length (delsub) = 5.000
obj fnct (2 = chi2; 3 = K-S; 4 = Kuiper) = 3
convergence tolerance (tol95) = 0.1079679
convergence tolerance (toler) = 0.0657912
number of standard deviations to fit age 2.0
measured age = 203.00
sigma of error in measured age = 9.60
number of tracks measured = 155
intermediate output every 50 forward models
random number generator seed = 13
system number generator urand(iseed)
expansion factor (alpha) = 1.300
reposition factor for explicit bound (delta) = 0.0010
original track length (xl0) 15.500
initial mean radius of length ellipse (xl3e) = 0.000
conventional mean data
empirical model of age reduction
track length reduction coefs.:
-4.86999989 0.00016800 -28.12000084 0.00000000 0.34999999
2.70000005
component variance coefs.:
0.78990000 0.00303500 -0.00229830 0.00000000

	temperature bounds		rate bounds		delt
1	50.00	200.00	15.00	0.00	10.00
2	25.00	175.00	12.50	0.00	10.00
3	25.00	150.00	10.00	0.00	10.00
4	25.00	150.00	12.50	0.00	10.00
5	25.00	125.00	11.50	0.00	10.00
6	10.00	100.00	9.00	0.00	10.00
7	10.00	25.00	0.00	4.00	10.00
8	15.00	50.00	0.00	6.00	10.00
9	25.00	100.00	0.00	8.00	10.00

10	25.00	125.00	0.00	7.50	10.00
11	25.00	125.00	7.50	0.00	10.00
12	25.00	125.00	7.50	0.00	10.00
13	25.00	100.00	8.00	0.00	10.00
14	20.00	90.00	7.00	0.00	10.00
15	20.00	80.00	6.00	0.00	10.00
16	20.00	70.00	6.00	0.00	10.00
17	10.00	55.00	4.50	0.00	10.00
18	10.00	40.00	3.00	0.00	10.00
19	10.00	25.00	0.00	3.00	10.00
20	10.00	40.00	0.00	4.00	10.00
21	10.00	50.00	4.00	4.00	10.00
22	10.00	60.00	4.00	4.00	10.00
23	10.00	60.00	4.00	4.00	10.00
24	10.00	55.00	4.00	4.00	10.00
25	10.00	55.00	4.00	4.00	10.00
26	10.00	50.00	4.00	4.00	10.00
27	10.00	50.00	4.00	4.00	10.00
28	10.00	45.00	4.00	0.00	10.00
29	10.00	45.00	4.00	0.00	10.00
30	10.00	40.00	4.00	0.00	10.00
31	10.00	25.00			

HEATING/COOLING SELECTION SUMMARY:

REGION	TIME RANGE MA	# OF EVENTS HEATING	COOLING	NHP	NCP
1	300.0- 240.0	NO	MONOTONIC	0	-1
2	240.0- 200.0	MONOTONIC	NO	-1	0
3	200.0- 120.0	NO	MONOTONIC	0	-1
4	120.0- 100.0	MONOTONIC	NO	-1	0
5	100.0- 30.0	1	MONOTONIC	1	-1
6	30.0- 0.0	NO	MONOTONIC	0	-1

NUMBER OF FORWARD RANDOM TRIALS, ITER = 269724
max obj function = 0.107965
CONVERGENCE AT 0.05 SIGNIFICANCE LEVEL
number of forward models: 250
STOP DATES - MONTH: 4 DAY: 4 YEAR: 2003

STOP TIME : 15 HR/S 29 MIN 7 S

TOTAL EXECUTION TIME = 0.706286 HOURS OR 42.3772 MINUTES

MODEL RESULTS AT .05 SIGNIFICANCE LEVEL

TIME (MY)	TIME (MA)	EXP MEAN TEMPERATURE (DEG C)	MIN OBJ TEMPERATURE (DEG C)	LOWER TEMP BOUND	UPPER TEMP BOUND
0.00	300.00	123.26	57.66	50.16	194.04
10.00	290.00	109.35	55.57	33.01	164.93
20.00	280.00	100.13	52.46	29.28	149.79
30.00	270.00	89.33	44.73	26.18	149.61
40.00	260.00	74.60	44.25	25.05	124.53
50.00	250.00	53.64	38.94	10.97	99.00
60.00	240.00	19.40	22.05	10.13	24.99
70.00	230.00	41.90	31.80	15.20	49.84
80.00	220.00	87.97	84.76	25.02	99.96
90.00	210.00	99.56	104.45	35.62	108.56
100.00	200.00	106.81	106.98	100.44	115.84
110.00	190.00	92.08	85.54	36.71	107.00
120.00	180.00	74.65	35.15	30.66	99.66
130.00	170.00	61.57	31.63	24.78	84.99
140.00	160.00	52.18	30.79	20.01	72.69
150.00	150.00	44.80	24.52	20.00	69.57
160.00	140.00	35.56	19.37	10.19	54.77
170.00	130.00	25.26	15.96	10.05	39.98
180.00	120.00	17.64	10.18	10.00	24.88
190.00	110.00	26.61	10.22	10.13	39.65
200.00	100.00	35.03	10.26	10.23	49.99
210.00	90.00	39.71	10.51	10.21	59.56
220.00	80.00	45.29	28.61	10.03	59.90
230.00	70.00	46.71	30.30	10.91	54.94
240.00	60.00	48.23	50.62	12.81	54.97
250.00	50.00	45.00	49.97	21.82	49.99
260.00	40.00	42.67	49.78	21.39	49.99
270.00	30.00	35.86	42.58	10.46	44.77
280.00	20.00	31.32	28.61	10.25	44.76
290.00	10.00	26.24	27.70	10.01	39.73
300.00	0.00	18.15	24.57	10.01	25.00

START DATE - MONTH: 4 DAY: 4 YEAR: 2003

START TIME: 15 HR/S 53 MIN 24 S

McCumber Pt 013
model 1993-2 1 hp init 15.5 apt surf

LASLETT ET AL ANNEALING MODEL FOR DURANGO APATITE

AFTINV32 v. 1.3 (AUGUST 3, 2000)
32-bit Watcom F77 v. 10.6 compiled for Windows 95
as a Windows NT windowed executable
code optimized for an Intel Pentium processor
Original source code developed by Sean Willett
Source code modified by Dale Issler

inversion control parameters:

MONTE CARLO RANDOM SEARCH METHOD USED
number of solutions (l) = 250
number of timesteps (m) = 30
number of parameters (m+1) = 31
NUMERICAL ACCURACY (%), ACUR = 0.1000000
timestep length (delsub) = 5.000
obj fnct (2 = chi2; 3 = K-S; 4 = Kuiper) = 3
convergence tolerance (tol95) = 0.1278985
convergence tolerance (toler) = 0.0779361
number of standard deviations to fit age 2.0
measured age = 207.00
sigma of error in measured age = 10.30
number of tracks measured = 110
intermediate output every 50 forward models
random number generator seed = 13
system number generator urand(iseed)
expansion factor (alpha) = 1.300
reposition factor for explicit bound (delta) = 0.0010
original track length (xl0) 15.500
initial mean radius of length ellipse (xl3e) = 0.000
conventional mean data
empirical model of age reduction
track length reduction coefs.:
-4.86999989 0.00016800 -28.12000084 0.00000000 0.34999999
2.70000005
component variance coefs.:
0.78990000 0.00303500 -0.00229830 0.00000000

	temperature bounds		rate bounds		delt
1	50.00	200.00	15.00	0.00	10.00
2	25.00	175.00	12.50	0.00	10.00
3	25.00	150.00	10.00	0.00	10.00
4	25.00	150.00	12.50	0.00	10.00
5	25.00	125.00	11.50	0.00	10.00
6	10.00	100.00	9.00	0.00	10.00
7	10.00	25.00	0.00	4.00	10.00
8	15.00	50.00	0.00	6.00	10.00
9	25.00	100.00	0.00	8.00	10.00

10	25.00	125.00	0.00	7.50	10.00
11	25.00	125.00	7.50	0.00	10.00
12	25.00	125.00	7.50	0.00	10.00
13	25.00	100.00	8.00	0.00	10.00
14	20.00	90.00	7.00	0.00	10.00
15	20.00	80.00	6.00	0.00	10.00
16	20.00	70.00	6.00	0.00	10.00
17	10.00	55.00	4.50	0.00	10.00
18	10.00	40.00	3.00	0.00	10.00
19	10.00	25.00	0.00	3.00	10.00
20	10.00	40.00	0.00	4.00	10.00
21	10.00	50.00	4.00	4.00	10.00
22	10.00	60.00	4.00	4.00	10.00
23	10.00	60.00	4.00	4.00	10.00
24	10.00	55.00	4.00	4.00	10.00
25	10.00	55.00	4.00	4.00	10.00
26	10.00	50.00	4.00	4.00	10.00
27	10.00	50.00	4.00	4.00	10.00
28	10.00	45.00	4.00	0.00	10.00
29	10.00	45.00	4.00	0.00	10.00
30	10.00	40.00	4.00	0.00	10.00
31	10.00	25.00			

HEATING/COOLING SELECTION SUMMARY:

REGION	TIME RANGE MA	# OF EVENTS HEATING	COOLING	NHP	NCP
1	300.0- 240.0	NO	MONOTONIC	0	-1
2	240.0- 200.0	MONOTONIC	NO	-1	0
3	200.0- 120.0	NO	MONOTONIC	0	-1
4	120.0- 100.0	MONOTONIC	NO	-1	0
5	100.0- 30.0	1	MONOTONIC	1	-1
6	30.0- 0.0	NO	MONOTONIC	0	-1

NUMBER OF FORWARD RANDOM TRIALS, ITER = 91279
max obj function = 0.127836
CONVERGENCE AT 0.05 SIGNIFICANCE LEVEL
number of forward models: 250
STOP DATES - MONTH: 4 DAY: 4 YEAR: 2003

STOP TIME : 16 HR/S 4 MIN 36 S

TOTAL EXECUTION TIME = 0.186700 HOURS OR 11.2020 MINUTES

MODEL RESULTS AT .05 SIGNIFICANCE LEVEL

TIME (MY)	TIME (MA)	EXP MEAN TEMPERATURE (DEG C)	MIN OBJ TEMPERATURE (DEG C)	LOWER TEMP BOUND	UPPER TEMP BOUND
0.00	300.00	123.44	130.15	50.16	199.29
10.00	290.00	110.46	124.14	33.46	167.09
20.00	280.00	99.83	122.97	28.58	148.21
30.00	270.00	89.55	97.96	26.65	134.91
40.00	260.00	72.06	90.18	25.05	121.19
50.00	250.00	50.70	81.50	10.91	97.93
60.00	240.00	19.16	17.06	10.13	24.99
70.00	230.00	42.17	49.26	15.49	49.90
80.00	220.00	88.64	84.76	25.02	99.91
90.00	210.00	99.09	91.33	33.71	108.10
100.00	200.00	106.12	112.78	98.14	119.54
110.00	190.00	89.55	54.41	37.28	105.23
120.00	180.00	73.42	53.21	26.65	99.90
130.00	170.00	59.10	26.98	22.25	89.57
140.00	160.00	50.04	24.91	20.38	77.83
150.00	150.00	41.90	22.64	20.16	65.52
160.00	140.00	33.18	21.91	11.47	53.39
170.00	130.00	24.59	16.94	10.01	39.47
180.00	120.00	16.70	15.69	10.00	24.82
190.00	110.00	23.30	26.00	10.00	39.71
200.00	100.00	30.51	26.42	10.01	49.76
210.00	90.00	34.52	28.39	10.01	59.38
220.00	80.00	40.02	31.22	10.04	59.56
230.00	70.00	42.02	32.65	10.02	54.99
240.00	60.00	43.61	49.43	10.08	54.97
250.00	50.00	41.01	49.49	10.65	49.99
260.00	40.00	39.96	47.06	10.39	49.99
270.00	30.00	35.62	32.65	10.04	44.98
280.00	20.00	31.52	26.26	10.02	44.00
290.00	10.00	26.21	23.17	10.01	39.61
300.00	0.00	17.69	17.71	10.00	24.79

START DATE - MONTH: 4 DAY: 4 YEAR: 2003

START TIME: 16 HR/S 28 MIN 6 S

Rainy Cove 045
model 1993-2 1 hp init 15.5 apt surf

LASLETT ET AL ANNEALING MODEL FOR DURANGO APATITE

AFTINV32 v. 1.3 (AUGUST 3, 2000)
32-bit Watcom F77 v. 10.6 compiled for Windows 95
as a Windows NT windowed executable
code optimized for an Intel Pentium processor
Original source code developed by Sean Willett
Source code modified by Dale Issler

inversion control parameters:

MONTE CARLO RANDOM SEARCH METHOD USED
number of solutions (l) = 250
number of timesteps (m) = 30
number of parameters (m+1) = 31
NUMERICAL ACCURACY (%), ACUR = 0.1000000
timestep length (delsub) = 5.000
obj fnct (2 = chi2; 3 = K-S; 4 = Kuiper) = 3
convergence tolerance (tol95) = 0.1151778
convergence tolerance (toler) = 0.0701846
number of standard deviations to fit age 2.0
measured age = 239.00
sigma of error in measured age = 9.00
number of tracks measured = 136
intermediate output every 50 forward models
random number generator seed = 13
system number generator urand(iseed)
expansion factor (alpha) = 1.300
reposition factor for explicit bound (delta) = 0.0010
original track length (xl0) 15.500
initial mean radius of length ellipse (xl3e) = 0.000
conventional mean data
empirical model of age reduction
track length reduction coefs.:
-4.86999989 0.00016800 -28.12000084 0.00000000 0.34999999
2.70000005
component variance coefs.:
0.78990000 0.00303500 -0.00229830 0.00000000

	temperature bounds		rate bounds		delt
1	50.00	200.00	15.00	0.00	10.00
2	25.00	175.00	12.50	0.00	10.00
3	25.00	150.00	10.00	0.00	10.00
4	25.00	150.00	12.50	0.00	10.00
5	25.00	125.00	11.50	0.00	10.00
6	10.00	100.00	9.00	0.00	10.00
7	10.00	25.00	0.00	4.00	10.00
8	15.00	50.00	0.00	6.00	10.00
9	25.00	100.00	0.00	8.00	10.00

10	25.00	125.00	0.00	7.50	10.00
11	25.00	125.00	7.50	0.00	10.00
12	25.00	125.00	7.50	0.00	10.00
13	25.00	100.00	8.00	0.00	10.00
14	20.00	90.00	7.00	0.00	10.00
15	20.00	80.00	6.00	0.00	10.00
16	20.00	70.00	6.00	0.00	10.00
17	10.00	55.00	4.50	0.00	10.00
18	10.00	40.00	3.00	0.00	10.00
19	10.00	25.00	0.00	3.00	10.00
20	10.00	40.00	0.00	4.00	10.00
21	10.00	50.00	4.00	4.00	10.00
22	10.00	60.00	4.00	4.00	10.00
23	10.00	60.00	4.00	4.00	10.00
24	10.00	55.00	4.00	4.00	10.00
25	10.00	55.00	4.00	4.00	10.00
26	10.00	50.00	4.00	4.00	10.00
27	10.00	50.00	4.00	4.00	10.00
28	10.00	45.00	4.00	0.00	10.00
29	10.00	45.00	4.00	0.00	10.00
30	10.00	40.00	4.00	0.00	10.00
31	10.00	25.00			

HEATING/COOLING SELECTION SUMMARY:

REGION	TIME RANGE MA	# OF EVENTS HEATING	COOLING	NHP	NCP
1	300.0- 240.0	NO	MONOTONIC	0	-1
2	240.0- 200.0	MONOTONIC	NO	-1	0
3	200.0- 120.0	NO	MONOTONIC	0	-1
4	120.0- 100.0	MONOTONIC	NO	-1	0
5	100.0- 30.0	1	MONOTONIC	1	-1
6	30.0- 0.0	NO	MONOTONIC	0	-1

NUMBER OF FORWARD RANDOM TRIALS, ITER = 16281
max obj function = 0.115111
CONVERGENCE AT 0.05 SIGNIFICANCE LEVEL
number of forward models: 250
STOP DATES - MONTH: 4 DAY: 4 YEAR: 2003

STOP TIME : 16 HR/S 30 MIN 17 S

TOTAL EXECUTION TIME = 0.036421 HOURS OR 2.1852 MINUTES

MODEL RESULTS AT .05 SIGNIFICANCE LEVEL

TIME (MY)	TIME (MA)	EXP MEAN TEMPERATURE (DEG C)	MIN OBJ TEMPERATURE (DEG C)	LOWER TEMP BOUND	UPPER TEMP BOUND
0.00	300.00	137.56	173.87	50.24	198.80
10.00	290.00	120.95	161.94	33.71	167.50
20.00	280.00	108.05	67.00	30.30	149.94
30.00	270.00	97.01	36.53	26.49	147.91
40.00	260.00	81.30	29.98	25.12	124.93
50.00	250.00	58.26	26.69	11.91	97.64
60.00	240.00	19.47	16.14	10.01	24.96
70.00	230.00	38.73	48.91	15.55	49.94
80.00	220.00	69.32	71.19	26.05	96.79
90.00	210.00	75.21	78.02	26.49	97.31
100.00	200.00	82.84	82.91	62.95	100.89
110.00	190.00	75.33	73.44	43.29	88.39
120.00	180.00	69.26	68.94	25.18	83.41
130.00	170.00	62.36	65.78	20.20	80.28
140.00	160.00	55.31	59.07	20.14	73.24
150.00	150.00	49.36	40.98	20.07	67.96
160.00	140.00	37.56	34.83	11.30	54.56
170.00	130.00	26.51	31.75	10.05	39.64
180.00	120.00	17.63	19.32	10.01	25.00
190.00	110.00	25.04	28.52	10.10	39.42
200.00	100.00	33.52	35.02	10.36	49.75
210.00	90.00	41.78	43.44	10.42	59.83
220.00	80.00	47.00	47.03	10.26	59.92
230.00	70.00	47.31	47.33	10.40	54.99
240.00	60.00	47.72	51.20	10.26	55.00
250.00	50.00	44.10	47.01	12.04	49.98
260.00	40.00	41.57	41.59	13.51	49.99
270.00	30.00	36.36	38.73	11.20	44.98
280.00	20.00	32.13	36.61	10.03	44.72
290.00	10.00	27.24	31.52	10.00	39.84
300.00	0.00	18.00	24.05	10.00	24.77

START DATE - MONTH: 4 DAY: 4 YEAR: 2003

START TIME: 16 HR/S 36 MIN 44 S

Partridge Island 046
model 1993-2 1 hp init 15.5 apt surf

LASLETT ET AL ANNEALING MODEL FOR DURANGO APATITE

```
 AFTINV32 v. 1.3 (AUGUST 3, 2000)
 32-bit Watcom F77 v. 10.6 compiled for Windows 95
 as a Windows NT windowed executable
 code optimized for an Intel Pentium processor
 Original source code developed by Sean Willett
 Source code modified by Dale Issler


  inversion control parameters:
 ------------------------------------------------
 ***MONTE CARLO RANDOM SEARCH METHOD USED***
 number of solutions (l) =          250
 number of timesteps (m) =           30
 number of parameters (m+1) =           31
 NUMERICAL ACCURACY (%), ACUR =        0.1000000
 timestep length (delsub) =  5.000
 obj fnct (2 = chi2; 3 = K-S; 4 = Kuiper) =            3
 convergence tolerance (tol95) =        0.1205549
 convergence tolerance (toler) =        0.0734612
 number of standard deviations to fit age 2.0
 measured age  =  210.00
 sigma of error in measured age  =   8.90
 number of tracks measured =          124
 intermediate output every           50 forward models
 random number generator seed =           13
 system number generator urand(iseed)
 expansion factor (alpha) = 1.300
 reposition factor for explicit bound (delta) = 0.0010
 original track length (xl0) 15.500
 initial mean radius of length ellipse (xl3e) =   0.000
 conventional mean data
 empirical model of age reduction
 track length reduction coefs.:
 -4.86999989   0.00016800 -28.12000084   0.00000000   0.34999999
2.70000005
 component variance coefs.:
  0.78990000   0.00303500  -0.00229830   0.00000000
```

	temperature bounds		rate bounds		delt
1	50.00	200.00	15.00	0.00	10.00
2	25.00	175.00	12.50	0.00	10.00
3	25.00	150.00	10.00	0.00	10.00
4	25.00	150.00	12.50	0.00	10.00
5	25.00	125.00	11.50	0.00	10.00
6	10.00	100.00	9.00	0.00	10.00
7	10.00	25.00	0.00	4.00	10.00
8	15.00	50.00	0.00	6.00	10.00
9	25.00	100.00	0.00	8.00	10.00

10	25.00	125.00	0.00	7.50	10.00
11	25.00	125.00	7.50	0.00	10.00
12	25.00	125.00	7.50	0.00	10.00
13	25.00	100.00	8.00	0.00	10.00
14	20.00	90.00	7.00	0.00	10.00
15	20.00	80.00	6.00	0.00	10.00
16	20.00	70.00	6.00	0.00	10.00
17	10.00	55.00	4.50	0.00	10.00
18	10.00	40.00	3.00	0.00	10.00
19	10.00	25.00	0.00	3.00	10.00
20	10.00	40.00	0.00	4.00	10.00
21	10.00	50.00	4.00	4.00	10.00
22	10.00	60.00	4.00	4.00	10.00
23	10.00	60.00	4.00	4.00	10.00
24	10.00	55.00	4.00	4.00	10.00
25	10.00	55.00	4.00	4.00	10.00
26	10.00	50.00	4.00	4.00	10.00
27	10.00	50.00	4.00	4.00	10.00
28	10.00	45.00	4.00	0.00	10.00
29	10.00	45.00	4.00	0.00	10.00
30	10.00	40.00	4.00	0.00	10.00
31	10.00	25.00			

HEATING/COOLING SELECTION SUMMARY:

REGION	TIME RANGE MA	# OF EVENTS HEATING	COOLING	NHP	NCP
1	300.0- 240.0	NO	MONOTONIC	0	-1
2	240.0- 200.0	MONOTONIC	NO	-1	0
3	200.0- 120.0	NO	MONOTONIC	0	-1
4	120.0- 100.0	MONOTONIC	NO	-1	0
5	100.0- 30.0	1	MONOTONIC	1	-1
6	30.0- 0.0	NO	MONOTONIC	0	-1

NUMBER OF FORWARD RANDOM TRIALS, ITER = 24074
max obj function = 0.120536
CONVERGENCE AT 0.05 SIGNIFICANCE LEVEL
number of forward models: 250
STOP DATES - MONTH: 4 DAY: 4 YEAR: 2003

STOP TIME : 16 HR/S 39 MIN 38 S

TOTAL EXECUTION TIME = 0.048317 HOURS OR 2.8990 MINUTES

MODEL RESULTS AT .05 SIGNIFICANCE LEVEL

TIME (MY)	TIME (MA)	EXP MEAN TEMPERATURE (DEG C)	MIN OBJ TEMPERATURE (DEG C)	LOWER TEMP BOUND	UPPER TEMP BOUND
0.00	300.00	129.95	145.76	50.00	191.74
10.00	290.00	117.34	50.57	30.06	166.69
20.00	280.00	104.99	43.87	26.35	149.83
30.00	270.00	96.66	36.71	26.01	143.90
40.00	260.00	82.14	30.22	25.10	124.50
50.00	250.00	56.87	19.47	11.54	97.93
60.00	240.00	19.03	14.97	10.03	24.94
70.00	230.00	41.21	46.92	16.24	49.94
80.00	220.00	85.64	74.59	25.40	99.91
90.00	210.00	94.65	102.21	37.54	105.77
100.00	200.00	101.52	105.52	72.98	112.65
110.00	190.00	90.23	73.18	37.48	104.71
120.00	180.00	78.40	72.56	28.18	98.18
130.00	170.00	67.60	68.67	20.65	89.52
140.00	160.00	56.78	66.09	20.35	79.15
150.00	150.00	47.47	43.49	20.22	69.86
160.00	140.00	36.33	36.33	10.86	54.53
170.00	130.00	26.62	35.45	10.51	39.68
180.00	120.00	17.75	18.68	10.00	24.91
190.00	110.00	25.28	31.82	10.01	39.95
200.00	100.00	32.46	32.69	10.01	49.94
210.00	90.00	39.19	32.80	10.01	59.94
220.00	80.00	44.09	41.36	10.23	59.99
230.00	70.00	44.46	46.00	10.15	54.97
240.00	60.00	45.09	46.50	10.11	54.98
250.00	50.00	42.23	47.83	11.85	49.98
260.00	40.00	39.93	48.43	11.40	49.99
270.00	30.00	34.74	33.22	10.05	44.97
280.00	20.00	30.77	28.96	10.03	44.74
290.00	10.00	27.02	27.39	10.00	40.00
300.00	0.00	17.62	22.91	10.00	24.95

APPENDIX C.

Apatite FT model inversion control parameters used, and resulting model temperature history summaries for the (U-Th)/He constrained thermal models for the southern Canadian Atlantic margin.

```
START DATE - MONTH:  3 DAY:  4 YEAR: 2004

START TIME: 10 HR/S   50 MIN    45 S

Martin Head 010 1 heat pulse init 15
dep at 240

LASLETT ET AL ANNEALING MODEL FOR DURANGO APATITE


 AFTINV32 v. 1.3 (AUGUST 3, 2000)
 32-bit Watcom F77 v. 10.6 compiled for Windows 95
 as a Windows NT windowed executable
 code optimized for an Intel Pentium processor
 Original source code developed by Sean Willett
 Source code modified by Dale Issler


  inversion control parameters:
 ---------------------------------------------------
 ***MONTE CARLO RANDOM SEARCH METHOD USED***
 number of solutions (l) =          250
 number of timesteps (m) =           29
 number of parameters (m+1) =           30
 NUMERICAL ACCURACY (%), ACUR =        0.1000000
 timestep length (delsub) =  2.000
 obj fnct (2 = chi2; 3 = K-S; 4 = Kuiper) =            3
 convergence tolerance (tol95) =        0.1079679
 convergence tolerance (toler) =        0.0657912
 number of standard deviations to fit age 2.0
 measured age  =  203.00
 sigma of error in measured age  =   9.60
 number of tracks measured =          155
 intermediate output every           50 forward models
 random number generator seed =           91
 system number generator urand(iseed)
 expansion factor (alpha) = 1.300
 reposition factor for explicit bound (delta) = 0.0010
 original track length (xl0) 15.000
 initial mean radius of length ellipse (xl3e) =   0.000
 conventional mean data
 empirical model of age reduction
 track length reduction coefs.:
 -4.86999989   0.00016800 -28.12000084   0.00000000   0.34999999
2.70000005
 component variance coefs.:
  0.78990000   0.00303500  -0.00229830   0.00000000

     temperature bounds         rate bounds           delt
```

1	100.00	200.00	10.00	0.00	20.00
2	0.00	180.00	18.00	0.00	10.00
3	0.00	150.00	15.00	0.00	10.00
4	0.00	120.00	12.00	0.00	10.00
5	0.00	80.00	8.00	0.00	10.00
6	0.00	20.00	0.00	5.00	10.00
7	0.00	50.00	0.00	10.00	10.00
8	0.00	100.00	0.00	12.50	10.00
9	0.00	125.00	0.00	15.00	10.00
10	0.00	150.00	15.00	0.00	10.00
11	0.00	140.00	14.00	0.00	10.00
12	0.00	120.00	12.00	0.00	10.00
13	0.00	100.00	10.00	0.00	10.00
14	0.00	90.00	9.00	0.00	10.00
15	0.00	80.00	8.00	0.00	10.00
16	0.00	60.00	6.00	0.00	10.00
17	0.00	40.00	4.00	0.00	10.00
18	0.00	20.00	0.00	3.00	10.00
19	0.00	30.00	0.00	3.90	10.00
20	0.00	39.00	3.90	4.00	10.00
21	0.00	40.00	4.00	4.80	10.00
22	0.00	48.00	4.80	4.90	10.00
23	0.00	49.00	4.90	5.00	10.00
24	0.00	50.00	5.00	4.90	10.00
25	0.00	49.00	4.90	4.80	10.00
26	0.00	48.00	4.80	4.00	10.00
27	0.00	40.00	4.00	0.00	10.00
28	0.00	39.00	3.90	0.00	10.00
29	0.00	30.00	3.00	0.00	10.00
30	0.00	20.00			

HEATING/COOLING SELECTION SUMMARY:

REGION	TIME RANGE MA	# OF EVENTS HEATING	COOLING	NHP	NCP
1	300.0- 240.0	NO	MONOTONIC	0	-1
2	240.0- 200.0	MONOTONIC	NO	-1	0
3	200.0- 120.0	NO	MONOTONIC	0	-1
4	120.0- 100.0	MONOTONIC	NO	-1	0
5	100.0- 30.0	1	MONOTONIC	1	-1
6	30.0- 0.0	NO	MONOTONIC	0	-1

NUMBER OF FORWARD RANDOM TRIALS, ITER = 246678
max obj function = 0.107855
CONVERGENCE AT 0.05 SIGNIFICANCE LEVEL
number of forward models: 250
STOP DATES - MONTH: 3 DAY: 4 YEAR: 2004

STOP TIME : 12 HR/S 22 MIN 23 S

TOTAL EXECUTION TIME = 1.527161 HOURS OR 91.6296 MINUTES

MODEL RESULTS AT .05 SIGNIFICANCE LEVEL

TIME (MY)	TIME (MA)	EXP MEAN TEMPERATURE (DEG C)	MIN OBJ TEMPERATURE (DEG C)	LOWER TEMP BOUND	UPPER TEMP BOUND
0.00	300.00	149.03	189.07	100.10	198.27
20.00	280.00	99.61	25.49	15.25	179.32
30.00	270.00	78.01	18.12	5.26	137.17
40.00	260.00	63.21	16.58	5.00	117.80
50.00	250.00	32.49	12.38	0.78	76.88
60.00	240.00	12.97	11.32	0.00	20.00
70.00	230.00	36.79	45.24	0.02	49.84
80.00	220.00	89.35	97.91	1.13	99.94
90.00	210.00	101.17	103.81	6.70	112.27
100.00	200.00	107.60	106.79	102.03	116.49
110.00	190.00	86.75	36.58	13.64	105.96
120.00	180.00	67.74	32.53	1.34	102.23
130.00	170.00	50.89	26.57	1.06	79.77
140.00	160.00	42.70	17.84	0.52	71.34
150.00	150.00	35.38	15.78	0.49	59.20
160.00	140.00	27.66	13.24	0.27	52.56
170.00	130.00	20.49	11.06	0.07	39.78
180.00	120.00	9.93	9.68	0.01	19.94
190.00	110.00	16.36	10.74	0.05	29.98
200.00	100.00	23.29	26.96	0.12	39.00
210.00	90.00	26.73	38.89	0.27	39.83
220.00	80.00	33.98	46.41	0.16	47.98
230.00	70.00	37.10	44.82	0.02	48.97
240.00	60.00	39.11	44.59	0.21	49.80
250.00	50.00	38.19	34.01	2.63	48.99
260.00	40.00	35.42	19.52	2.67	48.00
270.00	30.00	28.52	17.67	0.75	39.77
280.00	20.00	23.46	15.54	0.14	38.71
290.00	10.00	16.80	15.00	0.03	29.59
300.00	0.00	10.13	14.36	0.00	19.79

START DATE - MONTH: 3 DAY: 5 YEAR: 2004

START TIME: 9 HR/S 48 MIN 56 S

MacCumber Point 013 heat pulse, init 15 microns dep at 240

LASLETT ET AL ANNEALING MODEL FOR DURANGO APATITE

AFTINV32 v. 1.3 (AUGUST 3, 2000)
32-bit Watcom F77 v. 10.6 compiled for Windows 95
as a Windows NT windowed executable
code optimized for an Intel Pentium processor
Original source code developed by Sean Willett
Source code modified by Dale Issler

inversion control parameters:

MONTE CARLO RANDOM SEARCH METHOD USED
number of solutions (l) = 250
number of timesteps (m) = 29
number of parameters (m+1) = 30
NUMERICAL ACCURACY (%), ACUR = 0.1000000
timestep length (delsub) = 2.000
obj fnct (2 = chi2; 3 = K-S; 4 = Kuiper) = 3
convergence tolerance (tol95) = 0.1278985
convergence tolerance (toler) = 0.0779361
number of standard deviations to fit age 2.0
measured age = 207.00
sigma of error in measured age = 10.30
number of tracks measured = 110
intermediate output every 50 forward models
random number generator seed = 91
system number generator urand(iseed)
expansion factor (alpha) = 1.300
reposition factor for explicit bound (delta) = 0.0010
original track length (xl0) 15.000
initial mean radius of length ellipse (xl3e) = 0.000
conventional mean data
empirical model of age reduction
track length reduction coefs.:
-4.86999989 0.00016800 -28.12000084 0.00000000 0.34999999
2.70000005
component variance coefs.:
0.78990000 0.00303500 -0.00229830 0.00000000

	temperature bounds		rate bounds		delt
1	100.00	200.00	10.00	0.00	20.00
2	0.00	180.00	18.00	0.00	10.00
3	0.00	150.00	15.00	0.00	10.00
4	0.00	120.00	12.00	0.00	10.00
5	0.00	80.00	8.00	0.00	10.00
6	0.00	20.00	0.00	5.00	10.00
7	0.00	50.00	0.00	10.00	10.00
8	0.00	100.00	0.00	12.50	10.00
9	0.00	125.00	0.00	15.00	10.00

10	0.00	150.00	15.00	0.00	10.00
11	0.00	140.00	14.00	0.00	10.00
12	0.00	120.00	12.00	0.00	10.00
13	0.00	100.00	10.00	0.00	10.00
14	0.00	90.00	9.00	0.00	10.00
15	0.00	80.00	8.00	0.00	10.00
16	0.00	60.00	6.00	0.00	10.00
17	0.00	40.00	4.00	0.00	10.00
18	0.00	20.00	0.00	3.00	10.00
19	0.00	30.00	0.00	3.90	10.00
20	0.00	39.00	3.90	4.00	10.00
21	0.00	40.00	4.00	4.80	10.00
22	0.00	48.00	4.80	4.90	10.00
23	0.00	49.00	4.90	5.00	10.00
24	0.00	50.00	5.00	4.90	10.00
25	0.00	49.00	4.90	4.80	10.00
26	0.00	48.00	4.80	4.00	10.00
27	0.00	40.00	4.00	0.00	10.00
28	0.00	39.00	3.90	0.00	10.00
29	0.00	30.00	3.00	0.00	10.00
30	0.00	20.00			

HEATING/COOLING SELECTION SUMMARY:

REGION	TIME RANGE MA	# OF EVENTS HEATING	COOLING	NHP	NCP
1	300.0- 240.0	NO	MONOTONIC	0	-1
2	240.0- 200.0	MONOTONIC	NO	-1	0
3	200.0- 120.0	NO	MONOTONIC	0	-1
4	120.0- 100.0	MONOTONIC	NO	-1	0
5	100.0- 30.0	1	MONOTONIC	1	-1
6	30.0- 0.0	NO	MONOTONIC	0	-1

NUMBER OF FORWARD RANDOM TRIALS, ITER = 96961
max obj function = 0.127873
CONVERGENCE AT 0.05 SIGNIFICANCE LEVEL
number of forward models: 250
STOP DATES - MONTH: 3 DAY: 5 YEAR: 2004

STOP TIME : 10 HR/S 14 MIN 53 S

TOTAL EXECUTION TIME = 0.432491 HOURS OR 25.9495 MINUTES

MODEL RESULTS AT .05 SIGNIFICANCE LEVEL

TIME (MY)	TIME (MA)	EXP MEAN TEMPERATURE (DEG C)	MIN OBJ TEMPERATURE (DEG C)	LOWER TEMP BOUND	UPPER TEMP BOUND
0.00	300.00	151.37	159.07	100.25	199.16
20.00	280.00	97.66	76.43	9.94	179.32
30.00	270.00	80.04	49.38	6.05	147.37
40.00	260.00	59.27	47.13	2.94	117.00
50.00	250.00	35.79	47.04	1.58	77.60
60.00	240.00	12.57	9.02	0.08	19.97
70.00	230.00	36.77	9.66	0.28	49.96
80.00	220.00	88.44	86.09	5.17	99.96
90.00	210.00	98.78	101.04	11.01	114.59
100.00	200.00	107.04	110.16	100.37	120.84
110.00	190.00	87.48	29.87	18.49	105.79
120.00	180.00	70.65	28.19	0.89	100.57
130.00	170.00	52.43	27.50	0.68	91.19
140.00	160.00	42.27	24.11	0.56	68.65
150.00	150.00	35.11	23.80	0.20	59.75
160.00	140.00	27.41	21.19	0.06	54.25
170.00	130.00	18.97	5.20	0.01	39.78
180.00	120.00	8.16	3.25	0.00	19.65
190.00	110.00	14.60	7.92	0.01	29.99
200.00	100.00	21.22	11.72	0.02	38.42
210.00	90.00	24.73	8.83	0.03	39.91
220.00	80.00	30.49	8.31	0.02	47.98
230.00	70.00	33.22	3.58	0.02	48.97
240.00	60.00	32.80	0.05	0.05	49.37
250.00	50.00	31.42	19.35	1.49	48.44
260.00	40.00	30.23	45.80	0.89	46.66
270.00	30.00	25.81	30.18	0.06	39.49
280.00	20.00	21.28	25.01	0.02	38.21
290.00	10.00	15.84	18.46	0.01	29.85
300.00	0.00	9.26	17.20	0.00	19.99

START DATE - MONTH: 6 DAY: 22 YEAR: 2004

START TIME: 16 HR/S 25 MIN 56 S

Malpeque 021 model 2
model 2004-2 heatpulse with init len of 15 no Triassic burial

LASLETT ET AL ANNEALING MODEL FOR DURANGO APATITE

AFTINV32 v. 1.3 (AUGUST 3, 2000)
32-bit Watcom F77 v. 10.6 compiled for Windows 95
as a Windows NT windowed executable
code optimized for an Intel Pentium processor
Original source code developed by Sean Willett
Source code modified by Dale Issler

inversion control parameters:

MONTE CARLO RANDOM SEARCH METHOD USED
number of solutions (l) = 250
number of timesteps (m) = 30
number of parameters (m+1) = 31
NUMERICAL ACCURACY (%), ACUR = 0.1000000
timestep length (delsub) = 2.000
obj fnct (2 = chi2; 3 = K-S; 4 = Kuiper) = 3
convergence tolerance (tol95) = 0.1196061
convergence tolerance (toler) = 0.0728830
number of standard deviations to fit age 2.0
measured age = 247.00
sigma of error in measured age = 11.20
number of tracks measured = 126
intermediate output every 50 forward models
random number generator seed = 91
system number generator urand(iseed)
expansion factor (alpha) = 1.300
reposition factor for explicit bound (delta) = 0.0010
original track length (xl0) 15.000
initial mean radius of length ellipse (xl3e) = 0.000
conventional mean data
empirical model of age reduction
track length reduction coefs.:
-4.86999989 0.00016800 -28.12000084 0.00000000 0.34999999
2.70000005
component variance coefs.:
0.78990000 0.00303500 -0.00229830 0.00000000

	temperature bounds		rate bounds		delt
1	100.00	150.00	10.00	0.00	10.00
2	50.00	150.00	15.00	0.00	10.00
3	0.00	100.00	10.00	0.00	10.00
4	0.00	20.00	0.00	5.00	10.00
5	0.00	50.00	0.00	10.00	10.00
6	0.00	100.00	0.00	15.00	10.00
7	0.00	150.00	15.00	0.00	10.00
8	0.00	140.00	14.00	0.00	10.00
9	0.00	130.00	13.00	0.00	10.00

10	0.00	120.00	12.00	0.00	10.00
11	0.00	110.00	11.00	0.00	10.00
12	0.00	100.00	10.00	0.00	10.00
13	0.00	90.00	9.00	0.00	10.00
14	0.00	80.00	8.00	0.00	10.00
15	0.00	75.00	7.50	0.00	10.00
16	0.00	70.00	7.00	0.00	10.00
17	0.00	65.00	6.50	0.00	10.00
18	0.00	60.00	6.00	0.00	10.00
19	0.00	20.00	0.00	3.00	10.00
20	0.00	30.00	0.00	4.00	10.00
21	0.00	40.00	4.00	5.00	10.00
22	0.00	50.00	5.00	5.00	10.00
23	0.00	50.00	5.00	5.00	10.00
24	0.00	50.00	5.00	5.00	10.00
25	0.00	50.00	5.00	5.00	10.00
26	0.00	50.00	5.00	5.00	10.00
27	0.00	50.00	5.00	5.00	10.00
28	0.00	50.00	5.00	0.00	10.00
29	0.00	40.00	4.00	0.00	10.00
30	0.00	30.00	3.00	0.00	10.00
31	0.00	20.00			

HEATING/COOLING SELECTION SUMMARY:

REGION	TIME RANGE MA	# OF EVENTS HEATING	COOLING	NHP	NCP
1	300.0- 270.0	NO	MONOTONIC	0	-1
2	270.0- 240.0	MONOTONIC	NO	-1	0
3	240.0- 120.0	NO	MONOTONIC	0	-1
4	120.0- 100.0	MONOTONIC	NO	-1	0
5	100.0- 30.0	1	MONOTONIC	1	-1
6	30.0- 0.0	NO	MONOTONIC	0	-1

NUMBER OF FORWARD RANDOM TRIALS, ITER = 2331
max obj function = 0.119440
CONVERGENCE AT 0.05 SIGNIFICANCE LEVEL
number of forward models: 250
STOP DATES - MONTH: 6 DAY: 22 YEAR: 2004

STOP TIME : 16 HR/S 26 MIN 41 S

TOTAL EXECUTION TIME = 0.012459 HOURS OR 0.7475 MINUTES

MODEL RESULTS AT .05 SIGNIFICANCE LEVEL

TIME (MY)	TIME (MA)	EXP MEAN TEMPERATURE (DEG C)	MIN OBJ TEMPERATURE (DEG C)	LOWER TEMP BOUND	UPPER TEMP BOUND
0.00	300.00	124.80	126.53	100.14	149.85
10.00	290.00	104.41	121.30	50.19	149.37
20.00	280.00	52.27	25.71	0.87	97.72
30.00	270.00	12.16	19.41	0.00	19.95
40.00	260.00	37.30	41.91	0.25	49.96
50.00	250.00	73.81	72.20	1.92	99.19
60.00	240.00	83.47	73.40	7.46	114.86
70.00	230.00	75.26	71.44	4.63	101.33
80.00	220.00	67.60	64.69	1.14	93.23
90.00	210.00	60.61	52.85	0.24	88.64
100.00	200.00	53.50	45.28	0.03	81.64
110.00	190.00	47.26	37.75	0.02	67.92
120.00	180.00	41.47	31.28	0.00	67.68
130.00	170.00	36.68	21.78	0.00	58.47
140.00	160.00	31.55	14.26	0.00	57.35
150.00	150.00	26.62	10.04	0.00	55.55
160.00	140.00	21.22	8.86	0.00	55.13
170.00	130.00	16.06	5.95	0.00	52.29
180.00	120.00	8.02	0.32	0.00	19.79
190.00	110.00	15.04	0.60	0.01	29.87
200.00	100.00	23.28	2.91	0.01	39.36
210.00	90.00	30.77	4.45	0.01	49.97
220.00	80.00	34.86	4.55	0.02	49.98
230.00	70.00	37.65	5.35	0.19	50.00
240.00	60.00	38.82	6.39	0.26	49.99
250.00	50.00	38.63	10.62	0.14	49.99
260.00	40.00	36.48	26.64	0.12	49.97
270.00	30.00	33.30	49.52	0.07	49.99
280.00	20.00	25.86	36.47	0.05	39.79
290.00	10.00	16.96	22.98	0.05	29.97
300.00	0.00	10.41	11.93	0.02	19.95

START DATE - MONTH: 3 DAY: 3 YEAR: 2004

START TIME: 22 HR/S 11 MIN 48 S

Digby D-1 60.7 m, limit upper T to 50 C after 100 Ma
Model 2004-1 1 heat pulse with 15.0 initial length

LASLETT ET AL ANNEALING MODEL FOR DURANGO APATITE

AFTINV32 v. 1.3 (AUGUST 3, 2000)
32-bit Watcom F77 v. 10.6 compiled for Windows 95
as a Windows NT windowed executable
code optimized for an Intel Pentium processor
Original source code developed by Sean Willett
Source code modified by Dale Issler

inversion control parameters:

```
***MONTE CARLO RANDOM SEARCH METHOD USED***
number of solutions (l) =          250
number of timesteps (m) =           35
number of parameters (m+1) =           36
NUMERICAL ACCURACY (%), ACUR =        0.1000000
timestep length (delsub) =  2.000
obj fnct (2 = chi2; 3 = K-S; 4 = Kuiper) =            3
convergence tolerance (tol95) =        0.0999941
convergence tolerance (toler) =        0.0609323
number of standard deviations to fit age 2.0
measured age  =  244.00
sigma of error in measured age  =   7.20
number of tracks measured =          181
intermediate output every           50 forward models
random number generator seed =           91
system number generator urand(iseed)
expansion factor (alpha) = 1.300
reposition factor for explicit bound (delta) = 0.0010
original track length (xl0) 15.000
initial mean radius of length ellipse (xl3e) =   0.000
conventional mean data
empirical model of age reduction
track length reduction coefs.:
-4.86999989   0.00016800 -28.12000084   0.00000000   0.34999999
2.70000005
component variance coefs.:
 0.78990000   0.00303500  -0.00229830   0.00000000
```

	temperature bounds		rate bounds		delt
1	0.00	200.00	19.00	0.00	10.00
2	0.00	50.00	0.00	9.00	10.00
3	0.00	100.00	0.00	11.50	10.00
4	30.00	125.00	0.00	12.00	10.00
5	50.00	150.00	0.00	10.00	10.00
6	100.00	150.00	5.00	0.00	10.00
7	100.00	150.00	10.00	0.00	10.00
8	50.00	125.00	7.50	0.00	10.00
9	50.00	125.00	7.50	0.00	10.00

10	50.00	125.00	9.50	0.00	10.00
11	25.00	100.00	9.00	0.00	10.00
12	0.00	100.00	0.00	9.00	10.00
13	0.00	100.00	0.00	9.00	10.00
14	0.00	100.00	0.00	9.00	10.00
15	0.00	100.00	0.00	9.00	10.00
16	0.00	100.00	9.00	0.00	10.00
17	0.00	90.00	8.00	0.00	10.00
18	0.00	85.00	7.50	0.00	10.00
19	0.00	80.00	7.00	0.00	10.00
20	0.00	75.00	7.00	0.00	10.00
21	0.00	70.00	6.50	0.00	10.00
22	0.00	65.00	6.00	0.00	10.00
23	0.00	60.00	5.50	0.00	10.00
24	0.00	20.00	0.00	2.50	10.00
25	0.00	30.00	0.00	3.00	10.00
26	0.00	40.00	3.00	5.00	10.00
27	0.00	50.00	5.00	5.00	10.00
28	0.00	50.00	5.00	4.50	10.00
29	0.00	50.00	4.50	4.50	10.00
30	0.00	50.00	4.50	4.00	10.00
31	0.00	50.00	4.00	4.00	10.00
32	0.00	50.00	4.00	3.50	10.00
33	0.00	50.00	3.50	0.00	10.00
34	0.00	40.00	3.50	0.00	10.00
35	0.00	30.00	3.00	0.00	10.00
36	0.00	20.00			

HEATING/COOLING SELECTION SUMMARY:

REGION	TIME RANGE MA	# OF EVENTS HEATING	COOLING	NHP	NCP
1	350.0- 340.0	NO	MONOTONIC	0	-1
2	340.0- 300.0	MONOTONIC	NO	-1	0
3	300.0- 240.0	NO	MONOTONIC	0	-1
4	240.0- 200.0	MONOTONIC	NO	-1	0
5	200.0- 120.0	NO	MONOTONIC	0	-1
6	120.0- 100.0	MONOTONIC	NO	-1	0
7	100.0- 30.0	1	MONOTONIC	1	-1
8	30.0- 0.0	NO	MONOTONIC	0	-1

NUMBER OF FORWARD RANDOM TRIALS, ITER = 5968
max obj function = 0.099824
CONVERGENCE AT 0.05 SIGNIFICANCE LEVEL
number of forward models: 250
STOP DATES - MONTH: 3 DAY: 3 YEAR: 2004

STOP TIME : 22 HR/S 14 MIN 36 S

TOTAL EXECUTION TIME = 0.046633 HOURS OR 2.7980 MINUTES

MODEL RESULTS AT .05 SIGNIFICANCE LEVEL

TIME (MY)	TIME (MA)	EXP MEAN TEMPERATURE (DEG C)	MIN OBJ TEMPERATURE (DEG C)	LOWER TEMP BOUND	UPPER TEMP BOUND
0.00	350.00	94.90	57.49	1.05	192.62
10.00	340.00	37.00	48.40	0.17	49.65
20.00	330.00	84.23	75.61	2.69	99.89
30.00	320.00	105.66	113.62	30.30	124.89
40.00	310.00	117.96	119.11	50.25	147.12
50.00	300.00	125.25	128.97	101.82	149.91
60.00	290.00	118.86	122.66	100.12	149.89
70.00	280.00	92.65	66.68	51.13	124.20
80.00	270.00	84.16	63.51	50.59	117.96
90.00	260.00	75.01	61.43	50.08	100.22
100.00	250.00	64.89	32.04	26.35	97.34
110.00	240.00	52.87	28.51	1.00	74.07
120.00	230.00	58.50	59.39	1.83	76.89
130.00	220.00	63.69	60.27	7.91	88.31
140.00	210.00	69.53	72.63	19.72	89.44
150.00	200.00	75.56	73.20	45.45	92.47
160.00	190.00	68.58	67.06	36.04	81.31
170.00	180.00	61.35	62.41	5.55	75.64
180.00	170.00	55.56	59.82	3.46	70.71
190.00	160.00	49.66	59.07	0.02	67.85
200.00	150.00	43.57	53.50	0.01	64.46
210.00	140.00	36.03	38.51	0.01	60.89
220.00	130.00	28.77	17.66	0.01	53.47
230.00	120.00	11.05	12.08	0.00	20.00
240.00	110.00	16.66	22.99	0.03	29.58
250.00	100.00	25.69	31.27	0.05	39.60
260.00	90.00	33.68	49.05	0.06	50.00
270.00	80.00	38.53	48.62	0.18	50.00
280.00	70.00	41.19	37.75	0.06	49.99
290.00	60.00	42.18	35.99	3.04	49.99
300.00	50.00	41.46	34.65	7.05	49.99
310.00	40.00	40.01	29.38	3.33	50.00
320.00	30.00	36.83	29.00	0.25	50.00
330.00	20.00	28.09	26.30	0.20	39.91
340.00	10.00	19.45	21.05	0.13	29.86
350.00	0.00	11.68	18.56	0.02	19.96

START DATE - MONTH: 3 DAY: 9 YEAR: 2004

START TIME: 15 HR/S 45 MIN 48 S

PE-143 Mahone Bay
model 2004-1 hp init 15

LASLETT ET AL ANNEALING MODEL FOR DURANGO APATITE

AFTINV32 v. 1.3 (AUGUST 3, 2000)
32-bit Watcom F77 v. 10.6 compiled for Windows 95
as a Windows NT windowed executable
code optimized for an Intel Pentium processor
Original source code developed by Sean Willett
Source code modified by Dale Issler

inversion control parameters:

MONTE CARLO RANDOM SEARCH METHOD USED
number of solutions (l) = 250
number of timesteps (m) = 35
number of parameters (m+1) = 36
NUMERICAL ACCURACY (%), ACUR = 0.1000000
timestep length (delsub) = 2.000
obj fnct (2 = chi2; 3 = K-S; 4 = Kuiper) = 3
convergence tolerance (tol95) = 0.1072855
convergence tolerance (toler) = 0.0653754
number of standard deviations to fit age 2.0
measured age = 217.00
sigma of error in measured age = 6.50
number of tracks measured = 157
intermediate output every 50 forward models
random number generator seed = 91
system number generator urand(iseed)
expansion factor (alpha) = 1.300
reposition factor for explicit bound (delta) = 0.0010
original track length (xl0) 15.000
initial mean radius of length ellipse (xl3e) = 0.000
conventional mean data
empirical model of age reduction
track length reduction coefs.:
-4.86999989 0.00016800 -28.12000084 0.00000000 0.34999999
2.70000005
component variance coefs.:
0.78990000 0.00303500 -0.00229830 0.00000000

	temperature bounds		rate bounds		delt
1	0.00	200.00	20.00	0.00	10.00
2	0.00	50.00	0.00	10.00	10.00
3	0.00	100.00	0.00	12.50	10.00
4	30.00	125.00	0.00	12.00	10.00
5	50.00	150.00	0.00	10.00	10.00
6	100.00	150.00	5.00	0.00	10.00
7	100.00	149.00	9.90	0.00	10.00
8	50.00	140.00	9.00	0.00	10.00
9	50.00	130.00	8.00	0.00	10.00

10	50.00	125.00	12.50	0.00	10.00
11	0.00	125.00	12.50	0.00	10.00
12	0.00	120.00	12.00	0.00	10.00
13	0.00	120.00	12.00	0.00	10.00
14	0.00	110.00	11.00	0.00	10.00
15	0.00	110.00	11.00	0.00	10.00
16	0.00	100.00	10.00	0.00	10.00
17	0.00	90.00	9.00	0.00	10.00
18	0.00	85.00	8.50	0.00	10.00
19	0.00	80.00	8.00	0.00	10.00
20	0.00	75.00	7.50	0.00	10.00
21	0.00	70.00	7.00	0.00	10.00
22	0.00	65.00	6.50	0.00	10.00
23	0.00	60.00	6.00	0.00	10.00
24	0.00	20.00	0.00	3.00	10.00
25	0.00	30.00	0.00	4.00	10.00
26	0.00	40.00	4.00	4.90	10.00
27	0.00	49.00	4.90	5.00	10.00
28	0.00	50.00	4.50	5.00	10.00
29	5.00	50.00	5.00	4.50	10.00
30	0.00	50.00	5.00	5.00	10.00
31	0.00	50.00	5.00	5.00	10.00
32	0.00	50.00	5.00	4.90	10.00
33	0.00	49.00	4.90	0.00	10.00
34	0.00	40.00	4.00	0.00	10.00
35	0.00	30.00	3.00	0.00	10.00
36	0.00	20.00			

HEATING/COOLING SELECTION SUMMARY:

REGION	TIME RANGE MA	# OF EVENTS HEATING	COOLING	NHP	NCP
1	350.0- 340.0	NO	MONOTONIC	0	-1
2	340.0- 300.0	MONOTONIC	NO	-1	0
3	300.0- 120.0	NO	MONOTONIC	0	-1
4	120.0- 100.0	MONOTONIC	NO	-1	0
5	100.0- 30.0	1	MONOTONIC	1	-1
6	30.0- 0.0	NO	MONOTONIC	0	-1

NUMBER OF FORWARD RANDOM TRIALS, ITER = 7996
max obj function = 0.107189
CONVERGENCE AT 0.05 SIGNIFICANCE LEVEL
number of forward models: 250
STOP DATES - MONTH: 3 DAY: 9 YEAR: 2004

STOP TIME : 15 HR/S 48 MIN 47 S

TOTAL EXECUTION TIME = 0.049719 HOURS OR 2.9831 MINUTES

MODEL RESULTS AT .05 SIGNIFICANCE LEVEL

TIME (MY)	TIME (MA)	EXP MEAN TEMPERATURE (DEG C)	MIN OBJ TEMPERATURE (DEG C)	LOWER TEMP BOUND	UPPER TEMP BOUND
0.00	350.00	72.92	29.17	1.57	160.16
10.00	340.00	37.47	24.26	0.87	49.96
20.00	330.00	84.85	98.65	1.47	99.86
30.00	320.00	111.41	107.18	31.66	124.98
40.00	310.00	129.05	135.51	57.07	147.56
50.00	300.00	136.78	141.95	109.76	149.92
60.00	290.00	131.83	139.64	108.44	148.60
70.00	280.00	125.94	120.13	103.80	139.71
80.00	270.00	120.44	118.33	102.36	129.99
90.00	260.00	116.48	116.76	101.19	124.97
100.00	250.00	112.62	115.51	97.98	124.94
110.00	240.00	106.64	109.53	75.34	119.72
120.00	230.00	99.93	104.38	29.14	119.33
130.00	220.00	88.71	100.88	14.05	109.28
140.00	210.00	77.88	27.30	4.40	102.79
150.00	200.00	65.57	23.18	4.25	94.32
160.00	190.00	54.48	18.64	0.98	86.15
170.00	180.00	45.72	13.36	0.15	67.00
180.00	170.00	38.41	2.46	0.15	57.25
190.00	160.00	32.88	0.58	0.01	52.07
200.00	150.00	27.16	0.22	0.01	49.11
210.00	140.00	22.27	0.12	0.00	45.68
220.00	130.00	16.64	0.08	0.00	40.12
230.00	120.00	8.28	0.04	0.00	19.97
240.00	110.00	15.18	15.20	0.04	29.86
250.00	100.00	22.53	23.45	0.04	39.37
260.00	90.00	26.18	27.78	0.17	48.41
270.00	80.00	28.69	35.49	0.14	49.94
280.00	70.00	27.85	39.76	2.00	47.18
290.00	60.00	25.33	30.63	0.00	47.73
300.00	50.00	22.47	26.65	0.00	42.21
310.00	40.00	19.18	21.54	0.00	37.35
320.00	30.00	17.42	16.42	0.00	37.09
330.00	20.00	13.38	8.24	0.00	33.29
340.00	10.00	9.52	5.81	0.00	28.88
350.00	0.00	6.20	5.01	0.00	19.82

START DATE - MONTH: 3 DAY: 9 YEAR: 2004

START TIME: 22 HR/S 0 MIN 3 S

FT95-063 Halifax
model 2004-1 hp init 15

LASLETT ET AL ANNEALING MODEL FOR DURANGO APATITE

AFTINV32 v. 1.3 (AUGUST 3, 2000)
32-bit Watcom F77 v. 10.6 compiled for Windows 95
as a Windows NT windowed executable
code optimized for an Intel Pentium processor
Original source code developed by Sean Willett
Source code modified by Dale Issler

inversion control parameters:

MONTE CARLO RANDOM SEARCH METHOD USED
number of solutions (l) = 250
number of timesteps (m) = 35
number of parameters (m+1) = 36
NUMERICAL ACCURACY (%), ACUR = 0.1000000
timestep length (delsub) = 2.000
obj fnct (2 = chi2; 3 = K-S; 4 = Kuiper) = 3
convergence tolerance (tol95) = 0.1090165
convergence tolerance (toler) = 0.0664301
number of standard deviations to fit age 2.0
measured age = 205.60
sigma of error in measured age = 6.20
number of tracks measured = 152
intermediate output every 50 forward models
random number generator seed = 91
system number generator urand(iseed)
expansion factor (alpha) = 1.300
reposition factor for explicit bound (delta) = 0.0010
original track length (xl0) 15.000
initial mean radius of length ellipse (xl3e) = 0.000
conventional mean data
empirical model of age reduction
track length reduction coefs.:
-4.86999989 0.00016800 -28.12000084 0.00000000 0.34999999
2.70000005
component variance coefs.:
0.78990000 0.00303500 -0.00229830 0.00000000

	temperature bounds		rate bounds		delt
1	0.00	200.00	20.00	0.00	10.00
2	0.00	50.00	0.00	10.00	10.00
3	0.00	100.00	0.00	12.50	10.00
4	30.00	125.00	0.00	12.00	10.00
5	50.00	150.00	0.00	10.00	10.00
6	100.00	150.00	5.00	0.00	10.00
7	100.00	149.00	9.90	0.00	10.00
8	50.00	140.00	9.00	0.00	10.00
9	50.00	130.00	8.00	0.00	10.00

10	50.00	125.00	12.50	0.00	10.00
11	0.00	125.00	12.50	0.00	10.00
12	0.00	120.00	12.00	0.00	10.00
13	0.00	120.00	12.00	0.00	10.00
14	0.00	110.00	11.00	0.00	10.00
15	0.00	110.00	11.00	0.00	10.00
16	0.00	100.00	10.00	0.00	10.00
17	0.00	90.00	9.00	0.00	10.00
18	0.00	85.00	8.50	0.00	10.00
19	0.00	80.00	8.00	0.00	10.00
20	0.00	75.00	7.50	0.00	10.00
21	0.00	70.00	7.00	0.00	10.00
22	0.00	65.00	6.50	0.00	10.00
23	0.00	60.00	6.00	0.00	10.00
24	0.00	20.00	0.00	3.00	10.00
25	0.00	30.00	0.00	4.00	10.00
26	0.00	40.00	4.00	4.90	10.00
27	0.00	49.00	4.90	5.00	10.00
28	0.00	50.00	4.50	5.00	10.00
29	5.00	50.00	5.00	4.50	10.00
30	0.00	50.00	5.00	5.00	10.00
31	0.00	50.00	5.00	5.00	10.00
32	0.00	50.00	5.00	4.90	10.00
33	0.00	49.00	4.90	0.00	10.00
34	0.00	40.00	4.00	0.00	10.00
35	0.00	30.00	3.00	0.00	10.00
36	0.00	20.00			

HEATING/COOLING SELECTION SUMMARY:

REGION	TIME RANGE MA	# OF EVENTS HEATING	COOLING	NHP	NCP
1	350.0- 340.0	NO	MONOTONIC	0	-1
2	340.0- 300.0	MONOTONIC	NO	-1	0
3	300.0- 120.0	NO	MONOTONIC	0	-1
4	120.0- 100.0	MONOTONIC	NO	-1	0
5	100.0- 30.0	1	MONOTONIC	1	-1
6	30.0- 0.0	NO	MONOTONIC	0	-1

NUMBER OF FORWARD RANDOM TRIALS, ITER = 4661
max obj function = 0.108874
CONVERGENCE AT 0.05 SIGNIFICANCE LEVEL
number of forward models: 250
STOP DATES - MONTH: 3 DAY: 9 YEAR: 2004

STOP TIME : 22 HR/S 1 MIN 47 S

TOTAL EXECUTION TIME = 0.029011 HOURS OR 1.7406 MINUTES

MODEL RESULTS AT .05 SIGNIFICANCE LEVEL

TIME (MY)	TIME (MA)	EXP MEAN TEMPERATURE (DEG C)	MIN OBJ TEMPERATURE (DEG C)	LOWER TEMP BOUND	UPPER TEMP BOUND
0.00	350.00	90.30	36.41	0.90	181.76
10.00	340.00	36.70	31.62	0.35	49.97
20.00	330.00	83.56	71.96	3.06	99.51
30.00	320.00	110.38	124.82	30.11	124.93
40.00	310.00	128.49	129.52	51.68	148.14
50.00	300.00	136.77	132.40	111.56	149.71
60.00	290.00	131.81	128.58	107.62	148.95
70.00	280.00	126.02	127.65	107.08	139.56
80.00	270.00	121.07	126.52	104.43	129.92
90.00	260.00	117.07	120.17	102.34	124.93
100.00	250.00	113.80	118.72	97.30	124.91
110.00	240.00	109.25	118.21	89.37	119.69
120.00	230.00	104.19	109.78	75.63	119.29
130.00	220.00	96.30	97.78	54.70	109.42
140.00	210.00	88.62	91.95	0.81	108.52
150.00	200.00	79.33	58.27	0.50	98.60
160.00	190.00	70.33	56.44	0.05	89.62
170.00	180.00	61.95	49.88	0.04	83.48
180.00	170.00	53.46	45.84	0.03	76.06
190.00	160.00	46.65	33.00	0.02	70.88
200.00	150.00	39.80	32.38	0.02	64.53
210.00	140.00	32.01	27.06	0.02	60.60
220.00	130.00	24.54	26.02	0.01	58.17
230.00	120.00	10.11	19.61	0.00	19.90
240.00	110.00	17.06	24.97	0.00	29.99
250.00	100.00	24.96	28.04	0.01	39.87
260.00	90.00	32.18	29.27	0.01	48.98
270.00	80.00	35.95	47.12	0.16	49.81
280.00	70.00	37.29	43.67	5.01	49.59
290.00	60.00	35.86	41.59	5.01	49.99
300.00	50.00	35.14	39.08	1.07	49.95
310.00	40.00	33.21	37.92	0.37	49.76
320.00	30.00	29.48	23.58	0.16	48.13
330.00	20.00	22.56	22.35	0.13	39.36
340.00	10.00	16.14	11.73	0.11	29.86
350.00	0.00	9.86	11.21	0.03	19.90

APPENDIX D.

Apatite FT model inversion control parameters used, and resulting model temperature history summaries for the eastern Ellesmere Island, Nares Strait, Kane Basin, and western Greenland outcrop samples.

```
START DATE - MONTH:  1 DAY: 30 YEAR: 2004

START TIME: 10 HR/S   18 MIN     0 S

Na-03 Nares Devon Island gneiss
test 15.0 heat pulse

LASLETT ET AL ANNEALING MODEL FOR DURANGO APATITE

  AFTINV32 v. 1.3 (AUGUST 3, 2000)
 32-bit Watcom F77 v. 10.6 compiled for Windows 95
 as a Windows NT windowed executable
 code optimized for an Intel Pentium processor
 Original source code developed by Sean Willett
 Source code modified by Dale Issler

   inversion control parameters:
 --------------------------------------------------
 ***MONTE CARLO RANDOM SEARCH METHOD USED***
 number of solutions (l) =          250
 number of timesteps (m) =           19
 number of parameters (m+1) =           20
 NUMERICAL ACCURACY (%), ACUR =        0.1000000
 timestep length (delsub) =  2.000
 obj fnct (2 = chi2; 3 = K-S; 4 = Kuiper) =            3
 convergence tolerance (tol95) =        0.1151778
 convergence tolerance (toler) =        0.0701846
 number of standard deviations to fit age 2.0
 measured age  =  207.00
 sigma of error in measured age  =   7.20
 number of tracks measured =          136
 intermediate output every           50 forward models
 random number generator seed =           91
 system number generator urand(iseed)
 expansion factor (alpha) = 1.300
 reposition factor for explicit bound (delta) = 0.0010
 original track length (xl0) 15.000
 initial mean radius of length ellipse (xl3e) =   0.000
 conventional mean data
 empirical model of age reduction
 track length reduction coefs.:
 -4.86999989   0.00016800 -28.12000084   0.00000000   0.34999999
2.70000005
 component variance coefs.:
  0.78990000   0.00303500  -0.00229830   0.00000000

      temperature bounds          rate bounds           delt
   1        0.00      200.00       10.00        0.00       20.00
   2        0.00      200.00       10.00        0.00       20.00
```

3	0.00	200.00	10.00	0.00	20.00
4	0.00	200.00	10.00	0.00	20.00
5	0.00	200.00	10.00	0.00	20.00
6	0.00	200.00	10.00	0.00	20.00
7	0.00	200.00	10.00	0.00	20.00
8	0.00	200.00	10.00	0.00	20.00
9	0.00	200.00	10.00	0.00	20.00
10	0.00	175.00	8.75	0.00	20.00
11	0.00	150.00	7.50	0.00	20.00
12	0.00	125.00	6.25	0.00	20.00
13	0.00	100.00	5.00	0.00	20.00
14	0.00	100.00	5.00	5.00	20.00
15	0.00	100.00	5.00	4.00	20.00
16	0.00	80.00	4.00	3.00	20.00
17	0.00	60.00	3.00	2.00	20.00
18	0.00	40.00	2.00	0.00	20.00
19	0.00	20.00	1.00	0.00	20.00
20	0.00	5.00			

HEATING/COOLING SELECTION SUMMARY:

REGION	TIME RANGE MA	# OF EVENTS HEATING	COOLING	NHP	NCP
1	380.0- 120.0	NO	MONOTONIC	0	-1
2	120.0- 40.0	1	MONOTONIC	1	-1
3	40.0- 0.0	NO	MONOTONIC	0	-1

NUMBER OF FORWARD RANDOM TRIALS, ITER = 10261
max obj function = 0.115028
CONVERGENCE AT 0.05 SIGNIFICANCE LEVEL
number of forward models: 250
STOP DATES - MONTH: 1 DAY: 30 YEAR: 2004

STOP TIME : 10 HR/S 21 MIN 5 S

TOTAL EXECUTION TIME = 0.051403 HOURS OR 3.0842 MINUTES

MODEL RESULTS AT .05 SIGNIFICANCE LEVEL

TIME (MY)	TIME (MA)	EXP MEAN TEMPERATURE (DEG C)	MIN OBJ TEMPERATURE (DEG C)	LOWER TEMP BOUND	UPPER TEMP BOUND
0.00	380.00	187.53	199.73	124.99	200.00
20.00	360.00	182.90	199.71	118.66	199.99
40.00	340.00	177.04	194.63	117.28	199.99
60.00	320.00	169.95	186.10	110.46	199.88
80.00	300.00	161.37	178.89	105.16	199.75
100.00	280.00	152.18	175.93	97.32	199.74
120.00	260.00	140.28	158.64	92.99	198.59
140.00	240.00	117.95	91.97	63.20	194.95
160.00	220.00	89.10	76.56	14.11	105.70
180.00	200.00	78.60	75.44	9.58	95.44
200.00	180.00	69.57	69.27	4.03	86.33
220.00	160.00	61.17	61.65	0.05	78.66
240.00	140.00	53.35	61.32	0.04	72.06
260.00	120.00	45.45	50.63	0.02	68.25
280.00	100.00	50.54	54.39	0.04	77.35
300.00	80.00	56.04	43.91	2.47	79.03
320.00	60.00	46.93	38.01	3.26	59.98
340.00	40.00	27.30	29.39	0.07	39.59
360.00	20.00	11.86	20.00	0.02	20.00
380.00	0.00	2.35	4.73	0.01	4.98

START DATE - MONTH: 2 DAY: 2 YEAR: 2004

START TIME: 23 HR/S 10 MIN 55 S

Na-04 Devon Island gneiss
test 15.0 1 heat pulse

LASLETT ET AL ANNEALING MODEL FOR DURANGO APATITE

AFTINV32 v. 1.3 (AUGUST 3, 2000)
32-bit Watcom F77 v. 10.6 compiled for Windows 95
as a Windows NT windowed executable
code optimized for an Intel Pentium processor
Original source code developed by Sean Willett
Source code modified by Dale Issler

inversion control parameters:

MONTE CARLO RANDOM SEARCH METHOD USED
number of solutions (l) = 250
number of timesteps (m) = 19
number of parameters (m+1) = 20
NUMERICAL ACCURACY (%), ACUR = 0.1000000
timestep length (delsub) = 2.000
obj fnct (2 = chi2; 3 = K-S; 4 = Kuiper) = 3
convergence tolerance (tol95) = 0.1056348
convergence tolerance (toler) = 0.0643694
number of standard deviations to fit age 2.0
measured age = 191.00
sigma of error in measured age = 8.90
number of tracks measured = 162
intermediate output every 50 forward models
random number generator seed = 91
system number generator urand(iseed)
expansion factor (alpha) = 1.300
reposition factor for explicit bound (delta) = 0.0010
original track length (xl0) 15.000
initial mean radius of length ellipse (xl3e) = 0.000
conventional mean data
empirical model of age reduction
track length reduction coefs.:
-4.86999989 0.00016800 -28.12000084 0.00000000 0.34999999
2.70000005
component variance coefs.:
0.78990000 0.00303500 -0.00229830 0.00000000

	temperature bounds		rate bounds		delt
1	0.00	200.00	10.00	0.00	20.00
2	0.00	200.00	10.00	0.00	20.00
3	0.00	200.00	10.00	0.00	20.00
4	0.00	200.00	10.00	0.00	20.00
5	0.00	200.00	10.00	0.00	20.00
6	0.00	200.00	10.00	0.00	20.00
7	0.00	200.00	10.00	0.00	20.00
8	0.00	200.00	10.00	0.00	20.00
9	0.00	200.00	10.00	0.00	20.00
10	0.00	175.00	8.75	0.00	20.00
11	0.00	150.00	7.50	0.00	20.00
12	0.00	125.00	6.25	0.00	20.00
13	0.00	100.00	5.00	0.00	20.00
14	0.00	100.00	5.00	5.00	20.00

15	0.00	100.00	5.00	4.00	20.00
16	0.00	80.00	4.00	3.00	20.00
17	0.00	60.00	3.00	2.00	20.00
18	0.00	40.00	2.00	0.00	20.00
19	0.00	20.00	1.00	0.00	20.00
20	0.00	5.00			

HEATING/COOLING SELECTION SUMMARY:

REGION	TIME RANGE MA	# OF EVENTS HEATING	COOLING	NHP	NCP
1	380.0- 120.0	NO	MONOTONIC	0	-1
2	120.0- 40.0	1	MONOTONIC	1	-1
3	40.0- 0.0	NO	MONOTONIC	0	-1

NUMBER OF FORWARD RANDOM TRIALS, ITER = 9062
max obj function = 0.105579
CONVERGENCE AT 0.05 SIGNIFICANCE LEVEL
number of forward models: 250
STOP DATES - MONTH: 2 DAY: 2 YEAR: 2004

STOP TIME : 23 HR/S 14 MIN 13 S

TOTAL EXECUTION TIME = 0.054884 HOURS OR 3.2930 MINUTES

MODEL RESULTS AT .05 SIGNIFICANCE LEVEL

TIME (MY)	TIME (MA)	EXP MEAN TEMPERATURE (DEG C)	MIN OBJ TEMPERATURE (DEG C)	LOWER TEMP BOUND	UPPER TEMP BOUND
0.00	380.00	188.77	198.78	138.91	200.00
20.00	360.00	185.11	197.39	135.18	200.00
40.00	340.00	179.85	190.84	124.97	200.00
60.00	320.00	173.74	188.67	112.10	199.99
80.00	300.00	166.56	184.07	110.66	199.91
100.00	280.00	158.68	181.25	105.40	199.48
120.00	260.00	146.77	176.15	101.89	198.95
140.00	240.00	133.97	130.69	89.04	197.94
160.00	220.00	112.95	111.80	10.48	185.40
180.00	200.00	88.19	44.45	9.06	113.80
200.00	180.00	77.52	42.87	4.03	93.55
220.00	160.00	67.98	30.92	1.04	85.48
240.00	140.00	59.30	24.87	0.70	81.20
260.00	120.00	50.73	22.25	0.19	70.40
280.00	100.00	55.86	77.36	0.23	79.34
300.00	80.00	61.77	46.94	20.22	79.11
320.00	60.00	48.41	45.50	3.71	59.99
340.00	40.00	26.88	27.40	0.07	39.80
360.00	20.00	11.25	15.71	0.02	19.96
380.00	0.00	2.24	3.74	0.01	5.00

```
START DATE - MONTH:  2 DAY:  3 YEAR: 2004

START TIME: 21 HR/S   41 MIN    16 S

Na05 Devon Island gneiss
test 15.0 1 heat pulse

LASLETT ET AL ANNEALING MODEL FOR DURANGO APATITE

 AFTINV32 v. 1.3 (AUGUST 3, 2000)
 32-bit Watcom F77 v. 10.6 compiled for Windows 95
 as a Windows NT windowed executable
 code optimized for an Intel Pentium processor
 Original source code developed by Sean Willett
 Source code modified by Dale Issler


  inversion control parameters:
 --------------------------------------------------
 ***MONTE CARLO RANDOM SEARCH METHOD USED***
 number of solutions (l) =          250
 number of timesteps (m) =           19
 number of parameters (m+1) =           20
 NUMERICAL ACCURACY (%), ACUR =        0.1000000
 timestep length (delsub) =  2.000
 obj fnct (2 = chi2; 3 = K-S; 4 = Kuiper) =            3
 convergence tolerance (tol95) =        0.0956471
 convergence tolerance (toler) =        0.0582834
 number of standard deviations to fit age 2.0
 measured age  =  174.00
 sigma of error in measured age  =   8.40
 number of tracks measured =          198
 intermediate output every           50 forward models
 random number generator seed =           91
 system number generator urand(iseed)
 expansion factor (alpha) = 1.300
 reposition factor for explicit bound (delta) = 0.0010
 original track length (xl0) 15.000
 initial mean radius of length ellipse (xl3e) =   0.000
 conventional mean data
 empirical model of age reduction
 track length reduction coefs.:
 -4.86999989   0.00016800 -28.12000084   0.00000000   0.34999999
2.70000005
 component variance coefs.:
  0.78990000   0.00303500  -0.00229830   0.00000000

      temperature bounds         rate bounds            delt
   1        0.00      200.00       10.00        0.00       20.00
   2        0.00      200.00       10.00        0.00       20.00
   3        0.00      200.00       10.00        0.00       20.00
   4        0.00      200.00       10.00        0.00       20.00
   5        0.00      200.00       10.00        0.00       20.00
   6        0.00      200.00       10.00        0.00       20.00
   7        0.00      200.00       10.00        0.00       20.00
   8        0.00      200.00       10.00        0.00       20.00
   9        0.00      200.00       10.00        0.00       20.00
  10        0.00      175.00        8.80        0.00       20.00
```

11	0.00	150.00	7.50	0.00	20.00
12	0.00	125.00	6.20	0.00	20.00
13	0.00	100.00	5.00	0.00	20.00
14	0.00	100.00	5.00	5.00	20.00
15	0.00	100.00	5.00	4.00	20.00
16	0.00	80.00	4.00	3.00	20.00
17	0.00	60.00	3.00	2.00	20.00
18	0.00	40.00	2.00	0.00	20.00
19	0.00	20.00	1.00	0.00	20.00
20	0.00	5.00			

HEATING/COOLING SELECTION SUMMARY:

REGION	TIME RANGE MA	# OF EVENTS HEATING	COOLING	NHP	NCP
1	380.0- 120.0	NO	MONOTONIC	0	-1
2	120.0- 40.0	1	MONOTONIC	1	-1
3	40.0- 0.0	NO	MONOTONIC	0	-1

NUMBER OF FORWARD RANDOM TRIALS, ITER = 13065
max obj function = 0.095622
CONVERGENCE AT 0.05 SIGNIFICANCE LEVEL
number of forward models: 250
STOP DATES - MONTH: 2 DAY: 3 YEAR: 2004

STOP TIME : 21 HR/S 46 MIN 55 S

TOTAL EXECUTION TIME = 0.094275 HOURS OR 5.6565 MINUTES

MODEL RESULTS AT .05 SIGNIFICANCE LEVEL

TIME (MY)	TIME (MA)	EXP MEAN TEMPERATURE (DEG C)	MIN OBJ TEMPERATURE (DEG C)	LOWER TEMP BOUND	UPPER TEMP BOUND
0.00	380.00	191.65	194.56	142.19	200.00
20.00	360.00	188.51	194.27	132.72	200.00
40.00	340.00	184.51	165.41	130.55	200.00
60.00	320.00	179.64	164.51	123.18	199.99
80.00	300.00	172.50	160.47	115.33	199.94
100.00	280.00	165.34	153.52	104.83	199.86
120.00	260.00	155.46	145.31	103.74	199.80
140.00	240.00	142.85	113.51	95.96	198.54
160.00	220.00	126.52	111.27	79.15	198.22
180.00	200.00	102.66	89.84	11.41	169.74
200.00	180.00	84.13	62.34	2.69	101.60
220.00	160.00	75.07	52.36	1.24	93.67
240.00	140.00	67.47	50.60	0.09	84.85
260.00	120.00	60.14	30.47	0.09	79.37
280.00	100.00	70.49	70.14	4.69	89.16
300.00	80.00	72.47	76.30	45.29	79.74
320.00	60.00	50.11	53.34	17.19	59.92
340.00	40.00	28.86	36.56	1.39	39.86
360.00	20.00	10.99	12.51	0.11	19.98
380.00	0.00	2.53	2.91	0.01	4.96

START DATE - MONTH: 3 DAY: 25 YEAR: 2004

START TIME: 14 HR/S 47 MIN 52 S

Na-55 Leffert Glacier gneiss
cooling only 15 micron initial length

LASLETT ET AL ANNEALING MODEL FOR DURANGO APATITE

AFTINV32 v. 1.3 (AUGUST 3, 2000)
32-bit Watcom F77 v. 10.6 compiled for Windows 95
as a Windows NT windowed executable
code optimized for an Intel Pentium processor
Original source code developed by Sean Willett
Source code modified by Dale Issler

inversion control parameters:

MONTE CARLO RANDOM SEARCH METHOD USED
number of solutions (l) = 250
number of timesteps (m) = 19
number of parameters (m+1) = 20
NUMERICAL ACCURACY (%), ACUR = 0.1000000
timestep length (delsub) = 5.000
obj fnct (2 = chi2; 3 = K-S; 4 = Kuiper) = 3
convergence tolerance (tol95) = 0.1333979
convergence tolerance (toler) = 0.0812872
number of standard deviations to fit age 2.0
measured age = 271.00
sigma of error in measured age = 8.90
number of tracks measured = 101
intermediate output every 50 forward models
random number generator seed = 91
system number generator urand(iseed)
expansion factor (alpha) = 1.300
reposition factor for explicit bound (delta) = 0.0010
original track length (xl0) 15.000
initial mean radius of length ellipse (xl3e) = 0.000
conventional mean data
empirical model of age reduction
track length reduction coefs.:
-4.86999989 0.00016800 -28.12000084 0.00000000 0.34999999
2.70000005
component variance coefs.:
0.78990000 0.00303500 -0.00229830 0.00000000

	temperature bounds		rate bounds		delt
1	0.00	200.00	10.00	0.00	20.00
2	0.00	200.00	10.00	0.00	20.00
3	0.00	200.00	10.00	0.00	20.00
4	0.00	200.00	10.00	0.00	20.00
5	0.00	200.00	10.00	0.00	20.00
6	0.00	200.00	10.00	0.00	20.00
7	0.00	200.00	10.00	0.00	20.00
8	0.00	200.00	10.00	0.00	20.00
9	0.00	200.00	10.00	0.00	20.00

10	0.00	150.00	7.50	0.00	20.00
11	0.00	150.00	7.50	0.00	20.00
12	0.00	120.00	6.00	0.00	20.00
13	0.00	120.00	6.00	0.00	20.00
14	0.00	100.00	5.00	0.00	20.00
15	0.00	100.00	5.00	0.00	20.00
16	0.00	80.00	4.00	0.00	20.00
17	0.00	60.00	3.00	0.00	20.00
18	0.00	40.00	2.00	0.00	20.00
19	0.00	20.00	1.00	0.00	20.00
20	0.00	10.00			

HEATING/COOLING SELECTION SUMMARY:

REGION	TIME RANGE MA		# OF EVENTS HEATING	COOLING	NHP	NCP
1	380.0-	0.0	NO	MONOTONIC	0	-1

NUMBER OF FORWARD RANDOM TRIALS, ITER = 4285479
max obj function = 0.133337
CONVERGENCE AT 0.05 SIGNIFICANCE LEVEL
number of forward models: 250
STOP DATES - MONTH: 3 DAY: 25 YEAR: 2004

STOP TIME : 21 HR/S 33 MIN 49 S

TOTAL EXECUTION TIME = 6.765825 HOURS OR 405.9495 MINUTES

MODEL RESULTS AT .05 SIGNIFICANCE LEVEL

TIME (MY)	TIME (MA)	EXP MEAN TEMPERATURE (DEG C)	MIN OBJ TEMPERATURE (DEG C)	LOWER TEMP BOUND	UPPER TEMP BOUND
0.00	380.00	156.18	132.43	101.48	198.46
20.00	360.00	142.40	121.45	94.76	198.17
40.00	340.00	124.76	105.62	87.31	197.93
60.00	320.00	103.73	96.87	81.43	160.65
80.00	300.00	90.75	89.23	79.07	102.06
100.00	280.00	85.68	84.74	72.76	96.60
120.00	260.00	80.86	80.72	68.68	89.80
140.00	240.00	76.72	79.52	65.01	87.87
160.00	220.00	72.81	77.89	59.51	83.36
180.00	200.00	69.16	76.12	55.92	83.18
200.00	180.00	65.63	67.84	52.44	80.54
220.00	160.00	62.27	65.94	50.81	77.95
240.00	140.00	58.51	60.20	45.93	73.39
260.00	120.00	54.00	54.13	42.24	64.81
280.00	100.00	49.27	52.97	38.19	60.46
300.00	80.00	44.62	52.96	34.52	58.76
320.00	60.00	38.53	39.46	12.27	54.67
340.00	40.00	29.38	36.87	2.87	39.75
360.00	20.00	12.96	10.03	0.11	19.88
380.00	0.00	5.04	4.71	0.01	9.94

```
START DATE - MONTH:  1 DAY: 29 YEAR: 2004

START TIME: 23 HR/S    7 MIN    58 S

na-56 15 micron test
cooling only

LASLETT ET AL ANNEALING MODEL FOR DURANGO APATITE

 AFTINV32 v. 1.3 (AUGUST 3, 2000)
 32-bit Watcom F77 v. 10.6 compiled for Windows 95
 as a Windows NT windowed executable
 code optimized for an Intel Pentium processor
 Original source code developed by Sean Willett
 Source code modified by Dale Issler


  inversion control parameters:
 ------------------------------------------------
 ***MONTE CARLO RANDOM SEARCH METHOD USED***
 number of solutions (l) =          250
 number of timesteps (m) =           19
 number of parameters (m+1) =           20
 NUMERICAL ACCURACY (%), ACUR =        0.1000000
 timestep length (delsub) =  2.000
 obj fnct (2 = chi2; 3 = K-S; 4 = Kuiper) =            3
 convergence tolerance (tol95) =        0.0944731
 convergence tolerance (toler) =        0.0575680
 number of standard deviations to fit age 2.0
 measured age  =  317.00
 sigma of error in measured age  =  20.30
 number of tracks measured =          203
 intermediate output every           50 forward models
 random number generator seed =           91
 system number generator urand(iseed)
 expansion factor (alpha) = 1.300
 reposition factor for explicit bound (delta) = 0.0010
 original track length (xl0) 15.000
 initial mean radius of length ellipse (xl3e) =   0.000
 conventional mean data
 empirical model of age reduction
 track length reduction coefs.:
 -4.86999989   0.00016800 -28.12000084   0.00000000   0.34999999
2.70000005
 component variance coefs.:
  0.78990000   0.00303500  -0.00229830   0.00000000

      temperature bounds          rate bounds            delt
   1        0.00      200.00       10.00        0.00       20.00
   2        0.00      200.00       10.00        0.00       20.00
   3        0.00      200.00       10.00        0.00       20.00
   4        0.00      200.00       10.00        0.00       20.00
   5        0.00      200.00       10.00        0.00       20.00
   6        0.00      150.00        7.50        0.00       20.00
   7        0.00      150.00        7.50        0.00       20.00
   8        0.00      150.00        7.50        0.00       20.00
   9        0.00      150.00        7.50        0.00       20.00
  10        0.00      150.00        7.50        0.00       20.00
```

11	0.00	120.00	6.00	0.00	20.00
12	0.00	120.00	6.00	0.00	20.00
13	0.00	120.00	6.00	0.00	20.00
14	0.00	100.00	5.00	0.00	20.00
15	0.00	100.00	5.00	0.00	20.00
16	0.00	80.00	4.00	0.00	20.00
17	0.00	60.00	3.00	0.00	20.00
18	0.00	40.00	2.00	0.00	20.00
19	0.00	20.00	1.00	0.00	20.00
20	0.00	10.00			

HEATING/COOLING SELECTION SUMMARY:

REGION	TIME RANGE MA		# OF EVENTS HEATING	COOLING	NHP	NCP
1	380.0-	0.0	NO	MONOTONIC	0	-1

NUMBER OF FORWARD RANDOM TRIALS, ITER = 9248
max obj function = 0.094446
CONVERGENCE AT 0.05 SIGNIFICANCE LEVEL
number of forward models: 250
STOP DATES - MONTH: 1 DAY: 29 YEAR: 2004

STOP TIME : 23 HR/S 12 MIN 8 S

TOTAL EXECUTION TIME = 0.069305 HOURS OR 4.1583 MINUTES

MODEL RESULTS AT .05 SIGNIFICANCE LEVEL

TIME (MY)	TIME (MA)	EXP MEAN TEMPERATURE (DEG C)	MIN OBJ TEMPERATURE (DEG C)	LOWER TEMP BOUND	UPPER TEMP BOUND
0.00	380.00	151.53	123.18	79.11	199.95
20.00	360.00	139.28	107.78	71.88	199.24
40.00	340.00	119.42	106.16	65.28	195.52
60.00	320.00	104.70	92.29	64.56	195.11
80.00	300.00	84.26	85.15	59.69	101.77
100.00	280.00	76.94	79.73	51.72	93.96
120.00	260.00	70.16	72.49	46.76	86.89
140.00	240.00	63.93	66.82	35.15	84.96
160.00	220.00	56.54	60.12	24.02	72.29
180.00	200.00	48.13	56.93	2.33	69.44
200.00	180.00	37.87	56.28	0.84	57.77
220.00	160.00	28.68	1.62	0.38	51.36
240.00	140.00	20.49	1.27	0.09	40.76
260.00	120.00	13.43	0.92	0.01	34.40
280.00	100.00	8.24	0.81	0.00	24.12
300.00	80.00	4.66	0.23	0.00	16.09
320.00	60.00	2.75	0.10	0.00	13.72
340.00	40.00	1.63	0.07	0.00	10.04
360.00	20.00	1.04	0.04	0.00	6.07
380.00	0.00	0.58	0.03	0.00	4.44

START DATE - MONTH: 1 DAY: 29 YEAR: 2004

START TIME: 22 HR/S 52 MIN 26 S

na-70 15 micron test
cooling only

LASLETT ET AL ANNEALING MODEL FOR DURANGO APATITE

AFTINV32 v. 1.3 (AUGUST 3, 2000)
32-bit Watcom F77 v. 10.6 compiled for Windows 95
as a Windows NT windowed executable
code optimized for an Intel Pentium processor
Original source code developed by Sean Willett
Source code modified by Dale Issler

inversion control parameters:

MONTE CARLO RANDOM SEARCH METHOD USED
number of solutions (l) = 250
number of timesteps (m) = 19
number of parameters (m+1) = 20
NUMERICAL ACCURACY (%), ACUR = 0.1000000
timestep length (delsub) = 2.000
obj fnct (2 = chi2; 3 = K-S; 4 = Kuiper) = 3
convergence tolerance (tol95) = 0.1314864
convergence tolerance (toler) = 0.0801224
number of standard deviations to fit age 2.0
measured age = 278.00
sigma of error in measured age = 9.10
number of tracks measured = 104
intermediate output every 50 forward models
random number generator seed = 91
system number generator urand(iseed)
expansion factor (alpha) = 1.300
reposition factor for explicit bound (delta) = 0.0010
original track length (xl0) 15.000
initial mean radius of length ellipse (xl3e) = 0.000
conventional mean data
empirical model of age reduction
track length reduction coefs.:
-4.86999989 0.00016800 -28.12000084 0.00000000 0.34999999
2.70000005
component variance coefs.:
0.78990000 0.00303500 -0.00229830 0.00000000

	temperature bounds		rate bounds		delt
1	0.00	200.00	10.00	0.00	20.00
2	0.00	200.00	10.00	0.00	20.00
3	0.00	200.00	10.00	0.00	20.00
4	0.00	200.00	10.00	0.00	20.00
5	0.00	200.00	10.00	0.00	20.00
6	0.00	150.00	7.50	0.00	20.00
7	0.00	150.00	7.50	0.00	20.00
8	0.00	150.00	7.50	0.00	20.00
9	0.00	150.00	7.50	0.00	20.00
10	0.00	150.00	7.50	0.00	20.00

11	0.00	120.00	6.00	0.00	20.00
12	0.00	120.00	6.00	0.00	20.00
13	0.00	120.00	6.00	0.00	20.00
14	0.00	100.00	5.00	0.00	20.00
15	0.00	100.00	5.00	0.00	20.00
16	0.00	80.00	4.00	0.00	20.00
17	0.00	60.00	3.00	0.00	20.00
18	0.00	40.00	2.00	0.00	20.00
19	0.00	20.00	1.00	0.00	20.00
20	0.00	10.00			

HEATING/COOLING SELECTION SUMMARY:

REGION	TIME RANGE MA		# OF EVENTS HEATING	COOLING	NHP	NCP
1	380.0-	0.0	NO	MONOTONIC	0	-1

NUMBER OF FORWARD RANDOM TRIALS, ITER = 38359
max obj function = 0.131482
CONVERGENCE AT 0.05 SIGNIFICANCE LEVEL
number of forward models: 250
STOP DATES - MONTH: 1 DAY: 29 YEAR: 2004

STOP TIME : 23 HR/S 1 MIN 23 S

TOTAL EXECUTION TIME = 0.149158 HOURS OR 8.9495 MINUTES

MODEL RESULTS AT .05 SIGNIFICANCE LEVEL

TIME (MY)	TIME (MA)	EXP MEAN TEMPERATURE (DEG C)	MIN OBJ TEMPERATURE (DEG C)	LOWER TEMP BOUND	UPPER TEMP BOUND
0.00	380.00	164.58	164.67	99.32	199.96
20.00	360.00	154.96	152.07	96.20	199.76
40.00	340.00	142.80	110.38	95.08	199.75
60.00	320.00	122.28	109.54	82.38	190.86
80.00	300.00	97.89	84.86	73.54	145.95
100.00	280.00	85.38	67.88	59.23	97.26
120.00	260.00	77.62	67.83	57.84	93.40
140.00	240.00	71.21	58.59	49.37	83.96
160.00	220.00	64.89	54.21	45.69	77.86
180.00	200.00	58.35	48.80	39.70	70.14
200.00	180.00	51.98	48.14	37.55	63.66
220.00	160.00	46.37	43.22	26.35	59.46
240.00	140.00	40.10	41.28	19.50	53.97
260.00	120.00	34.27	41.19	11.44	46.74
280.00	100.00	28.14	36.64	2.62	42.52
300.00	80.00	22.34	31.30	1.54	38.12
320.00	60.00	16.80	26.28	0.22	35.58
340.00	40.00	11.65	14.69	0.10	31.33
360.00	20.00	7.13	5.76	0.01	19.61
380.00	0.00	3.63	2.54	0.01	9.89

START DATE - MONTH: 2 DAY: 2 YEAR: 2004

START TIME: 9 HR/S 37 MIN 12 S

Na-74 Bowman Island granite
test 15.0 cooling only

LASLETT ET AL ANNEALING MODEL FOR DURANGO APATITE

AFTINV32 v. 1.3 (AUGUST 3, 2000)
32-bit Watcom F77 v. 10.6 compiled for Windows 95
as a Windows NT windowed executable
code optimized for an Intel Pentium processor
Original source code developed by Sean Willett
Source code modified by Dale Issler

inversion control parameters:

MONTE CARLO RANDOM SEARCH METHOD USED
number of solutions (l) = 250
number of timesteps (m) = 19
number of parameters (m+1) = 20
NUMERICAL ACCURACY (%), ACUR = 0.1000000
timestep length (delsub) = 2.000
obj fnct (2 = chi2; 3 = K-S; 4 = Kuiper) = 3
convergence tolerance (tol95) = 0.1104634
convergence tolerance (toler) = 0.0673118
number of standard deviations to fit age 2.0
measured age = 270.00
sigma of error in measured age = 13.00
number of tracks measured = 148
intermediate output every 50 forward models
random number generator seed = 91
system number generator urand(iseed)
expansion factor (alpha) = 1.300
reposition factor for explicit bound (delta) = 0.0010
original track length (xl0) 15.000
initial mean radius of length ellipse (xl3e) = 0.000
conventional mean data
empirical model of age reduction
track length reduction coefs.:
-4.86999989 0.00016800 -28.12000084 0.00000000 0.34999999
2.70000005
component variance coefs.:
0.78990000 0.00303500 -0.00229830 0.00000000

	temperature bounds		rate bounds		delt
1	0.00	200.00	10.00	0.00	20.00
2	0.00	200.00	10.00	0.00	20.00
3	0.00	200.00	10.00	0.00	20.00
4	0.00	200.00	10.00	0.00	20.00
5	0.00	200.00	10.00	0.00	20.00
6	0.00	200.00	10.00	0.00	20.00
7	0.00	200.00	10.00	0.00	20.00
8	0.00	200.00	10.00	0.00	20.00
9	0.00	200.00	10.00	0.00	20.00
10	0.00	175.00	8.80	0.00	20.00

11	0.00	150.00	7.50	0.00	20.00
12	0.00	125.00	6.20	0.00	20.00
13	0.00	100.00	5.00	0.00	20.00
14	0.00	100.00	5.00	0.00	20.00
15	0.00	100.00	5.00	0.00	20.00
16	0.00	80.00	4.00	0.00	20.00
17	0.00	60.00	3.00	0.00	20.00
18	0.00	40.00	2.00	0.00	20.00
19	0.00	20.00	1.00	0.00	20.00
20	0.00	5.00			

HEATING/COOLING SELECTION SUMMARY:

REGION	TIME RANGE MA		# OF EVENTS HEATING	COOLING	NHP	NCP
1	380.0-	0.0	NO	MONOTONIC	0	-1

NUMBER OF FORWARD RANDOM TRIALS, ITER = 155672
max obj function = 0.110416
CONVERGENCE AT 0.05 SIGNIFICANCE LEVEL
number of forward models: 250
STOP DATES - MONTH: 2 DAY: 2 YEAR: 2004

STOP TIME : 10 HR/S 28 MIN 17 S

TOTAL EXECUTION TIME = 0.851403 HOURS OR 51.0842 MINUTES

MODEL RESULTS AT .05 SIGNIFICANCE LEVEL

TIME (MY)	TIME (MA)	EXP MEAN TEMPERATURE (DEG C)	MIN OBJ TEMPERATURE (DEG C)	LOWER TEMP BOUND	UPPER TEMP BOUND
0.00	380.00	161.03	100.74	100.25	199.82
20.00	360.00	153.03	100.37	98.96	198.88
40.00	340.00	142.79	94.34	92.01	197.30
60.00	320.00	127.80	91.97	80.01	193.28
80.00	300.00	99.88	91.86	79.15	144.92
100.00	280.00	89.83	91.22	72.81	101.76
120.00	260.00	83.54	86.14	70.89	92.96
140.00	240.00	78.26	74.02	65.16	89.70
160.00	220.00	72.99	69.71	57.87	85.70
180.00	200.00	68.20	64.62	54.41	80.77
200.00	180.00	63.92	62.60	47.26	77.19
220.00	160.00	59.07	52.81	44.26	73.14
240.00	140.00	53.54	51.00	36.10	69.49
260.00	120.00	47.78	50.90	29.48	61.43
280.00	100.00	41.92	48.87	25.76	57.05
300.00	80.00	35.27	35.75	16.45	49.08
320.00	60.00	28.18	27.49	2.07	44.49
340.00	40.00	21.38	23.59	0.42	39.85
360.00	20.00	11.40	16.73	0.23	19.98
380.00	0.00	2.51	1.21	0.01	4.97

START DATE - MONTH: 2 DAY: 3 YEAR: 2004

START TIME: 22 HR/S 11 MIN 42 S

Na-57 Cape Faraday dyke
test 15.0 1 heat pulse

LASLETT ET AL ANNEALING MODEL FOR DURANGO APATITE

AFTINV32 v. 1.3 (AUGUST 3, 2000)
32-bit Watcom F77 v. 10.6 compiled for Windows 95
as a Windows NT windowed executable
code optimized for an Intel Pentium processor
Original source code developed by Sean Willett
Source code modified by Dale Issler

inversion control parameters:

MONTE CARLO RANDOM SEARCH METHOD USED
number of solutions (l) = 250
number of timesteps (m) = 19
number of parameters (m+1) = 20
NUMERICAL ACCURACY (%), ACUR = 0.1000000
timestep length (delsub) = 2.000
obj fnct (2 = chi2; 3 = K-S; 4 = Kuiper) = 3
convergence tolerance (tol95) = 0.1360818
convergence tolerance (toler) = 0.0829226
number of standard deviations to fit age 2.0
measured age = 160.00
sigma of error in measured age = 10.40
number of tracks measured = 97
intermediate output every 50 forward models
random number generator seed = 91
system number generator urand(iseed)
expansion factor (alpha) = 1.300
reposition factor for explicit bound (delta) = 0.0010
original track length (xl0) 15.000
initial mean radius of length ellipse (xl3e) = 0.000
conventional mean data
empirical model of age reduction
track length reduction coefs.:
-4.86999989 0.00016800 -28.12000084 0.00000000 0.34999999
2.70000005
component variance coefs.:
0.78990000 0.00303500 -0.00229830 0.00000000

	temperature bounds		rate bounds		delt
1	0.00	200.00	10.00	0.00	20.00
2	0.00	200.00	10.00	0.00	20.00
3	0.00	200.00	10.00	0.00	20.00
4	0.00	200.00	10.00	0.00	20.00
5	0.00	200.00	10.00	0.00	20.00
6	0.00	200.00	10.00	0.00	20.00
7	0.00	200.00	10.00	0.00	20.00
8	0.00	200.00	10.00	0.00	20.00
9	0.00	200.00	10.00	0.00	20.00
10	0.00	175.00	8.80	0.00	20.00

11	0.00	150.00	7.50	0.00	20.00
12	0.00	125.00	6.20	0.00	20.00
13	0.00	100.00	5.00	0.00	20.00
14	0.00	100.00	5.00	5.00	20.00
15	0.00	100.00	5.00	4.00	20.00
16	0.00	80.00	4.00	3.00	20.00
17	0.00	60.00	3.00	2.00	20.00
18	0.00	40.00	2.00	0.00	20.00
19	0.00	20.00	1.00	0.00	20.00
20	0.00	5.00			

HEATING/COOLING SELECTION SUMMARY:

REGION	TIME RANGE MA	# OF EVENTS HEATING	COOLING	NHP	NCP
1	380.0- 120.0	NO	MONOTONIC	0	-1
2	120.0- 40.0	1	MONOTONIC	1	-1
3	40.0- 0.0	NO	MONOTONIC	0	-1

NUMBER OF FORWARD RANDOM TRIALS, ITER = 4371
max obj function = 0.135951
CONVERGENCE AT 0.05 SIGNIFICANCE LEVEL
number of forward models: 250
STOP DATES - MONTH: 2 DAY: 3 YEAR: 2004

STOP TIME : 22 HR/S 12 MIN 42 S

TOTAL EXECUTION TIME = 0.016666 HOURS OR 1.0000 MINUTES

MODEL RESULTS AT .05 SIGNIFICANCE LEVEL

TIME (MY)	TIME (MA)	EXP MEAN TEMPERATURE (DEG C)	MIN OBJ TEMPERATURE (DEG C)	LOWER TEMP BOUND	UPPER TEMP BOUND
0.00	380.00	193.05	178.96	147.05	200.00
20.00	360.00	190.00	172.99	137.45	200.00
40.00	340.00	186.65	172.86	131.98	200.00
60.00	320.00	182.78	166.33	124.43	200.00
80.00	300.00	177.53	150.48	113.99	199.99
100.00	280.00	171.44	144.84	108.49	199.99
120.00	260.00	162.51	144.52	100.19	199.92
140.00	240.00	153.13	140.27	98.87	199.90
160.00	220.00	141.06	131.58	89.09	199.89
180.00	200.00	121.44	97.77	72.71	172.36
200.00	180.00	100.23	84.40	21.87	147.78
220.00	160.00	85.18	73.96	0.01	102.61
240.00	140.00	77.48	64.77	0.00	95.14
260.00	120.00	69.86	51.66	0.00	88.22
280.00	100.00	75.80	84.75	20.97	98.67
300.00	80.00	69.18	58.82	15.41	79.94
320.00	60.00	48.92	49.90	4.06	59.94
340.00	40.00	28.63	24.09	1.39	39.86
360.00	20.00	11.80	6.01	0.23	19.97
380.00	0.00	2.45	4.90	0.01	4.91

START DATE - MONTH: 2 DAY: 11 YEAR: 2004

START TIME: 21 HR/S 43 MIN 37 S

Na-58 Orne Island dyke
cool only init 15

LASLETT ET AL ANNEALING MODEL FOR DURANGO APATITE

AFTINV32 v. 1.3 (AUGUST 3, 2000)
32-bit Watcom F77 v. 10.6 compiled for Windows 95
as a Windows NT windowed executable
code optimized for an Intel Pentium processor
Original source code developed by Sean Willett
Source code modified by Dale Issler

inversion control parameters:

MONTE CARLO RANDOM SEARCH METHOD USED
number of solutions (l) = 250
number of timesteps (m) = 18
number of parameters (m+1) = 19
NUMERICAL ACCURACY (%), ACUR = 0.1000000
timestep length (delsub) = 1.000
obj fnct (2 = chi2; 3 = K-S; 4 = Kuiper) = 3
convergence tolerance (tol95) = 0.1374862
convergence tolerance (toler) = 0.0837784
number of standard deviations to fit age 2.0
measured age = 84.40
sigma of error in measured age = 6.20
number of tracks measured = 95
intermediate output every 50 forward models
random number generator seed = 91
system number generator urand(iseed)
expansion factor (alpha) = 1.300
reposition factor for explicit bound (delta) = 0.0010
original track length (xl0) 15.000
initial mean radius of length ellipse (xl3e) = 0.000
conventional mean data
empirical model of age reduction
track length reduction coefs.:
-4.86999989 0.00016800 -28.12000084 0.00000000 0.34999999
2.70000005
component variance coefs.:
0.78990000 0.00303500 -0.00229830 0.00000000

	temperature bounds		rate bounds		delt
1	0.00	200.00	20.00	0.00	10.00
2	0.00	200.00	20.00	0.00	10.00
3	0.00	200.00	20.00	0.00	10.00
4	0.00	200.00	20.00	0.00	10.00
5	0.00	200.00	20.00	0.00	10.00
6	0.00	200.00	20.00	0.00	10.00
7	0.00	200.00	20.00	0.00	10.00
8	0.00	200.00	20.00	0.00	10.00
9	0.00	200.00	20.00	0.00	10.00
10	0.00	150.00	15.00	0.00	10.00

11	0.00	150.00	15.00	0.00	10.00
12	0.00	120.00	12.00	0.00	10.00
13	0.00	120.00	12.00	0.00	10.00
14	0.00	100.00	10.00	0.00	10.00
15	0.00	80.00	8.00	0.00	10.00
16	0.00	60.00	6.00	0.00	10.00
17	0.00	40.00	4.00	0.00	10.00
18	0.00	20.00	2.00	0.00	10.00
19	0.00	5.00			

HEATING/COOLING SELECTION SUMMARY:

REGION	TIME RANGE MA		# OF EVENTS HEATING	COOLING	NHP	NCP
1	180.0-	0.0	NO	MONOTONIC	0	-1

NUMBER OF FORWARD RANDOM TRIALS, ITER = 3805
max obj function = 0.137269
CONVERGENCE AT 0.05 SIGNIFICANCE LEVEL
number of forward models: 250
STOP DATES - MONTH: 2 DAY: 11 YEAR: 2004

STOP TIME : 21 HR/S 44 MIN 29 S

TOTAL EXECUTION TIME = 0.014423 HOURS OR 0.8654 MINUTES

MODEL RESULTS AT .05 SIGNIFICANCE LEVEL

TIME (MY)	TIME (MA)	EXP MEAN TEMPERATURE (DEG C)	MIN OBJ TEMPERATURE (DEG C)	LOWER TEMP BOUND	UPPER TEMP BOUND
0.00	180.00	183.29	167.53	122.72	200.00
10.00	170.00	179.79	140.54	121.76	200.00
20.00	160.00	176.10	138.13	118.91	200.00
30.00	150.00	171.70	137.25	114.98	200.00
40.00	140.00	165.91	132.67	108.93	199.97
50.00	130.00	159.64	126.93	103.44	199.97
60.00	120.00	153.19	126.55	101.00	199.55
70.00	110.00	145.55	119.20	95.41	198.34
80.00	100.00	135.67	116.64	65.39	198.08
90.00	90.00	107.24	91.52	53.24	146.66
100.00	80.00	89.42	86.40	48.14	113.99
110.00	70.00	75.35	83.06	36.61	102.07
120.00	60.00	63.85	43.10	20.29	93.03
130.00	50.00	50.93	41.56	9.76	85.96
140.00	40.00	41.83	36.55	0.97	67.03
150.00	30.00	33.62	26.61	0.32	54.07
160.00	20.00	25.01	21.61	0.17	39.94
170.00	10.00	12.02	15.03	0.05	19.96
180.00	0.00	2.58	4.21	0.00	4.98

START DATE - MONTH: 1 DAY: 31 YEAR: 2004

START TIME: 21 HR/S 24 MIN 41 S

Na-61 Manson Island sill
test 15.0 heat pulse

LASLETT ET AL ANNEALING MODEL FOR DURANGO APATITE

AFTINV32 v. 1.3 (AUGUST 3, 2000)
32-bit Watcom F77 v. 10.6 compiled for Windows 95
as a Windows NT windowed executable
code optimized for an Intel Pentium processor
Original source code developed by Sean Willett
Source code modified by Dale Issler

inversion control parameters:

MONTE CARLO RANDOM SEARCH METHOD USED
number of solutions (l) = 250
number of timesteps (m) = 19
number of parameters (m+1) = 20
NUMERICAL ACCURACY (%), ACUR = 0.1000000
timestep length (delsub) = 2.000
obj fnct (2 = chi2; 3 = K-S; 4 = Kuiper) = 3
convergence tolerance (tol95) = 0.1135397
convergence tolerance (toler) = 0.0691864
number of standard deviations to fit age 2.0
measured age = 203.00
sigma of error in measured age = 12.30
number of tracks measured = 140
intermediate output every 50 forward models
random number generator seed = 91
system number generator urand(iseed)
expansion factor (alpha) = 1.300
reposition factor for explicit bound (delta) = 0.0010
original track length (xl0) 15.000
initial mean radius of length ellipse (xl3e) = 0.000
conventional mean data
empirical model of age reduction
track length reduction coefs.:
-4.86999989 0.00016800 -28.12000084 0.00000000 0.34999999
2.70000005
component variance coefs.:
0.78990000 0.00303500 -0.00229830 0.00000000

	temperature bounds		rate bounds		delt
1	0.00	200.00	10.00	0.00	20.00
2	0.00	200.00	10.00	0.00	20.00
3	0.00	200.00	10.00	0.00	20.00
4	0.00	200.00	10.00	0.00	20.00
5	0.00	200.00	10.00	0.00	20.00
6	0.00	200.00	10.00	0.00	20.00
7	0.00	200.00	10.00	0.00	20.00
8	0.00	200.00	10.00	0.00	20.00
9	0.00	200.00	10.00	0.00	20.00
10	0.00	175.00	8.80	0.00	20.00

11	0.00	150.00	7.50	0.00	20.00
12	0.00	125.00	6.20	0.00	20.00
13	0.00	100.00	5.00	0.00	20.00
14	0.00	100.00	5.00	5.00	20.00
15	0.00	100.00	5.00	4.00	20.00
16	0.00	80.00	4.00	3.00	20.00
17	0.00	60.00	3.00	2.00	20.00
18	0.00	40.00	2.00	0.00	20.00
19	0.00	20.00	1.00	0.00	20.00
20	0.00	5.00			

HEATING/COOLING SELECTION SUMMARY:

REGION	TIME RANGE MA	# OF EVENTS HEATING	COOLING	NHP	NCP
1	380.0- 120.0	NO	MONOTONIC	0	-1
2	120.0- 40.0	1	MONOTONIC	1	-1
3	40.0- 0.0	NO	MONOTONIC	0	-1

NUMBER OF FORWARD RANDOM TRIALS, ITER = 3392
max obj function = 0.113529
CONVERGENCE AT 0.05 SIGNIFICANCE LEVEL
number of forward models: 250
STOP DATES - MONTH: 1 DAY: 31 YEAR: 2004

STOP TIME : 21 HR/S 25 MIN 47 S

TOTAL EXECUTION TIME = 0.018351 HOURS OR 1.1010 MINUTES

MODEL RESULTS AT .05 SIGNIFICANCE LEVEL

TIME (MY)	TIME (MA)	EXP MEAN TEMPERATURE (DEG C)	MIN OBJ TEMPERATURE (DEG C)	LOWER TEMP BOUND	UPPER TEMP BOUND
0.00	380.00	190.90	198.62	140.34	200.00
20.00	360.00	187.49	191.46	135.30	200.00
40.00	340.00	182.87	186.69	123.51	200.00
60.00	320.00	177.35	168.02	117.83	199.99
80.00	300.00	170.97	167.36	106.32	199.98
100.00	280.00	163.63	165.89	99.73	199.79
120.00	260.00	153.01	152.78	94.04	199.74
140.00	240.00	141.68	118.28	64.63	198.59
160.00	220.00	125.22	89.96	52.34	197.17
180.00	200.00	90.56	76.44	28.81	140.23
200.00	180.00	73.41	63.91	4.99	98.93
220.00	160.00	60.27	62.81	1.88	86.74
240.00	140.00	48.19	35.42	1.13	78.17
260.00	120.00	35.33	28.20	0.00	61.56
280.00	100.00	31.20	27.28	0.00	63.94
300.00	80.00	26.14	11.16	0.01	52.03
320.00	60.00	24.81	16.73	0.01	49.52
340.00	40.00	21.55	29.37	0.04	39.69
360.00	20.00	9.82	0.16	0.03	19.97
380.00	0.00	2.27	0.02	0.02	4.95

```
START DATE - MONTH:  1 DAY: 31 YEAR: 2004

START TIME: 22 HR/S   52 MIN    40 S

Na-75 Thule dyke
test 15.0 cooling only

LASLETT ET AL ANNEALING MODEL FOR DURANGO APATITE

 AFTINV32 v. 1.3 (AUGUST 3, 2000)
 32-bit Watcom F77 v. 10.6 compiled for Windows 95
 as a Windows NT windowed executable
 code optimized for an Intel Pentium processor
 Original source code developed by Sean Willett
 Source code modified by Dale Issler


  inversion control parameters:
 --------------------------------------------------
 ***MONTE CARLO RANDOM SEARCH METHOD USED***
 number of solutions (l) =          250
 number of timesteps (m) =           19
 number of parameters (m+1) =           20
 NUMERICAL ACCURACY (%), ACUR =        0.1000000
 timestep length (delsub) =  2.000
 obj fnct (2 = chi2; 3 = K-S; 4 = Kuiper) =            3
 convergence tolerance (tol95) =        0.1083141
 convergence tolerance (toler) =        0.0660021
 number of standard deviations to fit age 2.0
 measured age   =  197.00
 sigma of error in measured age  =  14.70
 number of tracks measured =          154
 intermediate output every           50 forward models
 random number generator seed =           91
 system number generator urand(iseed)
 expansion factor (alpha) = 1.300
 reposition factor for explicit bound (delta) = 0.0010
 original track length (xl0) 15.000
 initial mean radius of length ellipse (xl3e) =   0.000
 conventional mean data
 empirical model of age reduction
 track length reduction coefs.:
 -4.86999989   0.00016800 -28.12000084   0.00000000   0.34999999
2.70000005
 component variance coefs.:
  0.78990000   0.00303500  -0.00229830   0.00000000

      temperature bounds          rate bounds            delt
   1        0.00      200.00       10.00        0.00       20.00
   2        0.00      200.00       10.00        0.00       20.00
   3        0.00      200.00       10.00        0.00       20.00
   4        0.00      200.00       10.00        0.00       20.00
   5        0.00      200.00       10.00        0.00       20.00
   6        0.00      200.00       10.00        0.00       20.00
   7        0.00      200.00       10.00        0.00       20.00
   8        0.00      200.00       10.00        0.00       20.00
   9        0.00      200.00       10.00        0.00       20.00
  10        0.00      175.00        8.75        0.00       20.00
```

11	0.00	150.00	7.50	0.00	20.00
12	0.00	125.00	6.25	0.00	20.00
13	0.00	100.00	5.00	0.00	20.00
14	0.00	100.00	5.00	0.00	20.00
15	0.00	100.00	5.00	0.00	20.00
16	0.00	80.00	4.00	0.00	20.00
17	0.00	60.00	3.00	0.00	20.00
18	0.00	40.00	2.00	0.00	20.00
19	0.00	20.00	1.00	0.00	20.00
20	0.00	5.00			

HEATING/COOLING SELECTION SUMMARY:

REGION	TIME RANGE MA	# OF EVENTS HEATING	COOLING	NHP	NCP
1	380.0- 0.0	NO	MONOTONIC	0	-1

NUMBER OF FORWARD RANDOM TRIALS, ITER = 4022
max obj function = 0.108231
CONVERGENCE AT 0.05 SIGNIFICANCE LEVEL
number of forward models: 250
STOP DATES - MONTH: 1 DAY: 31 YEAR: 2004

STOP TIME : 22 HR/S 54 MIN 4 S

TOTAL EXECUTION TIME = 0.023233 HOURS OR 1.3940 MINUTES

MODEL RESULTS AT .05 SIGNIFICANCE LEVEL

TIME (MY)	TIME (MA)	EXP MEAN TEMPERATURE (DEG C)	MIN OBJ TEMPERATURE (DEG C)	LOWER TEMP BOUND	UPPER TEMP BOUND
0.00	380.00	188.87	158.81	125.73	200.00
20.00	360.00	185.22	158.26	117.08	200.00
40.00	340.00	180.74	151.00	110.19	199.99
60.00	320.00	174.81	148.54	106.60	199.99
80.00	300.00	168.63	139.14	102.85	199.98
100.00	280.00	159.83	134.28	97.21	199.97
120.00	260.00	149.26	125.36	82.85	199.64
140.00	240.00	136.71	103.05	80.00	198.84
160.00	220.00	122.19	86.43	73.62	198.22
180.00	200.00	93.46	83.26	66.92	131.01
200.00	180.00	83.13	77.84	61.25	98.58
220.00	160.00	75.35	71.59	53.34	90.21
240.00	140.00	68.26	64.37	43.85	84.28
260.00	120.00	60.98	62.35	36.75	77.08
280.00	100.00	53.27	44.43	21.65	70.57
300.00	80.00	44.38	39.99	17.89	63.37
320.00	60.00	35.47	28.22	0.68	55.06
340.00	40.00	24.62	25.62	0.29	39.40
360.00	20.00	11.20	16.83	0.03	19.99
380.00	0.00	2.51	0.58	0.00	5.00

START DATE - MONTH: 2 DAY: 4 YEAR: 2004

START TIME: 9 HR/S 49 MIN 36 S

na-76 Carey Islands
test 15.0 1 heat pulse

LASLETT ET AL ANNEALING MODEL FOR DURANGO APATITE

AFTINV32 v. 1.3 (AUGUST 3, 2000)
32-bit Watcom F77 v. 10.6 compiled for Windows 95
as a Windows NT windowed executable
code optimized for an Intel Pentium processor
Original source code developed by Sean Willett
Source code modified by Dale Issler

inversion control parameters:

MONTE CARLO RANDOM SEARCH METHOD USED
number of solutions (l) = 250
number of timesteps (m) = 19
number of parameters (m+1) = 20
NUMERICAL ACCURACY (%), ACUR = 0.1000000
timestep length (delsub) = 2.000
obj fnct (2 = chi2; 3 = K-S; 4 = Kuiper) = 3
convergence tolerance (tol95) = 0.1022565
convergence tolerance (toler) = 0.0623109
number of standard deviations to fit age 2.0
measured age = 253.00
sigma of error in measured age = 16.20
number of tracks measured = 173
intermediate output every 50 forward models
random number generator seed = 91
system number generator urand(iseed)
expansion factor (alpha) = 1.300
reposition factor for explicit bound (delta) = 0.0010
original track length (xl0) 15.000
initial mean radius of length ellipse (xl3e) = 0.000
conventional mean data
empirical model of age reduction
track length reduction coefs.:
-4.86999989 0.00016800 -28.12000084 0.00000000 0.34999999
2.70000005
component variance coefs.:
0.78990000 0.00303500 -0.00229830 0.00000000

	temperature bounds		rate bounds		delt
1	0.00	200.00	10.00	0.00	20.00
2	0.00	200.00	10.00	0.00	20.00
3	0.00	200.00	10.00	0.00	20.00
4	0.00	200.00	10.00	0.00	20.00
5	0.00	200.00	10.00	0.00	20.00
6	0.00	200.00	10.00	0.00	20.00
7	0.00	200.00	10.00	0.00	20.00
8	0.00	200.00	10.00	0.00	20.00
9	0.00	200.00	10.00	0.00	20.00
10	0.00	175.00	8.75	0.00	20.00

11	0.00	150.00	7.50	0.00	20.00
12	0.00	125.00	6.25	0.00	20.00
13	0.00	100.00	5.00	5.00	20.00
14	0.00	100.00	5.00	5.00	20.00
15	0.00	100.00	5.00	4.00	20.00
16	0.00	80.00	4.00	3.00	20.00
17	0.00	60.00	3.00	2.00	20.00
18	0.00	40.00	2.00	0.00	20.00
19	0.00	20.00	1.00	0.00	20.00
20	0.00	5.00			

HEATING/COOLING SELECTION SUMMARY:

REGION	TIME RANGE MA	# OF EVENTS HEATING	COOLING	NHP	NCP
1	380.0- 140.0	NO	MONOTONIC	0	-1
2	140.0- 40.0	1	MONOTONIC	1	-1
3	40.0- 0.0	NO	MONOTONIC	0	-1

NUMBER OF FORWARD RANDOM TRIALS, ITER = 57035
max obj function = 0.102078
CONVERGENCE AT 0.05 SIGNIFICANCE LEVEL
number of forward models: 250
STOP DATES - MONTH: 2 DAY: 4 YEAR: 2004

STOP TIME : 10 HR/S 11 MIN 23 S

TOTAL EXECUTION TIME = 0.363019 HOURS OR 21.7811 MINUTES

MODEL RESULTS AT .05 SIGNIFICANCE LEVEL

TIME (MY)	TIME (MA)	EXP MEAN TEMPERATURE (DEG C)	MIN OBJ TEMPERATURE (DEG C)	LOWER TEMP BOUND	UPPER TEMP BOUND
0.00	380.00	162.87	107.01	50.85	199.96
20.00	360.00	152.17	102.58	25.77	199.11
40.00	340.00	139.38	101.13	14.35	198.62
60.00	320.00	123.93	95.09	4.97	196.95
80.00	300.00	99.77	94.29	4.67	175.41
100.00	280.00	79.33	88.73	0.37	103.22
120.00	260.00	71.24	86.89	0.24	97.11
140.00	240.00	62.58	84.96	0.05	86.56
160.00	220.00	55.10	72.24	0.04	81.33
180.00	200.00	47.49	37.66	0.01	79.02
200.00	180.00	41.26	34.79	0.00	70.83
220.00	160.00	34.09	24.76	0.00	66.38
240.00	140.00	27.45	22.13	0.00	57.44
260.00	120.00	68.75	20.37	0.01	97.70
280.00	100.00	85.16	90.50	47.35	97.00
300.00	80.00	71.04	56.78	4.31	80.00
320.00	60.00	46.90	55.53	1.67	59.97
340.00	40.00	27.28	36.31	0.22	39.90
360.00	20.00	11.20	2.92	0.00	19.94
380.00	0.00	2.37	2.85	0.00	4.99

START DATE - MONTH: 2 DAY: 2 YEAR: 2004

START TIME: 21 HR/S 50 MIN 14 S

Na-77 Dundas Mtn sill
test 15.0 cooling only

LASLETT ET AL ANNEALING MODEL FOR DURANGO APATITE

AFTINV32 v. 1.3 (AUGUST 3, 2000)
32-bit Watcom F77 v. 10.6 compiled for Windows 95
as a Windows NT windowed executable
code optimized for an Intel Pentium processor
Original source code developed by Sean Willett
Source code modified by Dale Issler

inversion control parameters:

MONTE CARLO RANDOM SEARCH METHOD USED
number of solutions (l) = 250
number of timesteps (m) = 19
number of parameters (m+1) = 20
NUMERICAL ACCURACY (%), ACUR = 0.1000000
timestep length (delsub) = 2.000
obj fnct (2 = chi2; 3 = K-S; 4 = Kuiper) = 3
convergence tolerance (tol95) = 0.1031455
convergence tolerance (toler) = 0.0628526
number of standard deviations to fit age 2.0
measured age = 207.00
sigma of error in measured age = 13.70
number of tracks measured = 170
intermediate output every 50 forward models
random number generator seed = 91
system number generator urand(iseed)
expansion factor (alpha) = 1.300
reposition factor for explicit bound (delta) = 0.0010
original track length (xl0) 15.000
initial mean radius of length ellipse (xl3e) = 0.000
conventional mean data
empirical model of age reduction
track length reduction coefs.:
-4.86999989 0.00016800 -28.12000084 0.00000000 0.34999999
2.70000005
component variance coefs.:
0.78990000 0.00303500 -0.00229830 0.00000000

	temperature bounds		rate bounds		delt
1	0.00	200.00	10.00	0.00	20.00
2	0.00	200.00	10.00	0.00	20.00
3	0.00	200.00	10.00	0.00	20.00
4	0.00	200.00	10.00	0.00	20.00
5	0.00	200.00	10.00	0.00	20.00
6	0.00	200.00	10.00	0.00	20.00
7	0.00	200.00	10.00	0.00	20.00
8	0.00	200.00	10.00	0.00	20.00
9	0.00	200.00	10.00	0.00	20.00
10	0.00	175.00	8.75	0.00	20.00

11	0.00	150.00	7.50	0.00	20.00
12	0.00	125.00	6.25	0.00	20.00
13	0.00	100.00	5.00	0.00	20.00
14	0.00	100.00	5.00	0.00	20.00
15	0.00	100.00	5.00	0.00	20.00
16	0.00	80.00	4.00	0.00	20.00
17	0.00	60.00	3.00	0.00	20.00
18	0.00	40.00	2.00	0.00	20.00
19	0.00	20.00	1.00	0.00	20.00
20	0.00	5.00			

HEATING/COOLING SELECTION SUMMARY:

REGION	TIME RANGE MA		# OF EVENTS HEATING	COOLING	NHP	NCP
1	380.0-	0.0	NO	MONOTONIC	0	-1

NUMBER OF FORWARD RANDOM TRIALS, ITER = 5478
max obj function = 0.102904
CONVERGENCE AT 0.05 SIGNIFICANCE LEVEL
number of forward models: 250
STOP DATES - MONTH: 2 DAY: 2 YEAR: 2004

STOP TIME : 21 HR/S 52 MIN 19 S

TOTAL EXECUTION TIME = 0.034737 HOURS OR 2.0842 MINUTES

MODEL RESULTS AT .05 SIGNIFICANCE LEVEL

TIME (MY)	TIME (MA)	EXP MEAN TEMPERATURE (DEG C)	MIN OBJ TEMPERATURE (DEG C)	LOWER TEMP BOUND	UPPER TEMP BOUND
0.00	380.00	188.88	198.03	131.89	200.00
20.00	360.00	185.05	193.91	126.78	200.00
40.00	340.00	180.60	193.80	115.95	199.98
60.00	320.00	174.01	190.89	106.50	199.98
80.00	300.00	165.96	188.04	103.28	199.86
100.00	280.00	159.23	175.05	97.32	199.47
120.00	260.00	149.12	174.93	93.29	199.14
140.00	240.00	135.36	113.53	70.46	195.30
160.00	220.00	112.69	102.27	65.29	182.34
180.00	200.00	84.46	90.79	56.02	112.38
200.00	180.00	73.53	74.70	48.08	93.54
220.00	160.00	63.95	60.95	42.08	85.74
240.00	140.00	55.17	48.10	34.29	73.10
260.00	120.00	46.95	44.28	27.91	63.00
280.00	100.00	39.06	42.78	11.41	52.62
300.00	80.00	32.02	37.20	6.13	48.07
320.00	60.00	24.44	25.13	0.17	36.70
340.00	40.00	17.74	21.69	0.01	33.58
360.00	20.00	10.32	12.78	0.01	19.85
380.00	0.00	2.38	4.45	0.01	4.98

START DATE - MONTH: 4 DAY: 29 YEAR: 2004

START TIME: 22 HR/S 44 MIN 2 S

Na-78 Dundas mtn sill
cooling only init 15

LASLETT ET AL ANNEALING MODEL FOR DURANGO APATITE

AFTINV32 v. 1.3 (AUGUST 3, 2000)
32-bit Watcom F77 v. 10.6 compiled for Windows 95
as a Windows NT windowed executable
code optimized for an Intel Pentium processor
Original source code developed by Sean Willett
Source code modified by Dale Issler

inversion control parameters:

MONTE CARLO RANDOM SEARCH METHOD USED
number of solutions (l) = 250
number of timesteps (m) = 19
number of parameters (m+1) = 20
NUMERICAL ACCURACY (%), ACUR = 0.1000000
timestep length (delsub) = 2.000
obj fnct (2 = chi2; 3 = K-S; 4 = Kuiper) = 3
convergence tolerance (tol95) = 0.0989180
convergence tolerance (toler) = 0.0602765
number of standard deviations to fit age 2.0
measured age = 219.00
sigma of error in measured age = 11.20
number of tracks measured = 185
intermediate output every 50 forward models
random number generator seed = 91
system number generator urand(iseed)
expansion factor (alpha) = 1.300
reposition factor for explicit bound (delta) = 0.0010
original track length (xl0) 15.000
initial mean radius of length ellipse (xl3e) = 0.000
conventional mean data
empirical model of age reduction
track length reduction coefs.:
-4.86999989 0.00016800 -28.12000084 0.00000000 0.34999999
2.70000005
component variance coefs.:
0.78990000 0.00303500 -0.00229830 0.00000000

	temperature bounds		rate bounds		delt
1	0.00	200.00	10.00	0.00	20.00
2	0.00	200.00	10.00	0.00	20.00
3	0.00	200.00	10.00	0.00	20.00
4	0.00	200.00	10.00	0.00	20.00
5	0.00	200.00	10.00	0.00	20.00
6	0.00	200.00	10.00	0.00	20.00
7	0.00	200.00	10.00	0.00	20.00
8	0.00	200.00	10.00	0.00	20.00
9	0.00	200.00	10.00	0.00	20.00

10	0.00	175.00	8.75	0.00	20.00
11	0.00	150.00	7.50	0.00	20.00
12	0.00	125.00	6.25	0.00	20.00
13	0.00	100.00	5.00	0.00	20.00
14	0.00	100.00	5.00	0.00	20.00
15	0.00	100.00	5.00	0.00	20.00
16	0.00	80.00	4.00	0.00	20.00
17	0.00	60.00	3.00	0.00	20.00
18	0.00	40.00	2.00	0.00	20.00
19	0.00	20.00	1.00	0.00	20.00
20	0.00	5.00			

HEATING/COOLING SELECTION SUMMARY:

REGION	TIME RANGE MA		# OF EVENTS HEATING	COOLING	NHP	NCP
1	380.0-	0.0	NO	MONOTONIC	0	-1

NUMBER OF FORWARD RANDOM TRIALS, ITER = 10261
max obj function = 0.098824
CONVERGENCE AT 0.05 SIGNIFICANCE LEVEL
number of forward models: 250
STOP DATES - MONTH: 4 DAY: 29 YEAR: 2004

STOP TIME : 22 HR/S 48 MIN 6 S

TOTAL EXECUTION TIME = 0.067789 HOURS OR 4.0673 MINUTES

MODEL RESULTS AT .05 SIGNIFICANCE LEVEL

TIME (MY)	TIME (MA)	EXP MEAN TEMPERATURE (DEG C)	MIN OBJ TEMPERATURE (DEG C)	LOWER TEMP BOUND	UPPER TEMP BOUND
0.00	380.00	186.43	196.42	120.81	200.00
20.00	360.00	182.56	191.37	120.29	200.00
40.00	340.00	177.05	185.08	115.44	199.98
60.00	320.00	170.08	180.78	106.50	199.97
80.00	300.00	160.44	179.49	98.91	199.65
100.00	280.00	153.33	150.65	97.32	199.53
120.00	260.00	139.12	127.99	81.52	199.14
140.00	240.00	120.30	89.04	70.46	190.34
160.00	220.00	89.09	78.09	61.34	118.63
180.00	200.00	77.15	62.00	53.26	97.25
200.00	180.00	67.61	55.96	47.69	86.56
220.00	160.00	58.68	53.86	40.16	77.14
240.00	140.00	50.99	50.80	29.83	63.90
260.00	120.00	43.73	44.77	27.49	55.83
280.00	100.00	37.18	36.78	21.92	49.68
300.00	80.00	30.75	33.02	6.77	44.28
320.00	60.00	24.20	21.14	0.08	37.82
340.00	40.00	17.48	17.31	0.01	32.60
360.00	20.00	10.29	13.88	0.01	19.68
380.00	0.00	2.37	0.24	0.01	5.00

START DATE - MONTH: 2 DAY: 11 YEAR: 2004

START TIME: 9 HR/S 25 MIN 22 S

Na-10 Herbert Island dyke initial 15 micron cooling only

LASLETT ET AL ANNEALING MODEL FOR DURANGO APATITE

AFTINV32 v. 1.3 (AUGUST 3, 2000)
32-bit Watcom F77 v. 10.6 compiled for Windows 95
as a Windows NT windowed executable
code optimized for an Intel Pentium processor
Original source code developed by Sean Willett
Source code modified by Dale Issler

inversion control parameters:

MONTE CARLO RANDOM SEARCH METHOD USED
number of solutions (l) = 250
number of timesteps (m) = 19
number of parameters (m+1) = 20
NUMERICAL ACCURACY (%), ACUR = 0.1000000
timestep length (delsub) = 2.000
obj fnct (2 = chi2; 3 = K-S; 4 = Kuiper) = 3
convergence tolerance (tol95) = 0.1173291
convergence tolerance (toler) = 0.0714955
number of standard deviations to fit age 2.0
measured age = 225.00
sigma of error in measured age = 13.10
number of tracks measured = 131
intermediate output every 50 forward models
random number generator seed = 91
system number generator urand(iseed)
expansion factor (alpha) = 1.300
reposition factor for explicit bound (delta) = 0.0010
original track length (xl0) 15.000
initial mean radius of length ellipse (xl3e) = 0.000
conventional mean data
empirical model of age reduction
track length reduction coefs.:
-4.86999989 0.00016800 -28.12000084 0.00000000 0.34999999
2.70000005
component variance coefs.:
0.78990000 0.00303500 -0.00229830 0.00000000

	temperature bounds		rate bounds		delt
1	0.00	200.00	10.00	0.00	20.00
2	0.00	200.00	10.00	0.00	20.00
3	0.00	200.00	10.00	0.00	20.00
4	0.00	200.00	10.00	0.00	20.00
5	0.00	200.00	10.00	0.00	20.00
6	0.00	200.00	7.50	0.00	20.00
7	0.00	200.00	7.50	0.00	20.00
8	0.00	150.00	7.50	0.00	20.00
9	0.00	150.00	7.50	0.00	20.00
10	0.00	150.00	7.50	0.00	20.00

11	0.00	120.00	6.00	0.00	20.00
12	0.00	120.00	6.00	0.00	20.00
13	0.00	120.00	6.00	0.00	20.00
14	0.00	100.00	5.00	0.00	20.00
15	0.00	100.00	5.00	0.00	20.00
16	0.00	80.00	4.00	0.00	20.00
17	0.00	60.00	3.00	0.00	20.00
18	0.00	40.00	2.00	0.00	20.00
19	0.00	20.00	1.00	0.00	20.00
20	0.00	10.00			

HEATING/COOLING SELECTION SUMMARY:

REGION	TIME RANGE MA		# OF EVENTS HEATING	COOLING	NHP	NCP
1	380.0-	0.0	NO	MONOTONIC	0	-1

NUMBER OF FORWARD RANDOM TRIALS, ITER = 3950
max obj function = 0.117127
CONVERGENCE AT 0.05 SIGNIFICANCE LEVEL
number of forward models: 250
STOP DATES - MONTH: 2 DAY: 11 YEAR: 2004

STOP TIME : 9 HR/S 26 MIN 34 S

TOTAL EXECUTION TIME = 0.020033 HOURS OR 1.2020 MINUTES

MODEL RESULTS AT .05 SIGNIFICANCE LEVEL

TIME (MY)	TIME (MA)	EXP MEAN TEMPERATURE (DEG C)	MIN OBJ TEMPERATURE (DEG C)	LOWER TEMP BOUND	UPPER TEMP BOUND
0.00	380.00	184.45	172.09	129.22	199.99
20.00	360.00	179.16	160.01	119.32	199.95
40.00	340.00	172.63	156.40	113.47	199.94
60.00	320.00	163.92	124.28	104.47	199.90
80.00	300.00	152.75	112.69	96.83	199.90
100.00	280.00	143.29	110.90	90.00	199.59
120.00	260.00	128.32	103.56	62.63	193.81
140.00	240.00	103.00	94.83	62.44	146.95
160.00	220.00	86.38	83.24	56.34	109.82
180.00	200.00	76.02	60.03	54.74	92.94
200.00	180.00	67.62	55.02	43.84	88.80
220.00	160.00	58.95	53.46	37.68	77.53
240.00	140.00	51.49	50.88	34.30	67.35
260.00	120.00	43.32	43.76	5.64	60.51
280.00	100.00	35.33	38.42	2.75	52.88
300.00	80.00	28.59	30.88	0.55	45.45
320.00	60.00	22.07	16.63	0.34	40.93
340.00	40.00	15.55	12.16	0.01	31.88
360.00	20.00	8.94	5.09	0.01	19.64
380.00	0.00	3.89	0.19	0.01	9.91

START DATE - MONTH: 2 DAY: 10 YEAR: 2004

START TIME: 22 HR/S 17 MIN 22 S

Na-18 Haklyut Island dyke initial 15 micron cooling only

LASLETT ET AL ANNEALING MODEL FOR DURANGO APATITE

AFTINV32 v. 1.3 (AUGUST 3, 2000)
32-bit Watcom F77 v. 10.6 compiled for Windows 95
as a Windows NT windowed executable
code optimized for an Intel Pentium processor
Original source code developed by Sean Willett
Source code modified by Dale Issler

inversion control parameters:

MONTE CARLO RANDOM SEARCH METHOD USED
number of solutions (l) = 250
number of timesteps (m) = 19
number of parameters (m+1) = 20
NUMERICAL ACCURACY (%), ACUR = 0.1000000
timestep length (delsub) = 2.000
obj fnct (2 = chi2; 3 = K-S; 4 = Kuiper) = 3
convergence tolerance (tol95) = 0.1076251
convergence tolerance (toler) = 0.0655823
number of standard deviations to fit age 2.0
measured age = 268.00
sigma of error in measured age = 16.00
number of tracks measured = 156
intermediate output every 50 forward models
random number generator seed = 91
system number generator urand(iseed)
expansion factor (alpha) = 1.300
reposition factor for explicit bound (delta) = 0.0010
original track length (xl0) 15.000
initial mean radius of length ellipse (xl3e) = 0.000
conventional mean data
empirical model of age reduction
track length reduction coefs.:
-4.86999989 0.00016800 -28.12000084 0.00000000 0.34999999
2.70000005
component variance coefs.:
0.78990000 0.00303500 -0.00229830 0.00000000

	temperature bounds		rate bounds		delt
1	0.00	200.00	10.00	0.00	20.00
2	0.00	200.00	10.00	0.00	20.00
3	0.00	200.00	10.00	0.00	20.00
4	0.00	200.00	10.00	0.00	20.00
5	0.00	200.00	10.00	0.00	20.00
6	0.00	150.00	7.50	0.00	20.00
7	0.00	150.00	7.50	0.00	20.00
8	0.00	150.00	7.50	0.00	20.00
9	0.00	150.00	7.50	0.00	20.00
10	0.00	150.00	7.50	0.00	20.00

11	0.00	120.00	6.00	0.00	20.00
12	0.00	120.00	6.00	0.00	20.00
13	0.00	120.00	6.00	0.00	20.00
14	0.00	100.00	5.00	0.00	20.00
15	0.00	100.00	5.00	0.00	20.00
16	0.00	80.00	4.00	0.00	20.00
17	0.00	60.00	3.00	0.00	20.00
18	0.00	40.00	2.00	0.00	20.00
19	0.00	20.00	1.00	0.00	20.00
20	0.00	10.00			

HEATING/COOLING SELECTION SUMMARY:

REGION	TIME RANGE MA		# OF EVENTS HEATING	COOLING	NHP	NCP
1	380.0-	0.0	NO	MONOTONIC	0	-1

NUMBER OF FORWARD RANDOM TRIALS, ITER = 15058
max obj function = 0.107479
CONVERGENCE AT 0.05 SIGNIFICANCE LEVEL
number of forward models: 250
STOP DATES - MONTH: 2 DAY: 10 YEAR: 2004

STOP TIME : 22 HR/S 22 MIN 35 S

TOTAL EXECUTION TIME = 0.086981 HOURS OR 5.2188 MINUTES

MODEL RESULTS AT .05 SIGNIFICANCE LEVEL

TIME (MY)	TIME (MA)	EXP MEAN TEMPERATURE (DEG C)	MIN OBJ TEMPERATURE (DEG C)	LOWER TEMP BOUND	UPPER TEMP BOUND
0.00	380.00	172.15	127.86	99.32	199.99
20.00	360.00	164.25	123.26	96.20	199.99
40.00	340.00	155.41	116.31	91.48	199.86
60.00	320.00	142.68	101.43	86.57	199.82
80.00	300.00	117.03	93.57	74.55	190.41
100.00	280.00	97.23	81.83	63.24	137.30
120.00	260.00	86.05	81.32	62.22	103.28
140.00	240.00	79.22	79.55	58.81	92.81
160.00	220.00	72.88	72.73	51.12	87.39
180.00	200.00	66.66	58.76	44.45	84.39
200.00	180.00	60.24	51.87	38.59	74.46
220.00	160.00	54.25	44.84	33.25	70.54
240.00	140.00	47.13	41.77	24.88	61.53
260.00	120.00	40.26	34.63	16.45	58.07
280.00	100.00	32.89	34.51	2.62	54.73
300.00	80.00	25.22	34.19	0.29	42.31
320.00	60.00	18.90	27.47	0.08	39.42
340.00	40.00	13.15	13.45	0.04	29.03
360.00	20.00	7.59	8.71	0.01	19.51
380.00	0.00	3.70	6.87	0.01	9.90

START DATE - MONTH: 2 DAY: 10 YEAR: 2004

START TIME: 21 HR/S 19 MIN 9 S

na-63 15 micron initial length
cooling only

LASLETT ET AL ANNEALING MODEL FOR DURANGO APATITE

AFTINV32 v. 1.3 (AUGUST 3, 2000)
32-bit Watcom F77 v. 10.6 compiled for Windows 95
as a Windows NT windowed executable
code optimized for an Intel Pentium processor
Original source code developed by Sean Willett
Source code modified by Dale Issler

inversion control parameters:

MONTE CARLO RANDOM SEARCH METHOD USED
number of solutions (1) = 250
number of timesteps (m) = 19
number of parameters (m+1) = 20
NUMERICAL ACCURACY (%), ACUR = 0.1000000
timestep length (delsub) = 2.000
obj fnct (2 = chi2; 3 = K-S; 4 = Kuiper) = 3
convergence tolerance (tol95) = 0.1093729
convergence tolerance (toler) = 0.0666473
number of standard deviations to fit age 2.0
measured age = 264.00
sigma of error in measured age = 9.10
number of tracks measured = 151
intermediate output every 50 forward models
random number generator seed = 91
system number generator urand(iseed)
expansion factor (alpha) = 1.300
reposition factor for explicit bound (delta) = 0.0010
original track length (xl0) 15.000
initial mean radius of length ellipse (xl3e) = 0.000
conventional mean data
empirical model of age reduction
track length reduction coefs.:
-4.86999989 0.00016800 -28.12000084 0.00000000 0.34999999
2.70000005
component variance coefs.:
0.78990000 0.00303500 -0.00229830 0.00000000

	temperature bounds		rate bounds		delt
1	0.00	200.00	10.00	0.00	20.00
2	0.00	200.00	10.00	0.00	20.00
3	0.00	200.00	10.00	0.00	20.00
4	0.00	200.00	10.00	0.00	20.00
5	0.00	200.00	10.00	0.00	20.00
6	0.00	150.00	7.50	0.00	20.00
7	0.00	150.00	7.50	0.00	20.00
8	0.00	150.00	7.50	0.00	20.00
9	0.00	150.00	7.50	0.00	20.00
10	0.00	150.00	7.50	0.00	20.00

11	0.00	120.00	6.00	0.00	20.00
12	0.00	120.00	6.00	0.00	20.00
13	0.00	120.00	6.00	0.00	20.00
14	0.00	100.00	5.00	0.00	20.00
15	0.00	100.00	5.00	0.00	20.00
16	0.00	80.00	4.00	0.00	20.00
17	0.00	60.00	3.00	0.00	20.00
18	0.00	40.00	2.00	0.00	20.00
19	0.00	20.00	1.00	0.00	20.00
20	0.00	10.00			

HEATING/COOLING SELECTION SUMMARY:

REGION	TIME RANGE MA		# OF EVENTS HEATING	COOLING	NHP	NCP
1	380.0-	0.0	NO	MONOTONIC	0	-1

NUMBER OF FORWARD RANDOM TRIALS, ITER = 29703
max obj function = 0.109362
CONVERGENCE AT 0.05 SIGNIFICANCE LEVEL
number of forward models: 250
STOP DATES - MONTH: 2 DAY: 10 YEAR: 2004

STOP TIME : 21 HR/S 29 MIN 3 S

TOTAL EXECUTION TIME = 0.164984 HOURS OR 9.8990 MINUTES

MODEL RESULTS AT .05 SIGNIFICANCE LEVEL

TIME (MY)	TIME (MA)	EXP MEAN TEMPERATURE (DEG C)	MIN OBJ TEMPERATURE (DEG C)	LOWER TEMP BOUND	UPPER TEMP BOUND
0.00	380.00	170.38	130.06	110.76	199.97
20.00	360.00	162.39	129.32	106.02	199.95
40.00	340.00	153.52	119.59	99.08	199.93
60.00	320.00	143.89	105.42	91.73	199.82
80.00	300.00	120.08	98.54	80.13	199.61
100.00	280.00	92.62	92.05	66.33	128.61
120.00	260.00	83.30	85.78	63.34	94.89
140.00	240.00	77.28	78.07	54.44	90.58
160.00	220.00	70.55	70.64	53.11	82.41
180.00	200.00	64.04	64.28	44.45	79.26
200.00	180.00	58.06	52.71	41.54	73.13
220.00	160.00	51.70	50.26	33.21	64.01
240.00	140.00	45.66	39.56	24.88	60.15
260.00	120.00	39.25	37.68	19.53	55.77
280.00	100.00	32.22	32.24	13.75	46.59
300.00	80.00	25.57	27.44	3.25	42.23
320.00	60.00	19.62	25.45	0.60	34.08
340.00	40.00	13.95	25.42	0.10	28.98
360.00	20.00	8.51	14.42	0.01	19.74
380.00	0.00	4.07	8.77	0.01	9.81

START DATE - MONTH: 2 DAY: 11 YEAR: 2004

START TIME: 9 HR/S 33 MIN 38 S

Na-64 Kap Trautwine gneiss initial 15 micron cooling only

LASLETT ET AL ANNEALING MODEL FOR DURANGO APATITE

AFTINV32 v. 1.3 (AUGUST 3, 2000)
32-bit Watcom F77 v. 10.6 compiled for Windows 95
as a Windows NT windowed executable
code optimized for an Intel Pentium processor
Original source code developed by Sean Willett
Source code modified by Dale Issler

inversion control parameters:

MONTE CARLO RANDOM SEARCH METHOD USED
number of solutions (l) = 250
number of timesteps (m) = 19
number of parameters (m+1) = 20
NUMERICAL ACCURACY (%), ACUR = 0.1000000
timestep length (delsub) = 2.000
obj fnct (2 = chi2; 3 = K-S; 4 = Kuiper) = 3
convergence tolerance (tol95) = 0.1069492
convergence tolerance (toler) = 0.0651704
number of standard deviations to fit age 2.0
measured age = 189.00
sigma of error in measured age = 5.90
number of tracks measured = 158
intermediate output every 50 forward models
random number generator seed = 91
system number generator urand(iseed)
expansion factor (alpha) = 1.300
reposition factor for explicit bound (delta) = 0.0010
original track length (xl0) 15.000
initial mean radius of length ellipse (xl3e) = 0.000
conventional mean data
empirical model of age reduction
track length reduction coefs.:
-4.86999989 0.00016800 -28.12000084 0.00000000 0.34999999
2.70000005
component variance coefs.:
0.78990000 0.00303500 -0.00229830 0.00000000

	temperature bounds		rate bounds		delt
1	0.00	200.00	10.00	0.00	20.00
2	0.00	200.00	10.00	0.00	20.00
3	0.00	200.00	10.00	0.00	20.00
4	0.00	200.00	10.00	0.00	20.00
5	0.00	200.00	10.00	0.00	20.00
6	0.00	200.00	7.50	0.00	20.00
7	0.00	200.00	7.50	0.00	20.00
8	0.00	150.00	7.50	0.00	20.00
9	0.00	150.00	7.50	0.00	20.00
10	0.00	150.00	7.50	0.00	20.00

11	0.00	120.00	6.00	0.00	20.00
12	0.00	120.00	6.00	0.00	20.00
13	0.00	120.00	6.00	0.00	20.00
14	0.00	100.00	5.00	0.00	20.00
15	0.00	100.00	5.00	0.00	20.00
16	0.00	80.00	4.00	0.00	20.00
17	0.00	60.00	3.00	0.00	20.00
18	0.00	40.00	2.00	0.00	20.00
19	0.00	20.00	1.00	0.00	20.00
20	0.00	10.00			

HEATING/COOLING SELECTION SUMMARY:

REGION	TIME RANGE MA	# OF EVENTS HEATING	COOLING	NHP	NCP
1	380.0- 0.0	NO	MONOTONIC	0	-1

NUMBER OF FORWARD RANDOM TRIALS, ITER = 19329
max obj function = 0.106849
CONVERGENCE AT 0.05 SIGNIFICANCE LEVEL
number of forward models: 250
STOP DATES - MONTH: 2 DAY: 11 YEAR: 2004

STOP TIME : 9 HR/S 42 MIN 33 S

TOTAL EXECUTION TIME = 0.148597 HOURS OR 8.9158 MINUTES

MODEL RESULTS AT .05 SIGNIFICANCE LEVEL

TIME (MY)	TIME (MA)	EXP MEAN TEMPERATURE (DEG C)	MIN OBJ TEMPERATURE (DEG C)	LOWER TEMP BOUND	UPPER TEMP BOUND
0.00	380.00	187.93	159.79	130.39	200.00
20.00	360.00	184.09	152.39	124.92	200.00
40.00	340.00	178.36	138.82	115.08	199.98
60.00	320.00	172.25	138.16	112.65	199.89
80.00	300.00	165.98	130.88	111.84	199.86
100.00	280.00	157.80	120.42	104.83	199.37
120.00	260.00	144.08	119.26	99.88	199.26
140.00	240.00	117.38	115.30	96.06	149.74
160.00	220.00	102.78	93.95	74.68	145.05
180.00	200.00	89.74	83.97	70.17	101.31
200.00	180.00	81.95	74.44	65.72	92.73
220.00	160.00	75.79	70.80	62.14	87.50
240.00	140.00	69.66	67.89	54.42	82.46
260.00	120.00	63.52	67.26	48.04	74.58
280.00	100.00	57.16	60.63	43.97	68.16
300.00	80.00	50.56	54.56	30.72	64.91
320.00	60.00	42.38	44.73	18.12	59.21
340.00	40.00	29.14	29.69	4.09	39.96
360.00	20.00	12.51	16.68	0.05	20.00
380.00	0.00	5.07	1.37	0.05	9.97

START DATE - MONTH: 2 DAY: 11 YEAR: 2004

START TIME: 14 HR/S 56 MIN 3 S

Na-35 Pavy Fm., Cape Back
heat pulse to 35 Ma, init len of 15

LASLETT ET AL ANNEALING MODEL FOR DURANGO APATITE

AFTINV32 v. 1.3 (AUGUST 3, 2000)
32-bit Watcom F77 v. 10.6 compiled for Windows 95
as a Windows NT windowed executable
code optimized for an Intel Pentium processor
Original source code developed by Sean Willett
Source code modified by Dale Issler

inversion control parameters:

MONTE CARLO RANDOM SEARCH METHOD USED
number of solutions (l) = 250
number of timesteps (m) = 12
number of parameters (m+1) = 13
NUMERICAL ACCURACY (%), ACUR = 0.1000000
timestep length (delsub) = 1.000
obj fnct (2 = chi2; 3 = K-S; 4 = Kuiper) = 3
convergence tolerance (tol95) = 0.1191401
convergence tolerance (toler) = 0.0725990
number of standard deviations to fit age 2.0
measured age = 61.00
sigma of error in measured age = 3.80
number of tracks measured = 127
intermediate output every 50 forward models
random number generator seed = 91
system number generator urand(iseed)
expansion factor (alpha) = 1.300
reposition factor for explicit bound (delta) = 0.0010
original track length (xl0) 15.000
initial mean radius of length ellipse (xl3e) = 0.000
conventional mean data
empirical model of age reduction
track length reduction coefs.:
-4.86999989 0.00016800 -28.12000084 0.00000000 0.34999999
2.70000005
component variance coefs.:
0.78990000 0.00303500 -0.00229830 0.00000000

	temperature bounds		rate bounds		delt
1	0.00	5.00	0.00	15.00	5.00
2	0.00	80.00	15.00	15.00	5.00
3	0.00	80.00	15.00	13.00	5.00
4	0.00	80.00	13.00	12.00	5.00
5	0.00	60.00	12.00	10.00	5.00
6	0.00	60.00	10.00	0.00	5.00
7	0.00	40.00	8.00	0.00	5.00
8	0.00	30.00	6.00	0.00	5.00
9	0.00	25.00	5.00	0.00	5.00
10	0.00	20.00	4.00	0.00	5.00

11	0.00	15.00	3.00	0.00	5.00
12	0.00	10.00	2.00	0.00	5.00
13	0.00	5.00			

HEATING/COOLING SELECTION SUMMARY:

REGION	TIME RANGE MA	# OF EVENTS HEATING	COOLING	NHP	NCP
1	60.0- 55.0	1	NO	1	0
2	55.0- 35.0	1	MONOTONIC	1	-1
3	35.0- 0.0	NO	MONOTONIC	0	-1

NUMBER OF FORWARD RANDOM TRIALS, ITER = 323
max obj function = 0.119117
CONVERGENCE AT 0.05 SIGNIFICANCE LEVEL
number of forward models: 250
STOP DATES - MONTH: 2 DAY: 11 YEAR: 2004

STOP TIME : 14 HR/S 56 MIN 8 S

TOTAL EXECUTION TIME = 0.001403 HOURS OR 0.0842 MINUTES

MODEL RESULTS AT .05 SIGNIFICANCE LEVEL

TIME (MY)	TIME (MA)	EXP MEAN TEMPERATURE (DEG C)	MIN OBJ TEMPERATURE (DEG C)	LOWER TEMP BOUND	UPPER TEMP BOUND
0.00	60.00	2.65	4.18	0.00	4.99
5.00	55.00	33.05	67.31	0.00	67.31
10.00	50.00	27.38	12.69	0.00	56.24
15.00	45.00	24.17	12.45	0.01	52.48
20.00	40.00	21.36	4.82	0.14	47.35
25.00	35.00	19.92	3.29	0.19	52.33
30.00	30.00	15.08	2.44	0.04	35.34
35.00	25.00	11.99	2.31	0.01	22.84
40.00	20.00	9.11	2.02	0.01	21.05
45.00	15.00	6.78	1.11	0.00	16.81
50.00	10.00	4.45	0.66	0.00	13.95
55.00	5.00	2.63	0.07	0.00	9.86
60.00	0.00	1.34	0.04	0.00	4.79

START DATE - MONTH: 2 DAY: 11 YEAR: 2004

START TIME: 15 HR/S 0 MIN 21 S

Na-36 Pavy Fm., Cape Back
heat pulse to 35 Ma, init len of 15

LASLETT ET AL ANNEALING MODEL FOR DURANGO APATITE

AFTINV32 v. 1.3 (AUGUST 3, 2000)
32-bit Watcom F77 v. 10.6 compiled for Windows 95
as a Windows NT windowed executable
code optimized for an Intel Pentium processor
Original source code developed by Sean Willett
Source code modified by Dale Issler

inversion control parameters:

MONTE CARLO RANDOM SEARCH METHOD USED
number of solutions (l) = 250
number of timesteps (m) = 12
number of parameters (m+1) = 13
NUMERICAL ACCURACY (%), ACUR = 0.1000000
timestep length (delsub) = 1.000
obj fnct (2 = chi2; 3 = K-S; 4 = Kuiper) = 3
convergence tolerance (tol95) = 0.1056348
convergence tolerance (toler) = 0.0643694
number of standard deviations to fit age 2.0
measured age = 62.40
sigma of error in measured age = 3.10
number of tracks measured = 162
intermediate output every 50 forward models
random number generator seed = 91
system number generator urand(iseed)
expansion factor (alpha) = 1.300
reposition factor for explicit bound (delta) = 0.0010
original track length (xl0) 15.000
initial mean radius of length ellipse (xl3e) = 0.000
conventional mean data
empirical model of age reduction
track length reduction coefs.:
-4.86999989 0.00016800 -28.12000084 0.00000000 0.34999999
2.70000005
component variance coefs.:
0.78990000 0.00303500 -0.00229830 0.00000000

	temperature bounds		rate bounds		delt
1	0.00	5.00	0.00	15.00	5.00
2	0.00	80.00	15.00	15.00	5.00
3	0.00	80.00	15.00	13.00	5.00
4	0.00	80.00	13.00	12.00	5.00
5	0.00	60.00	12.00	10.00	5.00
6	0.00	60.00	10.00	0.00	5.00
7	0.00	40.00	8.00	0.00	5.00
8	0.00	30.00	6.00	0.00	5.00
9	0.00	25.00	5.00	0.00	5.00
10	0.00	20.00	4.00	0.00	5.00

11	0.00	15.00	3.00	0.00	5.00
12	0.00	10.00	2.00	0.00	5.00
13	0.00	5.00			

HEATING/COOLING SELECTION SUMMARY:

REGION	TIME RANGE MA	# OF EVENTS HEATING	COOLING	NHP	NCP
1	60.0- 55.0	1	NO	1	0
2	55.0- 35.0	1	MONOTONIC	1	-1
3	35.0- 0.0	NO	MONOTONIC	0	-1

NUMBER OF FORWARD RANDOM TRIALS, ITER = 1722
max obj function = 0.105634
CONVERGENCE AT 0.05 SIGNIFICANCE LEVEL
number of forward models: 250
STOP DATES - MONTH: 2 DAY: 11 YEAR: 2004

STOP TIME : 15 HR/S 0 MIN 40 S

TOTAL EXECUTION TIME = 0.005330 HOURS OR 0.3198 MINUTES

MODEL RESULTS AT .05 SIGNIFICANCE LEVEL

TIME (MY)	TIME (MA)	EXP MEAN TEMPERATURE (DEG C)	MIN OBJ TEMPERATURE (DEG C)	LOWER TEMP BOUND	UPPER TEMP BOUND
0.00	60.00	2.72	2.43	0.04	5.00
5.00	55.00	52.62	66.45	0.64	79.22
10.00	50.00	48.86	62.83	0.55	79.19
15.00	45.00	43.66	16.80	0.20	79.65
20.00	40.00	35.01	4.00	0.22	58.73
25.00	35.00	30.57	5.87	0.26	52.33
30.00	30.00	22.41	4.17	0.18	38.53
35.00	25.00	16.61	3.56	0.01	29.55
40.00	20.00	11.63	2.70	0.00	23.86
45.00	15.00	7.80	1.67	0.00	18.17
50.00	10.00	4.87	0.83	0.00	14.32
55.00	5.00	2.94	0.83	0.00	9.87
60.00	0.00	1.54	0.70	0.00	4.89

START DATE - MONTH: 2 DAY: 11 YEAR: 2004

START TIME: 15 HR/S 4 MIN 21 S

Na-48 Pavy Fm., south of Cape Baird
heat pulse to 35 Ma, init len of 15

LASLETT ET AL ANNEALING MODEL FOR DURANGO APATITE

AFTINV32 v. 1.3 (AUGUST 3, 2000)
32-bit Watcom F77 v. 10.6 compiled for Windows 95
as a Windows NT windowed executable
code optimized for an Intel Pentium processor
Original source code developed by Sean Willett
Source code modified by Dale Issler

inversion control parameters:

MONTE CARLO RANDOM SEARCH METHOD USED
number of solutions (l) = 250
number of timesteps (m) = 12
number of parameters (m+1) = 13
NUMERICAL ACCURACY (%), ACUR = 0.1000000
timestep length (delsub) = 1.000
obj fnct (2 = chi2; 3 = K-S; 4 = Kuiper) = 3
convergence tolerance (tol95) = 0.1147616
convergence tolerance (toler) = 0.0699310
number of standard deviations to fit age 2.0
measured age = 58.20
sigma of error in measured age = 3.80
number of tracks measured = 137
intermediate output every 50 forward models
random number generator seed = 91
system number generator urand(iseed)
expansion factor (alpha) = 1.300
reposition factor for explicit bound (delta) = 0.0010
original track length (xl0) 15.000
initial mean radius of length ellipse (xl3e) = 0.000
conventional mean data
empirical model of age reduction
track length reduction coefs.:
-4.86999989 0.00016800 -28.12000084 0.00000000 0.34999999
2.70000005
component variance coefs.:
0.78990000 0.00303500 -0.00229830 0.00000000

	temperature bounds		rate bounds		delt
1	0.00	5.00	0.00	15.00	5.00
2	0.00	80.00	15.00	15.00	5.00
3	0.00	80.00	15.00	13.00	5.00
4	0.00	80.00	13.00	12.00	5.00
5	0.00	60.00	12.00	10.00	5.00
6	0.00	60.00	10.00	0.00	5.00
7	0.00	40.00	8.00	0.00	5.00
8	0.00	30.00	6.00	0.00	5.00
9	0.00	25.00	5.00	0.00	5.00
10	0.00	20.00	4.00	0.00	5.00

11	0.00	15.00	3.00	0.00	5.00
12	0.00	10.00	2.00	0.00	5.00
13	0.00	5.00			

HEATING/COOLING SELECTION SUMMARY:

REGION	TIME RANGE MA	# OF EVENTS HEATING	COOLING	NHP	NCP
1	60.0- 55.0	1	NO	1	0
2	55.0- 35.0	1	MONOTONIC	1	-1
3	35.0- 0.0	NO	MONOTONIC	0	-1

NUMBER OF FORWARD RANDOM TRIALS, ITER = 420
max obj function = 0.114548
CONVERGENCE AT 0.05 SIGNIFICANCE LEVEL
number of forward models: 250
STOP DATES - MONTH: 2 DAY: 11 YEAR: 2004

STOP TIME : 15 HR/S 4 MIN 26 S

TOTAL EXECUTION TIME = 0.001403 HOURS OR 0.0842 MINUTES

MODEL RESULTS AT .05 SIGNIFICANCE LEVEL

TIME (MY)	TIME (MA)	EXP MEAN TEMPERATURE (DEG C)	MIN OBJ TEMPERATURE (DEG C)	LOWER TEMP BOUND	UPPER TEMP BOUND
0.00	60.00	2.76	0.45	0.00	4.91
5.00	55.00	38.14	60.40	0.00	66.99
10.00	50.00	34.44	56.24	0.13	76.92
15.00	45.00	32.72	35.57	0.37	78.66
20.00	40.00	27.13	24.70	2.26	54.49
25.00	35.00	25.48	16.29	1.02	43.83
30.00	30.00	21.25	6.43	0.10	35.34
35.00	25.00	17.44	5.68	0.06	29.48
40.00	20.00	13.98	4.63	0.03	24.88
45.00	15.00	10.89	3.70	0.00	19.97
50.00	10.00	7.04	2.46	0.00	14.87
55.00	5.00	4.36	1.88	0.00	9.86
60.00	0.00	1.98	1.45	0.00	4.98

START DATE - MONTH: 2 DAY: 11 YEAR: 2004

START TIME: 15 HR/S 8 MIN 16 S

Na-48b Pavy Fm., south of Cape Baird
heat pulse to 35 Ma, init len of 15

LASLETT ET AL ANNEALING MODEL FOR DURANGO APATITE

AFTINV32 v. 1.3 (AUGUST 3, 2000)
32-bit Watcom F77 v. 10.6 compiled for Windows 95
as a Windows NT windowed executable
code optimized for an Intel Pentium processor
Original source code developed by Sean Willett
Source code modified by Dale Issler

inversion control parameters:

MONTE CARLO RANDOM SEARCH METHOD USED
number of solutions (l) = 250
number of timesteps (m) = 12
number of parameters (m+1) = 13
NUMERICAL ACCURACY (%), ACUR = 0.1000000
timestep length (delsub) = 1.000
obj fnct (2 = chi2; 3 = K-S; 4 = Kuiper) = 3
convergence tolerance (tol95) = 0.1079679
convergence tolerance (toler) = 0.0657912
number of standard deviations to fit age 2.0
measured age = 56.00
sigma of error in measured age = 3.30
number of tracks measured = 155
intermediate output every 50 forward models
random number generator seed = 91
system number generator urand(iseed)
expansion factor (alpha) = 1.300
reposition factor for explicit bound (delta) = 0.0010
original track length (xl0) 15.000
initial mean radius of length ellipse (xl3e) = 0.000
conventional mean data
empirical model of age reduction
track length reduction coefs.:
-4.86999989 0.00016800 -28.12000084 0.00000000 0.34999999
2.70000005
component variance coefs.:
0.78990000 0.00303500 -0.00229830 0.00000000

	temperature bounds		rate bounds		delt
1	0.00	5.00	0.00	15.00	5.00
2	0.00	80.00	15.00	15.00	5.00
3	0.00	80.00	15.00	13.00	5.00
4	0.00	80.00	13.00	12.00	5.00
5	0.00	60.00	12.00	10.00	5.00
6	0.00	60.00	10.00	0.00	5.00
7	0.00	40.00	8.00	0.00	5.00
8	0.00	30.00	6.00	0.00	5.00
9	0.00	25.00	5.00	0.00	5.00

10	0.00	20.00	4.00	0.00	5.00
11	0.00	15.00	3.00	0.00	5.00
12	0.00	10.00	2.00	0.00	5.00
13	0.00	5.00			

HEATING/COOLING SELECTION SUMMARY:

REGION	TIME RANGE MA	# OF EVENTS HEATING	COOLING	NHP	NCP
1	60.0- 55.0	1	NO	1	0
2	55.0- 35.0	1	MONOTONIC	1	-1
3	35.0- 0.0	NO	MONOTONIC	0	-1

NUMBER OF FORWARD RANDOM TRIALS, ITER = 638
max obj function = 0.107756
CONVERGENCE AT 0.05 SIGNIFICANCE LEVEL
number of forward models: 250
STOP DATES - MONTH: 2 DAY: 11 YEAR: 2004

STOP TIME : 15 HR/S 8 MIN 24 S

TOTAL EXECUTION TIME = 0.002245 HOURS OR 0.1347 MINUTES

MODEL RESULTS AT .05 SIGNIFICANCE LEVEL

TIME (MY)	TIME (MA)	EXP MEAN TEMPERATURE (DEG C)	MIN OBJ TEMPERATURE (DEG C)	LOWER TEMP BOUND	UPPER TEMP BOUND
0.00	60.00	2.62	3.37	0.02	5.00
5.00	55.00	52.68	59.80	0.64	79.22
10.00	50.00	50.48	56.05	0.41	79.37
15.00	45.00	48.33	63.44	0.39	79.77
20.00	40.00	40.60	56.90	1.10	59.51
25.00	35.00	38.01	7.13	2.27	59.16
30.00	30.00	28.35	5.89	0.84	39.80
35.00	25.00	20.88	4.47	0.14	29.99
40.00	20.00	15.84	3.27	0.01	24.90
45.00	15.00	11.37	3.21	0.01	19.92
50.00	10.00	7.65	3.12	0.00	14.89
55.00	5.00	4.29	1.55	0.00	9.97
60.00	0.00	2.02	1.14	0.00	4.98

START DATE - MONTH: 3 DAY: 22 YEAR: 2004

START TIME: 15 HR/S 19 MIN 10 S

Na-32 Cape Lawrence Archer Fiord Fm.
cooling only 15 initial

LASLETT ET AL ANNEALING MODEL FOR DURANGO APATITE

AFTINV32 v. 1.3 (AUGUST 3, 2000)
32-bit Watcom F77 v. 10.6 compiled for Windows 95
as a Windows NT windowed executable
code optimized for an Intel Pentium processor
Original source code developed by Sean Willett
Source code modified by Dale Issler

inversion control parameters:

MONTE CARLO RANDOM SEARCH METHOD USED
number of solutions (l) = 250
number of timesteps (m) = 20
number of parameters (m+1) = 21
NUMERICAL ACCURACY (%), ACUR = 0.1000000
timestep length (delsub) = 1.000
obj fnct (2 = chi2; 3 = K-S; 4 = Kuiper) = 3
convergence tolerance (tol95) = 0.1062858
convergence tolerance (toler) = 0.0647662
number of standard deviations to fit age 2.0
measured age = 63.40
sigma of error in measured age = 2.30
number of tracks measured = 160
intermediate output every 50 forward models
random number generator seed = 91
system number generator urand(iseed)
expansion factor (alpha) = 1.300
reposition factor for explicit bound (delta) = 0.0010
original track length (xl0) 15.000
initial mean radius of length ellipse (xl3e) = 0.000
conventional mean data
empirical model of age reduction
track length reduction coefs.:
-4.86999989 0.00016800 -28.12000084 0.00000000 0.34999999
2.70000005
component variance coefs.:
0.78990000 0.00303500 -0.00229830 0.00000000

	temperature bounds		rate bounds		delt
1	0.00	200.00	20.00	0.00	5.00
2	0.00	200.00	20.00	0.00	5.00
3	0.00	200.00	20.00	0.00	5.00
4	0.00	200.00	20.00	0.00	5.00
5	0.00	200.00	20.00	0.00	5.00
6	0.00	200.00	20.00	0.00	5.00
7	0.00	200.00	20.00	0.00	5.00
8	0.00	200.00	20.00	0.00	5.00
9	0.00	200.00	20.00	0.00	5.00
10	0.00	200.00	20.00	0.00	5.00

11	0.00	200.00	20.00	0.00	5.00
12	0.00	200.00	20.00	0.00	5.00
13	0.00	200.00	20.00	0.00	5.00
14	0.00	200.00	20.00	0.00	5.00
15	0.00	200.00	20.00	0.00	5.00
16	0.00	200.00	20.00	0.00	5.00
17	0.00	150.00	20.00	0.00	5.00
18	0.00	100.00	20.00	0.00	5.00
19	0.00	20.00	4.00	0.00	5.00
20	0.00	10.00	2.00	0.00	5.00
21	0.00	5.00			

HEATING/COOLING SELECTION SUMMARY:

REGION	TIME RANGE MA		# OF EVENTS HEATING	COOLING	NHP	NCP
1	100.0-	0.0	NO	MONOTONIC	0	-1

NUMBER OF FORWARD RANDOM TRIALS, ITER = 74668
max obj function = 0.106275
CONVERGENCE AT 0.05 SIGNIFICANCE LEVEL
number of forward models: 250
STOP DATES - MONTH: 3 DAY: 22 YEAR: 2004

STOP TIME : 15 HR/S 33 MIN 46 S

TOTAL EXECUTION TIME = 0.243433 HOURS OR 14.6060 MINUTES

MODEL RESULTS AT .05 SIGNIFICANCE LEVEL

TIME (MY)	TIME (MA)	EXP MEAN TEMPERATURE (DEG C)	MIN OBJ TEMPERATURE (DEG C)	LOWER TEMP BOUND	UPPER TEMP BOUND
0.00	100.00	164.11	191.89	116.30	199.95
5.00	95.00	159.63	191.84	115.73	199.90
10.00	90.00	154.33	188.65	111.38	199.81
15.00	85.00	148.26	185.37	108.29	199.69
20.00	80.00	141.56	182.89	107.13	199.14
25.00	75.00	135.66	178.84	103.28	179.45
30.00	70.00	129.37	174.50	102.28	179.31
35.00	65.00	115.74	125.95	28.33	168.32
40.00	60.00	89.11	82.89	7.23	119.29
45.00	55.00	67.56	79.53	0.10	102.94
50.00	50.00	35.97	24.11	0.09	83.01
55.00	45.00	26.27	0.01	0.01	57.83
60.00	40.00	19.43	0.01	0.01	44.49
65.00	35.00	14.30	0.00	0.00	35.05
70.00	30.00	10.24	0.00	0.00	24.26
75.00	25.00	7.16	0.00	0.00	17.80
80.00	20.00	5.10	0.00	0.00	14.41
85.00	15.00	3.54	0.00	0.00	10.62
90.00	10.00	2.41	0.00	0.00	10.41
95.00	5.00	1.48	0.00	0.00	8.12
100.00	0.00	0.84	0.00	0.00	4.98

START DATE - MONTH: 2 DAY: 11 YEAR: 2004

START TIME: 14 HR/S   4 MIN   59 S

Na-66 Nares Mt.Moore/Mt. Lawson
heat pulse to 35 Ma, init len of 15

LASLETT ET AL ANNEALING MODEL FOR DURANGO APATITE

AFTINV32 v. 1.3 (AUGUST 3, 2000)
32-bit Watcom F77 v. 10.6 compiled for Windows 95
as a Windows NT windowed executable
code optimized for an Intel Pentium processor
Original source code developed by Sean Willett
Source code modified by Dale Issler

inversion control parameters:

MONTE CARLO RANDOM SEARCH METHOD USED
number of solutions (l) = 250
number of timesteps (m) = 12
number of parameters (m+1) = 13
NUMERICAL ACCURACY (%), ACUR = 0.1000000
timestep length (delsub) = 1.000
obj fnct (2 = chi2; 3 = K-S; 4 = Kuiper) = 3
convergence tolerance (tol95) = 0.1168892
convergence tolerance (toler) = 0.0712274
number of standard deviations to fit age 2.0
measured age = 60.20
sigma of error in measured age = 3.90
number of tracks measured = 132
intermediate output every 50 forward models
random number generator seed = 91
system number generator urand(iseed)
expansion factor (alpha) = 1.300
reposition factor for explicit bound (delta) = 0.0010
original track length (xl0) 15.000
initial mean radius of length ellipse (xl3e) = 0.000
conventional mean data
empirical model of age reduction
track length reduction coefs.:
-4.86999989 0.00016800 -28.12000084 0.00000000 0.34999999
2.70000005
component variance coefs.:
 0.78990000 0.00303500 -0.00229830 0.00000000

	temperature bounds		rate bounds		delt
1	0.00	5.00	0.00	15.00	5.00
2	0.00	75.00	15.00	15.00	5.00
3	0.00	75.00	15.00	13.00	5.00
4	0.00	65.00	13.00	12.00	5.00
5	0.00	60.00	12.00	10.00	5.00
6	0.00	50.00	10.00	0.00	5.00
7	0.00	40.00	8.00	0.00	5.00
8	0.00	30.00	6.00	0.00	5.00
9	0.00	25.00	5.00	0.00	5.00
10	0.00	20.00	4.00	0.00	5.00

11	0.00	15.00	3.00	0.00	5.00
12	0.00	10.00	2.00	0.00	5.00
13	0.00	5.00			

HEATING/COOLING SELECTION SUMMARY:

REGION	TIME RANGE MA	# OF EVENTS HEATING	COOLING	NHP	NCP
1	60.0- 55.0	1	NO	1	0
2	55.0- 35.0	1	MONOTONIC	1	-1
3	35.0- 0.0	NO	MONOTONIC	0	-1

NUMBER OF FORWARD RANDOM TRIALS, ITER = 1631
max obj function = 0.116791
CONVERGENCE AT 0.05 SIGNIFICANCE LEVEL
number of forward models: 250
STOP DATES - MONTH: 2 DAY: 11 YEAR: 2004

STOP TIME : 14 HR/S 5 MIN 14 S

TOTAL EXECUTION TIME = 0.004042 HOURS OR 0.2425 MINUTES

MODEL RESULTS AT .05 SIGNIFICANCE LEVEL

TIME (MY)	TIME (MA)	EXP MEAN TEMPERATURE (DEG C)	MIN OBJ TEMPERATURE (DEG C)	LOWER TEMP BOUND	UPPER TEMP BOUND
0.00	60.00	2.72	2.43	0.00	5.00
5.00	55.00	44.53	63.25	0.00	74.28
10.00	50.00	40.95	59.75	0.12	74.30
15.00	45.00	34.28	15.91	0.51	64.57
20.00	40.00	27.88	3.23	0.17	56.32
25.00	35.00	23.90	4.89	1.02	43.60
30.00	30.00	18.30	3.38	0.11	35.34
35.00	25.00	14.73	2.86	0.01	24.23
40.00	20.00	11.39	2.14	0.00	21.40
45.00	15.00	8.56	1.31	0.00	19.35
50.00	10.00	5.95	0.64	0.00	14.44
55.00	5.00	3.44	0.64	0.00	9.89
60.00	0.00	1.58	0.54	0.00	4.98

APPENDIX E.

Apatite compositional data (oxide wt. %) for the Nares Strait/Kane Basin region of Ellesmere Island and western Greenland. All analyses were done using a Jeol JXA 8200 Superprobe at Dalhousie University. Data acquisition was done using a wavelength dispersive system (WDS) with a 5 μm beam diameter, 15.0 kV accelerating voltage, and 2.0 $x10^{-8}$ A current settings.

O	F	Na	Mg	P	S	Cl	Ca	Mn	Fe	Sr	Y	La	Ce	Total	Comment
38.425	3.792	0.114	0.002	18	0.087	0.381	38.58	0.016	0.037	0	0	0.227	0.425	100.09	Dur F_ap1
38.045	3.534	0.109	0.003	17.97	0.088	0.376	38.84	0	0.012	0	0	0.212	0.425	99.618	Dur F_ap2
38.488	3.369	0.1	1E-04	17.96	0.064	0.36	39	0.009	0.012	0.006	0	0.227	0.355	99.951	Dur F_ap3
37.857	3.662	0.144	0.002	17.88	0.125	0.402	38.84	0	0.036	0	0	0.24	0.501	99.691	dur-1
37.772	3.34	0.146	0	17.94	0.154	0.41	38.85	0	0.019	0	0	0.205	0.428	99.263	dur-2
38.781	3.518	0.131	0	17.61	0.12	0.324	38.91	0	0.02	0	0	0.213	0.527	100.16	Dur Ap1
38.249	3.626	0.134	0	17.96	0.09	0.35	38.88	0.001	0.025	0.007	0	0.262	0.499	100.07	Dur Ap2
38.055	3.767	0.127	0	17.87	0.093	0.361	39.04	0.009	0.008	0	0	0.287	0.444	100.07	dur20
37.867	3.336	0.135	0.004	17.43	0.107	0.414	39.13	0.027	0.032	0	0	0.342	0.514	99.339	dur21
37.774	3.451	0.131	0.01	17.37	0.107	0.386	39.07	0	0	0	0	0.253	0.521	99.072	dur22
37.888	3.411	0.115	0.011	17.35	0.108	0.387	39.37	0.012	0.013	0	0	0.303	0.472	99.435	dur23
37.836	3.394	0.108	0.013	17.37	0.105	0.405	39.37	0.014	0.038	0	0	0.322	0.462	99.428	dur24
37.96	3.528	0.149	0.005	17.87	0.084	0.415	39.36	0.014	0.035	0	0	0.211	0.421	100.06	dur25
37.576	3.446	0.115	0.002	17.85	0.077	0.397	38.9	0.028	0.023	0	0	0.227	0.44	99.08	dur26
38.325	3.589	0.119	0.001	17.92	0.057	0.412	39.09	0.014	0.038	0	0	0.23	0.485	100.29	dur27
38.02	3.756	0.148	0	17.91	0.143	0.385	38.9	0.025	0.029	0	0	0.223	0.463	100.01	dur29
37.602	3.376	0.146	0.003	17.86	0.138	0.356	39.12	0	0.044	0.004	0	0.282	0.44	99.368	dur30
37.625	3.398	0.143	0.004	17.92	0.13	0.362	39.24	0.005	0.018	0.012	0	0.24	0.491	99.586	dur-31
37.484	3.47	0.107	0.003	17.69	0.097	0.35	39.35	0.007	0.04	0.006	0	0.208	0.446	99.266	dur-32
37.383	3.365	0.109	0.013	17.17	0.088	0.375	39.3	0.03	0.016	0.003	0	0.223	0.45	98.532	dur33
37.219	3.314	0.12	0.008	17.47	0.094	0.417	39.09	0.018	0.025	0	0	0.287	0.47	98.531	dur34
38.035	3.393	0.163	0.005	17.77	0.136	0.402	39.15	0.004	0.031	0	0	0.278	0.511	99.878	dur35
37.96	3.319	0.108	0	17.8	0.085	0.415	39.21	0.008	0.021	0	0	0.248	0.429	99.608	dur36
37.923	**3.485**	**0.127**	**0.004**	**17.74**	**0.103**	**0.384**	**39.07**	**0.01**	**0.025**	**0.002**	**0**	**0.25**	**0.462**	**99.582**	**Average**

O	F	Na	Mg	P	S	Cl	Ca	Mn	Fe	La	Ce	Total	Comment
40.01	4.129	0.008	0	17.26	0	0.038	39.29	0.014	0.04	0.219	0.776	101.7874	na03b gr47
41.37	3.755	0	0	18.06	0.003	0.044	40.02	0.002	0.026	0.188	0.701	104.1726	na03b gr46
40.52	3.278	0	0.004	18.55	0.006	0.027	40.43	0	0.025	0.078	0.277	103.1953	na03b gr49
40.54	4.173	0	0.004	18.05	0.003	0.02	39.92	0.002	0.04	0.221	0.852	103.8244	na03b gr32
41.44	3.682	0	0.002	18.19	0.005	0.04	39.87	0.01	0.034	0.179	0.766	104.221	na03b gr33
40.44	3.563	0	0	18.3	0.003	0.027	39.77	0	0.029	0.045	0.495	102.6664	na03b gr42
40.33	3.681	0	0	18.02	0.004	0.041	39.76	0	0.041	0.171	0.718	102.7557	na03b gr43
41.49	3.435	0	9E-04	18.03	0.011	0.034	39.91	0.016	0.038	0.166	0.799	103.9244	na03b gr34

40.98	3.597	0	0.002	18.15	7E-04	0.044	39.67	0.012	0.053	0.138	0.755	103.3955	**na03b gr41**
40.12	3.352	0	0.01	18.17	0	0.034	40.23	0.01	0.029	0.008	0.432	102.4072	**na03b gr52**
40.76	3.521	0	0.003	18.24	0.006	0.035	39.66	0	0.026	0.162	0.606	103.0169	**na03b gr51**
40.19	3.456	0.007	6E-04	17.66	0	0.032	39.02	0.015	0.065	0.269	0.881	101.6023	**na03b gr50**
41.41	3.693	0	6E-04	18.15	0.001	0.033	40	0	0.034	0.157	0.687	104.1615	**na03b gr40**
40.94	3.654	0	0.007	18.28	0	0.036	39.9	0	0.028	0.081	0.602	103.5295	**na03b gr37**
40.85	3.509	0	0	18.24	0.011	0.04	40.04	0.004	0.043	0.156	0.58	103.4691	**na03b gr38**
40.66	3.414	0	0.002	18.18	0	0.033	39.37	0.009	0.032	0.131	0.775	102.6081	**na03b gr2**
41.13	3.428	0.005	0.006	17.94	0.002	0.046	39.43	0	0.032	0.261	0.844	103.1225	**na03b gr3**
40	3.658	0	0.003	17.96	0.004	0.027	39.69	0	0.062	0.195	0.808	102.4078	**na03b gr4**
40.42	3.446	0	0	18.01	7E-04	0.044	39.69	0.002	0.056	0.145	0.713	102.5229	**na03b gr1**
40.77	3.535	0	0	18.18	0.009	0.026	39.86	0	0.056	0.093	0.553	103.0804	**na03b gr12**
40.02	3.555	0	0	17.95	0.002	0.057	40	0	0.022	0.115	0.567	102.2816	**na03b gr11**
40.9	3.628	0.004	0	18.4	0.005	0.019	39.88	0.02	0.054	0.131	0.494	103.5396	**na03b gr13**
40.58	3.61	0	0	18.44	0	0.035	40.16	0.018	0.033	0.193	0.585	103.6669	**na03b gr14**
41.16	3.51	0	0	18.28	0.005	0.021	40.05	0	0.068	0.093	0.522	103.7082	**na03b gr19**
39.63	3.585	0	0	18.26	0	0.057	40.13	0	0.047	0.047	0.35	102.0982	**na03b gr26**
40.18	3.514	0.008	0	17.63	0	0.029	40.04	0	0.064	0.215	0.704	102.3852	**na03b gr25**
40.78	3.419	0.011	0	17.87	0	0.026	40.19	0	0.031	0.073	0.282	102.6715	**na03b gr22**
40.46	3.473	0	0	18.01	0.003	0.031	40.58	0.01	0.031	0	0.136	102.744	**na03b gr24**
40.08	3.618	0	0	17.63	0.005	0.041	39.96	5E-04	0.053	0.145	0.574	102.1287	**na03b gr5**
40.49	3.444	0	0	17.92	0.003	0.032	40.41	0.005	0.034	0.072	0.496	102.9245	**na03b gr6**
39.18	3.321	0	0	17.94	0.005	0.018	39.96	0	0.039	0.11	0.416	100.9834	**na03b gr7**
40.58	3.515	0	0	17.91	0.002	0.034	39.75	0.004	0.038	0.048	0.46	102.3316	**na03b gr21**
40.29	3.579	0	0	17.64	0.003	0.034	39.85	0.002	0.079	0.206	0.697	102.3713	**na03b gr10**
40.47	3.428	0.025	0	17.5	0.001	0.047	39.72	0	0.054	0.183	0.725	102.1658	**na03b gr9**
39.59	3.488	0	0	17.71	0	0.019	40.56	0	0.054	0.027	0.282	101.7374	**na03b gr8**
40.05	3.669	0.018	0	17.53	0.003	0.029	39.73	0.028	0.031	0.235	0.76	102.0947	**na03b gr23**
39.92	3.576	0	0	18.05	0.002	0.021	40.56	0	0.045	0.004	0.253	102.4346	**na03b gr17**
40.59	3.417	0	0	17.42	0.006	0.04	39.76	0.009	0.046	0.101	0.374	101.7617	**na03b gr15**
41.52	3.727	0.001	0.004	17.16	0	0.045	40.13	0.002	0.035	0.126	0.531	103.2773	**na03b gr18**
39.92	3.798	0.028	0	17.85	0.003	0.039	39.54	0.019	0.048	0.287	0.85	102.3825	**na03b gr16**
39.67	3.586	0	0	17.47	0	0.041	39.79	0.011	0.058	0.13	0.574	101.328	**na03b gr27**
39.27	3.291	0	0.005	18.02	0	0.033	39.86	0	0.046	0.122	0.706	101.3464	**na03b gr28**
40.47	**3.565**	**0.003**	**0.001**	**17.96**	**0.003**	**0.034**	**39.91**	**0.005**	**0.043**	**0.136**	**0.594**	**102.7199**	**Average**

O	F	Na	Mg	P	S	Cl	Ca	Mn	Fe	Sr	Y	La	Ce	Total	Comment
37.7	3.043	0.024	0.01	16.72	0	0.83	37.51	0.214	0.145	0	0.186	0.373	1.149	97.904	**na32 gr13**
38.984	3.175	0.16	0.021	17.33	0.09	0.302	38.98	0.081	0.042	0	0	0.134	0.634	99.932	**na32 gr14**
39.256	1.984	0.005	0	18.17	0.011	0.127	39.46	0.044	0.005	0	0	0	0.161	99.218	**na32 gr5**
38.886	3.146	0.035	0.02	17.29	0.006	0.489	39.27	0.162	0.158	0	0	0.001	0.211	99.668	**na32 gr4**
39.059	2.803	0.001	0	17	0.004	0.083	38.56	0.068	0.01	0	0	0	0.214	97.808	**na32 gr6**
39.058	2.795	0	0	18.08	0	0.038	40.06	0.057	0.003	0	0	0	0.03	100.11	**na32 gr7**
38.808	3.289	0.026	0	17.33	0.078	0.089	39.56	0.075	0	0	0	0.03	0.195	99.488	**na32 gr1**
38.664	3.343	0.027	0	17.47	0.017	0.07	39.92	0.048	0	0	0	0	0.1	99.65	**na32 gr3**
39.2	3.097	0.002	0	17.57	0.033	0.046	40.31	0.041	0	0	0	0	0.066	100.36	**na32 gr11**
38.302	2.871	0	0	18.13	0.001	0.028	40.11	0.053	0.008	0	0	0	0.039	99.539	**na32 gr10**
37.7	3.189	0.051	0.004	17.51	0.006	0.384	38.93	0.054	0.101	0	0.095	0.104	0.581	98.709	**na32 gr12**
39.016	3.04	0.066	0.006	17.65	0.007	0.326	39.53	0.089	0.057	0	0	0.103	0.357	100.25	**na32 gr20**
38.595	2.524	0	0	17.73	0.017	0.342	39.56	0.062	0	0	0	0	0.133	98.962	**na32 gr22**
38.53	3.574	0.019	0.076	18.26	0.003	0.163	39.75	0.023	0.308	0	0	0	0.153	100.86	**na32 gr23**
38.674	3.01	0.014	0	18.03	0.051	0.114	39.85	0.032	0.013	0	0	0	0.133	99.913	**na32 gr22**
38.782	2.822	0	0	17.19	0.023	0.076	40.03	0.046	0	0	0	0	0.073	99.047	**na32 gr26**
38.467	3.528	0.044	0	17.77	0	0.082	39.31	0.034	0.017	0	0.074	0.059	0.211	99.594	**na32 gr18**
39.209	3.47	0.029	0	17.93	0.043	0.169	39.79	0.043	0.016	0	0	0.03	0.295	101.02	**na32 gr17**
38.846	2.806	0	0	17.25	0.004	0.05	39.75	0.041	4E-04	0	0	0	0.022	98.768	**na32 gr19**
39.61	2.893	0	0	17.51	0.015	0.041	40.06	0.022	0.001	0	0	0	0.041	100.2	**na32 gr42**
38.824	3.053	0	0	17.42	0.007	0.012	40.19	0.035	0	0	0	0	0.044	99.585	**na32 gr43**
41.282	3.277	0.066	0.002	17.59	0.004	0.101	38.79	0.235	0.041	0	0	0	0.125	101.51	**na32 gr44**
38.156	3.622	0	0	16.69	0.004	0.035	39.37	0.049	0.051	0	0	0.001	0.287	98.269	**na32 gr45**
38.999	3.404	0.027	1E-04	17.92	0.062	0.051	40.15	0.03	0.002	0	0	0	0.179	100.83	**na32 gr39**
38.18	3.697	0.093	0.009	17.56	6E-04	0.197	38.53	0.065	0.244	0	0	0.234	0.944	99.748	**na32 gr33**
38.47	2.433	0.048	0.002	18.01	0.032	0.518	39.59	0.076	0	0	0	0	0.127	99.305	**na32 gr36**
38.534	3.208	0.049	0.003	17.07	0.008	0.154	39.19	0.117	0.013	0	0	0.124	0.455	98.921	**na32 gr37**
39.619	2.882	0.002	0	16.88	0.031	0.09	39.98	0.036	0	0	0	0.036	0.078	99.636	**na32 gr31**
38.489	3.425	0	0	17.56	0.007	0.188	39.53	0.067	0.02	0	0	0.024	0.295	99.604	**na32 gr30**
38.824	**3.083**	**0.027**	**0.005**	**17.54**	**0.019**	**0.179**	**39.5**	**0.069**	**0.043**	**0**	**0.012**	**0.043**	**0.253**	**99.6**	**Average**

O	F	Na	Mg	P	S	Cl	Ca	Mn	Fe	La	Ce	Total	Comment
34.1	2.615	0.002	0	15.92	0.009	0	37.34	0.006	0	0	0.094	90.7743	**na35 gr37**
34.75	3.04	0	0.012	16.7	0	0	37.14	0	0	0	0.052	92.7616	**na35 gr36**
34.19	3.327	0.007	0	16.71	0.004	0	36.76	0	0	0	0.04	92.5418	**na35 gr31**
35.9	3.116	0	0.008	16.7	0.007	0.008	36.35	0	0	0	0.09	93.1273	**na35 gr45**
34.41	3.51	0	0	17.25	0	0.008	37.57	0	0	0	0.031	93.9685	**na35 gr46**
34.99	2.363	0	0.002	17.04	0	0.002	36.91	0	0	0	0.057	92.1832	**na35 gr47**
33.23	2.843	0	0	17.05	0.001	0	36.62	0.014	0.004	0	0.085	91.9361	**na35 gr34**
35.51	2.096	0.01	0.004	16.41	0.014	0.024	37.39	0.005	0.004	0	0.099	92.133	**na35 gr26**
33.99	3.373	0.009	0.002	17.35	0	0.006	37.11	0.008	0.003	0	0.045	93.0997	**na35 gr23**
35.9	3.129	0	0.019	16.83	0.017	0.012	37.14	0.022	0.003	0	0.054	93.9772	**na35 gr22**
34.24	1.815	0.015	0.005	16.67	0.015	0.007	37.48	0.019	0.003	0	0	90.7467	**na35 gr51**
34.53	3.253	0	0.004	17.52	0	0	37.96	0.018	0	0	0.024	93.938	**na35 gr50**
34.95	2.713	0	0.012	17.15	0.003	0.007	37.37	0.007	0.017	0	0.026	93.2097	**na35 gr21**
34.33	4.123	0.05	0.004	17.12	0.002	0.002	37.41	0.012	0.007	0	0.061	93.8274	**na35 gr15**
34.99	4.011	0.025	0	16.1	0	0.002	36.72	0.014	0.014	0	0.018	93.684	**na35 gr12**
35.14	3.157	0.028	0.011	16.16	0.013	0.012	37.01	0.034	0.019	0.033	0.127	92.3101	**na35 gr4**
35.13	3.02	0.017	0	16.66	0.011	0.007	37.16	0	0.024	0	0.007	92.752	**na35 gr3**
35.36	2.578	0.013	0	16.44	0	0	37.79	0.023	0.035	0	0.025	92.4816	**na35 gr2**
35.07	3.176	0.019	0.003	16.29	0	0.009	37.27	0.031	0.017	0	0	93.0201	**na35 gr1**
35.11	3.101	0.004	0	16.62	0.007	0.003	36.9	0.005	0.027	0.01	0.039	92.6429	**na35 gr18**
35.1	2.831	0	0.007	16.63	0.004	0.028	37.29	0.022	9E-04	0.017	0.116	92.7873	**na35 gr7**
34.99	2.924	0.027	2E-04	16.73	0	0.016	37.17	0.026	0.017	0.014	0.122	92.7151	**na35 gr33**
34.66	3.635	0.012	0	17.3	0	0.006	37.47	0.013	0.012	0	0	94.0341	**na35 gr8**
34.59	3.517	0.016	0	16.51	0	0.003	37.72	0.019	9E-04	0	0.016	92.6453	**na35 gr40**
35.51	2.824	0.023	0.004	16.92	0	0.01	37.59	0.012	0.031	0	0.005	93.6876	**na35 gr39**
35.39	2.463	0.028	0	16.63	0	0.003	37.2	0.014	0.008	0	0	91.9592	**na35 gr42**
34.99	2.661	0.045	0.001	15.81	0.004	0.009	37.03	0	0	0	0	91.1605	**na35 gr25**
35.57	2.478	0.022	0.003	16.63	0.004	0.007	37	0.02	0.019	0.097	0.084	92.6868	**na35 gr9**
34.88	**2.989**	**0.013**	**0.004**	**16.71**	**0.004**	**0.007**	**37.21**	**0.012**	**0.009**	**0.006**	**0.047**	**92.74254**	**Average**

O	F	Na	Mg	P	S	Cl	Ca	Mn	Fe	Sr	Y	La	Ce	Total	Comment
39.28	1.76	0.071	0.005	17.16	0.034	0.018	38.93	0.018	0.012	0.62	0	0	0.205	98.106	**na48 gr10**
40.126	1.616	7E-04	0	17.5	0.009	0.006	38.82	0	0.018	0.502	0	0.023	0.351	98.974	**na48 gr11**
40.039	1.732	0.008	0	17.22	0.05	0.01	38.82	0.008	0.013	0.598	0	0	0.133	98.632	**na48 gr16**
40.484	1.783	0.011	0	17.69	0.011	0	39.78	0.004	0.003	0.27	0	0	0.077	100.11	**na48 gr29**
39.662	1.354	0.025	0	17.82	0.009	0.005	39.57	0.007	0.011	0.17	0	0	0.158	98.795	**na48 gr31**
38.927	2.96	0.014	0	17.64	0.015	0.01	38.85	0.006	0.003	0.853	0	0	0.236	99.508	**na48 gr32**
39.225	1.775	0	0	17.8	0.01	0	39.13	0	0.003	0.347	0	0	0.113	98.405	**na48 gr42**
39.185	2.295	0	0	17.72	0.006	5E-04	38.68	0	0	0.283	0	0	0.058	98.228	**na48 gr44**
39.761	1.999	0.11	0.026	17.37	0.011	0	37.56	0.002	0.006	0.37	0	0	0.309	97.532	**na48 gr41**
40.556	1.531	0.011	0	17	0.069	0.011	39.45	5E-04	0.018	0.628	0	0	0.13	99.403	**na48 gr45**
39.606	1.931	0.017	0	17.51	0.016	0.02	38.54	0.019	0.01	0.693	0	0.108	0.434	98.906	**na48 gr40**
40.45	1.776	0	0	17.76	0.004	0.005	39.36	0	0.011	0.612	0	0.076	0.294	100.35	**na48 gr6**
40.964	1.571	0.032	0.007	17.41	0.017	0.003	39.48	0	0.015	0.082	0	0	0.074	99.657	**na48 gr5**
39.679	2.34	0	0	18.02	0.012	0	39.41	0	0.016	0.406	0	0	0.069	99.953	**na48 gr39**
39.76	1.596	0.031	0.018	16.81	0.111	0.037	38.93	0	0.031	0.507	0	0	0.063	97.901	**na48 gr4**
40.69	1.687	0.012	0.039	17.32	0.2	0.082	39.36	0	0.028	0.31	0	0	0.077	99.805	**na48 gr1**
40.209	1.866	0.009	0.036	17.02	0.21	0.086	39.28	0	0.016	0.369	0	0	0.123	99.228	**na48 gr2**
38.758	3.188	0	0	18.08	0.009	0.003	39.47	0.006	0	0.828	0	0	0.05	100.39	**na48 gr3**
39.596	1.62	0	0	17.23	0.006	0.012	39.02	0	0.006	0.626	0	0.053	0.323	98.495	**na48 gr51**
39.722	2.075	0.015	0.007	17.33	0.106	0.004	39.53	0.001	0.019	0.579	0	0	0.125	99.518	**na48 gr34**
38.843	1.683	0.017	0	16.9	0.011	0.015	38.65	0	0.006	0.687	0	0.282	0.594	97.694	**na48 gr33**
39.169	2.734	0	0	17.91	0.025	0.003	38.6	0.015	0.012	1.672	0	0	0.117	100.25	**na48 gr26**
39.115	2.088	0	0	17.69	0.001	0	38.97	5E-04	0.011	1.15	0	0.028	0.197	99.258	**na48 gr22**
40.032	1.609	0.012	0.002	17.86	0.012	0	39.09	0.015	0.036	0.388	0	0.015	0.237	99.31	**na48 gr9**
39.522	1.977	0.02	0	17.25	0.063	0.006	38.61	0.003	0.021	0.667	0	0	0.153	98.295	**na48 gr12**
38.646	3.433	0.006	0	17.69	0.004	0	39.06	0.009	0.012	1.583	0	0	0.143	100.58	**na48 gr20**
40.16	1.8	0.003	0	16.9	0.093	0.022	39.55	0.01	0.004	0.657	0	0	0.038	99.234	**na48 gr27**
37.591	1.546	0	0	17.12	0.016	0.001	37.78	0.007	0	0.539	0	0.141	0.454	95.185	**na48 gr8**
39.381	2.035	0.019	0	17.96	0.014	0.007	39.39	0	0.007	0.315	0	0.012	0.286	99.431	**na48 gr7**
39.574	2.42	0.035	0	17.68	0.015	0	38.63	0	0	0.702	0	0	0.25	99.31	**na48 gr17**
39.624	**1.993**	**0.016**	**0.005**	**17.48**	**0.039**	**0.012**	**39.01**	**0.004**	**0.012**	**0.6**	**0**	**0.025**	**0.196**	**99.015**	**Average**

O	F	Na	Mg	P	S	Cl	Ca	Mn	Fe	Sr	Y	La	Ce	Total	Comment
39.076	3.708	0	0.144	16.84	0.014	0.123	38.3	0.046	0.364	0	0	0	0.22	98.834	**na56 gr26**
38.591	3.826	0	0.146	17.74	0	0.101	39.55	0.039	0.306	0.032	0	0	0.126	100.46	**na56 gr25**
38.848	3.568	0	0.149	17.55	0.006	0.109	39.27	0.054	0.304	0.016	0	0.004	0.157	100.03	**na56 gr24**
38.669	3.579	0	0.142	17.61	0.009	0.106	39.37	0.044	0.333	0	0	0.007	0.192	100.07	**na56 gr23**
38.965	3.526	0	0.128	16.7	0.009	0.105	39.29	0.054	0.284	0	0	0.005	0.154	99.224	**na56 gr44**
38.904	3.632	0	0.154	17.63	6E-04	0.103	39.6	0.048	0.32	0	0	0	0.154	100.54	**na56 gr42**
38.625	3.52	0	0.128	16.93	0	0.103	39.46	0.047	0.337	0	0	0	0.148	99.301	**na56 gr43**
38.804	3.712	0	0.118	17.8	0	0.109	39.43	0.034	0.308	0.008	0	0.019	0.151	100.49	**na56 gr33**
39.444	4.048	0	0.144	18.08	0	0.161	39.28	0.046	0.323	0.034	0	0.015	0.132	101.71	**na56 gr27**
38.794	3.567	0	0.144	17.93	0.009	0.126	39.34	0.057	0.315	0.034	0	0	0.14	100.46	**na56 gr28**
38.926	3.573	0	0.162	18.2	0.008	0.098	39.32	0.038	0.318	0.042	0	0	0.1	100.78	**na56 gr29**
38.202	3.639	0	0.152	18.03	0.017	0.123	39.13	0.041	0.305	0	0	0	0.137	99.771	**na56 gr32**
38.732	3.558	0	0.143	18.23	0.013	0.129	39.39	0.043	0.324	0.05	0	0	0.109	100.72	**na56 gr34**
38.719	3.614	0	0.13	17.86	0.01	0.149	39.45	0.059	0.305	0.05	0	0.005	0.184	100.53	**na56 gr35**
38.665	3.472	0	0.137	18.28	0.009	0.119	39.47	0.048	0.309	0.023	0	0	0.106	100.64	**na56 gr36**
38.873	3.592	0	0.144	17.95	0.005	0.11	39.4	0.053	0.319	0.052	0	0	0.087	100.58	**na56 gr3**
38.61	3.647	0	0.133	18.02	0.004	0.137	39.14	0.036	0.302	0.023	0	0.027	0.17	100.24	**na56 gr6**
38.897	3.567	0	0.167	17.81	0	0.117	39.16	0.057	0.325	0	0	0	0.111	100.21	**na56 gr1**
38.844	3.874	0	0.145	18.05	0	0.131	39.32	0.048	0.282	0.034	0	0	0.114	100.85	**na56 gr2**
39.33	3.523	0	0.134	18.21	0.008	0.12	39.34	0.049	0.289	0.05	0	0	0.16	101.21	**na56 gr8**
39.337	3.49	0	0.142	17.06	0.017	0.108	37.71	0.04	0.288	0.028	0	0	0.106	98.325	**na56 gr11**
38.558	3.588	0	0.159	17.92	0.005	0.132	39.51	0.06	0.314	0	0	0	0.089	100.34	**na56 gr19**
38.682	3.387	0	0.17	17.62	0.013	0.111	39.23	0.032	0.318	0.023	0	0.005	0.132	99.726	**na56 gr12**
38.802	3.445	0	0.169	18.21	0.014	0.087	39.39	0.038	0.314	0.015	0	0.021	0.145	100.65	**na56 gr13**
38.506	3.562	0	0.166	17.71	0	0.121	39.15	0.057	0.34	0.031	0	0	0.136	99.777	**na56 gr15**
39.099	3.493	0	0.169	18.18	0.006	0.115	39.85	0.034	0.312	0.071	0	0	0.159	101.49	**na56 gr19**
39.086	3.559	6E-04	0.077	18.14	0.007	0.119	39.9	0.039	0.257	0.031	0	0	0.159	101.37	**na56 gr18**
39.353	3.675	0	0.162	18.23	0.015	0.11	39.27	0.04	0.322	0.025	0	0	0.12	101.33	**na56 gr17**
38.623	3.538	0.011	0.087	17.78	0.006	0.115	39.57	0.071	0.252	0.009	0	0.004	0.112	100.18	**na56 gr16**
38.913	3.7	0	0.15	18.19	0.013	0.148	39.37	0.036	0.291	0.001	0	0	0.117	100.93	**na56 gr20**
39.018	3.466	0	0.166	18.05	0.005	0.12	39.38	0.044	0.311	0.039	0	0	0.114	100.72	**na56 gr21**
38.855	**3.601**	**4E-04**	**0.144**	**17.82**	**0.007**	**0.118**	**39.3**	**0.046**	**0.309**	**0.023**	**0**	**0.004**	**0.137**	**100.37**	**Average**

O	F	Na	Mg	P	S	Cl	Ca	Mn	Fe	Sr	Y	La	Ce	Total	Comment
38	3.231	0	0.09	17.78	0.007	0.121	39.67	0.025	0.209	0.009	0	0	0.147	99.289	**na57 gr26**
39.542	2.951	0	0.072	17.33	0.005	0.265	39.51	0.031	0.234	0.058	0	0.012	0.128	100.14	**na57 gr23**
38.291	2.946	0.042	0.052	18.07	0.005	0.267	39.41	0.045	0.152	0.042	0	0.024	0.187	99.528	**na57 gr24**
39.005	3.304	0.007	0.089	17.62	0.004	0.138	39.48	0.039	0.255	0.052	0	0	0.146	100.14	**na57 gr25**
39.405	3.23	0	0.12	17.69	0.004	0.132	39.4	0.051	0.252	0.052	0	0	0.114	100.45	**na57 gr22**
38.679	3.274	0	0.157	18.03	0.002	0.168	39.54	0.068	0.333	0	0	0	0.058	100.31	**na57 gr17**
38.224	3.242	0	0.156	17.44	0.004	0.126	39.24	0.051	0.302	0.023	0	0	0.122	98.92	**na57 gr19**
38.977	3.027	0.021	0.066	17.53	0.013	0.255	39.61	0.051	0.213	0	0	0.047	0.131	99.938	**na57 gr21**
38.586	3.11	0	0.153	18.19	0.01	0.202	39.26	0.048	0.309	0.028	0	0	0.09	99.985	**na57 gr20**
38.657	3.086	0	0.144	17.99	0.009	0.228	39.51	0.056	0.292	0.001	0	0.016	0.076	100.07	**na57 gr18**
39.044	3.299	0	0.106	17.36	0.006	0.141	39.4	0.034	0.264	0.017	0	0	0.134	99.802	**na57 gr16**
37.983	2.948	0	0.106	17.41	0.013	0.223	39.31	0.042	0.291	0.042	0	0.014	0.199	98.58	**na57 gr15**
38.912	3.285	0	0.152	18.03	0.013	0.173	39.39	0.04	0.32	0.063	0	0	0.086	100.46	**na57 gr14**
37.488	2.964	0	0.135	17.11	0.012	0.214	39.26	0.036	0.318	0.063	0	0	0.131	97.732	**na57 gr13**
39.093	3.338	0	0.146	18.19	0.021	0.132	39.45	0.045	0.331	0.052	0	0	0.097	100.9	**na57 gr28**
38.951	3.283	0	0.141	18.37	0.016	0.155	39.4	0.06	0.34	0.012	0	0	0.14	100.86	**na57 gr29**
38.697	3.228	0	0.108	18.28	0.01	0.169	39.57	0.06	0.278	0.025	0	0	0.139	100.56	**na57 gr32**
38.374	3.207	0	0.108	18.03	0.008	0.134	39.4	0.058	0.297	0	0	0	0.109	99.722	**na57 gr31**
38.597	3.515	0	0.169	18.13	0.009	0.094	39.03	0.06	0.293	0	0	0	0.096	99.985	**na57 gr10**
38.485	3.095	0	0.119	18.13	0.003	0.228	39.43	0.045	0.3	0.012	0	0	0.126	99.972	**na57 gr3**
38.757	3.077	0.05	0.028	18.06	0.002	0.181	39.76	0.047	0.15	0	0	0	0.218	100.33	**na57 gr2**
38.692	3.224	0	0.113	18.34	0.012	0.133	39.34	0.057	0.309	0.004	0	0	0.159	100.39	**na57 gr4**
38.422	2.912	0.001	0.108	18.24	0.011	0.193	39.61	0.064	0.301	0.041	0	0	0.07	99.978	**na57 gr5**
37.944	3.304	0	0.114	18.23	0.007	0.125	39.33	0.051	0.315	0	0	0	0.11	99.537	**na57 gr6**
37.71	2.938	1E-04	0.077	18.27	0.008	0.117	39.5	0.054	0.275	0.017	0	0	0.092	99.057	**na57 gr1**
38.581	**3.161**	**0.005**	**0.113**	**17.91**	**0.009**	**0.172**	**39.43**	**0.049**	**0.277**	**0.025**	**0**	**0.005**	**0.124**	**99.865**	**Average**

O	F	Na	Mg	P	S	Cl	Ca	Mn	Fe	Sr	Y	La	Ce	Total	Comment
37.538	3.473	0	0.118	18.28	0.01	0.105	39.23	0.057	0.369	0.036	0	0	0.17	99.384	**na58 gr25**
38.077	3.511	0	0.13	18.17	0.004	0.116	39.4	0.051	0.351	0.06	0	0	0.056	99.933	**na58 gr24**
38.777	3.618	0.003	0.118	17.95	0.003	0.12	39.69	0.068	0.357	0.036	0	0	0.168	100.91	**na58 gr27**
38.956	3.892	0	0.104	18.11	0.017	0.119	39.14	0.044	0.346	0.05	0	0	0.092	100.87	**na58 gr30**
39.209	3.773	0	0.116	18.18	6E-04	0.097	39.54	0.04	0.38	0.055	0	0	0.131	101.52	**na58 gr31**
38.839	3.78	0	0.132	17.99	0.009	0.094	39.06	0.027	0.368	0.047	0	0	0.039	100.39	**na58 gr1**
38.978	3.667	0	0.118	17.91	0	0.133	39.2	0.053	0.364	0	0	0	0.126	100.54	**na58 gr2**
38.315	3.569	0	0.124	18.25	0.009	0.126	39.48	0.046	0.361	0.015	0	0	0.132	100.43	**na58 gr3**
38.325	3.81	0	0.145	18.29	0.015	0.11	39.49	0.061	0.355	0	0	0	0.101	100.7	**na58 gr4**
38.078	3.676	0	0.116	18.07	0	0.103	39.61	0.048	0.367	0.031	0	0	0.162	100.27	**na58 gr5**
38.979	3.876	0	0.133	18.26	0.003	0.094	39.6	0.052	0.385	0.007	0	0	0.061	101.45	**na58 gr6**
38.419	3.71	0.002	0.154	18.31	0.006	0.102	39.54	0.044	0.362	0	0	0	0.047	100.69	**na58 gr7**
38.165	3.837	0	0.16	18.32	0.009	0.143	39.32	0.07	0.393	0.017	0	0	0.07	100.5	**na58 gr8**
39.078	3.705	0	0.167	18.36	0.008	0.091	39.77	0.055	0.371	0.017	0	0	0.051	101.67	**na58 gr9**
38.176	3.678	4E-04	0.129	18.21	0.009	0.114	39.23	0.04	0.363	0.007	0	0	0.141	100.09	**na58 gr10**
38.227	3.651	0	0.111	17.95	0.004	0.126	38.88	0.069	0.4	0.025	0	0	0.124	99.566	**na58 gr11**
38.792	3.665	0	0.144	18.08	0.004	0.129	39.42	0.05	0.416	0.001	0	0	0.151	100.85	**na58 gr12**
37.495	3.793	0	0.126	18.15	0.008	0.119	39.18	0.059	0.369	0.036	0	0	0.064	99.404	**na58 gr13**
39.097	3.702	0	0.157	18.28	0.009	0.115	39.55	0.053	0.338	0	0	0	0.075	101.37	**na58 gr14**
38.265	3.608	0	0.155	18.17	0.007	0.136	39.09	0.044	0.394	0	0	0	0.062	99.934	**na58 gr15**
38.062	3.62	0	0.135	18.06	0.01	0.122	39.34	0.044	0.392	0.044	0	0	0.132	99.959	**na58 gr16**
38.927	3.96	0	0.127	18.29	6E-04	0.125	39.72	0.05	0.364	0.017	0	0	0.135	101.72	**na58 gr17**
39.08	3.664	0	0.16	18.38	0.002	0.104	39.63	0.056	0.368	0.039	0	0	0.053	101.54	**na58 gr18**
38.378	3.792	0	0.125	17.96	0.012	0.123	39.3	0.059	0.37	0.05	0	0	0.123	100.29	**na58 gr19**
37.981	3.831	0	0.163	18.01	6E-04	0.128	39.4	0.061	0.364	0.023	0	0	0.09	100.06	**na58 gr20**
38.489	3.754	0.006	0.117	17.76	0.007	0.102	39.37	0.044	0.371	0.06	0	0	0.117	100.19	**na58 gr21**
38.474	3.721	0	0.157	18.3	0.009	0.112	39.33	0.079	0.387	0	0	0	0.106	100.67	**na58 gr22**
38.188	3.669	1E-04	0.123	18.03	0.006	0.104	39.35	0.042	0.363	0	0	0	0.12	99.998	**na58 gr23**
38.477	**3.714**	**4E-04**	**0.134**	**18.15**	**0.006**	**0.115**	**39.39**	**0.052**	**0.371**	**0.024**	**0**	**0**	**0.103**	**100.53**	**Average**

O	F	Na	Mg	P	S	Cl	Ca	Mn	Fe	Sr	Y	La	Ce	Total	Comment
40.334	2.251	0.098	0.036	17.32	0.06	0.028	39.06	0	0.06	0.579	0	0	0.176	99.994	**na66 gr27**
40.06	2.068	0.001	0	17.84	0.002	0	39.41	0.018	0.017	0.849	0	0	0.097	100.36	**na66 gr22**
39.063	2.511	0.047	0.016	16.77	0.068	0.051	38.8	0.015	0.057	0.955	0	0.024	0.452	98.835	**na66 gr23**
41.101	0.812	0.132	0.031	16.68	0.051	0.031	39.14	0.008	0.054	0.093	0	0	0.059	98.187	**na66 gr24**
40.145	2.213	0.085	0.035	16.53	0.061	0.041	39.42	0.012	0.054	0.567	0	0	0.109	99.273	**na66 gr8**
39.829	2.348	0.059	0.034	16.59	0.085	0.021	38.99	0.014	0.044	0.667	0	0	0.299	98.988	**na66 gr7**
38.22	3.287	0.032	6E-04	18.24	0.017	0.008	39.34	0.01	0.038	0.006	0	0	0.089	99.294	**na66 gr29**
38.269	2.336	0.033	0.035	17.17	0.089	0.068	38.59	0.051	0.055	1.142	0	0.256	0.68	98.775	**na66 gr6**
38.739	2.627	0.071	0.004	17.17	0.041	0	39.12	0.027	0.018	0.453	0	0.107	0.402	98.781	**na66 gr34**
39.539	2.054	0	0.004	17.64	0.01	0	39.13	0.008	0.021	1.114	0	0	0.076	99.589	**na66 gr37**
38.273	2.758	0.023	0.08	17.3	0.062	0.037	39.11	0.012	0.046	0.673	0	0.016	0.271	98.662	**na66 gr2**
40.006	1.685	0.137	0.004	16.48	0.018	0.005	38.59	0.017	0.003	0.724	0	0.094	0.365	98.124	**na66 gr1**
39.871	2.004	0.113	0.002	17.83	0.018	0.005	39.52	0.014	0.023	0.519	0	0	0.064	99.979	**na66 gr3**
39.15	2.246	0.007	0.001	17.71	0.012	0.015	39.47	0.02	0.018	0.521	0	0	0.128	99.306	**na66 gr4**
39.613	2.144	0.072	0.01	16.96	0.041	0.014	39.03	0.029	0.046	0.505	0	0.146	0.455	99.071	**na66 gr5**
39.452	1.926	0.017	0	17.44	0.008	0.009	39.02	0.028	0.005	0.889	0	0.058	0.164	99.019	**na66 gr12**
38.812	3.119	0	0.008	18.16	0.009	0	40.01	0	0.027	0	0	0	0.03	100.18	**na66 gr9**
39.187	1.565	0.025	0	17.74	0.011	0	39.26	0.025	0.014	0.591	0	0	0.175	98.591	**na66 gr11**
38.8	2.496	9E-04	0.004	17.36	0.013	0.009	38.77	0.027	0.014	1.466	0	0.03	0.153	99.146	**na66 gr10**
39.247	2.309	0.023	7E-04	17.99	0.016	0	39.45	0.019	0.024	0.475	0	0	0.086	99.638	**na66 gr13**
39.555	1.812	0	0.003	17.66	0.015	0.002	39	0.013	0.007	0.955	0	0.036	0.154	99.219	**na66 gr16**
39.502	1.893	0.05	0.009	17.68	0.024	0	39.66	0.016	0.031	0.395	0	0	0.123	99.387	**na66 gr18**
38.252	3.167	0.061	0.038	17.22	0.118	0.037	39.08	0.026	0.044	0.553	0	0.097	0.369	99.068	**na66 gr17**
40.718	2.356	0.036	0.006	17.41	0.022	0.016	39.1	0.027	0.016	0.734	0	0.066	0.12	100.63	**na66 gr20**
39.681	1.421	0.055	0.003	17.34	0.019	0.01	39.62	0.007	0.022	0.213	0	0	0.073	98.465	**na66 gr56**
38.251	3.191	0.024	0.006	17.94	0.024	0.006	39.67	0.021	0.075	0	0	0	0.067	99.276	**na66 gr58**
38.905	2.626	0.058	0.062	17.4	0.172	0.039	38.83	0.03	0.059	0.762	0	0.151	0.29	99.379	**na66 gr21**
38.387	3.127	0.024	0.103	17.39	0.035	0.187	38.78	0.03	0.085	0.644	0	0.127	0.296	99.21	**na66 gr14**
39.708	1.249	0.109	0.011	17.09	0.039	0.024	39.74	0.029	0.066	0.103	0	0	0.098	98.263	**na66 gr45**
38.707	2.599	0.096	0.009	17.29	0.037	0.004	38.73	0.027	0.023	0.703	0	0.102	0.417	98.746	**na66 gr46**
38.936	2.269	0.066	0.034	17	0.11	0.04	39	0.019	0.025	0.605	0	0.03	0.234	98.371	**na66 gr28**
39.300	**2.273**	**0.05**	**0.019**	**17.37**	**0.042**	**0.023**	**39.18**	**0.019**	**0.035**	**0.595**	**0**	**0.043**	**0.212**	**99.155**	**Average**

O	F	Na	Mg	P	S	Cl	Ca	Mn	Fe	Sr	Y	La	Ce	Total	Comment
38.332	3.592	7E-04	0.06	18.45	0.003	0.204	39.25	0.031	0.252	0.058	0	0	0.192	100.42	**Na75 gr5**
38.734	3.544	0	0.147	18.16	0	0.151	38.84	0.035	0.331	0.043	0	0	0.168	100.15	**Na75 gr7**
38.565	3.577	0	0.12	18.32	0.001	0.182	39.16	0.056	0.357	0	0	0	0.217	100.55	**Na75 gr6**
38.565	3.571	0	0.143	18.34	0	0.17	39.08	0.038	0.333	0.048	0	0	0.176	100.46	**Na75 gr9**
38.74	3.595	0	0.128	18.16	0.01	0.194	38.85	0.043	0.342	0	0	0	0.187	100.24	**Na75 gr8**
37.52	3.969	0	0.058	18.31	0	0.178	39.17	0.023	0.263	0.035	0	0	0.181	99.707	**Na75 gr4**
38.84	3.525	0	0.132	18.42	0	0.189	39.05	0.038	0.324	0.03	0	0	0.119	100.66	**Na75 gr3**
39.062	3.569	0	0.18	18.23	0	0.167	39.08	0.051	0.344	0.025	0	0	0.182	100.89	**Na75 gr2**
39.025	3.523	0	0.154	18.01	0.008	0.205	38.92	0.058	0.349	0.064	0	0	0.166	100.48	**Na75 gr1**
38.838	3.451	0	0.146	17.99	0.002	0.147	39.39	0.045	0.345	0.043	0	0	0.185	100.59	**Na75 gr11**
37.936	3.497	0	0.164	18.26	0.007	0.153	39.01	0.05	0.382	0.031	0	0	0.06	99.548	**Na75 gr10**
37.814	3.485	0	0.101	18.27	0.015	0.16	39.38	0.042	0.328	0.005	0	0	0.077	99.674	**Na75 gr51**
37.398	3.396	0	0.097	18.28	0.008	0.152	39.32	0.041	0.305	0.07	0	0	0.05	99.109	**Na75 gr42**
38.064	3.484	0	0.109	18.24	0.01	0.143	38.97	0.055	0.333	0.028	0	0	0.119	99.559	**Na75 gr39**
37.504	3.443	0	0.144	18.01	0.003	0.206	39.07	0.042	0.355	0.036	0	0	0.077	98.893	**Na75 gr38**
37.985	3.392	0	0.17	17.97	0.011	0.124	38.84	0.048	0.378	0	0	0	0.053	98.967	**Na75 gr35**
38.002	3.511	0.016	0.046	18.01	0.004	0.138	39.05	0.028	0.235	0.039	0	0	0.158	99.235	**Na75 gr24**
36.525	3.307	0	0.108	18.2	0.003	0.145	38.83	0.059	0.323	0.057	0	0	0.06	97.62	**Na75 gr25**
38.151	3.387	0	0.136	18.19	0.011	0.149	38.98	0.044	0.364	0.023	0	0	0.075	99.516	**Na75 gr32**
37.276	3.504	0	0.101	17.91	0.006	0.138	38.89	0.054	0.331	0.023	0	0	0.086	98.314	**Na75 gr31**
37.443	3.416	0	0.134	17.96	0	0.179	38.92	0.051	0.336	0.036	0	0	0.09	98.568	**Na75 gr30**
38.074	3.509	0	0.153	17.89	0.003	0.127	39.14	0.039	0.369	0.002	0	0	0.075	99.384	**Na75 gr29**
38.38	3.601	0	0.127	18.1	0	0.165	38.9	0.032	0.327	0.02	0	0	0.151	99.805	**Na75 gr22**
38.557	3.403	0	0.133	17.89	0	0.156	38.8	0.028	0.335	0.017	0	0	0.155	99.48	**Na75 gr23**
38.887	3.484	0	0.124	17.39	0	0.107	38.97	0.05	0.329	0.017	0	0	0.122	99.481	**Na75 gr26**
38.977	3.704	0	0.117	18.25	6E-04	0.167	38.59	0.054	0.331	0.09	0	0.015	0.086	100.38	**Na75 gr27**
38.756	3.601	0	0.147	18.2	0	0.16	39.14	0.05	0.332	0.004	0	0.032	0.16	100.58	**Na75 gr20**
38.179	3.576	0	0.152	18.05	0	0.135	38.85	0.026	0.341	0.014	0	0	0.137	99.463	**Na75 gr21**
38.941	3.55	0	0.125	18.2	6E-04	0.126	39.3	0.028	0.338	0.048	0	0	0.131	100.79	**Na75 gr17**
39.319	3.638	0	0.148	18.33	0.011	0.181	39.16	0.053	0.33	0.014	0	0	0.104	101.29	**Na75 gr16**
38.247	3.451	0	0.139	18.4	0.005	0.18	38.97	0.051	0.365	0.06	0	0.008	0.148	100.02	**Na75 gr14**
38.278	**3.524**	**5E-04**	**0.127**	**18.14**	**0.004**	**0.16**	**39.03**	**0.043**	**0.332**	**0.032**	**0**	**0.002**	**0.127**	**99.801**	**Average**

O	F	Na	Mg	P	S	Cl	Ca	Mn	Fe	La	Ce	Total	Comment
41.42	2.956	0	0.088	18.22	0.017	0.394	39.62	0.086	0.421	0	0.094	103.3166	**na76 gr10**
41.82	2.77	0	0.089	18.47	0.001	0.516	39.9	0.075	0.427	0	0.119	104.1814	**na76 gr9**
41.34	2.781	0	0.104	18.2	7E-04	0.478	39.65	0.059	0.426	0	0.143	103.175	**na76 gr8**
41.9	2.769	0.002	0.061	18.28	0	0.474	40.21	0.071	0.376	0	0.177	104.3443	**na76 gr6**
42.26	2.886	0	0.048	18.41	0.008	0.545	39.92	0.06	0.387	0	0.194	104.7171	**na76 gr5**
42.02	2.877	0	0.103	18.39	0	0.465	39.65	0.065	0.481	0	0.134	104.1762	**na76 gr4**
42.15	2.9	0	0.081	18.66	0	0.474	39.89	0.071	0.418	0	0.118	104.7598	**na76 gr3**
42.14	2.883	0	0.015	18.28	0.009	0.432	39.86	0.064	0.307	0.014	0.344	104.3768	**na76 gr2**
42.43	2.943	0	0.032	18.37	0.003	0.459	40.46	0.052	0.339	0	0.143	105.227	**na76 gr1**
42.24	2.989	0	0.077	18.42	0.001	0.476	39.88	0.077	0.407	0	0.164	104.7623	**na76 gr42**
41.08	2.674	0	0.119	18.08	0.004	0.446	39.83	0.085	0.45	0	0.169	102.9916	**na76 gr32**
42.24	2.993	0	0.05	18.47	0.01	0.434	40.16	0.065	0.377	0	0.067	104.861	**na76 gr40**
42.03	2.963	0	0.052	18.48	0.003	0.411	40.16	0.066	0.379	0	0.054	104.5946	**na76 gr41**
41.46	2.629	9E-04	0.034	18.39	7E-04	0.443	40.34	0.05	0.342	0	0.169	103.8656	**na76 gr31**
41.75	2.869	0	0.052	18.45	0.004	0.412	39.8	0.064	0.383	0	0.162	103.9427	**na76 gr30**
43.15	3.08	0	0.032	17.83	0.013	0.371	40.13	0.069	0.369	0	0.247	105.2966	**na76 gr27**
42.66	2.85	0	0.115	18.41	0	0.498	39.81	0.062	0.469	0	0.174	105.0559	**na76 gr28**
42.28	2.839	0	0.066	18.45	0.013	0.459	40.13	0.075	0.426	0	0.17	104.9417	**na76 gr17**
42	3.019	0	0.071	18.54	0	0.476	39.99	0.056	0.461	0	0.185	104.8346	**na76 gr16**
42.01	3.052	0	0.075	18.57	0	0.475	40.24	0.066	0.393	0	0.078	104.9504	**na76 gr18**
41.63	2.853	0.038	0.142	17.86	7E-04	0.258	39.05	0.05	0.57	0	0.258	102.7073	**na76 gr19**
42.41	3.063	0	0.092	18.25	0.008	0.412	39.45	0.067	0.474	0	0.134	104.3554	**na76 gr25**
42.84	3.179	0.016	0.02	18.4	0	0.385	40.14	0.058	0.219	0	0.204	105.4518	**na76 gr14**
41.83	3.011	0	0.061	18.11	0	0.424	39.75	0.08	0.389	0	0.102	103.7975	**na76 gr20**
42.41	3.121	0	0.059	18.59	0.004	0.392	39.84	0.074	0.38	0	0.116	104.9884	**na76 gr22**
41.96	3.041	0	0.061	18.15	0.004	0.4	39.42	0.059	0.363	0	0.134	103.5939	**na76 gr23**
41.9	2.985	0	0.043	18.63	0.005	0.438	40.28	0.051	0.322	0	0.099	104.7633	**na76 gr38**
41.73	3.079	0	0.032	18.36	0.002	0.408	39.99	0.065	0.339	0	0.121	104.1393	**na76 gr35**
42.47	3.169	0	0.039	17.93	0	0.463	39.47	0.075	0.299	0	0.172	104.0991	**na76 gr34**
38.33	2.721	0	0.046	18.39	0	0.434	39.8	0.07	0.365	0	0.126	100.3168	**na76 gr36**
41.94	2.971	0	0.09	17.76	0	0.391	40.19	0.083	0.457	0	0.175	104.0758	**na76 gr33**
42.23	3.077	0.05	0.003	18.48	0	0.395	39.69	0.038	0.234	0	0.223	104.4339	**na76 gr24**
41.94	**2.937**	**0.003**	**0.064**	**18.32**	**0.003**	**0.435**	**39.9**	**0.066**	**0.389**	**4E-04**	**0.155**	**104.2217**	**Average**

O	F	Na	Mg	P	S	Cl	Ca	Mn	Fe	Sr	Y	La	Ce	Total	Comment
38.251	2.432	0	0.098	17.44	0.012	0.441	38.75	0.073	0.255	0.078	0	0.002	0.312	98.138	**na77 gr14**
39.323	2.468	0	0.087	17.59	0.017	0.448	38.96	0.042	0.244	0.022	0	0	0.17	99.376	**na77 gr15**
38.788	2.328	0	0.059	17.97	0.025	0.689	39.17	0.054	0.196	0.089	0	0.028	0.193	99.586	**na77 gr13**
38.186	2.07	0.017	0.069	17.27	0.012	0.7	38.98	0.054	0.214	0.073	0	0.036	0.292	97.971	**na77 gr9**
38.837	2.179	0	0.076	17.64	0.013	0.724	39.07	0.04	0.228	0.076	0	0	0.207	99.095	**na77 gr8**
38.275	2.7	0	0.074	17.5	0.016	0.363	39.31	0.062	0.244	0.095	0	0.006	0.293	98.942	**na77 gr7**
37.974	2.262	0.003	0.053	17.5	0.015	0.512	39.16	0.067	0.183	0.116	0	0	0.281	98.13	**na77 gr2**
38.176	2.009	0.015	0.065	18.18	0.008	0.754	39.01	0.036	0.198	0.065	0	0.01	0.215	98.743	**na77 gr3**
38.877	2.199	0.003	0.078	17.75	0.019	0.739	39.3	0.039	0.233	0.086	0	0.029	0.214	99.566	**na77 gr1**
37.746	2.434	0.003	0.072	17.67	0.01	0.521	39.61	0.044	0.21	0.06	0	0	0.209	98.591	**na77 gr12**
38.967	2.279	0	0.089	17.93	0.013	0.616	39.26	0.066	0.247	0.068	0	0.017	0.24	99.794	**na77 gr4**
37.99	2.097	0.014	0.071	18.21	0.012	0.681	39.28	0.042	0.197	0.059	0	0.022	0.243	98.92	**na77 gr5**
39.161	2.496	0.008	0.082	18.06	0.015	0.331	39.24	0.054	0.239	0.054	0	0.012	0.206	99.964	**na77 gr6**
39.02	2.26	0.004	0.063	18.25	0.006	0.508	39.13	0.025	0.212	0.047	0	0.01	0.265	99.801	**na77 gr11**
38.772	2.507	6E-04	0.056	18.17	0	0.515	39.17	0.022	0.238	0.053	0	0	0.21	99.707	**na77 gr36**
39.82	2.394	0	0.055	17.99	0	0.518	39.27	0.029	0.201	0.047	0	0	0.277	100.61	**na77 gr10**
38.802	2.714	0	0.067	18.07	0.001	0.412	39.24	0.027	0.252	0.045	0	0	0.218	99.848	**na77 gr35**
39.358	2.25	0.042	0.025	17.98	0.005	0.2	39.3	0.034	0.15	0	0	0.082	0.343	99.77	**na77 gr31**
38.733	2.877	0	0.075	18.22	0	0.215	39.4	0.031	0.224	0.018	0	0	0.132	99.92	**na77 gr32**
38.609	2.271	0	0.071	18.21	0.004	0.669	39.02	0.027	0.218	0.023	0	0	0.14	99.27	**na77 gr33**
38.854	2.448	0	0.084	18.15	0.008	0.559	39.47	0.044	0.234	0	0	0	0.185	100.04	**na77 gr34**
38.841	2.351	0	0.049	18.11	0.002	0.419	39.24	0.031	0.168	0.01	0	0.014	0.223	99.464	**na77 gr29**
39.473	2.387	0.013	0.052	18.16	0.004	0.665	39.43	0.039	0.174	0.034	0	0	0.276	100.71	**na77 gr25**
38.48	2.53	0.003	0.052	18.25	0.002	0.508	39.26	0.039	0.18	0.037	0	0	0.228	99.569	**na77 gr26**
38.459	2.568	0	0.069	18.16	0.002	0.473	39.06	0.03	0.226	0.085	0	0.025	0.254	99.41	**na77 gr26**
38.541	2.003	0	0.091	18.24	6E-04	0.479	38.89	0.045	0.257	0.063	0	0	0.176	98.782	**na77 gr24**
38.952	2.482	0	0.065	18.26	0	0.486	39.49	0.028	0.221	0.031	0	0	0.148	100.16	**na77 gr23**
40.02	2.352	0	0.051	17.88	0.002	0.706	39.32	0.032	0.196	0.039	0	0	0.165	100.77	**na77 gr18**
38.6	2.52	0	0.064	18.22	0.005	0.53	39.11	0.025	0.212	0.029	0	0	0.15	99.455	**na77 gr19**
38.753	2.6	0	0.078	18.2	0	0.462	39.55	0.049	0.241	0.037	0	0	0.184	100.15	**na77 gr21**
39.981	2.379	0	0.073	18.17	0.001	0.599	39.53	0.047	0.212	0.045	0	0	0.206	101.25	**na77 gr22**
38.794	**2.382**	**0.004**	**0.068**	**17.98**	**0.007**	**0.53**	**39.23**	**0.041**	**0.216**	**0.051**	**0**	**0.009**	**0.221**	**99.532**	**Average**